

THE MECHANICS OF DRAWING POLYGONAL TUBE FROM  
ROUND ON A CYLINDRICAL PLUG

by

MARANGA wa MURIUKI

Submitted in fulfilment of the requirements for the degree of  
DOCTOR OF PHILOSOPHY

THE UNIVERSITY OF ASTON IN BIRMINGHAM

OCTOBER 1981

Supervisor:

Professor D.H. Sansome

THE MECHANICS OF DRAWING POLYGONAL TUBE FROM  
ROUND ON A CYLINDRICAL PLUG

Maranga wa Muriuki

Year: 1981

Submitted in fulfilment of the requirements for the degree of  
Doctor of Philosophy

SUMMARY

Economic factors such as the expense of raw materials, labour and power, are compelling manufacturers of polygonal section rod and tube to seek new production routes. One such method generating considerable industrial interest is the drawing of any regular polygonal tube from round stock on a cylindrical plug in a single pass. Although much work has been done on the drawing of round tube, no theoretical or experimental work has been done on the drawing of a polygonal tube directly from round stock on a cylindrical plug. This project studies this process experimentally and establishes a general theoretical solution based on the principle of least work of deformation.

The theoretical and experimental investigations shewed the practicability of the drawing process. The design of the die profile, i.e. the curves of the interpenetration between the undrawn circular workpiece and the drawn polygonal tube, with the bore remaining circular, was found to be critical. A gradual transformation of the external surface of the round stock to the final section with minimum energy dissipation was found to be essential.

A semi-analytical method, which was developed to determine the mean coefficient of friction in the drawing process, produced values which were comparable with those from the direct measurement using the split rotating die.

Upper and lower bound solutions were developed to predict the maximum and the minimum values of the draw force. The upper bound value over-estimates the actual load to effect the process; the lower bound on the other hand is an under-estimate. A computer programme was written to enumerate the results for a variety of drawing parameters including, for example, the mean coefficient of friction and the geometry of the deformation zone. The theoretical results compared well with the experimental data.

Key Words:        Tube drawing  
                  Polygonal drawing  
                  Energy method  
                  Upper bound  
                  Friction determination



FRONTISPIECE

CONTENTS

	Page
SUMMARY	
FRONTISPIECE	
CONTENTS .. .. .	ii
PLATES .. .. .	viii
NOTATION .. .. .	ix
CHAPTER 1 GENERAL INTRODUCTION .. .. .	1
CHAPTER 2 REVIEW OF THE LITERATURE	
2.1 Introduction .. .. .	4
2.2 Equilibrium approach in drawing .. .. .	6
2.2.1. Axisymmetric bar drawing .. .. .	6
2.2.2 Axisymmetric tube drawing .. .. .	7
2.3 Upper bound solution .. .. .	9
2.3.1 Plane (sheet) drawing .. .. .	12
2.3.2 Axisymmetric bar solution .. .. .	12
2.3.3 Drawing of section rods .. .. .	14
2.3.4 Tube drawing .. .. .	15
2.4 Visioplasticity .. .. .	15
2.5 Finite element analysis in plastic deformation	
2.5.1 Introduction .. .. .	20
2.5.2 Derivation of elastic stiffness matrix .. .. .	22
2.5.3 Derivation of plastic stiffness matrix .. .. .	23
2.6 Determination of the mean pressure and coefficient of friction	
2.6.1 Die rotation method .. .. .	24
2.6.2 Split die method .. .. .	25
2.6.3 Split rotating die .. .. .	25
2.6.4 Estimation of redundant work .. .. .	27

## CHAPTER 3 THEORY: THE MECHANICS OF DRAWING POLYGONAL

## TUBE FROM ROUND ON A CYLINDRICAL PLUG

3.1	Introduction .. .. .	28
3.2	Upper bound solution .. .. .	29
3.2.1	Deformation pattern .. .. .	30
3.2.2	Velocity field .. .. .	32
3.2.3	Strain rates .. .. .	37
3.2.4	Internal power of deformation .. .. .	39
3.2.5	Power loss in shearing the material at the inlet and exit shear surfaces .. .. .	45
3.2.6	Power loss in friction between the tool-workpiece interfaces .. .. .	48
3.2.7	Apparent strain method .. .. .	49
3.2.7.1	The mean equivalent strain .. .. .	54
3.2.7.2	The work hardening factor .. .. .	56
3.2.7.3	Evaluation of $I_1$ and $I_2$ .. .. .	57
3.3	Lower bound solution .. .. .	59
3.3.1	Deformation pattern .. .. .	59
3.3.2	Derivation of the lower bound solution .. .. .	60
3.4	Computer programme .. .. .	64

## CHAPTER 4 THE DERIVATION OF PROCESS PARAMETERS IN THE

## DRAWING OF POLYGONAL TUBE FROM ROUND STOCK ON

## A CYLINDRICAL PLUG

4.1	Introduction .. .. .	75
4.2	The mean coefficient of friction and the mean pressure	
4.2.1	Determination of the mean coefficient of friction and the mean die pressure from the estimated redundant work	
4.2.1.1	Theoretical analysis .. .. .	76
4.2.1.2	Derivation of the mean coefficient of friction and the mean die pressure .. .. .	79

4.2.2	Determination of the mean coefficient of friction and the mean die pressure by split rotating die method		
4.2.2.1	Introduction .. .. .	82	
4.2.2.2	The general derivation of the mean coefficient of friction and the mean pressure from the measurable forces	83	
4.3	Dies for drawing polygonal tubes from round stock on a cylindrical plug .. .. .	87	
4.3.1	Deforming shapes of polygonal tube drawing die		
4.3.1.1	Pyramidical plane shape die (shape A) .. .. .	88	
4.3.1.2	Elliptical plane surface die (shape B) .. .. .	89	
4.3.1.3	Triangular plane surface die (shape C) .. .. .	89	
4.3.1.4	Inverted parabolic surface die (shape D) .. .. .	89	
4.3.2	Dies used in the polygonal tube drawing experiments		
4.3.2.1	Introduction .. .. .	90	
4.3.2.2	Die manufacture .. .. .	91	
4.4	Material of round stock used in the tests		
4.4.1	Selection of tubing .. .. .	91	
4.4.2	The stress-strain relationship of the tube material .. .. .	94	
4.5	Plugs .. .. .	94	
4.6	Lubricants .. .. .	97	
CHAPTER 5 INSTRUMENTATION			
5.1	Introduction .. .. .	98	
✓ 5.2	The force/torque transducer at the tag holder ..	100	
5.3	The plug force transducer .. .. .	100	
5.4	The axial force transducer - the ring type .. ..	100	

	Page
5.5 The cup load cell - the force/torque transducer	103
5.6 Draw speed measurement .. .. .	103
5.7 Rotational speed measurement .. .. .	105
CHAPTER 6 EXPERIMENTAL PROCEDURE .. .. .	107
CHAPTER 7 RESULTS .. .. .	109
CHAPTER 8 DISCUSSION OF RESULTS	
8.1 Introduction .. .. .	128
8.2 Theoretical results	
8.2.1 Introduction .. .. .	129
8.2.2 Upper bound .. .. .	129
8.2.3 Lower bound .. .. .	131
8.2.4 Limitation of achievable reduction of area .. .. .	132
8.2.5 Mean pressure .. .. .	133
8.3 Experimental results	
8.3.1 Introduction .. .. .	134
8.3.2 Draw force .. .. .	135
8.3.3 Die geometry .. .. .	140
8.3.3.1 The shape of the deformation zone .. .. .	140
8.3.3.1 The optimal tube drawing dies ..	146
8.3.4 Evaluation of the mean coefficient of friction .. .. .	151
8.3.5 Evaluation of the mean pressure .. ..	152
8.4 Other observation	153
CHAPTER 9 CONCLUSIONS .. .. .	156
CHAPTER 10 SUGGESTIONS FOR FURTHER WORK .. .. .	159
REFERENCES .. .. .	163
ACKNOWLEDGEMENTS .. .. .	173
APPENDIX .. .. .	
A-1 Geometrical relations for the input tube and the required polygonal tube maintaining the same bore	A1

	Page
A-2 Preliminary selection of tubes .. .. .	A3
A-3 Stock of tubes used in the experiments .. .. .	A10
A-4 Theoretical results .. .. .	A14
A-5 Experimental results	
A-5.1 Drawing of poylgonal tube from round on a cylindrical plug .. .. .	A52
A-5.2 Tension tests of the drawn tubes .. .. .	A59
A-5.3 Determination of the mean coefficient of friction and pressure using the split rotating die .. .. .	A66
A-5.4 Determination of the mean coefficient of friction and pressure from the estimated redundant work and application of apparent strain method .. .. .	A67
A-6 Specifications for the equipment and instrumentation .. .. .	A69
A-7 Calibration curves .. .. .	A73
A-8 Deformation pattern for the upper bound solution of drawing polygonal tubes from round stock on a cylindrical plug .. .. .	A78
A-9 Lower bound - numerical integration .. .. .	A98
A-10 Parameters for the design of dies for drawing of polygonal tubes from round on a cylindrical plug ..	A103
A-11 Dies used in the experiments .. .. .	A112
A-12 Split rotating die .. .. .	A114
A-13 Main computer programme .. .. .	A119
A-14 Axisymmetric tube drawing solutions corresponding to the polygonal tube drawing .. .. .	A141
A-15 Computer sub-programmes to calculate the mean coefficient of friction in polygonal tube drawing using equations (4.10) and (4.19) .. .. .	A143

A-16	Hydraulic drawbench: Assembly and design of equipment .. .. .	A148
A-17	Mechanical drawings of parts for the 'Sheffield' drawbench assembly and other tube drawing accessories .. .. .	A155
A-18	Reduction in draw force with die rotation .. ..	A170

*Translation of the summary in Kikuyu*

## PLATES

- FRONTISPIECE 'Brookes' hydraulic drawbench
- 6.1 Instrumentation
  - 8.1 Conventional or industrial dies and sectional bar drawing dies used in the tube drawing experiments
  - 8.2 The shapes of the deformation zone of the conventional pyramidal die formed by radiused surfaces and the elliptical/conical surface die (elliptical shape 'B') for the drawing of a polygonal section directly from round stock
  - 8.3 Square section drawing dies (shape 'B')
  - 8.4 Hexagonal (6WB) and octagonal (8WB) elliptical tube drawing dies
  - 8.5 Square tube drawing
  - 8.6 Hexagonal tube drawing
  - 8.7 Octagonal and decagonal tube drawing
  - 8.8 Cross-section of tubes drawn through the square dies
  - 8.9 Tube sections drawn directly from round stock on a cylindrical plug through the hexagonal, octagonal, decagonal and round dies displayed in Plates 8.1 and 8.4
  - 8.10 Hexagonal die tips
  - 8.11 Square die tips
  - A-12.1 A cross-section through the split rotating die rig
  - A-12.2 The split rotating die drive system
  - A-12.3 Tube drawn through the square die tips
  - A-16.1 'Sheffield' hydraulic drawbench

## NOTATION

$D_b$	Diameter of the inlet circular section
$D_a$	Diameter of circle circumscribing the required polygonal tube
$H_a, A/C$	Diagonal length of the drawing die equal to the diameter of the circle circumscribing the polygon
$L$	Die length measured along the draw axis (die height)
$N_s$	Number of sides of the drawn polygon tube
$A/F$	Across flat length of the polygonal tube
$t_b$	Inlet tube wall thickness
$d_p (=2r_p)$	Plug diameter equal to the bore of the input stock
$A_b$	Cross-sectional area at entry
$A_a$	Cross-sectional area at exit
$A_r$	Ratio of cross-sectional area at entry to that at the exit
red, 'r'	Reduction of area
$t_a$	Maximum tube wall thickness along the major diagonal of the drawn tube
$\kappa$	Factor ( $0 \leq \kappa \leq \frac{1}{2}$ ) expressing tube wall thickness at the diagonals in terms of $H_a$ , i.e. $t_a = \kappa H_a$
$D_e$	Diameter of an equivalent circular section on a cylindrical plug at the exit
$\alpha_e$	The equivalent die semi-angle; it is the semi-angle of a conical die corresponding to the polygonal tube drawing die on a cylindrical plug, for the same reduction of area and the same die length
$\alpha_c$	Die semi-angle of the conical surface in a polygonal section drawing die

$\alpha_s$	Die semi-angle of the flat surface in a polygonal section drawing die
$\lambda_c$	Angle subtended by the conical surface of a symmetric section at the draw axis
$\lambda_s$	Angle subtended by the flat surface of a symmetric section at the draw axis
$\beta$	Included angle of a symmetric section of the die ( = $\lambda_c + \lambda_s$ )
$\rho, \theta, \phi$	General spherical co-ordinates
$\rho$	Radial distance from the virtual apex to the centroid of the assumed shape element at the inlet section
$\theta$	Inclination of the radius to the tube axis
$\psi$	The relative angular deflexion of an element measured in the $\rho - \theta$ plane
$\eta$	The relative lateral displacement of the assumed shape element at the outlet section referred to the inlet
$\dot{U}_\rho, \dot{U}_\theta, \dot{U}_\phi$	Velocities in $\rho, \theta,$ and $\phi$ directions respectively
$\mu_m, \mu$	The mean coefficient of friction at the die/tube and the plug/tube interfaces
$p_m, p$	Mean pressure at the die/tube and the plug/tube interfaces
$\sigma_{za}$	Mean draw stress
$k$	Mean yield stress in shear
$Y_m$	Mean yield stress in tension
$(\sigma_f)$	Flow stress of the material
$W$	Work done per unit volume of the material
$\sigma_o$	Stress at unit strain
$\dot{VOL}$	Volumetric rate
$J^*$	Actual externally supplied power
$V$	Volume of the deforming material
$\dot{\epsilon}_{ij}$	Strain rate

$\tau_s$	Shear stress at the sliding surfaces
$ \Delta v $	Velocity discontinuities at the sliding surfaces
$S_\Gamma$	Surface of velocity discontinuities
$T_i$	Pre-determined body tractions
$S_t$	Surface area subjected to pre-determined body tractions
$S_v$	Surface of prescribed velocity
$v_i$	Velocity at entry and exit surfaces having pre-determined body tractions
$u_i$	Discrete displacement function
$\hat{n}_j$	Unit outward normal
$\sigma_{ij}$	Stress tensor component
$\bar{\sigma}$	Generalised stress or $\sqrt{\frac{3}{2}} \{\sigma'_{ij} \sigma'_{ij}\}^{\frac{1}{2}}$
$\bar{\epsilon}$	Generalised strain or $\sqrt{\frac{2}{3}} \{\epsilon'_{ij} \epsilon'_{ij}\}^{\frac{1}{2}}$
$t$	Factor ( $-1 \leq t \leq 1$ ) selected to optimize the inlet and the exit shear surfaces by minimisation of the plastic work done
$N$	Number of hyperbolic curves banding the exit section
$M$	Number of sectors into which the inlet section is divided

General subscripts

a	exit parameter
b	entry parameter
p, 2	plug surface
d, 1	die surface
c	conical
s	flat or straight
m	mean
$\delta_{ij}$	Kronecker delta
$\nu$	Poisson's ratio

CHAPTER 1

GENERAL INTRODUCTION

## I. GENERAL INTRODUCTION

The drawing of polygonal tube directly from round stock on a cylindrical plug is of great value to industry. For instance, in the making of nuts such a process would bring significant savings in the cost of raw material, tooling, power and labour, and possibly impart improved mechanical properties to the metal.

An investigation of the mechanics of drawing polygonal tube from round on a cylindrical plug would provide information on the forces on the tools and an insight into the flow of the deforming metal. Such a study would lead to an optimal selection of tool profile, unveil the possibility of drawing defects and the limitations to the application of the process. An understanding of the mechanics of deformation also would lead to an efficient utilisation of material resources and draw-benches. A rigorous investigation requires that a wide range of experimental data be collected, explained theoretically, thus providing a valuable guide to the problems encountered in industry.

Many theories of axisymmetric tube drawing have been published but there is no known attempt to establish the theory on the drawing of a polygonal tube from round on a cylindrical plug. The project undertakes this subject to study the process experimentally and establish a theoretical solution.

Recently Kariyawasam (1) has investigated the drawing of a regular polygonal tube from round tube on a corresponding polygonal plug. His work followed that of an earlier research on the drawing of regular polygonal bars from round stock by Basily (2). The problems in both cases were solved numerically.

An interesting feature of the work in the theses of Basily,

Kariyawasam and in this thesis is the geometry of the deformation zone through which a workpiece of entirely circular cross-section transforms wholly or partly to a polygonal section in a single pass. A gradual transformation of the round stock to the final section is critical. In addition the deforming passage must affect the ease of manufacture, the associated drawing defects and the quality of the final product and also the power to effect the process with optimum efficiency. Therefore, the die has a complex shape.

Basily investigated die shapes formed by combining conical and plane surfaces having different inclinations to the axis. They were the pyramidal plane surfaces, elliptical plane/conical surfaces, triangular plane/conical surfaces and the inverted parabolic/conical surfaces. Since close pass tube drawing can be compared with the drawing of a solid section in which the central section is arrested, thereby introducing an undeformable frictional interface, similar die deforming shapes were investigated for tubing.

A review of drawing theories has been presented to form the basis of the approach finally adopted. Mathematical solutions similar to those of axisymmetric drawing are extremely difficult to derive for polygonal tube drawing; the flow pattern is too complicated. In this thesis two numerical solutions were established for the drawing of a regular polygonal tube from round tube on a cylindrical plug. Close pass draw was assumed. The first is based on equilibrium of forces and predicts the lower bound. The second solution was obtained from a velocity field that minimizes the energy required for the process and incorporates an apparent strain method which includes Coulomb friction. The two loads bound the actual force to effect the deformation for the given drawing parameters. The details of the derivation are given in Chapter 3. The details of the velocity fields and the computer programmes are discussed in Appendices A-8 and A-13.

To fulfil the objective of the experimental part, two hydraulic drawbenches were initially to be used. The author helped to instal and carry out the necessary modifications to one of the drawbenches. However, owing to the economic conditions the bench was abandoned eventually but since the work took a substantial fraction of the period intended for research, the details of the installation, design and assembly are included in Appendices A-16 and A-17. Equipment which was designed to measure the parameters included (i) the load cells at the die, tag and the plug ends and (ii) the device for measuring the draw speeds.

Detailed mechanical drawings are given in the appendix A-17.

Dies for the drawing of regular polygonal tube from round stock on a cylindrical plug are discussed in Chapter 4 and in the Appendix A-10

The mean coefficient of friction was determined by an instrumented rotating die. The analysis, in addition, required the measurement of the following parameters:-

- (i) the draw force
- (ii) the thrust force at the die
- (iii) the draw speed
- (iv) the plug force
- (v) the rotational speed and
- (vi) the rotational torque

The analyses of the equipment and the circuit diagrams to measure the above parameters are given in Chapter 5 and Appendix A-16. The calibration of the instrumentations is given in the Appendix A-7.

CHAPTER 2

REVIEW OF THE LITERATURE

## 2.1 INTRODUCTION

Drawing of metal is believed to have been used first by the Ancient Egyptians to draw ornamental wires. They cut strips from hammered metal sheets, lubricated them with animal fat and pulled them through a die, which had been made by abraiding a hole in a pebble, to produce a circular section (3). Today, the technique is widely used in industry to draw wire, rod, strip, tube, bi-metal tube, section, etc.

Cold drawing is a metal forming process which gives a close dimensional control, improves the degree of surface finish and may also introduce desirable effects on the mechanical properties of the metal. The strength of the drawn product limits the amount of deformation which can be achieved in any single stage. Thus any modification to improve the drawing process must reduce the tensile stress within the drawn product, enabling greater reductions per pass to be achieved. There is continued research in metal working establishments to improve methods to manufacture a product. A vast amount of literature on both the theoretical and experimental aspects of drawing processes has been published. The fundamental factors covered in the drawing theories include the mechanical properties of the work material, the geometry of the deforming passage and the friction at the tool-workpiece interface.

The analysis of plastic flow of metal has received attention by a number of investigators. In particular, solutions of axisymmetric drawing have been produced by Davis and Dokos (4), Sachs and Hoffman (5), Siebel (6), Maclellan (7), Wistrieck (8), Yang (9), Johnson and Sowerby (10), and Zimmerman and Avitzur (11) and Hill and Tupper (12). The plane strain theories have been discussed by Siebel (13), Hill (14), Green and Hill (15), and Green (16).

In practice, non-circular sections such as polygonal rods and tubes, channels, angles, etc., are commonly drawn. In such cases the flow is generally asymmetric and hence the analysis is complicated by comparison with the analyses for plane-strain deformation and the circular sections with axial symmetry. The symmetric drawing of polygonal rods, i.e. the cross-section of the billet and the product are geometrically similar, has been studied, theoretically only by Prakash and Juneja (17), and Prakash and Khan (18). The drawing of regular polygonal bar from round stock has been investigated theoretically and experimentally by Basily (2). An experimental and theoretical investigation on the drawing of polygonal tube from round stock on a corresponding polygonal plug has been reported by Kariyawasam (1). There is no known literature on the drawing of regular polygonal tube from round stock on a cylindrical plug in spite of the value of this shape of tube which finds uses in engineering and as raw material for nut manufacture. Therefore, this thesis undertakes this investigation.

Metal working theories can be grouped broadly under:-

- (i) equilibrium approach
- (ii) slip line field solution
- (iii) upper bound solution
- (iv) energy approach when the total work is decomposed into homogeneous, redundant and friction components
- (v) viscoplasticity and
- (vi) finite element method.

However, a comprehensive review is only presented for the equilibrium and the upper bound approaches which form the basis of the methods used to obtain the solutions for the drawing of a polygonal tube from round on a cylindrical plug in Chapter 3. The application of the viscoplasticity and the finite element techniques to metal working are discussed

briefly in sections 2.4 and 2.5. In addition, experimental methods to determine the mean coefficient of friction and the mean pressure are reviewed in section 2.6.

## 2.2 EQUILIBRIUM APPROACH IN DRAWING

The method is based on the equilibrium of forces, without paying attention to the internal flow restrictions. The loads determined are sometimes in agreement with practical values for some processes. The theory, nevertheless, must be applied with caution because under some circumstances the load is seriously under-estimated. The error arises when the external constraint causes appreciable internal distortion of the workpiece beyond that strictly necessary for the shape change.

### 2.2.1 Axisymmetric bar drawing

In 1927 Sachs (19), proposed a theory which proved the most important among the early theories on wire drawing. He assumed that plane cross-sections of the workpiece remained plane as they passed through the die, the stress distribution on such planes was uniform, the die surface was one of the principal planes, the yield stress was constant, Coulomb friction applied and the friction at the die-workpiece interface did not affect the stress distribution. By considering the equilibrium of longitudinal forces together with Tresca's yield criterion, he derived the following expression for the drawing stress:-

$$\sigma_{za} = Y_m \left( \frac{1 + \tilde{B}}{\tilde{B}} \right) \left[ 1 - \left( \frac{A_a}{A_b} \right)^{\tilde{B}} \right] \quad (2.1)$$

where,  $\tilde{B} = \mu \cot \alpha$

$A_b$ , and  $A_a$  are the cross-sectional areas at the inlet and exit respectively.

Later, other investigators such as Körber and Eichenger (20), Davis and Dokos (4), and Lunt and Maclellan (21) refined and improved

on this theory. In particular, Davis and Dokos extended the solution to the case where the material work-hardens linearly. However, Atkins and Caddell (22) have shown, using the power law, that for practical range of parameters the error is about 8% when the mean yield stress is used instead of taking into account the strain-hardening relationship in the governing force-balance differential equations prior to the integration. They have also given a method for incorporating an empirically determined redundant work factor into the above equation. Siebel (6), added a factor  $2/3\sigma Y_m$  to the above equation to account for redundant work. Johnson and Rowe (23), have given a general expression to account for redundant work in drawing of cylindrical stock.

Comprehensive reviews of the work of other investigators have been published by Wistrieck (8,24) and Maclellan (7).

#### 2.2.2. Axisymmetric tube drawing

The drawing of tubes is based on three fundamental metal working processes, viz. sinking, plug and mandrel drawing. In the sinking process the tube is drawn without any internal support in the bore with a resultant decrease in tube diameter, with ideally no change in wall thickness. In the fixed plug and the mandrel drawing processes, the major deformation is the reduction of the wall thickness.

The mandrel drawing process similar to plug drawing, but the difference between the processes lies in the fact that the mandrel moves with respect to both the tube and the die. Because of this the mechanics of the process are greatly altered by virtue of the fact that part of the drawing load is transmitted through the material. Sachs, Lubahn and Tracy (25), derived an equation for the drawing of thin-walled tubing with a moving mandrel to yield the draw stress:-

$$\sigma_{za} = Y_m \left( \frac{1 + B^*}{B^*} \right) \left[ 1 - \left( \frac{h_a}{h_b} \right)^{B^*} \right] \quad (2.2)$$

$$\text{where, } B^* = \frac{\mu_1 - \mu_2}{\tan\alpha_1 - \tan\alpha_2}$$

$\mu_1, \mu_2$  are the coefficients of friction at the die/ and the mandrel/tube interfaces respectively

$\alpha_1, \alpha_2$  are the semi-angles of the dies and the mandrel respectively

$h_b, h_a$  are the initial and final tube thicknesses respectively.

The solution was based on the following assumptions:-

normal stress acting on a transverse section is distributed uniformly over the cross-section; the normal pressures on the die and the mandrel are equal; the axial stress and the normal pressure are the principal stresses. The developed relation thus becomes less exact at large tool angles, and especially if the difference between the two angles is large. Sachs and Espey (26) later published their experimental work on tube drawing with a moving mandrel.

In the case of plug drawing, the direction of the friction forces between the plug and the tube is the same as that between the tube and the die. The solution is the same as for the mandrel drawing except that the parameter  $B^*$  changes to

$$B^* = \frac{\mu_1 + \mu_2}{\tan\alpha_1 - \tan\alpha_2}$$

In 1946, Sachs and Baldwin (27) derived a solution to the sinking of thin walled tubing:-

$$\sigma_{za} = Y_m' \left( \frac{1 + \tilde{B}}{\tilde{B}} \right) \left[ 1 - \left( \frac{D_a}{D_b} \right)^{\tilde{B}} \right] \quad (2.3)$$

where,  $\tilde{B} = \mu \cot\alpha$

$D_b$ ,  $D_a$  are the mean diameters at the inlet and the exit respectively  
 $Y'_m = mY_m$ , is the modified mean yield stress from the von Mises  
yield criterion applied to the complex state of stress occurring  
in tube sinking. The average value of  $m = 1.1$ .

The solution was based on the following assumptions:-

a shear stress produced by frictional force exists on the interface  
between the die and the tube; transverse sections are free from shear  
stresses; the normal stress acting on the transverse sections is  
uniformly distributed over the cross-section and is a principal stress;  
the wall thickness of the tube is small in comparison to the tube  
diameter; the wall thickness of the tube remains constant throughout  
the process; and the radial pressure on the die is small in comparison  
with the principal longitudinal and circumferential stresses.

Swift (28) and Chung and Swift (29) have put forward a theory  
which predicts the sinking loads, wall thicknesses and length increments.

All these theories proposed by Sachs and his collaborators were  
basically for stress determination and include friction and no redundant  
effect. In all cases, the stress distribution across the tube wall was  
assumed to remain constant which only applied to thin-walled tubing. A  
more general method of accounting for the effect of redundancy was pro-  
posed by Blazynski and Cole (30, 31) in their investigations of the  
sinking, mandrel and fixed plug drawing processes. The semi-empirical  
method is a modification of Hill and Tupper's concept of the equivalent  
total mean stress.

### 2.3 UPPER BOUND SOLUTION

In 1951 Prager and Hodge (32) derived the formulae for bounding  
loads for a rigid - perfectly plastic material. These were deduced

from work principles published by Hill (14).

The upper bound theorem for rigid-perfectly plastic solid states that among all admissible strain rate solutions the actual one, which is also statically admissible, minimizes the power to effect the given forming process. Drucker (33) extended the theorem to include the velocity discontinuities. With the additional usual assumptions that the material obeys von Mises yield criterion and the flow follows the Levy-Mises stress/strain relationship the complete upper bound expression becomes:-

$$J^* = 2k \int_V \sqrt{\dot{\epsilon}_{ij} \dot{\epsilon}_{ij}} dV + \int_{S_T} \tau |\Delta v| dS - \int_{S_t} T_i v_i dS \quad (2.4)$$

The lower bound theorem states that among all statically admissible stress field  $\sigma_{ij}$ , the actual one minimizes the expression,

$$I = \int_{S_v} \sigma_{ij} v_i \hat{n}_j dS \quad (2.5)$$

A statically admissible field is that one which satisfies the equilibrium equation and does not violate the yield criterion. Several admissible stress fields can be assumed aiming at getting the maximum value of power, I. As the power calculated becomes larger, it is presumed that the stress field associated with it is closer to the actual stress field. That the equilibrium solution which is in terms of a stress distribution is not kinematically admissible is readily apparent, unless the actual stress field has been used. The equilibrium methods discussed in section (2.2) are lower bound solutions. The solutions fail to take account of redundant deformation. For example, in drawing the error is proportionally significant for small reductions and large die angles.

Different kinematically admissible velocity fields can be assumed to determine the minimum value of  $J^*$ . For lower values of  $J^*$ , it is presumed that the velocity field that led to it is approaching an

actual velocity field.

The great advantage that kinematically admissible solutions have is that they do consider the modes in which it is possible for metal to flow, and hence more likely to give the correct results to metal working problems. In addition to predicting the loads (e.g. extrusion or drawing force), the understanding has led to the optimization of the process. The defects such as redundant deformation, central fracture and other defects, bulge formation, rough and eccentric flow, bar shaving, dead zone formation, etc., have been predicted. The elimination of some of these defects has been possible by proper choice of variables in the respective processes. As an example, Avitzur (34, 35) has applied the study to the central bursting defects in extrusion and wire drawing.

Incorporating friction in the upper bound integral (2.4), poses a problem. Coulomb friction could be allowed, when  $\tau = \mu p$  or the tangential stress at any point is proportional to the pressure  $p$ , between the die and the workpiece. However, the pressure  $p$  is usually unknown. An indirect method i.e. the apparent strain method has been used to incorporate friction in case of Coulomb friction (2). An alternative to this is to assume a constant shear stress  $\tau = mk$ , where  $0 < m < 1$ . The factor  $m$  takes a constant value for a given die and material under constant surface and temperature conditions. It is taken to be independent of velocity, also it does suffer from the disadvantage that the shear stress at the tools, rarely bears a constant relationship to the yield stress in shear of the workpiece.

The upper bound solution concerns the movement of the material through the deforming tool. The problem, therefore, is how to deduce such admissible velocity fields which conform to external boundaries without violating the continuity criterion. In the early development,

the deforming zone was sub-divided into rigid regions and a pattern of internal velocity discontinuities was found that was compatible with imposed velocity boundaries and which gave as low an energy dissipation as possible.

### 2.3.1 Plane (sheet) drawing

Hill (36) first illustrated the upper bound technique applied to plane-strain by a simple approximation to the slip-line analyses for wedge shaped dies.

Johnson and Mellor (37) have reviewed the application of the theorem to plane strain problems. In his original work Johnson (38) assumed that the basic deformation zone was built up of triangular elements similar to those deduced by slip-line solution. However, the material was considered rigid both inside and outside these triangles and the energy was dissipated along these discontinuities and the boundaries only.

Kudo (39) developed the concept of unit deforming regions. The workpiece is divided into suitable rectangular regions and each of these is then sub-divided into rigid triangles. The minimum energy dissipated along the discontinuities and the boundaries is calculated for a unit region algebraically or by scale drawing for various unit dimensions and frictional conditions. The optimal geometry for each sub-unit is thus determined for the deforming zone.

### 2.3.2 Axisymmetric bar solution

The solutions of plane strain conditions can be adapted to axial symmetry by supposing that the diagrams represent diametral sections of the workpiece.

In 1959 Alexander (40) when commenting on the plane strain upper bound solutions of Johnson (38), extended the method to represent the case of axial symmetry. He retained the velocity field proposed by Johnson but the deforming zone in this case is a single annular region which appears triangular in the plane of symmetry. Deformation was considered by shearing at the boundaries in addition to the homogeneous deformation within the deforming zones.

In 1960 Kudo (41) extended his previous solution of plane strain to axisymmetric problems where the unit rectangular regions were cylindrical. These were again sub-divided into sections which were triangular in the plane of symmetry. He considered the energy expended by deforming the material within the individual zones, as well as by shearing at the discontinuities and the boundaries.

Kobayashi (42) in 1963 proposed the replacement of Kudo's rectangular units by curved surfaces of velocity discontinuities. However, the difference between his solution and Kudo's was too small for critical comparison.

In 1965 Halling and Mitchell (43), extended Johnson's upper bound method by considering additional power dissipated in circumferential straining within the plastic zone. They extended this solution to incorporate work-hardening characteristics of the material.

Kobayashi and Thomsen (44) proposed a solution similar to the above by considering the velocity field to be composed of a variable number of separate triangles and assumed a constant value for the slope of the entry discontinuity. The solution was thus dependent on the initial choice of the slope.

Thomsen et al (45) have extensively reviewed the earlier work of Kudo in their book. Adie and Alexander (46) have proposed graphical

methods for obtaining kinematically admissible velocity fields for axisymmetric problems in which solid billets are used. This is an extension of the usefulness and applicability of Halling and Mitchell's approach.

An important contribution to the upper bound solution is the introduction of the spherical velocity field for the application to problems of axial symmetric workpieces. Kinematically admissible velocity fields are developed with suitable spherical surfaces of velocity discontinuity, dictated by the geometric boundaries such as in simple wire drawing, or found by minimising the total energy dissipation (11). Avitzur (47, 48) derived an upper bound solution in which he considered the deforming zone to be bounded by spherical shear surfaces with their centres at the virtual apex of the die. The flow through the die was thus expressed by  $\int_A^a$  kinematically admissible velocity field. The distinctive part of Avitzur's work is that he expresses the power of internal deformation as the homogeneous component multiplied by a factor greater than unity to account for the relative shearing of the material in the deforming zone. A large selection of problems has been detailed in his book (49).

### 2.3.3 Drawing of section rods

Juneja and Prakash (17) in 1975 obtained an upper bound solution for the symmetric drawing of polygonal sections, i.e. the original and the final cross-sections are geometrically similar. They assumed that the zone of plastic deformation is enclosed by two cylindrical surfaces of velocity discontinuity at entry and exit to the pyramidal portion of the die. In their solution they concluded that the draw load for the symmetric drawing of section rod is higher than that of the corresponding axisymmetric drawing. This draw load decreases rapidly to that of the axisymmetric solution by Avitzur (47), as the number of sides of the section increases. Prakash and Khan (18) in 1979

extended the problem to generalize the shape of the zone of plastic deformation and optimised the geometric factor denoting the shear surfaces to obtain the lowest upper bound value of the working stress.

Basily (2, 50) derived a numerical upper bound solution for the drawing of regular polygonal bars from round stock in a single pass. The material flows through the die where an initially circular cross-section deforms gradually to the required polygonal section at the exit. The velocity field was derived from a deformation pattern, constructed by conformal mapping with optimised inlet and exit shear surfaces.

#### 2.3.4 Tube drawing

In 1965, Avitzur (51) extended his wire drawing upper bound method of spherical velocity field to tube sinking through a conical die and tube expansion over a conical mandrel.

A general upper bound solution has been constructed for axisymmetric contained plastic flow that occurs in processes like drawing and extrusion of tubes and wires by Prakash and Juneja (52). They assumed plane velocity discontinuities at the entry and exit to the die. As particular examples, the solutions were applied to plastic flow through conical dies with plug or mandrel.

### 2.4 VISIOPLASTICITY

#### 2.4.1 Introduction

Visioplasticity is a semi-analytical technique based on the examination of a velocity field developed incrementally within the deforming body. This method of deriving the instantaneous motion of the particles making up the body was developed by Thomsen et al (54, 55, 56) and is analogous to photo-elastic techniques for analysing

stresses in elastic problems. The study obtains detailed analysis of the distribution of stress, strain and strain rates of the forming process using experimental flow data together with plastic stress-strain relationships.

The metal flow is observed by sectioning the billet on a meridian plane or a plane containing the major deformation. The surfaces are ground flat and polished on both sides of the cut; a regular pattern of square (or circular) grid is imprinted on one face by either mechanical or photographic means. The two halves are re-assembled and the distortion of the grid is observed with a microscope or an enlarged photograph after each incremental deforming step has been given to the billet. The displacement and hence the velocity of each element are thus determinable.

The instantaneous velocity at each point can be resolved into the components  $u$  and  $v$  in the axial and radial directions respectively (see fig. 2.1). A series of graphs showing the variation of  $u$  and  $v$  with the position co-ordinates are plotted (i.e.  $u$  versus  $z$ ,  $v$  versus  $r$ ,  $u$  versus  $r$  and  $v$  versus  $z$ ). The slope of the appropriate velocity/position curve gives the strain rate at a particular point.

$$\dot{\epsilon}_r = \frac{\delta v}{\delta r}; \quad \dot{\epsilon}_z = \frac{\delta u}{\delta z}; \quad \text{and} \quad \dot{\gamma}_{zr} = \frac{\delta u}{\delta r} + \frac{\delta v}{\delta z} \quad (2.6)$$

By the use of von Mises flow rules together with the force equilibrium of the element, the stress components are derived from the computed strain rates. It is apparent that the numerous calculations, graphical differentiations and integrations involved are laborious and time consuming. An extensive computer facility is therefore desirable. Also, to obtain reliable differentials it is necessary to smoothen the experimental data in both the axial and radial directions (57).

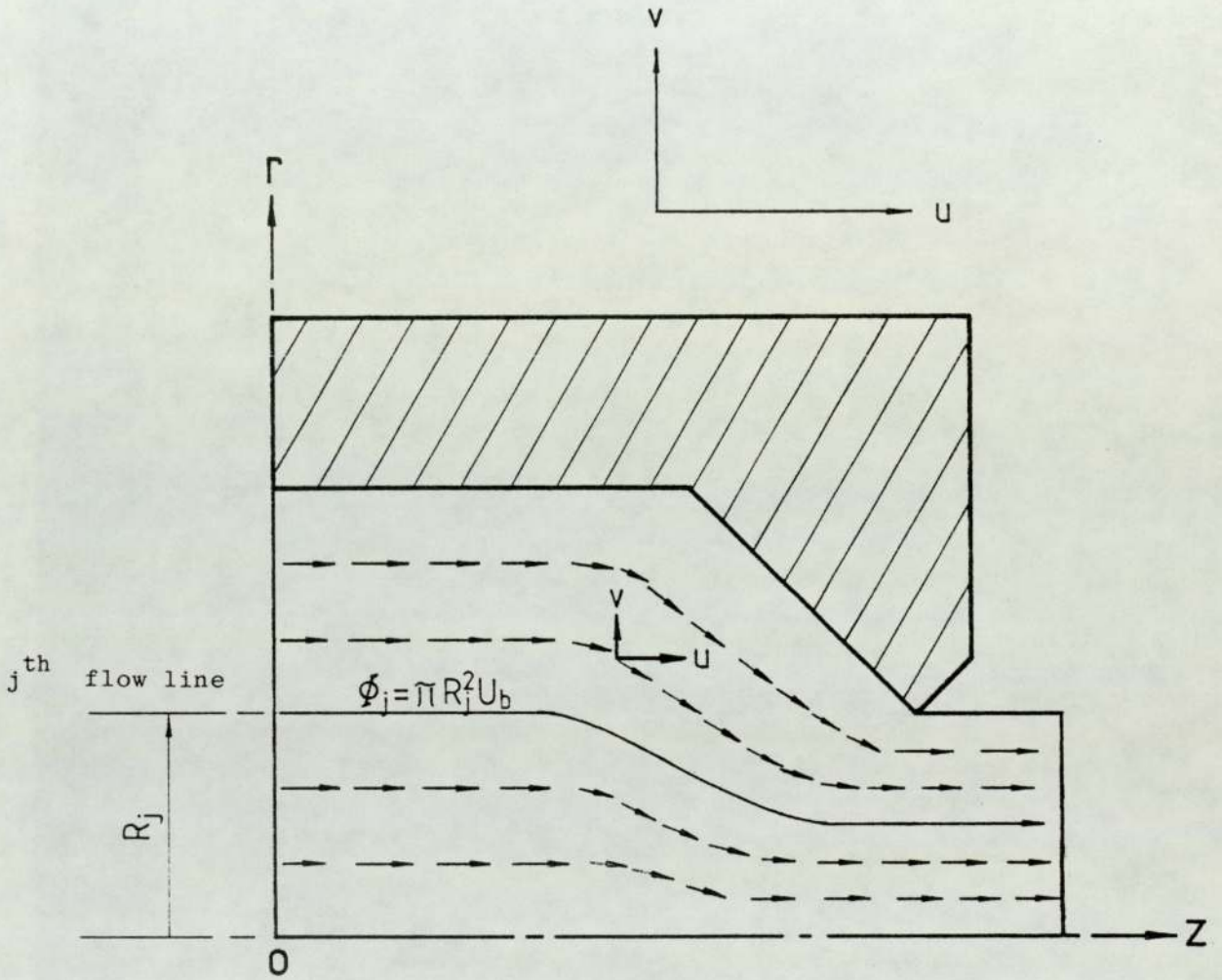


Fig. 2.1 A sketch showing the directions of the instantaneous velocity vectors deduced from the distortion of an etched grid (axial lines) for a billet subjected to 75% reduction of area.

An alternative method of analysing the resulting distorted grid is to fit a flow function  $\Phi$  to the data (58, 59, 60).  $\Phi$  is represented as some function of  $r$  and  $z$  having a number of adjustable parameters. For example, in Fig. 2.1, the value of the function  $\Phi_j$ , which is constant along the flow line  $j$ , can be obtained from the initial conditions outside the deformation zone, i.e.

$$\Phi_j = \pi R_j^2 |U_b| \quad (2.7)$$

Where,

$U_b$  is the ram speed (in case of extrusion or  $U_b = U_a (1 - r)$  in drawing) and ( $U_a =$  velocity of extrudate)

$R_j$  is the radius of the flow line before deformation starts.

The flow function  $\Phi = \Phi_j$  is expressed as a function of  $r$  and  $z$  from the co-ordinates of the observed points along the flow line, i.e.

$$\Phi = \sum_{n=1}^m A_n r^n \quad (2.8)$$

At each station (i.e.  $z =$  constant) the approximate polynomial (of order  $m$ ) describes the variation of  $\Phi$  with  $r$ . The changes in the polynomial coefficients ( $A_n$ ) downstream from one station to the next describes the variation of  $\Phi$  with  $z$ . A numerical routine is devised to select these coefficients in such a way as to give the best fit with the measured data.

Once it has been established that the function is reasonably accurate the velocity components are evaluated at each point,

$$\begin{aligned}
\dot{\epsilon}_r &= \frac{\delta v}{\delta r} = \frac{1}{2\pi r} \left( \frac{1}{r} \frac{\delta \phi}{\delta z} - \frac{\delta^2 \phi}{\delta r \delta z} \right) \\
\dot{\epsilon}_z &= \frac{\delta u}{\delta z} = \frac{1}{2\pi r} \frac{\delta^2 \phi}{\delta r \delta z} \\
\dot{\epsilon}_\theta &= \frac{v}{r} = -(\dot{\epsilon}_r + \dot{\epsilon}_z) = -\frac{1}{2\pi r} \cdot \frac{1}{r} \frac{\delta \phi}{\delta z} \\
\dot{\gamma}_{rz} &= \frac{\delta u}{\delta r} + \frac{\delta v}{\delta z} = -\frac{1}{2\pi r} \left( \frac{1}{r} \frac{\delta \phi}{\delta r} - \frac{\delta^2 \phi}{\delta r^2} + \frac{\delta^2 \phi}{\delta z^2} \right) \\
\dot{\gamma}_{r\theta} &= \dot{\gamma}_{z\theta} = 0
\end{aligned}
\tag{2.9}$$

The corresponding stress components are obtained by considering the equilibrium equation and von Mises flow rules:

$$\begin{aligned}
\sigma_z(r, z) &= \int_z^a \left[ \frac{\delta}{\delta r} \left( \frac{\dot{\gamma}_{rz}}{2\lambda} \right) + \frac{\dot{\gamma}_{rz}}{2r\lambda} \right] dz + \\
&\int_{r_0}^r \left[ \frac{\delta}{\delta r} \left( \frac{\dot{\epsilon}_z - \dot{\epsilon}_r}{\lambda} \right) - \frac{\delta}{\delta z} \left( \frac{\dot{\gamma}_{rz}}{2\lambda} \right) - \frac{\dot{\epsilon}_r - \dot{\epsilon}_\theta}{r\lambda} \right] dr \Big|_{z=a} \\
&+ \sigma_z(r_0, a) \\
\sigma_r(r, z) &= \sigma_z + \frac{2}{3} \bar{\sigma} \left( \frac{\dot{\epsilon}_r - \dot{\epsilon}_z}{\dot{\epsilon}} \right) \\
\sigma_\theta(r, z) &= \sigma_z + \frac{2}{3} \bar{\sigma} \left( \frac{\dot{\epsilon}_\theta - \dot{\epsilon}_z}{\dot{\epsilon}} \right) \\
\tau_{rz} &= \frac{1}{3} \bar{\sigma} \left( \frac{\dot{\gamma}_{rz}}{\dot{\epsilon}} \right)
\end{aligned}
\tag{2.10}$$

where,

$\sigma_z(r_0, a)$  is the axial stress at a reference point

$$\dot{\bar{\epsilon}} = \left\{ \frac{2}{3} \dot{\epsilon}'_{ij} \dot{\epsilon}'_{ij} \right\}^{\frac{1}{2}} \quad \text{and} \quad (a)$$

$$\bar{\sigma} = \left\{ \frac{3}{2} \sigma'_{ij} \sigma'_{ij} \right\}^{\frac{1}{2}} \quad (b)$$

$$\dot{\lambda} = \frac{3}{2} \left( \frac{\dot{\bar{\epsilon}}}{\bar{\sigma}} \right) \quad (c)$$

(2.11)

The viscoplasticity method provides information of the plastic flow process during the forming process and is a valuable tool for determining the distribution of strain rates and stress directly from experiments and plastic flow laws. The solution therefore is exact. However, the limitation is the laborious experimental work which must be performed first. The technique has only been applied effectively to axisymmetric bar and tubular extrusions and plane strain extrusion in most of the articles already referenced in this section. The method can be used in other metal forming processes for detailed investigations and checking the simpler predictive techniques such as upper bounds and approximate slip line fields.

## 2.5 FINITE ELEMENT ANALYSIS IN PLASTIC DEFORMATION

### 2.5.1 Introduction

In some cases of drawing, fracture of the product occurs at the die exit where the effect of elastic deformation is not negligible. The elastic spring-back after deformation at the throat could have important effects on the residual stress distribution. However, the conventional methods such as slip lines and upper bounds are not sufficient in such mixed elastic-plastic problems. The finite element technique is applied appropriately in such situations where elastic and plastic deformations are accounted for in separate régimes and the transition between them (using the governing criterion of yielding such

as von Mises criterion,  $\frac{1}{2} \sigma'_{ij} \sigma'_{ij} = k^2$ ).

The finite element method was developed extensively as a concept in structural mechanics when a loaded part was thought of as a system built up of numerous tiny connected structures of elements (61, 62). These elements can be put together in any configuration to simulate exceedingly complex shapes and boundary conditions. The application has recently extended to metalworking processes (63, 64, 65, 66, 67) to solve problems with irregular shaped boundaries and elastic-plastic conditions. In addition, the technique finds application in non-steady flow processes and is readily programmable to include realistic material properties such as strain hardening. However, even a relatively simple problem requires computer facilities.

The method can be summarised conveniently in the following steps:-

- (i) The deforming material is divided into a number of finite elements
- (ii) The elastic stiffness matrix  $[k^e]$  or the plastic stiffness matrix  $[k^p]$  is derived for a typical element
- (iii) The nodal forces and the displacement must be compatible with those of its neighbours. Therefore, the stiffness matrices  $[k^e]$  and  $[k^p]$  are assembled to form the 'global' stiffness matrix of the whole body. This overall matrix  $[K]$  relates the nodal load increment  $\{dL\}$  to the nodal displacement  $\{dU\}$ , i.e.

$$\{dL\} = [K]\{dU\} \quad (2.12)$$

- (iv) The solution of the resulting set of simultaneous equations is accomplished using a high speed computer. From the known nodal forces and the consequential displacements, the detailed distribution of stress and strain is developed.

The use of elastic-plastic method enables a complete stress analysis to be developed revealing the extent of the plastic zone. K. Iwata et al (67) applied the finite element technique to hydrostatic extrusion process using triangular elements for plane strain problem and ring elements for the axisymmetric case. Hydrostatic extrusion is characterised by the boundary condition that the radial support of the billet is given by the hydrostatic pressure. Their analysis revealed the existence of tensile stress zone on the surface of the extruded part behind the exit. The hydrostatically extruded product is known to fracture at the die exit, where the effect of the elastic deformation cannot be ignored (68).

The next two sections outline briefly the derivation of the elastic and plastic stiffness matrices.

### 2.5.2 Derivation of the elastic stiffness matrix $[k^e]$

For an elastic state of isotropic material the strain-stress relationship using Hooke's law is given in tensor notation as,

$$\epsilon_{ij} = \frac{\sigma'_{ij}}{2G} + \delta_{ij} (1 - 2\nu) \frac{\sigma_{ii}}{3E} \quad (2.13)$$

Where, E is the Young's modulus of elasticity

G is the modulus of rigidity

$\delta_{ij}$  is the Kronecker's delta

$\nu$  is the Poisson's ratio

Inverting equation (2.13) gives

$$\sigma_{ij} = 2G \left( \epsilon_{ij} + \delta_{ij} \frac{\nu}{1 - 2\nu} \epsilon_{ii} \right) \quad (2.14)$$

which in matrix form becomes,

$$\{\sigma\} = 2(1 + \nu) G [D^e] \{\epsilon\} \quad (2.15)$$

$[D^e]$  is known as the elastic stress-strain matrix, i.e. relates the elastic stress  $\{\sigma\}$  to the elastic strain  $\{\epsilon\}$ .

The stiffness matrix  $[k^e]$  for the elastic element is given by

$$[k^e] = \int_V [B]^T [D^e] [B] dV \quad (2.16)$$

where the matrix  $[B]$  expresses the strain vector  $\{\epsilon\}$  in terms of the nodal displacement  $\{U\}_o^e$ , i.e.

$$\{\epsilon\} = [B]\{U\}_o^e \quad (2.17)$$

### 2.5.3 Derivation of the plastic stiffness matrix $[k^p]$

For the yielded element the plastic stress-strain matrix  $[D^p]$  takes the place of the elastic stress-strain matrix  $[D^e]$  obtained in the last section. The method is based on inverting the complete Prandtl-Reuss equations of plasticity (14) in conjunction with von Mises yield criterion. The derivation is presented in detail in ref. (64); however, the important equations are reproduced below.

The Prandtl-Reuss equations for the deviatoric strain increment  $d\epsilon_{ij}$  during continued loading are:

$$d\epsilon'_{ij} = \sigma'_{ij} d\lambda + \frac{d\sigma'_{ij}}{2G} \quad (2.18)$$

where

$$d\lambda = \frac{3}{2} \frac{d\bar{\epsilon}^p}{\bar{\sigma}} = \frac{3}{2} \frac{d\bar{\sigma}}{\bar{\sigma}H'} \quad (2.19)$$

$$\text{and } \bar{\sigma} = \left( \frac{3}{2} \sigma'_{ij} \sigma'_{ij} \right)^{\frac{1}{2}} \quad (2.20)$$

$$\bar{d\epsilon}^p = \left( \frac{2}{3} d\epsilon_{ij}^p d\epsilon_{ij}^p \right)^{\frac{1}{2}} \quad (2.21)$$

$$H' = \frac{d\bar{\sigma}}{d\bar{\epsilon}^p} \quad (= \text{the slope of the graph of } \bar{\sigma} \text{ versus } \bar{d\epsilon}^p) \quad (2.22)$$

The von Mises yield criterion is given by

$$\sigma'_{ij} \sigma'_{ij} = \frac{2}{3} \bar{\sigma}^2 \quad (2.23)$$

By inverting equation (2.18), the total stress increment  $d\sigma'_{ij}$  is obtained,

$$d\sigma'_{ij} = 2G \left( d\epsilon_{ij} + \frac{\nu}{1-2\nu} \delta_{ij} d\epsilon_{ii} - \sigma'_{ij} \frac{\sigma'_{kl} d\epsilon_{kl}}{S} \right) \quad (2.24)$$

$$\text{where } S = \frac{2}{3} \bar{\sigma}^2 \left( 1 + \frac{H'}{2G} \right) \quad \text{and} \quad \sigma'_{kl} d\epsilon_{kl} = \sigma'_{ij} d\epsilon_{ij} \quad (2.25)$$

Equation (2.24) can be expressed in matrix form or

$$\{d\sigma\} = 2(1 + \nu)G[D^P]\{d\epsilon\} \quad (2.26)$$

where  $[D^P]$  is the plastic stress-strain matrix.

Similarly, the stiffness matrix for the plastic element is given by,

$$[k^P] = \int_V [B]^T [D^P] [B] dV \quad (2.27)$$

## 2.6 Determination of the mean pressure and the coefficient of friction

### 2.6.1 Die rotation method

When an axisymmetric die is continuously rotated about the axis while drawing, the measurement of the torque and the reduction in the drawing load can be used to determine the mean coefficient of friction.

Linicus and Sachs (69) evaluated the mean coefficient of friction in wire drawing from the measured reduction in draw load. Nishihara et al (70) are reported to have successfully evaluated the mean coefficient of friction for wire drawing through curved profile dies by the measurement of both the torque and the reduction in the draw load.

Sansome and Rothman (71) proposed a theory to explain the reduction

in load when the die is rotated. They also brought to light the difference between the mean coefficient of friction determined from the measurement of the rotating torque and from the reduction in the drawing force. The method is illustrated briefly in Appendix A-18.

### 2.6.2 Split die method

For drawing round wire or bar the die may be split into two halves along its axis and the pieces clamped together. The die separating force necessary to hold them together is measured concurrently with the drawing force (see Fig. 2.2). The method was proposed by Maclellan (7) to determine the mean coefficient of friction and the mean die pressure in wire drawing. He reports (72) that his results were unsuccessful because the lubricant penetrated between the two halves and gave rise to additional hydrostatic pressure of unknown magnitude. Wistreich (24) successfully improved on this method. The two halves of the die were pressed with a known force which was progressively reduced till they just started to separate; at which point the holding force was taken equal to the splitting force. Yang (9) reports that he has used the method satisfactorily. However, it is a bit laborious.

Lancaster and Rowe (73) used the plug technique in which two strips, separated by a flat bar were drawn simultaneously. This eliminated the dependence of the mean coefficient of friction on the die angle.

One drawback to the technique is that it cannot be used for a continuous process. There is also a possibility of the formation of fins when the die halves are not in contact.

### 2.6.3 Split rotating die

In polygonal bar or tube drawing it is not possible to rotate the die over the surface of the workpiece. The method reported in (2) was developed by Basily and Sansome to determine the mean coefficient of friction and the mean pressure in the drawing of polygonal bars from

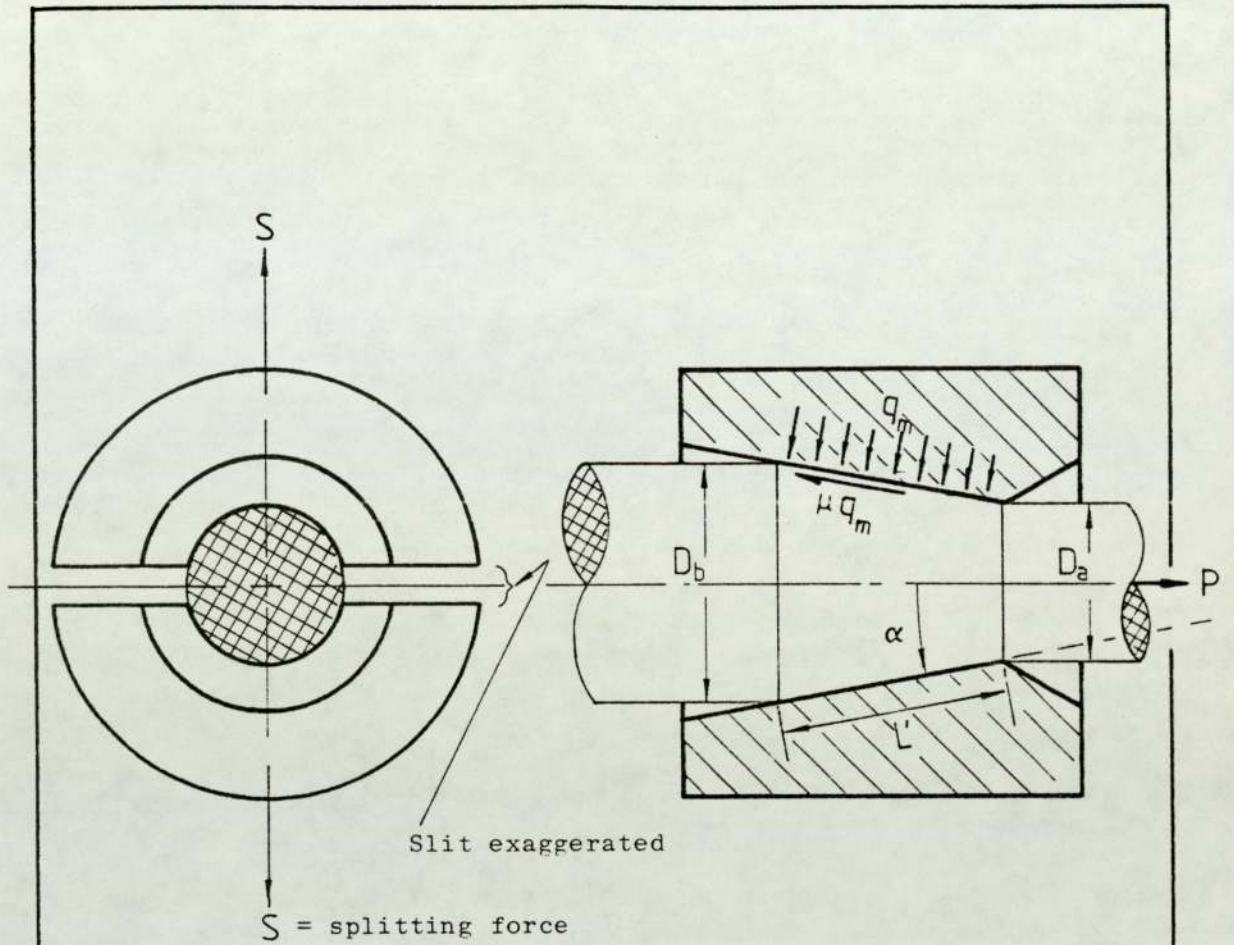


Fig. 2.2 Forces in wire drawing (Wistreich)

Using the above diagrams and the equilibrium of forces the following equations are derived:

$$P = (A_b - A_a)(1 + \mu \cot \alpha)q_m \quad (2.28)$$

$$S = \frac{1}{\pi} (A_b - A_a)(\cot \alpha - \mu)q_m \quad (2.29)$$

From equations (2.28) and (2.29),

$$\mu = \tan \left( \frac{P}{\pi S} - \alpha \right)$$

and

$$q_m = \frac{\pi S}{(A_b - A_a)(\cot \alpha - \mu)}$$

} (2.30)

round stock. Fingered die tips enclosed in the deforming metal while their external surfaces formed a surface around which a conical die rotated. This technique, adopted to determine the same parameters in the tube drawing process, is described in details in Chapter 4 and Appendix A-12.

#### 2.6.4 Estimation of redundant work

The mean coefficient of friction is determined indirectly from the experiments and theoretical analysis. The accuracy of the results is therefore dependent on the theory. The following method is based on the energy approach, where the total work done consists of three components:-

$$W = W_h + W_r + W_f \quad (2.31)$$

$W$  is the total work done per unit volume of the metal or the draw stress,  $W_h$  is the homogeneous work,  $W_r$  is the redundant work and  $W_f$  is the component to overcome friction on the tool-workpiece interface. The measurement of either  $W_r$  or  $W_f$  leads directly to the other, provided their interdependence is disregarded.

The redundant work can be determined by superimposing the stress-strain curve of the drawn metal onto the master curve of the undrawn metal. The area under the master stress-strain curve swept by the curve of the drawn material when shifted to line up with it, gives the redundant work (74, 75). To avoid likely graphical errors inherent in curve fitting, Basily and Sansome (76) expressed the master stress-strain curve of the undrawn metal mathematically. The redundant work was deduced analytically from the drawing parameters. The method relied on the application of the apparent strain (77) and the measured flow stress of the drawn bar. The method is described in detail in Chapter 4.

### CHAPTER 3

THEORY : THE MECHANICS OF DRAWING POLYGONAL TUBE  
DIRECTLY FROM ROUND ON A CYLINDRICAL PLUG

### 3.1 INTRODUCTION

The chapter develops the upper and the lower loads for the drawing of regular polygonal tube from round on a cylindrical plug. The derivations are confined to close pass drawing.

The object is to calculate the lower bound load, too low a load to deform the metal and also an upper bound which is certainly too high a load. As pointed out in Chapter 1, the deforming passage of the die is complex and therefore in both cases numerical integration will be used to obtain the solutions for any given drawing parameters. The actual load lies between the two limits; therefore the skill of application lies in choosing the deformation pattern for the upper bound solution which makes the difference between the two bounding loads as small as possible. The prediction of the bounding loads is of value in industry when planning and scheduling the work on draw benches. The method adopted facilitates the investigation of the effect of drawing on the deformation of the drawing process for both the forces involved and the deformation occurring within the material.

The upper bound solution is obtained by equating the external rates of doing work to the internal rate of doing work in a deformation mode satisfying the displacement boundary conditions. The development of the velocity pattern for the upper bound solution is described in section 3.2.2. Coulomb friction was incorporated in the upper bound expression by an apparent strain method presented in section 3.2.7.

The lower bound solution described in section 3.3 is based on the equilibrium of forces and Tresca's yield criterion. The solution is derived for the elliptical plane/conical surface die shape shown in Fig. 4.1 on page 77.

The computer programme presented in section 3.4 provides the results for both the upper and lower bound solutions for the drawing of polygonal tubes from round on a cylindrical plug, and also for the corresponding axisymmetric tube drawing for the purpose of comparison.

### 3.2 Upper bound solution for the drawing of polygonal tube from round on a cylindrical plug

In the upper bound solution the minimum energy required to deform the metal is calculated. The material is assumed to shear as it crosses the shear surfaces at the inlet and outlet regions of the deforming zone. Further relative shearing of the material elements in the deforming zone is considered in addition to the homogeneous deformation. The friction between the deforming metal and the tools is accounted for using Coulomb's relationship.

If a velocity field is assumed and the deforming material obeys von Mises yield criterion and the Levy-Mises flow rule, the upper bound solution, discussed in Chapter 2.3, indicates that the actual strain rate field  $\dot{\epsilon}_{ij}$  is the one that minimizes the expression,

$$J^* = \sqrt{\frac{2}{3}} Y_m \left( \int_V \sqrt{\dot{\epsilon}_{ij} \dot{\epsilon}_{ij}} dV + \int_{\Gamma} \tau |\Delta v| dS - \int_{S_t} T_i v_i dS \right) \quad (3.1)$$

The first term on the right represents the power to deform the material in the deformation zone, the second term calculates the rate of energy dissipation over the surfaces of velocity discontinuity including the tools/tube interfaces, and the last term covers the power to the pre-determined body tractions such as the back tension in wire drawing and front tension in extrusion.

The die passage through which an entirely circular tube transforms

to a regular polygonal tube with the bore unchanged, has a complex shape (e.g. Fig. 3.1). The associated flow is irregular and therefore a velocity field is derived from a conformally mapped deformation pattern. The circular section of the undrawn tube at entry is divided into triangular elements. As the tube is drawn through the deformation passage, the elements are assumed to be entirely transformed into triangular elements at the die exit plane. A constant reduction of area is maintained at each plane between the entry and the exit. A velocity pattern is thereby obtained and the value of  $J^*$ , the power to effect the process, is minimized for the given set of drawing parameters.

### 3.2.1 Deformation pattern for the drawing of a regular polygonal tube from round on a cylindrical plug

The method developed for obtaining the deformation pattern is based on conformally mapping each element in the inlet plane to the corresponding element at the exit plane. See Fig. 3.2.

At the exit plane (Fig. 3.2(a)), the cross-sectional area of the polygonal tube is banded by  $(N-2)$  hyperbolae, in each of which the focal distance  $a_i$  is adjusted to suit the asymptotes and such that the hyperbola corresponding to the outer surface is almost coincident with the flat surface of the polygonal tube. The innermost curve remains circular corresponding to the surface of the plug. The area between consecutive curves is calculated. Making the assumption of a constant reduction of area, the corresponding cross-sectional area at the inlet plane is determined and hence the radii bounding it. (See Fig. 3.2(b)).

The banded area at the inlet cross section of the tube is divided into  $(M-1)$  equal sectors. Each sector, say A B C D, is further

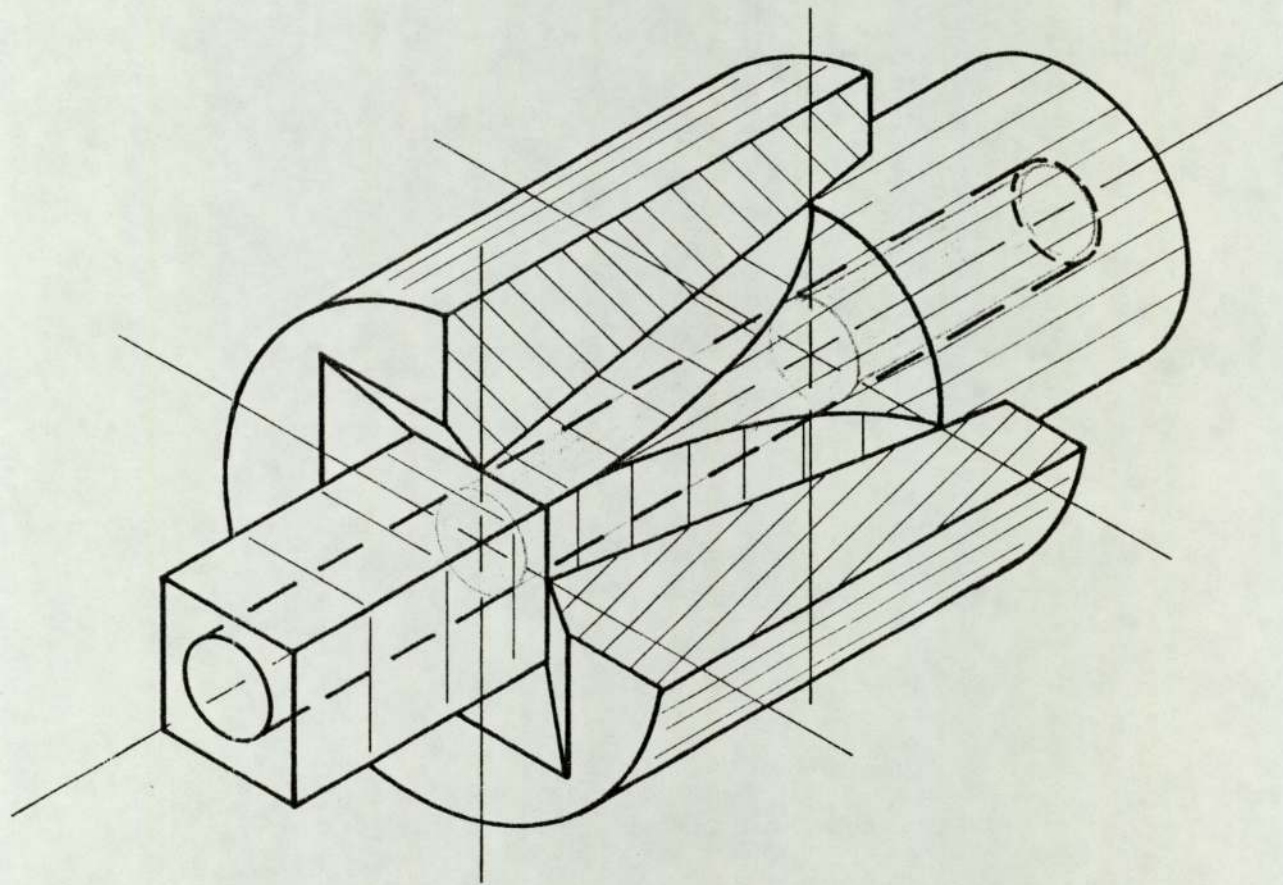


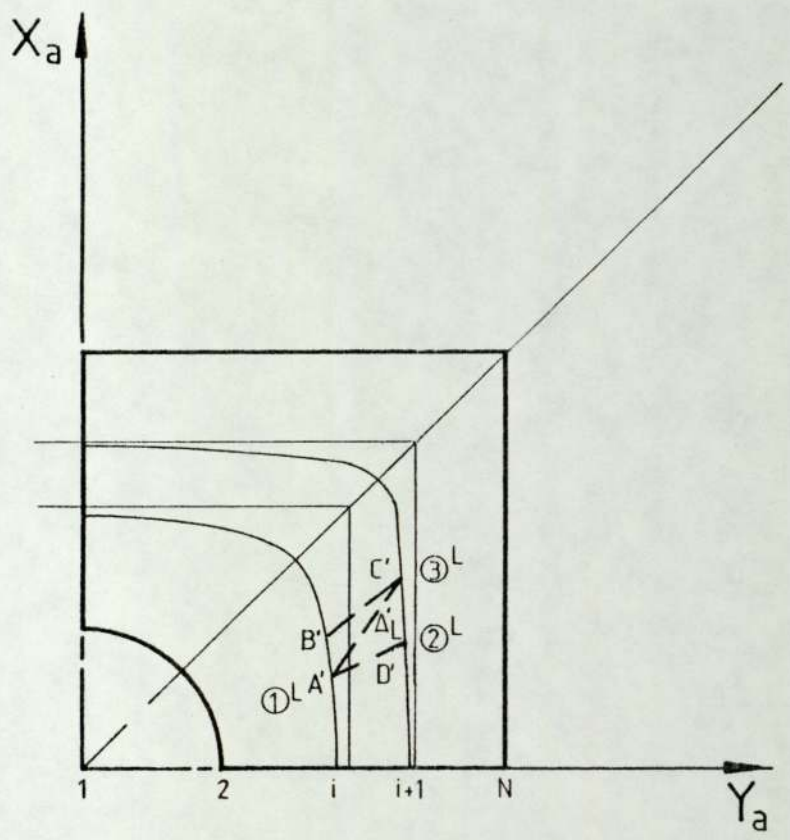
Fig. 3.1 The direct drawing of square tube directly from round stock on a cylindrical plug

divided into two triangles, the large triangle ADC and the small triangle ACB. The area of each triangle can be determined and, from the known co-ordinates of the vertices, the centroid is located.

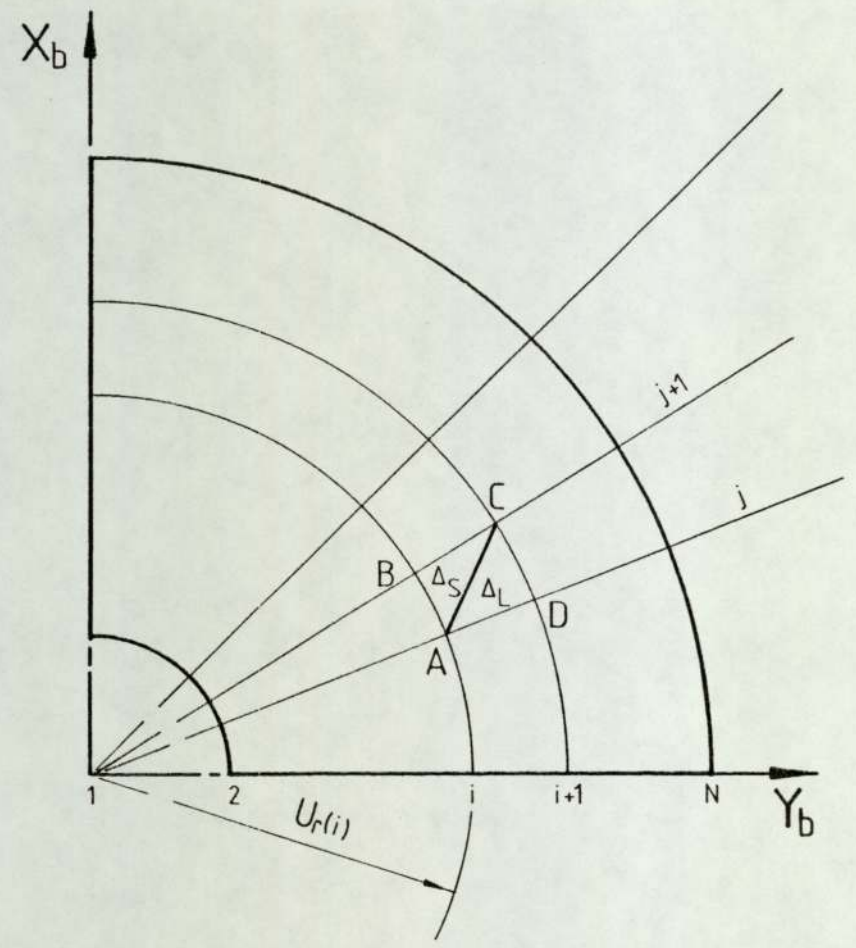
Assuming a constant reduction of area of the large triangle ADC on the inlet plane, the corresponding area of the large triangle A'D'C' on the exit plane can be determined. At the exit plane, let this triangle be defined by the co-ordinates  $(X_1, Y_1)$ ,  $(X_2, Y_2)$  and  $(X_3, Y_3)$  (or  $(X_a, Y_a)_{i,j}$ ,  $(X_a, Y_a)_{i+1,j}$  and  $(X_a, Y_a)_{i+1,j+1}$ ) of which  $(X_3, Y_3)$  lies on the hyperbola  $i+1$ . By starting with known vertices (1) and (2) or  $(X_1, Y_1)$  and  $(X_2, Y_2)$ , the third unknown vertex can be found by solving the equation of the triangle in which  $(X_1, Y_1)$ ,  $(X_2, Y_2)$  and the area are known and the third point satisfies the hyperbola  $i+1$ . Having determined the third vertex  $(X_3, Y_3)$  (or  $(X_a, Y_a)_{i+1,j+1}$ ) the point is then substituted for  $(X_2, Y_2)$  of the next triangle A'C'B', and the third point for this new triangle can be found in a similar manner. The procedure continues until the whole exit section is mapped into triangles. The centroids of the large and small triangles can now be located. The details of the mapping are given in the Appendices A-8.1, A-8.2 and A-8.3.

### 3.2.2 Velocity Field

Before meeting the die, a particle of the metal can be assumed to travel parallel to the tube axis and towards the die entry. Within the die the velocity of the particle is expressed 3-dimensionally by the spherical system of co-ordinates,  $\dot{U} = \dot{U}(U_\rho, U_\theta, U_\phi)$  and changes as the deformation proceeds. At the exit plane the deformed particle again travels parallel to the tube axis without deformation. A boundary exists which separates the undeformed metal from the zone where relative deformation occurs. The material shears at this surface and changes direction. A similar distortion exists at the



(a) Exit plane



(b) Entry plane

Fig. 3.2. Determination of the deformation pattern by conformal mapping of the elemental areas

exit, except that the streamlines pass through the boundary from the deformation zone into a region subject to an elastic distortion only.

There is generally no means for determining the shape or exact position of these boundaries. The surfaces normally assumed, are plane, spherical or conical (78). However, since the deformation mode of the problem is complex, a streamline on entry to the deformation zone is assumed to shear at a surface inclined at an angle  $t\theta$  to the draw axis. The position of the particle is defined on the spherical surface  $(\rho_b, \theta, \phi)$  (see Fig. 3.3). The parameter  $t$ , where  $-1 \leq t \leq 1$ , is used to optimise the shear surface by minimising the shear work. Similarly, a general pyramidal shear surface is defined at the exit of the deformation zone and the parameter  $t$  is used to optimise the geometry of the surface.

An 'entry' plane  $(X_b, Y_b)$  may be defined as the plane normal to the die axis through the point where the outermost tube elements ( $r = R_b$ ) first contact the die and start to deform. Similarly, the 'exit' plane  $(X_a, Y_a)$  may be said to be the plane normal to the draw axis through the point where the outermost material starts to flow parallel to the draw axis and deformation ceases.

Once a shear surface has been defined, a plane parallel to the 'exit' or 'entry' planes and passing through the centroid of the particle on the respective shear surfaces can be drawn. Such planes are denoted by  $(X'_a, Y'_a)$  and  $(X'_b, Y'_b)$  for the exit and inlet shear surfaces respectively. By joining the centroids of the corresponding triangular elements, the drawn vector defines the path travelled by the element and also the direction of flow.

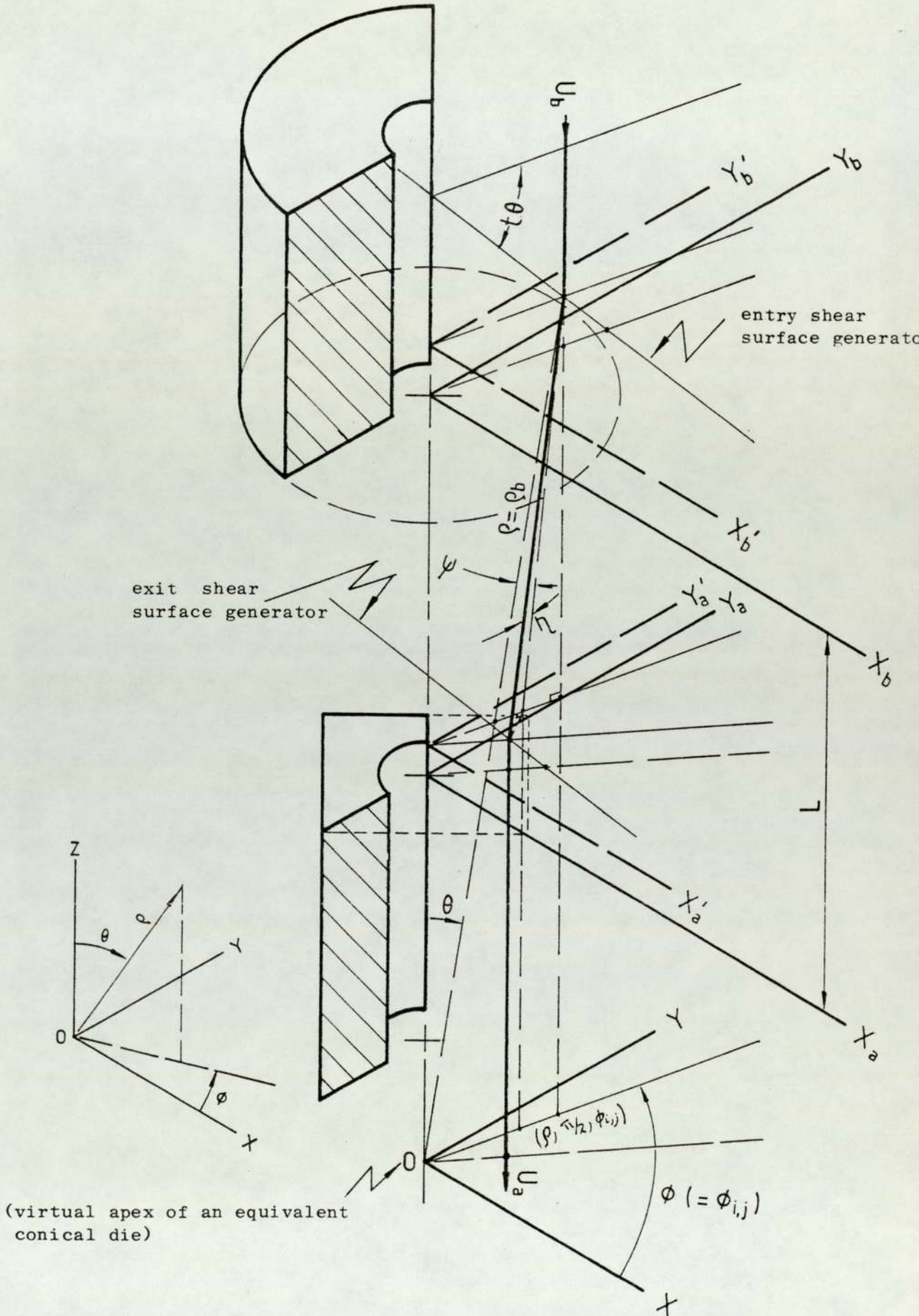


Fig. 3.3

Flow path of an elemental particle through the die for drawing polygonal tube from round stock on a cylindrical plug.

The values of the angular deflections  $\eta$  and  $\psi$  and the length of the flow path of a particle in the deformation zone  $Z_t$ , are calculated by the method shown in Appendices A-8.4 and A-8.5, and Fig. A-8.6 on page A93.

From the calculated angles and the flow path, the velocity field  $\dot{U}(\dot{U}_\rho, \dot{U}_\theta, \dot{U}_\phi)$  is established and therefore the strain rates.

If  $U_b$  is the velocity of an element before shear and  $\dot{U} = \dot{U}(\dot{U}_\rho, \dot{U}_\theta, \dot{U}_\phi)$  is the velocity immediately after shear, then for continuity of flow of the material, the component of velocity normal to the shear surface must be the same on each side, i.e.  $U_b \cos\theta = \dot{U} \cos\eta \cos\psi \cos(1-t)\theta$

$$\text{or } \dot{U} = U_b \cdot \frac{\cos\theta}{\cos\eta \cos\psi \cos(1-t)\theta} \quad (3.2)$$

Assuming a linear convergence of the die passage with an equivalent die semi-cone angle  $\alpha_e$ , then the virtual apex is the centre of the spherical system of co-ordinates  $\rho, \theta, \phi$ . (The equivalent semi-cone angle is discussed in Appendix A-10.) The cross-sectional area of the material at any radius  $\rho$  is given by,

$$A = \pi(\rho \sin\alpha_e)^2 - A_p \quad (3.3)$$

For a linear convergent die passage the velocity of an element at any radius  $\rho$  is given by:-

$$\dot{U} = U_b \cdot \left( \frac{\pi(\rho_b \sin\alpha_e)^2 - A_p}{\pi(\rho \sin\alpha_e)^2 - A_p} \right) \cdot \frac{\cos\theta}{\cos\eta \cos\psi \cos(1-t)\theta} \quad (3.4)$$

$$= U_b \cdot \left( \frac{\rho_b'}{\rho'} \right)^2 \frac{\cos\theta}{\cos\eta \cos\psi \cos(1-t)\theta}$$

where,

$$\rho_b'^2 = \rho_b^2 - \frac{A_p}{\pi \sin^2 \alpha_e}$$

$$\rho'^2 = \rho^2 - \frac{A_p}{\pi \sin^2 \alpha_e}$$
(3.5)

The velocity  $\dot{U}$  can be resolved into three components, namely  $\dot{U}_\rho$ ,  $\dot{U}_\theta$  and  $\dot{U}_\phi$ . From the geometry of Fig. 3.3 and Fig. A-8.7 (on page A96).

$$\dot{U}_\rho = U_b \left( \frac{\rho_b'}{\rho} \right)^2 \frac{\cos \theta}{\cos(1-t)\theta}$$

$$\dot{U}_\theta = \dot{U} \cos \eta \sin \psi$$

$$= U_b \cdot \left( \frac{\rho_b'}{\rho'} \right)^2 \frac{\cos \theta}{\cos(1-t)\theta} \cdot \tan \psi$$
(3.6)

$$U_\phi = \dot{U} \sin \eta$$

$$= U_b \left( \frac{\rho_b'}{\rho'} \right)^2 \frac{\cos \theta \cdot \tan \eta}{\cos(1-t)\theta \cdot \cos \psi}$$

### 3.2.3 Strain rates

Using the general spherical polar co-ordinates  $(\rho, \theta, \phi)$  and the velocity components  $\dot{U}_\rho$ ,  $\dot{U}_\theta$ , and  $\dot{U}_\phi$  in the directions of  $\rho$ ,  $\theta$  and  $\phi$  respectively, the strain rates are:-

$$\dot{\epsilon}_\rho = \frac{\dot{\delta U}_\rho}{\delta \rho}$$

$$\dot{\epsilon}_\theta = \frac{\dot{U}_\theta}{\rho} + \frac{1}{\rho} \cdot \frac{\delta \dot{U}_\theta}{\delta \theta}$$

$$\begin{aligned} \dot{\epsilon}_{\phi} &= \frac{\dot{U}_{\rho}}{\rho} + \frac{1}{\rho \sin\theta} \cdot \frac{\delta \dot{U}_{\theta}}{\delta \phi} + \cot\theta \cdot \frac{\dot{U}_{\theta}}{\rho} \\ \dot{\gamma}_{\rho\theta} &= \frac{\delta \dot{U}_{\theta}}{\delta \rho} - \frac{\dot{U}_{\theta}}{\rho} + \frac{1}{\rho} \cdot \frac{\delta \dot{U}_{\rho}}{\delta \theta} \\ \dot{\gamma}_{\theta\phi} &= \frac{1}{\rho} \cdot \frac{\delta \dot{U}_{\theta}}{\delta \theta} - \frac{\dot{U}_{\theta}}{\rho} \cdot \cot\theta + \frac{1}{\rho \sin\theta} \cdot \frac{\delta \dot{U}_{\theta}}{\delta \phi} \\ \dot{\gamma}_{\phi\rho} &= \frac{1}{\rho \sin\theta} \cdot \frac{\delta \dot{U}_{\rho}}{\delta \phi} + \frac{\delta \dot{U}_{\phi}}{\delta \rho} - \frac{\dot{U}_{\phi}}{\rho} \end{aligned} \quad (3.7)$$

The above equations are applied to the derived velocity expressions (equation 3.6) to yield the strain rates for the deformation pattern:-

$$\dot{\epsilon}_{\rho} = \frac{U_b}{\rho} \cdot \left( \frac{\rho_b'}{\rho'} \right)^2 \frac{\cos\theta}{\cos(1-t)\theta} - 2 \left( \frac{\rho}{\rho'} \right)^2 \quad (3.8a)$$

$$\begin{aligned} \dot{\epsilon}_{\theta} &= -\frac{1}{\rho} U_b \left( \frac{\rho_b'}{\rho'} \right)^2 \frac{\cos\theta}{\cos(1-t)\theta} \left\{ 1 + \tan\psi (-t \tan\theta + \right. \\ &\quad \left. \frac{1}{\cos\psi} + (1-t)\tan\theta) \right\} \end{aligned} \quad (3.8b)$$

$$\begin{aligned} \dot{\epsilon}_{\phi} &= -\frac{U_b}{\rho} \left( \frac{\rho_b'}{\rho'} \right)^2 \frac{\cos\theta}{\cos(1-t)\theta} \cdot \left\{ 1 + \frac{r_a}{\rho_b - \rho_E} \cdot \right. \\ &\quad \left. \frac{\cos(\phi - \phi_A)}{\cos\psi \sin\theta \cos\theta} + \frac{\tan\psi}{\tan\theta} \right\} \end{aligned} \quad (3.8c)$$

where

$$r_a = \sqrt{X_a^2 + Y_a^2}$$

$$\phi_A = \tan^{-1} \left( \frac{X_a}{Y_a} \right)$$

$$\rho_E = \rho_b - Z_s \sec\theta$$

and  $Z_s$  is given by equation A-8.31 on page A89.

$$\dot{\epsilon}_{\rho\theta} = -\frac{U_b}{\rho} \left( \frac{\rho_b'}{\rho'} \right)^2 \frac{\cos\theta}{\cos(1-t)\theta} \left\{ -\tan\psi \left( 2 \left( \frac{\rho}{\rho'} \right)^2 + 1 \right) - t \tan\theta + (1-t) \tan(1-t)\theta \right\} \quad (3.8d)$$

$$\dot{\epsilon}_{\theta\phi} = -\frac{U_b}{\rho} \left( \frac{\rho_b'}{\rho'} \right)^2 \frac{\cos\theta}{\cos(1-t)\theta} \cdot \frac{\tan\eta}{\cos\psi} \left\{ -t \tan\theta + \tan\psi + \tan\theta + (1-t) \tan(1-t)\theta - \frac{1}{\tan\theta} \right\} \quad (3.8e)$$

$$\dot{\epsilon}_{\phi\rho} = \frac{U_b}{\rho} \left( \frac{\rho_b'}{\rho'} \right)^2 \frac{\cos\theta}{\cos(1-t)\theta} \cdot \frac{\tan\eta}{\cos\psi} \left\{ 2 \left( \frac{\rho}{\rho'} \right)^2 + 1 \right\} \quad (3.8f)$$

#### 3.2.4. Internal power of deformation

The following assumptions are made when deriving the rate of work to deform the metal in the zone between the defined inlet and exit shear surfaces:-

- (i) The material obeys von Mises yield criterion,

$$\sigma'_{ij}\sigma'_{ij} - 2k^2 = 0 \quad (3.9)$$

where

$$\sigma'_{ij} = \sigma_{ij} - \frac{1}{3} \sigma_{kk} \delta_{ij} \quad (3.10)$$

- (ii) The flow follows Levy-Mises stress-strain relationship,

$$\dot{\epsilon}'_{ij} = d\lambda \sigma'_{ij} \quad (3.11)$$

where  $d\lambda$  is a positive constant of proportionality.

(iii) The material is non work-hardening, i.e. the yield stress of the material remains constant as the metal deforms.

(iv) The incompressibility condition is satisfied,

$$\text{i.e. } \epsilon_{ii} = 0 \quad (3.12)$$

(v) The elastic components of strain are ignored.

The rate of work required to deform material of elemental volume  $dV$  is given by

$$\dot{dW}_I = \sigma_{ij} \dot{\epsilon}_{ij} dV \quad (3.13)$$

∴ Power required to deform material of volume  $V$ ,

$$\dot{W}_I = \int_V \sigma_{ij} \dot{\epsilon}_{ij} dV \quad (3.14)$$

Multiplying each side of Levy-Mises flow rule (3.11) by  $\dot{\epsilon}_{ij}$  gives,

$$\dot{\epsilon}_{ij} \dot{\epsilon}_{ij} = d\lambda \sigma'_{ij} \dot{\epsilon}_{ij} \quad (3.15)$$

and by  $\sigma'_{ij}$  gives,

$$\sigma'_{ij} \dot{\epsilon}_{ij} = d\lambda \sigma'_{ij} \sigma'_{ij} \quad (3.16)$$

But from von Mises equation (3.9),

$$\sigma'_{ij} \sigma'_{ij} = 2k^2,$$

∴ equation (3.16) becomes

$$\sigma'_{ij} \dot{\epsilon}_{ij} = d\lambda 2k^2 \quad (3.17)$$

From the definition of  $\sigma'_{ij}$  and equation (3.12), the L.H.S. of

equation (3.17) gives,

$$\begin{aligned}
 \sigma'_{ij} \dot{\epsilon}_{ij} &= (\sigma_{ij} - \frac{1}{3} \sigma_{kk} \delta_{ij}) \dot{\epsilon}_{ij} \\
 &= \sigma_{ij} \dot{\epsilon}_{ij} - \frac{1}{3} \sigma_{kk} \epsilon_{ii} \\
 &= \sigma_{ij} \dot{\epsilon}_{ij}
 \end{aligned} \tag{3.18}$$

Equations (3.17) and (3.15) yield

$$\begin{aligned}
 \dot{\epsilon}_{ij} \dot{\epsilon}_{ij} &= d\lambda \cdot d\lambda \cdot 2k^2 = d\lambda^2 \cdot 2k^2 \\
 \text{or } d\lambda &= \sqrt{\left( \frac{\dot{\epsilon}_{ij} \dot{\epsilon}_{ij}}{2k^2} \right)}
 \end{aligned} \tag{3.19}$$

Using (3.19) and (3.18) in equation (3.17) gives the relationship

$$\sigma'_{ij} \dot{\epsilon}_{ij} = \sigma_{ij} \dot{\epsilon}_{ij} = \sqrt{2k} \sqrt{\dot{\epsilon}_{ij} \dot{\epsilon}_{ij}} \tag{3.20}$$

Substituting for  $\sigma_{ij} \dot{\epsilon}_{ij}$  in equation (3.14), and the total power

$$\dot{W}_I = \sqrt{2} \int_V k \sqrt{\dot{\epsilon}_{ij} \dot{\epsilon}_{ij}} dV \tag{3.21}$$

For constant k

$$\dot{W}_I = \sqrt{2}k \int_V \sqrt{\dot{\epsilon}_{ij} \dot{\epsilon}_{ij}} dV \tag{3.22}$$

Using a mean yield stress ( $Y_m$ ) for a strain hardening material (22), for von Mises condition,

$$k = \frac{Y_m}{\sqrt{3}}$$

$$\therefore \dot{W}_I = \sqrt{\frac{2}{3}} Y_m \int_V \sqrt{\dot{\epsilon}_{ij} \dot{\epsilon}_{ij}} dV \tag{3.23}$$

Substituting for strain rates defined in equations (3.7) and (3.8),

$$\begin{aligned}
 \dot{\epsilon}_{ij} \dot{\epsilon}_{ij} &= \dot{\epsilon}_1^2 + \dot{\epsilon}_2^2 + \dot{\epsilon}_j^2 + 2(\dot{\epsilon}_{12}^2 + \dot{\epsilon}_{23}^2 + \dot{\epsilon}_{31}^2) \\
 &= \dot{\epsilon}_\rho^2 + \dot{\epsilon}_\theta^2 + \dot{\epsilon}_\phi^2 + 2 \left\{ \left( \frac{\dot{\gamma}_{\rho\theta}}{2} \right)^2 + \left( \frac{\dot{\gamma}_{\theta\phi}}{2} \right)^2 + \left( \frac{\dot{\gamma}_{\phi\rho}}{2} \right)^2 \right\} \\
 &= \dot{\epsilon}_\rho^2 + \dot{\epsilon}_\theta^2 + \dot{\epsilon}_\phi^2 + \frac{1}{2} \left\{ \dot{\gamma}_{\rho\theta}^2 + \dot{\gamma}_{\theta\phi}^2 + \dot{\gamma}_{\phi\rho}^2 \right\}
 \end{aligned}$$

(3.24)

∴ the expression for the internal power of deformation becomes,

$$\begin{aligned}
 \dot{W}_I &= \frac{Y_m}{\sqrt{3}} \int_V \sqrt{2(\dot{\epsilon}_\rho^2 + \dot{\epsilon}_\theta^2 + \dot{\epsilon}_\phi^2) + (\dot{\gamma}_{\rho\theta}^2 + \dot{\gamma}_{\theta\phi}^2 + \dot{\gamma}_{\phi\rho}^2)} dV \\
 &= \frac{Y_m}{\sqrt{3}} \int_V \frac{U_b}{\rho} \left( \frac{\rho_b'}{\rho'} \right)^2 \frac{\cos t\theta}{\cos(1-t)\theta} \sqrt{K} dV
 \end{aligned} \tag{3.25}$$

where:

$$\begin{aligned}
 K &= \left\{ 2 \left[ 4 \left( \frac{\rho}{\rho'} \right)^4 + \left\{ 1 + \tan\psi \left[ -t \tan\theta + \right. \right. \right. \right. \\
 &\quad \left. \left. \left. \frac{1}{\cos\psi} + (1-t)\tan(1-t)\theta \right] \right\}^2 + \left\{ 1 + \frac{r_a}{\rho_b' - \rho_\epsilon} \right. \right. \\
 &\quad \left. \left. \frac{\cos(\phi - \phi_A)}{\cos\psi \cos\theta \sin\theta} + \frac{\tan\psi}{\tan\theta} \right\}^2 \right] + \left[ \left\{ -\tan\psi \left[ 2 \left( \frac{\rho}{\rho'} \right)^2 + 1 \right] - \right. \right. \\
 &\quad \left. \left. t \tan\theta + (1-t)\tan(1-t)\theta \right\}^2 + \left\{ \frac{\tan\eta}{\cos\psi} \left[ -t \tan\theta \right. \right. \right.
 \end{aligned}$$



But from equation (3.5),

$$\rho_b'^2 = \rho_b^2 - \frac{A_p}{\pi \sin^2 \alpha_e}$$

$$\therefore \left( \frac{\rho_b'}{\rho_b} \right)^2 = \frac{A_b}{\pi \rho_b^2 \sin^2 \alpha_e} = \frac{A_b}{\pi R_b^2},$$

then equation (3.30) becomes

$$W_I = \frac{Y_m}{\sqrt{3}} \cdot U_b \cdot \frac{A_b}{\pi R_b^2} \int_{\theta=\theta_1}^{\alpha_e} \int_{\phi=0}^{2\pi} \int_{\rho_a}^{\rho_b} \frac{\rho}{\rho'^2} \sqrt{K} d\rho \frac{\cos t \theta}{\cos(1-t)\theta} dA_b \quad (3.31)$$

$$= Y_m \cdot U_b \cdot A_b \cdot f(s) \quad (3.32)$$

where,

$$f(s) = \frac{1}{\pi \sqrt{3} R_b^2} \int_{\theta_1}^{\alpha_e} \int_{\phi=0}^{2\pi} \left[ \int_{\rho_a}^{\rho_b} \frac{\rho}{\rho'^2} \sqrt{K} d\rho \right] \frac{\cos t \theta}{\cos(1-t)\theta} \cdot dA_b \quad (3.33)$$

$f(s)$  is evaluated numerically by dividing the inlet section into  $N_s \times (M - 1) \times (N - 2)$  elemental areas which are themselves subdivided into large and small triangles, i.e. :-

$$f(s) = \frac{N_s}{\pi \sqrt{3} R_b^2} \left\{ \begin{array}{l} N \rightarrow \infty \\ M \rightarrow \infty \end{array} \sum_{i=1}^{N-2} \sum_{j=1}^{M-1} \left[ \int_{\rho_a}^{\rho_b} \frac{\rho}{\rho'^2} \sqrt{K} d\rho \right] \frac{\cos t \theta}{\cos(1-t)\theta} \cdot dA_b \right\} \quad (3.34)$$

3.2.5 Power loss in shearing the material at the inlet and exit shear surfaces.

The internal power  $\dot{W}_I$  derived in the last section, is required to overcome the homogenous deformation and the necessary relative shearing within the material itself during its progress through the die deforming passage. Power is also required to compensate for the losses due to the shearing of the material on both the inlet and exit shear surfaces.

The rate of working in crossing a shear boundary of the elemental surface area  $dA_s$  is given by:-

$$\dot{dW}_R = k \dot{U}^* dA_s \quad (3.35)$$

where,

$\dot{U}^*$  is the velocity discontinuity along the surface and

$k$  is the yield stress of the material in shear equal to

$$\frac{Y_m}{\sqrt{3}} \text{ by von Mises yield criterion.}$$

An elemental particle just before shear at entry travels parallel to the draw axis with a velocity  $U_b$  but after shearing, its velocity is defined by  $\dot{U}(U_\rho, U_\theta, U_\phi)$ . Therefore, in order for the particle to change direction the work material has been subjected to a velocity discontinuity  $\dot{U}^*$  tangential to the shear boundary. The resultant velocity of the tangential components on both sides of the shear surface gives the velocity discontinuity,

$$\dot{U}_{rb} = U_b \left\{ \left[ \frac{\cos\theta}{\cos(1-t)\theta} \cdot \frac{\tan\theta}{\cos\psi} \right]^2 + \left[ -\sin\theta + \cos\theta \tan\psi + \cos\theta \tan(1-t)\theta \right]^2 \right\}^{\frac{1}{2}} \quad (3.36)$$

A similar situation occurs at the exit shear boundary when the velocity of the particle just before shear is  $\dot{U}(\dot{U}_\rho, \dot{U}_\theta, \dot{U}_\phi)$ , but after shear the particle travels parallel to the tube axis with the velocity  $U_a$ . The resultant tangential velocity,

$$\dot{U}_{ra} = \dot{U}_{rb} \cdot \left( \frac{\rho_b'}{\rho_a'} \right)^2 \quad (3.37)$$

The details of the derivation of the velocity discontinuities are given in the appendix A-8.6.

The rate of work dissipation at the entry shear surface,

$$\begin{aligned} \dot{W}_{R_b} &= \int_{A_b} k \cdot \dot{U}_{rb} \cdot dA_s \\ &= \int_{A_b} k \cdot \dot{U}_{rb} \cdot \frac{dA_b}{\cos\theta} \end{aligned} \quad (3.38)$$

The rate of work dissipation at the exit shear surface,

$$\dot{W}_{R_a} = \int_{A_a} k \cdot \dot{U}_{ra} \cdot dA_s \quad (3.39)$$

An equivalent conical die passage has been assumed; consequently

$$\frac{dA_b}{dA_a} = \left( \frac{\rho_b'}{\rho_a'} \right)^2 \quad \text{and}$$

$$\dot{U}_{ra} = \left( \frac{\rho_b'}{\rho_a'} \right)^2 \cdot \dot{U}_{rb}$$

$$\begin{aligned} \dot{W}_{R_a} &= \int_{A_b} k \cdot \left( \frac{\rho_b'}{\rho_a'} \right)^2 \cdot \dot{U}_{rb} \cdot \left( \frac{\rho_a'}{\rho_b'} \right)^2 \cdot \frac{dA_b}{\cos\theta} \\ &= \int_{A_b} k \cdot \dot{U}_{rb} \cdot \frac{dA_b}{\cos\theta} \end{aligned} \quad (3.40)$$

The total power to shear the material at the inlet and exit boundaries is,

$$\begin{aligned} \dot{W}_R &= \dot{W}_{R_b} + \dot{W}_{R_a} \\ &= 2 \int_{A_b} k \cdot \dot{U}_{rb} \cdot \frac{dA_b}{\cos\theta} \end{aligned} \quad (3.41)$$

$$= \frac{2}{\sqrt{3}} Y_m \cdot U_b \int_{A_b} \left( \frac{\dot{U}_{rb}}{U_b} \right) \cdot \frac{dA_b}{\cos\theta}$$

$$= \frac{2}{\sqrt{3}} Y_m \cdot U_b \cdot A_b R(s) \quad (3.42)$$

where,

$$\begin{aligned} R(s) &= \frac{1}{A_b} \int_{A_b} \left\{ \left[ \frac{\cos\theta}{\cos(1-t)\theta} \cdot \frac{\tan\eta}{\cos\psi} \right]^2 + \left[ -\sin\theta + \right. \right. \\ &\quad \left. \left. \cos\theta \tan\psi + \cos\theta \tan(1-t)\theta \right]^2 \right\}^{\frac{1}{2}} \cdot \frac{dA_b}{\cos\theta} \end{aligned}$$

(3.43)

$$= \frac{N_s}{A_b} \sum_{M \rightarrow \infty}^{N_s \rightarrow \infty} \sum_{i=1}^{N-2} \sum_{j=1}^{M-1} \left\{ \left[ \frac{\cos\theta}{\cos(1-t)\theta} \cdot \frac{\tan\eta}{\cos\psi} \right]^2 + \right.$$

$$\left[ -\sin\theta + \cos\theta \tan\psi + \cos\theta \tan(1-t)\theta \right]^2 \Bigg\}^{\frac{1}{2}} \cdot \frac{dA_b}{\cos\theta} \quad (3.44)$$

Since  $t$  is an arbitrary parameter, values of  $-1 \leq t \leq 1$  will be used to select the value that gives the minimum  $R(s)$ . Hence the optimum shear surface for the given draw conditions.

### 3.2.6 Power loss in friction between the tool/workpiece interface

Friction occurs as the tube slides between the die and the plug. This implies that additional power is required to overcome the friction losses.

In the case of Coulomb friction, a mean coefficient of friction  $\mu$  is usually assumed for the given relative sliding surfaces. The rate of work loss is given by:-

$$\dot{W}_F = \int_{A_{s1}} \mu p U_s dA_s + \int_{A_{s2}} \mu p U_s dA_s \quad (3.45)$$

where, the first term on the right calculates the loss at the die/tube interface and the second term refers to the loss at the plug/tube interface.

In the above equation the mean die pressure and the mean plug pressure are unknown. It is usual to assume a mean value of pressure equal to that of the frictionless case. However, to overcome this difficulty  $\dot{W}_F$  can be obtained indirectly by the apparent strain method (77). The method, presented in the next section, enables the

calculation of the draw load, in case of Coulomb friction without obtaining the distribution of the pressure at the tube/tool interfaces.

### 3.2.7 Apparent strain method

This is an energy method, where the total work is divided into plastic and surface friction energy.

Friction produces shear stresses and strains at the workpiece interface and these have two principal effects on the work done. Energy is dissipated at the interface simply as a result of relative motion. If the shear stress at the surface is significant compared with the yield stress of the material, additional internal distortion results within the deformation zone. Both of these effects increase the work done.

The total work done per unit volume of the material is equated to an area under the equivalent stress-strain curve (see Fig. 3.5). The strains  $\bar{\epsilon}_a$  and  $\bar{\epsilon}_m$  corresponding to the total work and plastic work per unit volume are known as the apparent and the mean equivalent strains, respectively.

From the definition, work done per unit volume,

$$W = \int_0^{\bar{\epsilon}_a} \bar{\sigma} d\bar{\epsilon} = \bar{Y}_m \cdot \bar{\epsilon}_a \quad (3.46)$$

Assuming that the presence of friction at the die/tube and plug/tube interfaces has negligible effect on the plastic work, which is likely to be the case in cold drawing, then

$$\bar{\epsilon}_a = \bar{\epsilon}_m + \bar{\epsilon}_f \quad (3.47)$$

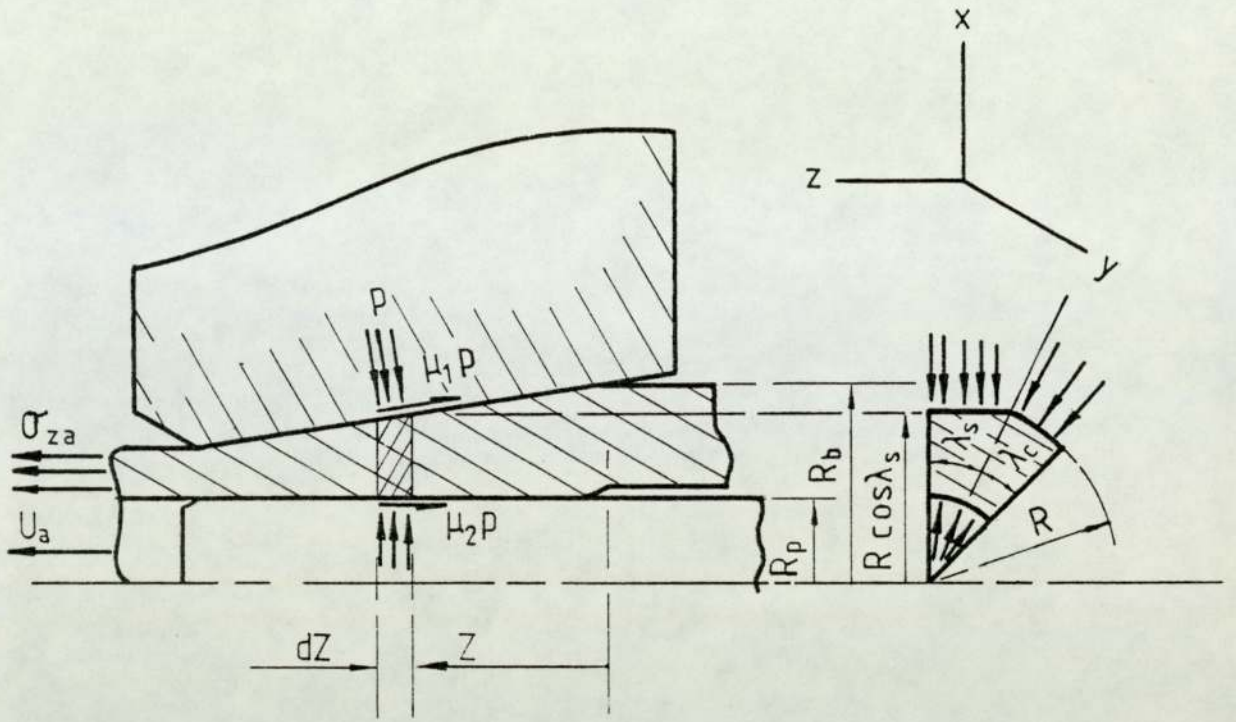


Fig. 3.4 Stress and the deformation pattern in the drawing of polygonal tube from round stock on a cylindrical plug for the apparent strain analysis.

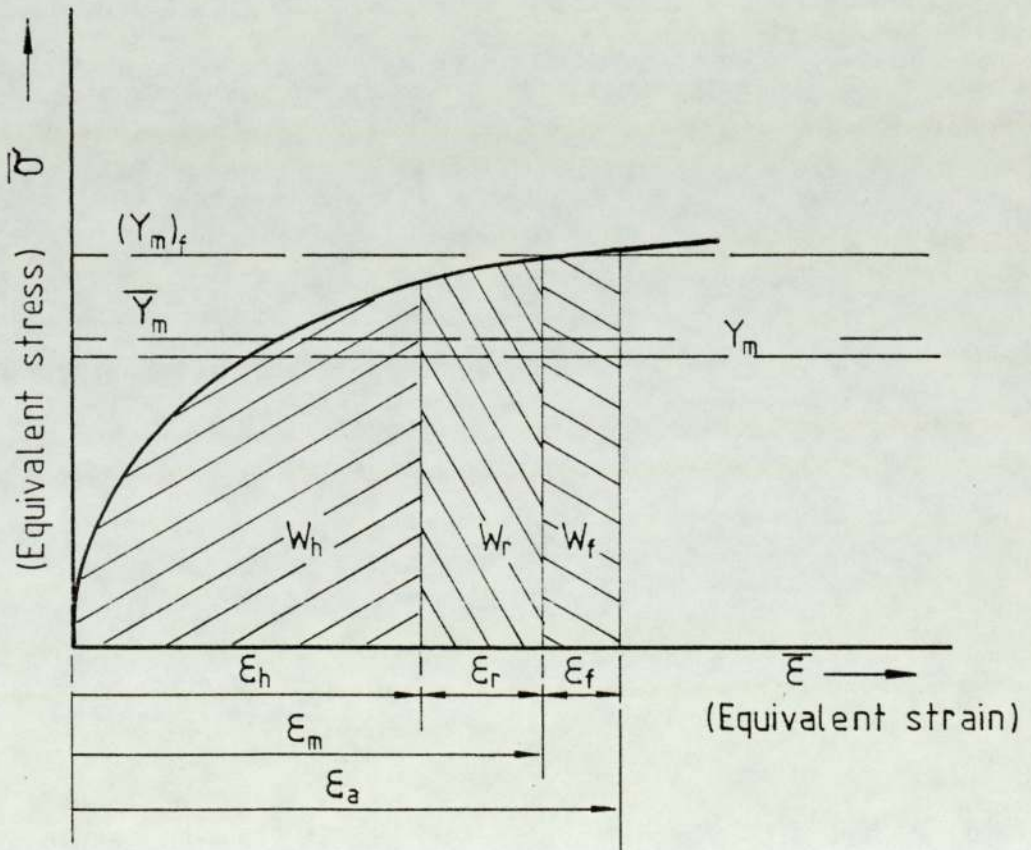


Fig. 3.5 The equivalent stress-strain diagram showing the terms used in the apparent strain analysis.

In a drawing process with no back-pull, the total work done per unit volume is equal to the draw stress,

$$\text{i.e. } W = \sigma_{za} \quad (3.48)$$

It is assumed that a mean coefficient of friction ( $\mu_m$ ) and the mean pressure ( $p_m$ ) occur at both the die/tube and plug/tube sliding surfaces. In the following derivations the subscripts  $c_1$ ,  $s_1$  and  $s_2$  denote conical, straight die and plug surfaces respectively.

From Fig. 3.4 for steady draw, the equilibrium of horizontal forces gives,

$$\sigma_{za} \cdot A_a = p_m \left\{ \sum (\mu_m \cos\alpha_s + \sin\alpha_s) dA_{s_1} + \right. \\ \left. \sum (\mu_m \cos\alpha_c + \sin\alpha_c) dA_{c_1} + \sum \mu_m dA_{s_2} \right\} \quad (3.49)$$

From equations (3.48) and (3.46),

$$\bar{\epsilon}_a = \frac{\sigma_{za}}{\bar{Y}_m} \quad (3.50)$$

Substituting for  $\sigma_{za}$  in (3.50) gives,

$$\bar{\epsilon}_a = \frac{\sigma_{za}}{\bar{Y}_m} = \frac{p_m}{\bar{Y}_m} \cdot \frac{1}{A_a} \left\{ \sum (\mu_m \cos\alpha_s + \sin\alpha_s) dA_{s_1} + \right. \\ \left. \sum (\mu_m \cos\alpha_c + \sin\alpha_c) dA_{c_1} + \sum \mu_m dA_{s_2} \right\}$$

$$\text{or } \bar{\epsilon}_a = \frac{p_m}{\bar{Y}_m} \cdot I_1 \quad (3.51)$$

$$\text{where } I_1 = \frac{1}{A_a} \left\{ \sum (\mu_m \cos \alpha_s + \sin \alpha_s) dA_{s_1} \right. \\ \left. + \sum (\mu_m \cos \alpha_c + \sin \alpha_c) dA_c + \sum \mu_m dA_{s_2} \right\} \quad (3.52)$$

From the definition of friction strain  $\bar{\epsilon}_f$ , work done against friction per unit volume of the material,

$$W_f = (Y_m)_f \cdot \bar{\epsilon}_f \quad (3.53)$$

Also the friction work can be determined by the energy dissipated as the material slides between the die and the plug surfaces. Using  $U_{c_1}$ ,  $U_{s_1}$  and  $U_{s_2}$  for the respective surface velocities:-

$$\dot{\text{VOL}} \times W_f = \mu_m \cdot p_m \cdot U_b \left\{ \sum \left( \frac{U_{s_1}}{U_b} \right) dA_{s_1} + \right. \\ \left. \sum \left( \frac{U_{c_1}}{U_b} \right) dA_{c_1} + \sum \left( \frac{U_{s_2}}{U_b} \right) dA_{s_2} \right\} \quad (3.54)$$

Substituting for  $W_f$  in the above equation.

$$\dot{\text{VOL}} \times (Y_m)_f \cdot \bar{\epsilon}_f = \mu_m \cdot p_m \cdot U_b \left\{ \sum \left( \frac{U_{s_1}}{U_b} \right) dA_{s_1} + \right. \\ \left. \sum \left( \frac{U_{c_1}}{U_b} \right) dA_{c_1} + \sum \left( \frac{U_{s_2}}{U_b} \right) dA_{s_2} \right\}$$

$$\therefore \bar{\epsilon}_f = \frac{p_m}{(Y_m)_f} \cdot \frac{\mu_m \cdot U_b}{\dot{\text{VOL}}} \left\{ \sum \left( \frac{U_{s_1}}{U_b} \right) dA_{s_1} + \right. \\ \left. \sum \left( \frac{U_{c_1}}{U_b} \right) dA_{c_1} + \sum \left( \frac{U_{s_2}}{U_b} \right) dA_{s_2} \right\}$$

$$\text{or } \bar{\epsilon}_f = \frac{P_m}{(Y_m)_f} \cdot I_2 \quad (3.55)$$

$$\text{where } I_2 = \frac{\mu_m U_b}{VOL} \left\{ \sum \left( \frac{U_{s1}}{U_b} \right) dA_{s1} + \sum \left( \frac{U_{c1}}{U_b} \right) dA_{c1} + \sum \left( \frac{U_{s2}}{U_b} \right) dA_{s2} \right\} \quad (3.56)$$

Dividing equation (3.51) by (3.55) yields

$$\frac{\bar{\epsilon}_a}{\bar{\epsilon}_f} = \frac{(Y_m)_f}{\bar{Y}_m} \cdot \frac{I_1}{I_2} = \frac{1}{B} \cdot \frac{I_1}{I_2}$$

$$\text{where, } B = \frac{\bar{Y}_m}{(Y_m)_f} \quad (3.57)$$

$$\therefore \bar{\epsilon}_f = B \cdot \frac{I_2}{I_1} \cdot \bar{\epsilon}_a = \Psi \cdot \bar{\epsilon}_a \quad (3.58)$$

$$\text{where, } \Psi = B \cdot \frac{I_2}{I_1} \quad (3.59)$$

By substituting the value of  $\bar{\epsilon}_f$  in equation (3.47) gives:-

$$\bar{\epsilon}_a = \bar{\epsilon}_m + \Psi \bar{\epsilon}_a$$

$$\text{or } \bar{\epsilon}_a = \frac{\bar{\epsilon}_m}{(1 - \Psi)} \quad (3.60)$$

From equations (3.51) and (3.60),

$$\begin{aligned}
 p_m &= \bar{Y}_m \cdot \frac{\bar{\epsilon}_a}{I_1} \\
 &= \bar{Y}_m \cdot \frac{\bar{\epsilon}_m}{I_1(1 - \psi)}
 \end{aligned}
 \tag{3.61}$$

$$\sigma_{za} = \bar{Y}_m \cdot \bar{\epsilon}_a = Y_m \cdot \frac{\bar{\epsilon}_m}{(1 - \psi)}
 \tag{3.62}$$

Therefore, if the value of  $\bar{\epsilon}_m$  is known, the draw stress (3.62) and the mean pressure (3.61) can be calculated from the geometry of the deforming passage together with the velocity distribution and mean coefficient of friction ( $I_1$  and  $I_2$ ) and the work hardening factor (B).  $\bar{\epsilon}_m$  can be derived from the total plastic work as shown in the next section.

### 3.2.7.1 The mean equivalent strain $\bar{\epsilon}_m$

If the metal undergoing deformation obeys von Mises yield criterion and Levy-Mises flow rules, the plastic work done per unit volume can be expressed as

$$W_p = \int_0^{\bar{\epsilon}_m} \bar{\sigma} \, d\bar{\epsilon}
 \tag{3.63}$$

where, 
$$\bar{\sigma} = \sqrt{\frac{3}{2}} \left\{ \sigma'_{ij} \sigma'_{ij} \right\}^{\frac{1}{2}}
 \tag{3.64}$$

$$d\bar{\epsilon} = d\bar{\epsilon}^p = \sqrt{\frac{2}{3}} \left\{ d\epsilon_{ij}^p \, d\epsilon_{ij}^p \right\}^{\frac{1}{2}}
 \tag{3.65}$$

The mean equivalent strain is defined as the strain which bounds an area under the equivalent stress-strain diagram (Fig. 3.5) equal to the total plastic work done per unit volume of the material.

$$\text{i.e. } W_p = \int_0^{\bar{\epsilon}_m} \bar{\sigma} d\bar{\epsilon} = Y_m \cdot \bar{\epsilon}_m \quad (3.66)$$

The plastic work ( $W_p$ ) can be considered to consist of the internal work of deformation ( $W_i$ ) and the redundant work ( $W_r$ ) of shearing the material at the assumed surfaces of discontinuities at both the inlet and the outlet boundaries.

$$\text{i.e. } W_p = W_i + W_r \quad (3.67)$$

or in terms of power,

$$W_p \times \dot{VOL} = \dot{W}_I + \dot{W}_R \quad (3.68)$$

From equations (3.32) and (3.42),

$$\dot{W}_I = Y_m \cdot U_b \cdot A_b \cdot f(s)$$

$$\text{and } \dot{W}_R = 2 \cdot \frac{Y_m}{\sqrt{3}} \cdot U_b \cdot A_b R(s)$$

∴ equation (3.66) becomes

$$(Y_m \cdot \bar{\epsilon}_m) \cdot \dot{VOL} = Y_m \cdot U_b \cdot A_b \cdot f(s) +$$

$$\frac{2}{\sqrt{3}} \cdot Y_m \cdot U_b \cdot A_b \cdot R(s)$$

$$\therefore \bar{\epsilon}_m = \frac{1}{\dot{VOL}} \left\{ \frac{Y_m}{Y_m} \cdot U_b \cdot A_b \cdot f(s) + \frac{2}{\sqrt{3}} \cdot \frac{Y_m}{Y_m} \cdot U_b \cdot A_b \cdot R(s) \right\}$$

(3.69)

The values of  $f(s)$  and  $R(s)$  are evaluated by the use of a computer and hence the value of the mean equivalent strain.

### 3.2.7.2 The work hardening factor B

The work hardening factor B (equation 3.57) is the ratio of the mean flow stress over the whole strain range ( $0 \sim \bar{\epsilon}_a$ ) to the mean flow stress over the strain range  $\bar{\epsilon}_m \sim \bar{\epsilon}_a$ . Therefore the value depends not only on the material characteristic but also on the process and the friction.

For a process where work done against friction or the coefficient of friction  $\mu$  is small, the strain range  $\bar{\epsilon}_m \sim \bar{\epsilon}_a$  is also small. In another instance the material is fully work-hardened. The mean flow stress over this range can be approximated therefore as,

$$(\bar{Y}_m)_f = \bar{\sigma}_{\bar{\epsilon}=\bar{\epsilon}_a} \quad (3.70)$$

By definition,

$$\bar{Y}_m \cdot \bar{\epsilon}_a = \int_0^{\bar{\epsilon}_a} f(\bar{\epsilon}) d\bar{\epsilon}$$

$$\text{or } \bar{Y}_m = \frac{1}{\bar{\epsilon}_a} \int_0^{\bar{\epsilon}_a} f(\bar{\epsilon}) d\bar{\epsilon} \quad (3.71)$$

$$\therefore B = \frac{\bar{Y}_m}{(\bar{Y}_m)_f} = \frac{\frac{1}{\bar{\epsilon}_a} \int_0^{\bar{\epsilon}_a} f(\bar{\epsilon}) d\bar{\epsilon}}{\bar{\sigma}_{\bar{\epsilon}=\bar{\epsilon}_a}} \quad (3.72)$$

If the equivalent stress-strain curve of the material follows the power law or

$$f(\bar{\epsilon}) = \sigma = \sigma_0 \bar{\epsilon}^n, \quad (3.73)$$

then equation (3.72) gives

$$B = \frac{1}{1+n} \quad (3.74)$$

### 3.2.7.3 Evaluation of $I_1$ and $I_2$

From equations (3.52) and (3.56),

$$I_1 = \frac{1}{A_a} \left\{ \sum (\mu_m \cos\alpha_s + \sin\alpha_s) dA_{s_1} + \sum (\mu_m \cos\alpha_c + \sin\alpha_c) dA_{c_1} + \sum \mu_m dA_{s_2} \right\}$$

$$I_2 = \mu_m \cdot \frac{U_b}{VOL} \left\{ \sum \left( \frac{U_{s_1}}{U_b} \right) dA_{s_1} + \sum \left( \frac{U_{c_1}}{U_b} \right) dA_{c_1} + \sum \left( \frac{U_{s_2}}{U_b} \right) dA_{s_2} \right\}$$

$I_1$  and  $I_2$  are found by integration over the whole sliding surface areas of the deforming tube.

However, to determine  $I_2$  the area and the velocity of every element on the relative sliding surface between the workpiece and the tools are required. The deforming die has a complex shape and therefore to determine the velocity at each point is a problem by

itself. The longitudinal velocity increases towards the die exit as well as circumferentially and the flow, especially at the intersection of the conical and the plane surfaces, is too complicated. An approximate method is therefore used to determine  $I_2$ . A mean sliding velocity is calculated from an idealised equivalent conical die (see appendix A-10).

If  $\bar{U}_{s_1}$  is the mean sliding velocity at the die surface,

$$\bar{U}_{s_1} = \frac{\int_{A_s} U dA_s}{\int_{A_s} dA_s} \quad (3.75)$$

For a convergent die passage and the continuity of flow,

$$U = \left( \frac{\rho_b'}{\rho'} \right)^2 U_b \cos \alpha_e \quad (3.76)$$

$$\text{and } dA_s = \rho \sin \alpha_e \cdot 2\pi d\rho$$

$$\begin{aligned} \therefore \bar{U}_{s_1} &= \frac{\int_{\rho} U_b \left( \frac{\rho_b'}{\rho'} \right)^2 \cdot \rho \sin \alpha_e \cdot 2\pi \cdot d\rho \cos \alpha_e}{\int_{\rho} \rho \sin \alpha_e \cdot 2\pi \cdot d\rho} \\ &= \frac{U_b \cdot (\rho_b' \sin \alpha_e)^2 \cdot \pi \cdot \ln \left( \frac{A_b}{A_a} \right) \cos \alpha_e}{\pi \sin^2 \alpha_e (\rho_b^2 - \rho_a^2)} \\ &= U_b \cdot \frac{\ln A_r \cos \alpha_e}{\left(1 - \frac{1}{A_r}\right)} \quad (3.77) \end{aligned}$$

For the tube/plug interface the mean velocity,

$$\begin{aligned}\bar{U}_{s_2} &= \frac{U_b + U_a}{2} \\ &= \frac{U_b}{2} (1 + A_r)\end{aligned}\tag{3.78}$$

3.3 The lower bound<sup>\*</sup> solution for the drawing of regular polygonal tube from round on a cylindrical plug.

The upper bound solution depends on the assumed velocity pattern in the deforming metal and is an over-estimate of the load required to effect the process. A lower bound solution which ignores the effects of redundant work is thus necessary; the actual load lies within the two limits.

By considering the equilibrium of forces of an elemental slug together with Tresca's yield criterion, the resulting stress expression is integrated numerically using a computer; also, the programme computes the mean pressure. The development of the computer programme is discussed in appendix A-9.

### 3.3.1 Deformation pattern of the lower bound solution

The four basic shapes of the die deforming zone are the pyramidal plane surface, the elliptical plane/conical surface, triangular plane/conical surface and the inverted parabolic/conical surface. These die shapes are shown in Fig. 4.1 on page 77.

However, the lower bound solution is developed only for the elliptical plane/conical surface die. The die has a gradual transition

\* see reference 81, page 171

from round and the surface equation is readily derived. The deforming passage is made from a cone of semi-angle ' $\alpha_c$ ' cut by ' $N_s$ ' planes equal to the number of sides of the polygonal tube required. Each of these planes is equally spaced around the tube axis and inclined at an angle ' $\alpha_s$ '. The construction of this die shape is given in details in Chapter 4, section 4.3.

### 3.3.2 Derivation of the lower bound solution

Fig. 3.6 shows a round tube deforming through the elliptical plane/conical surface die and on a cylindrical plug to produce a polygonal tube. The following geometrical relationships are derived:

(i) general parameters for the die

$$\rho = \frac{\pi}{N_s}$$

$$A_r = \frac{A_b}{A_a}$$

$$R_b = \frac{D_b}{2}$$

$$\alpha_c = \tan^{-1} \left( \frac{D_b - H_a}{2L} \right)$$

$$\alpha_s = \tan^{-1} \left( \frac{D_b - H_a / \cos \beta}{2L} \right)$$

$$L = \frac{D_b}{\tan \alpha_e} \left( 1 - \frac{1}{(D_b / D_e)} \right)$$

$$\text{where } \frac{D_e}{2} = \sqrt{\frac{A_a + A_p}{\pi}}$$

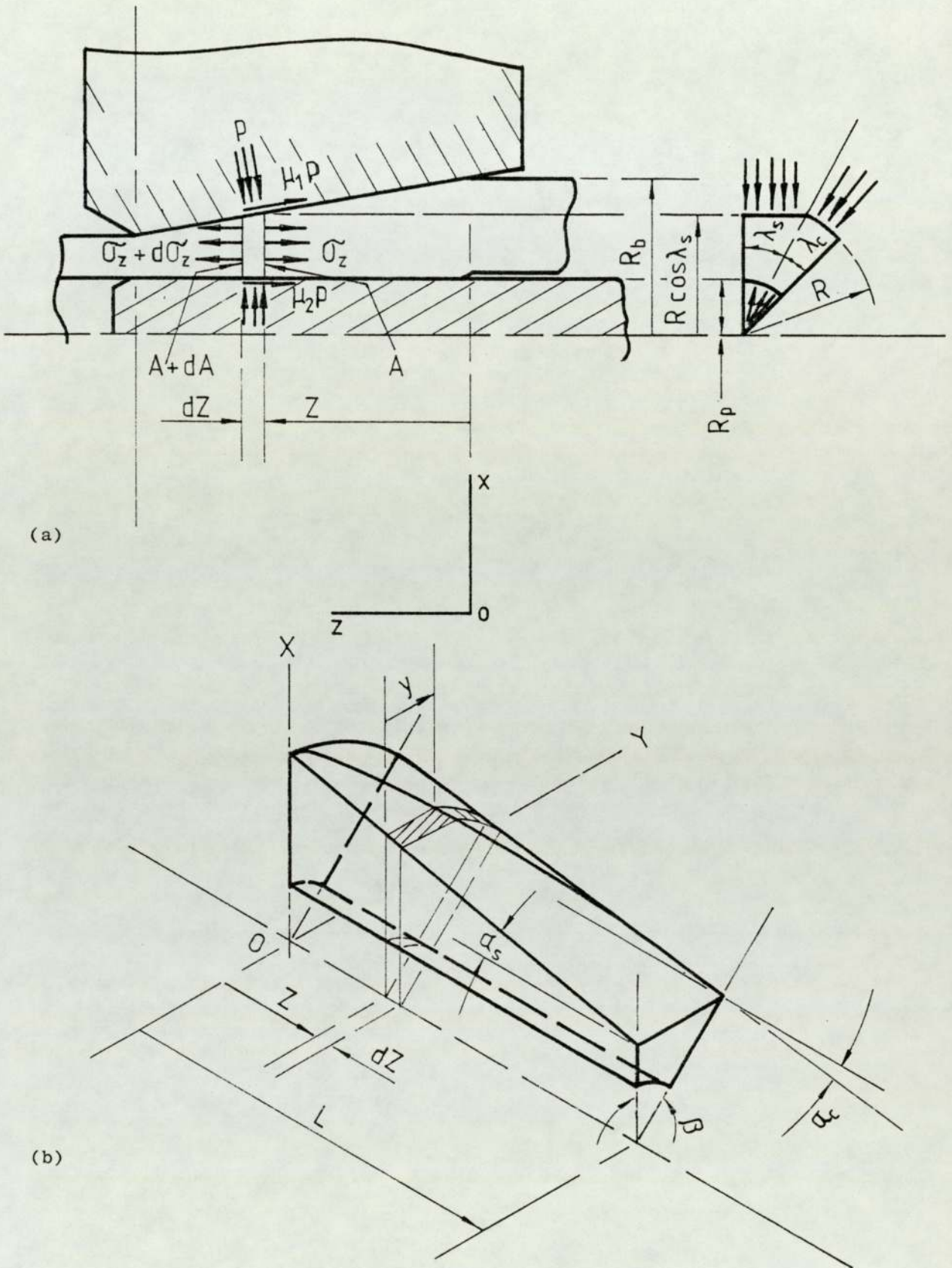


Fig. 3.6 Stress and deformation pattern for the lower bound solution for the drawing of polygonal tube from round stock on a cylindrical plug.

(ii) parameters for the elliptical plane surface

$$e = \frac{\cos\alpha_s}{\cos\alpha_c}$$

$$a = \frac{D_b}{2} \frac{\cos\alpha_c}{\sin(\alpha_c + \alpha_s)}$$

$$b = \frac{D_b}{2} \cdot \frac{1}{\sin(\alpha_c + \alpha_s)} \cdot \sqrt{\cos^2\alpha_c - \cos^2\alpha_s}$$

(iii) At any section Z,

$$R = R_b - Z \tan\alpha_c$$

$$R_s = R \cos\lambda_s$$

$$\sin\lambda_s = \frac{y}{R} = b \frac{\sqrt{2aZ \cos\alpha_s - Z^2}}{a \cos\alpha_s (R_b - Z \tan\alpha_c)}$$

$$\beta = \lambda_c + \lambda_s$$

$$A = \frac{1}{2} (R_b - Z \tan\alpha_c)^2 (\cos\lambda_s \sin\lambda_s + \lambda_c) - \frac{1}{2} \beta \cdot R_p^2$$

For an element between Z and Z + dZ,

$$\text{flat surface area } dA_{s_1} = y \frac{dZ}{\cos\alpha_s}$$

$$\text{conical surface area } dA_{c_1} = R \cdot \lambda_c \cdot \frac{dZ}{\cos\alpha_c}$$

$$\text{tube/plug surface area } dA_{s_2} = \beta \cdot R_p \cdot dZ$$

$$\frac{dA}{dZ} = -R \left\{ (\cos\lambda_s \sin\lambda_s + \lambda_c) \tan\alpha_c + \frac{b}{a} \cdot \frac{\sin^2\lambda_s}{\cos^2\lambda_s} \right\}$$

$$\frac{1}{R} \left( \frac{R (a \cos \alpha_s - Z)}{(2aZ \cos \alpha_s - Z^2)^{\frac{1}{2}}} + \tan \alpha_c \{ 2aZ \cos \alpha_s - Z^2 \}^{\frac{1}{2}} \right)$$

Resolving forces in the Z direction and for the equilibrium of

the element  $\sum F_z = 0$ ,

$$(\sigma_z + d\sigma_z) (A + dA) - \sigma_z \cdot A - p_1 (dA_{s_1} \sin \alpha_s + dA_{c_1} \sin \alpha_c) -$$

$$\mu_1 p_1 (dA_{s_1} \cos \alpha_s + dA_{c_1} \cos \alpha_c) - \mu_2 p_2 dA_{s_2} = 0$$

i.e.

$$Ad\sigma_z + d\sigma_z dA = -\sigma_z dA + p_1 \left\{ (\sin \alpha_s + \mu_1 \cos \alpha_s) dA_{s_1} + \right. \\ \left. (\sin \alpha_c + \mu_1 \cos \alpha_c) dA_{c_1} \right\} + \mu_2 p_2 dA_{s_2} \quad (3.79)$$

The following assumptions are made:-

- (i) a mean pressure  $p$  at both the die/tube and plug/tube interfaces,
- (ii) a mean coefficient of friction  $\mu_m$  at both the die/tube and plug/tube interfaces,
- (iii) the horizontal stress  $\sigma_z$  and the mean normal pressure  $p$  are the principal stresses and
- (iv) a mean yield stress  $Y$ .

Applying Tresca's yield criterion,

$$\sigma_z + p = Y$$

$$\text{or } p = Y - \sigma_z \quad (3.80)$$

∴ equation (3.79) becomes,

$$d\sigma_z (A + dA) = -\sigma_z dA + (Y - \sigma_z) \left\{ (\sin\alpha_s + \mu \cos\alpha_s) dA_{s_1} + (\sin\alpha_c + \mu \cos\alpha_c) dA_{c_1} + \mu dA_{s_2} \right\} \quad (3.81)$$

After simplifying and dividing through by Y, equation (3.81) yields,

$$d \left( \frac{\sigma_z}{Y} \right) = \frac{1}{(A + dA)} \left\{ - \left( \frac{\sigma_z}{Y} \right) dA + \left[ 1 - \left( \frac{\sigma_z}{Y} \right) \right] \left[ (\sin\alpha_s + \mu_m \cos\alpha_s) dA_{s_1} + (\sin\alpha_c + \mu_m \cos\alpha_c) dA_{c_1} + \mu_m dA_{s_2} \right] \right\} \quad (3.82)$$

A computer programme was developed to solve equation (3.82) numerically. The value of the mean pressure was obtained from equation (3.80).

The development of the numerical integration is presented in the appendix A-9. The detailed computer programme is given in the appendix A-13.

### 3.4 The computer programme

The flow chart for the computer programme shown in Fig. 3.7 consists of:-

- the input statement;
- three major 'do' loops;
- the four sub-programmes; and
- the print-out statements of the results.

The input consists mainly of the incoming and outgoing stock dimensions, the stress-strain properties of the material and the drawing velocity.

The three major 'do' loops generate the number of sides of the required polygon (1), the equivalent die semi-angle (2) and the mean coefficient of friction (3(a,b,c)).

The four sub-programmes are:-

- (i) the development of the deformation pattern and hence the velocity field,
- (ii) the upper bound solution for the polygonal tube drawing,
- (iii) the lower bound solution for the polygonal tube drawing, and
- (iv) the upper and the lower bound solutions for the corresponding axisymmetric tube drawing on a cylindrical plug.

The main parts of the upper bound solution for the drawing of regular polygonal tubes from round stock are:-

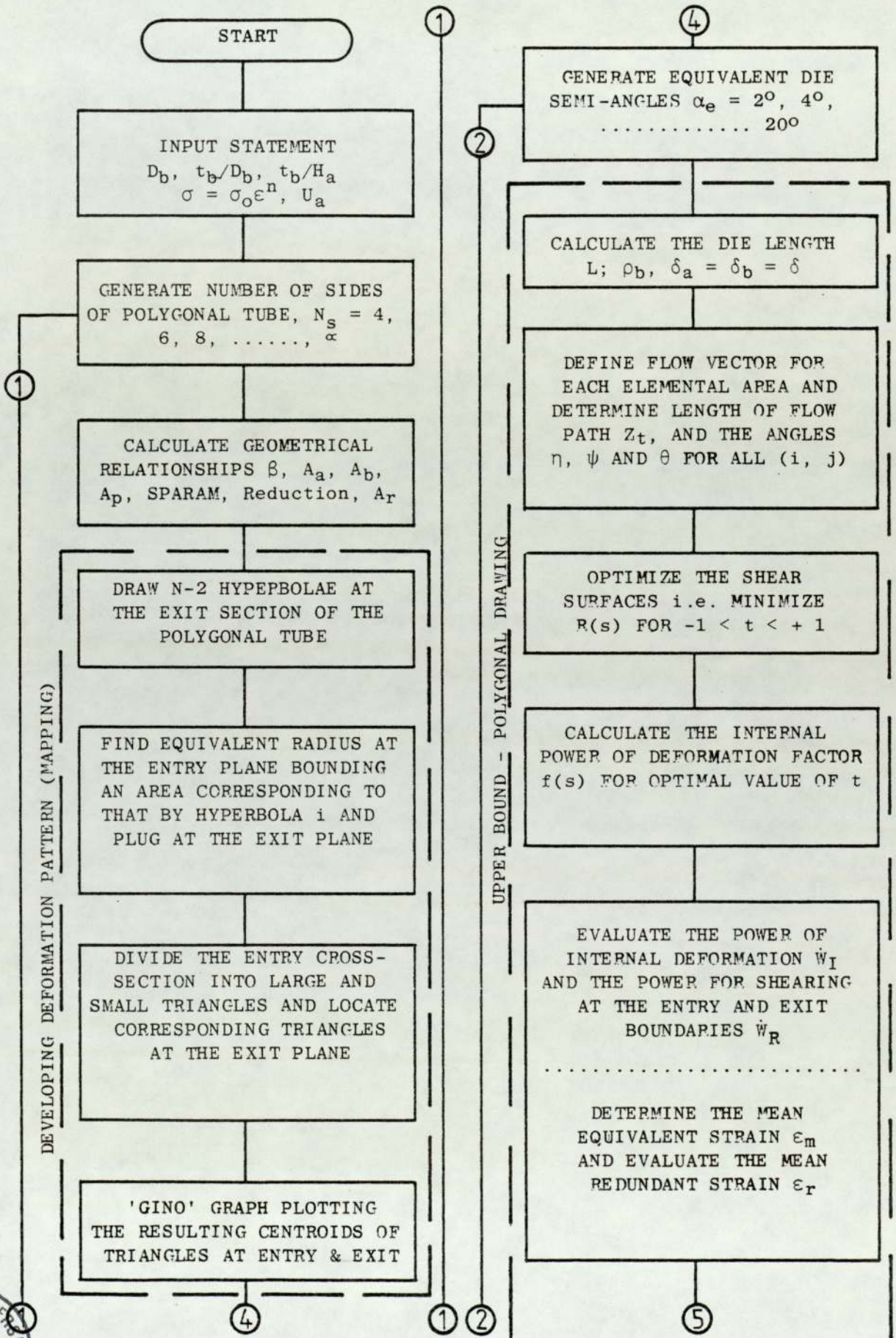
- (a) the optimisation of the entry and exit shear surfaces,
- (b) the calculation of the mean equivalent strain,
- (c) the calculation of the apparent strain factors  $I_1$  and  $I_2$  given by equations (3.52) and (3.56) respectively,
- (d) the calculation of the power loss at the workpiece-tool interface, and
- (e) finally, the tabulation of the mean draw stress and the mean die pressure.

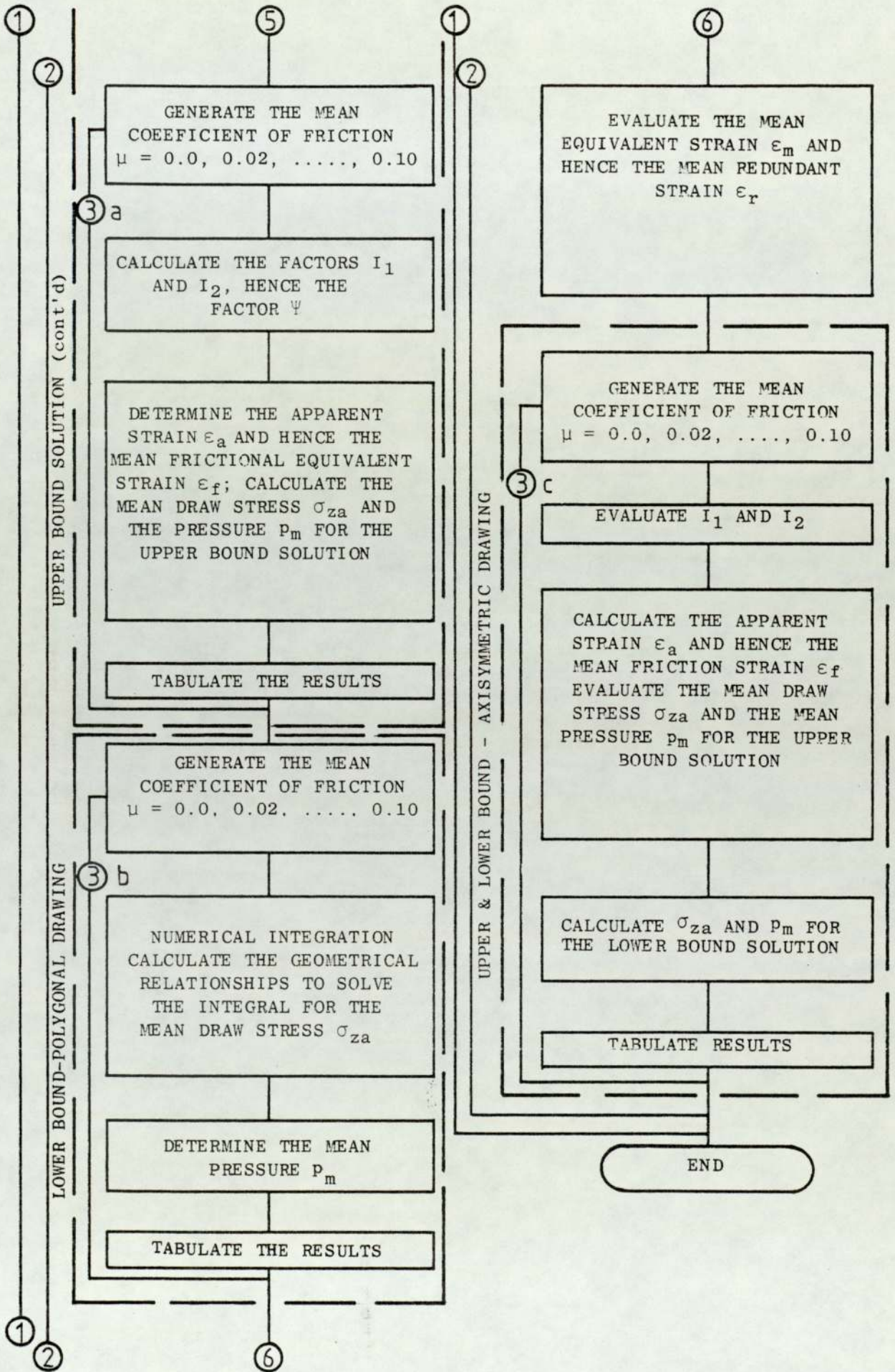
The equations for the upper and the lower bound solutions for the axisymmetric tube drawing on a cylindrical plug are reproduced in Appendix A-14.

The complete programme is presented in Appendix A-13 and Table 3.1 on page 73, shows the layout of the computer print-out. The solutions to the upper and the lower bound for the drawing of polygonal tubes from a range of input tubing are tabulated in Appendix A-4.

Sampled graphical output of the mapped entry and exit tubular sections are shown in Fig. 3.8, 3.9, 3.10 and 3.11. The centroids of the large triangles at entry for  $j = \text{constant}$  (shown in Fig. 3.2(b) on page 33 and the nomenclature as defined in the Appendix A-8.2 on page A81), are joined by straight lines. The areas encompassed by the circular arcs on entry map into areas bordered by hyperbolic curves at the exit.

Fig. 3.7 The flow chart for the computer programme for the drawing of polygonal tube from round stock on a cylindrical plug





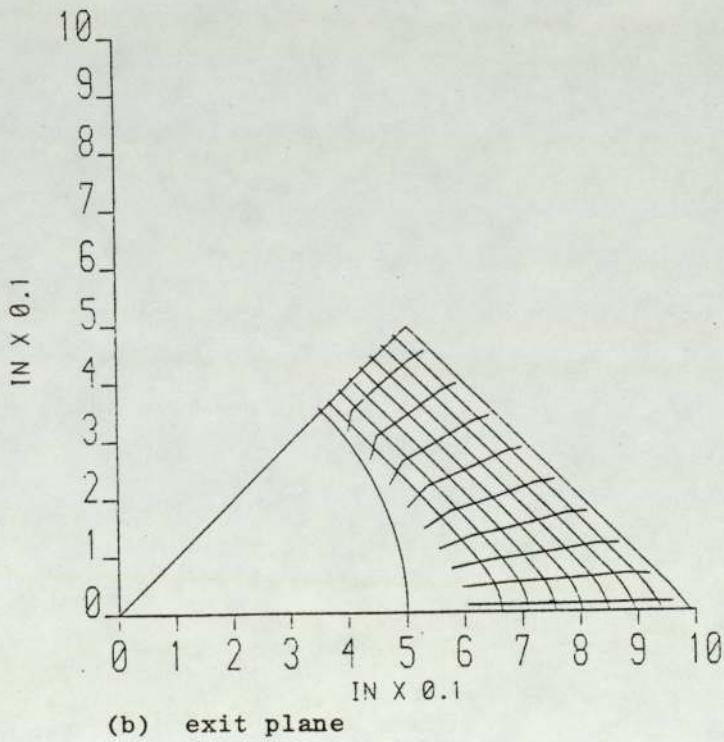
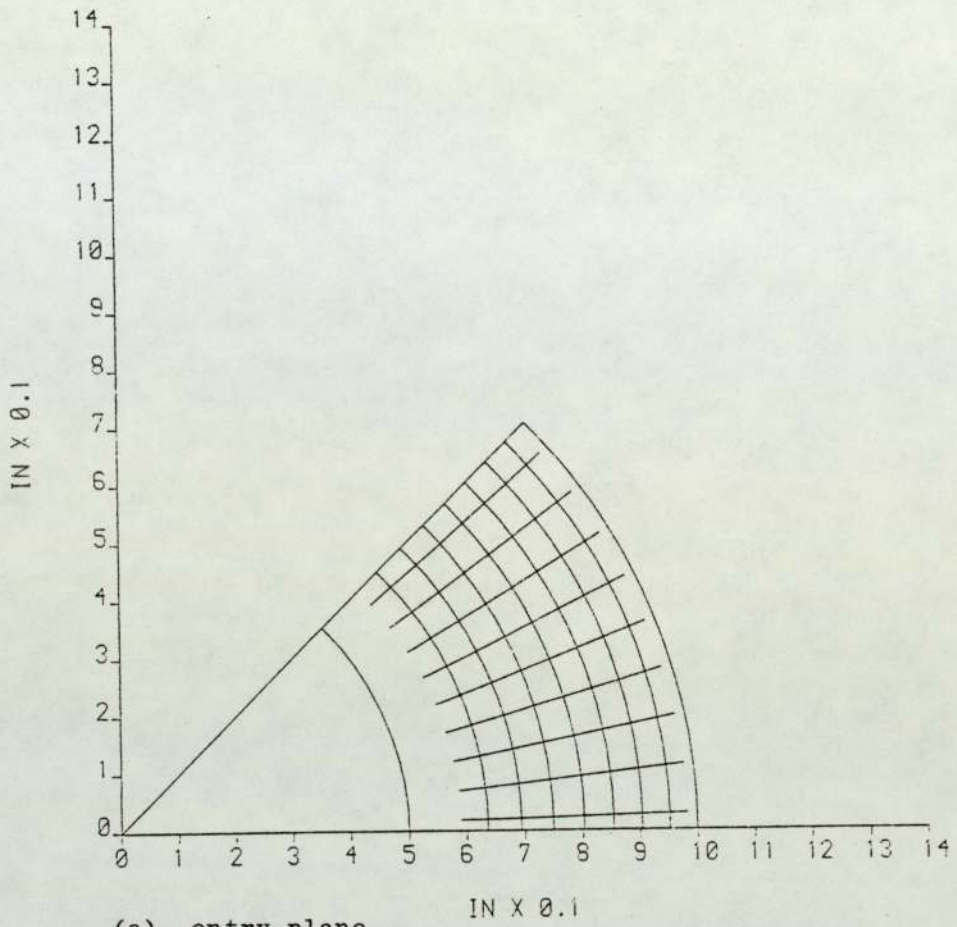


Fig. 3.8 Deformation pattern of the symmetric section of the square tube for the reduction in area of 48.45%

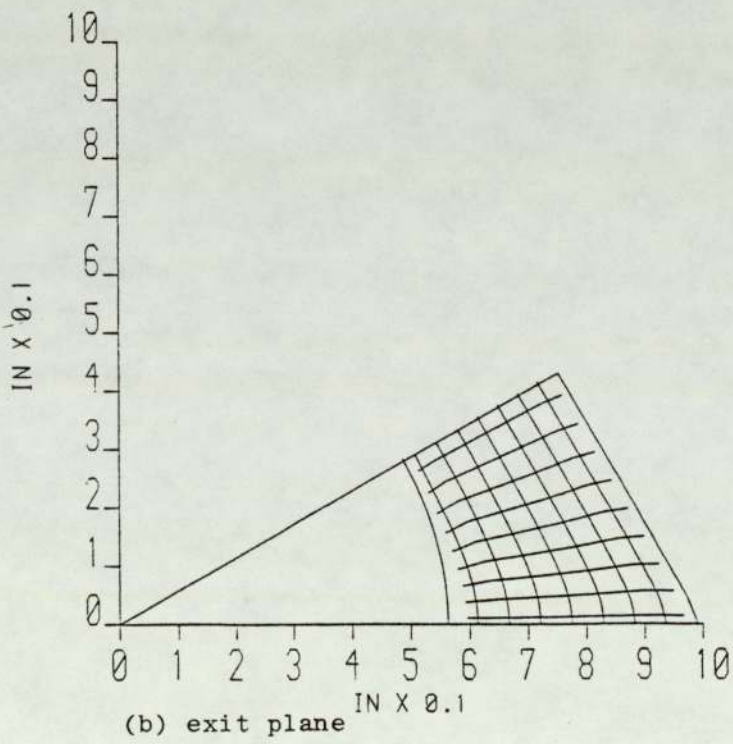
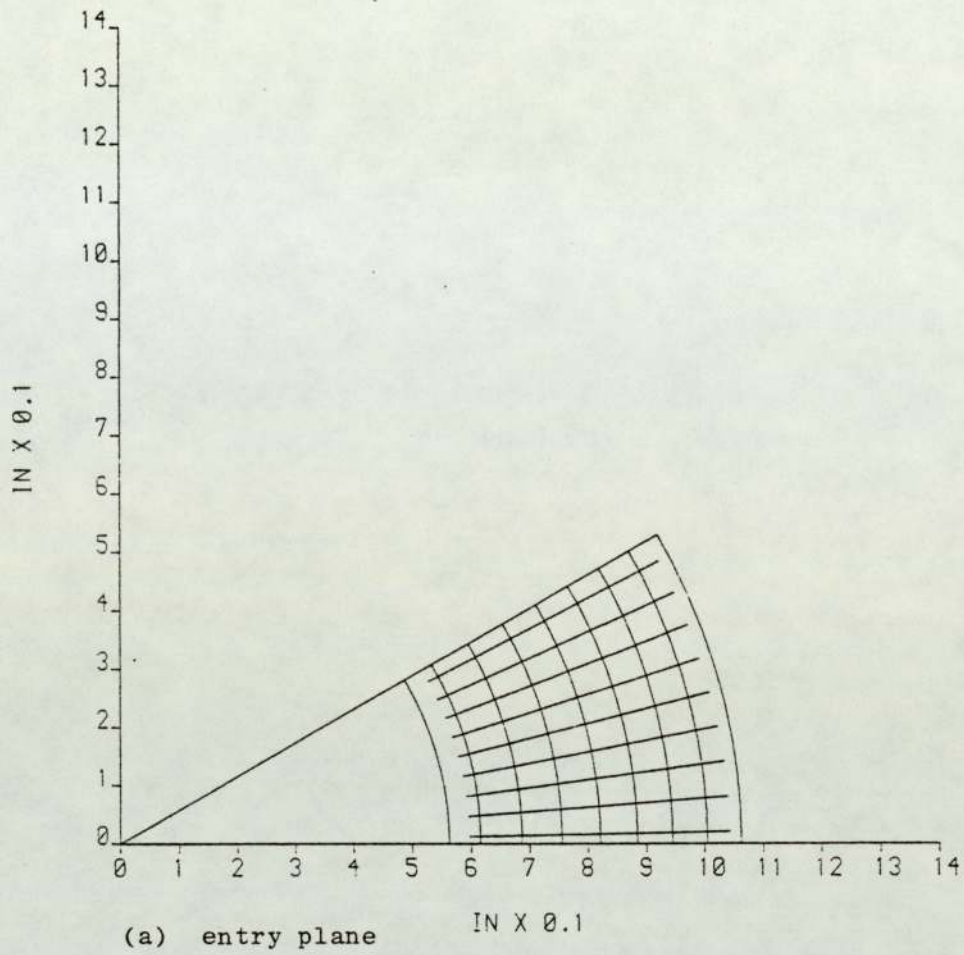


Fig. 3.9 Deformation pattern of the symmetric section of the hexagonal tube for the reduction in area of 37.16%

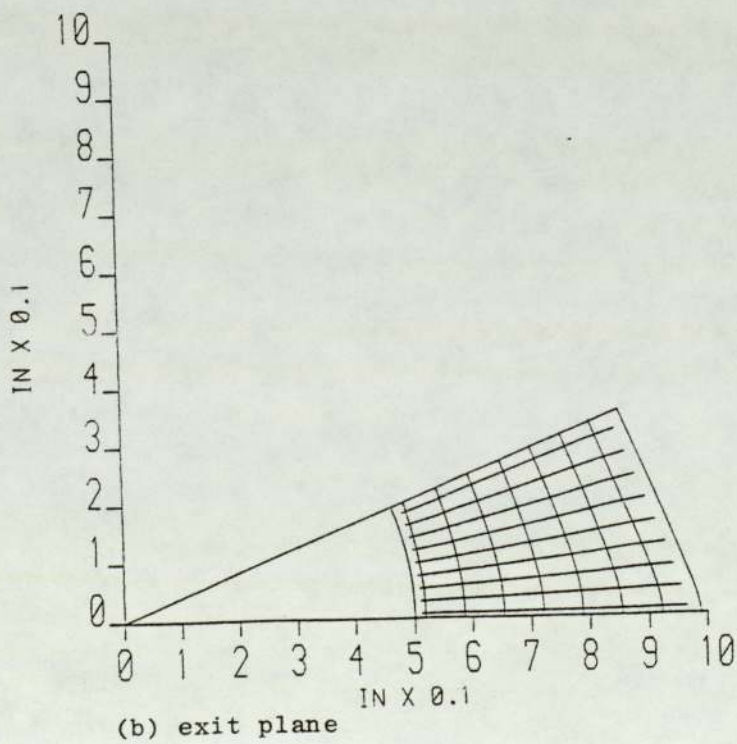
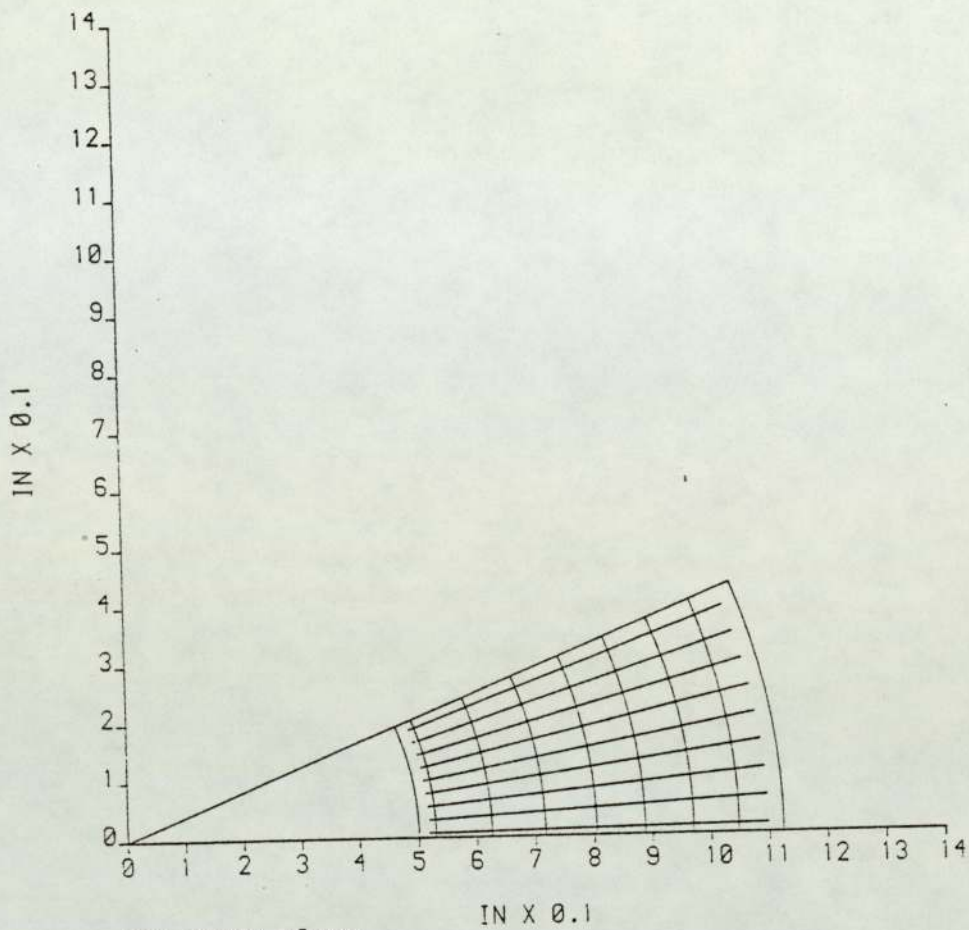
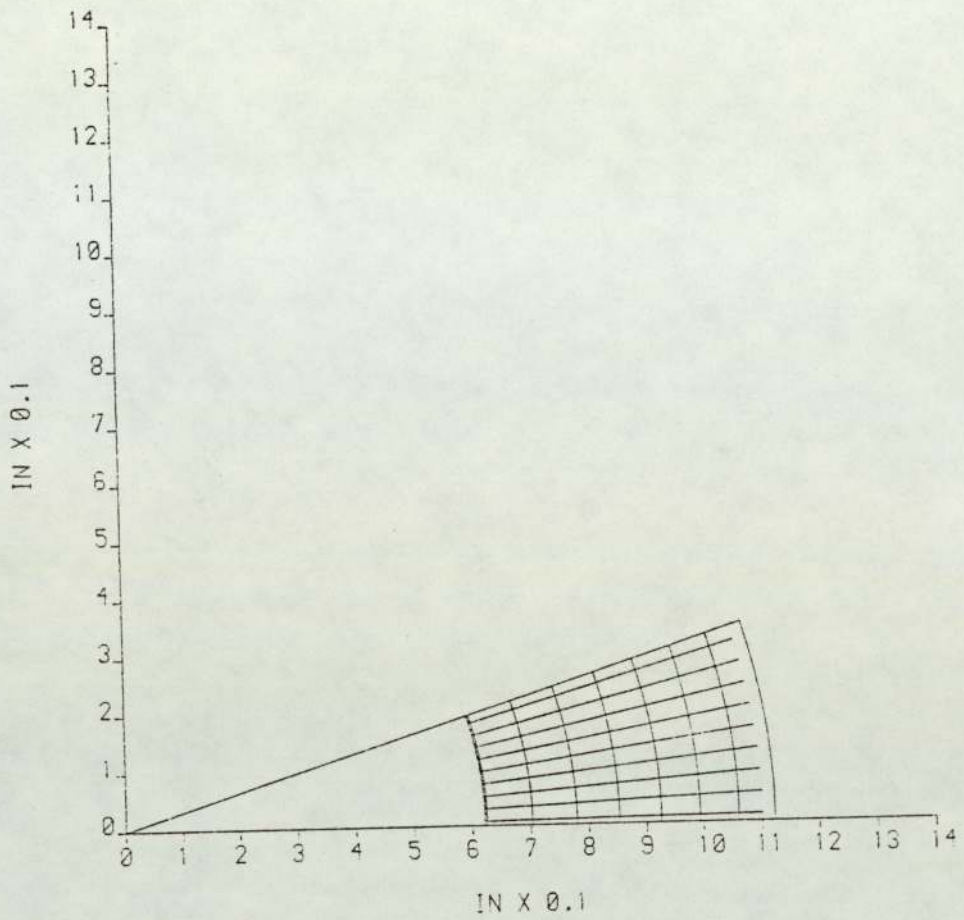
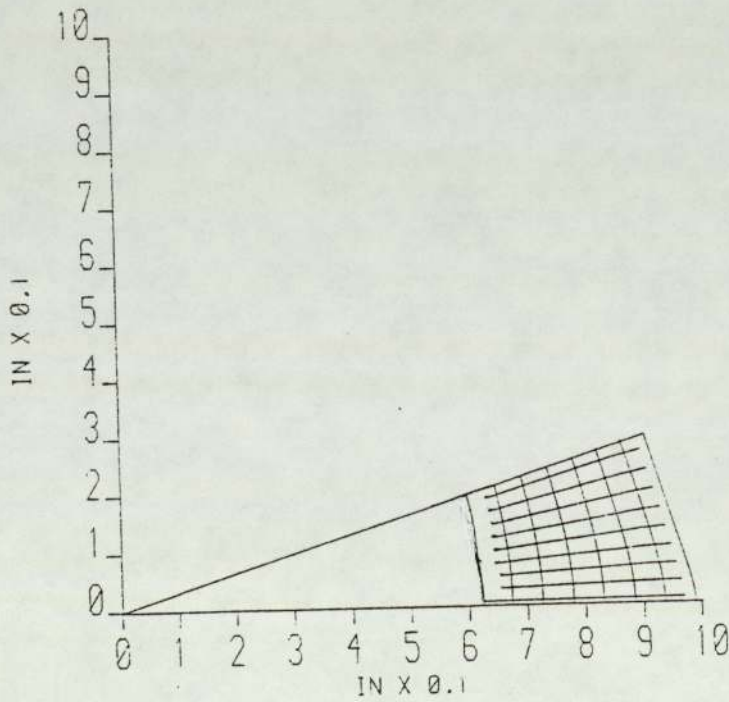


Fig. 3.10 Deformation pattern of the symmetric section of the octagonal tube for the reduction in area of 35.97%



(a) entry plane



(b) exit plane

Fig. 3.11 Deformation pattern of the symmetric section of the decagonal tube for the reduction in area of 37.73%

TABLE 3.1 The format of the computer output for the drawing of hexagonal tube directly from round stock of outer diameter  $1 \frac{1}{16}$  in by  $\frac{1}{4}$  in gauge for a reduction in area of 37.16 %

(a) Equivalent die semi-angle

$$\alpha_e = 7^\circ$$

```

229 SEMI-DIE ANGLE = 7 DEGREES
230 DIE HEIGHT = 0.6235 INCHES

***** UPPER BOUND SOLUTION FOR POLYGONAL DRAWING *****
236 PARAMETER T SHEAR FACTOR R(S)
238 0.100 2.348942
239 0.200 1.942522
240 0.300 1.538379
241 0.400 1.139642
242 0.500 0.764234
243 0.600 0.532495
244 0.700 0.531900
245 0.800 0.704429
246 0.900 1.012386
247 1.000 1.383204

250 OPTIMAL T = 0.700 AND MINIMUM R(S) = 0.531900
253 THE VALUE OF F'(S) = 57.827114

256 REDUNDANT STRAIN = 0.110485
257 INTERNAL WORK STRAIN = 0.564826
259 THE MEAN EQUIVALENT STRAIN = 0.675311
261 THE HOMOG. EQUIVALENT STRAIN = 0.464555

264 COEFFICIENT APPARENT YIELD STRESS DRAW FORCE DRAW STRESS MEAN DIE-PRESS DRAW POWER DRAW/YIELD MEAN-PRESS/YIELD
265 OF FRICTION STRAIN (TONF/SQ IN) (TONF) (TONF/SQ IN) (TONF/SQ IN) (HP-POWER) STRESS STRESS RATIO
267 0.000 0.675311 37.1951 10.0728 25.1182 42.4793 10.256 0.67531 1.14207
268 0.020 0.779491 38.4316 11.9824 29.8802 40.2389 12.200 0.80334 1.04703
269 0.040 0.863972 39.3840 13.6452 34.0266 38.0680 13.893 0.91482 0.96659
270 0.060 0.938112 40.1438 15.1019 37.6594 36.0341 15.377 1.01248 0.89763
271 0.080 1.002378 40.7459 16.3866 40.8629 34.1557 16.665 1.09861 0.83785
272 0.100 1.058619 41.2857 17.5267 43.7059 32.4315 17.845 1.17504 0.78554

**** THE LOWER BOUND SOLUTION OF SECTION DRAWING ****
279 COEFFICIENT YIELD STRESS DRAW LOAD DRAW STRESS DIE PRESSURE PLUG PRESSURE DRAW/YIELD DIE P/YIELD PLUG P/YIELD
280 OF FRICTION (TONF/SQ IN) (TONF) (TONF/SQ IN) (TONF/SQ IN) (TONF/SQ IN) STRESS RATIO STRESS STRESS
281 0.000 34.1018 6.4230 16.0170 27.7824 27.6505 0.46968 0.81469 0.41022
282 0.020 34.1018 7.6245 19.0254 26.2453 26.0884 0.55790 0.76962 0.72251
283 0.040 34.1018 8.6869 21.6698 24.8183 24.6193 0.63545 0.72777 0.72252
284 0.060 34.1018 9.6208 23.9912 23.4928 23.2943 0.70352 0.68890 0.68358
285 0.080 34.1018 10.4368 26.0261 22.2607 22.0452 0.76319 0.65277 0.64645
286 0.100 34.1018 11.1510 27.8070 21.1148 20.8844 0.81541 0.61917 0.61241

290 LOWER AND UPPER BOUND SOLUTIONS FOR AXISYMMETRIC DRAWING
293 THE HOMOG. EQUIVALENT STRAIN = 0.464555
294 THE REDUNDANT EQUIVALENT STRAIN = 0.107512
295 THE MEAN EQUIVALENT STRAIN = 0.572067

297 I UPPER BOUND SOLUTION I LOWER BOUND SOLUTION I
298 COEFF OF FRICTION YIELD STRESS DRAW FORCE DRAW STRESS MEAN DIE-PRESS APPARENT PRESS/YIELD YIELD STRESS DRAW/YIELD PRESS/YI
299 FRICTION (TONF/SQ IN) (TONF) (TONF/SQ IN) (TONF/SQ IN) STRAIN STRESS RATIO (TONF/SQ IN) STRESS -STRESS
301 0.000 35.7900 8.2105 20.4743 34.6255 0.572067 0.96746 34.1018 0.3656 0.6344
302 0.020 36.9797 9.7670 24.3558 32.7993 0.658626 0.88695 34.1018 0.4569 0.5431
303 0.040 37.6951 11.1224 27.7356 31.0298 0.731885 0.81881 34.1018 0.5373 0.4627
304 0.060 38.0272 12.1098 30.6997 29.3720 0.794691 0.76039 34.1018 0.6079 0.3921
305 0.080 39.2259 13.3570 33.3079 27.8409 0.849132 0.70976 34.1018 0.6698 0.3302
306 0.100 39.7261 14.2863 35.6253 26.4354 0.896774 0.66544 34.1018 0.7242 0.2758

```

TABLE 3.1 (Continued)

(b) Equivalent die semi-angle

$$\alpha_e = 8^\circ$$

149 SEMI-DIE ANGLE = 8 DEGREES  
 150 DIE FLIGHT = 0.5447 INCHES

\*\*\*\*\* UPPER BOUND SOLUTION FOR POLYGONAL DRAWING \*\*\*\*\*

156 PARAMETER T SHEAR FACTOR R(S)

156	0.100	2.885796
159	0.200	2.220902
160	0.300	1.758706
161	0.400	1.302743
162	0.500	0.873551
163	0.600	0.607953
164	0.700	0.607396
165	0.800	0.805672
166	0.900	1.158330
167	1.000	1.582750

170 OPTIMAL T = 0.700 AND MINIMUM R(S) = 0.607396

173 THE VALUE OF F'(S) = 57.527196

176 REDUNDANT STRAIN = 0.126299  
 177 INTERNAL WORK STRAIN = 0.561896

179 THE MEAN EQUIVALENT STRAIN = 0.688195

181 THE HOMOGL. EQUIVALENT STRAIN = 0.464555

184	COEFFICIENT OF FRICTION	APPARENT STRAIN	YIELD STRESS (TONF/SQ IN)	DRAW FORCE (TONF)	DRAW STRESS (TONF/SQ IN)	MEAN DIE-PRESS (TONF/SQ IN)	DRAW POWER (H-POWER)	DRAW/YIELD STRESS	MEAN-PRESS/YIELD STRESS RATIO
187	0.300	0.688195	37.3586	10.3101	25.7100	43.4801	10.498	0.68820	1.16386
188	0.320	0.760443	38.4654	12.0385	30.0200	41.4951	12.257	0.80356	1.07876
189	0.340	0.860120	39.3431	13.5703	33.8398	39.5503	13.317	0.90581	1.00527
190	0.360	0.929053	40.0593	14.9339	37.2404	37.7015	15.205	0.99684	0.94114
191	0.380	0.990810	40.6562	16.1539	40.2826	35.7691	16.448	1.07827	0.88471
192	0.400	1.045066	41.1624	17.2506	43.0174	34.3568	17.564	1.15147	0.83466

\*\*\*\* THE LOWER BOUND SOLUTION OF SECTION DRAWING \*\*\*\*

199	COEFFICIENT OF FRICTION	YIELD STRESS (TONF/SQ IN)	DRAW LOAD (TONF)	DRAW STRESS (TONF/SQ IN)	DIE PRESSURE (TONF/SQ IN)	PLUG PRESSURE (TONF/SQ IN)	DRAW/YIELD STRESS RATIO	DIE P/YIELD STRESS	PLUG P/YIELD STRESS
200	0.300	34.1018	6.4230	16.0170	27.7790	27.4505	0.48968	0.81459	0.81082
201	0.320	34.1018	7.4854	18.6661	26.4292	26.2793	0.54757	0.77501	0.77061
202	0.340	34.1018	8.4348	21.0336	25.1645	24.9953	0.61679	0.73792	0.73296
203	0.360	34.1018	9.2823	23.1470	23.9788	23.7924	0.67876	0.70315	0.69769
204	0.380	34.1018	10.0380	25.0315	22.8667	22.6650	0.73402	0.67054	0.66463
205	0.400	34.1018	10.7111	26.7100	21.8232	21.6078	0.78324	0.63994	0.63363

LOWER AND UPPER BOUND SOLUTIONS FOR AXISYMMETRIC DRAWING

213 THE HOMOGL. EQUIVALENT STRAIN = 0.464555  
 214 THE REDUNDANT EQUIVALENT STRAIN = 0.119364  
 215 THE MEAN EQUIVALENT STRAIN = 0.583919

217	UPPER BOUND SOLUTION					LOWER BOUND SOLUTION				
218	COEFF OF FRICTION	YIELD STRESS (TONF/SQ IN)	DRAW FORCE (TONF)	DRAW STRESS (TONF/SQ IN)	MEAN DIE-PRESS (TONF/SQ IN)	APPARENT STRAIN	PRESS/YIELD STRESS RATIO	YIELD STRESS (TONF/SQ IN)	DRAW/YIELD STRESS	PRESS/YIELD STRESS
221	0.300	35.9607	8.4205	20.9981	35.5115	0.583919	0.98751	34.1018	0.3656	0.6344
222	0.320	37.0261	9.4322	24.5183	33.8903	0.662189	0.91531	34.1018	0.4460	0.5340
223	0.340	37.8710	11.0832	27.6380	32.3019	0.729794	0.85295	34.1018	0.5179	0.4421
224	0.360	39.3603	12.1970	30.4154	30.7920	0.788774	0.79854	34.1018	0.5822	0.4178
225	0.380	39.7149	13.1934	32.9000	29.3770	0.840681	0.75066	34.1018	0.6395	0.3605
226	0.400	39.8222	14.0891	35.1336	28.0602	0.886715	0.70819	34.1018	0.6907	0.3093

CHAPTER 4

THE DERIVATION OF PROCESS PARAMETERS IN THE  
DRAWING OF POLYGONAL TUBE DIRECTLY FROM  
ROUND STOCK ON A CYLINDRICAL PLUG

#### 4.1. INTRODUCTION

The method adopted for the experimental part of the project had two main objectives:

1. A laboratory investigation of the relationship between the deformation occurring when drawing polygonal tube and the following parameters:
  - (i) the draw force
  - (ii) the plug force
  - (iii) the mean die pressure and the mean plug pressure
  - (iv) the mean coefficient of friction
  - (v) the mean equivalent strain and
  - (vi) the reduction of area.
  
2. To optimize the drawing process for industrial applications based on the study of the inter-relationship of the following parameters:
  - (i) the shape of the deformation zone
  - (ii) the mean equivalent die semi-angle
  - (iii) the mean coefficient of friction and
  - (iv) the reduction of area achievable.

To fulfil the first objective, the draw force and the plug force were measured by two load cells at the tag holder and the rear of the drawbench respectively. In addition, another load cell was installed to measure the thrust at the die. The design of the load cells are presented in Appendices A-16 and A-17.

The mean coefficient of friction and the mean pressure were determined by two methods. In one method the values were established indirectly by estimating the redundant work occurring in the process

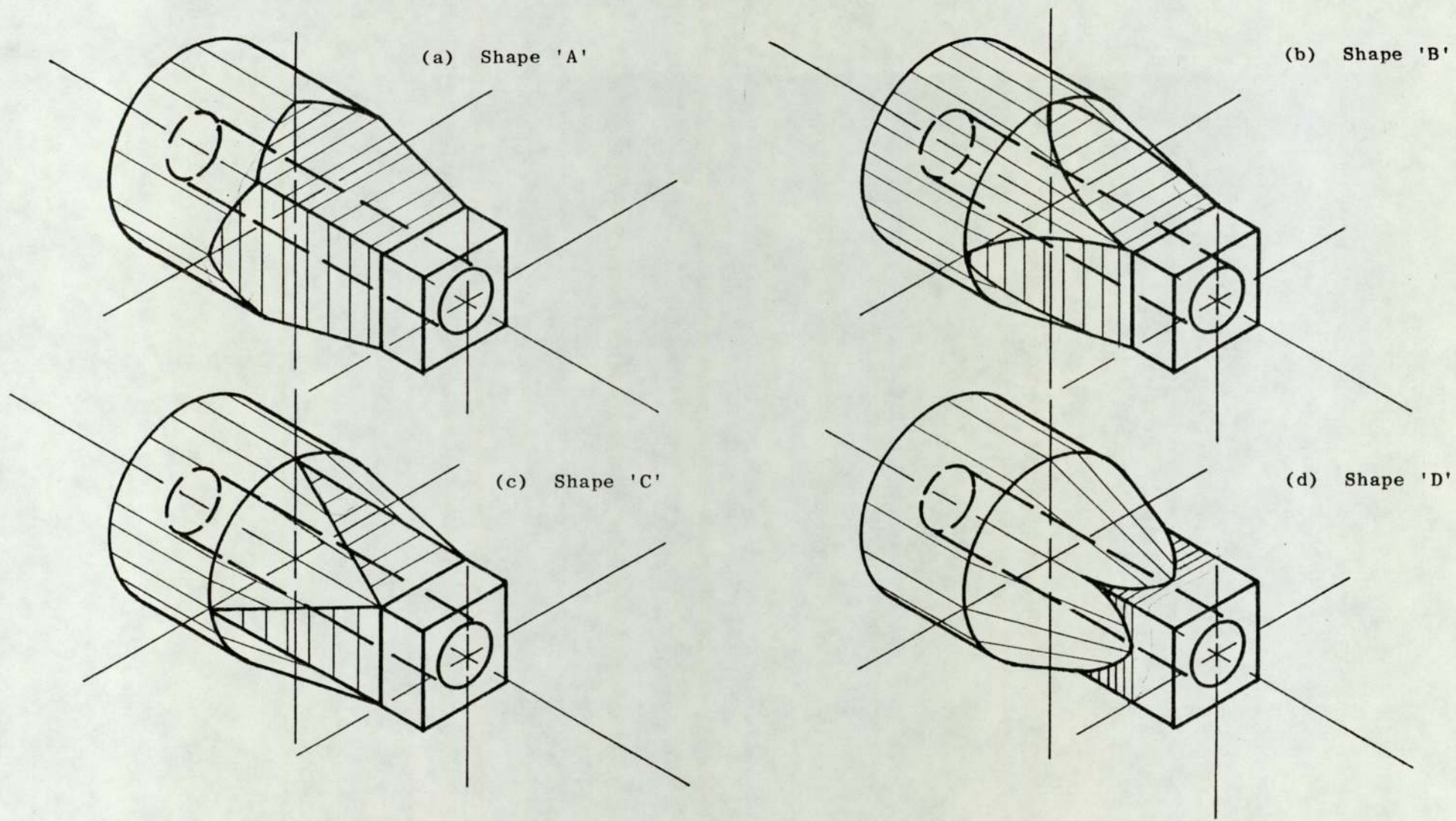
and applying the apparent strain method of analysis; in the other method the values were determined directly and continuously by an instrumented split rotating die rig. The details of the two methods are given in section 4.2.

In the drawing of polygonal tube from round stock on a cylindrical plug, the geometry of the deforming zone through which an entirely circular section transforms partly to a polygonal tube in a single pass forms the core of the problem. A gradual transformation of the round stock to the final section with minimal energy dissipation is critical. The second objective was concerned, therefore, with the investigations of different die deforming profiles to give the required shape of the tube. In this thesis, four different die deforming shapes, shown in figure 4.1, were used. To establish the optimum die profile, draw tests were carried out on the different die passages, maintaining the same speed and the lubricant. The experimental work showed that the die profile exhibiting the least amount of work done also produced a polygonal tube with sharp corners and better surface finish. Dies of the same profile but different semi-angles were used in further tests and the resulting loads compared, to establish the optimum equivalent die semi-angle. An extensive discussion on the design of the dies for the drawing of polygonal sections directly from round stock is given in section 4.3.

The selection of the drawing tube material, the design of the corresponding plugs and the selection of the drawing lubricant are presented in detail in sections 4.4, 4.5 and 4.6 respectively.

#### 4.2. THE MEAN COEFFICIENT OF FRICTION AND THE MEAN DIE PRESSURE

4.2.1. Determination of the mean coefficient of friction and the mean die pressure from the estimated redundant work



(a) Pyramidical shape die

(b) Elliptical plane surface die

(c) Triangular plane surface die

(d) Inverted parabolic plane surface die

Fig. 4.1 Isometric drawing of the general features of the four basic shapes of the die deforming zone for the direct drawing of polygonal (square) tube from round.

#### 4.2.1.1. Theoretical analysis

As already discussed in section 3.2.7, and shown in figure 3.5, the total work  $W$ , expended in a particular deformation can be regarded as a sum of three components:

$$W = W_h + W_r + W_f \quad (4.1)$$

where:

$W_h$  represents the work component due to homogeneous plastic deformation,

$W_r$  the component due to redundant deformation, i.e. the internal distortion inessential to the change of shape and

$W_f$  is the component due to friction at the tool/workpiece interface.

$W_h$  is derived simply from the stress-strain curve with the equivalent strain corresponding to the reduction of area.  $W$ , the total work per unit volume of the metal is given by the draw stress and the only two unknowns are  $W_r$  and  $W_f$ . However,  $W_r$  and  $W_f$  are not entirely separable because the flow constraint will be influenced by the friction at the tool surface; so  $W_r$  will depend upon the coefficient of friction. But in cold drawing there is negligible interaction between redundant work and friction and therefore, the measurement of either  $W_r$  or  $W_f$  leads to the derivation of the other.

If stress-strain tests on the undrawn material are performed and the resulting true stress-strain curve compared with that for the drawn material, the curve for the drawn metal rises above that of the undrawn material. So when the curve for the drawn metal is translated in the direction of the increasing strain until the two

curves fit, the amount by which the curve has moved may be taken to represent the redundant strain and the redundant work  $W_r$ , is calculated from the displaced area under the curve of the undrawn metal (74, 75). This graphical method of fitting the two curves is subject to error if the metal does not work-harden rapidly.

Consequently, to overcome this weakness in the technique, the master stress-strain curve is expressed mathematically and the mean redundant strain and the redundant work in the drawing process are deduced analytically. The semi-analytical method adopted in this investigation was developed by Basily and Sansome (76) to determine the same parameters in the drawing of polygonal rod from round.

#### 4.2.1.2. Derivation of the mean coefficient of friction and the mean die pressure.

If the stress-strain curve of the undrawn metal fits the exponential law,  $\sigma = \sigma_o \epsilon^n$ , then the energy components can be expressed thus:

$$W_h = \int_0^{\epsilon_h} \sigma d\epsilon = \frac{\sigma_o \epsilon_h^{n+1}}{(n+1)} \quad (a)$$

$$W_r = \int_{\epsilon_h}^{\epsilon_m} \sigma d\epsilon = \frac{\sigma_o}{n+1} \left\{ \epsilon_m^{n+1} - \epsilon_h^{n+1} \right\} \quad (b) \quad (4.2)$$

$$W_f = \int_{\epsilon_m}^{\epsilon_a} \sigma d\epsilon = W - \frac{\sigma_o}{n+1} \epsilon_m^{n+1} \quad (c)$$

where  $\epsilon_h$ ,  $\epsilon_m$  and  $\epsilon_a$  are the homogeneous, the mean equivalent and the apparent strain respectively.

$$\text{The homogeneous strain, } \epsilon_h = \ln\left(\frac{1}{1-r}\right) \quad (4.3)$$

The mean equivalent strain  $\epsilon_m$  is the actual strain occurring in the material after drawing taking into account the homogeneous and the redundant work during the drawing operation. This strain corresponds to the flow stress of the drawn metal given by:

$$\epsilon_m = \left(\frac{\sigma_f}{\sigma_o}\right)^{\frac{1}{n}} \quad (4.4)$$

The flow stress is obtained from the tension tests conducted on the drawn metal.

The apparent strain  $\epsilon_a$ , is an imaginary equivalent strain which bounds an area under the stress-strain diagram equal to the total work done per unit volume of the metal, i.e.

$$\epsilon_a = \left\{ \left( \frac{W}{\sigma_o} \right)^{(n+1)} \right\}^{\frac{1}{(n+1)}} \quad (4.5)$$

Substituting values of  $\epsilon_h$ ,  $\epsilon_m$  and  $\epsilon_a$  in the equations (4.2), the energy components become thus:

$$W_h = \frac{\sigma_o}{n+1} \left\{ \ln\left(\frac{1}{1-r}\right) \right\}^{n+1} \quad (a)$$

$$W_r = \frac{\sigma_o}{n+1} \left\{ \left( \frac{\sigma_f}{\sigma_o} \right)^{\frac{n+1}{n}} - \left[ \ln\left(\frac{1}{1-r}\right) \right]^{n+1} \right\} \quad (b) \quad (4.6)$$

$$W_f = W - \frac{\sigma_o}{n+1} \left( \frac{\sigma_f}{\sigma_o} \right)^{\frac{n+1}{n}} \quad (c)$$

It is assumed that Coulomb friction obtains in cold drawing and it is postulated that a mean coefficient of friction and a mean

pressure occur at both the die/tube and the plug/tube sliding surfaces.

By considering the equilibrium of the horizontal forces of the whole deforming zone (figure 3.4), the work done per unit volume is given by:

$$W = \frac{1}{A_a} \cdot p_m \left\{ \sum (\mu_m \cos\alpha_s + \sin\alpha_s) dA_{s_1} + \sum (\mu_m \cos\alpha_c + \sin\alpha_c) dA_c + \sum \mu_m dA_{s_2} \right\} \quad (4.7)$$

Similarly, the frictional work per unit volume can be obtained,

$$W_f = \mu_m \cdot p_m \cdot U_b \left\{ \sum \left( \frac{U_{s_1}}{U_b} \right) dA_{s_1} + \sum \left( \frac{U_{s_c}}{U_b} \right) dA_c + \sum \left( \frac{U_{s_2}}{U_b} \right) dA_{s_2} \right\} \frac{1}{VOL} \quad (4.8)$$

Dividing equation (4.7) by equation (4.8) to eliminate  $p_m$  gives:

$$\frac{W}{W_f} = \frac{1}{A_a} \left\{ \sum (\mu_m \cos\alpha_s + \sin\alpha_s) dA_{s_1} + \sum (\mu_m \cos\alpha_c + \sin\alpha_c) dA_c + \sum \mu_m dA_{s_2} \right\} \frac{1}{\mu_m \cdot U_b \left\{ \sum \left( \frac{U_{s_1}}{U_b} \right) dA_{s_1} + \sum \left( \frac{U_{s_c}}{U_b} \right) dA_c + \sum \left( \frac{U_{s_2}}{U_b} \right) dA_{s_2} \right\} \frac{1}{VOL}} \quad (4.9)$$

The above equation simplifies to yield:

$$\mu_m = \frac{W_f}{A_a} \sum (\sin \alpha_s dA_{s_1} + \sin \alpha_c dA_c)$$

$$\frac{W \cdot U_b \left\{ \sum \left[ \left( \frac{U_{s_1}}{U_b} \right) dA_{s_1} + \left( \frac{U_c}{U_b} \right) dA_c + \left( \frac{U_{s_2}}{U_b} \right) dA_{s_2} \right] \right\}}{VOL} -$$

$$\frac{W_f}{A_a} \left\{ \sum \left( \cos \alpha_s dA_{s_1} + \cos \alpha_c dA_c + dA_{s_2} \right) \right\} \quad (4.10)$$

The mean die pressure is calculated from either equation (4.7) or (4.8).

#### 4.2.2. Determination of the mean coefficient of friction and the mean die pressure by the split rotating die method

##### 4.2.2.1. Introduction

The direct measurement of the mean coefficient of friction and the mean die pressure for the drawing of polygonal tube from round on a cylindrical plug was made using the split rotating die rig (see Plates: A-12.1, A-12.2 and 8.11) designed by Basily and Sansome (2). A brief description of the general features is given in the Appendix A-12.

The most unusual feature of the split rotating die rig is the die inserts. The inserts, equal to the number of faces in the polygonal section required, enclose a convergent die passage while their exterior surfaces form a conical surface around which a conical die rotates. A set of six such die tips designed to form a pyramidal die passage is shown in Plate 8.10 and on page A117. The flexibility of the rotating die rig allows for the investigations of different polygonal sections, equivalent die semi-angles and the input stock with a range of outside diameters.

The forces on both the die insert (Q) and the conical die (R)

were continuously measured by load cells installed in the rig. The mean coefficient of friction and the mean die pressure were derived from the two measured forces.

4.2.2.2. The general derivation of the mean coefficient of friction and the mean pressure from the measurable forces

The reason for rotating the conical die relative to the die inserts is to rotate the friction vector between the conical die and the die inserts through  $90^\circ$  relative to the draw axis, i.e. the component of the friction force between the conical die and the die inserts along the axis of the tube vanishes. The general principle of the rotating die is illustrated in figure 4.2.

By considering the equilibrium of the forces in the direction of the tube axis, the mean coefficient of friction and the mean die pressure are determined. Resolving forces in the Z and X directions of the exploded diagram, figure 4.2 (b):

(iv) PLUG

$$\sum F_z = 0, \quad -F_p + F_{34} = 0$$

$$\text{For Coulomb friction, } F_{34} = \mu_{34} N_{34}$$

$$\therefore F_p = \mu_{34} N_{34} \quad (4.11)$$

(iii) TUBE

$$\sum F_z = 0,$$

$$P - F_{34} - F_{23} \cos \alpha_s - N_{23} \sin \alpha_s = 0$$

$$\text{where, } F_{23} = \mu_{23} N_{23}$$

$$\therefore P - \mu_{34} N_{34} - (\mu_{23} \cos \alpha_s + \sin \alpha_s) N_{23} = 0 \quad (4.12)$$

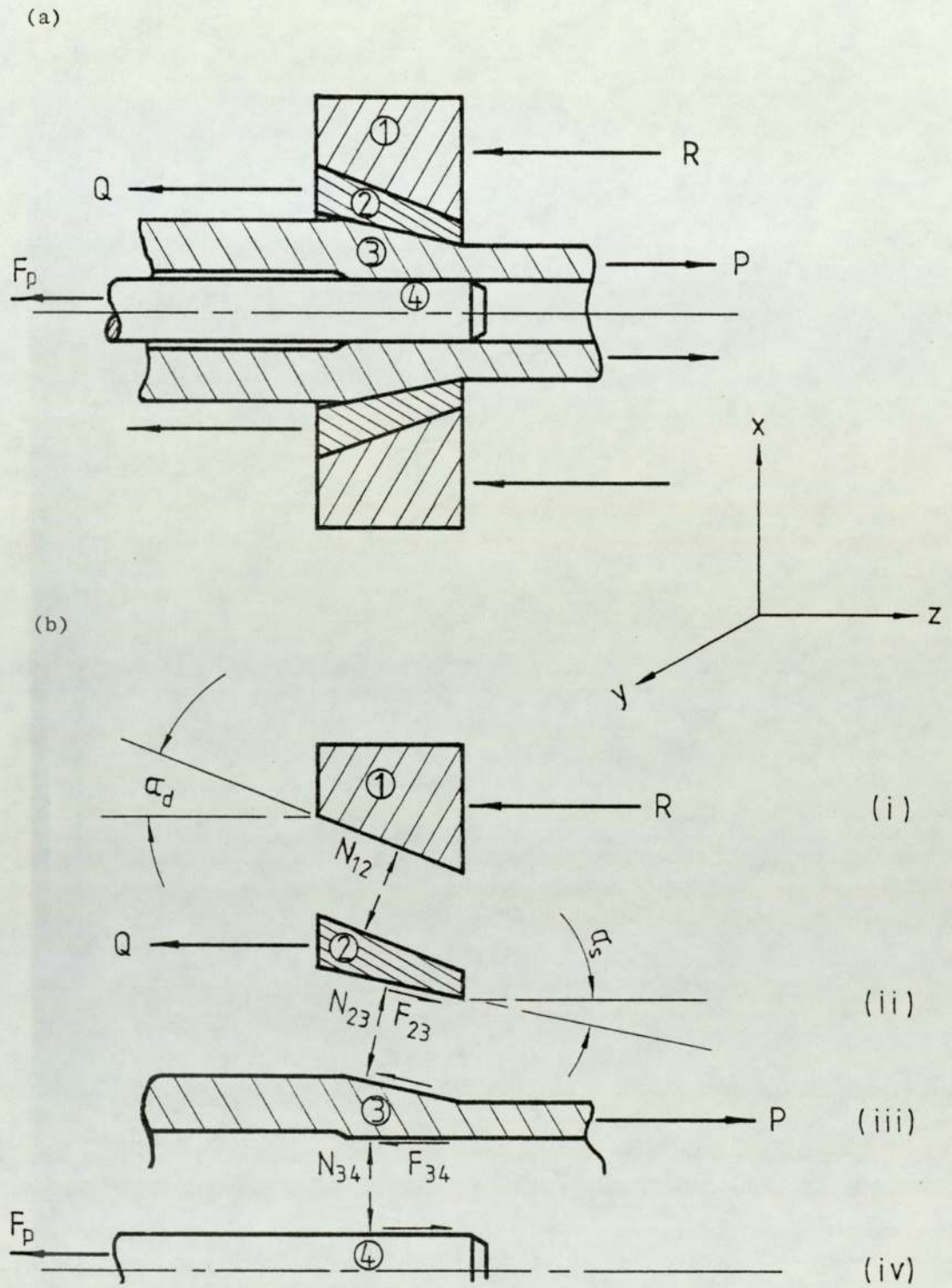


Fig. 4.2 The general principles of the split rotating die for the direct determination of the mean coefficient of friction.

$$\sum F_x = 0,$$

$$N_{34} - N_{23} \cos\alpha_s + F_{23} \sin\alpha_s = 0$$

or:

$$N_{34} - N_{23} \cos\alpha_s + \mu_{23} N_{23} \sin\alpha_s = 0$$

$$\therefore N_{34} - (\cos\alpha_s - \mu_{23} \sin\alpha_s) N_{23} = 0 \quad (4.13)$$

(ii) DIE TIPS

$$\sum F_z = 0$$

$$-Q + F_{23} \cos\alpha_s + N_{23} \sin\alpha_s - N_{12} \sin\alpha_d = 0$$

or:

$$-Q + (\mu_{23} \cos\alpha_s + \sin\alpha_s) N_{23} - N_{12} \sin\alpha_d = 0 \quad (4.14)$$

$$\sum F_y = 0,$$

$$N_{23} (\cos\alpha_s - \mu_{23} \sin\alpha_s) - N_{12} \cos\alpha_d = 0 \quad (4.15)$$

From figure 4.2(a), the equilibrium of forces in the horizontal direction gives:

$$P - Q - R - F_p = 0 \quad (4.16)$$

Equations (4.11), (4.12), (4.13), (4.14) and (4.15) were solved simultaneously to yield:

$$\begin{aligned} & \frac{P}{Q} (\mu_{23} \cos\alpha_s + \sin\alpha_s - \tan\alpha_d (\cos\alpha_s - \mu_{23} \sin\alpha_s)) \\ &= \mu_{34} (\cos\alpha_s - \mu_{23} \sin\alpha_s) - (\mu_{23} \cos\alpha_s + \sin\alpha_s) \end{aligned} \quad (4.17)$$

Assuming  $\mu_{12} = \mu_{23} = \mu_{34} = \mu$ , equation (4.17) reduces to:

$$\mu^2 + \frac{P}{Q} \left( \frac{1}{\tan\alpha_s} + \tan\alpha_d \right) \mu + \frac{P}{Q} \left( 1 - \frac{\tan\alpha_d}{\tan\alpha_s} \right) + 1 = 0 \quad (4.18)$$

The solution of the quadratic equation yields

$$\mu = \frac{-b \pm \sqrt{b^2 - 4ac}}{2a} \quad (4.19)$$

where:  $a = 1$

$$b = \frac{P}{Q} \left( \frac{1}{\tan \alpha_s} + \tan \alpha_d \right) \quad (4.20)$$

$$c = \frac{P}{Q} \left( 1 - \frac{\tan \alpha_d}{\tan \alpha_s} \right)$$

$$\text{and } \frac{P}{Q} = 1 + \frac{R}{Q} + \frac{F}{Q} \quad (4.21)$$

The mean pressure:

$$\begin{aligned} p_m &= \frac{N_3}{A_s} \\ &= \frac{P}{(1-\mu^2) \sin \alpha_s} \cdot \frac{1}{A_s} \end{aligned} \quad (4.22)$$

where:  $A_s$  = tube-die tips contact area

$$= N_s \cdot \frac{R_b^2}{4} \cdot \frac{1}{\sin \alpha_s} \left\{ -\sin 2\theta_1 + 2 \left( \frac{\pi}{2} - \theta_1 \right) \right\} \quad (4.23)$$

$$\text{for } \theta_1 = \sin^{-1} \left\{ 1 - \left( \frac{L}{R_b} \right) \tan \alpha_s \right\} \quad (4.24)$$

Using figures 4.2b(i), the applied torque ( $T_a$ ) is given by:

$$\begin{aligned} T_a &= \bar{r} \cdot \mu N_{12} \\ &= \bar{r} \mu \frac{P}{\cos \alpha_d} \left\{ \frac{1}{1 - \frac{\mu + \tan \alpha_s}{1 - \mu \tan \alpha_d}} \right\} \end{aligned} \quad (4.25)$$

where  $\bar{r}$  is the mean radius of the conical die.

The specifications of the split rotating dies used in the investigations are:

(a) for the square die tips

$$\begin{aligned}\alpha_d &= 8.1^\circ \\ \alpha_s &= 5.7^\circ \\ \bar{r} &= 0.755 \text{ in}\end{aligned}\tag{4.26}$$

(b) for the hexagonal die tips

$$\begin{aligned}\alpha_d &= 8.1^\circ \\ \alpha_s &= 6.7^\circ \\ \bar{r} &= 0.755 \text{ in}\end{aligned}\tag{4.27}$$

#### 4.3. DIES FOR DRAWING POLYGONAL TUBES FROM ROUND STOCK ON A CYLINDRICAL PLUG

In order to establish the effectiveness of the theoretical work, dies for the drawing of polygonal tube directly from round stock on a cylindrical plug were designed. It was shown in the bar drawing work (2), when a circular workpiece transformed to a polygonal section in a single pass, that the factor having the greatest effect on the draw forces was the shape of the deformation zone. The solid bar represents the limiting condition of a tube, the relative wall thickness being  $t_b/D_b = 0.5$ . Thus it asserts that in the process of tube drawing where a circular cross-section deforms through a single die to a polygonal tube with the bore remaining unchanged, the factor having the greatest influence on the die design is the geometry of the deforming zone. Another factor that minimises the draw force for the combination of the drawing lubricant and the reduction of area achieved, is the optimum die angle.

However, for the direct drawing die the conventional term semi-cone angle is inapplicable, since the actual die semi-angle changes from a minimum at the diagonals of the die to a maximum at the mid sides of the section. Additionally, the semi-angles are dependent on the shape of the die deforming passage. The term equivalent semi-angle, ' $\alpha_e$ ' has been defined as the semi-angle of a conical die for the axisymmetric tube drawing which produces the same reduction of area as the polygonal tube drawing die, the die lengths being equal and the bore remaining unchanged in both cases. This definition facilitates the comparison of the polygonal tube drawing with the same number of sides and of different number of sides as well. Since close pass drawing is assumed, the definition applies to the drawing of solid sections from round too. Details of the equivalent die semi-angle are discussed in Appendix A-10.

#### 4.3.1 Deforming shapes of the polygonal tube drawing die

The transformation of a circular tube at the entry plane of the die to a polygonal tube at the exit on a cylindrical plug, can take various forms during its progress through the deformation passage. The four basic shapes, illustrated in figure 4.1, take into account the method of manufacture, industrial interest and the applicability of the theoretical analyses to the die geometry.

##### 4.3.1.1 Pyramidal plane shape die (Shape A)

The shape of the deformation zone of this die, which is comparable with section to section <sup>drawing</sup> used in industry and shown in figure 4.1(a), is generated from the number of planes which is equal to the number of sides of the polygonal tube. These planes form a truncated pyramid having sides inclined equally to the tube axis. The angle of the inclination of each plane to

the tube axis depends on the outer diameter of the tube for a given die length and the equivalent semi-angle ' $\alpha_e$ '.

#### 4.3.1.2 Elliptical plane surface die (Shape B)

The shape of the deforming zone of this die, Fig. 4.1(b) is generated from a number of inclined planes which is equal to the number of sides of the polygonal tube required. Each of these planes cut the cone in an ellipse. In this way the deformation zone will be formed from the elliptical planes and the remaining portions of the main cone surface. The inclination of each plane to the tube axis depends on the die length for the given tube outer diameter and the equivalent semi-angle.

#### 4.3.1.3 Triangular plane surface die (Shape C)

The shape of the deforming zone, Fig. 4.1(c), is generated by combining  $N_s$  number of asymmetric cones around the tube axis. The apex of each cone is placed at the corner of the polygonal tube required in such a way that the cones have a common base approximating to a circle in the plane normal to the tube axis. (The diameter of the approximate circles corresponds to that of the incoming tube.) The remaining gap between successive cones will take the shape of triangular plane. The angle of inclination of these planes and the geometrical parameters of the cones depend on the die length for a given tube outer diameter and the equivalent semi-angle.

#### 4.3.1.4 Inverted parabolic plane surface die (Shape D)

The shape of the deforming zone, Fig. 4.1(d), is generated from the axial intersection of a conical surface with a prism which forms the required polygon. Each plane surface of the polygonal tube intersects the main cone in a parabola. The main cone angle depends on the die length for a given tube outer diameter and the equivalent

semi-angle.

#### 4.3.2 Dies used in the polygonal tube drawing experiments

##### 4.3.2.1 Introduction

The die deforming shapes A and D, illustrated in figure 4.1, allow different inlet diameters to be drawn while maintaining their deforming pattern but with increasing inlet diameters the equivalent die semi-angle will increase. The deforming die passages B and C are fixed for a given outside diameter tubing. So, if a larger outside diameter tube is drawn through the die, i.e. larger than that for which the die was designed, a new combined mode of deformation occurs.

The dies with the four basic shapes were used in the preliminary drawing tests to establish the optimum profile. This set of dies originally was designed for polygonal bar drawing from round stock (2) and is summarized in Table A-11 on page A113.

The die passages B and C are designed to provide a gradual transition in shape from the round section at the die entry to the final shape of the polygon at the exit. In addition to exhibiting a relatively lower drawing force, the resulting drawn tube had sharper corners compared with the shapes A and D.

The optimal deforming profile, the elliptical shape B, was selected for the new set of dies in the investigation of the polygonal tube drawing from round on a cylindrical plug. From the established theory, an optimal equivalent die semi-angle of  $8^{\circ}$  was arrived at for the range of tubing available for the experiments. The shapes of section tubes investigated were the square, the hexagon, the octagon and the decagon. The design parameters and the mechanical drawings of these dies are given in Appendix A-10.

#### 4.3.2.2. Die manufacture

Tungsten carbide is an excellent die material because of its resistance to wear, its ability to maintain a high polish and its reluctance to pick-up; it also reduces the variation in friction to a minimum for most workpiece metals. Normally, in the laboratory by comparison with the industry, relatively few tubes are drawn for experimental purposes and therefore, the use of tungsten carbide is rarely warranted. Tool steel (ARNE) is readily available, is less expensive, and it is cheaper to machine to the different die shapes compared with tungsten carbide.

A die insert of alloy steel was shrink fitted into a bolster of EN24. The three dies (mechanical drawings shown in Appendix A-10.2) were manufactured by Aston Services Ltd.

#### 4.4. MATERIAL OF ROUND STOCK USED IN THE TESTS

##### 4.4.1 Selection of the tubing

Mild steel was selected as the appropriate material for the tubes. The choice is in line with the previous research on the mechanics of drawing polygonal bars from round and the drawing of polygonal tube from round on the corresponding polygonal plug. Therefore, for comparisons to be drawn, mild steel was again selected as the experimental metal.

Mild steel has excellent workability, a relatively low work hardening rate and is widely used since it is relatively inexpensive. Another factor is that if expensive low strength non-ferrous material had been selected, large diameter tube would have been necessary to operate the drawbench under reasonable loads. High strength non-ferrous material has the drawback of not being able to withstand large strains, i.e. large reductions of area.

The constituent elements of the mild steel for the tubing are given in Appendix A-3.1.

In selecting the sizes of the tubes for the experimental investigations, the geometrical dimensions of the outgoing stock were fixed. The major diagonal of the polygonal tube  $H_a$ , was fixed at 1 inch and close pass drawing was used in the calculations. Using the geometrical relations of the cross-sections at the entry and the exit to the die given in Appendix A-1, the reduction of area can be expressed thus:

$$r = 1 - \frac{1/(t_b/H_a)^2 \left\{ \text{SPARAM} - \frac{\pi}{2} (1-2\kappa)^2 \right\}}{\pi \left\{ 1/(t_b/D_b) - 1 \right\}} \quad (4.28)$$

SPARAM is the geometrical factor for the outgoing polygonal section,

$$N_s \cos\beta \cdot \sin\beta / 4$$

$H_a$  is the diagonal length of the polygon and

$\kappa$  is a factor expressing the maximum wall thickness in terms of the diagonal length.

A range of tubes in commercial catalogues was selected and a table of the gauge ( $t_b$ ) against the outside diameter ( $D_b$ ) was drawn for each polygonal section showing the reduction of area. Other information readily available was the cross-section area of the tube, the internal diameter, the thickness of the wall along the diagonal of the drawn section, and the ratio of the gauge to the outside diameter ( $t_b/D_b$ ). See Appendix A-2.

To minimise the number of tube sizes in the tests, graphs of the number of sides of the polygon ( $N_s$ ) versus the reduction of area were drawn. A family of  $t_b/D_b$  curves for a fixed outside diameter of 1 in, 1 1/16 in, 1 1/8 in, 1 3/16 in and 1 1/4 in are shown in Appendix (p. A8) A-2. The tensile yield stress eventually limits the reduction of area

per pass. In practice it is not usual to draw tubes with over 50% reduction of area. Therefore, this criterion was used to reduce the number of tube sizes required. It was noted that in order to draw square sections at a reasonably low reduction of area, thick walled tubing would be required. However, for economic reasons, only those sizes readily in stock were used in the experiments (Table A-3.1 on page A10). Consequently, to obtain feasible reductions of area for some sections, for example the square and the hexagon, some amount of sink was anticipated.

One batch of tubes for the preliminary tests was obtained from 'Lebas Tube Ltd'. The seamless tubes specifically ordered for drawing experiments were cold drawn, pickled and limed before delivery. The tubes were cut into lengths of  $4\frac{1}{2}$  feet and labelled.

The second batch of tubes, mainly from 'British and General Tube Co.Ltd.' was delivered as drawn, cut into short lengths of  $2\frac{1}{2}$  to 3 ft, labelled and separate arrangements made for annealing and swaging.

One set of tubes for the drawing of square sections was swaged to a 0.69 in diameter for a length of 8 in; the other batch used for the drawing of hexagonal, octagonal, decagonal and round sections were push-pointed to a 0.85 in diameter for a length of 8 in. The swaging of the thin walled tubes was carried out on the Denison testing machine; a die specially designed for this purpose is shown on page A167.

#### 4.4.2 The stress-strain relationship of the tube material

The power law  $\sigma = \sigma_0 \epsilon^n$ , expressing the true stress-strain relation of the tubular material (79, 80) can be re-written:

$$\ln(\sigma) = \ln(\sigma_0) + n \ln(\epsilon) \quad (4.29)$$

From the tension tests, if the graph of  $\ln(\sigma)$  vs  $\ln(\epsilon)$  is plotted and the initial 5% plastic strain disregarded as non-representative, a reasonably straight line is obtained. The slope of the line gives the strain hardening exponent 'n' which is numerically equal to the plastic instability strain; the value of ' $\sigma_0$ ' is obtained by extrapolating the same line to intersect the stress axis at unit strain.

The uniaxial stress-strain tests were carried out on full sections of the tube. The tubular specimens, plugged at the ends, were gripped between the jaws of the Denison testing machine. The Baldwin extensometer was used together with the Denison chart servomechanism for the plotting of a load-elongation diagram. The true stress-strain curve of the mild steel for the tubing, reproduced from equation (4.29), is shown in figure 4.3. These curves are extrapolated from strain values of 0.1.

#### 4.5 Plugs

Close pass occurs when there is no sink on to the plug. Thus the plug must fit the bore prior to drawing. However, in practice it is difficult to obtain a close fit between the tube and the plug. A reduction in the outer diameter following sinking will produce a condition of close pass in the deforming zone of the tool.

From the table of selected tubes, a set of nine plugs was designed for the nominal diameters of 3/4 in, 11/16 in, 5/8 in, 9/16 in, 1/2 in, 7/16 in, 3/8 in, 5/16 in and 1/4 in. The nominal

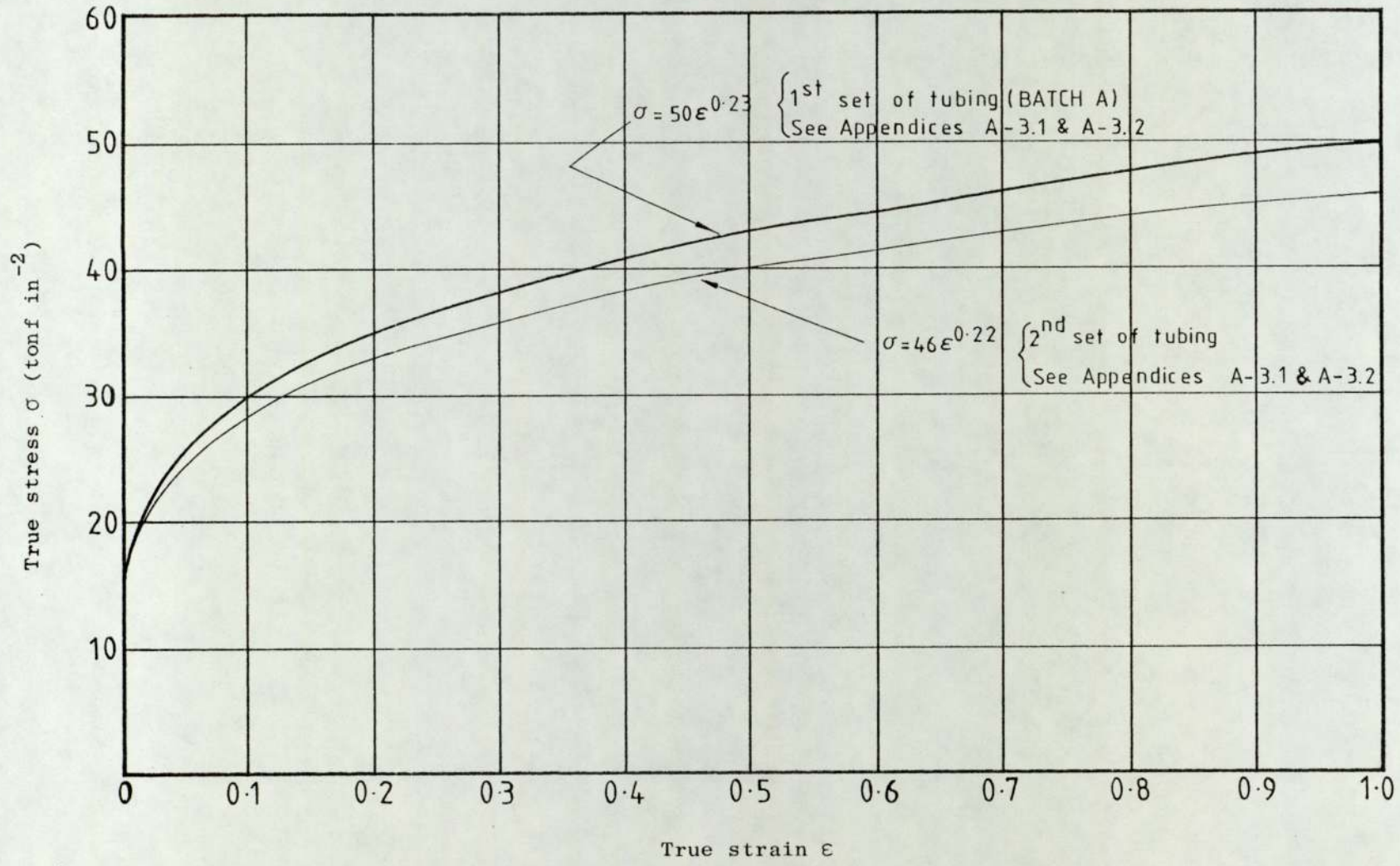


Fig. 4.3 The true stress-strain diagram for the mild steel of the tubes

diameters were ground to a 0.005 in to 0.010 in clearance.

As a first attempt, plugs of nominal diameters 1/2 in, 9/16 in, 5/8 in, 11/16 in, and 3/4 in were manufactured from Sverker 3. This is a high carbon chromium alloy tool steel with tungsten, recommended for applications demanding maximum wear resistance, and hence little variation of the coefficient of friction. The plugs were heat treated to 64 RC, ground and lapped in the Departmental workshop. The lengths of the plugs were such that their positions in the die could be adjusted to protrude by 1/8 in at the exit plane and not less than 1/8 in at the entry for the range of tube sizes under investigation. The 1/2 in diameter plug was made exceptionally longer to satisfy the above conditions when drawing with the split rotating die. A silver steel sleeve was soldered onto the end of a 3/8 in diameter high speed steel rod to hold the plugs. The plugs with 3/8 in clearance bore slid through the bar from the opposite end. The plug backstop and the plugs are shown in Appendix A-17, page A168. This plug bar arrangement failed to draw the higher reductions of area; the plug force was higher than expected and at the loads the plug bar material, high speed steel is notch sensitive.

As a result of this experience, all the plugs were manufactured integral with the bars and were ground to size (see Appendix A-17, page A169). The plug ends were heat treated to the appropriate hardness to resist wear and attain high compressive strength. The special plug backstop designed to withstand about 5 tonf, facilitated the adjustment of the plug position in the die.

#### 4.6 LUBRICANTS

The lubricant to be used in tube drawing is expected to meet favourably the following conditions:

- must generally separate the surfaces;
- must provide low coefficient of friction;
- must generally be non-corrosive and non-toxic;
- must not breakdown at the stress and the localised temperatures;
- must generally be readily removed; and
- must not be abrasive.

The drawing oil TD50, which is widely used in industry in arduous conditions had been used successfully in the investigations of drawing polygonal sections from round bar, and has therefore been adopted for <sup>this</sup> tube drawing. The effectiveness of soap and oil 717 as <sub>^</sub>lubricants in the drawing of polygonal sections directly from round stock had been extensively reported (2).

CHAPTER 5

INSTRUMENTATION

## 5.1 INTRODUCTION

The following quantities were measured on the "Brookes" bench:

- (i) the draw force
- (ii) the plug force
- (iii) the draw speed
- (iv) the axial thrust on the rotating conical die
- (v) the drag force on the die inserts and
- (vi) the rotational speed of the conical die.

The following quantities were to have<sup>been</sup> measured on the "Sheffield" drawbench<sup>†</sup>:

- (i) the draw force
- (ii) the plug force
- (iii) the draw speed and
- (vi) the axial thrust on the die.

Some of the above quantities were not directly involved in the calculations of the results for the direct drawing of polygonal tubes from round stock. However, to be able to compare results, it was important to keep these quantities fixed throughout the experiments. For example, in the split rotating die experiment, the rotational speed of the conical die had no direct effect on the balance of forces in the axial direction, but the frictional force changed at different speeds;

### <sup>†</sup> Footnote

The load and draw speed transducers on the two benches were similar; however, the instruments on the "Sheffield" rig were not calibrated and the entire experimental work was performed on the operating 'Brookes' Drawbench (see Appendix A-16).

the generated heat affected the viscosity of the lubricant. Therefore, by keeping the record of the rotational speed the general effect could be estimated.

Although it was envisaged that the measurement of the different drawing parameters would be made essentially under steady conditions, the data recording was continuous. An ultra-violet beam recorder with d.c. transducers was used, and continuously screened cables avoided the cross-coupling effect. The ten-turn wirewound resistors with good temperature stability provided smooth variation and ensured accurate control of the null balance.

The bridge circuit of each transducer consisted of a set of metal foil strain gauges from the same batch. However, owing to the built-in inequality on resistance or the tolerance, a trimming resistance was generally essential for the initial bridge balance.

A high degree of repeatability and accuracy is required in measuring drawing parameters in order that a reliable comparison of experimental and theoretical solutions can be made. The testing machines used in the calibration of the load transducers had been maintained according to B.S. 1610: 1964 ('load verification of testing machines') and B.S. 5781: 1979 ('specification for measurement and calibration systems').

The load cell at the tag holder and the cup load cell of the split rotating die rig had foil gauges for the measurement of torques in addition to the axial loads. However, calibration of the torque transducer was not carried out in each case.

The calibration curves of the load transducers are given in Appendix A-7.

## 5.2 THE FORCE/TORQUE TRANSDUCER AT THE TAG HOLDER

The combined load cell of the rod type installed on the bench measured the draw force and the rotational torque on the tag when determining the mean coefficient of friction using the split rotating die rig. The bridge circuit for the transducer is given in Figure 5.1.

Calibration of the load cell under the direct tensile load was done on a 50 tonf range of the "Denison" testing hydraulic machine. Special adaptors, shown on pages A161, A162 and A163, were required. Readings were taken for both the increasing and decreasing load. The calibration curve is shown in Figure A-7.1.

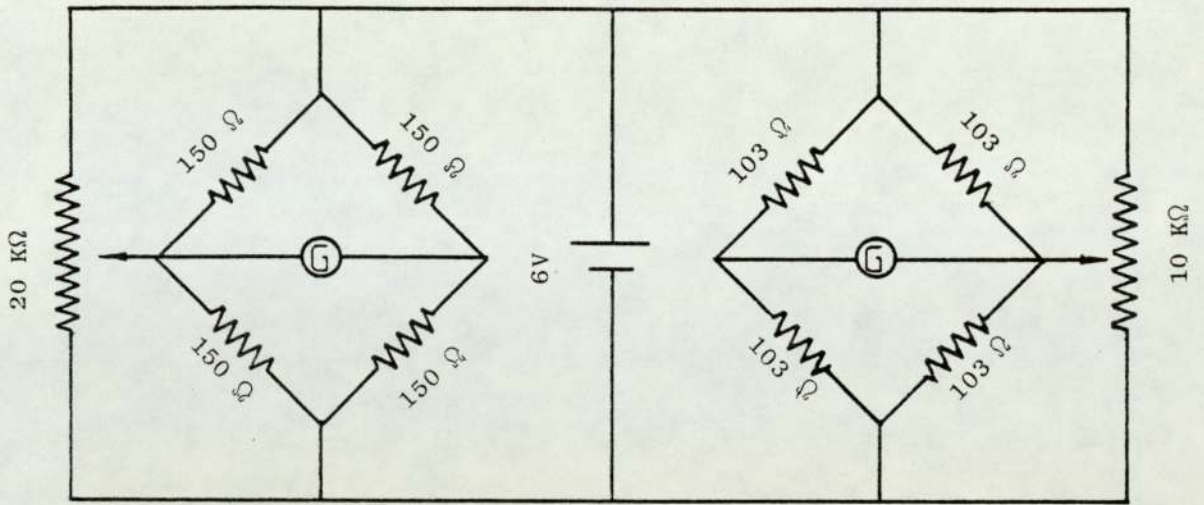
## 5.3 THE PLUG FORCE TRANSDUCER

The bridge circuit for the transducer is shown in Figure 5.2. The output signal of the torque bridge passed through a 'SGA 300 KAP' amplifier. This type of amplifier with zero setting device provided a bridge supply voltage which was virtually independent of the source. In addition the device had potentiometers for zero, span and bridge supply voltage adjustments.

The load transducer was calibrated under the compressive force on the "Denison" hydraulic testing machine for both an increasing and a decreasing load. The calibration curve is given in Figure A-7.2.

## 5.4 THE AXIAL FORCE TRANSDUCER - THE RING TYPE

The die load cell, described in Section A-16.3.2.1.3 and the load cell for the measurement of the axial thrust on the conical die of the split rotating die rig (described in Appendix A-12), were formed from a continuous ring which strained in terms of bending and torsion when subjected to an axial thrust.



torque bridge

force bridge

Fig. 5.1 Circuit diagram of the tag load transducers.

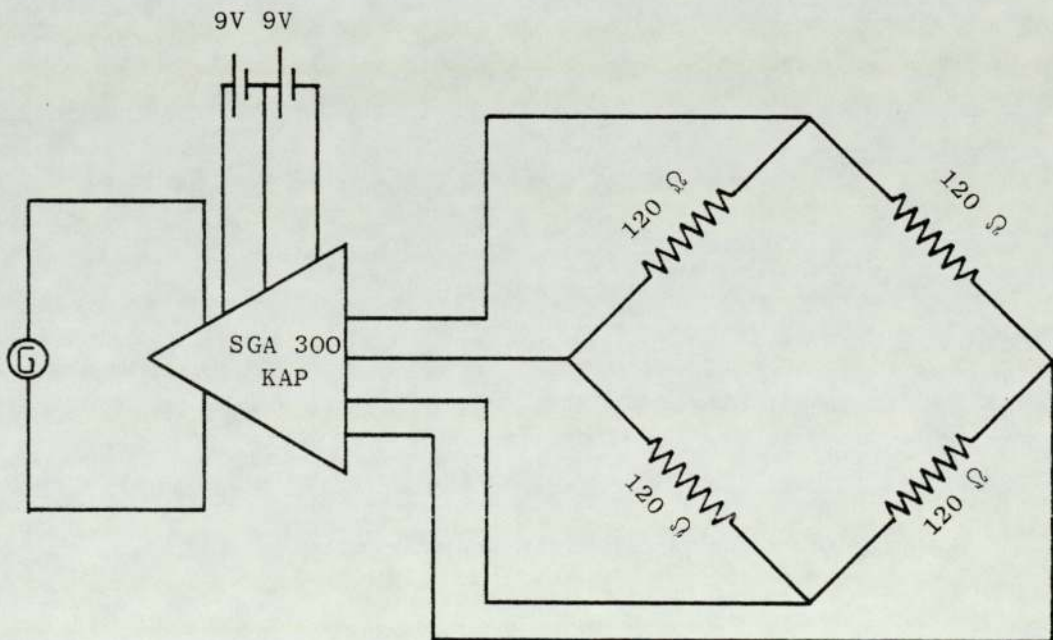


Fig. 5.2 Circuit diagram of the plug load transducer.

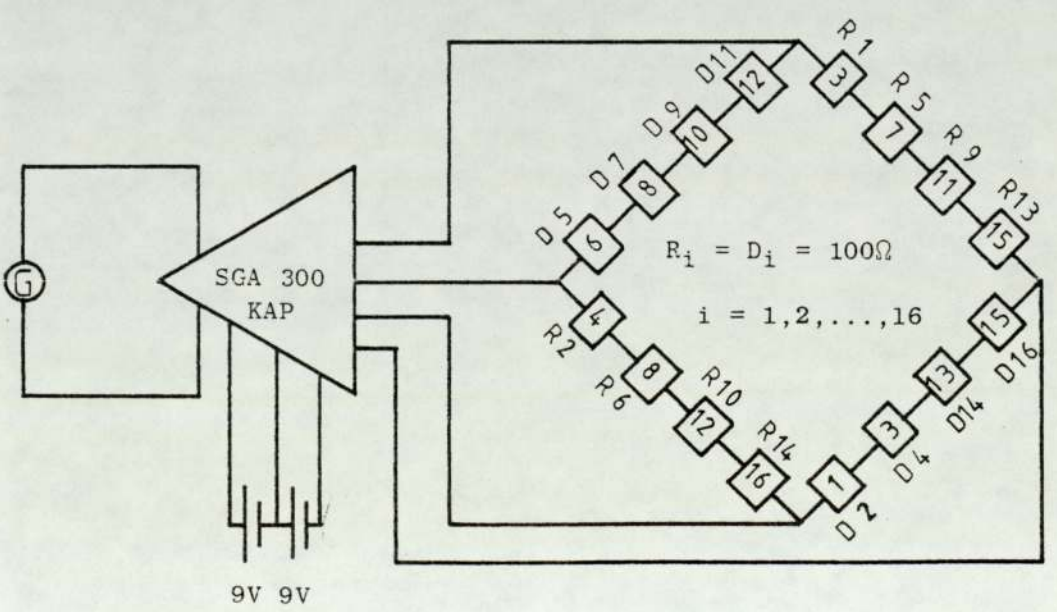
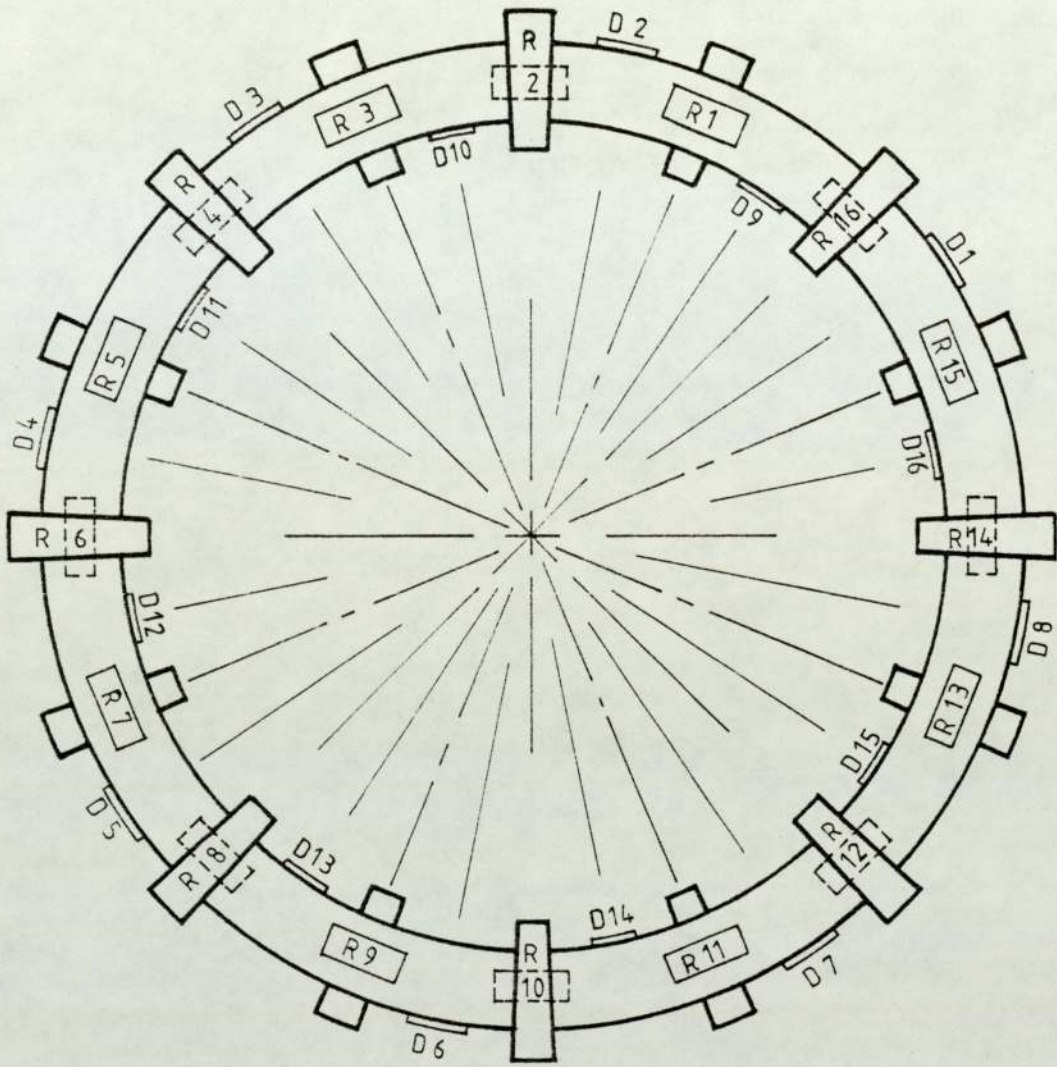


Fig. 5.3 Strain gauge arrangement and the circuit diagrams of the ring load cell in the split rotating die rig.

The bending stress and the strain distribution were derived in Ref (2).

The active strain gauges were bonded in positions of maximum bending moment derived from the stress analysis. Dummy gauges were bonded also on both the outside and the inside surfaces of the ring in positions of zero bending moment. The dummy gauges compensated for both the temperature and the residual bending strains. The arrangement of the gauges as shown in Figure 5.3, compensated for the offset loading.

The load cell was calibrated under the direct compressive force on the "Denison" testing machine. Readings were taken for both an increasing and a decreasing load. The calibration curve for the transducer is given in Figure A-7.3.

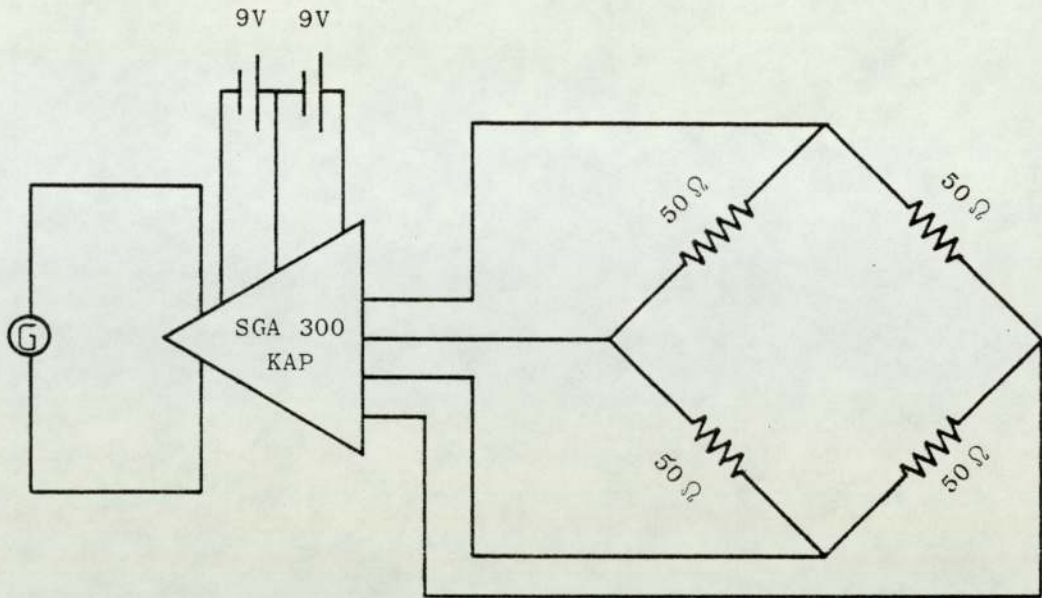
#### 5.5 THE CUP LOAD CELL - THE FORCE/TORQUE TRANSDUCER

The cup load cell of the split rotating die rig was designed to measure the drag force on the die inserts and the rotational torque (see Appendix A-12). The bridge circuits for this combined force/torque transducer are shown in Figure 5.4.

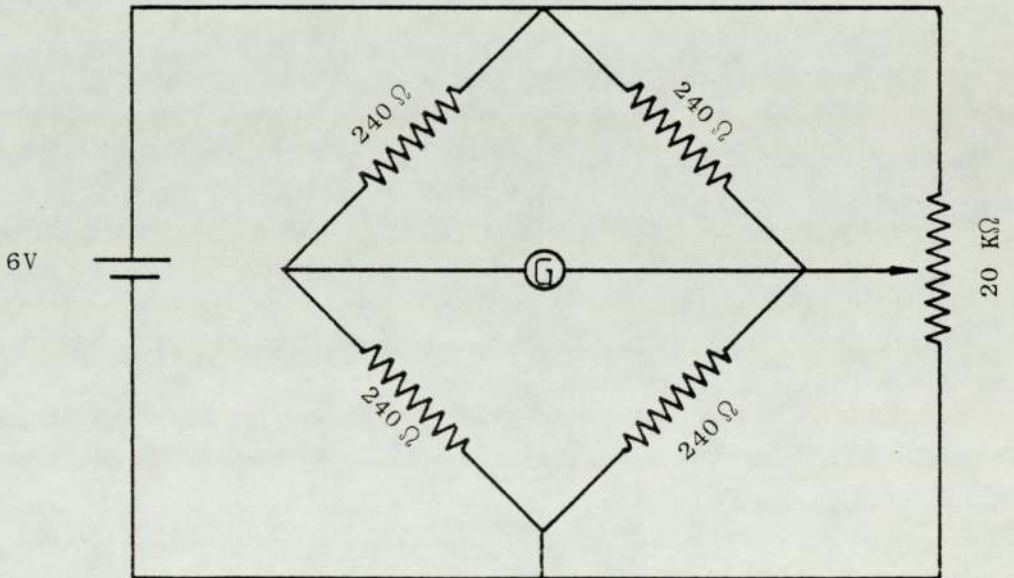
The calibration of the axial force bridge was carried out under the compressive load on the "Denison" testing machine.

#### 5.6 DRAW SPEED MEASUREMENT

The control valve on the "Brookes" drawbench was calibrated coarsely and for a more accurate speed check, a manual speed calibration was found to be adequate, since the draw load is not critically dependent on the draw speed. Two marks were made on the drawbench at a known distance apart. The time taken to travel this



(a) Torque bridge



(b) Axial force bridge

Fig. 5.4 Circuit diagram of the cup load cell of split rotating die rig.

distance was measured using a stop-watch. The mean speed was calculated and checked against the dial value on the control valve.

#### 5.7 ROTATIONAL SPEED MEASUREMENT

The speed of the conical die installed in the split rotating die rig was measured through the tachogenerator arrangement shown in Figure 5.5. The drive of the tachogenerator was provided by the output shaft of the variable speed driving unit while the drive for the conical die was provided by the reduction gear unit (see Plate A-12.2).

The calibration of the rotational speed transducer was carried out on the drawbench. The speed of the output shaft of the gear reduction unit was derived using a stop-watch and a circular plate rotating together with the shaft. The dial reading of the variable speed belt drive was noted and the corresponding deflexion of the galvanometer of the tachogenerator circuit was recorded on the U-V chart. A reproducible deflexion-speed curve was obtained as shown in Figure A-7.5.

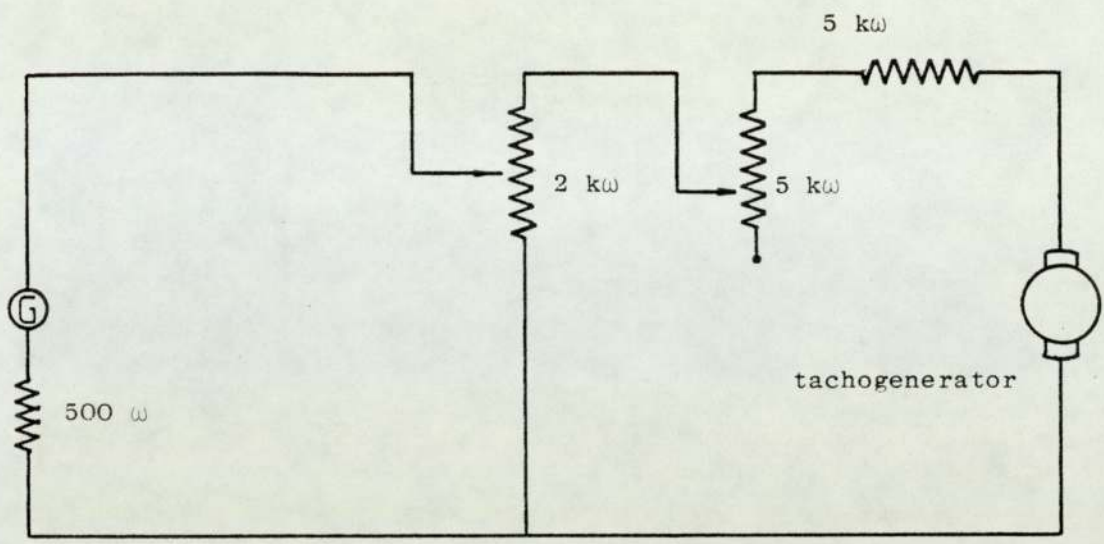


Figure 5.5. Rotational speed transducer

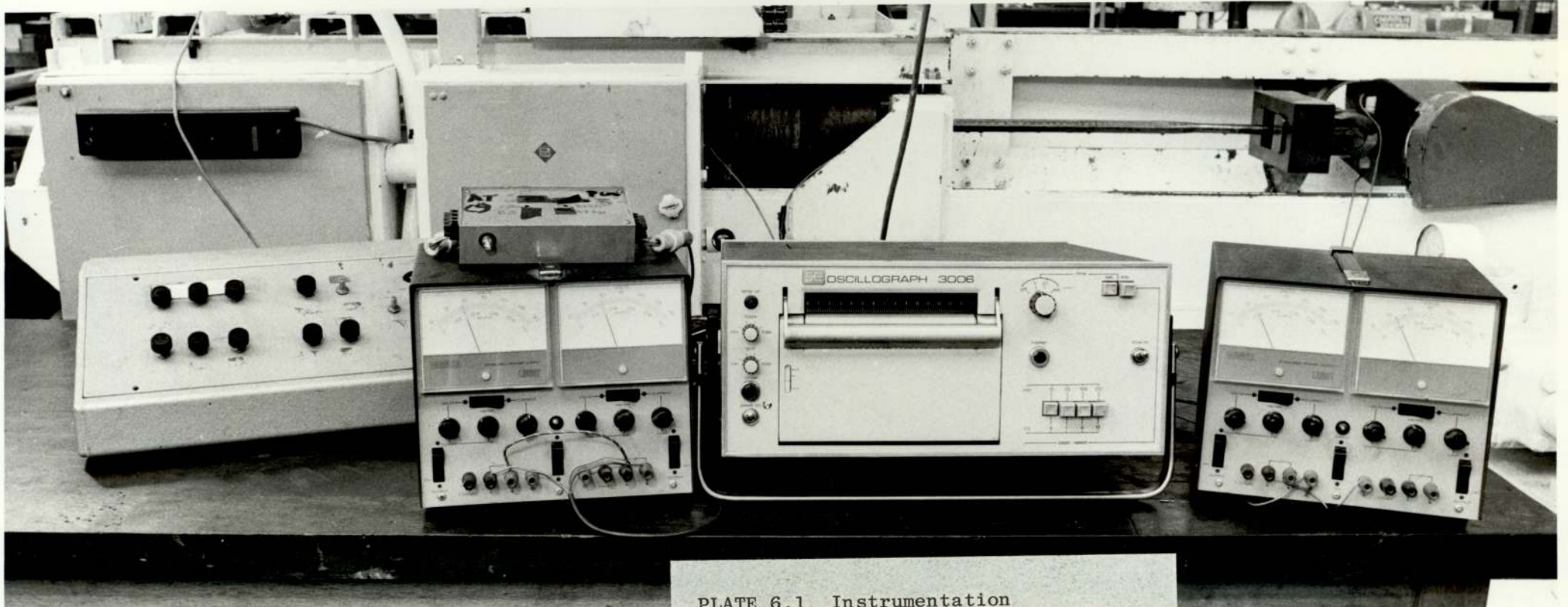


PLATE 6.1 Instrumentation

CHAPTER 6

EXPERIMENTAL PROCEDURE

## 6. EXPERIMENTAL PROCEDURE

Before the start of the experiments the instruments were allowed to warm up for about one hour. The supply voltage was set at the appropriate value of 6.5 or 9.5 volts and checked periodically against a digital voltmeter. The bridge circuits were balanced.

The tubing was examined visually; the external and the internal surfaces were cleaned with 'Inhibisol' to remove the grease and any abrasive particles. The tubular specimen was allowed to dry, inclined at an angle, and some of the lubricant TD 50 poured into the bore. To ensure effective lubrication, the tube was rotated continuously when applying the oil. The outside of the tube was brushed with oil so as to leave an excess coat of the lubricant at the die entry.

The plug bar length was adjusted such that the plug end just protruded by about 1/16 inch beyond the throat when the die was in position. The tagged end of the drawing tube was gripped by the wedge-shaped jaw of the dog assembly before inserting the plug.

The drawn tube was allowed to cool, examined for defects, measured and labelled. The information recorded immediately after each drawing test included the specification of the die, the input stock dimensions, the plug size, the reduction of area, the draw speed, the date and the number of the test, brief notes on the quality of the drawn product in the light of the conditions of the die and the plug, etc. The records proved invaluable later in the project for reference and identification of the product.

The drawn tube was sawn into lengths appropriate for tensile tests to determine the mean flow stress. The tensile tests were carried out on the polygonal tube sections gripped between the jaws of the 'Denison'

hydraulic testing machine. Short lengths of mild steel bars machined to the size of the tube bore plugged the ends of the test specimen.

In some tests, in order to investigate the transition zone from round to the polygonal tube, the drawing was stopped leaving about six inches of the tube undrawn. Most of the drawn tube was sawn off leaving a length of about four inches. The abrasive edge was filed off and the piece cleaned. Before retracting it from the die, the lubricant was applied generously to the drawn tube to reduce the die wear and facilitate extraction. Finally, the plug was knocked out of the tube.

In the measurement of the mean coefficient of friction and the mean die pressure using the split rotating die, the tubing was prepared as described in paragraph 2. The conical die and the die tips were cleaned, dried and lubricated using the same oil as that in the other tests. As in the previous tests, the position of the plug with respect to the die exit plane was adjusted to project by about 1/16 inch.

The tube was drawn for a short length before the rotary drive was switched on while the drawing continued. Different rotor speeds could be set by drawing and stopping at intervals of one foot. Before the end of the undrawn tube was reached, the rotary drive was switched off and the drawing stopped. The die inserts were easily removed from the casing of the rotating rig.

CHAPTER 7

RESULTS

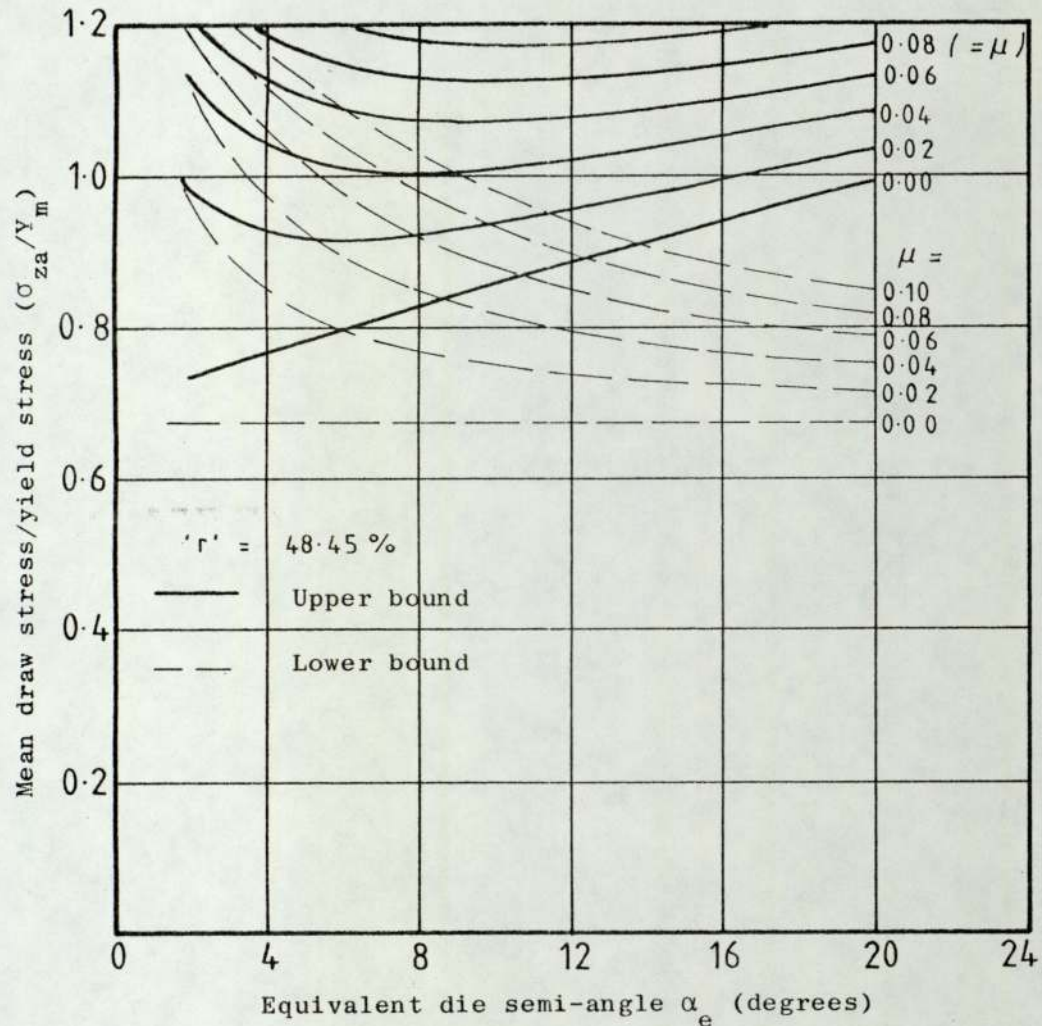


Fig. 7.1 Variation of the mean draw stress with the die semi-angle and coefficient of friction for the upper and lower bound solutions in the drawing of square tube directly from round.

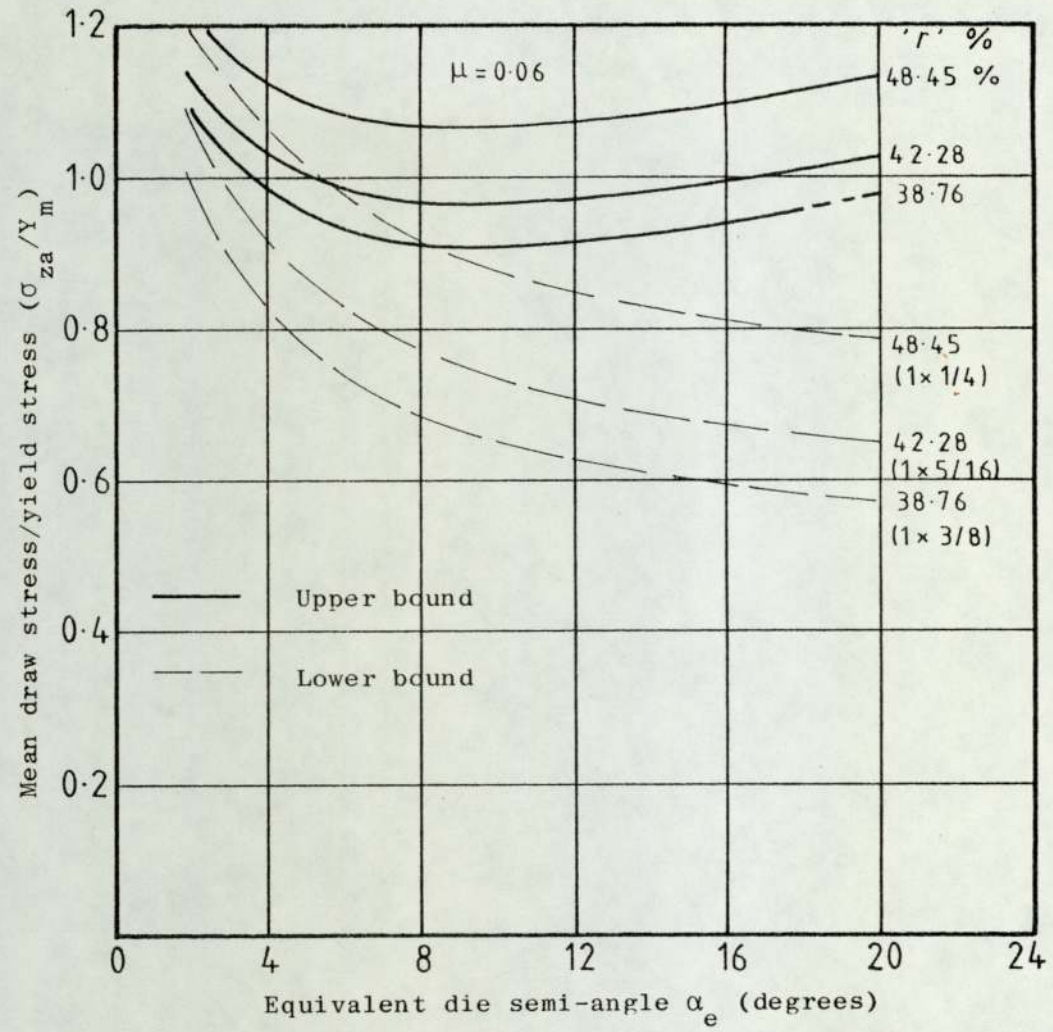


Fig. 7.2 Variation of the mean draw stress with the die semi-angle and the reduction of area for the upper and lower bound solutions in the drawing of square tube directly from round.

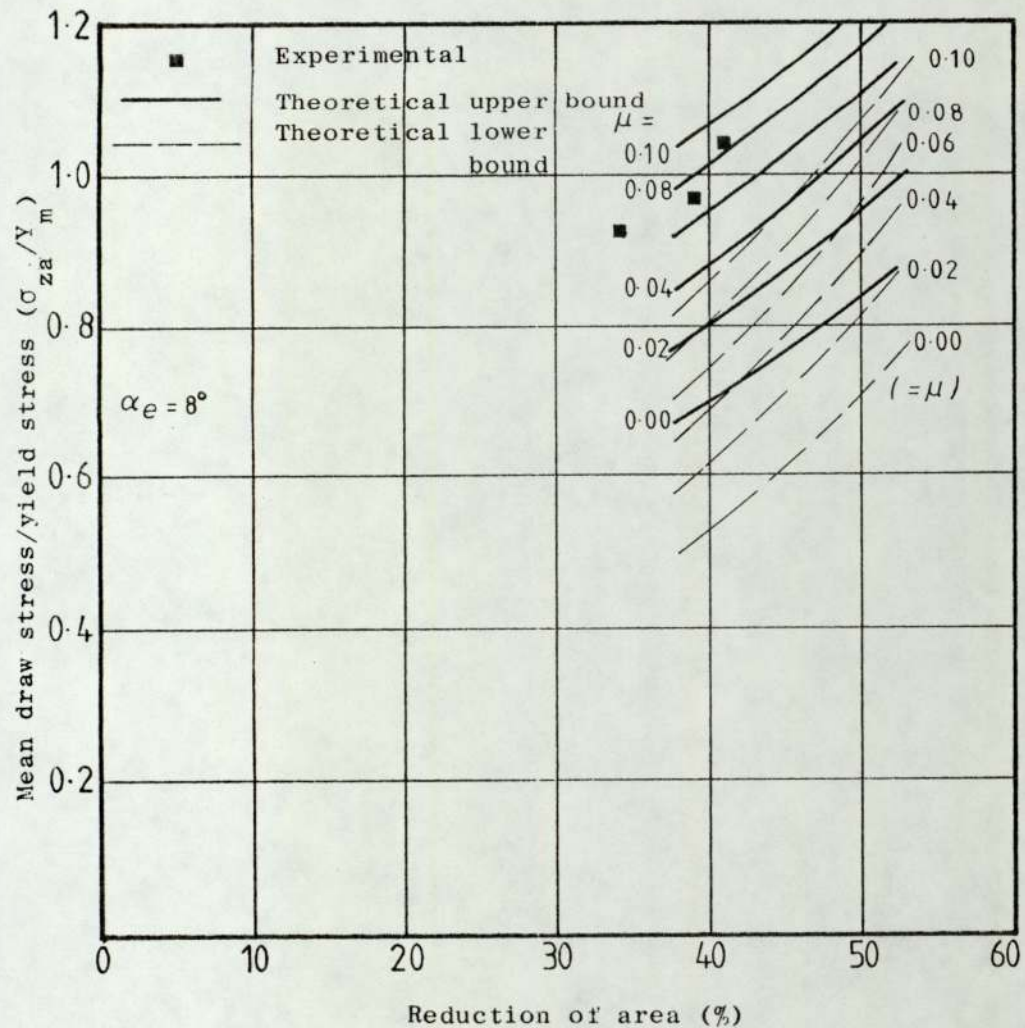


Fig. 7.3 Comparison between the experimental and theoretical draw stress from the upper and lower bound solutions in the drawing of square tube directly from round stock.

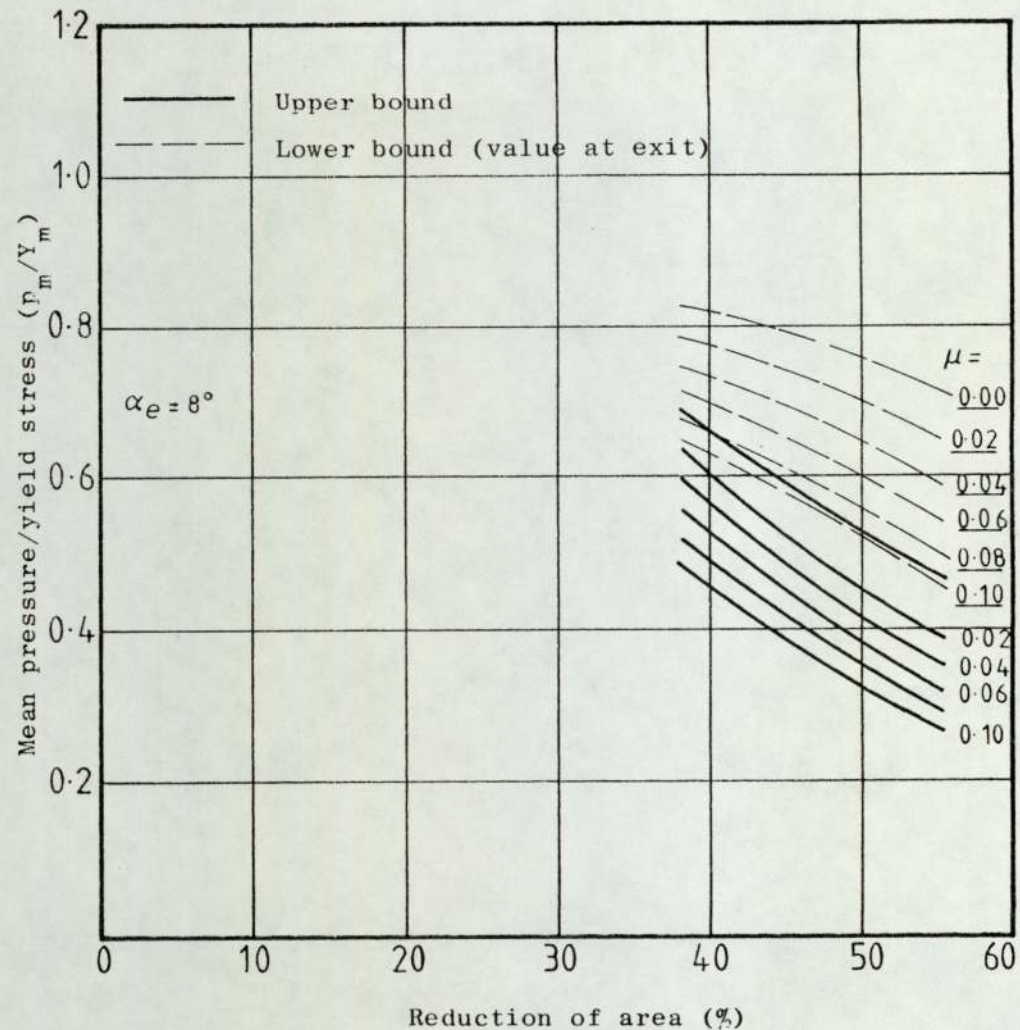


Fig. 7.4 Variation of the mean pressure with reduction of area and coefficient of friction for the upper and lower bound solutions in the drawing of square tube directly from round stock.

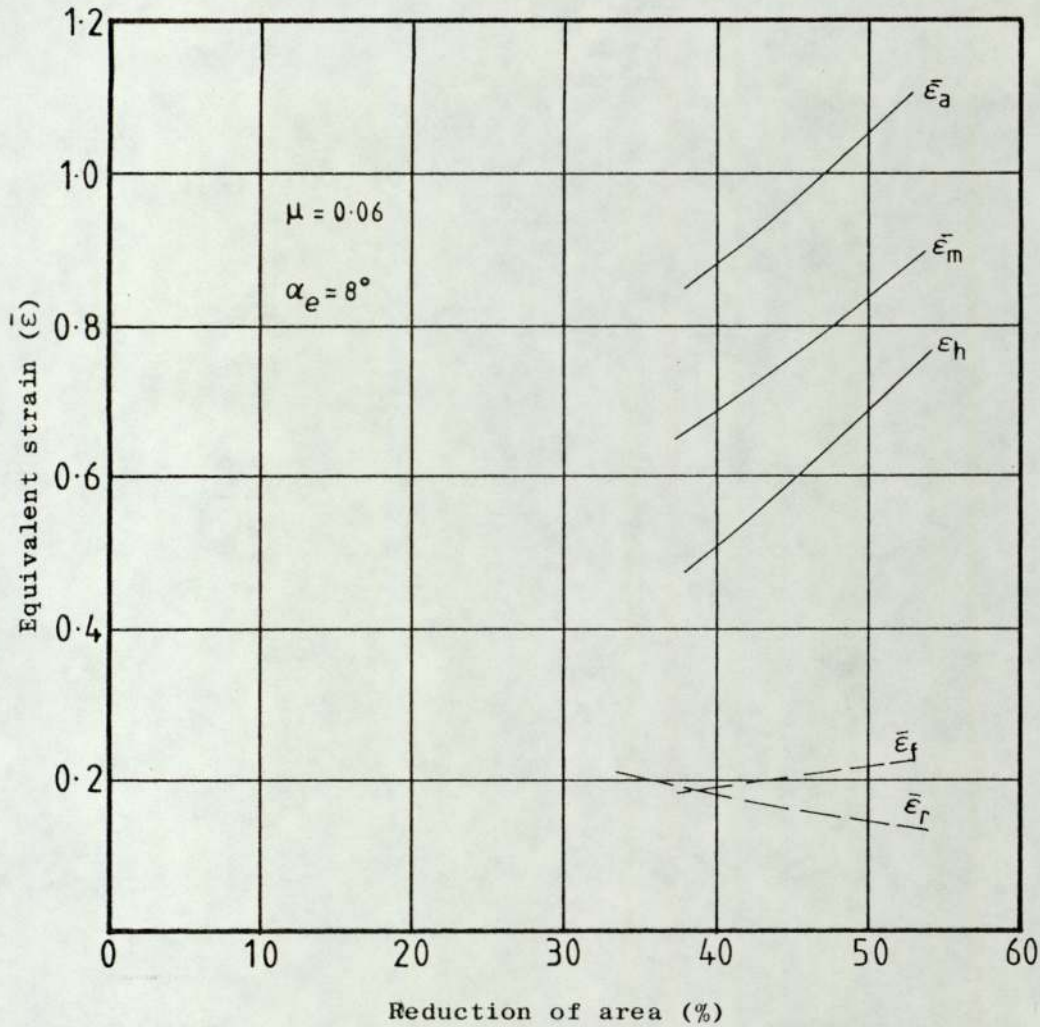


Fig. 7.5 Variation of apparent strain and the equivalent strain components with reduction of area in the drawing of square tube directly from round stock on a cylindrical plug.

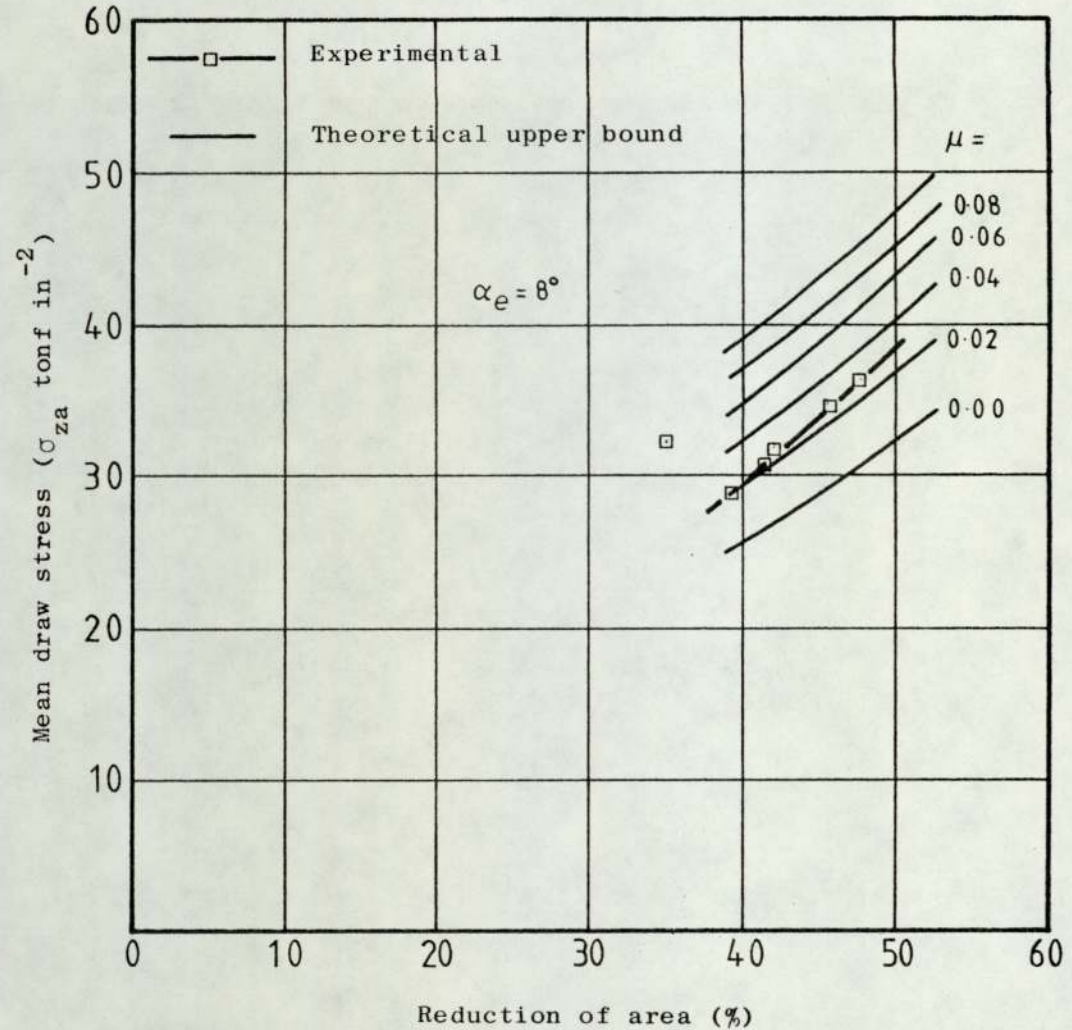


Fig. 7.6 Comparison between the measured draw stress and the values predicted by the upper bound theory for drawing of square tube directly from round stock on a cylindrical plug.

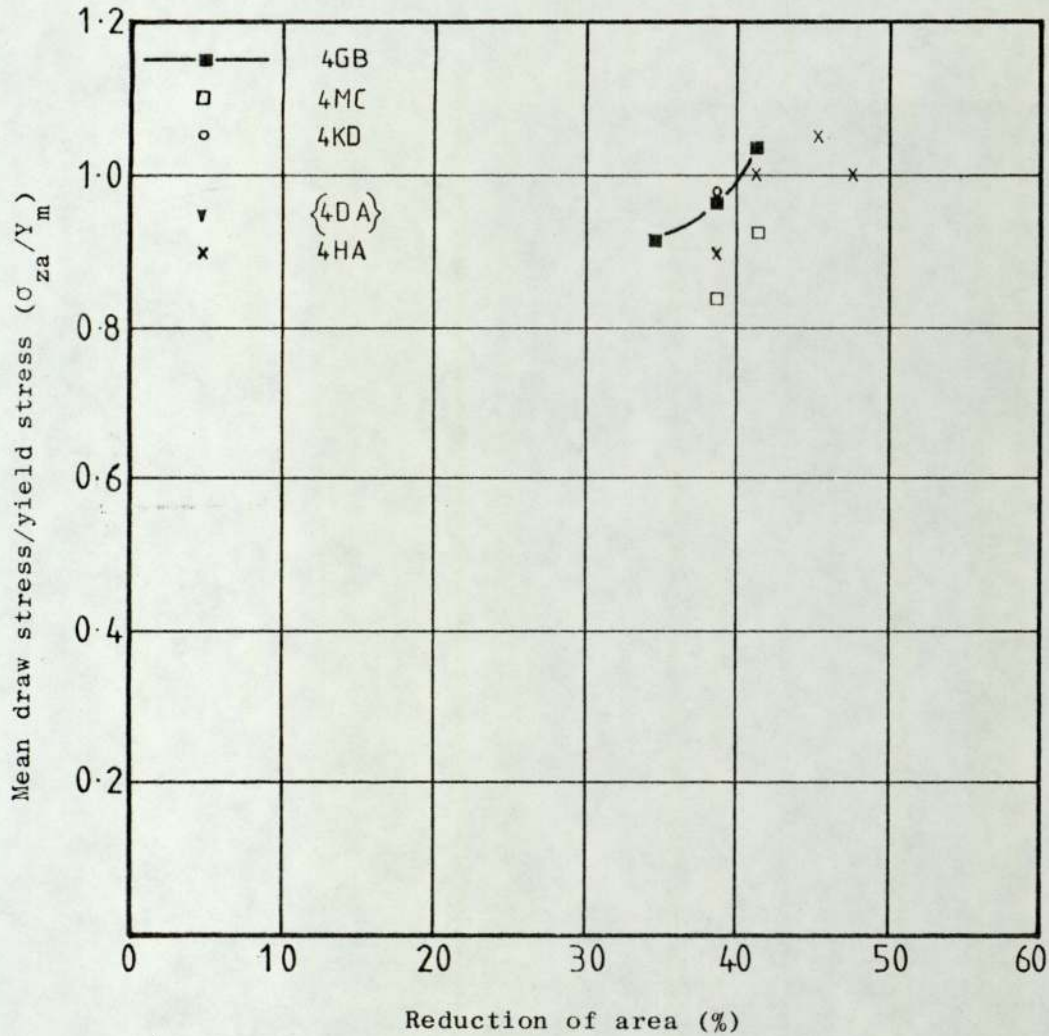


Fig.7.7 Experimental draw stress/yield stress versus reduction of area from the drawing of square tube directly from round using different profiled dies.

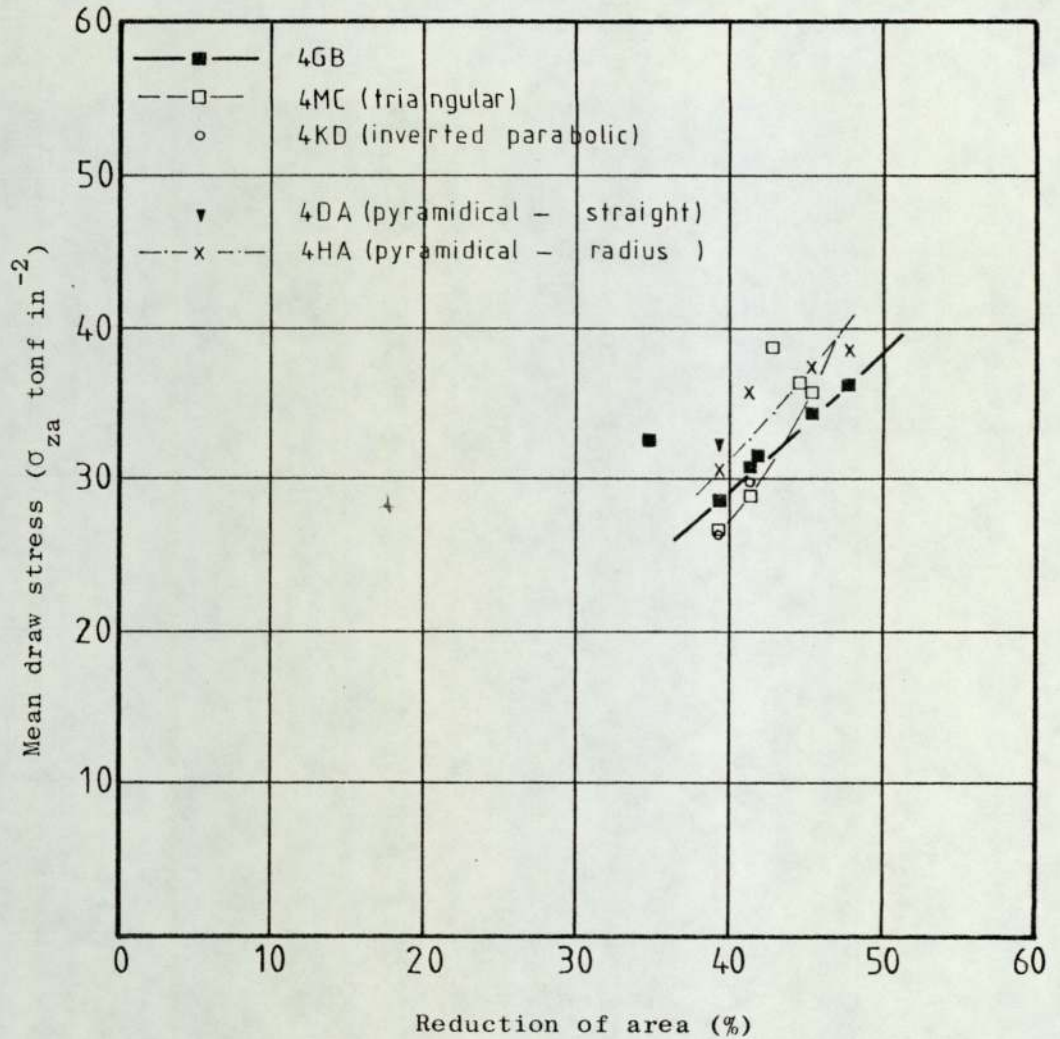


Fig.7.8 A comparison of the draw stress from the different shaped square dies.

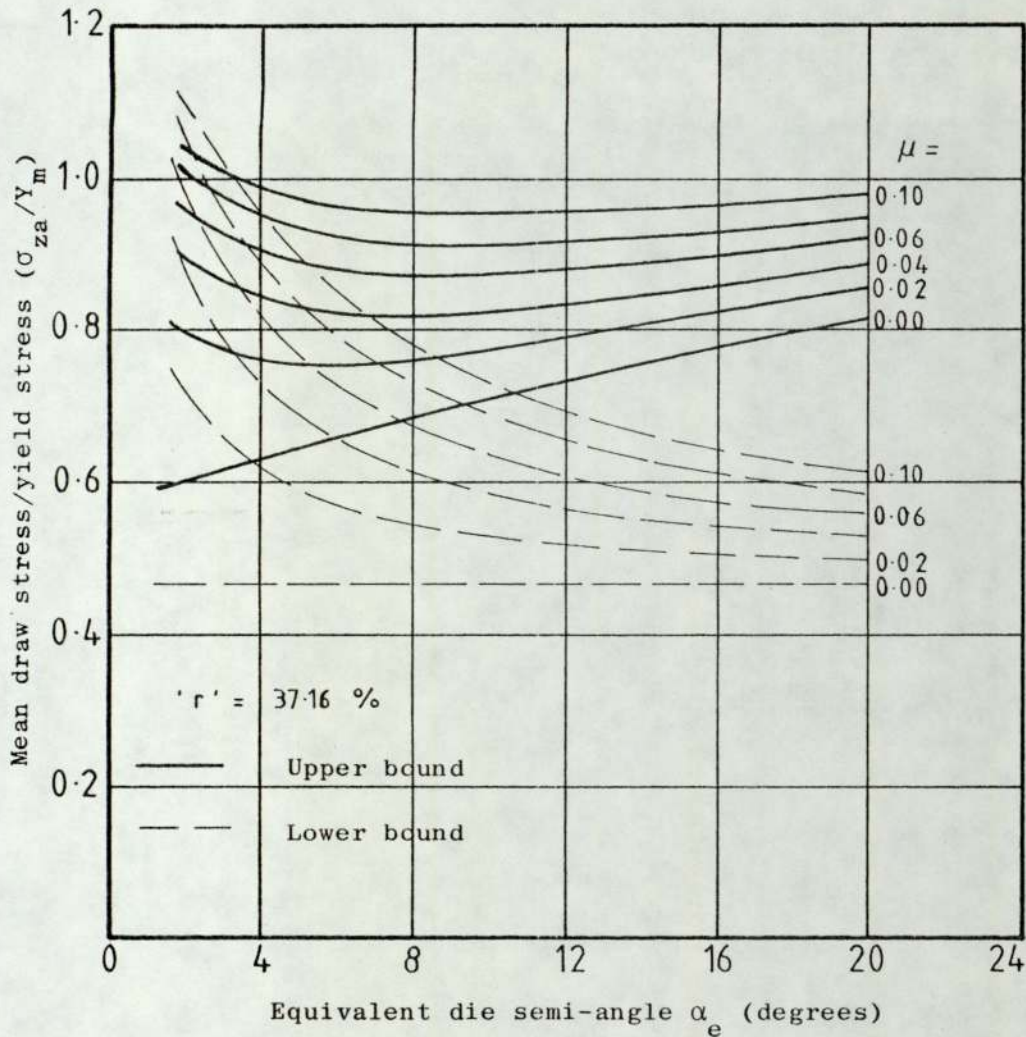


Fig. 7.9 Variation of the mean draw stress with the die semi-angle and coefficient of friction for the upper and lower bound solutions in the drawing of hexagonal tube directly from round.

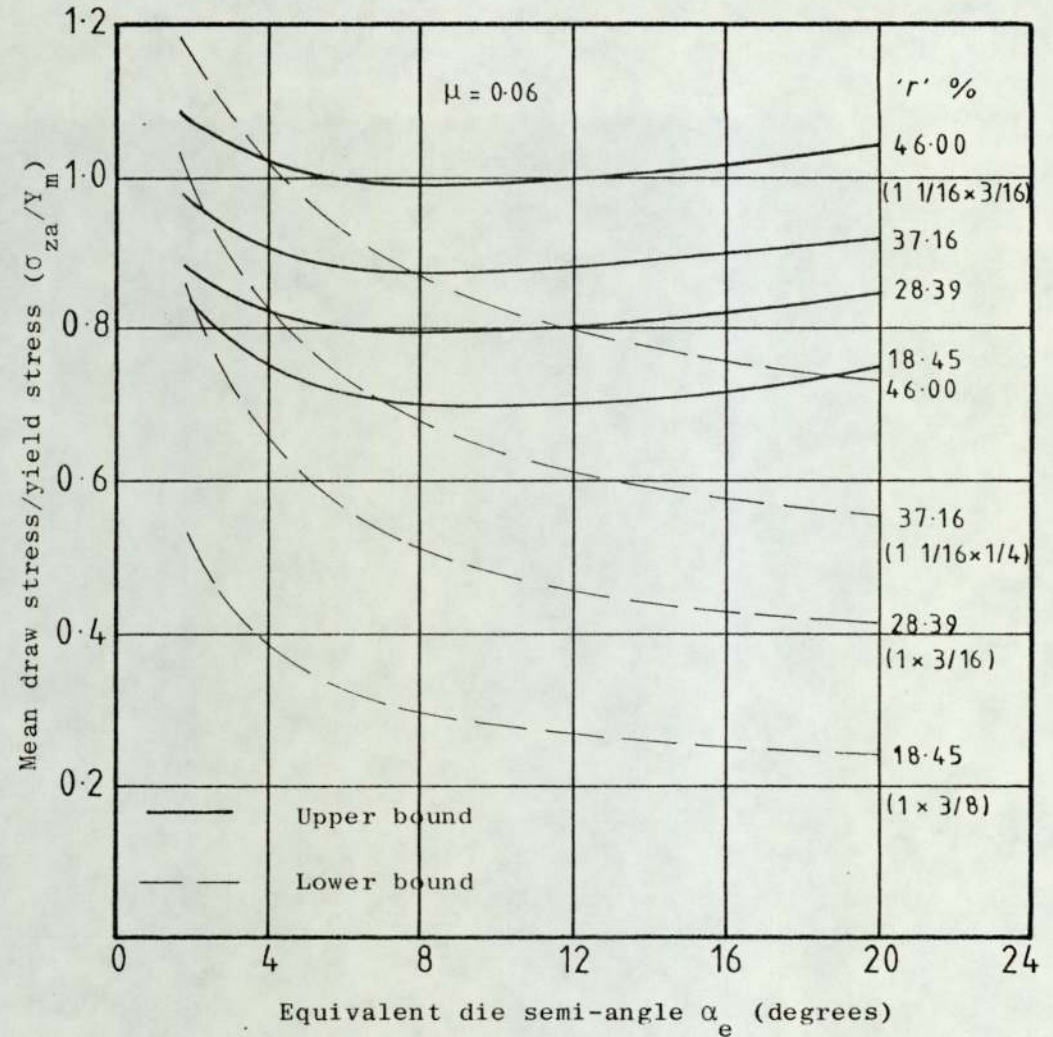


Fig. 7.10 Variation of the mean draw stress with the die semi-angle and the reduction of area for the upper and lower bound solutions in the drawing of hexagonal tube directly from round.

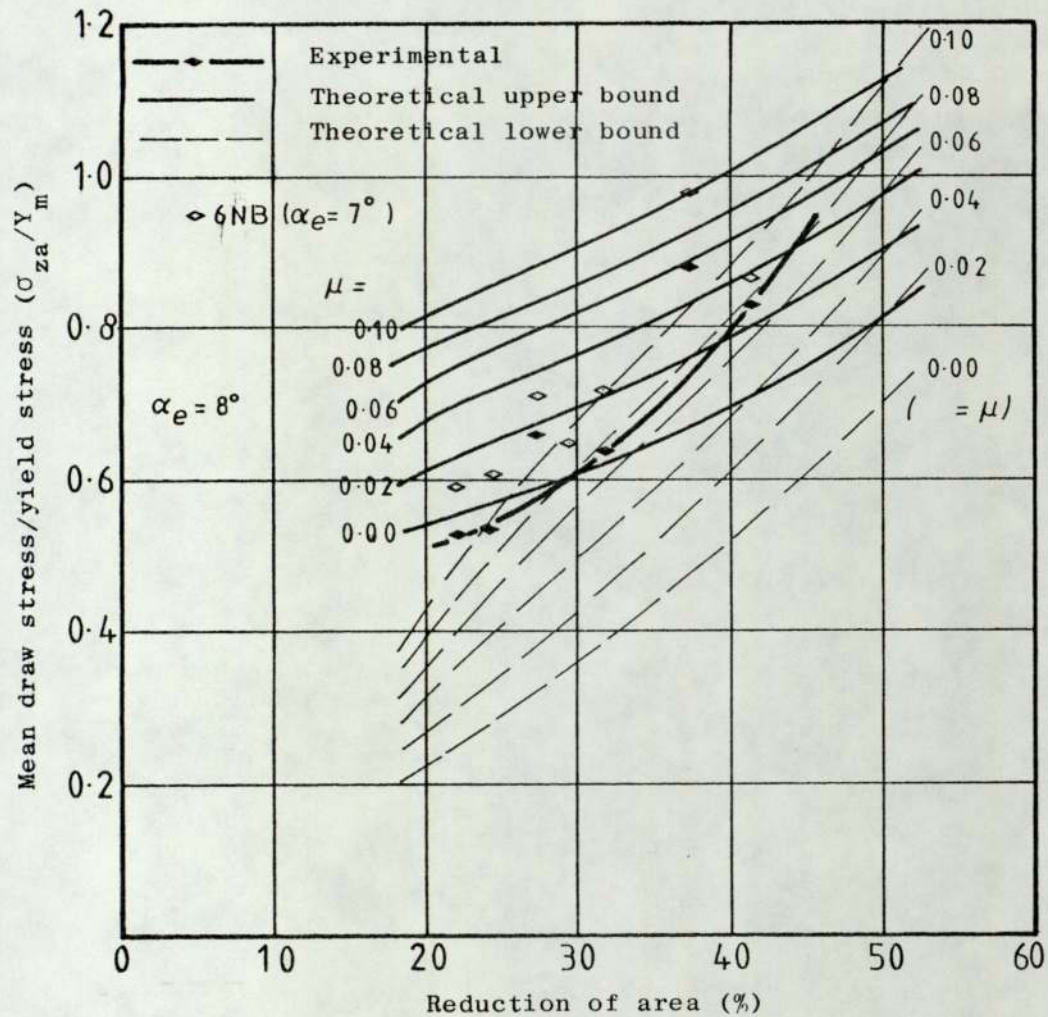


Fig. 7.11 Comparison between the experimental and theoretical draw stress from the upper and lower bound solutions in the drawing of hexagonal tube directly from round stock.

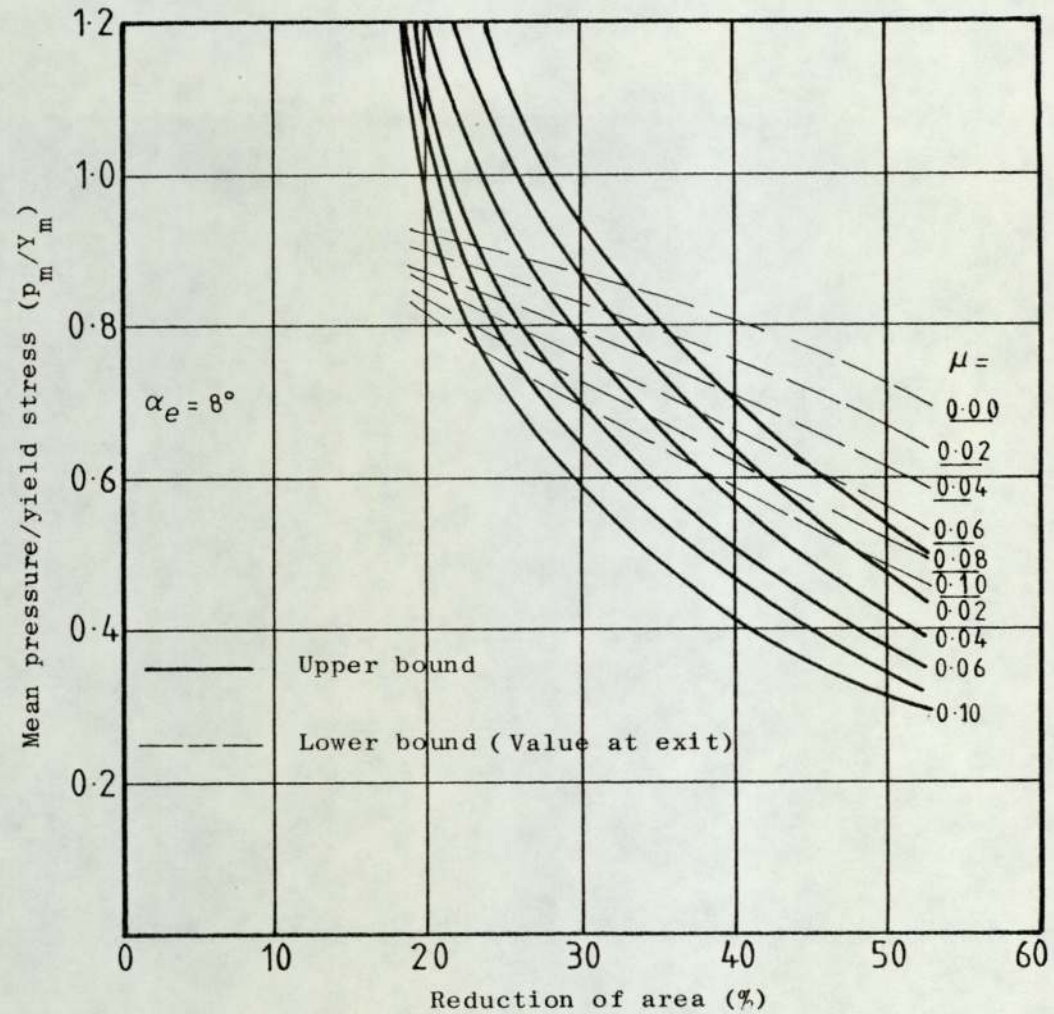


Fig. 7.12 Variation of the mean pressure with reduction of area and coefficient of friction for the upper and lower bound solutions in the drawing of hexagonal tube directly from round stock.

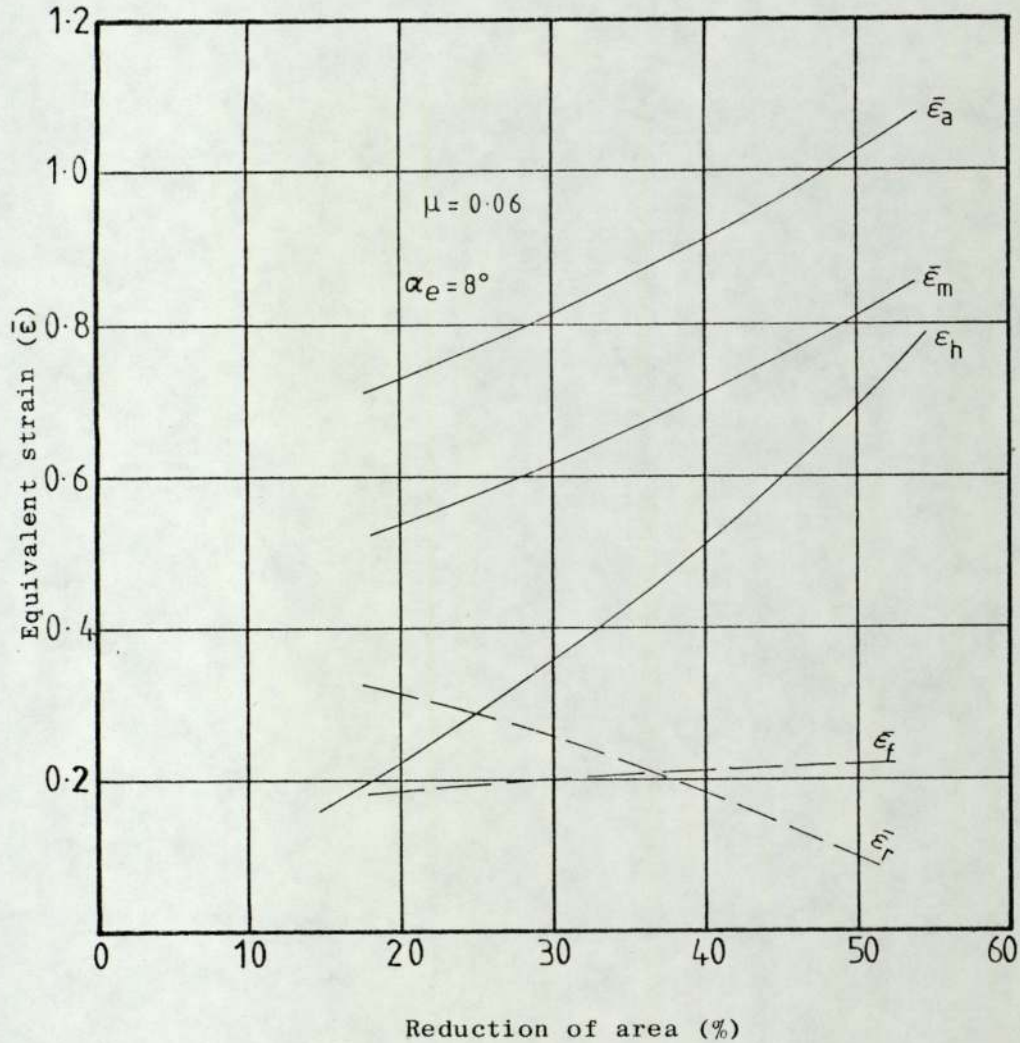


Fig. 7.13 Variation of apparent strain and the equivalent strain components with reduction of area in the drawing of hexagonal tube directly from round stock on a cylindrical plug.

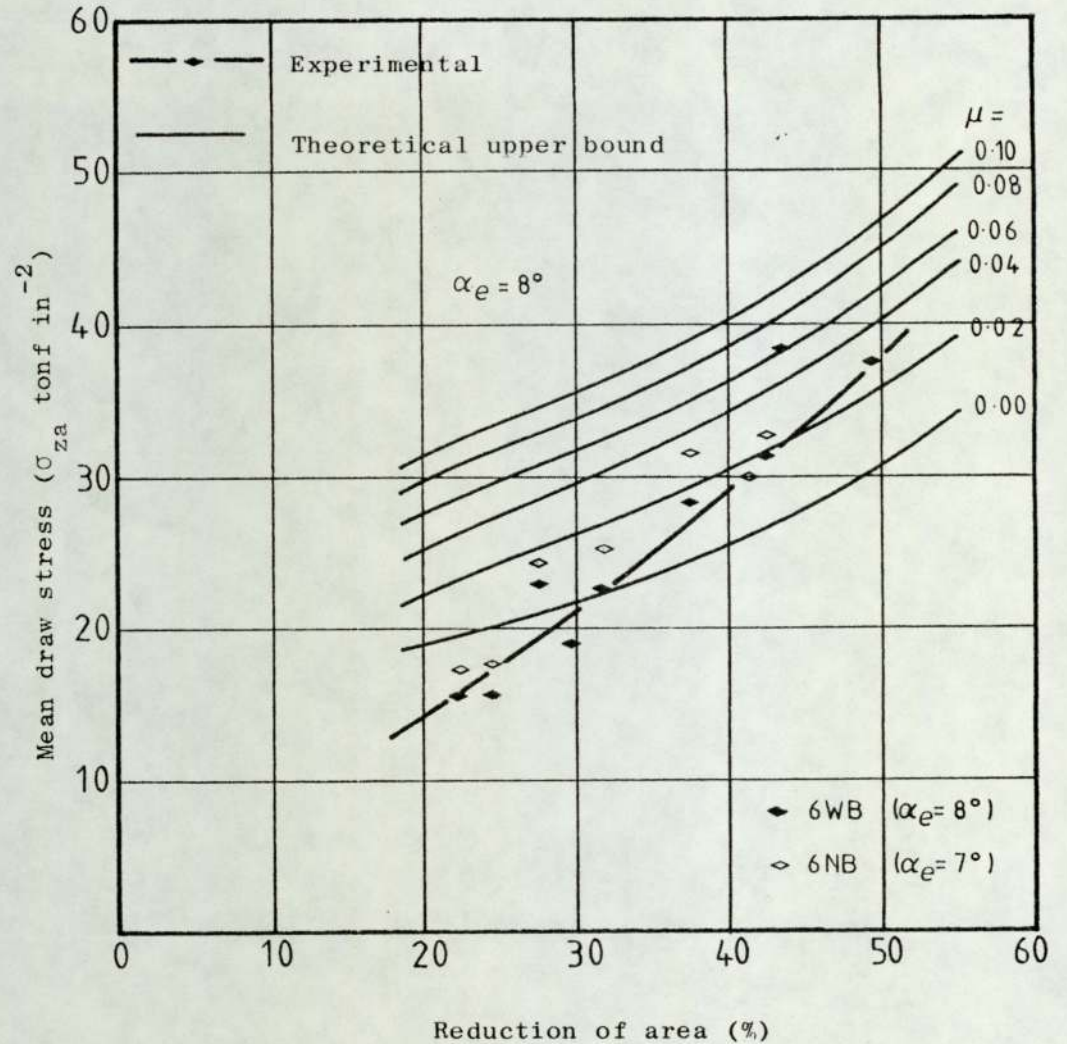


Fig. 7.14 Comparison between the measured draw stress and the values predicted by the upper bound theory for drawing of hexagonal tube directly from round stock on a cylindrical plug.

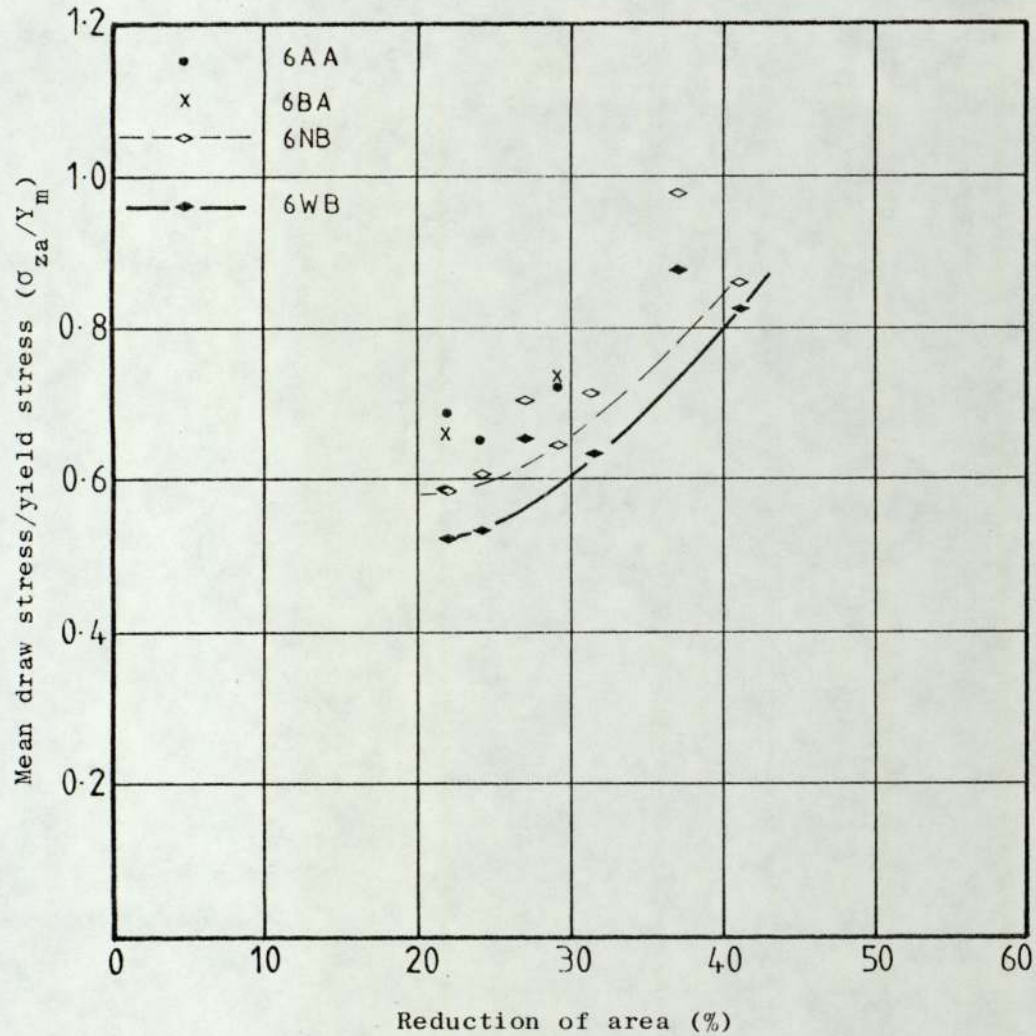


Fig. 7.15 Experimental draw stress/yield stress versus reduction of area from the drawing of hexagonal tube directly from round using different profiled dies.

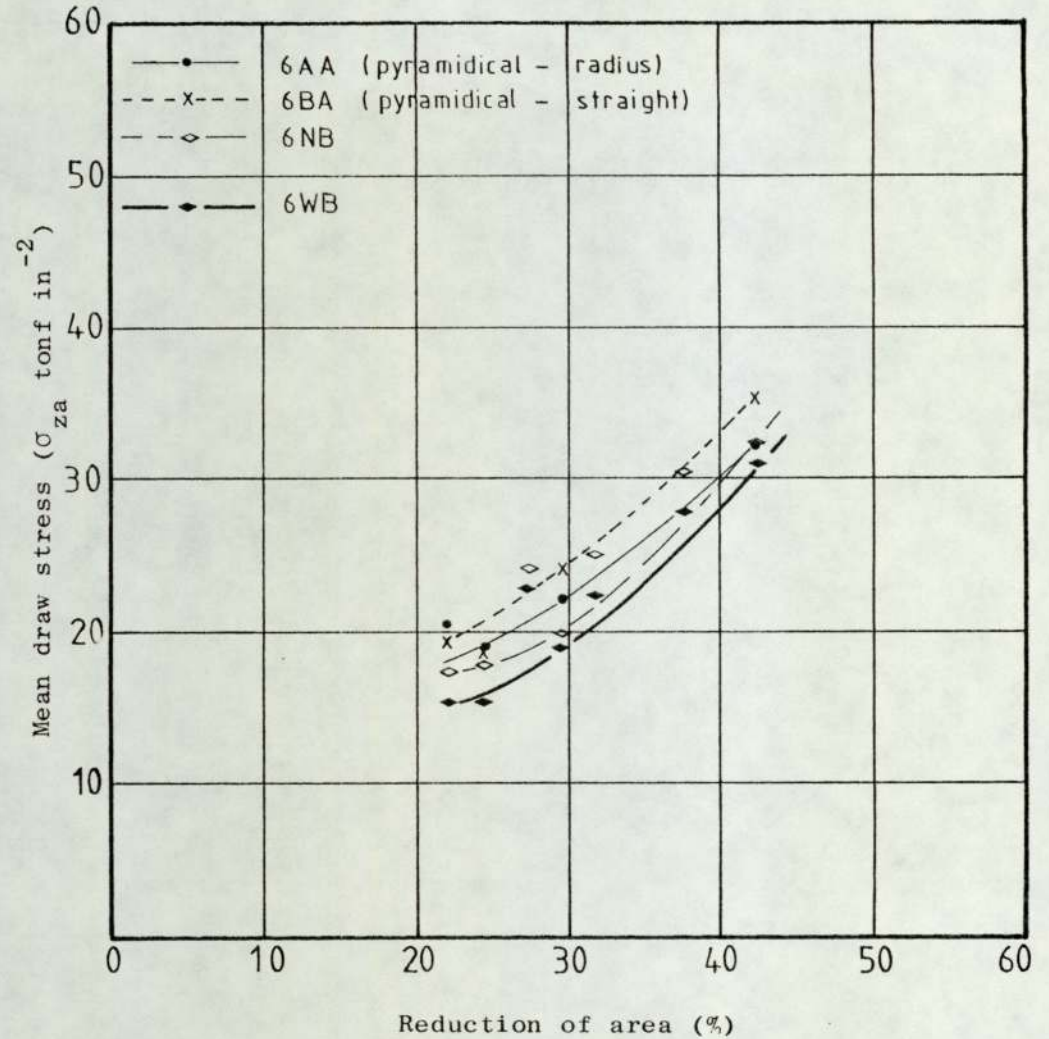


Fig. 7.16 A comparison of the draw stress from the different shaped hexagonal dies.

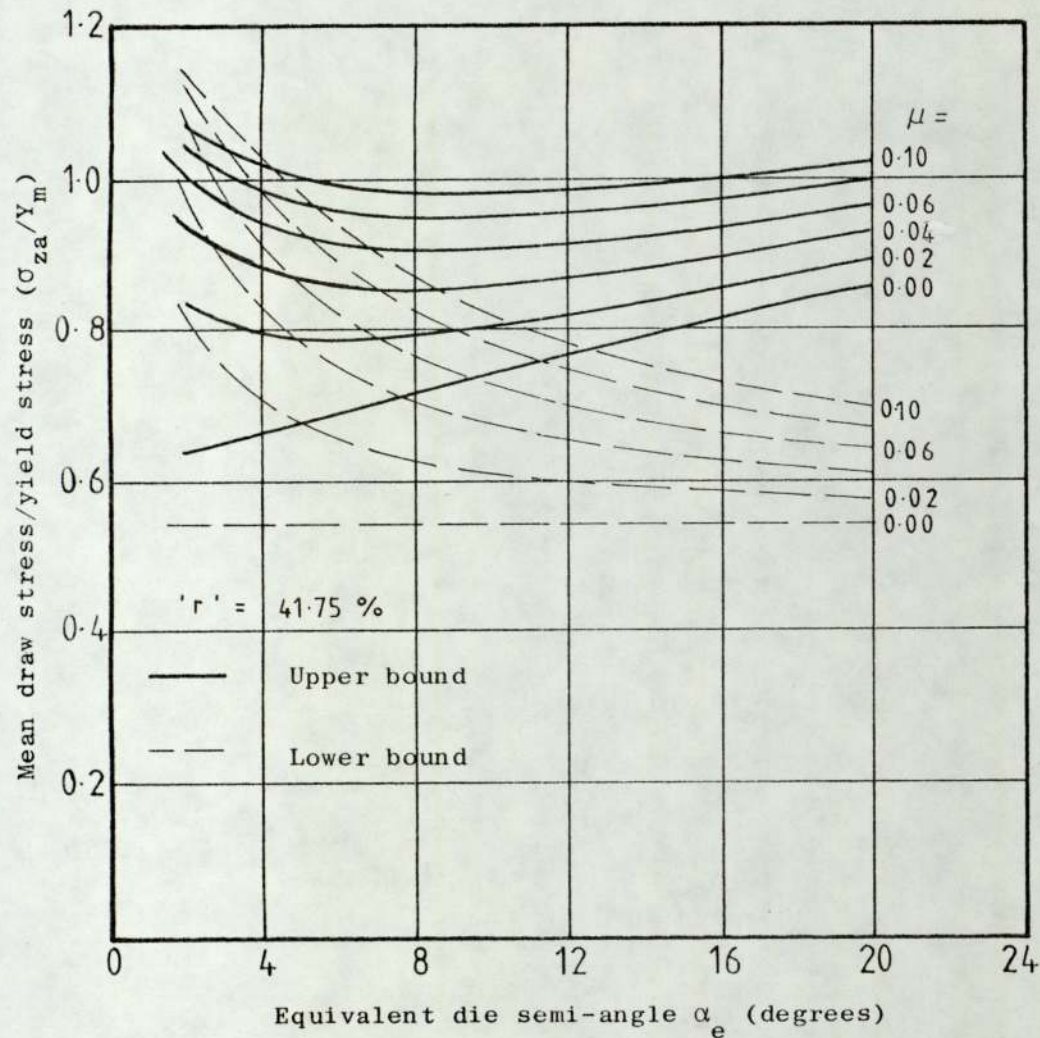


Fig. 7.17 Variation of the mean draw stress with the die semi-angle and coefficient of friction for the upper and lower bound solutions in the drawing of octagonal tube directly from round.

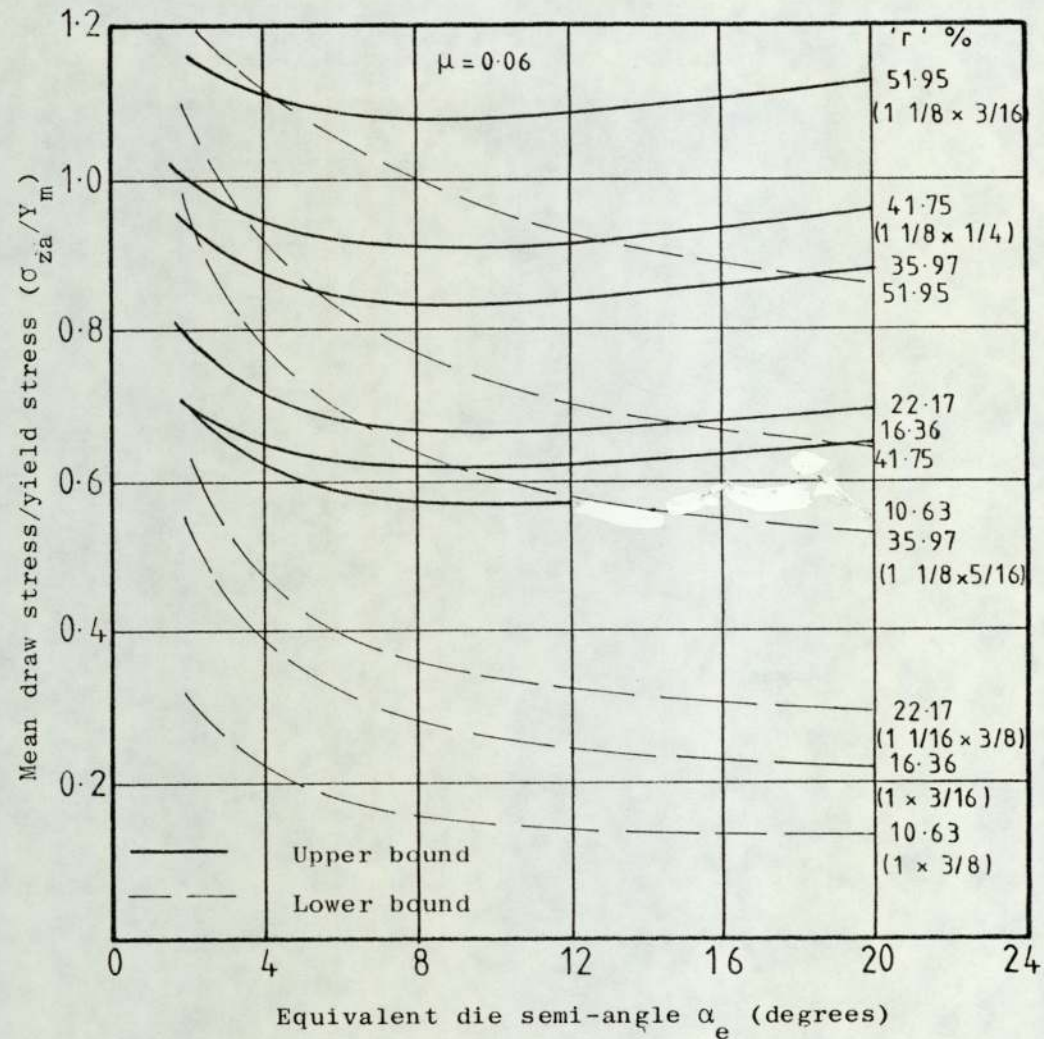


Fig. 7.18 Variation of the mean draw stress with the die semi-angle and the reduction of area for the upper and lower bound solutions in the drawing of octagonal tube directly from round.

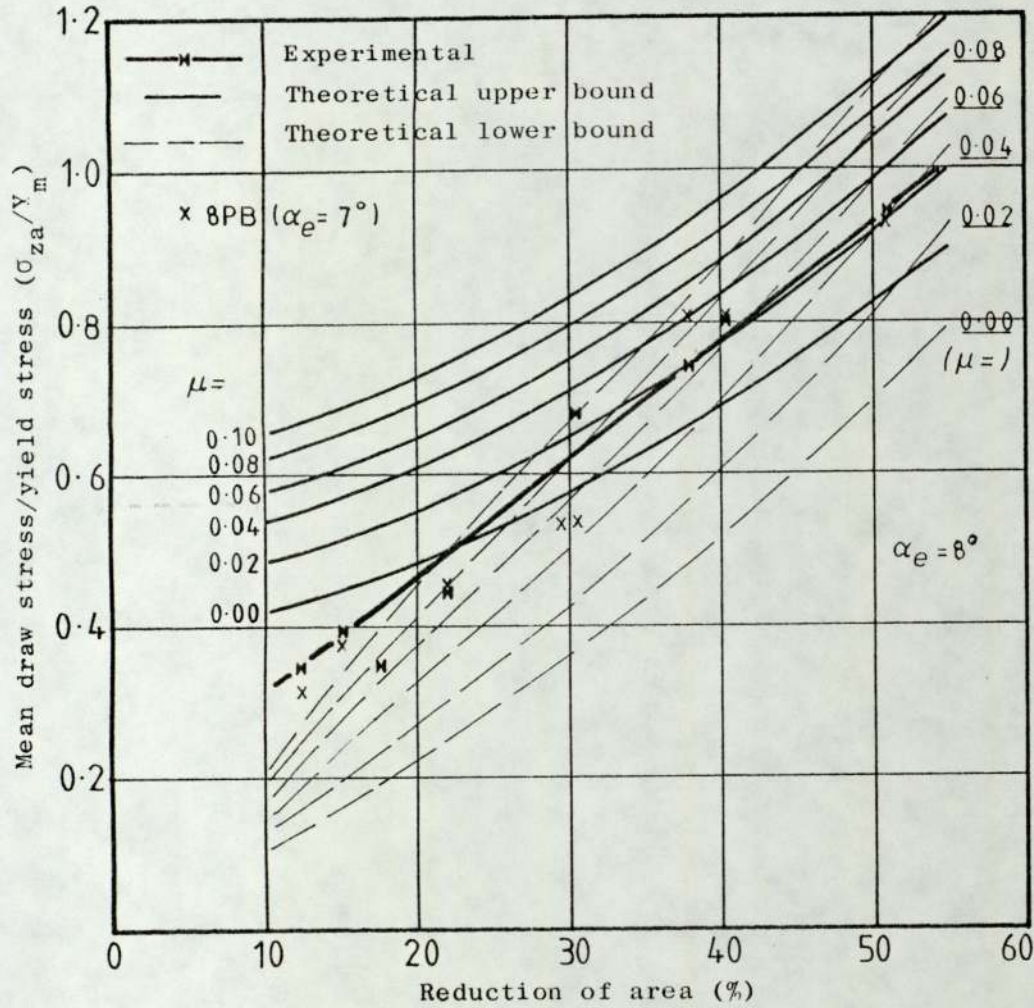


Fig. 7.19 Comparison between the experimental and theoretical draw stress from the upper and lower bound solutions in the drawing of octagonal tube directly from round stock.

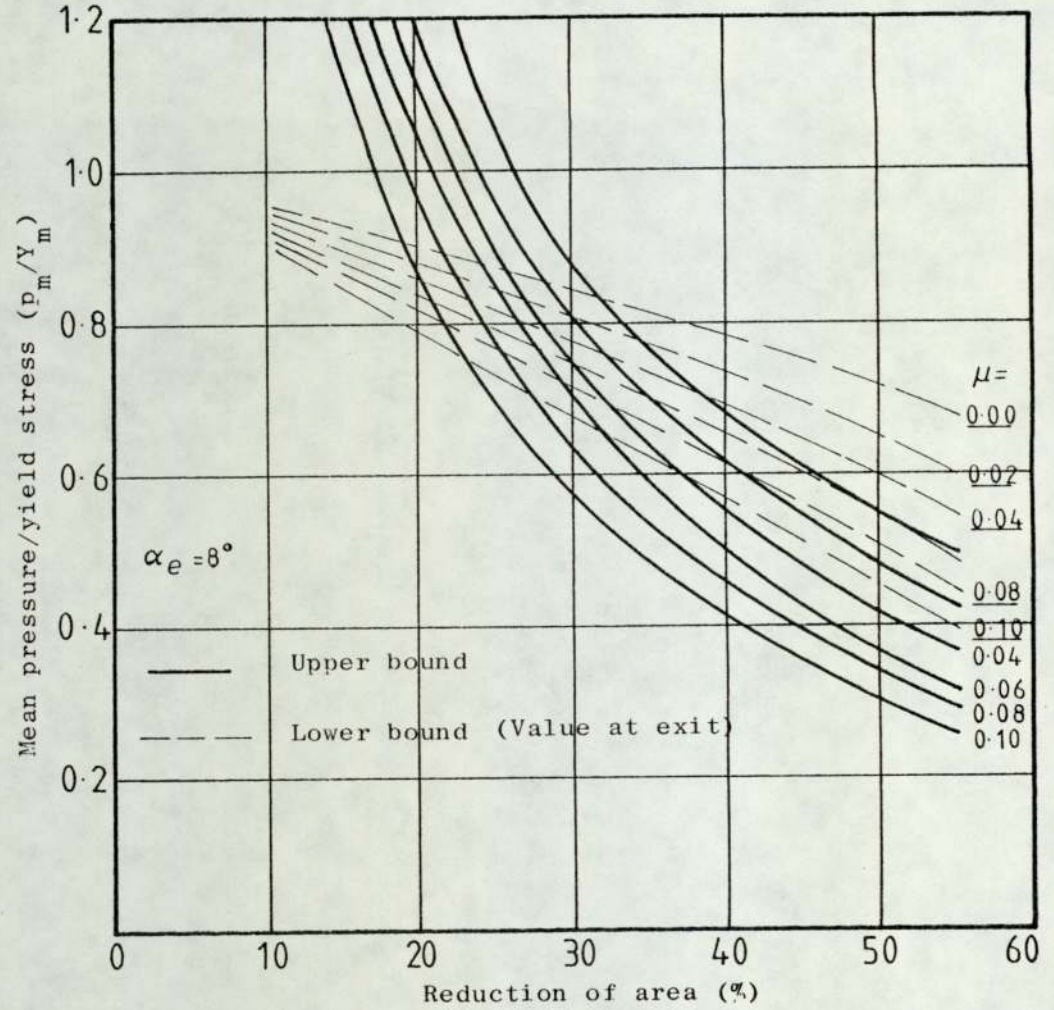


Fig. 7.20 Variation of the mean pressure with reduction of area and coefficient of friction for the upper and lower bound solutions in the drawing of octagonal tube directly from round stock.

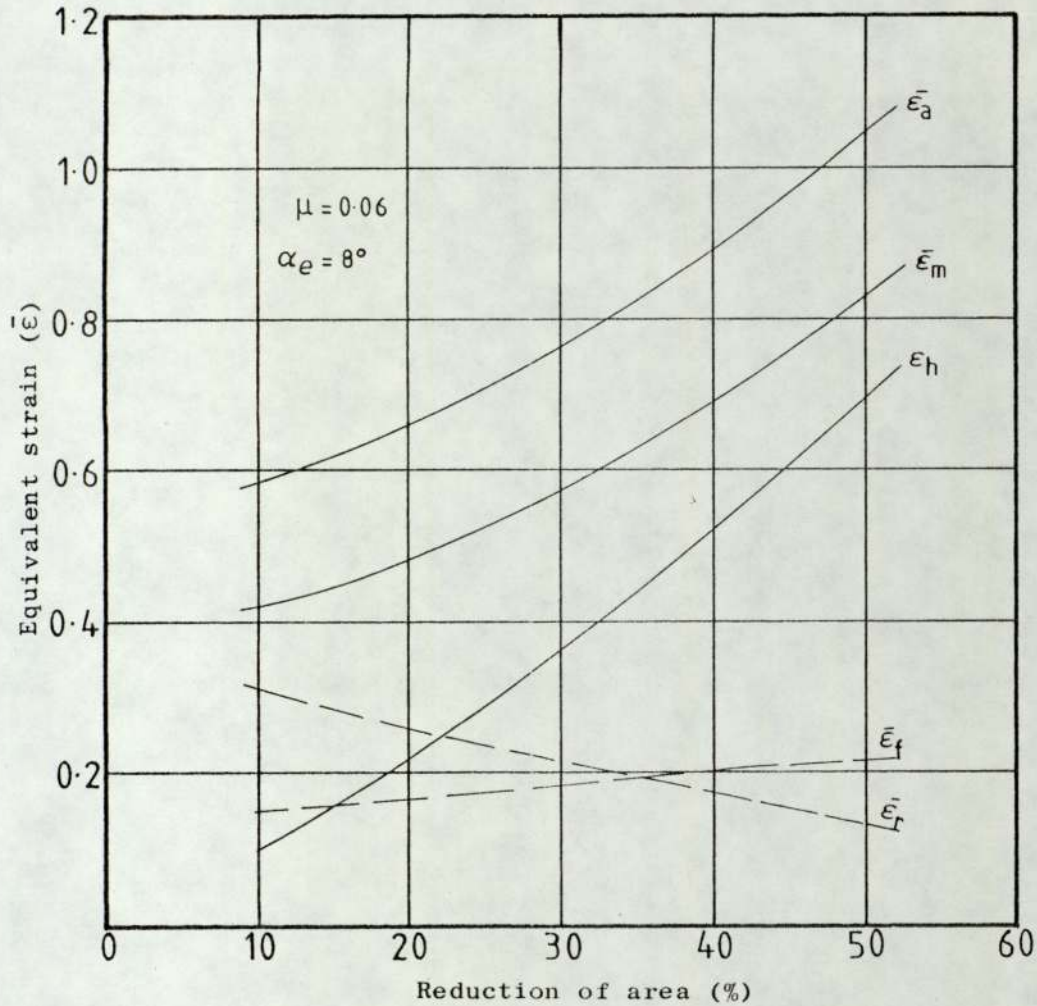


Fig. 7.21 Variation of apparent strain and the equivalent strain components with reduction of area in the drawing of octagonal tube directly from round stock on a cylindrical plug.

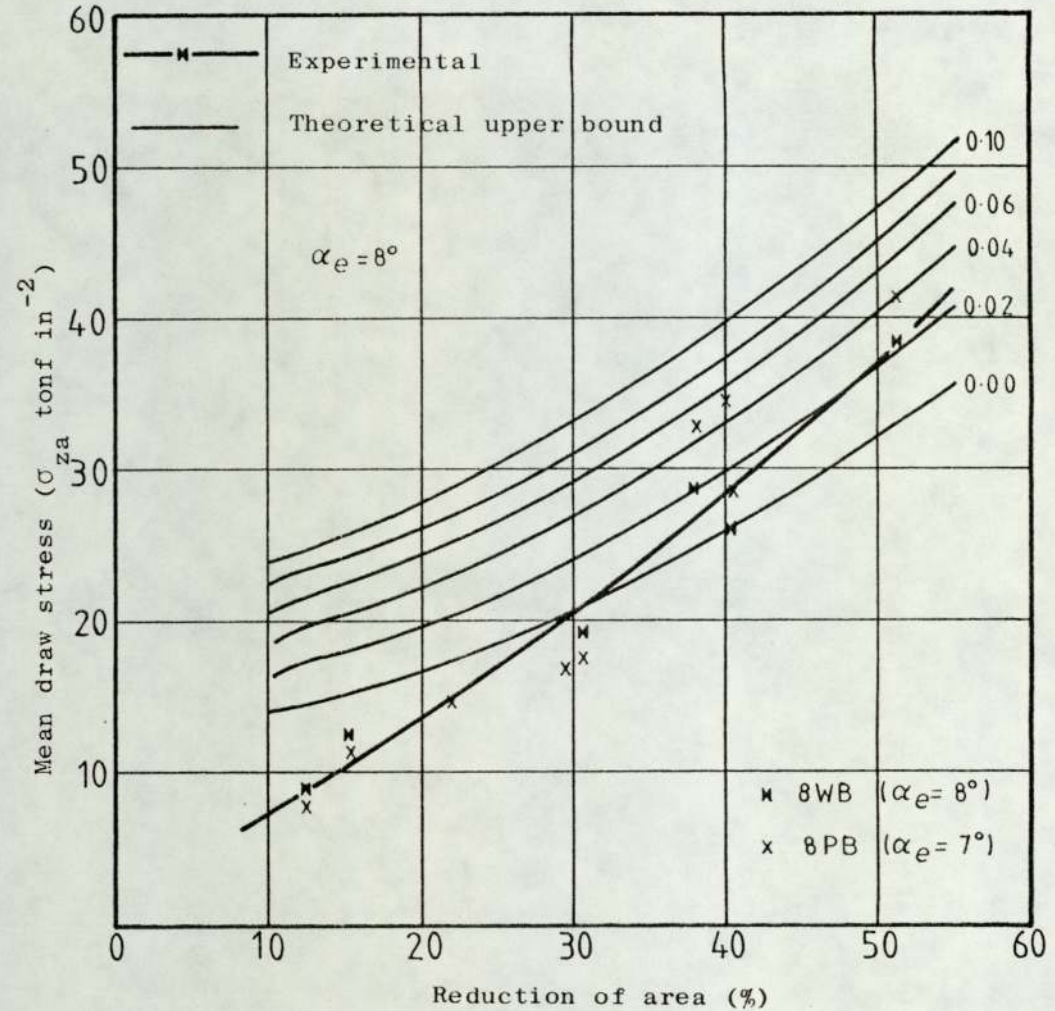


Fig. 7.22 Comparison between the measured draw stress and the values predicted by the upper bound theory for drawing of octagonal tube directly from round stock on a cylindrical plug.

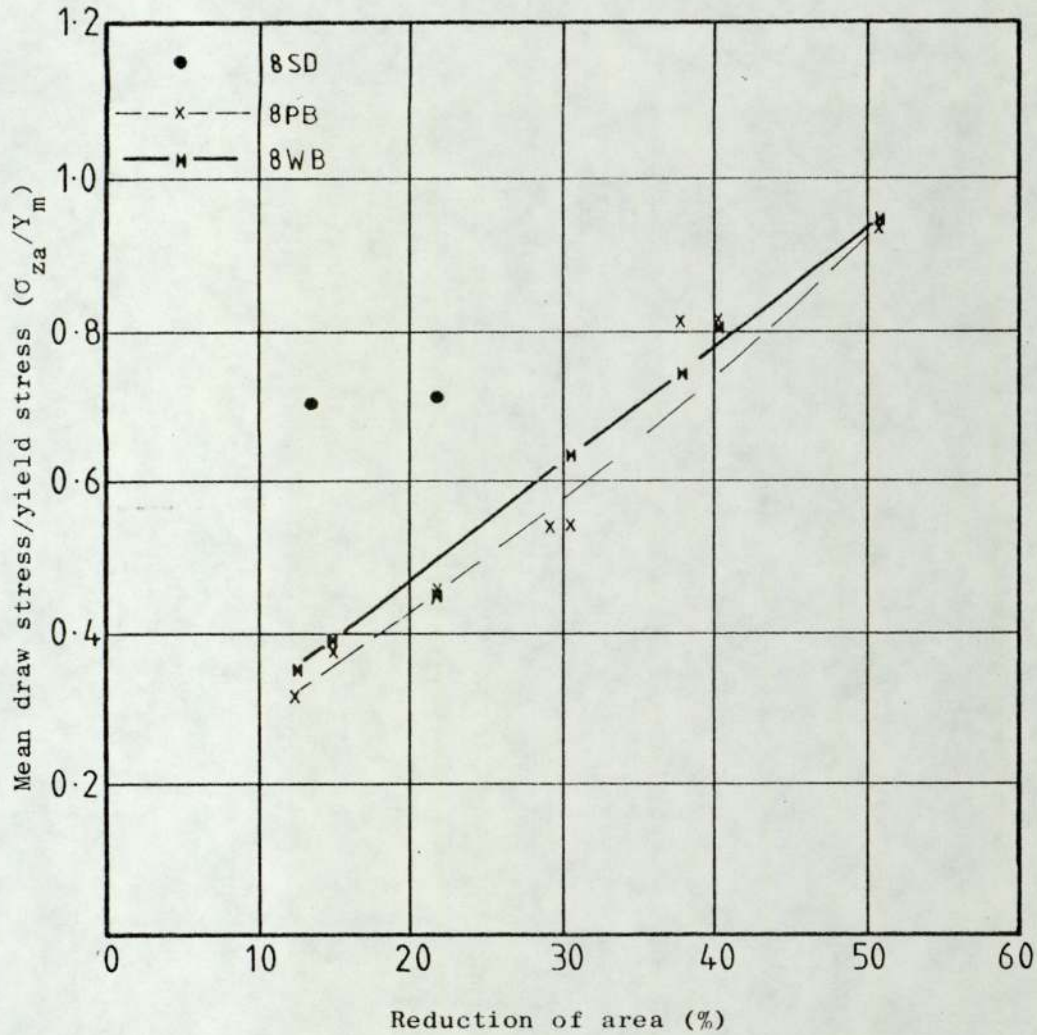


Fig. 7.23 Experimental draw stress/yield stress versus reduction of area from the drawing of octagonal tube directly from round using different profiled dies.

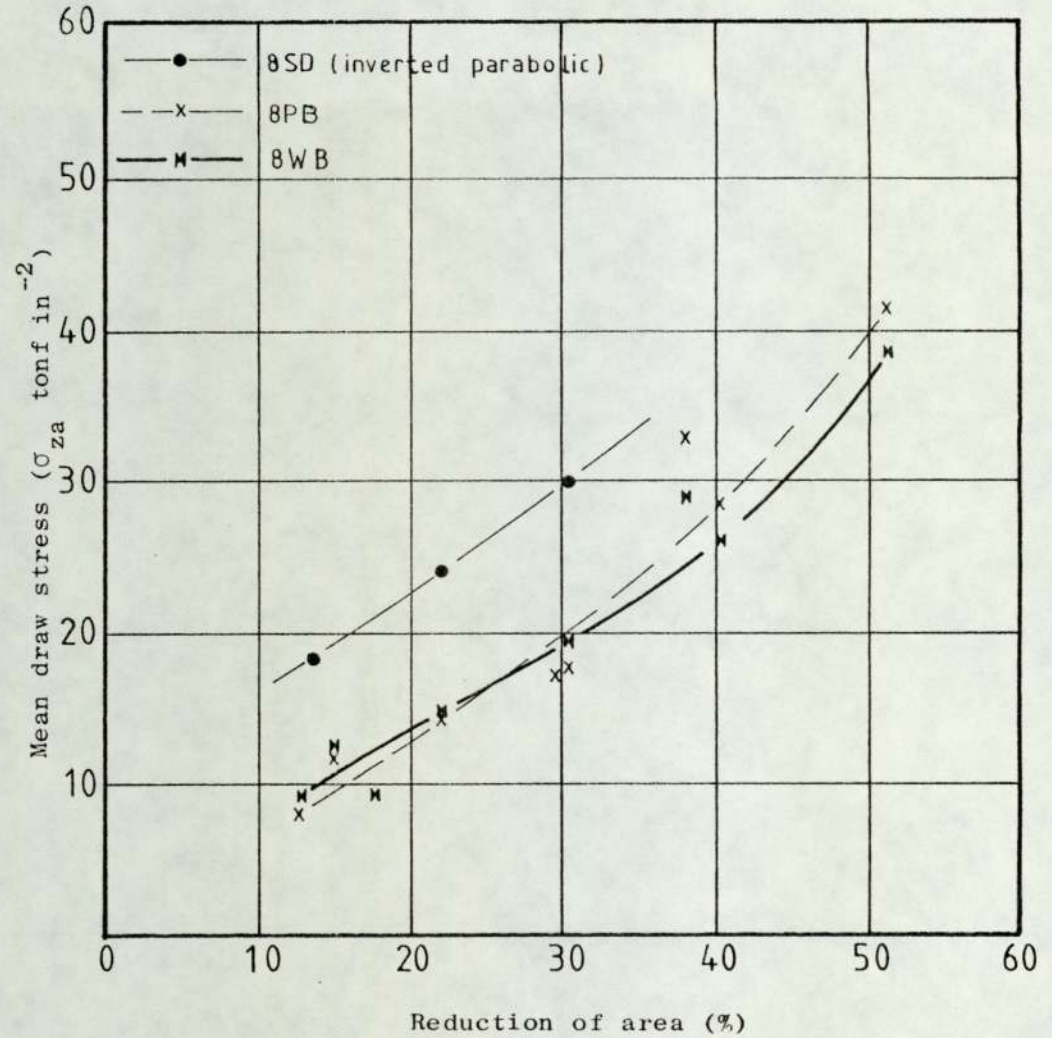


Fig. 7.24 A comparison of the draw stress from the different shaped octagonal dies.

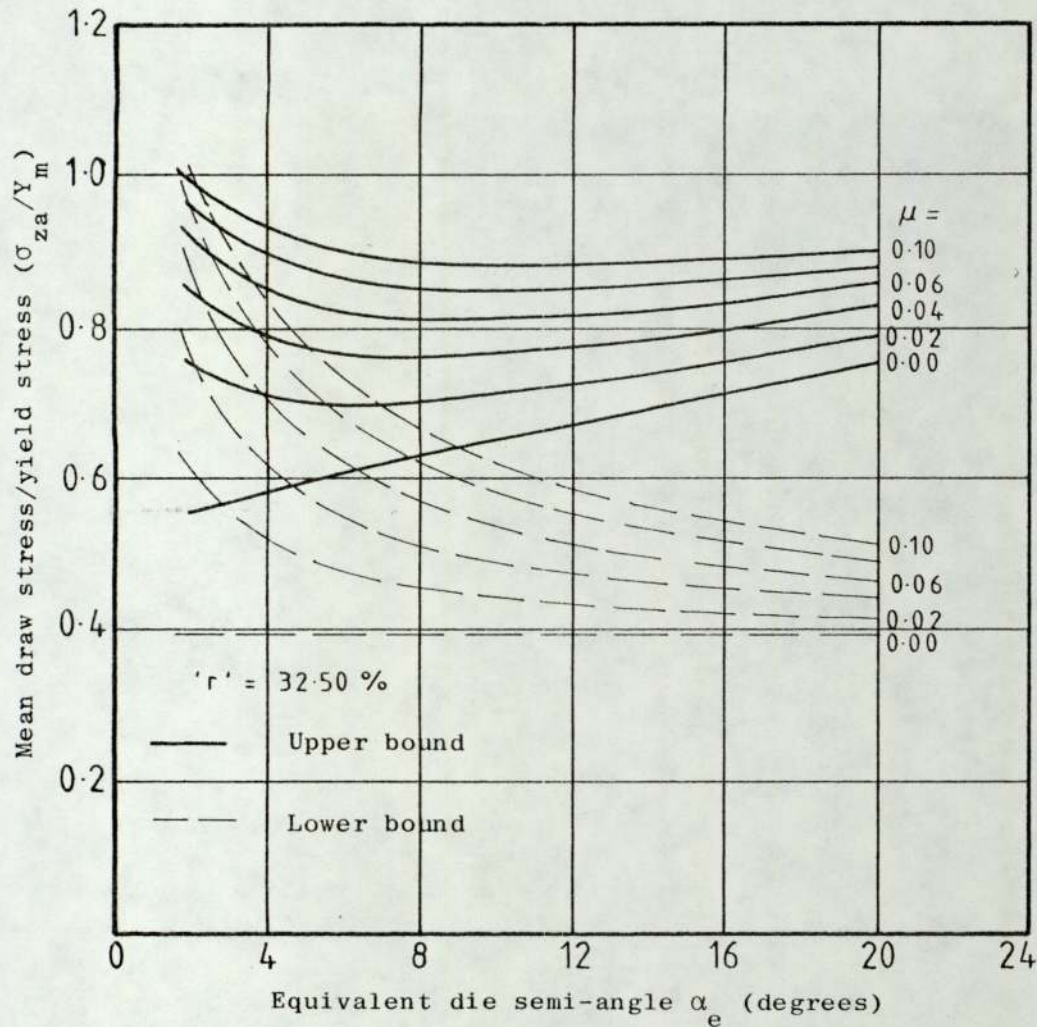


Fig. 7.25 Variation of the mean draw stress with the die semi-angle and coefficient of friction for the upper and lower bound solutions in the drawing of decagonal tube directly from round.

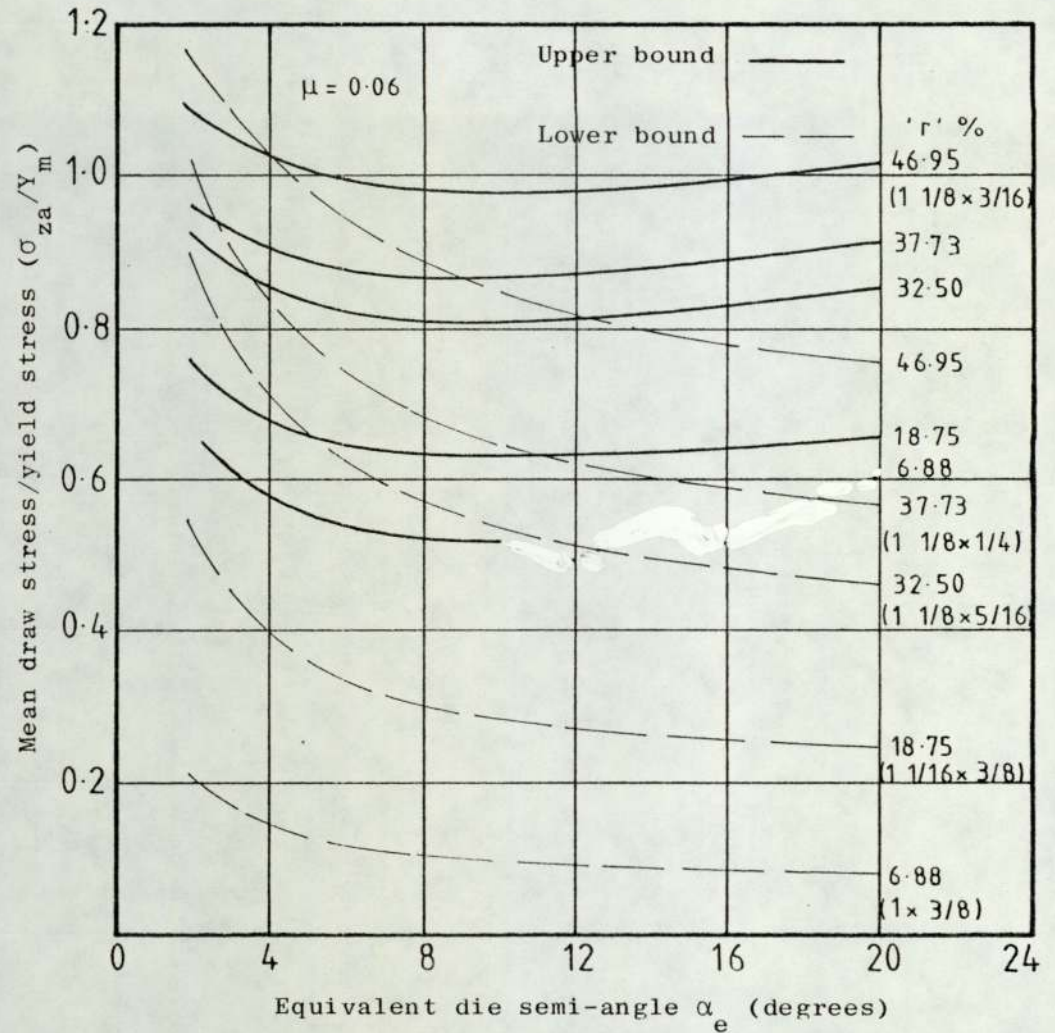


Fig. 7.26 Variation of the mean draw stress with the die semi-angle and the reduction of area for the upper and lower bound solutions in the drawing of decagonal tube directly from round.

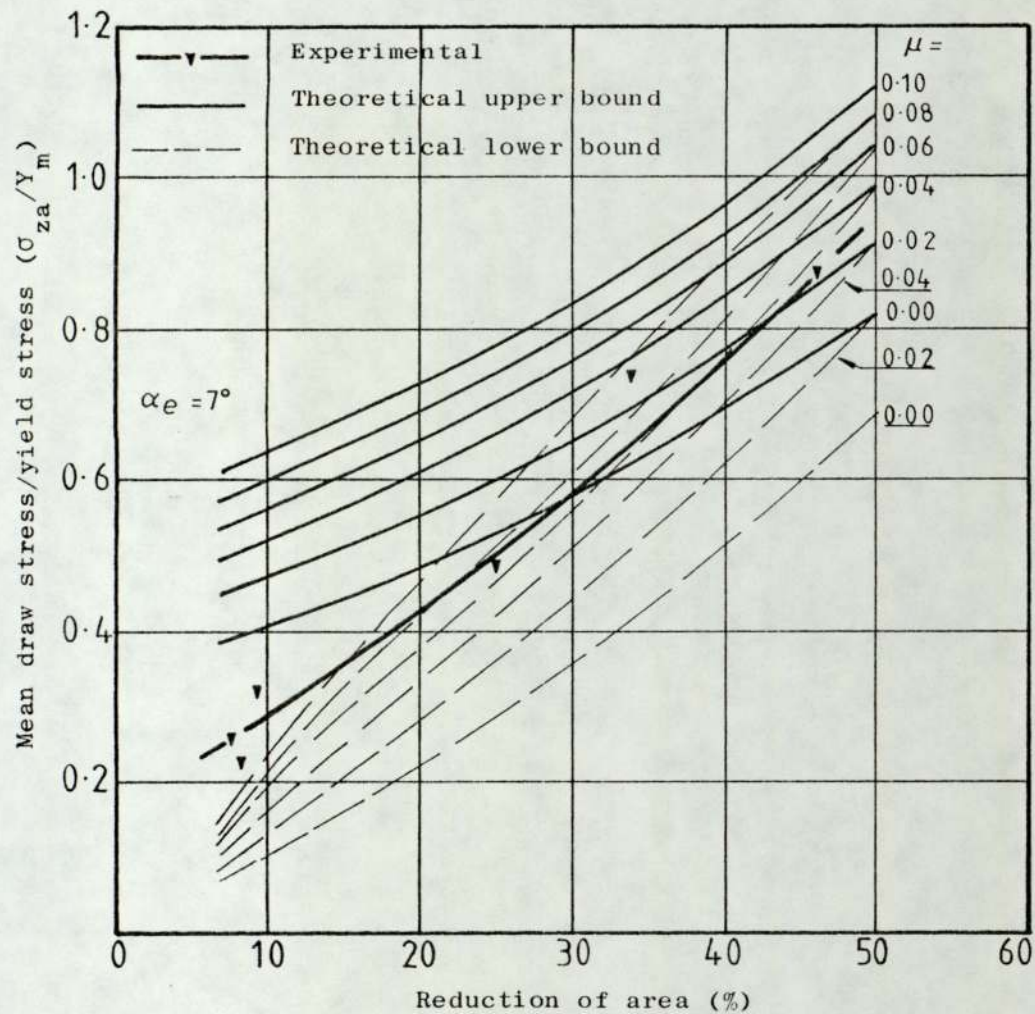


Fig. 7.27 Comparison between the experimental and theoretical draw stress from the upper and lower bound solutions in the drawing of decagonal tube directly from round stock.

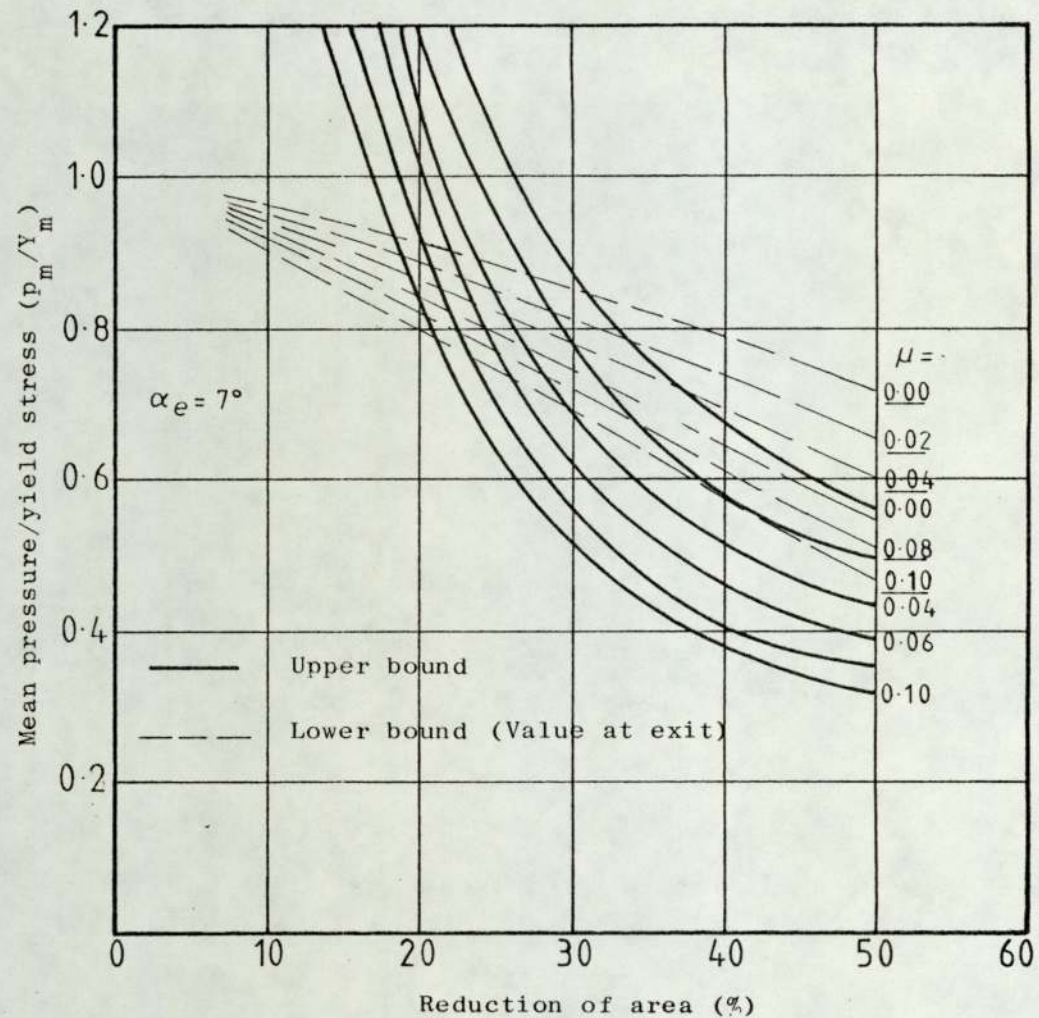


Fig. 7.28 Variation of the mean pressure with reduction of area and coefficient of friction for the upper and lower bound solutions in the drawing of decagonal tube directly from round stock.

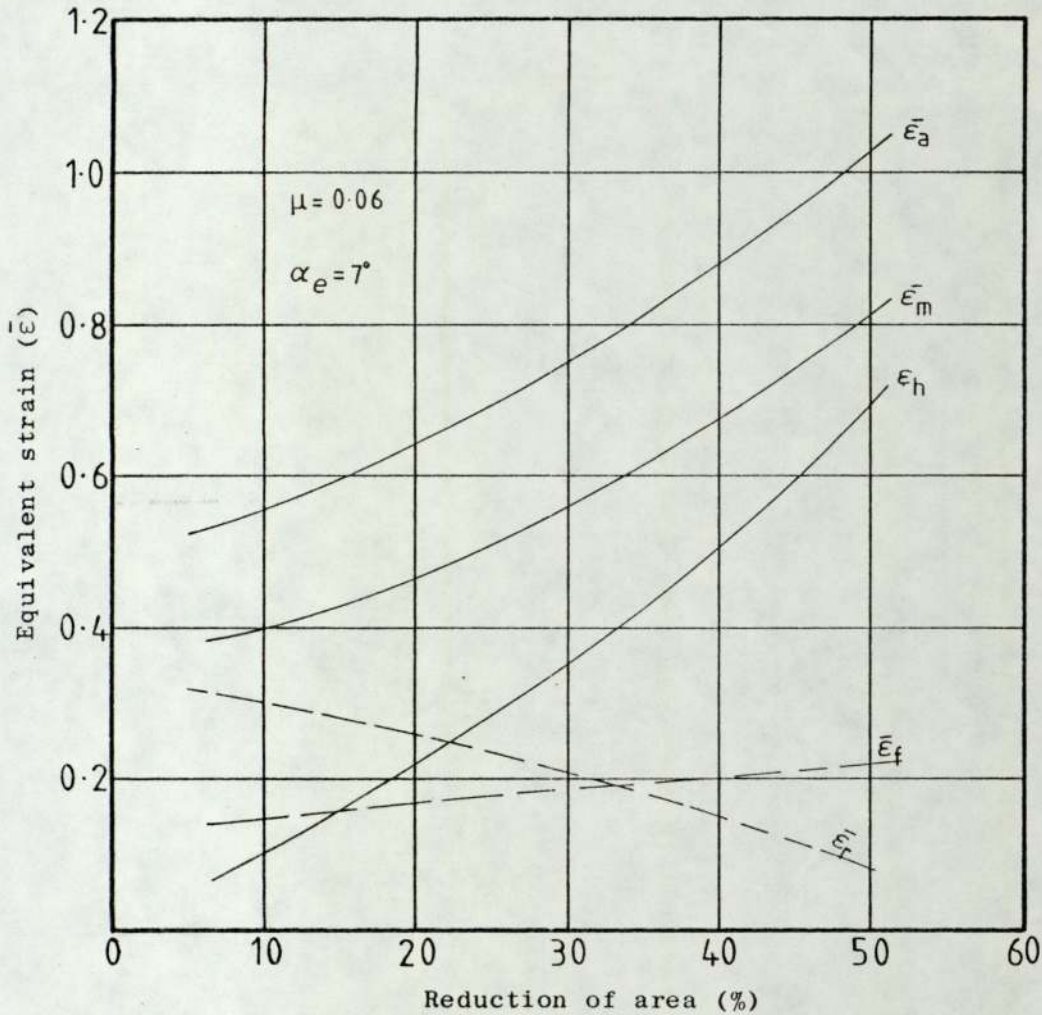


Fig. 7.29 Variation of apparent strain and the equivalent strain components with reduction of area in the drawing of decagonal tube directly from round stock on a cylindrical plug.

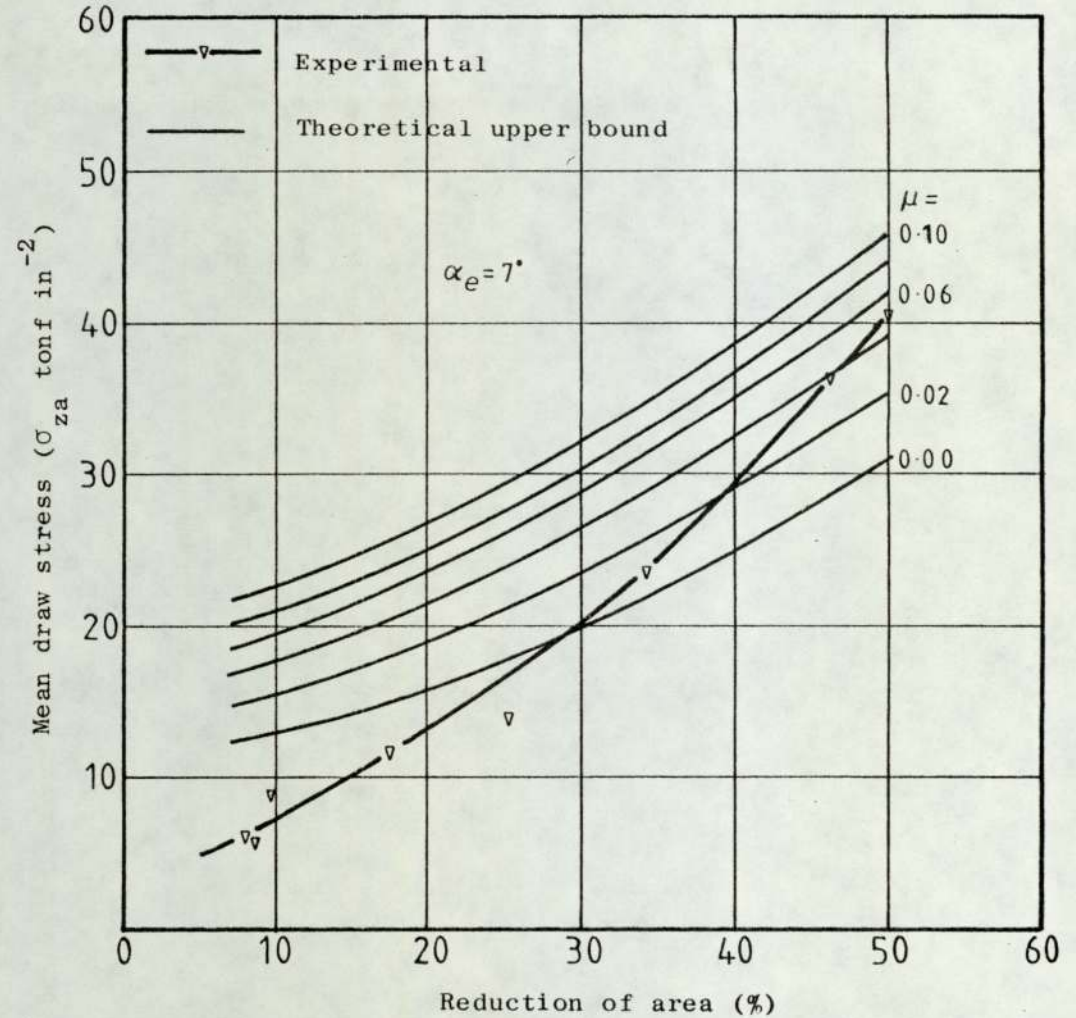


Fig. 7.30 Comparison between the measured draw stress and the values predicted by the upper bound theory for drawing of decagonal tube directly from round stock on a cylindrical plug.

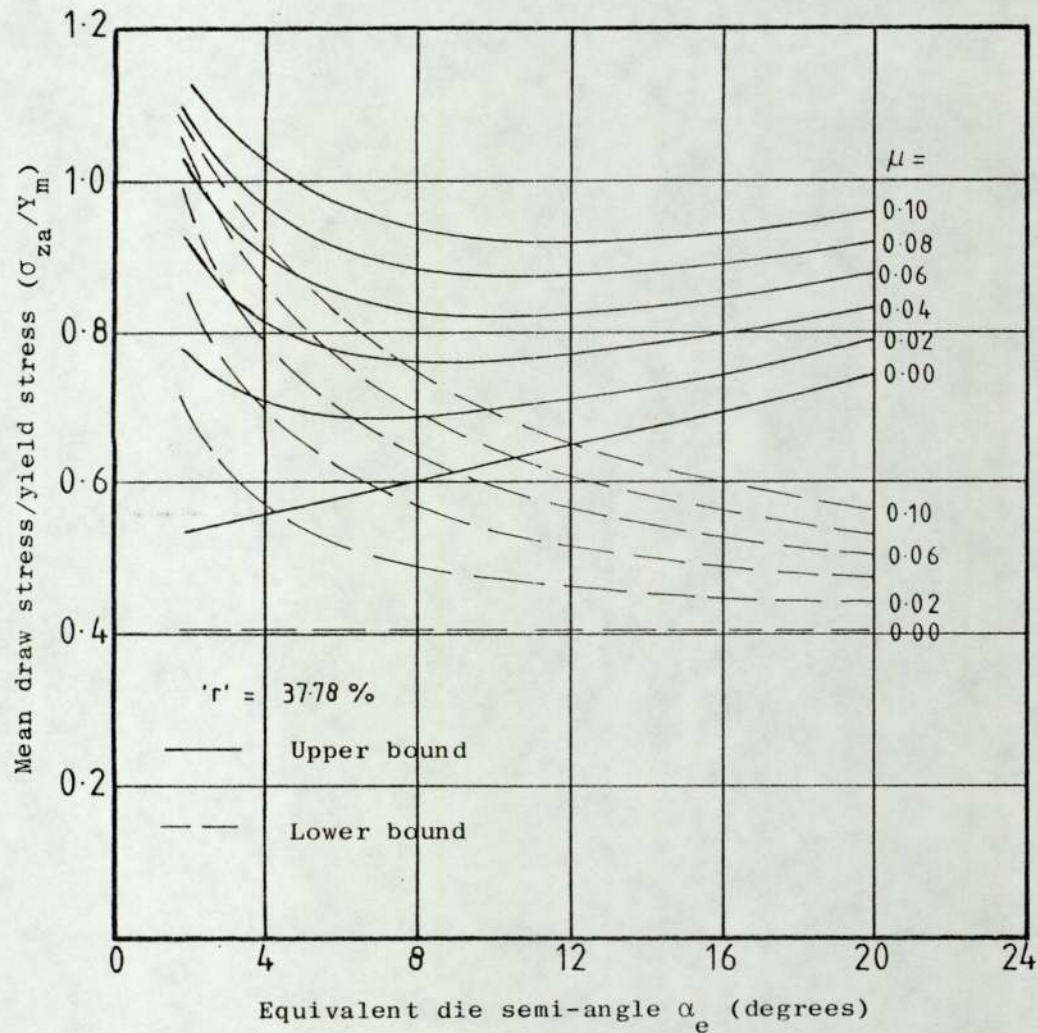


Fig. 7.31 Variation of the mean draw stress with the die semi-angle and coefficient of friction for the upper and lower bound solutions in the drawing of round tube directly from round.

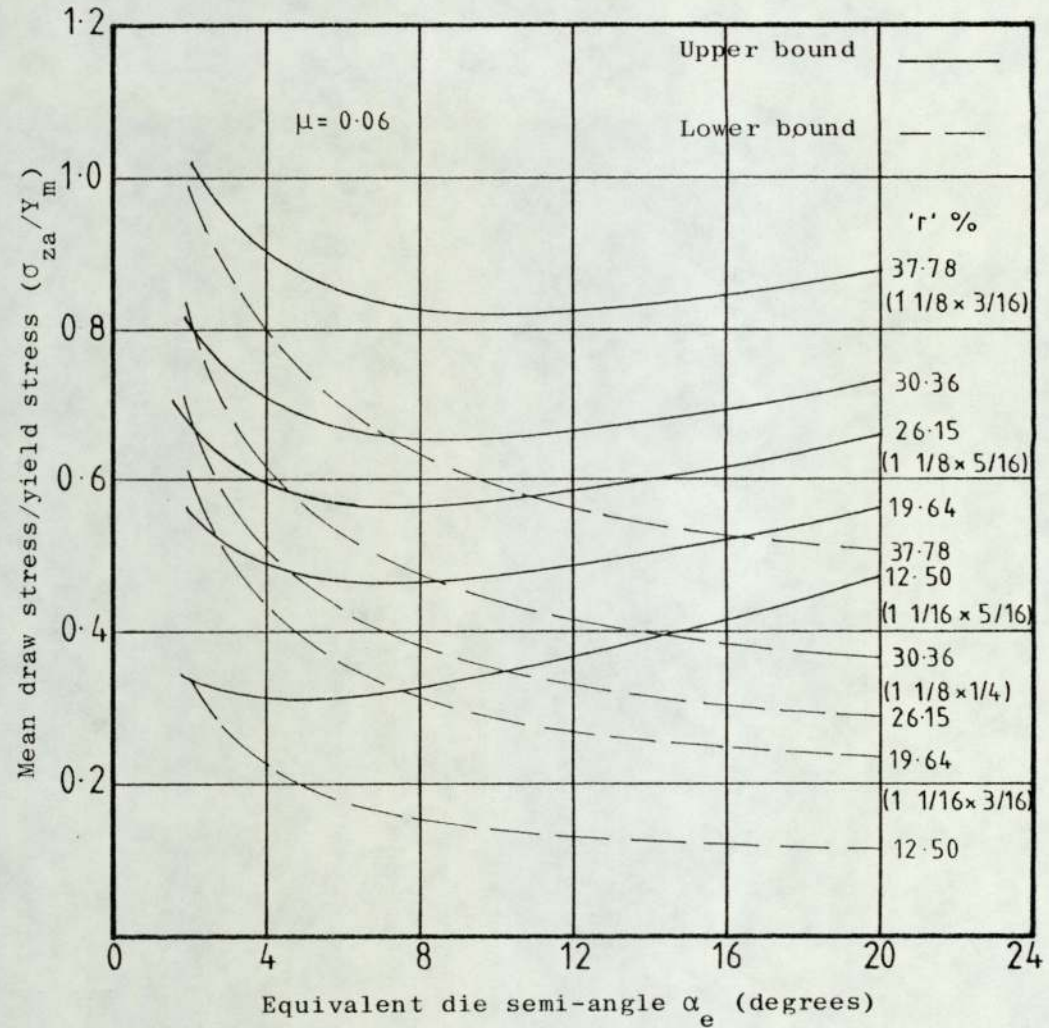


Fig. 7.32 Variation of the mean draw stress with the die semi-angle and the reduction of area for the upper and lower bound solutions in the drawing of round tube directly from round.

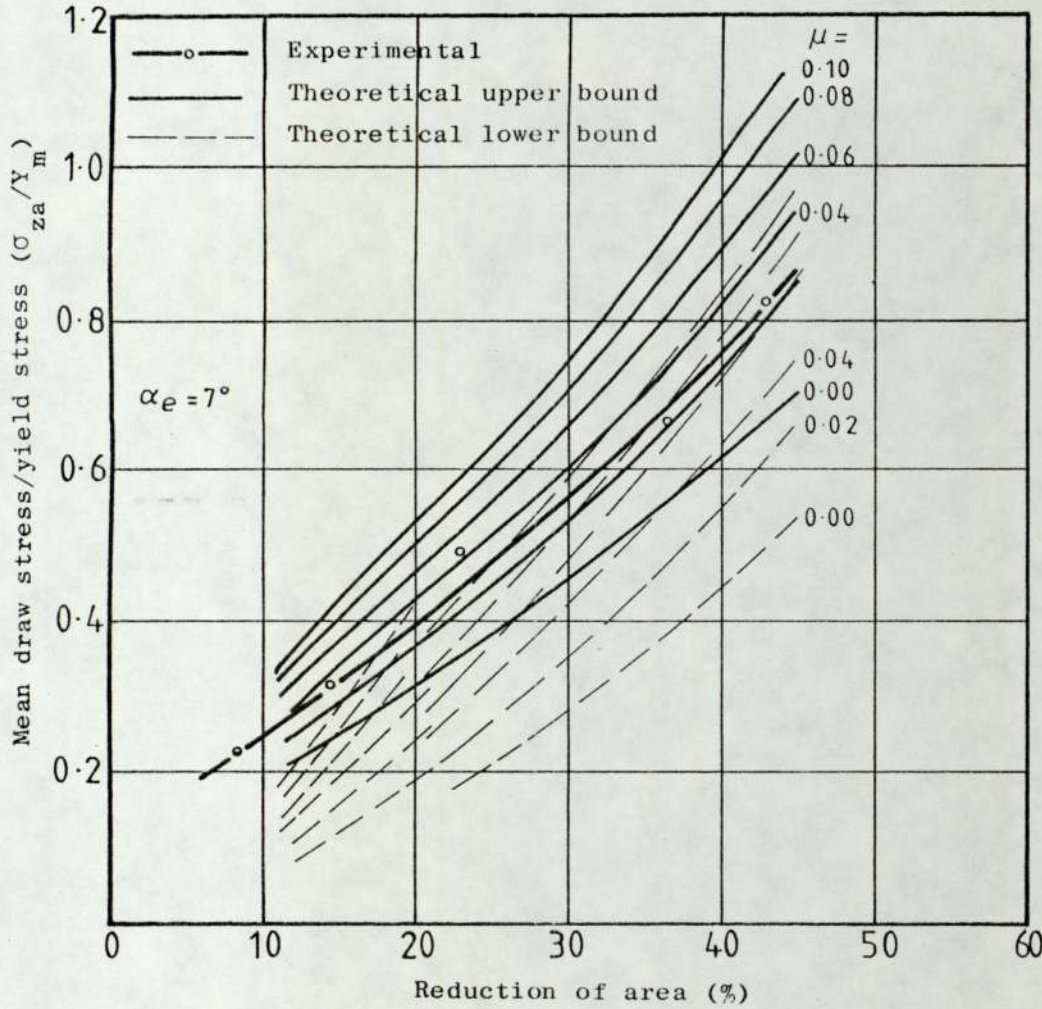


Fig. 7.33 Comparison between the experimental and theoretical draw stress from the upper and lower bound solutions in the drawing of round tube directly from round stock.

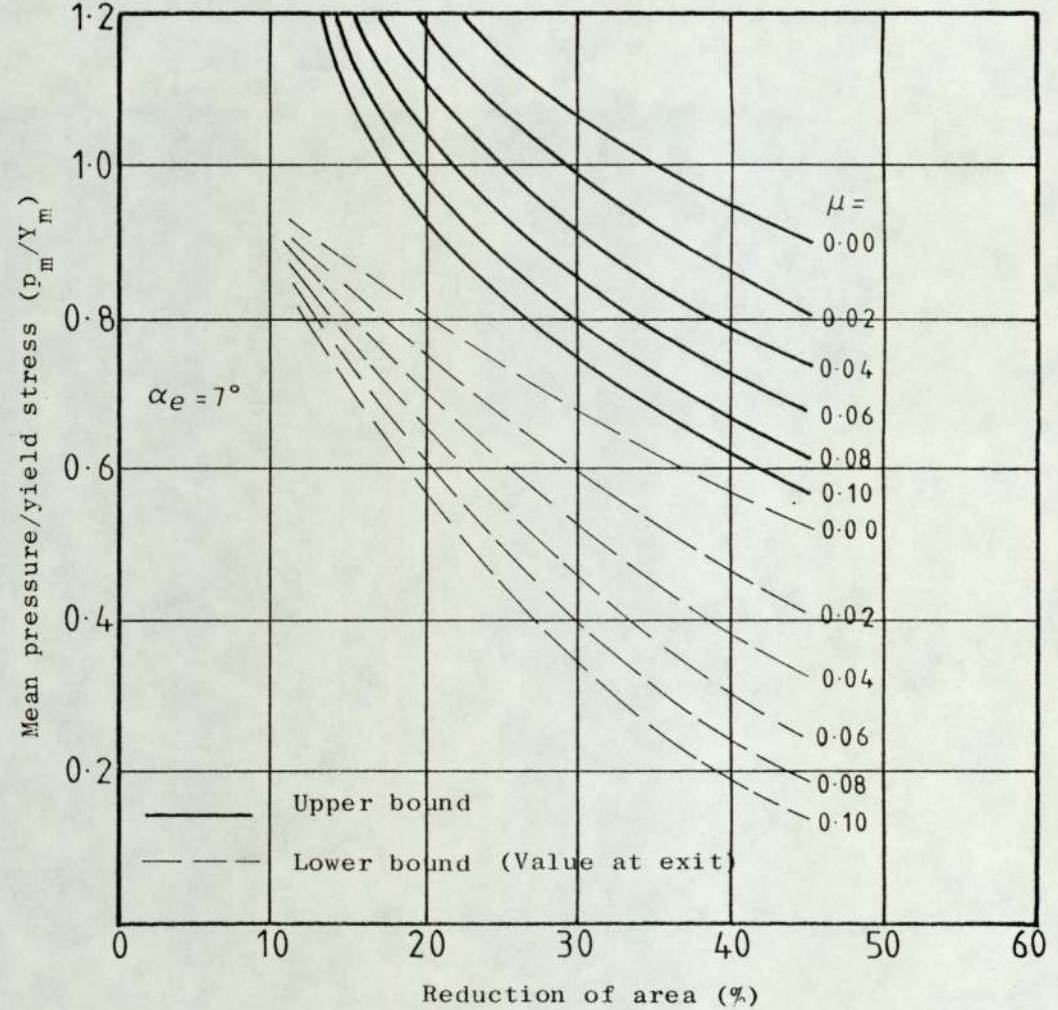


Fig. 7.34 Variation of the mean pressure with reduction of area and coefficient of friction for the upper and lower bound solutions in the drawing of round tube directly from round stock.

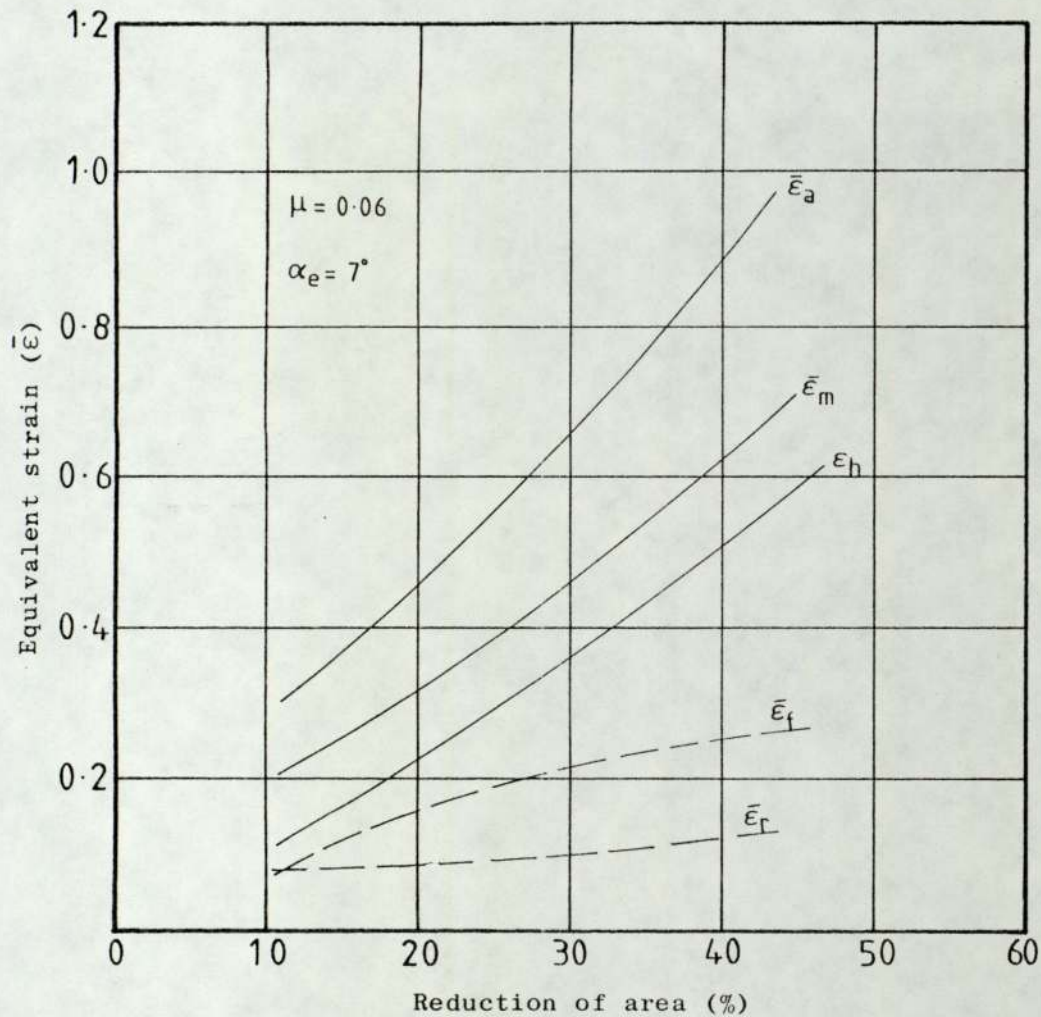


Fig. 7.35 Variation of apparent strain and the equivalent strain components with reduction of area in the drawing of round tube directly from round stock on a cylindrical plug.

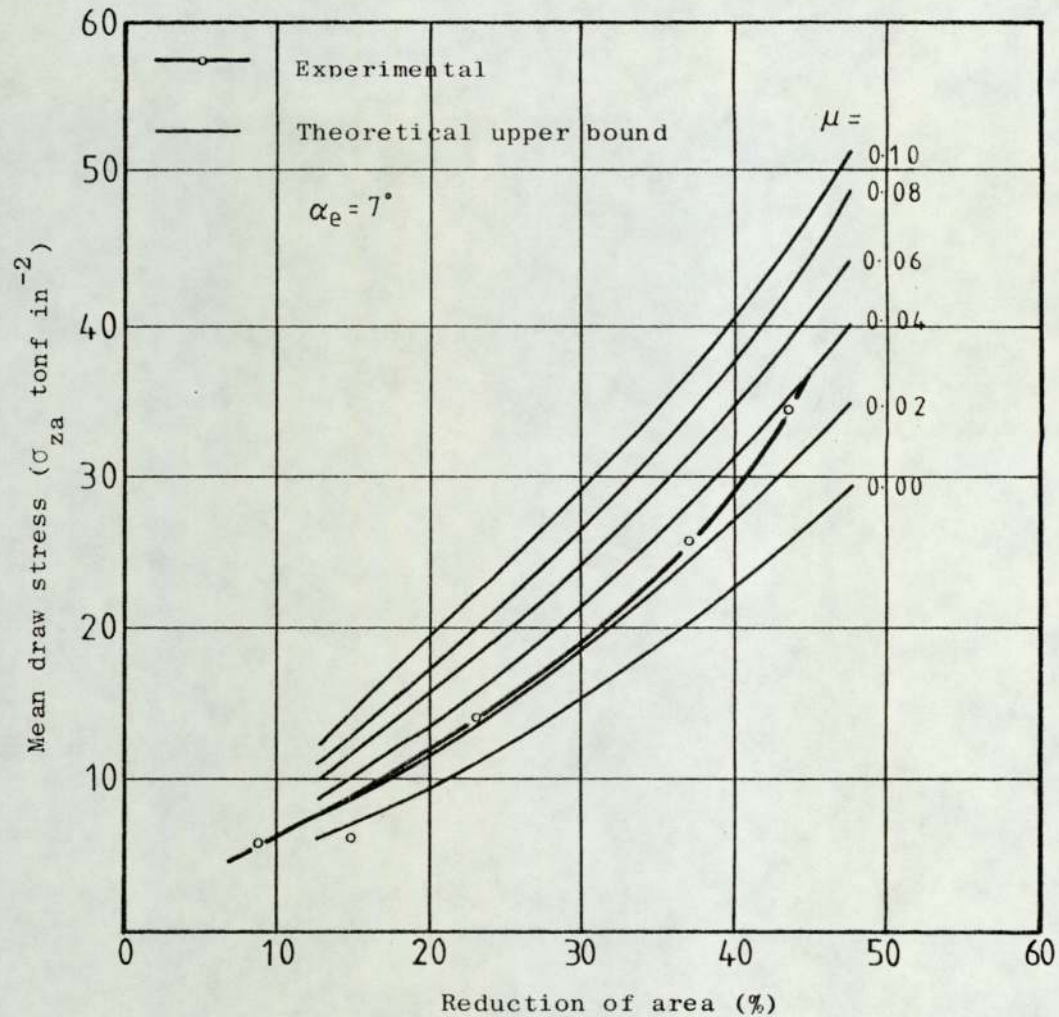


Fig. 7.36 Comparison between the measured draw stress and the values predicted by the upper bound theory for drawing of round tube directly from round stock on a cylindrical plug.

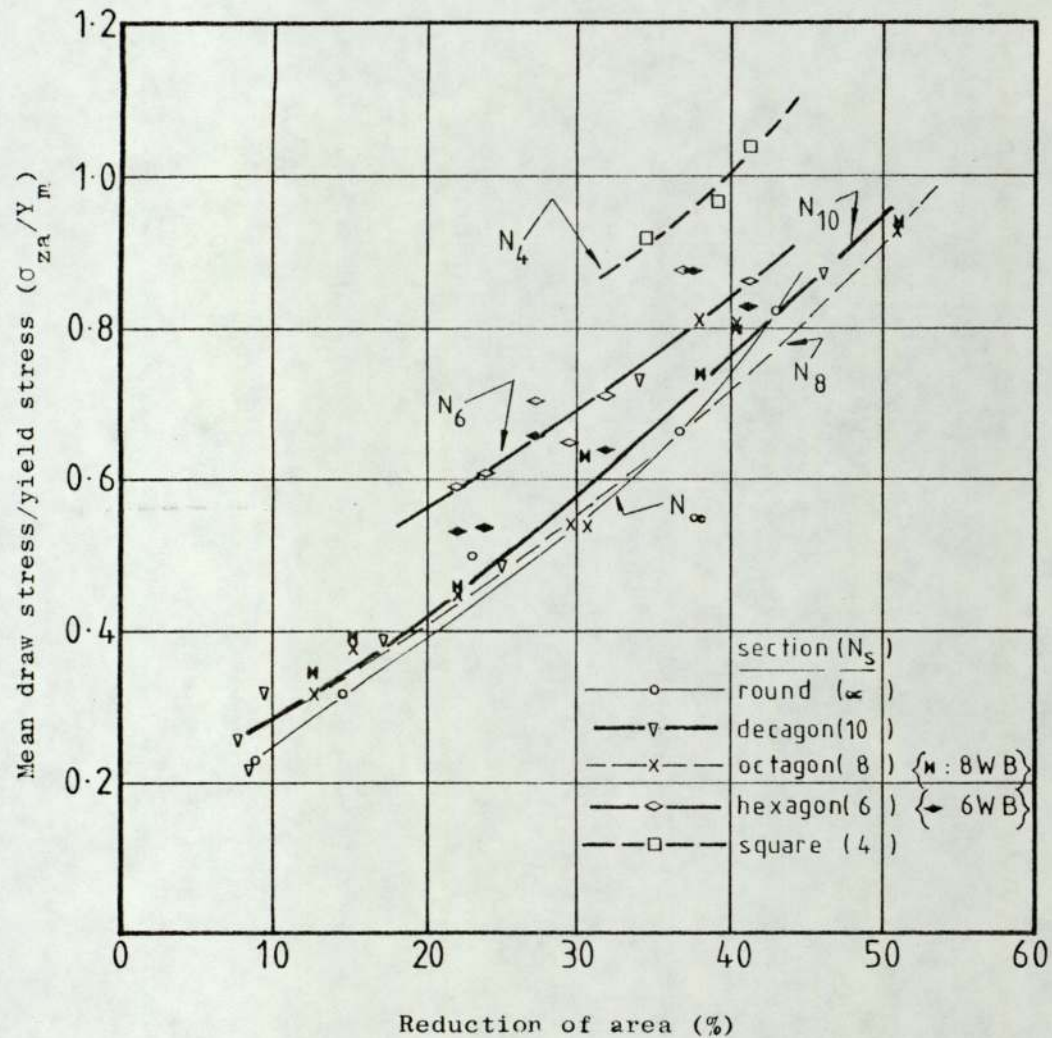


Fig. 7.37 Mean draw stress versus the reduction of area for the drawing of square, hexagonal, octagonal, decagonal and round tube directly from round on a cylindrical plug.

CHAPTER 8

DISCUSSION OF RESULTS

## 8.1 INTRODUCTION

The results of the investigation of drawing polygonal tube from round stock on a cylindrical plug are discussed under three main headings, namely:

- (i) theoretical results
- (ii) experimental results, and
- (iii) other observations.

The theoretical account deals with the effect of the following parameters on the drawing processes:

- draw force
- mean pressure
- mean coefficient of friction
- limitation of achievable reduction of area, and
- equivalent die semi-angle.

Further, the upper bound solution facilitated the design of an optimal tube drawing die to give a superior drawn section and dissipate the least amount of work in the forming process.

The experimental part of the project provided data to establish the accuracy and reliability of the adopted theoretical method of analysis. In addition, this section of the project evaluated the drawing process as a basis for industrial application. It was pointed out in Chapters 3 and 4 that the transformation of a round tube in a single die to form a polygonal section with the bore remaining circular can take various shapes. Preliminary tests were carried out on the available section rod drawing dies (see Table A-11.1 on page A113) to select a geometrical die passage which produced a polygonal tube with sharp corners whilst dissipating the least amount of energy to effect the deformation. On the basis of the theoretical analysis, dies of this optimal profile were manufactured for the tube drawing

processes.

The last section of the Chapter discusses formation of pick up, tensile failure and effects of excessive deviation from the close pass drawing on the quality of the output section.

## 8.2. THEORETICAL RESULTS

### 8.2.1 Introduction

The theoretical analysis of drawing a regular polygonal tube directly from round with the bore remaining the same resulted in expressions which were solved numerically using a computer. The two solutions, the lower and the upper bound, predict the draw loads to within reasonable limits of the experimental values. Further, the optimisation of the die design using the developed upper bound solution was achieved satisfactorily.

### 8.2.2 Upper bound

The upper bound solution was obtained from a velocity field that minimizes the energy to effect the deformation and incorporates an apparent strain method to include Coulomb friction. The velocity pattern was developed by conformal mapping of triangular elements from entry plane to the positions at the exit plane. Therefore, the solution accounts for the mode of deformation.

Figures 7.1, 7.9, 7.17, 7.25 and 7.31 show the variation of the total draw stress against the equivalent die semi-angle ' $\alpha_e$ ' predicted by the upper bound solution and the lower bound solution. As expected the value of the draw stress from the upper bound is higher compared with that from the lower bound solution. The lower bound solution neglects the redundant work whilst the upper bound solution accounts for the work of shear at both the entry and exit to the deformation zone together with the relative shearing within the

metal.

The results of the upper and the lower bound solutions for a given area reduction were plotted for a range of mean coefficients of friction. Each of the curves for the upper bound solution exhibits a minimum value of the draw load. This is explained by the variation in magnitude of the redundant and frictional work components with the die semi-angle. The friction work increases with decreasing die semi-angle due to the larger contact area on the shallower die; on the other hand increasing the die semi-angle to reduce the contact area increases the redundant work. As seen in the same diagrams (e.g. Figure 7.1), the optimum equivalent die semi-angle increases with increasing value of the mean coefficient of friction. It is apparent that increasing the mean coefficient of friction causes a higher total draw stress. This higher total draw stress produced by the increase in friction may be minimized by reducing the contact length of the die, i.e. increasing the die semi-angle.

Figures 7.5, 7.13, 7.21, 7.29 and 7.35 show that the redundant strain decreases and the frictional strain component increases with the increase in reduction of area for a given value of the mean coefficient of friction. For a given tube outer diameter increasing the bore size increases the plug-tube contact area which increases the friction component. The redundant work decreases with increase in reduction of area because of the shallower depth of shear planes at the exit and entry to the deformation zone. Although the upper bound solution gives overall results which approximate quite closely to the experimental values, it should be treated with caution when analysing the individual components since these will change quantitatively with the selected velocity field. However, this statement should not render the variation of the strain components with reduction of area ineffective.

Figures 7.2, 7.10, 7.18, 7.26 and 7.32 show the variation of the optimal die semi-angle with the reduction of area for a mean coefficient of friction,  $\mu = 0.06$ . In close pass drawing a change in reduction of area is brought about by altering the bore size or the die size or both for a given tubing outer diameter. In this thesis, the diagonal length of the section dies was standardized at 1 inch; therefore, changes of area reductions were achieved by changing the bore size for any given tube stock. Hence an increase in reduction of area causes a larger plug contact area which increases friction. In order to balance the increase in friction it is generally expected that the contact length of the die-tube interface would be reduced, i.e. an increase in the die semi-angle. However, this increase in the die semi-angle is distinctively evident at high reductions of area where the increased frictional strain component is markedly high. Also in the case of square section where the outer diameter of the input stock equals the diagonal length of the die and the work of shear is proportionally high, the change in the die semi-angle with increased reduction of area is fairly slight (see Figure 7.2).

### 8.2.3 Lower bound

The lower bound analysis was based on the equilibrium of forces of an elemental slug of the material undergoing plastic deformation; it led to the formulation of the differential equation (3.82) involving the stress system produced and the physical configuration. The method does not however, take into account, an increase in the drawing stress produced by the onset of redundant shearing and as a result it underestimates the magnitude of the draw forces especially at large equivalent die semi-angles where the redundant work is at its greatest. The draw load obtained by the integration of the basic differential equation (3.82) can be shown, for the case of  $N_s^0 = \infty$ , to comprise

approximately of a constant term and a second term which incorporates the mean coefficient of friction and the die semi-angle. The latter originates from the integration of the frictional force at the tool-workpiece interfaces and apparently decreases with die semi-angle (i.e. shorter contact lengths). The former term represents the homogeneous component which is virtually a constant for a given reduction of area. (At low values of die semi-angles the lower bound solutions exceed the upper bound values and it is realized that this is inadmissible.)

Although the lower bound analysis over-simplifies the mechanics of the process by ignoring the effect of the pattern of flow, the analysis involved is usually straightforward and forms an important conjugate in the upper bound analysis. In general, as shown in Figures 7.3, 7.11, 7.19, 7.27 and 7.33, the draw stress of the lower bound solution rises rapidly at higher reductions of area where the friction component has the greatest effect.

#### 8.2.4 Limitation of achievable reduction of area

The upper limit of the possible reduction of area can be read directly from the upper bound solution of drawing a polygonal tube from round on a cylindrical plug, since the draw stress cannot exceed the mean yield stress of the drawn metal.

Unlike the situation of axisymmetric drawing on a cylindrical plug (i.e. close pass drawing), there is a minimum reduction of area, for a given tube outer diameter, in the direct drawing of section tube. In the polygonal tube drawing on a plug, the material cannot expand laterally (to fill up the corners) and therefore the diagonal of the drawn tube is smaller than or at its greatest equal to the outer diameter of the input stock. This is illustrated below thus:  
In case of polygonal tube drawing from a stock of outer diameter

$$D_a = H_a,$$

$$\text{Area at entry, } A_b = \frac{\pi}{4} H_a^2 - A_p \quad (8.1)$$

$$\begin{aligned} \text{Area at exit, } A_a &= \frac{H_a}{\sqrt{2}} \frac{H_a}{\sqrt{2}} - A_p \\ &= \frac{H_a^2}{2} - A_p \end{aligned} \quad (8.2)$$

$$\text{Therefore, reduction of area 'r' = } 1 - \frac{\frac{H_a^2}{2} - A_p}{\frac{\pi}{4} H_a^2 - A_p} \quad (8.3)$$

Using a solid bar as a limiting case of a tube then  $A_p = 0$ , and the minimum allowable reduction of area for the 'tubing' becomes:

$$'r' = 36.34\%$$

The limiting reductions of area, based on geometry, for other sections are given in Figure A-2.1 together with a family of curves for a range of  $t_b/D_b$ , where the outer diameter of the input stock equals the diagonal length of the section die.

#### 8.2.5 Mean pressure

Figures 7.4, 7.12, 7.20, 7.28 and 7.34 show the variation of the mean die pressure with the reduction of area for a range of mean coefficients of friction. The die pressure predicted by either the upper or the lower bound solution decreases with increase in reduction of area and the value of the mean coefficient of friction for a given draw section. † The variation of the mean pressure with friction can be illustrated by considering the Tresca's yield criterion which expresses the pressure at exit to the die in terms of the draw stress and the mean yield stress, i.e:

$$\sigma_{za} + p = Y_m \quad (8.4)$$

For a given reduction of area, the draw stress  $\sigma_{za}$  is always greater at higher values of coefficient of friction because of the larger friction component. For example:

†

Please see page 155a for a continuation of the discussion.

$$\sigma_{za} \mu=0.03 > \sigma_{za} \mu=0.02 \quad (8.5)$$

Using equation (8.4), the above relation becomes:

$$\left| Y_m - p \right|_{\mu=0.03} > \left| Y_m - p \right|_{\mu=0.02} \quad (8.6)$$

But  $Y_m$  is a constant for the same reduction of area:

the above inequality becomes:

$$-p \mu=0.03 > -p \mu=0.02$$

or:

$$p \mu=0.03 < p \mu=0.02 \quad (8.7)$$

### 8.3 EXPERIMENTAL RESULTS

#### 8.3.1 Introduction

The main objective of the experimental part of the project was to correlate the theoretical predictions with the actual data. The performance of different geometrical shapes of draw dies including those employed in conventional industrial processes (see Plates 8.1 and 8.2) was evaluated in order to find a die profile to produce a successful draw with minimum draw force. Using this ideal geometrical shape, further three dies for the hexagon, octagon and the square were manufactured for tube drawing to establish the reliability of the predictions from the theory.

The other parameter affecting the draw load and the mean pressure is the mean coefficient of friction which was determined experimentally using the split rotating die rig. The semi-analytical method, developed in Chapter 4 to determine the mean coefficient of friction from the estimated redundant work in the drawing process and the application of the apparent strain analysis, produced results which compared well with the directly measured values. However, the values

of the mean die pressure were lower than those predicted by either the upper or the lower bound solutions.

### 8.3.2 Draw force

The theoretical and experimental results are tabulated in Appendices A-4 and A-5. A sample of the theoretical data is compared with that obtained from experiments in Table 8.1. The upper bound overestimates the experimental values by an average of 11.34%, 9.64% and 8.65% for the hexagonal, octagonal and decagonal tubes respectively. Figures 7.6, 7.14, 7.22, 7.30 and 7.36 show a more general comparison of the measured and calculated values of the mean draw stress for the various polygonal sections and a range of reductions of area.

The theory was developed for a close pass drawing. However, in practice a small amount of sink is unavoidable in the early stages of the draw (in this thesis the range of tubes available to give the desired range of reductions of area was limited especially for the square and the hexagon); and to counteract the effect of the proportion of sink present in different reductions of area, the draw load was expressed as a ratio of the mean yield stress of the drawn metal. This technique also has a slight advantage of minimizing the influence of the initial yield stress of the undrawn tube on the results. The geometrical shape of the deformation zone changes for some die shapes when tubing outer diameter is different from that used in the design; this is associated with increased level of redundancy.

The experimental and theoretical draw loads are plotted together in Figures 7.3, 7.11, 7.19, 7.27 and 7.33. As shown in these figures the upper bound tends to give a better estimation of the total draw loads at high reductions of area. In close pass drawing, low reductions of area were obtained from thick-walled tubing where the stock outer diameter approaches that of the diagonal length of the

Table 8.1 Comparison between the measured and calculated draw loads in the drawing of polygonal tubes directly from round stock on a cylindrical plug

Tube o.d.(in) x gauge (in)	Test number	Tube section	Die	Equivalent die semi- angle ( $\alpha_e$ degrees)	Reduction of area** (%)	Mean draw stress $\sigma_{za}$ (tonf in <sup>-2</sup> )		$\frac{(\sigma)_{theo} - (\sigma)_{act}}{(\sigma)_{act}} \times 100$ (%)
						Theoretical ( $\sigma$ ) theo	Experimental ( $\sigma$ ) actual	
1 1/8 x 1/4	107	hexagon	6WB	8	41.75	41.9386	37.5856†	11.34
						{1.0222}	-	-
1 1/8 x 3/16	078	octagon	8WB	8	51.95	44.7000	38.5130	16.00
						{1.0781}	{0.9475}	{13.88}
1 1/8 x 3/16	072	octagon	8PB	7	51.95	44.8384	41.4832	8.09
						{1.0808}	{0.9351}	{15.58}
1 1/8 x 1/4	012*	octagon	8PB	7	41.75	36.4959	34.8106	4.84
						{0.9145}	{0.8230}	{16.00}
1 1/8 x 3/16	066	decagon	10QB	7	46.95	40.1880	36.4340	10.34
						{0.9889}	{0.8694}	{13.74}
1 1/8 x 1/4	016*	decagon	10QB	7	37.73	34.4829	32.2413	6.95
						{0.8734}	{0.8143}	{7.27}
1 1/8 x 3/16	062	round	∞RA	7	37.78	32.6882	25.8447	26.50
						{0.8363}	{0.6641}	{25.92}

{ } denotes the stress expressed as a ratio of the yield stress and the corresponding % over-estimate of the actual value

\* test number with asterisk denotes first batch of tubes (Appendix A-3.2)

\*\* reduction of area in the actual experiment is slightly lower

† the tag broke and the load is therefore an instantaneous value

section die. As shown in Figures 7.5, 7.13, 7.21, 7.29 and 7.35, the relative shearing of the metal in the deformation zone and at the entry and exit shear surfaces contributed considerably to the total work at low reductions of area. It is thought that an improved velocity pattern would be needed by finer triangular network during conformal mapping. However, this would be accomplished at the expense of increased computer time (the time for 282 elemental triangles was 1500 m.u).

The reliability of the experimental results is indubitable since they were obtained with reliable instruments calibrated under the standard methods together with standard material heat treated purposely for the experiments. Any major discrepancy would therefore be attributed to the theoretical analysis. The upper and the lower bound solutions were built up on several assumptions to simplify the complex analytical expressions in the application of the energy method and in incorporating the apparent strain method to include Coulomb friction. In the analysis, an equivalent circular mode on the external surfaces was introduced which is not the true shape of the deformation zone. However, the shape factors  $f(s)$  and  $R(s)$  (equations 3.34 and 3.44) accounted for the actual shape of the output section tube in the case of the internal work of deformation and the redundant work at the entry and exit shear surfaces respectively. The friction work factor  $I_2$  (equation 3.56) required the integration of the elemental surface velocities which was beyond the scope of the research. Another assumption that was used in both solutions is the close pass drawing, whereas in practice there is always some amount of draft.

As was expected the experimental data are enveloped by the upper and the lower bound solutions and thus indicates the reliability of two solutions developed for predicting the draw loads. It was brought

out in the last paragraph that the main weakness in the developed upper bound solution is that it does not embody the actual identity of the shape of the deformation zone. However, the overall agreement of the theoretical and experimental values proves the validity of the adopted theory in the analysis of polygonal tube drawing directly from round stock on a cylindrical plug.

The total draw force versus the reduction of area for different shapes of section tubes is shown in Figure 7.37. For a given reduction of area, the square section exhibits the highest draw stress followed by the hexagonal tube. However, as the number of sides of the drawn section increases (i.e. the octagon, decagon and round) the observed trend is not consistent over the entire range of area reductions. It does not generally follow that for a given reduction of area, the section with the fewer number of sides experiences a draw stress higher than that of the following section with higher number of sides or vice versa. The non-consistent pattern could be explained by the variation of the redundant work and frictional work components with reduction of area for the different shapes of tubes. By changing the tubing outer diameter, plug size or both, it is possible to draw a tube section of sides  $N_s(i+2)$  with a reduction of area equal to that of a section with less number of sides  $N_s(i)$ . In the situation where the bore size is kept constant, the reduction of area can be varied by changing the outer diameter of the input tube and the method becomes analogous to that of the solid bar drawing (ref (2)). Table 8.2 gives the areas of the die-stock interfaces for a series of stock outer diameters calculated for an elliptical plane surface die. It shows that for a given reduction of area, the die-workpiece contact surface of a section  $N_s(i)$  is less than that for the corresponding section with higher number of sides  $N_s(i+2)$ . In case of a solid section it would be argued that increased

Table 8.2 Comparison of areas of the elliptical die-workpiece interface for the different shapes of sections under the same reduction of area

Reduction of area (%)	$N_S(i)$ section	$N_S(i+2)$ section
	(Stock o.d. (in))	(Corresponding stock o.d. (in))
	{die-workpiece surface area (in <sup>2</sup> )}	{die-workpiece surface area (in <sup>2</sup> )}
36.34	square	hexagon
	(1)	(1.1397)
	{2.5069}	{3.1190}
43.61	square	hexagon
	(1 1/16)	(1.2110)
	{3.3832}	{4.2201}
17.30	hexagon	octagon
	(1)	(1.0434)
	{1.1503}	{1.2331}
9.97	octagon	decagon
	(1)	(1.0193)
	{0.6547}	{0.6743}
20.25	octagon	decagon
	(1 1/16)	(1.0830)
	{1.4955}	{1.5436}
26.09	decagon	round
	(1 1/8)	(1.1632)
	{2.1451}	{2.2752}
17.13	decagon	round
	(1 1/16)	(1.0985)
	{1.2582}	{1.3321}

friction work for the section with  $N_s(i+2)$  sides would outweigh the higher redundant work at low reductions of area for a section with  $N_s(i)$  sides. In this particular thesis, the reductions of area were obtained by varying the outer diameter of the tube, the plug diameter or both. The amount of redundant work and the friction work components will vary with different  $t_b/D_b$  of the input stock even though the same reduction of area is involved in the particular section.

### 8.3.3 Die geometry

As discussed in section 4.3, die geometry is the factor having the greatest effect on the successful drawing of the polygonal tube directly from round stock. The geometry embodies the shape of the deformation zone and the equivalent die semi-angle. The effect of the latter on the drawing process is discussed together with dies designed for tube drawing.

#### 8.3.3.1 The shape of the deformation zone

The section rod dies used in the tests are shown in Plates 8.1 and 8.2. The details of their design from the point of view of the profile, material and the nomenclature are presented in Appendix A-11. The three additional dies manufactured for tube drawing are also displayed in Plates 8.3 and 8.4. Plate 8.3 includes two square section dies which burst during the drawing process.†

A sample of the output sectional tubes from different dies are presented in Plates 8.5 to 8.9. The absolute values of the draw

† The tube drawing die 4WB burst into bits during its first draw and the failure was attributed to the misalignment of the bolster and the pellet axes when shrink-fitting. The section rod drawing die 4JB disintegrated into four parts when experimenting with a steel solid bar of a relatively higher yield stress than that expected to be used with the die.

loads for the square, hexagonal and octagonal dies are compared in Tables 8.3, 8.4 and 8.5 respectively. A further comparison of the performance of these dies is made graphically in Figures 7.7 and 7.8 (square), 7.15 and 7.16 (hexagon) and Figures 7.23 and 7.24 (octagon), and numerically in Tables 8.6 and 8.7 for the hexagonal and octagonal draw.

The drawing of a square tube directly from round on a plug proved to be the severest of all sections; for any given tube size, the material elements suffer the greatest lateral displacement as they flow through the deformation zone. A further problem was the high reductions of area involved; the feasible reductions of area were over 40%. The available thick walled tubing (size 1 in o.d. x  $\frac{1}{4}$  in gauge) for the square gave reductions of area of 48.45% for the close pass draw. Whenever excessive amounts of sink were introduced to obtain feasible reductions, various problems were experienced. The corner sharpness of the drawn polygon was inferior.†† The pre-sunk bore might not form back to round, which was especially noticeable when the outer diameter of input stock was nearer or equal to the diagonal length of the section die. Where the diameter of the tubing was greater than the diagonal of the section die, the increased level of sinking which was intimately associated with increased redundant work caused the tube breakage at the throat to the die.

To use a very thick walled tube to obtain lower permissible reductions of area (i.e. almost a solid bar) would introduce a further problem commonly found in fixed plug drawing, i.e. chatter. The

†† Corner sharpness may be defined as of that section which completely filled the drawing die. However, some roundness of the output section was inevitable in most cases when the number of sides equals 4 or 6 and the word 'sharpness' was coined for comparative purpose.

Table 8.3 Comparison of the measured draw and plug forces from the different square drawing dies

Tube size outer dia- meter (in) x gauge (in)	Internal diameter (in)	Plug diameter (in)	Reduction of area %	Test No. (for reference)	Draw load (tonf) (Plug force (tonf))				Draw stress, $\sigma_{za}$ (tonf in <sup>-2</sup> ) (Mean yield stress, $Y_m$ (tonf in <sup>-2</sup> ) {Draw stress/mean yield stress}			
					Die 4HA	Die 4KD	Die 4MC	Die 4GB	Die 4HA	Die 4KD	Die 4MC	Die 4GB
1 x 3/16	0.625	0.488	34.61	- ; - - ; 103	-	-	-	10.0968	-	-	-	32.2619
								(1.5093)				(35.1218)
												{0.9186}
1 x 7/32	0.5625	0.470	39.19	126;125 124;102	10.4032	8.5968	8.7097	9.4355	31.8623	26.3296	26.6754	28.8984
					(01.8056)	(1.0833)	(1.3796)	(0.9722)	(35.5142)	(26.8306)	(31.6713)	(29.9333)
									{0.8972}	{0.9813}	{0.8423}	{0.9654}
1 x 7/32	0.5625	0.485	41.28	130;129 128;138	11.2903	9.4355	9.2097	9.6772	35.8133	29.9297	29.2134	30.6971
					(1.4815)	(1.3889†)	(1.2685)	(1.3426)	(35.4651)	-	(31.5646)	(29.6035)
									{1.0098}		{0.9255}	{1.0369}
1 x 1/4	0.490	0.470	45.29	132; - 131,104	12.2581	-	11.7742	11.1290	37.5432	-	36.0612†	35.5672†
					(1.9599)		(2.2222†)	(0.8333†)	35.7736			
									{1.0495}			
1 x 1/4	0.490	0.470	47.56	133; - - ; -	12.1371	-	-	-	38.7813	-	-	-
					(1.7940)				(38.5334)			
									{1.0064}			

† short length of drawn tube broke (or instantaneous loads)

Die	Shape	Remarks
4HA	Pyramidal (radius)	Industrial with land
4KD	Inverted parabolic	Section bar drawing
4MC	Triangular	Section bar drawing
4GB	Elliptical	Section tube drawing

Table 8.4 Comparison of the draw loads from the different hexagonal drawing dies

Tube size outer diameter (in) x gauge (in)	Internal diameter (in)	Plug diameter (in)	Reduction of area (%)	Test No (for reference)	Draw Force (tonf) (Draw stress $\sigma_{za}$ (tonf in <sup>-2</sup> ))				Mean yield stress (tonf in <sup>-2</sup> ) (Draw stress/mean yield stress)			
					Die 6BA	Die 6AA	Die 6NB	Die 6WB	Die 6BA	Die 6AA	Die 6NB	Die 6WB
1 x 1/4	0.490	0.485	22.13	136; 135 083; 088	9.0726 (19.5122)	9.6169 (20.6925)	8.1720 (17.5835)	7.3064 (15.7211)	29.3285 (0.6656)	30.0165 (0.6894)	29.6414 (0.5932)	29.5976 (0.5312)
1 x 7/32	0.5625	0.577	24.41	119; 118 084; 089	7.7419 (19.0767)	7.8360 (19.3086)	7.3185 (18.0335)	6.3710 (15.6986)	29.1403 (0.6547)	29.6398 (0.6514)	29.6219 (0.6088)	29.2124 (0.5374)
1 x 3/16	0.625	0.620	27.37	- ; - 085; 090	-	-	8.5484 (24.5931)	8.0376 (23.1237)	-	-	34.7238 (0.7082)	35.1014 (0.6588)
1 1/16 x 7g (0.177)	0.7085	0.620	29.41	121; 120 018; 044	8.3266 (23.4330)	7.8226 (22.5050)	7.1048 (20.4401)	6.6734 (19.1981)	32.3915 (0.7395)	30.9460 (0.7272)	31.3922 (0.6511)	-
1.040 x 0.235	0.570	0.557	31.71	- ; + 115; 114	-	-	10.2621 (25.2866)	9.1935 (22.6536)	-	-	35.3379 (0.7156)	35.4403 (0.6392)
1 1/16 x 8g (0.160)	0.7425	0.682	37.35	- ; - 086; 092	-	-	8.7634 (30.8363)	8.0645 (28.3769)	-	-	31.4409 (0.9808)	32.1920 (0.8815)
1 1/16 x 7g (0.176)	0.7086	0.682	42.28	032; 031 047; 059	10.1075 (35.5657)	9.2645 (32.5994)	9.3548 (32.9173)	8.8710 (31.2476)	-	-	-	-

† short length of drawn tube broke (or instantaneous loads)

Die	Shape	Remarks
6BA	Pyramidal (straight)	Industrial die with land
6AA	Pyramidal (radius)	Industrial die with land
6NB	Elliptical	Section bar drawing
6WB	Elliptical	Section tube drawing

Table 8.5 Comparison of the measured draw loads from the different octagonal drawing dies

Tube size outer dia- meter (in) x gauge (in)	Internal diameter (in)	Plug diameter (in)	Reduction of area (%)	Test No (for reference)	Draw force (tonf)			Mean yield stress $Y_m$ (tonf in <sup>-2</sup> ) (Draw stress / yield stress)		
					(Draw stress, $\sigma_{za}$ (tonf in <sup>-2</sup> )	Die 8SD	Die 8PB	Die 8WB	Die 8SD	Die 8PB
1 x 1/4	0.490	0.485	12.48	- ,068 073	-	4.2200 (8.0786)	4.8387 (9.2631)	-	25.5203 (0.3166)	26.3611 (0.3514)
1 x 7/32	0.5625	0.557	13.68	116; 069 074	8.5484 (18.4455)	3.9314 (8.4831)	4.2338 (9.1356)	33.6891 (0.7154)	24.0575 (0.3526)	26.0606 (0.3506)
1 x 3/16	0.625	0.620	15.34	- ; 070 075	-	4.7581 (11.7425)	5.1613 (12.7376)	-	30.8370 (0.3808)	32.1543 (0.3961)
1.040 x 0.235	0.570	0.557	22.02	117; 112 113	11.1693 (24.1009)	6.8952 (14.8782)	6.9355 (14.9652)	26.2930 (0.7015)	32.4826 (0.4580)	33.2793 (0.4497)
1 1/16 x 7g(0.177)	0.7085	0.682	30.58	053; 082 081	10.2419 (29.9645)	6.1021 (17.4733)	6.6935 (19.5829)	-	32.9337 (0.5420)	30.6807 (0.6383)
1 1/8 x 3/16	0.750	0.682	38.10	- ; 071 076	-	11.2500 (32.9137)	9.8790 (28.9026)	-	40.6743 (0.8092)	39.0518 (0.7401)
1 1/16 x 8g (0.160)	0.748	0.745	40.22	- ; 079 077	-	7.7218 (28.4733)	7.1371 (26.3173)	-	35.1844 (0.8093)	32.8293 (0.8016)
1 1/8 x 3/16	0.750	0.745	50.89	- ; 072 078	-	11.2500 (41.4832)	10.4516 (38.5391)	-	44.4484 (0.9333)	40.6752 (0.9475)
1 1/8 x 8g (0.160)**	0.805	0.745		055; 028 -	12.9032† (47.5791)	11.2097 (41.3345)	-	-	39.1239 (1.0565)	-
1 1/16 x** 10g(0.128)	0.806	0.740	26.28	054; 010 -	9.3548 (34.4948)	6.5726 (23.7256)	-	-	36.7613 (0.6454)	-

†Short length of drawn stock (or instantaneous loads); \*\* first batch of tubes

Die	Shape	Remarks
8SD	Inverted parabolic	Section bar drawing
8PB	Elliptical	Section bar drawing
8WB	Elliptical	Section tube drawing

resulting thinner plug bar might suffer from severe elastic extension and relaxation during the draw and thereby causing a variation in the draw load.

The persistent breakage of tube due to high reductions of area involved coupled with the physical limitations mentioned above for the square tube drawing, were major drawbacks in establishing a conclusive mode of the die passage. Despite these problems, the elliptical plane surface square die 4GB produced a series of tubes (see Plates 8.5 and 8.8) with relatively 'sharper' corners than those of other geometrical shapes. The measured draw loads were in some cases slightly higher than those recorded from either the inverted parabolic or the triangular plane surface dies (see Table 8.3).

The industrial pyramidal die (4HA) successfully drew tubes with reductions of area of 47.56%. The die passage formed by radiused surfaces has a variable mean equivalent die semi-angle and is complicated and tedious to analyse. Unlike other plane surface/conical surface dies, it is harder to machine and therefore, too expensive for research work. The corner 'sharpness' of the tube drawn through the industrial die was, however, inferior to that of the triangular die for the same reduction of area.

In general, the other polygonal sections showed the elliptical plane surface to be the optimal profile (see Plates 8.6, 8.7 and 8.9). It produced better cornered sections whilst dissipating the least amount of energy under the same draw conditions. The shape of the deformation zone of this die provides a gradual change in shape and a simultaneous reduction of area; it has a further advantage of being easily machined.

The inverted parabolic die (8SD) produced the highest draw load for the octagonal set of dies. Also this die profile 'D' (conventional die for hydrostatic extrusion of section rods) produced the most distorted section tube (see 4KD in Plate 8.5). These characteristics were due to the sudden change in shape through which the material had to undergo and consequently increased redundant work.

The straight pyramidal die shape 'A' (conventional die for symmetric drawing of section rods) was unsuccessful in producing a square tube due to the tensile failure (4DA in Plate 8.5). The hexagonal dies 6AA and 6BA produced section tubes with relatively inferior corners to those exhibited by the draw dies formed by the elliptical plane surfaces. Furthermore, the loads were higher than those of the elliptical plane surface dies for the same reduction of area.

The triangular die (4MC) produced tubes with corner 'sharpness' comparable with those from the elliptical plane surface die (4GB).

#### 8.3.3.2 The optimal tube drawing dies

(The effect of the die semi-angle on the draw loads and the quality of the drawn tube)

Having selected the optimal shape of the deformation zone, the other important factor was the optimum die semi-angle ' $\alpha_e$ '. The effect of this parameter was assessed by designing dies as predicted by the upper bound theory for drawing polygonal tubes directly from round stock; their performances were compared with those of the available section rod drawing dies of the same geometrical shape (i.e. elliptical plane surface). The square (4JB), the hexagonal (6NB) and the octagonal (8PB) solid section drawing dies were designed for an equivalent angle of  $7^\circ$  (it is shown in Appendix A-10

that the definition of the equivalent die semi-angle for a solid section drawing die is equally applicable to the tube drawing case when the bore of the stock remains unchanged).

It was shown in section 8.2.2 during the discussion of the upper bound solution that for a given tube size and a mean coefficient of friction, the graph of the total draw load against the equivalent die semi-angle has a minimum point. Therefore, for a curve corresponding to a mean coefficient of friction obtained experimentally or otherwise, the optimum die semi-angle can be interpolated. The die semi-angle corresponding to the mean coefficient of friction of  $\mu = 0.06$  for the square, hexagonal and octagonal curves give an optimal die semi-angle of  $8^\circ$  for different reductions of area for each particular polygon. The same equivalent die semi-angle was maintained so as to be able to compare results from different draw sections. The outer diameter of the input stock used in the design of the solid section dies for the individual polygon was retained.

The square die 4JB (see Plate 8.3) was not available during the final tests with the last batch of tubes which was specially heat treated for tube drawing experiments. The die designed for the square draw (4GB) did not perform as expected and one major aspect contributing to this failure is the lack of thick-walled tubes to give low and feasible reductions of area.

The results of the hexagonal dies 6NB and 6WB are compared in Table 8.6. In general, the optimal tube drawing die (6WB) showed a marked improvement of 5% to 13% reduction in draw stress for area reductions ranging from 22.13% to 42.28%. The drawn tubes are displayed in Plates 8.6 and 8.9 and they indicate clearly an improvement in the surface finish and the corner 'sharpness' (the hexagonal die 6NB made from tool steel had been used in the previous

Table 8.6 The effect of the equivalent die semi-angle on the draw loads for the hexagonal die of elliptical profile.

Tube size outer diameter (in) x gauge (in)	Internal diameter (in)	Plug diameter (in)	Reduction of area (%)	Test number (for reference)	Draw force (tonf) (Draw stress, $\sigma_{za}$ (tonf in <sup>-2</sup> ))		Mean yield stress $Y_m$ , (tonf in <sup>-2</sup> ) (Draw stress/ $Y_m$ )		$\frac{(\sigma_{za})_{NB} - (\sigma_{za})_{WB}}{(\sigma_{za})_{NB}} \times 100$	$\frac{(\frac{\sigma_{za}}{Y_m})_{NB} - (\frac{\sigma_{za}}{Y_m})_{WB}}{(\frac{\sigma_{za}}{Y_m})_{NB}} \times 100$
					Die 6NB	Die 6WB	Die 6NB	Die 6WB		
1 x 1/4	0.490	0.485	22.13	083;088	8.1720	7.3064	29.6414	29.5976	10.59	
					(17.5835)	15.7211	(0.5932)	(0.5312)		10.45
1 x 7/32	0.5625	0.557	24.41	084;089	7.3185	6.3710	29.6219	29.2124	12.95	
					(18.0335)	(15.6986)	(0.6088)	(0.5374)		11.73
1 x 3/16	0.625	0.620	27.37	084;090	8.5484	8.0376	34.7238	35.1015	05.97	
					(24.5931)	(23.1237)	(0.7082)	(0.6588)		6.98
1 1/16 x 7g (0.177)	0.7085	0.620	29.41	018;044	7.1048	6.6734	31.3922	-	06.07	
					(20.4401)	(19.1981)	(0.6511)			-
1.040x 0.235	0.570	0.557	31.71	115;114	10.2621	9.1935	35.3379	35.4403	10.41	
					(25.2866)	(22.6536)	(0.7156)	(0.6392)		10.68
1 1/16x8g (0.160)	0.7425	0.682	37.35	086;092	8.7634	8.0645	31.4409	32.1920	07.97	
					(30.8363)	(28.3769)	(0.9808)	(0.8815)		10.12
1 1/16x7g (0.176)	0.7085	0.682	42.28	047;059	9.3548	8.8710	-	-	05.07	
					(32.9173)	(31.2476)				-

Die	$\alpha_e$	Design stock (o.d. (in))	Remarks
6NB	7	1.125	Section bar drawing die (tool steel)
6WB	8	1.125	Section tube drawing die (tool steel)

- 148 -

research work of rod and tube drawing and suffered from persistent formation of pickup). The dimensions of the drawn product across flats (A/F) and across corners (A/C)<sup>†</sup> agreed fairly well, and therefore apart from the severe pickup on the section rod drawing die the improvement was attributed confidently to the change in the die semi-angle.

The results of the elliptical plane dies 8PB and 8WB are shown in Table 8.7. The optimal tube drawing die showed a remarkable improvement in the draw loads especially at high reductions of area. However, at low reductions of area (where generally the outer diameter of the input stock is less than the die design input stock), the results were reversed. The trend could be explained as follows: For a given tube size, the shallower die 8PB has increased frictional surface; increasing the die angle (8WB) reduces the friction surface but has the effect of increased redundant component. It was shown in section 8.2.2. that at low reductions of area, the redundant work component predominates and therefore in general the shallower die (8PB) is better for drawing tubes at low reductions of area than the tube drawing die (8WB).

An improvement of the draw loads of 7% to 12% was recorded for the tube drawing die. Plates 8.7 and 8.9 also show an improvement in the surface finish and the corner 'sharpness'. When the drawn products were compared dimensionally,<sup>††</sup> the tubes from the section rod drawing

† Mean A/C (in) 6WB :	1.000	6NB :	1.000
A/F (in) 6WB :	0.870	6NB :	0.870
†† Mean A/C (in) 8WB :	1.000	8PB :	1.006
A/F (in) 8WB :	0.930	8PB :	0.950

Table 8.7 The effect of the equivalent die semi-angle on the draw loads for the octagonal die of elliptical profile

Tube size outer diameter (in) x gauge (in)	Internal diameter (in)	Plug diameter (in)	Reduction of area (%)	Test No (for reference)	Draw force (tonf) (Draw stress, $\sigma_{za}$ (tonf in <sup>-2</sup> ))		Mean yield stress $Y_m$ (tonf in <sup>-2</sup> ) (Draw stress/ $Y_m$ )		$\frac{(\sigma_{za})_{PB} - (\sigma_{za})_{WB}}{(\sigma_{za})_{PB}}$ x 100 %	$\frac{\left(\frac{\sigma_{za}}{Y_m}\right)_{PB} - \left(\frac{\sigma_{za}}{Y_m}\right)_{WB}}{\left(\frac{\sigma_{za}}{Y_m}\right)_{PB}} \times 100$
					Die 8PB	Die 8WB	Die 8PB	Die 8WB		
					1 x 1/4	0.490	0.485	12.48	068;073	4.2200 (8.0786)
1 x 7/32	0.5625	0.557	13.68	069;074	3.9314 (8.4831)	4.2338 (9.1356)	24.0575 (0.3526)	26.0606 (0.3506)	{07.69}	00.57
1 x 3/16	0.625	0.620	15.34	070;075	4.7581 (11.7425)	5.1613 (12.7376)	30.8370 (0.3808)	32.1543 (0.3961)	{08.47}	{04.02}
1.040 x 0.235	0.570	0.557	22.02	112;113	6.8952 (14.8782)	6.9355 (14.9652)	32.4826 (0.4580)	33.2793 (0.4497)	{00.58}	01.81
1 1/16 x 7g (0.177)	0.7085	0.682	30.58	082;081	6.1021 (17.4733)	6.6935 (19.5829)	32.9337 (0.5421)	30.6807 (0.6383)	{11.37}	{17.74}
1 1/8 x 3/16	0.750	0.682	38.10	071;076	11.2500 (32.9137)	9.8790 (28.9026)	40.6743 (0.8092)	39.0518 (0.7401)	12.19	08.54
1 1/16 x 8g	0.748	0.745	40.22	079;077	7.7218 (28.4733)	7.1371 (26.3173)	35.1844 (0.8093)	32.8293 (0.8016)	07.52	00.95
1 1/8 x 3/16	0.750	0.745	50.89	072;078	11.2500 (41.4832)	10.4516 (38.5391)	44.4484 (0.9333)	40.6752 (0.9475)	07.10	{01.52}

{ } denotes (%) increase of draw load over the section bar drawing die

Die	$\alpha_e^o$	Design stock o.d. (in)	Remarks
8PB	7	1.125	Bar drawing die (tool steel)
8WB	8	1.125	Tube drawing die (tool steel)

die 8PB were found to be slightly larger. If this could not be attributed to the springback after drawing, then reductions of area from the section rod die were slightly lower than indicated. This adds a further credit to the tube drawing die.

In general the improvement of the draw loads and the surface finish for the hexagonal and octagonal tube drawing dies could be claimed, in turn, to be due to the differences in the equivalent die semi-angles.

#### 8.3.4 Evaluation of the mean coefficient of friction

The mean coefficient of friction as pointed out in Chapter 4 was determined using two methods, namely direct measurement and semi-analytically.

##### 8.3.4.1 Direct measurement

The mean coefficient of friction from the square split die from repetitive tests was 0.042 (see Table A-5.3). One of the die tips designed for the hexagonal drawing with the rotating rig broke during the first attempt (see Plate 8.10). The results were therefore limited to the square section where only two reductions were accomplished with a fair amount of sink.

The failure of the hexagonal die tips was possibly due to faulty heat treatment as has also been demonstrated in Ref. 2 (see Plate 8.11). There was no time to verify this claim but possible improvements are suggested in Chapter 10.

##### 8.3.4.2 Semi-analytical method

A sample of the experimental results is displayed in Tables A-5.4.1 and A-5.4.2. The values of the mean coefficients of friction in the drawing of various polygonal tubes compare reasonably with

those reported elsewhere (2). The results of the square section compare fairly with the directly measured value of 0.042.

### 8.3.5 Evaluation of the mean pressure

The mean die pressure was determined by the two methods, i.e. the split rotating die method and the semi-analytical technique as discussed in Chapter 4.

The values of the mean pressure from the split rotating die method are presented in Table A-5.3.1. The two feasible reductions of area produced consistent values of the mean pressures evaluated using equation 4.22.

Tables A-5.4.1 and A-5.4.2 give a sample of the mean pressure values obtained by the semi-analytical method. The values were dependent on the successful integration of the die-tube and tube-plug elemental velocities over the entire deformation zone given by  $I_1$  and  $I_2$  (or equations 3.52 and 3.56); an equivalent mode was used to estimate the mean velocity at the tool-workpiece surface. However, the values of the mean pressures obtained were lower than those of the upper and the lower bound solutions. For example, using test No. 021:

Section : hexagonal

Die : 6NB ( $\alpha_e = 7^\circ$ )

Tube size : 1 in x 3/16 in

Reduction of area: 28.39%

Theoretical mean pressure: 27.223 tonf in<sup>-2</sup>

Semi-analytical mean pressure: 11.893 tonf in<sup>-2</sup>

. . . deviation of the upper bound solution from the value obtained semi-analytically:

$$= \frac{27.223 - 11.893}{11.893} = 129\%$$

Further work is suggested in Chapter 10 to obtain the velocity distribution at the tool-workpiece interfaces which would facilitate the numerical integration of the friction factor  $I_2$ .

#### 8.4 Other observations

In general, the process of drawing a polygonal tube from round on a cylindrical plug has been accomplished successfully. However, there are some practical aspects that deserve attention, namely the formation of pickup, the tensile failure, the rounding of corners and the bore not forming circular whenever a high proportion of sink is present.

The pickup on the internal wall of the tube was not readily evident except when asperities welded onto the plug. This form of defect was noticed especially when drawing with the square dies using smaller diameter plugs.

Occasionally pickup was evident on the dies; the dies intended for research were made from tool steel which is prone to pickup after a number of drawing tests and, especially so, when heavy reductions are involved. Pickup on the dies or plugs could have been due to the breakdown of lubricant under high pressure in some parts of the deformation zone or could easily have been caused by small scale (or the swarf from swaged tag) which scour away the protective surface film, leaving bare metal. If two such surfaces come into contact under the working pressure they tend to weld together resulting in fragments of the workpiece being torn away by the subsequent shearing and left firmly adhered to the tool. The act of shearing exposes more nascent surface which usually projects through the surrounding lubricant film so that pickup becomes cummulatively worse. Whenever such situations arose reconditioning of the die was effected.

In general, the tensile fracture occurred when drawing with high reductions of area and was in fact a characteristic of the square tube tests. Another form of tensile failure that was noticed occasionally and when dealing with heavy reductions of area was the breakage of the drawn tube whenever drawing had been interrupted by intermittent stoppages. This could have been caused by either the breakdown of the hydrodynamic lubrication or the presence of residual stresses.

Under certain conditions of drawing a thick lubricant film separating the workpiece and the die can be established by the viscous force acting on the fluid; the breakdown of the film may cause metal to metal contact which results in high friction at the resumption of the draw. The hydrodynamic lubrication is favoured by a small angle between the workpiece and the die (thus forming the wedging action) and the relative high speeds. The tests in the laboratory were conducted at a relatively low speed of  $5 \text{ ft min}^{-1}$  but the geometry of the die passage may have created the conditions for hydrodynamic lubrication to be possible to some degree. An elliptical die is a combination of the plane surfaces and conical faces with a smaller conical angle.

On the other hand, there may be a variation in the pattern of residual stresses during the drawing operation and at the intermediate stoppages. The latter causes the tube to be gripped tighter with consequential increase in friction at the resumption of the drawing operation.

The corners of the drawn section were not as sharp as expected and especially when the results were compared with those of the solid sections in Ref. (2). Although close pass drawing was assumed, in practice there is always some amount of sink. The proportion of sink is often more significant at low reductions of area and when the

number of sides of the polygonal tube approaches that of the square. If the diameter of the input tubing is equal to that of the diagonal length of the drawing die, the drawn tube is then not likely to fill up the corners of the section die. Wherever there is sinking, the preformed bore takes the shape of the section die (see Plate 8.6, test 093) and on contact with a circular plug reshapes to round. Obviously redundancy is associated with the level of sink present in a given pass and the consequential increase in draw load is likely to cause the breakage of the tube. Furthermore, if the proportion of sink is high there may not be enough material to fill up the corners back to circular on contact with the plug. These problems were encountered greatly in the square drawing.

(continued from page 133 'mean pressure')

The theoretical pressure ratio curves of the upper bound analysis exhibit values greater than unity at low reductions of area (e.g. Fig. 7.34, page 125). By extrapolation when the reduction of area tends to zero the value of the mean pressure ratio rises to infinity, which is inadmissible. The theoretical reason for the rise in the mean pressure ratio curve follows from equation (3.61), page 54:

$$\frac{p_m}{\bar{Y}_m} = \frac{\bar{\epsilon}_m}{I_1(1-\Psi)}$$

When  $\mu = 0.0$ ,  $\Psi = 0$  ( $\Psi$  is zero, given by equation (3.59) because  $I_2 = 0$  (equation (3.56)).

$$\therefore \frac{p_m}{\bar{Y}_m} = \frac{\bar{\epsilon}_m}{I_1}$$

If, for example the axisymmetric case is considered (Appendix A-14, page A141),

$$I_1 = \frac{A_b - A_a}{A_a} \quad (\text{equation A-14.2, page A141})$$

$$= \frac{\text{red}}{1 - \text{red}}$$

$$\therefore \text{When red} = 5\%, \quad \frac{p_m}{\bar{Y}_m} = 19\bar{\epsilon}_m$$

$$\text{or when red} = 0\% \quad , \quad \frac{p_m}{\bar{Y}_m} = \infty$$

(extreme case)

The foregoing example shows that the validity of the results evaluated from equation (3.61) breaks down as the reduction of area decreases to low values. This may be explained by the fact that at low reductions of area the plastic relationship assembled in the upper bound theory is no longer applicable and the size of the deformation zone is such that elastic distortions can no longer be ignored. Because of this consideration it is thought inadvisable to plot mean pressure ratios greater than 1.2. Wistreich (24) has plotted values of pressure ratios (experimental-theoretical) greater than 1.2 and Basily (2) obtained theoretical pressure ratios up to 1.4.



PLATE 3.1 Conventional or industrial dies and sectional bar drawing dies used in the tube drawing experiments (see Table A-11.1 for details of nomenclature, design, etc.)



NEW DESIGN DIE

CONVENTIONAL DESIGN DIE

PLATE 3.2 The shapes of the deformation zone of the conventional pyramidal die formed by radiused surfaces and the elliptical/conical surface die (elliptical shape 'B') for the drawing of a polygonal section directly from round stock

4WB



4JB



4GB



PLATE 8.3. Square section drawing dies (shape 'B')

- (i) 4WB: Tube drawing die that burst during its first draw due to misalignment of the pellet and the bolster axes during shrink-fitting
- (ii) 4JB: Section bar drawing die which disintegrated into bits when attempting to draw a steel bar with a yield stress of about 45 tonf in<sup>-2</sup>
- (iii) 4GB: Tube drawing die



PLATE 8.4 Hexagonal (6WB) and octagonal (8WB) elliptical tube drawing dies

(ii) & (iii)



1 x 7/32; 4DA(pyramidal); test no.127  
int. dia : 0.562 ; plug size : 0.470 ; red : 39.19 %



1 x 1/4 ; 4GB(elliptical) ; test no.104  
int. dia : 0.490 ; plug size : 0.485 ; red : 45.29 %



1 x 1/4 ; 4MC(triangular); test no.131; red : 45.29 %



1 x 1/4 ; 4HA(pyramidal) ; test no.132; red : 45.29 %



1 x 1/4 ; 4JB(elliptical) ; test no.035  
int. dia : 0.500 ; plug size : 0.495 ; red : 48.45 %

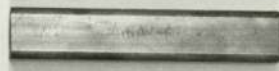


1 x 7/32 ; 4KD(inverted parabolic); test no.129  
int. dia : 0.562 ; plug size : 0.485 ; red : 41.28 %

(i) & (iv)



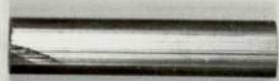
1 x 7/32 ; square ; red : 41.28 %  
int. dia : 0.562 ; plug size : 0.485



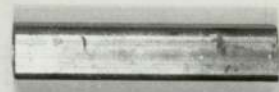
4GB; test no.138



4MC; test no.128



4HA; test no.130



4JB; test no.036  
(plug size : 0.495; red : 43.44 %)



4KD; test no.125  
(plug size : 0.470; red : 39.19 %)

PLATE 8.5 Square tube drawing  
The photograph shows:

- (i) tubes drawn through different dies
- (ii) transition zone exhibited by various die profiles, and
- (iii) mode of tensile fracture
- (iv) the comparison of the surface finish, corner 'sharpness' and the bore roundness when the condition of drawing is the same

(iv)



1 1/8 x 3/16; 6WB; Test no. 093  
int. dia : 0.750; plug size : 0.682; red: 48.54 %



1 1/8 x 8g; 6WB; Test no. 041  
int. dia: 0.805; plug size : 0.682; red: 41.14 %



(ii)

1 1/16 x 10g; 6WB; Test no. 095  
int. dia : 0.806; plug size : 0.745; red : 43.16 %



1 1/16 x 7/32; 6NB; Test no. 017  
int. dia : 0.625; plug size : 0.620; red : 40.05 %

(iii)



6WB; Test no. 045

(i)



1 x 7/32; hexagon; red : 24.41 %  
int. dia : 0.562; plug size : 0.557



6AA; Test no. 118



6BA; Test no. 119



6NB; Test no. 084



6WB; Test no. 089

PLATE 8.6 Hexagonal tube drawing

The photograph shows:

- (i) tubes drawn through industrial (6AA & 6BA) & section drawing dies
- (ii) effect of drawing at high reductions of area with a fair amount of sink (test 095)
- (iii) effect of equivalent die semi-angle on product under same drawing conditions, and
- (iv) transition zone when there is an excessive amount of sink (test 093)



1 1/8 x 3/16; 10QB(elliptical); Test no. 027  
int. dia : 0.750; plug size : 0.745; red : 45.89



(i.v) 1 3/16 x 1/4; 10QB(elliptical); Test no. 111  
int. dia : 0.687; plug size : 0.682; red : 49.80%



(i)

1.040 x 0.235; octagon; red : 22.02 %  
int. dia : 0.570 ; plug size : 0.557



(iii) 1 1/8 x 8g; 8SD(inverted parabolic); Test no. 055  
int. dia : 0.805; plug size : 0.745; red : 44.09 %



8SD; Test no. 117



1 1/8 x 3/16; 8PB(elliptical); red : 50.89 %  
int. dia : 0.750; plug size : 0.745; Test no. 072



8PB; Test no. 112

(ii)



8WB(elliptical) Test no. 078



8WB; Test no. 113

PLATE 3.7. Octagonal and decagonal tube drawing

The photograph shows:

- (i) tubes drawn through inverted parabolic & elliptical octagonal dies
- (ii) effect of equivalent die semi-angle on drawn tube
- (iii) transition zone on inverted parabolic die (test 055)
- (iv) transition of external surface when tube drawn through decagonal die has o.d. equal to that of the design stock (test 111)

					
o.d. x gauge	1 x 1/4		1 x 7/32		1 x 3/16
int. dia	0.490		0.562		0.625
4GB					
plug dia			0.470	0.485	0.488
red (%)			39.19	41.28	34.61
4MC					
plug dia			0.470	0.485	
red (%)			39.19	41.28	
4KD					
plug dia			0.470		
red (%)			39.19		
4HA					
plug dia	0.470	0.485	0.470	0.485	
red (%)	45.29	47.56	39.19	41.28	
4JB					
plug dia	0.470			0.495	
red (%)	45.29			43.44	

PLATE 8.8 Cross-section of tubes drawn through the square dies

o.d.	1			1 1/16			1 1/8	
gauge	0.255	0.219	0.187	0.160	0.176	0.219	0.187	0.250
int dia	0.490	0.562	0.625	0.745	0.708	0.625	0.750	0.625
6WB								
plug dia	0.485	0.557	0.620	0.682	0.682	0.620	0.620	
red (%)	22.13	24.41	27.37	37.35	42.28	40.05	37.06	
6NB								
6BA								
plug dia	0.485	0.557			0.620			
red (%)	22.13	24.41			29.41			
6AA								
8WB								
plug dia	0.485	0.557	0.620	0.745	0.682	0.620	0.745	0.620
red (%)	12.48	13.68	15.34	40.22	30.58	30.12	50.89	40.33
8PB								
8SD								
10QB								
plug dia	0.485	0.557	0.620	0.745	0.682	0.620	0.745	0.620
red (%)	07.85	08.54	09.56	34.13	24.97	25.35	45.89	37.02
alphaRA								
plug dia				0.745	0.682		0.745	0.620
red (%)				22.96	14.68		36.72	29.64

PLATES 8.9 Tube sections drawn directly from round stock on a cylindrical plug through the hexagonal, octagonal, decagonal and round dies displayed in Plates 8.1 & 8.4

(i)

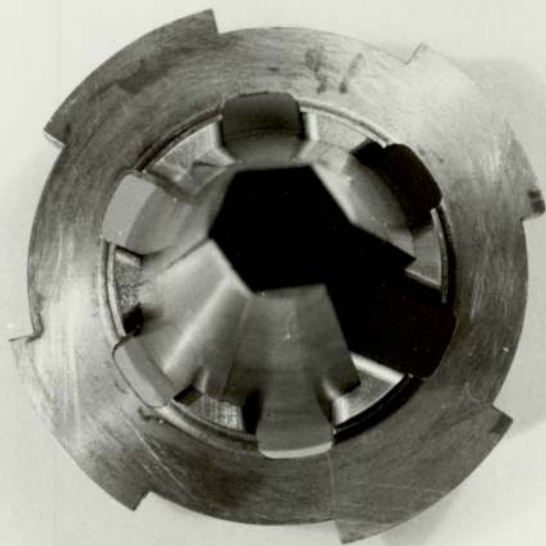


PLATE 3.10 Hexagonal die tips  
(i) enclosing a pyramidal passage  
and  
(ii) showing the breakage of one of the  
fingers was accelerated possibly  
by the rough swaged tag

(ii)



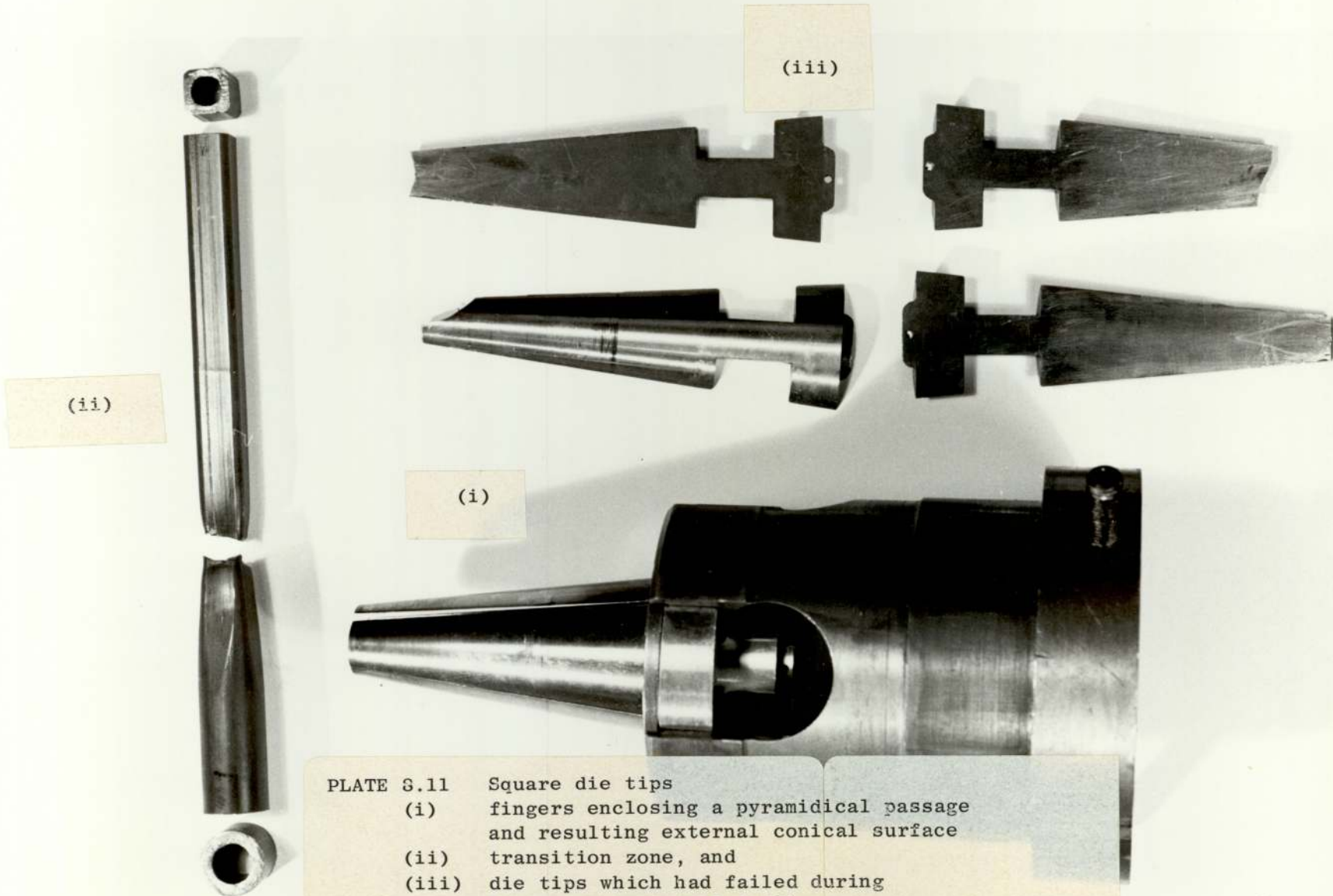


PLATE 3.11

Square die tips

- (i) fingers enclosing a pyramidal passage and resulting external conical surface
- (ii) transition zone, and
- (iii) die tips which had failed during tests reported in Ref (2)

CHAPTER 9

CONCLUSIONS

## 9. CONCLUSIONS

An extensive investigation of the mechanics of drawing polygonal tube from round stock on a cylindrical plug has been accomplished successfully both theoretically and experimentally to enable the following conclusions to be drawn:

1. The theoretical and experimental analyses have shown the feasibility of drawing regular polygonal tubes from round stock on a cylindrical plug in a single pass.
2. Generally there is good agreement between the theoretical and experimental values.

The lower bound solution and the upper bound solution bracket the experimental value to within close limits. For a given draw condition, the derived upper bound solution predicts a higher value of draw stress due to the account taken for redundant work whilst the simpler lower bound under-estimates the draw stress as it neglects the redundant effect.

3. A comparison of the performance of the various geometrical shapes of section dies used in other industrial application and in the drawing of a section bar directly from round showed the optimum geometrical profile to be elliptical. This die shape produced polygonal tubes with the sharpest corners whilst dissipating the least amount of energy. Consequently, a set of elliptical shaped dies was designed for the investigations of the polygonal tube drawing process.
4. Unlike the axisymmetric tube drawing problem, the shape of the die deforming passage forms an integral part of the analysis of the drawing of polygonal tube directly from round stock on a cylindrical plug.

5. Drawing of a square tube proved to be the severest of all polygonal sections. In addition to the limitations imposed by high reductions of area, the material suffers the greatest lateral displacement as the external surface of the workpiece transforms from round to a square with the bore remaining circular.
6. The optimisation of the equivalent die semi-angle as predicted by the upper bound solution produced satisfactory results. The optimal section dies designed for tubing showed notable performance over those for drawing polygonal bars directly from round stock. A reduction in the draw load was observed together with a distinct improvement on the corner sharpness of the sections when using hexagonal and octagonal rod- and tube-drawing dies. However, similar conclusive results cannot be claimed for the square sections due to high reductions of area encountered. The level of sink in the tubes drawn through the two square dies vitiated the conditions of drawing; the tubes so drawn were from different casts (the rod drawing die had burst before the final tests).
7. The semi-analytical method, which was developed to determine the mean coefficient of friction from the estimated redundant work and the apparent strain method, produced results which compared well with those from the direct measurement using the split rotating die. Although the experimental data available were only by the square die tips, the semi-analytical technique can be generalised to hold true in determining the mean coefficient of friction for other polygonal sections.
8. The understanding of the drawing process from the experimental and theoretical investigations is undoubtedly of practical value to manufacturers of nut blanks who would make substantial savings in raw material and capital investment in some stations of the production line. The developed theory and the accompanying

computer program form a useful guide when producing draw schedules and in the design of draw tools and the selection of the drawbench for the required dimensional series of the input-output stock.

CHAPTER 10

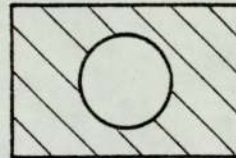
SUGGESTIONS FOR FURTHER WORK

10. SUGGESTIONS FOR FURTHER WORK

On the basis of the present study of mechanics of drawing regular polygonal tube directly from round stock on a cylindrical plug, further work is suggested as follows:-

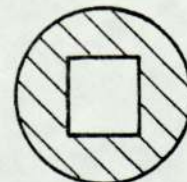
1. Irregular polygonal tube drawing

The derived theoretical solution could be generalised to account for drawing of irregular polygonal sections directly from round stock. In this class are the rectangular sections where, for a given input tube, the effect of changing the breadth to length ratio of the drawn section on the process loads would be of great interest.



2. Circular tube drawing from round on a polygonal plug in a single pass

In this case the forming die is conical but the plug takes one of the shapes already discussed for polygonal tube drawing dies (see Section 4.3). The study of the process (where the bore changes directly from round to a polygon whilst the external surface remains circular) requires the definition of an equivalent conical angle " $\alpha_e$ " for the plug and the conventional conical angle " $\alpha$ " for the die. The combination of the two angles and the shape of plug would constitute the major factors to be investigated for optimal drawing that gives the least work of deformation and a superior quality of the drawn section.



### 3. Polygonal tube drawing with back-pull

In the axisymmetric case, drawing with back-pull reduces the rate of die wear which is related to lower levels of die pressure (Blazynski (2), Chapter 6). This effect could be investigated in the drawing of polygonal tube with back-pull. For example, the input stock could be passed through an axially symmetric drawing die prior to the polygonal die. The study could include the determination of the proportion of draw loads and the estimation of the die pressures acting on the two dies.

The problem could be extended to the case where back-tension is provided by a polygonal die (i.e. polygonal tube drawing in tandem). Where the draw stress becomes exceedingly high (e.g. in square drawing) to offset the advantages of back-tension, it is suggested to use an input stock which had been drawn through a corresponding polygonal die in a separate operation (i.e. polygonal tube drawing in sequence).

### 4. Use of ultrasonic vibrations in polygonal tube drawing

When drawing with square and hexagonal sections high reductions of area were involved which resulted occasionally in tube breakage. Ultrasonic vibrations of the tools plastically deforming metals have the effect of reducing process loads and consequently greater reductions of area can be attained (Ref. (3)). Therefore, to overcome the problem of drawing at high reductions of area, it is suggested to investigate the effect of ultrasonic vibrations in the polygonal tube drawing process by vibrating the die radially or the plug axially. The vibrations also reduce

the coefficient of friction and thereby increase the tool life.

5. Evaluation of residual stresses in polygonal tube drawing

In polygonal tube drawing directly from round stock, the material deforms non-uniformly and residual stresses are bound to occur. To evaluate the level of disparity it is suggested that a metallurgical study of, say, the grain distortion across the drawn section be carried out.

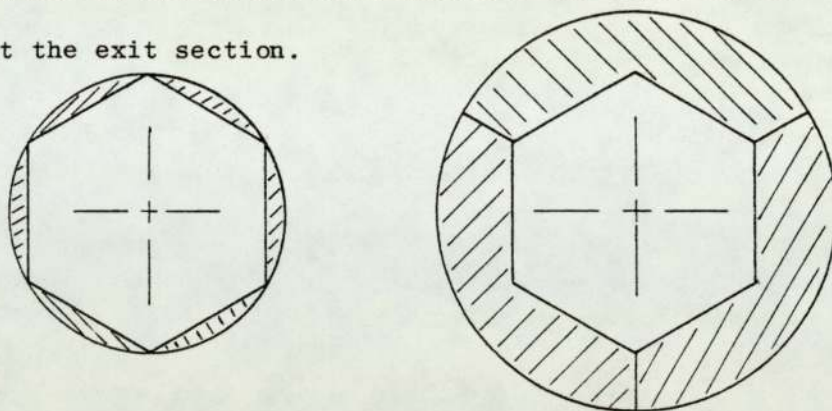
6. Visioplasticity in polygonal tube drawing

When applying the apparent strain analysis, expressions with surface velocities were simplified by introducing a mean velocity of an equivalent circular mode of the external configuration of the deformation zone. An improvement on the solution is suggested by obtaining the surface velocity distribution using visioplastic techniques. Further study using the methods is proposed; splitting the specimen through two planes of symmetry (i.e. across flats and across diagonals) will give further insight to the flow of metal and redundant deformation.

7. Inserts of the split rotating die

High reductions of area limited the range of tests when determining the mean coefficient of friction using the split rotating die for the square section. One of the hexagonal fingered die tips designed to fit the existing conical die, failed during the first draw. Even though the failure could have been due to heat treatment, the cross-section of the insert at the tip was fairly thin. When designing hexagonal,

octagonal and decagonal inserts it is suggested to use fewer number of splits and also increase the depth of the metal at the exit section.



8. Drawbenches (Appendix A-16)

'Sheffield' drawbench has been designed specifically for tube drawing; it is a stiffer bench than the 'Brookes' drawbench which is suitable for drawing solid bars. Since in polygonal tube drawing high reductions of area are encountered, a slight bending moment on the drawn tube which acts on the tag increases the stress to the point where the tube breaks. It is suggested that comparative studies be carried out on the drawing of tubes using the two drawbenches.

## REFERENCES

1. KARIYAWASAM, V.P.           The mechanics of drawing polygonal tube from round on a plug. Ph.D. thesis (1980) University of Aston in Birmingham.
2. BASILY, B.B.                The mechanics of drawing polygonal section rod from round bar. Ph.D. thesis (1976) University of Aston in Birmingham.
3. SANSOME, D.H.             People, pence and plasticity. Inaugural lecture, University of Aston (4th March 1975).
4. DAVIS, E.A. &             The theory of wire drawing. J. Appl. Mech. 1944, vol. 11, A-193 to A-198.  
DOKOS, S.J.
5. HOFFMAN, O. &             An introduction to the theory of plasticity for engineers. Mcgraw-Hill Press, New York (1953). Chapters 15, 16 and 17.  
SACHS, G.
6. SIEBEL, E.                 Stahl u Eisen (Iron and Steel), 1947, vol. 66 - 67, pp. 171 - 180.
7. MACLELLAN, G.D.S.         Critical survey of wire industry. J. Iron Steel Inst. 1948, vol. 158, pp. 347 - 356.
8. WISTRIECH, J.G.          The fundamentals of wire drawing. Met. Rev. 1958, vol. 3 (10), pp. 97 - 142.
9. YANG, C.T.                 On the mechanics of wire drawing. Trans. ASME, series B, 1961, vol. 83 pp. 523 - 530.
10. JOHNSON, W. &          Wire drawing: A survey of theories. Wire SOWERBY, R.                 Industry, 1969, vol. 36, pp. 137 - 144 and 249 - 256.

11. ZIMMERMAN, Z. & AVITZUR, B. Metal flow through converging dies - a lower upper bound approach using generalised boundaries of the plastic zone. Trans. ASME, series B (Feb. 1970), vol. 92, pp. 119-129.
12. HILL, R. & TUPPER, S.J. New theory of plastic deformation in wire drawing. J. Iron Steel Inst. (1948), vol. 159, pp. 353-359.
13. SIEBEL, E. Application to shaping processes of Henky's laws of equilibrium. J. Iron and Steel Inst. (1947), vol. 155, pp. 526-534.
14. HILL, R. Mathematical theory of plasticity. Clarence Press (1950).
15. GREEN, A.P. & HILL, R. Calculations on influence of friction and die geometry in sheet drawing. J. Mech. Phys. Solids (1952), vol. 1. pp. 31-36.
16. GREEN, A.P. Plane theories of drawing. Proc. Inst. Mech. Engrs. (1960), vol. 174 (31), pp. 847-864.
17. JUNEJA, B.L. & PRAKASH, R. An analysis for drawing and extrusion of polygonal sections. Int. J. MTDR (1975), vol. 15, pp. 1-30.
18. PRAKASH, R. & KHAN, Q.M. An analysis of plastic flow through polygonal converging dies with generalised boundaries of zone of plastic deformation. Int. J. MTDR (1979), vol. 19, pp. 1-19.
19. SACHS, G. Z. ang. math. mech. (1927), vol. 7, pp. 235-236.
20. KÖRBER, F. & EICHENGER, A. Mitt. K.-W. I. Eisenf. (1940), vol. 22 (5), pp. 57-79.

21. LUNT, R.W. & MACLELLAN, G.D.S. An extension of wire drawing, with special reference to the contributions of K.B. Lewis, J. Inst. Met. (1946), vol. 72, pp. 65-96.
22. ATKINS, A.G. & CADDELL, R.M. The incorporation of work hardening and redundant work in rod drawing analyses. Int. J. Mech. Sci. (1968), vol. 10, pp. 15-28.
23. JOHNSON, R.W. & ROWE, G.W. Redundant work in drawing cylindrical stock. J. Inst. Met. (1968), vol. 96, pp. 97-105.
24. WISTRIECH, J.G. Investigation of the mechanics of wire drawing. Proc. Inst. Mech. Engrs. (1955), vol. 169, pp. 654-665.
25. SACHS, G., LUBAHN, J.D. & TRACY, D.P. Drawing thin-walled tubing with a moving mandrel through a single stationary die. J. Appl. Mech. (Dec. 1944), vol. 11, pp. A-199 to A-210.
26. ESPEY, G. & SACHS, G. Experimentation on tube drawing with a moving mandrel. Trans. ASME & J. Appl. Mech. (vol. 14), 1947, vol. 69, pp. A-81 to A-87.
27. SACHS, G. & BALDWIN, W.M. Stress analysis of tube sinking. Trans. ASME (1946), vol. 68, pp. 655-662.
28. SWIFT, H.W. Stresses and strains in tube drawing. Phil. Mag. series 7 (Sept. 1949), vol. 40 (308), pp. 883-902.
29. CHUNG, S.Y. & SWIFT, H.W. A theory of tube sinking. J. Iron Steel Inst. (1952), vol. 170, pp. 29-36.

30. BLAZYNSKI, T.Z. & COLE, I.M. An investigation of the plug drawing. Proc. Inst. Mech. Engrs. (1960), vol. 174, pp. 797-812.
31. BLAZYNSKI, T.Z. & COLE, I.M. An investigation of the sinking and mandrel drawing processes. Proc. Inst. Mech. Engrs. (1963-64), vol. 198 (part 1, No. 33), pp. 894-906.
32. PRAGER, W. & HODGE, P.G. Theory of perfectly plastic solids. Wiley, 1951. Chapter 8.
33. DRUCKER, D.C. & PROVIDENCE, R.L. Coulomb friction, plasticity and limit loads. J. Appl. Mech. (Mar. 1954), vol. 21, pp. 71-74.
34. AVITZUR, B. An analysis of central bursting defects in extrusion and wire drawing. Trans. ASME series B (1968), vol. 90, pp. 79-91.
35. ZIMMERMAN, Z. & AVITZUR, B. An analysis of the effect of strain hardening on central bursting defects in drawing and extrusion. Trans. series B (1970), vol. 92, pp. 135-145.
36. HILL, R. On the state of stress in a plastic-rigid body at the yield point. Phil. Mag. (1951), vol. 42, pp. 868-
37. JOHNSON, W. & MELLOR, P.B. Engineering plasticity. Van Nostrand, 1975. Chapter 13.
38. JOHNSON, W. Estimation of upper bound loads for extrusion and coining operations. Proc. Inst. Mech. Engrs. (1959), vol. 173, pp. 61-72.
39. KUDO, H. An upper bound approach to plane-strain forging and extrusion - I. Int. J. Mech. Sci. (1960), vol. 1, pp. 57-83.

40. ALEXANDER, J.M. Proc. Inst. Mech. Engrs. (1959), vol. 173, pp. 85-91.
41. KUDO, H. Some analytical and experimental studies of axisymmetric cold forging and extrusion - I. Int. J. Mech. Sci. (1960), vol. 2, pp. 102 -127.
42. KOBAYASHI, S. Upper bound solutions of axisymmetric forming problems - II. ASME WA-81, Winter Annual Meeting, Nov. 1963, paper No. 63.
43. HALLING, J. & MITCHELL, L.A. An upper bound solution for axisymmetric extrusion. Int. J. Mech. Sci. (1965), vol. 7, pp. 277-295.
44. KOBAYASHI, S. & THOMSEN, E.G. Upper bound and lower bound solutions to axisymmetric compression and extrusion problems. Int. J. Mech. Sci. (1965), vol. 7, pp. 127-143.
45. THOMSEN, E.G., YANG, C.T. & KOBAYASHI, S. Mechanics of plastic deformation in metal processing. MacMillan Press, 1965.
46. ADIE, J.G. & ALEXANDER, J.M. A graphical method of obtaining hodographs for upper bound solution to axisymmetric problems. Int. J. Mech. Sci. (1967), vol. 9, pp. 349-357.
47. AVITZUR, B. Analysis of wire drawing and extrusion through conical dies of large cone angle. Trans. ASME series B (1964), vol. 86, pp. 305-316.
48. AVITZUR, B. Analysis of wire drawing and extrusion through conical dies of small cone angle. Trans. ASME series B (1963), vol. 85, pp. 89-96.

49. AVITZUR, B. Metal forming: processes and analysis.  
Magraw-Hill Book Company, New York, 1968.
50. BASILY, B.B. & Some theoretical considerations for the  
SANSOME, D.H. direct drawing of section rod from round.  
Int. J. Mech. Sci. (1976), vol. 18, pp.201-208.
51. AVITZUR, B. Tube sinking and expanding. Trans. ASME  
series B (1965), vol. 87, pp. 71-79.
52. PRAKASH, R. & A general solution to axisymmetric contained  
JUNEJA, B.L. plastic flow processes. Proc. Brit. Conf.  
Engg. Prod., I.I.T. Delhi (Dec. 1976),  
pp. C-93 to C-107.
53. THOMSEN, E.G. & Experimental stress determination within a  
LAPSEY, J.T. metal during plastic flow. Proc. Soc. Exp.  
Stress Analysis (1952), vol. XI (No.2),  
pp. 59-68.
54. FRISCH, J. & Experimental study of metal extrusion at  
THOMSEN, E.G. various strain rates. Trans. ASME (1954),  
vol. 76, pp. 599-606.
55. THOMSEN, E.G. A new approach to metal forming problems -  
Experimental stress analysis for a tubular  
extrusion. Trans. ASME (1955), vol. 77,  
pp. 515-522.
56. SHABAIK, A.H. & Computer application to visioelasticity method.  
THOMSEN, E.G. Trans. ASME series B (May 1967), vol. 89,  
pp. 339-349.

57. MEDRANO, R.E. & GILLIS, P.P. Visioplasticity techniques in axisymmetric extrusion. *J. Strain Analysis* (1972), vol.7, pp. 170-177.
58. SHABAİK, A.H. & THOMSEN, E.G. A theoretical method for the analysis of metalworking problems. *Trans. ASME series B* (1968), vol. 90, pp. 343-352.
59. METHA, H.S., SHABAİK, A.H. & KOBAYASHI, S. Analysis of tube extrusion. *Trans. ASME series B* (1970), vol. 92, pp. 403-411.
60. ZIENKIEWICZ, O.C. *Finite element method in engineering science.* McGraw-Hill Co., London 1971.
61. PAULSEN, C.W. *Finite element analysis.* *Machine Design* (1971), vol. 43 (3 parts): Sept. 30 (No.24) pp. 46-52, Oct. 14 (No. 25) pp. 146-150, Oct. 28 (No. 26) pp. 90-94.
62. MARCAL, P.V. & KING, I.P. Elastic-plastic analysis of two dimensional stress systems by the finite element method. *Int. J. Mech. Sci.* (1967), vol. 9, pp. 143-155.
63. YAMADA, Y., YOSHIMURA, N. & SAKURAI, T. Plastic stress strain matrix and its application for the solution of elastic-plastic problems by finite element method. *Int. J. Mech. Sci.* (1968), vol. 10, pp. 343-354.
64. LEE, C.H. & KOBAYASHI, S. Elastoplastic flat punch indentation by the finite element method. *Int. J. Mech. Sci.* (1970), vol. 12, pp. 349-370.

65. ZIENKIEWICZ, O.C. & GODBOLE, P.N. Flow of plastic and visco-plastic solids with special reference to extrusion and forming processes. Int. J. Num. Meth. Engng. (1974), vol. 8, pp. 3-16.
66. HARTLEY, P., STURGESS, C.E.N. & ROWE, G.W. Friction in finite element analyses of metal-forming processes. Int. J. Mech. Sci. (1979), vol. 21, pp. 301-311.
67. IWATA, K., OSAKADA, K. & FUJINO, S. Analysis of hydrostatic extrusion by the finite element method. Trans. ASME series B (1972), vol. 94, pp. 697-703.
68. FIORENTINO, R.J., RICHARDSON, B.D. & SABROFF, A.M. Hydrostatic extrusion of billet materials - Role of die design and residual stress distribution. Metal Forming (1969), vol. 36 (no. 9), pp. 243-252.
69. LINICUS, W. & SACHS, G. Mitt. Dt. Mater. Anst. 'Spanlose formug der metalle', 1931, vol. 16, pp. 36-67.
70. NISHIHARA, T., KAKUZEN, M. & Tech. Rep. Eng. Inst. Kyoto University (1955), vol. 5, Rep. No.22, 75.
71. ROTHMAN, D. & SANSOME, D.H. An investigation of rod drawing with die rotation. Int. J. MTDR (1970), vol. 10, pp. 179-192.
72. MACLELLAN, G.D.S. Some friction effects in wire drawing. J.Inst. Met. (1952-53), vol. 81, pp. 1-13.
73. LANCASTER, P.R. & ROWE, G.W. (ii) Comparison of theoretical and experimental drawing stresses and the evaluation of the coefficient of friction. Proc. Inst. Mech. Engrs. (1963-64), vol. 178 (part 1, No.2), pp. 69-89.

74. TROZERA, T.A. On non-homogeneous work for wire drawing.  
Trans. ASM (1964), vol. 57, pp.309-323.
75. ATKINS, A.G. & The influence of redundant work when drawing  
CADDELL, R.M. rods through conical dies. Trans. ASME  
series B (1968) vol. 90, pp. 411-418.
76. BASILY, B.B. & 17th Int. MTDR Conf. (Sept. 1976)  
SANSOME, D.H.
77. THOMPSON, P.J. & Apparent strain method for analysis of  
SANSOME, D.H. steady-state metal-working operations.  
Metals Technology (Nov. 1976), vol.  
pp. 497-502.
78. PUGH, H.L.D Redundant work and friction in the hydrostatic  
extrusion of pure aluminium and aluminium  
alloy. J. Mech.Eng.Sci. (1964), vol. 6  
(No. 4), pp. 362-370.
79. VOCE, E. The relationship between stress and strain  
for homogeneous deformation. J.Inst. Metals  
(1948), vol. 74, pp. 537-562.
80. ERASMUS, L.A. Mechanical properties: significance of tensile  
test results. Metallurgia & Metal Forming  
(1975), vol. 42, pp. 94-97.
81. CADDELL, R. M. et al International Journal of Mechanical Engineering  
Education (1980), vol. 8.

#### BIBLIOGRAPHY

1. ROWE, G.W. Principles of industrial metalworking  
processes. Edward Arnold, 1977.



### ACKNOWLEDGEMENTS

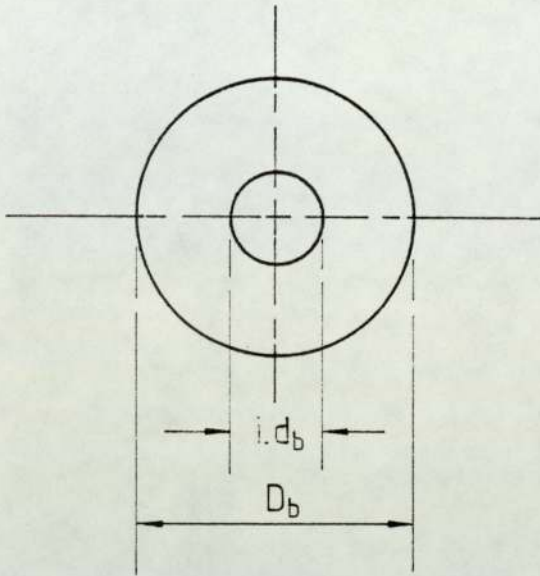
I am grateful to the Commonwealth Scholarship Commission for the grant to study at the University of Aston in Birmingham, and to the University of Nairobi (Kenya) for the study leave. I owe special thanks to Professor D.H. Sansome for the continued interest, support and discussion during the research and the preparation of the manuscript. I am heavily indebted to Mr. G.M. Jones, Mr. S. Twamley and the technical staff of the Production Engineering machine shop and the Communication Media Unit. I also extend my appreciation to Mrs. J. Neale and Mrs. E.A. Copeland for their effort and patience in typing the thesis.

Finally I wish to thank my wife Wanjiku and daughter Wanjugu, who tolerated 'energies', 'upper bounds', 'polygonal drawing', 'friction' and other things over the period of research.

APPENDIX

A-1 Geometrical relations for the input tube and the required polygonal tube maintaining the same bore

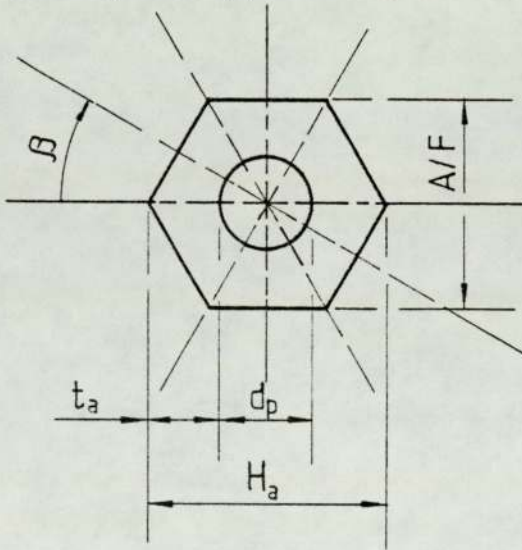
(a) Input tube section



$$A_b = \pi t_b^2 \left( \frac{1}{t_b/D_b} - 1 \right)$$

$$A_p = \frac{\pi}{4} d_p^2$$

(b) Output polygonal tube section



$$t_a = \kappa H_a, \text{ where } 0 < \kappa < \frac{1}{2}$$

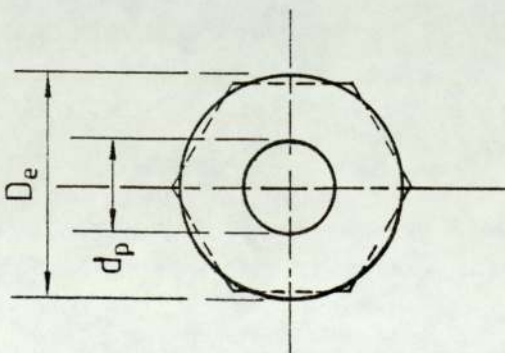
$$\text{and } \kappa = \frac{1}{2}(1 - d_p/H_a)H_a$$

$$A_a = H_a^2 \left( \text{SPARAM} - \frac{\pi}{4}(1 - 2\kappa)^2 \right)$$

$$\text{SPARAM} = N_s \cos \phi \cdot \sin \phi / 4$$

$$\phi = \beta = \text{included angle of the symmetric section } (= \frac{\pi}{N_s})$$

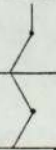
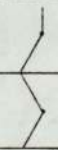
(c) Equivalent output section for axisymmetric drawing



$$D_e = 2R_e = \sqrt{(A_a + A_p)4/\pi}$$

Reduction of area,

$$'r' = 1 - A_a/A_b$$

No. of sides (Ns)	Section name	$\beta (= \pi/Ns \text{ rad})$ (degrees)	SPARAM	A/F ( $H_a = 1 \text{ in}$ )
3	triangular	60	0.3248	0.7500**
4	square	45	0.5000	0.7071
5	pentagon	36	0.5944	0.8090
6	hexagon	30	0.6495	0.8660
7	heptagon	25.71	0.6840	0.9010
8	octagon	22.5	0.7071	0.9239
9	nonagon	20	0.7231	0.9397
10	decagon	18	0.7347	0.9510
11	unidecagon	16.36	0.7434	0.9595
12	duodecagon	15	0.7500	0.9659
				
				
$\infty$	circular	0	0.7854	1.0000

\*\* the altitude of triangular section

A-2 PRELIMINARY SELECTION OF TUBES

TABLE No. A-2.1 Drawing square tube from round on a cylindrical plug

INPUT GAUGE ( $t_b$ in)		INPUT TUBE OUTER DIAMETER ( $D_b$ in)							
		1	$1 \frac{1}{16}$	$1 \frac{1}{8}$	$1 \frac{3}{16}$	$1 \frac{1}{4}$	$1 \frac{5}{16}$	$1 \frac{3}{8}$	$1 \frac{7}{16}$
$\frac{1}{16}$	$t_b/D_b$	0.0625	0.0588	0.0555	0.0526	0.0500	0.0476	0.0454	0.0435
	$1/A_b$	5.432	5.091	4.7882	4.524	4.289	4.073	3.875	3.706
	i.d. <sub>b</sub>	0.872	0.9345	0.997	1.0595	1.122	1.1875	1.25	1.3125
	$\kappa$	0.064	0.033	0.0015	-	-	-	-	-
	'r'	-	-	-	-	-	-	-	-
$\frac{1}{8}$	$t_b/D_b$	0.1250	0.1176	0.1110	0.1052	0.100	0.095	0.091	0.0869
	$1/A_b$	2.9103	2.715	2.5462	2.3951	2.2635	2.1385	2.0394	1.9388
	i.d. <sub>b</sub>	0.744	0.8065	0.869	0.9315	0.994	1.0625	1.125	1.1875
	$\kappa$	0.128	0.097	0.0655	0.0342	-	-	-	-
	'r'	0.8139	-	-	-	-	-	-	-
$\frac{3}{16}$	$t_b/D_b$	0.1875	0.1765	0.1667	0.1579	0.150	0.1428	0.1364	0.1304
	$1/A_b$	2.0894	1.9406	1.8113	1.6977	1.5978	1.5083	1.430	1.3577
	i.d. <sub>b</sub>	0.625	0.6875	0.750	0.8125	0.875	0.9375	1.00	1.0625
	$\kappa$	0.1875	0.1562	0.125	0.094	0.0625	0.312	-	-
	'r'	0.5963	0.7500	0.8946	-	-	-	-	-
$\frac{1}{4}$	$t_b/D_b$	0.25	0.2353	0.2222	0.2105	0.20	0.1905	0.1818	0.1739
	$1/A_b$	1.6976	1.5671	1.4549	1.3579	1.2732	1.1985	1.1316	1.0721
	i.d. <sub>b</sub>	0.50	0.5625	0.625	0.6875	0.75	0.8125	0.875	0.9375
	$\kappa$	0.25	0.2187	0.1875	0.1562	0.125	0.094	0.0625	0.0312
	'r'	0.4845	0.6058	0.7188	0.8251	0.9259	-	-	-
$\frac{5}{16}$	$t_b/D_b$	0.3125	0.2941	0.2778	0.2631	0.25	0.2381	0.2273	0.2174
	$1/A_b$	1.4816	1.3580	1.2538	1.1637	1.0865	1.0186	0.9588	0.9055
	i.d. <sub>b</sub>	0.375	0.4375	0.50	0.5625	0.625	0.6875	0.75	0.8125
	$\kappa$	0.3125	0.2812	0.25	0.2187	0.1875	0.1562	0.125	0.0875
	'r'	0.4228	0.5252	0.6193	0.7072	0.7901	0.8689	-	-
$\frac{3}{8}$	$t_b/D_b$	0.375	0.3529	0.3333	0.3158	0.30	0.2857	0.2727	0.2609
	$1/A_b$	1.3581	1.2344	1.1316	1.0448	0.9701	0.9054	0.8487	0.7990
	i.d. <sub>b</sub>	0.25	0.3125	0.375	0.4375	0.50	0.5625	0.625	0.6875
	$\kappa$	0.375	0.3437	0.3125	0.2812	0.25	0.2187	0.1875	0.1562
	'r'	0.3876	0.4775	0.5591	0.6347	0.7245	0.7724	0.8360	0.8972
$\frac{7}{16}$	$t_b/D_b$	0.4375	0.4118	0.3889	0.3684	0.35	0.3333	0.3182	0.3043
	$1/A_b$	1.2934	1.1643	1.0583	0.9670	0.8955	0.8314	0.7761	0.7274
	i.d. <sub>b</sub>	0.125	0.1875	0.25	0.3125	0.375	0.4375	0.50	0.5675
	$\kappa$	0.4375	0.4062	0.375	0.3437	0.3125	0.3812	0.25	0.2187
	'r'	0.3692	0.4500	0.5228	0.5709	0.6511	0.7093	0.7643	0.8171
$\frac{1}{2}$	$t_b/D_b$	-	0.4706	0.4444	0.4210	0.400	0.3809	0.3636	0.3478
	$1/A_b$	-	1.1318	1.0184	0.9258	0.8488	0.7834	0.7274	0.6790
	i.d. <sub>b</sub>	-	0.0625	0.125	0.1875	0.25	0.3125	0.375	0.4375
	$\kappa$	-	0.4687	0.4375	0.4062	0.375	0.3437	0.3125	0.2812
	'r'	-	0.4376	0.5033	0.5626	0.6173	0.6684	0.7166	0.7626
$\frac{5}{8}$	$t_b/D_b$								
	$1/A_b$								
	i.d. <sub>b</sub>								
	$\kappa$								
	'r'								

TABLE No. A-2.2 Drawing hexagonal tube from round on a cylindrical plug

INPUT GAUGE ( $t_b$ in)		INPUT TUBE OUTER DIAMETER ( $D_b$ in)							
		1	$1 \frac{1}{16}$	$1 \frac{1}{8}$	$1 \frac{3}{16}$	$1 \frac{1}{4}$	$1 \frac{5}{16}$	$1 \frac{3}{8}$	$1 \frac{7}{16}$
$\frac{1}{16}$	$t_b/D_b$	0.0625	0.0588	0.0555	0.0526	0.0500	0.0476	0.0454	0.0435
	$l/A_b$	5.432	5.091	4.7882	4.524	4.289	4.073	3.875	3.706
	i.d <sub>b</sub>	0.872	0.9345	0.997	1.0595	1.122	1.1875	1.25	1.3125
	$\kappa$	0.064	0.033	0.0015	-	-	-	-	-
	'r'	0.7159	-	-	-	-	-	-	-
$\frac{1}{8}$	$t_b/D_b$	0.1250	0.1176	0.1110	0.1052	0.100	0.095	0.091	0.0869
	$l/A_b$	2.9103	2.715	2.5462	2.3951	2.2635	2.1385	2.0394	1.9388
	i.d <sub>b</sub>	0.744	0.8065	0.869	0.9315	0.994	1.0625	1.125	1.1875
	$\kappa$	0.128	0.097	0.0655	0.0342	-	-	-	-
	'r'	0.3749	0.6218	0.8564	-	-	-	-	-
$\frac{3}{16}$	$t_b/D_b$	0.1875	0.1765	0.1667	0.1579	0.150	0.1428	0.1364	0.1304
	$l/A_b$	2.0894	1.9406	1.8113	1.6977	1.5978	1.5083	1.430	1.3577
	i.d <sub>b</sub>	0.625	0.6875	0.750	0.8125	0.875	0.9375	1.00	1.0625
	$\kappa$	0.1875	0.1562	0.125	0.094	0.0625	0.312	-	-
	'r'	0.2840	0.4601	0.6237	0.7764	0.9230	-	-	-
$\frac{1}{4}$	$t_b/D_b$	0.25	0.2353	0.2222	0.2105	0.20	0.1905	0.1818	0.1739
	$l/A_b$	1.6976	1.5671	1.4549	1.3579	1.2732	1.1985	1.1316	1.0721
	i.d <sub>b</sub>	0.50	0.5625	0.625	0.6875	0.75	0.8125	0.875	0.9375
	$\kappa$	0.25	0.2187	0.1875	0.1562	0.125	0.094	0.0625	0.0312
	'r'	0.2306	0.3717	0.5014	0.6222	0.7355	0.8421	-	-
$\frac{5}{16}$	$t_b/D_b$	0.3125	0.2941	0.2778	0.2631	0.25	0.2381	0.2273	0.2174
	$l/A_b$	1.4816	1.3580	1.2538	1.1637	1.0865	1.0186	0.9588	0.9055
	i.d <sub>b</sub>	0.375	0.4375	0.50	0.5625	0.625	0.6875	0.75	0.8125
	$\kappa$	0.3125	0.2812	0.25	0.2187	0.1875	0.1562	0.125	0.0875
	'r'	0.2013	0.3222	0.4318	0.5334	0.6276	0.8009	0.8807	-
$\frac{3}{8}$	$t_b/D_b$	0.375	0.3529	0.3333	0.3158	0.30	0.2857	0.2727	0.2609
	$l/A_b$	1.3581	1.2344	1.1316	1.0448	0.9701	0.9054	0.8487	0.7990
	i.d <sub>b</sub>	0.25	0.3125	0.375	0.4375	0.50	0.5625	0.625	0.6875
	$\kappa$	0.375	0.3437	0.3125	0.2812	0.25	0.2187	0.1875	0.1562
	'r'	0.1846	0.2929	0.3899	0.4785	0.5889	0.6370	0.7091	0.7777
$\frac{7}{16}$	$t_b/D_b$	0.4375	0.4118	0.3889	0.3684	0.35	0.3333	0.3182	0.3043
	$l/A_b$	1.2934	1.1643	1.0583	0.9670	0.8955	0.8314	0.7761	0.7274
	i.d <sub>b</sub>	0.125	0.1875	0.25	0.3125	0.375	0.4375	0.50	0.5675
	$\kappa$	0.4375	0.4062	0.375	0.3437	0.3125	0.3812	0.25	0.2187
	'r'	0.1758	0.2759	0.3646	0.4461	0.5172	0.5850	0.6483	0.7083
$\frac{1}{2}$	$t_b/D_b$	-	0.4706	0.4444	0.4210	0.400	0.3809	0.3636	0.3478
	$l/A_b$	-	1.1318	1.0184	0.9258	0.8488	0.7834	0.7274	0.6790
	i.d <sub>b</sub>	-	0.0625	0.125	0.1875	0.25	0.3125	0.375	0.4375
	$\kappa$	-	0.4687	0.4375	0.4062	0.375	0.3437	0.3125	0.2812
	'r'	-	0.2684	0.3510	0.4242	0.4904	0.5512	0.6078	0.6611
$\frac{5}{8}$	$t_b/D_b$								
	$l/A_b$								
	i.d <sub>b</sub>								
	$\kappa$								
	'r'								

TABLE No. A-2.3 Drawing octagonal tube from round on a cylindrical plug

INPUT GAUGE ( $t_b$ in)		INPUT TUBE OUTER DIAMETER ( $D_b$ in)							
		1	$1 \frac{1}{16}$	$1 \frac{1}{8}$	$1 \frac{3}{16}$	$1 \frac{1}{4}$	$1 \frac{5}{16}$	$1 \frac{3}{8}$	$1 \frac{7}{16}$
$\frac{1}{16}$	$t_b/D_b$	0.0625	0.0588	0.0555	0.0526	0.0500	0.0476	0.0454	0.0435
	$l/A_b$	5.432	5.091	4.7882	4.524	4.289	4.073	3.875	3.706
	i.d <sub>b</sub>	0.872	0.9345	0.997	1.0595	1.122	1.1875	1.25	1.3125
	$\kappa$	0.064	0.033	0.0015	-	-	-	-	-
	'r'	0.4030	0.8880	-	-	-	-	-	-
$\frac{1}{8}$	$t_b/D_b$	0.1250	0.1176	0.1110	0.1052	0.100	0.095	0.091	0.0869
	$l/A_b$	2.9103	2.715	2.5462	2.3951	2.2635	2.1385	2.0394	1.9388
	i.d <sub>b</sub>	0.744	0.8065	0.869	0.9315	0.994	1.0625	1.125	1.1875
	$\kappa$	0.128	0.097	0.0655	0.0342	-	-	-	-
	'r'	0.2072	0.4654	0.7097	0.9396	-	-	-	-
$\frac{3}{16}$	$t_b/D_b$	0.1875	0.1765	0.1667	0.1579	0.150	0.1428	0.1364	0.1304
	$l/A_b$	2.0894	1.9406	1.8113	1.6977	1.5978	1.5083	1.430	1.3577
	i.d <sub>b</sub>	0.625	0.6875	0.750	0.8125	0.875	0.9375	1.00	1.0625
	$\kappa$	0.1875	0.1562	0.125	0.094	0.0625	0.312	-	-
	'r'	0.1636	0.3483	0.5195	0.6786	0.8310	-	-	-
$\frac{1}{4}$	$t_b/D_b$	0.25	0.2353	0.2222	0.2105	0.20	0.1905	0.1818	0.1739
	$l/A_b$	1.6976	1.5671	1.4549	1.3579	1.2732	1.1985	1.1316	1.0721
	i.d <sub>b</sub>	0.50	0.5625	0.625	0.6875	0.75	0.8125	0.875	0.9375
	$\kappa$	0.25	0.2187	0.1875	0.1562	0.125	0.094	0.0625	0.0312
	'r'	0.1329	0.2815	0.4176	0.5440	0.6622	0.7731	-	-
$\frac{5}{16}$	$t_b/D_b$	0.3125	0.2941	0.2778	0.2631	0.25	0.2381	0.2273	0.2174
	$l/A_b$	1.4816	1.3580	1.2538	1.1637	1.0865	1.0186	0.9588	0.9055
	i.d <sub>b</sub>	0.375	0.4375	0.50	0.5625	0.625	0.6875	0.75	0.8125
	$\kappa$	0.3125	0.2812	0.25	0.2187	0.1875	0.1562	0.125	0.0875
	'r'	0.1159	0.2440	0.3596	0.4664	0.5651	0.6579	0.7456	0.8285
$\frac{3}{8}$	$t_b/D_b$	0.375	0.3529	0.3333	0.3158	0.30	0.2857	0.2727	0.2609
	$l/A_b$	1.3581	1.2344	1.1316	1.0448	0.9701	0.9054	0.8487	0.7990
	i.d <sub>b</sub>	0.25	0.3125	0.375	0.4375	0.50	0.5625	0.625	0.6875
	$\kappa$	0.375	0.3437	0.3125	0.2812	0.25	0.2187	0.1875	0.1562
	'r'	0.1064	0.2218	0.3245	0.4184	0.5365	0.5859	0.6603	0.7317
$\frac{7}{16}$	$t_b/D_b$	0.4375	0.4118	0.3889	0.3684	0.35	0.3333	0.3182	0.3043
	$l/A_b$	1.2934	1.1643	1.0583	0.9670	0.8955	0.8314	0.7761	0.7274
	i.d <sub>b</sub>	0.125	0.1875	0.25	0.3125	0.375	0.4375	0.50	0.5675
	$\kappa$	0.4375	0.4062	0.375	0.3437	0.3125	0.3812	0.25	0.2187
	'r'	0.1013	0.2088	0.3036	0.3904	0.4656	0.5371	0.6036	0.6665
$\frac{1}{2}$	$t_b/D_b$	-	0.4706	0.4444	0.4210	0.400	0.3809	0.3636	0.3478
	$l/A_b$	-	1.1318	1.0184	0.9258	0.8488	0.7834	0.7274	0.6790
	i.d <sub>b</sub>	-	0.0625	0.125	0.1875	0.25	0.3125	0.375	0.4375
	$\kappa$	-	0.4687	0.4375	0.4062	0.375	0.3437	0.3125	0.2812
	'r'	-	0.2032	0.2924	0.3709	0.4415	0.5061	0.5660	0.6220
$\frac{5}{8}$	$t_b/D_b$								
	$l/A_b$								
	i.d <sub>b</sub>								
	$\kappa$								
	'r'								

TABLE No. A-2.4 Drawing decagonal tube from round on a cylindrical plug

INPUT GAUGE ( $t_b$ in)		INPUT TUBE OUTER DIAMETER ( $D_b$ in)							
		1	$1 \frac{1}{16}$	$1 \frac{1}{8}$	$1 \frac{3}{16}$	$1 \frac{1}{4}$	$1 \frac{5}{16}$	$1 \frac{3}{8}$	$1 \frac{7}{16}$
$\frac{1}{16}$	$t_b/D_b$	0.0625	0.0588	0.0555	0.0526	0.0500	0.0476	0.0454	0.0435
	$l/A_b$	5.432	5.091	4.7882	4.524	4.289	4.073	3.875	3.706
	i.d <sub>b</sub>	0.872	0.9345	0.997	1.0595	1.122	1.1875	1.25	1.3125
	$\kappa$	0.064	0.033	0.0015	-	-	-	-	-
	'r'	0.2529	0.7473	-	-	-	-	-	-
$\frac{1}{8}$	$t_b/D_b$	0.1250	0.1176	0.1110	0.1052	0.100	0.095	0.091	0.0869
	$l/A_b$	2.9103	2.715	2.5462	2.3951	2.2635	2.1385	2.0394	1.9388
	i.d <sub>b</sub>	0.744	0.8065	0.869	0.9315	0.994	1.0625	1.125	1.1875
	$\kappa$	0.128	0.097	0.0655	0.0342	-	-	-	-
	'r'	0.1268	0.3904	0.6394	0.8744	-	-	-	-
$\frac{3}{16}$	$t_b/D_b$	0.1875	0.1765	0.1667	0.1579	0.150	0.1428	0.1364	0.1304
	$l/A_b$	2.0894	1.9406	1.8113	1.6977	1.5978	1.5083	1.430	1.3577
	i.d <sub>b</sub>	0.625	0.6875	0.750	0.8125	0.875	0.9375	1.00	1.0625
	$\kappa$	0.1875	0.1562	0.125	0.094	0.0625	0.312	-	-
	'r'	0.1059	0.2947	0.4694	0.6313	0.7868	-	-	-
$\frac{1}{4}$	$t_b/D_b$	0.25	0.2353	0.2222	0.2105	0.20	0.1905	0.1818	0.1739
	$l/A_b$	1.6976	1.5671	1.4549	1.3579	1.2732	1.1985	1.1316	1.0721
	i.d <sub>b</sub>	0.50	0.5625	0.625	0.6875	0.75	0.8125	0.875	0.9375
	$\kappa$	0.25	0.2187	0.1875	0.1562	0.125	0.094	0.0625	0.0312
	'r'	0.0860	0.2382	0.3774	0.5065	0.6270	0.7400	-	-
$\frac{5}{16}$	$t_b/D_b$	0.3125	0.2941	0.2778	0.2631	0.25	0.2381	0.2273	0.2174
	$l/A_b$	1.4816	1.3580	1.2538	1.1637	1.0865	1.0186	0.9588	0.9055
	i.d <sub>b</sub>	0.375	0.4375	0.50	0.5625	0.625	0.6875	0.75	0.8125
	$\kappa$	0.3125	0.2812	0.25	0.2187	0.1875	0.1562	0.125	0.0875
	'r'	0.0750	0.2065	0.3249	0.4343	0.5351	0.6298	0.7191	0.8036
$\frac{3}{8}$	$t_b/D_b$	0.375	0.3529	0.3333	0.3158	0.30	0.2857	0.2727	0.2609
	$l/A_b$	1.3581	1.2344	1.1316	1.0448	0.9701	0.9054	0.8487	0.7990
	i.d <sub>b</sub>	0.25	0.3125	0.375	0.4375	0.50	0.5625	0.625	0.6875
	$\kappa$	0.375	0.3437	0.3125	0.2812	0.25	0.2187	0.1875	0.1562
	'r'	0.0688	0.1877	0.2935	0.3895	0.5116	0.5598	0.6368	0.7096
$\frac{7}{16}$	$t_b/D_b$	0.4375	0.4118	0.3889	0.3684	0.35	0.3333	0.3182	0.3043
	$l/A_b$	1.2934	1.1643	1.0583	0.9670	0.8955	0.8314	0.7761	0.7274
	i.d <sub>b</sub>	0.125	0.1875	0.25	0.3125	0.375	0.4375	0.50	0.5675
	$\kappa$	0.4375	0.4062	0.375	0.3437	0.3125	0.3812	0.25	0.2187
	'r'	0.0656	0.1767	0.2744	0.3637	0.4409	0.5142	0.5821	0.6464
$\frac{1}{2}$	$t_b/D_b$	-	0.4706	0.4444	0.4210	0.400	0.3809	0.3636	0.3478
	$l/A_b$	-	1.1318	1.0184	0.9258	0.8488	0.7834	0.7274	0.6790
	i.d <sub>b</sub>	-	0.0625	0.125	0.1875	0.25	0.3125	0.375	0.4375
	$\kappa$	-	0.4687	0.4375	0.4062	0.375	0.3437	0.3125	0.2812
	'r'	-	0.1719	0.2643	0.3453	0.4180	0.4845	0.5459	0.6032
$\frac{5}{8}$	$t_b/D_b$								
	$l/A_b$								
	i.d <sub>b</sub>								
	$\kappa$								
	'r'								

TABLE No. A-2.5 Drawing round tube from round on a cylindrical plug

INPUT GAUGE ( $t_b$ in)		INPUT TUBE OUTER DIAMETER ( $D_b$ in)							
		1	$1 \frac{1}{16}$	$1 \frac{1}{8}$	$1 \frac{3}{16}$	$1 \frac{1}{4}$	$1 \frac{5}{16}$	$1 \frac{3}{8}$	$1 \frac{7}{16}$
$1/16$	$t_b/D_b$	0.0625	0.0588	0.0555	0.0526	0.0500	0.0476	0.0454	0.0435
	$l/A_b$	5.432	5.091	4.7882	4.524	4.289	4.073	3.875	3.706
	i.d <sub>b</sub>	0.872	0.9345	0.997	1.0595	1.122	1.1875	1.25	1.3125
	$\kappa$	0.064	0.033	0.0015	-	-	-	-	-
	'r'	-	0.4965	0.9973	-	-	-	-	-
$1/8$	$t_b/D_b$	0.1250	0.1176	0.1110	0.1052	0.100	0.095	0.091	0.0869
	$l/A_b$	2.9103	2.715	2.5462	2.3951	2.2635	2.1385	2.0394	1.9388
	i.d <sub>b</sub>	0.744	0.8065	0.869	0.9315	0.994	1.0625	1.125	1.1875
	$\kappa$	0.128	0.097	0.0655	0.0342	-	-	-	-
	'r'	-	0.2566	0.5139	0.7582	-	-	-	-
$3/16$	$t_b/D_b$	0.1875	0.1765	0.1667	0.1579	0.150	0.1428	0.1364	0.1304
	$l/A_b$	2.0894	1.9406	1.8113	1.6977	1.5978	1.5083	1.430	1.3577
	i.d <sub>b</sub>	0.625	0.6875	0.750	0.8125	0.875	0.9375	1.00	1.0625
	$\kappa$	0.1875	0.1562	0.125	0.094	0.0625	0.312	-	-
	'r'	-	0.1991	0.3802	0.5481	0.7081	-	-	-
$1/4$	$t_b/D_b$	0.25	0.2353	0.2222	0.2105	0.20	0.1905	0.1818	0.1739
	$l/A_b$	1.6976	1.5671	1.4549	1.3579	1.2732	1.1985	1.1316	1.0721
	i.d <sub>b</sub>	0.50	0.5625	0.625	0.6875	0.75	0.8125	0.875	0.9375
	$\kappa$	0.25	0.2187	0.1875	0.1562	0.125	0.094	0.0625	0.0312
	'r'	-	0.1610	0.3072	0.4396	0.5643	0.6810	-	-
$5/16$	$t_b/D_b$	0.3125	0.2941	0.2778	0.2631	0.25	0.2381	0.2273	0.2174
	$l/A_b$	1.4816	1.3580	1.2538	1.1637	1.0865	1.0186	0.9588	0.9055
	i.d <sub>b</sub>	0.375	0.4375	0.50	0.5625	0.625	0.6875	0.75	0.8125
	$\kappa$	0.3125	0.2812	0.25	0.2187	0.1875	0.1562	0.125	0.0875
	'r'	-	0.1396	0.2631	0.3769	0.4815	0.5796	0.6719	0.7560
$3/8$	$t_b/D_b$	0.375	0.3529	0.3333	0.3158	0.30	0.2857	0.2727	0.2609
	$l/A_b$	1.3581	1.2344	1.1316	1.0448	0.9701	0.9054	0.8487	0.7990
	i.d <sub>b</sub>	0.25	0.3125	0.375	0.4375	0.50	0.5625	0.625	0.6875
	$\kappa$	0.375	0.3437	0.3125	0.2812	0.25	0.2187	0.1875	0.1562
	'r'	-	0.1269	0.2378	0.3380	0.4669	0.5152	0.5950	0.6702
$7/16$	$t_b/D_b$	0.4375	0.4118	0.3889	0.3684	0.35	0.3333	0.3182	0.3043
	$l/A_b$	1.2934	1.1643	1.0583	0.9670	0.8955	0.8314	0.7761	0.7274
	i.d <sub>b</sub>	0.125	0.1875	0.25	0.3125	0.375	0.4375	0.50	0.5675
	$\kappa$	0.4375	0.4062	0.375	0.3437	0.3125	0.3812	0.25	0.2187
	'r'	-	0.1193	0.2222	0.3160	0.3968	0.4732	0.5438	0.6105
$1/2$	$t_b/D_b$	-	0.4706	0.4444	0.4210	0.400	0.3809	0.3636	0.3478
	$l/A_b$	-	1.1318	1.0184	0.9258	0.8488	0.7834	0.7274	0.6790
	i.d <sub>b</sub>	-	0.0625	0.125	0.1875	0.25	0.3125	0.375	0.4375
	$\kappa$	-	0.4687	0.4375	0.4062	0.375	0.3437	0.3125	0.2812
	'r'	-	0.1162	0.2141	0.2997	0.3762	0.4459	0.5100	0.5700
$5/8$	$t_b/D_b$								
	$l/A_b$								
	i.d <sub>b</sub>								
	$\kappa$								
	'r'								

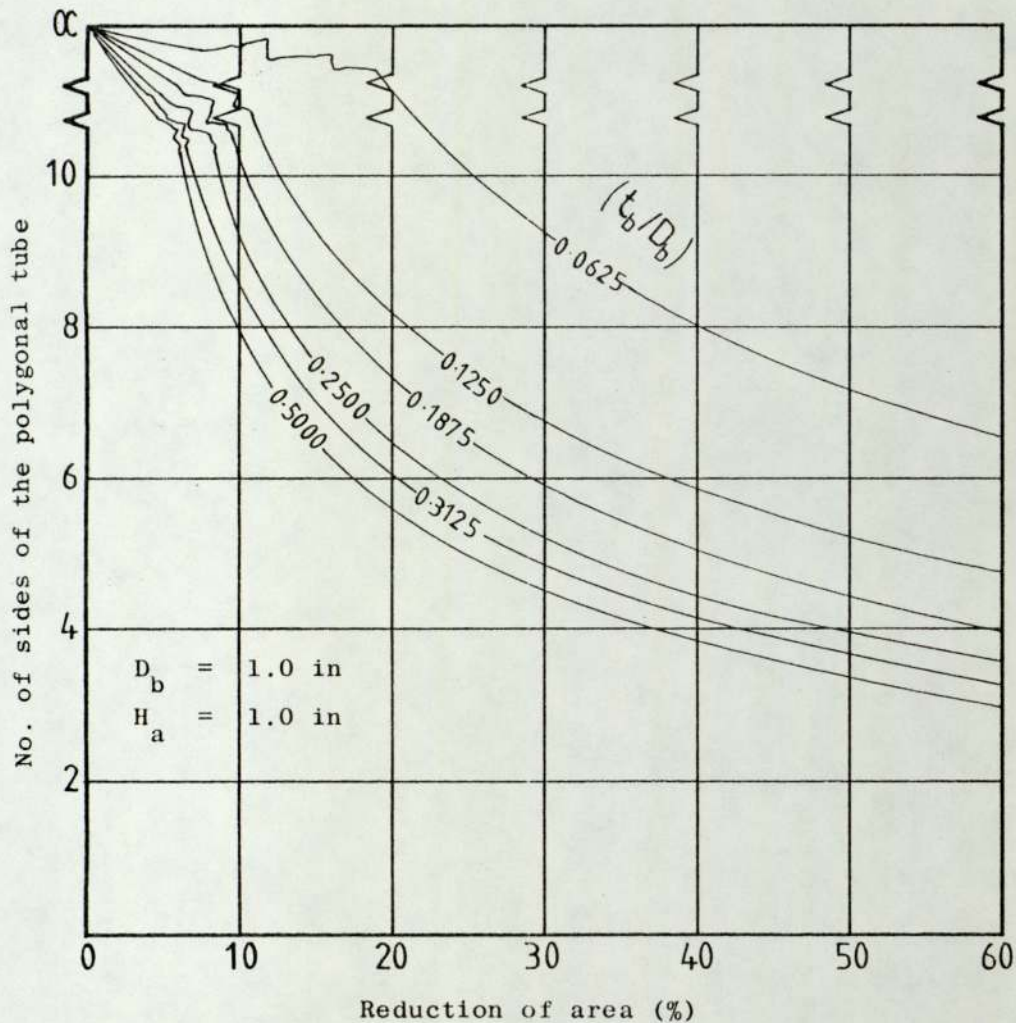


Fig. A-2.1 Reduction of area versus the number of sides for different  $t_b/D_b$  input stock tubing from the consideration of geometry (exit die diagonal 1 in).

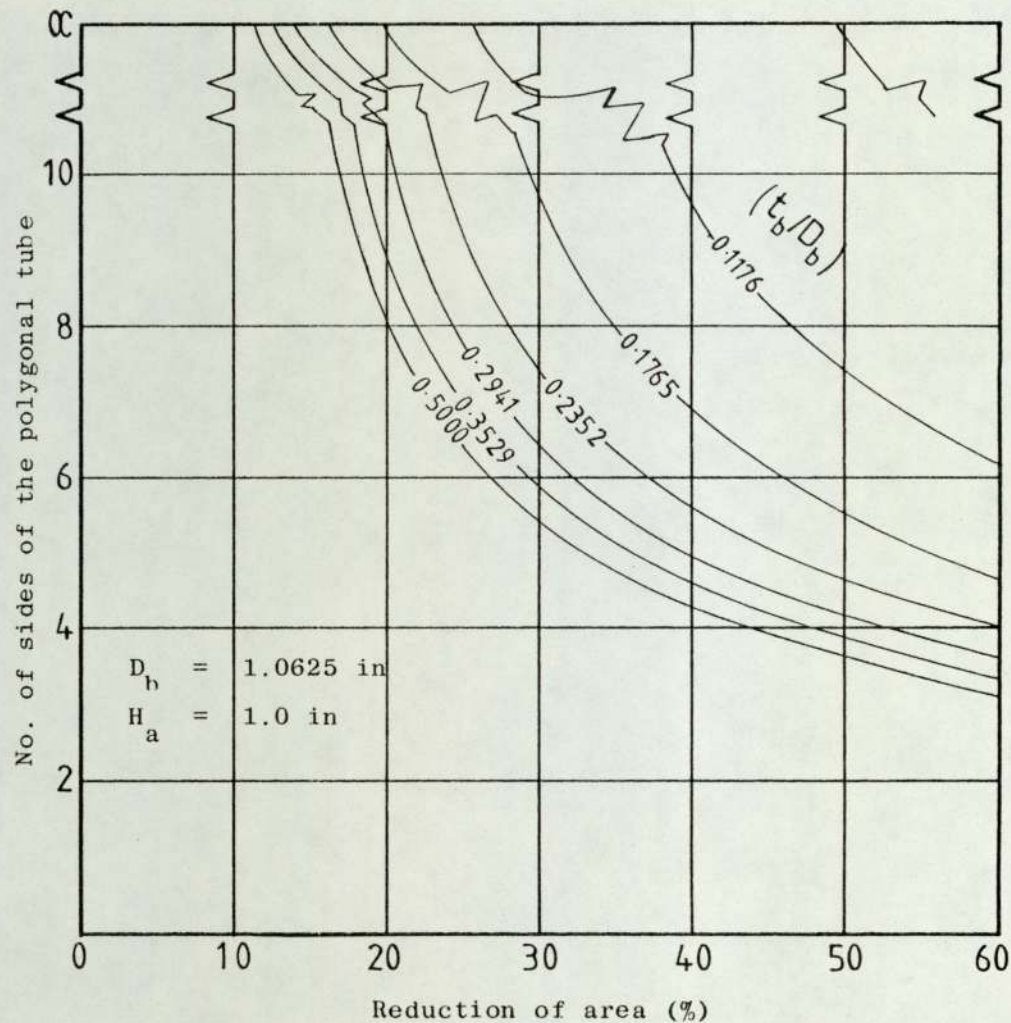


Fig. A-2.2 Reduction of area versus the number of sides for different  $t_b/D_b$  input stock tubing from the consideration of geometry (exit die diagonal 1 in).

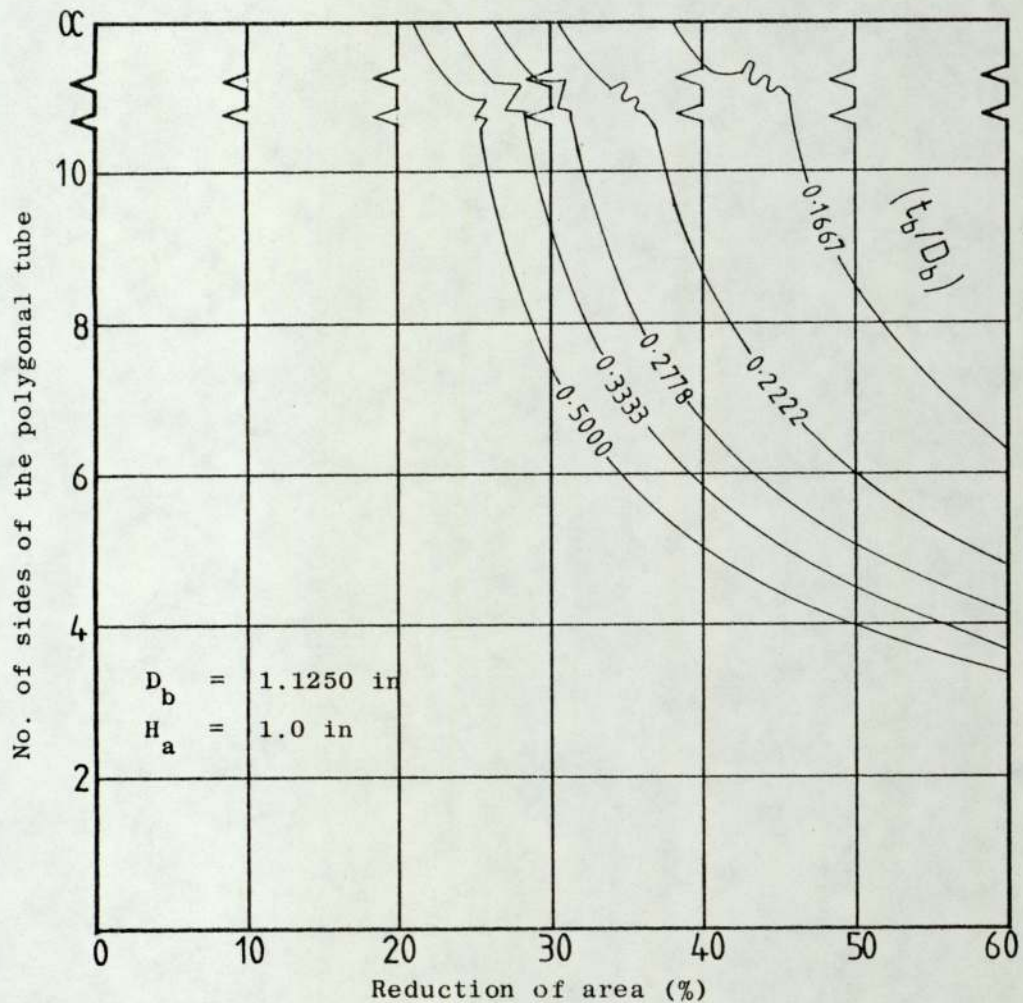


Fig. A-2.3 Reduction of area versus the number of sides for different  $t_b/D_b$  input stock tubing from consideration of geometry (exit die diagonal 1 in).

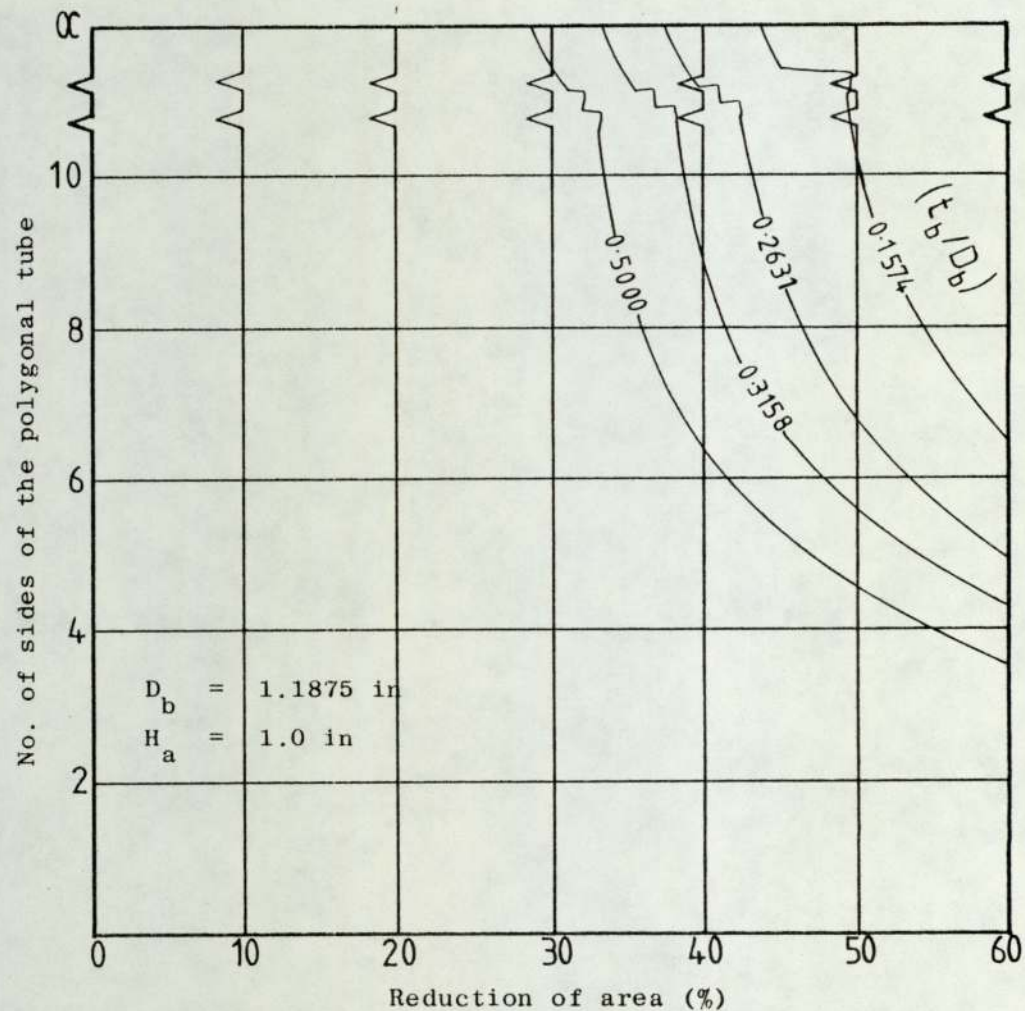


Fig. A-2.4 Reduction of area versus the number of sides for different  $t_b/D_b$  input stock tubing from the consideration of geometry (exit die diagonal 1 in).

A-3 STOCK OF TUBES USED IN THE EXPERIMENTS

TABLE No. A-3.1 Reductions of areas (%) for the stock of tubes in the drawing of polygonal tubes from round

S/ No	TUBE SPECIFICATION			NOMINAL PLUG DIAMETER (d <sub>n</sub> in)							
	Code	Nominal. o.d. (in) x gauge(in)	int. dia. (in)	3/8	7/16	1/2	9/16	5/8	11/16	3/4	
Square Tube	1	a176	1 x 7g	0.648	14.49	23.25	33.35	44.80	57.59	-	-
	2	a187	1 x 3/16	0.625	18.60	26.94	36.55	47.45	59.63	-	-
	3	a219	1 x 7/32	0.562	27.44	34.87	43.44	53.16	-	-	-
	4	a250	1 x 1/4	0.50	33.87	40.64	48.45	-	-	-	-
	7	b219	1 1/16 x 7/32	0.624	32.82	39.69	47.63	56.63	-	-	-
	12	a150	1 x .150	0.70	-	12.70	24.19	37.21	51.76	-	-
	13	a120	1 x .120	0.760	-	-	8.47	24.19	41.76	-	-
Hexagonal Tube	5	b128	1 1/16 x 10g	0.806	-	-	-	-	8.80	25.95	44.72
	6	b160	1 1/16 x 8g	0.742	-	-	-	11.61	24.45	38.66	54.21
	7	b219	1 1/16 x 7/32	0.624	7.03	13.91	21.84	30.84	40.90	-	-
	8	c160	1 1/8 x 8g	0.805	-	-	-	17.33	29.35	42.63	57.18
	9	c187	1 1/8 x 3/16	0.750	2.39	9.61	17.94	27.39	37.94	49.61	62.39
	10	c250	1 1/8 x 1/4	0.625	21.56	27.36	34.06	41.65	50.13	-	-
	11	b177	1 1/16 x .177	0.708	-	-	-	18.56	30.40	43.48	-
Octagonal Tube	5	b128	1 1/16 x 10g	0.806	-	-	-	-	-	10.62	29.39
	6	b160	1 1/16 x 8g	0.742	-	-	-	-	11.76	25.96	41.51
	7	b219	1 1/16 x 7/32	0.624	-	3.98	11.91	20.91	30.96	-	-
	8	c160	1 1/8 x 8g	0.805	-	-	-	5.45	17.47	30.75	45.30
	9	c187	1 1/8 x 3/16	0.750	-	-	7.51	16.95	27.51	39.18	51.95
	10	c250	1 1/8 x 1/4	0.625	13.18	18.98	25.68	33.27	41.75	-	-
	11	b177	1 1/16 x .177	0.708	-	-	-	6.86	18.70	31.78	-
Decagonal Tube	5	b128	1 1/16 x 10g	0.806	-	-	-	-	-	3.26	22.04
	6	b160	1 1/16 x 8g	0.742	-	-	-	-	5.67	19.87	35.42
	7	b219	1 1/16 x 7/32	0.624	-	-	-	16.14	26.20	-	-
	8	c160	1 1/8 x 8g	0.805	-	-	-	-	11.78	25.06	39.61
	9	c187	1 1 1/8 x 3/16	0.750	-	-	2.51	11.95	22.50	34.17	46.95
	10	c250	1 1/8 x 1/4	0.625	9.16	14.96	21.66	29.25	37.73	-	-
	11	b177	1 1/16 x .177	0.708	-	-	-	1.25	13.09	25.63	-
Circular Tube	5	b128	1 1/16 x 10g	0.806	-	-	-	-	-	-	8.56
	6	b160	1 1/16 x 8g	0.742	-	-	-	-	-	8.70	24.26
	7	b219	1 1/16 x 7/32	0.624	-	-	-	7.41	17.46	-	-
	8	c160	1 1/8 x 8g	0.805	-	-	-	-	1.33	14.61	29.16
	9	c187	1 1/8 x 3/16	0.750	-	-	-	2.78	13.33	25.00	37.78
	10	c250	1 1/8 x 1/4	0.625	1.79	7.59	14.29	21.87	30.36	-	-
	11	b177	1 1/16 x .177	0.708	-	-	-	-	-	15.88	-

A-3.1. Quontavac analyses on the tube material

(1) Stock from Lebas Tube Ltd

(a) Batch A

Element	C	S	Si	P	Mn	Ni	Cr	Mo	Co	Cu	Sn
%	0.11	0.038	0.13	0.021	0.43	0.25	0.12	0.04	0.03	0.19	0.016

(b) Batch B

Element	C	S	Si	P	Mn	Ni	Cr	Mo	Co	Cu	Sn
%	0.12	0.045	0.13	0.020	0.56	0.09	0.115	0.03	N/D	0.24	0.05

(2)\* Stock from Lebas Tube Ltd and British and General Tube Co Ltd

(c) Batch C (Lebas Tube Ltd)

The analysis was similar to Batch A above.

(d) Batch D (British and General Tube Ltd)

The results of the chemical analysis were not available.

\* This second stock of tubing was received as drawn and the heat treatment carried out under a separate arrangement.

A-3.2. Test reference (labelling)

Tube o.d. x gauge  (in x in)	Code	Serial Number			
		1st set of tubing		2nd set of tubing	
		BATCH A	BATCH B	BATCH C	BATCH D
1 x 7g	a176	1			
1 x 3/16	a187	2			14
1 x 7/32	a219	3		15	
1 x 1/4	a250	4			16
1 1/16 x 10g	a128	5			
1 1/16 x 8g	b160	6			17
1 1/16 x 7g	b177		11		
1 1/16 x 7/32	b219	7			
1 1/8 x 8g	c160	8			
1 1/18 x 3/16	c187	9			19
1 1/18 x 1/4	c250	10			
1.040 x 0.235	b <sup>-</sup> 235				20 <sup>-</sup>
1 3/16 x 1/4	d250				20 <sup>+</sup>

Code: 1st letter refers to tube o.d. (in)

a : 1; b : 1 1/16; c : 1 1/8; d : 1 3/16

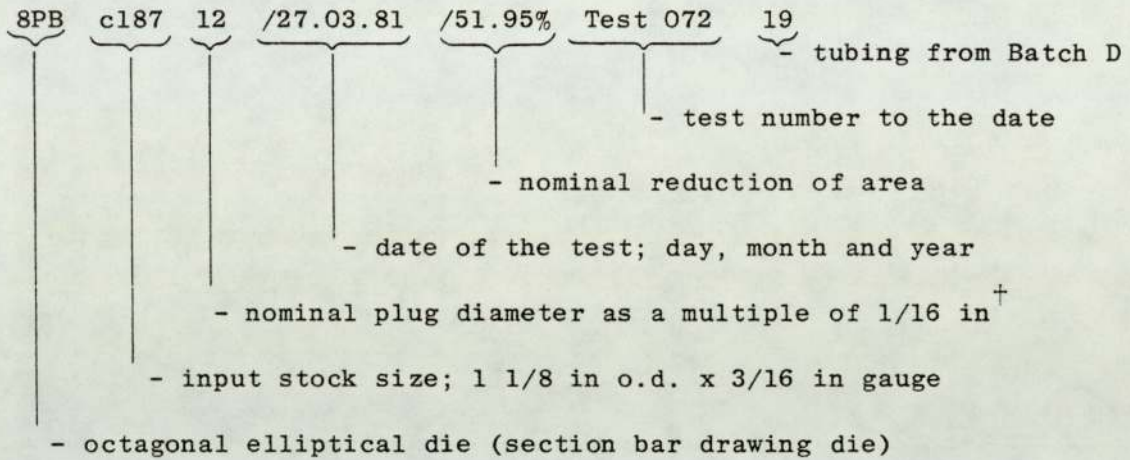
The three digits denote the gauge size as a multiple of 1/1000 in. e.g. a219 represents 1 in o.d. x 0.219 in (or simply 1 x 7/32).

Whenever the tube from Batch A was annealed under the arrangement for heat treating the 2nd set of tubing, this was denoted by superscript h added to the 1st letter.

e.g. b<sup>h</sup>219: 1 1/16 x 7/32 tubing from Batch A annealed together with the 2nd stock of tubes.

Examples

- (i) For quick reference and easy identification of the drawn sections, the tubes were labelled as shown in the example below:



<sup>†</sup> Nominal plug diameters were expressed as multiples of 1/16 in, except the following plugs:

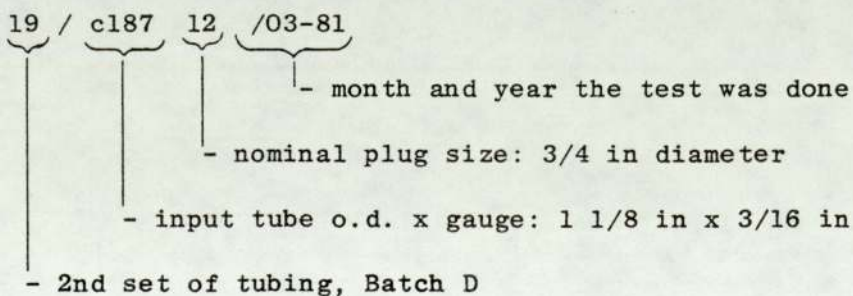
0.485 (31/64 in) denoted by 7\*\* (or 7\*\*/16)

0.470 (15/32 in) denoted by 7\* (or 7\*/16)

0.488 denoted by 8<sup>-</sup> (or 8<sup>-</sup>/16)

- (ii) Test reference in Appendix A-5

For the example above, the format of the tube (test) reference has been re-expressed as:



The test number, the die designate and the reduction of area appear in separate columns.

A-4 THEORETICAL RESULTS:

Upper and lower bound solutions for the drawing  
of polygonal <sup>tube</sup> from round on a cylindrical plug  
^

TABLE No. A-4.1.1

The upper and the lower bound solutions for the drawing of square tube from round on a cylindrical plug.

Input tube size : 1.0000 in o.d. x 0.3750 in gauge  
 Reduction of area : 38.76%

Equivalent die semi-angle $\alpha_e$	Mean coeff. of friction $\mu$	UPPER BOUND						LOWER BOUND		
		Draw force	Mean draw stress	Mean die pressure	Mean yield stress	Mean draw stress/ yield stress	Mean die pressure/ yield stress	Mean yield stress	Mean draw stress/ yield stress	Mean die pressure/ yield stress
		P tonf	$\sigma_{za}$ tonf in <sup>-2</sup>	$P_m$ tonf in <sup>-2</sup>	$\bar{Y}_m$ tonf in <sup>-2</sup>			$Y_m$ tonf in <sup>-2</sup>		
2	0.00	09.873	21.896	22.229	36.245	0.6041	0.6133	34.532	0.4985	0.8240
	0.02	13.202	30.831	17.436	38.659	0.8506	0.4811		0.7377	0.6946
	0.04	16.345	36.273	14.217	39.861	1.0008	0.3922		0.8971	0.5910
	0.06	17.999	39.918	11.971	40.586	1.1013	0.3303		1.0013	0.5076
	0.08	19.176	42.527	10.327	41.073	1.1733	0.2849		1.0677	0.4400
	0.10	20.059	44.485	09.077	41.423	1.2273	0.2504		1.1085	0.3848
4	0.00	10.479	23.240	23.667	36.654	0.6340	0.6457	34.532	0.4985	0.8239
	0.02	12.907	28.626	20.861	38.122	0.7810	0.5691		0.6299	0.7556
	0.04	14.751	32.714	18.562	39.093	0.8925	0.5064		0.7375	0.6946
	0.06	16.194	35.915	16.683	39.786	0.9798	0.4552		0.8253	0.6400
	0.08	17.353	38.484	15.134	40.308	1.0499	0.4129		0.8968	0.5910
	0.10	18.303	40.591	13.838	40.714	1.1074	0.3775		0.9545	0.5471
6	0.00	11.064	24.538	25.118	37.031	0.6626	0.6783	34.532	0.4985	0.8237
	0.02	12.852	28.503	23.068	38.091	0.7697	0.6229		0.5888	0.7774
	0.04	14.329	31.779	21.267	38.880	0.8582	0.5743		0.6679	0.7344
	0.06	15.568	34.525	19.696	39.492	0.9323	0.5319		0.7371	0.6945
	0.08	16.620	36.859	18.323	39.981	0.9953	0.4948		0.7976	0.6575
	0.10	17.524	38.865	17.119	40.382	1.0495	0.4623		0.8503	0.6230
7	0.00	11.349	25.170	25.852	37.209	0.6764	0.6948	34.532	0.4985	0.8236
	0.02	12.941	28.701	24.027	38.141	0.7713	0.6457		0.5765	0.7839
	0.04	14.290	31.693	22.391	38.860	0.8517	0.6018		0.6422	0.7463
	0.06	15.446	34.257	20.935	39.434	0.9206	0.5626		0.7083	0.7112
	0.08	16.447	36.476	19.640	39.903	0.9803	0.5278		0.7638	0.6783
	0.10	17.321	38.414	18.485	40.294	1.0324	0.4968		0.8131	0.6473
8	0.00	11.6303	25.793	26.594	37.381	0.6900	0.7114	34.532	0.4985	0.8234
	0.02	13.071	28.988	24.939	38.212	0.7755	0.6672		0.5671	0.7884
	0.04	14.316	31.749	23.434	38.873	0.8493	0.6269		0.6298	0.7553
	0.06	15.401	34.155	22.074	39.412	0.9137	0.5905		0.6845	0.7240
	0.08	16.354	36.262	20.847	39.860	0.9702	0.5577		0.7365	0.6944
	0.10	17.197	38.140	19.739	40.239	1.0203	0.5280		0.7826	0.6664
10	0.00	12.183	27.019	28.114	37.709	0.7165	0.7455	34.532	0.4985	0.8231
	0.02	13.405	29.729	26.700	38.394	0.7884	0.7080		0.5537	0.7950
	0.04	14.490	32.136	25.387	38.962	0.8522	0.6732		0.6048	0.7681
	0.06	15.460	34.287	24.175	39.440	0.9092	0.6411		0.6520	0.7424
	0.08	16.331	36.218	23.059	39.849	0.9604	0.6115		0.6956	0.7178
	0.10	17.117	37.961	22.032	40.204	1.0067	0.5864		0.7358	0.6943

TABLE No. A-4.1.1. .... (continued)

The upper and the lower bound solutions for the drawing of square tube from round on a cylindrical plug.

Input tube size : 1.000 in o.d. x 0.3750 in gauge  
 Reduction of area : 38.7%

Equivalent die semi-angle $\alpha_0$	Mean coeff. of friction $\mu$	UPPER BOUND					LOWER BOUND			
		Draw force	Mean draw stress	Mean die pressure	Mean yield stress	Mean draw stress	Mean die pressure	Mean yield stress	Mean draw stress	Mean die pressure
		P tonf	$\sigma_{za}$ tonf in <sup>-2</sup>	$P_m$ tonf in <sup>-2</sup>	$\bar{Y}_m$ tonf in <sup>-2</sup>	/yield stress	/yield stress	$Y_m$ tonf in <sup>-2</sup>	/yield stress	/yield stress
12	0.00	12.733	28.238	29.710	38.024	0.7426	0.7813	34.532	0.4985	0.8227
	0.02	13.804	30.614	28.454	38.607	0.8056	0.7483		0.5446	0.7992
	0.04	14.774	32.965	27.273	39.104	0.8617	0.7173		0.5878	0.7766
	0.06	15.655	34.719	26.168	39.533	0.9131	0.6882		0.6283	0.7549
	0.08	16.459	36.502	25.136	39.908	0.9600	0.6610		0.6662	0.7339
	0.10	17.195	38.135	24.172	40.238	1.0029	0.6357		0.7017	0.7137
14	0.00	13.298	29.492	31.431	38.337	0.7693	0.8199	34.532	0.4985	0.8222
	0.02	14.260	31.626	30.285	38.845	0.8250	0.7900		0.5380	0.8021
	0.04	15.143	33.584	29.197	39.287	0.8760	0.7616		0.5754	0.7826
	0.06	15.956	35.386	28.168	39.675	0.9230	0.7348		0.6107	0.7638
	0.08	16.706	37.049	27.198	40.020	0.9664	0.7094		0.6442	0.7455
	0.10	17.400	38.589	26.283	40.328	1.0066	0.6856		0.6758	0.7278
16	0.00	13.858	30.734	33.232	38.636	0.7955	0.8601	34.532	0.4985	0.8216
	0.02	14.736	32.681	32.165	39.085	0.8459	0.8325		0.5330	0.8041
	0.04	15.550	34.387	31.146	39.483	0.8926	0.8062		0.5658	0.7870
	0.06	16.307	36.164	30.176	39.838	0.9360	0.7810		0.5971	0.7704
	0.08	17.011	37.727	29.253	40.157	0.9765	0.7572		0.6269	0.7543
	0.10	17.669	39.185	28.377	40.445	1.0142	0.7345		0.6554	0.7386
18	0.00	14.471	32.093	35.259	38.952	0.8239	0.9052	34.532	0.4985	0.8210
	0.02	15.285	33.899	34.247	39.356	0.8703	0.8792		0.5290	0.8055
	0.04	16.046	35.586	33.276	39.717	0.9136	0.8543		0.5582	0.7903
	0.06	16.759	37.166	32.346	40.044	0.9542	0.8304		0.5863	0.7755
	0.08	17.427	38.649	31.457	40.340	0.9922	0.8076		0.6131	0.7610
	0.10	18.055	40.041	30.607	40.610	1.0280	0.7858		0.6388	0.7470
20	0.00	16.324	36.203	40.461	39.846	0.9056	1.0154	34.532	0.4985	0.8204
	0.02	17.149	38.032	39.411	40.218	0.9545	0.9891		0.5258	0.8064
	0.04	17.924	39.752	38.399	40.554	0.9976	0.9637		0.5521	0.7928
	0.06	18.655	41.372	37.426	40.861	1.0383	0.9392		0.5774	0.7794
	0.08	19.345	42.901	36.491	41.141	1.0767	0.9158		0.6017	0.7664
	0.10	19.996	44.346	35.593	41.399	1.1129	0.8933		0.6252	0.7536
22	0.00									
	0.02									
	0.04									
	0.06									
	0.08									
	0.10									

TABLE No. A-4.1.2

The upper and the lower bound solutions for the drawing of square tube from round on a cylindrical plug.

Input tube size : 1.000 in o.d. x 0.8125 in gauge  
 Reduction of area : 42.28 %

Equivalent die semi-angle $\alpha$	Mean coeff. of friction $\mu$	UPPER BOUND					LOWER BOUND			
		Draw force P	Mean draw stress $\sigma_{za}$	Mean die pressure $P_m$	Mean yield stress $\bar{Y}_m$	Mean draw stress/ yield stress	Mean die pressure/ yield stress	Mean yield stress $Y_m$	Mean draw stress/ yield stress	Mean die pressure/ yield stress
		tonf	tonf in <sup>-2</sup>	tonf in <sup>-2</sup>	tonf in <sup>-2</sup>			tonf in <sup>-2</sup>		
2	0.00	09.300	23.875	20.808	36.841	0.6481	0.5648	35.459	0.5590	0.8051
	0.02	12.996	33.368	15.370	39.238	0.9056	0.4172		0.8313	0.6537
	0.04	15.047	38.626	12.094	40.335	1.0484	0.3283		0.9939	0.5883
	0.06	16.345	41.960	09.950	40.969	1.1389	0.2701		1.0894	0.4495
	0.08	17.241	44.258	08.446	41.383	1.2013	0.2293		1.1381	0.3805
	0.10	17.895	45.938	07.334	41.785	1.2469	0.1991		1.1626	0.3263
4	0.00	09.864	25.322	22.137	37.251	0.6798	0.5942	35.459	0.5590	0.8050
	0.02	12.147	31.182	18.855	38.741	0.8371	0.5061		0.7120	0.7241
	0.04	13.780	35.374	16.349	39.673	0.9496	0.4389		0.8310	0.6536
	0.06	15.003	38.514	14.405	40.313	1.0339	0.3867		0.9231	0.5921
	0.08	15.842	40.950	12.863	40.782	1.0993	0.3453		0.9936	0.5383
	0.10	16.709	42.894	11.613	41.140	1.1515	0.3118		1.0471	0.4910
6	0.00	10.410	26.723	23.482	37.631	0.7101	0.6240	35.459	0.5590	0.8045
	0.02	12.107	31.080	21.055	38.717	0.8259	0.5595		0.6650	0.7497
	0.04	13.450	34.527	19.030	39.492	0.7175	0.5057		0.7547	0.6994
	0.06	14.536	37.316	17.337	40.074	0.9916	0.4607		0.8306	0.6536
	0.08	15.433	39.617	15.907	40.529	1.0528	0.4227		0.8945	0.6117
	0.10	16.185	41.547	14.688	40.893	1.1041	0.3903		0.9482	0.5733
7	0.00	10.676	27.407	24.164	37.811	0.7248	0.6391	35.459	0.5590	0.8046
	0.02	12.192	31.299	21.994	38.762	0.8278	0.5817		0.6508	0.7571
	0.04	13.429	34.472	20.137	39.480	0.9117	0.5326		0.7304	0.7132
	0.06	14.454	37.106	18.546	40.032	0.9814	0.4905		0.7994	0.6727
	0.08	15.319	39.324	17.175	40.472	1.0400	0.4542		0.8591	0.6351
	0.10	16.045	41.217	15.985	40.832	1.0901	0.4228		0.9105	0.6003
8	0.00	10.939	28.081	24.853	37.984	0.7393	0.6543	35.459	0.5590	0.8045
	0.02	12.314	31.611	22.880	38.841	0.8322	0.6024		0.6399	0.7627
	0.04	13.462	34.558	21.158	39.499	0.9098	0.5570		0.7113	0.7238
	0.06	14.434	37.052	19.656	40.021	0.9755	0.5175		0.7744	0.6874
	0.08	15.266	39.189	18.340	40.446	1.0317	0.4828		0.8300	0.6535
	0.10	15.986	41.038	17.181	40.798	1.0804	0.4523		0.8789	0.6217
10	0.00	11.453	29.401	26.260	38.314	0.7674	0.6854	35.459	0.5590	0.8041
	0.02	12.623	32.405	24.566	39.023	0.8458	0.6112		0.6242	0.7705
	0.04	13.634	34.999	23.047	39.593	0.9135	0.6015		0.6834	0.7388
	0.06	14.514	37.258	21.686	40.062	0.9724	0.5660		0.7370	0.7088
	0.08	15.287	39.243	20.465	40.456	1.0242	0.5341		0.7854	0.6803
	0.10	15.971	40.999	19.367	40.791	1.0701	0.5055		0.8223	0.6584

TABLE No. A-4.1.2

..... (continued)

The upper and the lower bound solutions for the drawing of square tube from round on a cylindrical plug.

Input tube size : 1.0000 in o.d. x 0.3125 in gauge  
 Reduction of area : 42.28 %

Equivalent die semi-angle $\alpha_0$	Mean coeff. of friction $\mu$	UPPER BOUND					LOWER BOUND			
		Draw force P tonf	Mean draw stress $\sigma_{za}$ tonf in <sup>-2</sup>	Mean die pressure $P_m$ tonf in <sup>-2</sup>	Mean yield stress $\bar{Y}_m$ tonf in <sup>-2</sup>	Mean draw stress /yield stress	Mean die pressure /yield stress	Mean yield stress $Y_m$ tonf in <sup>-2</sup>	Mean draw stress /yield stress	Mean die pressure /yield stress
12	0.00	11.957	30.695	27.721	38.627	0.9747	0.7177	35.459	0.5590	0.8036
	0.02	12.985	33.334	26.213	39.231	0.8630	0.6786		0.6136	0.7756
	0.04	13.893	35.664	24.836	39.734	0.9233	0.6430		0.6639	0.7489
	0.06	14.700	37.736	23.581	40.159	0.9770	0.6105		0.7102	0.7233
	0.08	15.422	39.590	22.439	40.523	1.0249	0.5808		0.7529	0.6989
	0.10	16.072	41.257	21.388	40.839	1.0681	0.5537		0.7922	0.6756
14	0.00	12.460	31.985	29.258	38.927	0.8217	0.7516	35.459	0.5590	0.8031
	0.02	13.383	34.355	27.881	39.455	0.8825	0.7162		0.6058	0.7791
	0.04	14.212	36.483	26.607	39.904	0.9372	0.6835		0.6549	0.7560
	0.06	14.960	38.404	25.430	40.292	0.9865	0.6533		0.6902	0.7338
	0.08	15.638	40.145	24.343	40.630	1.0313	0.6254		0.7282	0.7124
	0.10	16.256	41.731	23.338	40.927	1.0720	0.5995		0.7636	0.6919
16	0.00	12.974	33.306	30.909	39.225	0.8491	0.7880	35.459	0.5590	0.8025
	0.02	13.818	35.471	29.626	39.693	0.9043	0.7553		0.5999	0.7815
	0.04	14.585	37.440	28.427	40.099	0.9545	0.7247		0.6384	0.7612
	0.06	15.285	39.238	27.309	40.455	1.0003	0.6962		0.6746	0.7416
	0.08	15.927	40.885	26.266	40.770	1.0423	0.6696		0.7087	0.7227
	0.10	16.517	42.400	25.294	41.050	1.0809	0.6448		0.7408	0.7044
18	0.00	13.434	34.487	32.580	39.483	0.8735	0.8236	35.459	0.5590	0.8018
	0.02	14.211	36.481	31.308	39.904	0.9239	0.7929		0.5952	0.7832
	0.04	14.924	38.312	30.171	40.274	0.9703	0.7641		0.6295	0.7651
	0.06	15.582	40.000	29.101	40.602	1.0131	0.7371		0.6621	0.7476
	0.08	16.189	41.559	28.097	40.896	1.0526	0.7116		0.6929	0.7306
	0.10	16.752	43.005	27.153	41.160	1.0892	0.6877		0.7222	0.7141
20	0.00	13.953	35.820	34.356	39.766	0.9007	0.8639	35.459	0.5590	0.8010
	0.02	14.679	37.681	33.197	40.148	0.9476	0.8348		0.5916	0.7843
	0.04	15.350	39.405	32.102	40.488	0.9909	0.8073		0.6223	0.7681
	0.06	15.973	41.005	31.066	40.792	1.0311	0.7812		0.6518	0.7523
	0.08	16.554	42.494	30.087	41.067	1.0686	0.7566		0.6790	0.7369
	0.10	17.095	43.883	29.162	41.317	1.1035	0.7333		0.7067	0.7220
22	0.00									
	0.02									
	0.04									
	0.06									
	0.08									
	0.10									

TABLE No. A- 4.1.3. The upper and the lower bound solutions for the drawing of square tube from round on a cylindrical plug.

Input tube size : 1.000 in o.d. x 0.2500 in gauge  
 Reduction of area : 48.45 %

Equivalent die semi-angle $\alpha_p$	Mean coeff. of friction $\mu$	UPPER BOUND					LOWER BOUND			
		Draw force P tonf	Mean draw stress $\sigma_{za}$ tonf in <sup>-2</sup>	Mean die pressure $p_m$ tonf in <sup>-2</sup>	Mean yield stress $\bar{Y}_m$ tonf in <sup>-2</sup>	Mean draw stress/ yield stress	Mean die pressure /yield stress	Mean yield stress $Y_m$ tonf in <sup>-2</sup>	Mean draw stress/ yield stress	Mean die pressure /yield stress
2	0.00	08.406	27.685	18.699	37.883	0.7308	0.4936	37.031	0.6746	0.7704
	0.02	11.529	37.968	12.905	40.205	1.0023	0.3407		0.9826	0.5891
	0.04	13.059	43.128	09.793	41.182	1.1384	0.2585		1.1322	0.4613
	0.06	14.034	46.220	07.880	41.723	1.2201	0.2080		1.1970	0.3697
	0.08	14.659	48.278	06.589	42.066	1.2744	0.1739		1.2178	0.3030
	0.10	15.105	49.747	05.660	42.305	1.3132	0.1494		1.2168	0.2534
4	0.00	08.889	29.276	19.835	38.284	0.7647	0.5181	37.031	0.6746	0.7702
	0.02	10.865	45.784	16.231	39.759	0.9347	0.4240		0.8547	0.6716
	0.04	12.188	40.141	13.685	40.829	1.0485	0.3575		0.9824	0.5890
	0.06	13.134	43.255	11.812	41.205	1.1298	0.3085		1.0714	0.5137
	0.08	13.843	45.590	10.384	41.615	1.1908	0.2712		1.1320	0.4613
	0.10	14.394	47.404	09.260	41.922	1.2382	0.2419		1.1719	0.4118
6	0.00	09.357	30.8179	20.985	38.655	0.7972	0.5429	37.031	0.6746	0.7700
	0.02	10.840	35.699	18.291	39.741	0.9235	0.4732		0.8010	0.7023
	0.04	11.956	39.374	16.169	40.482	1.0186	0.4183		0.9019	0.6423
	0.06	12.825	42.236	14.472	41.020	1.0926	0.3744		0.9819	0.5889
	0.08	13.520	44.526	13.089	41.430	1.1519	0.3386		1.0449	0.5414
	0.10	14.089	46.399	11.943	41.753	1.2003	0.3090		1.0939	0.4991
7	0.00	09.586	31.570	21.570	38.832	0.8130	0.5555	37.031	0.6746	0.7698
	0.02	10.913	35.941	19.152	39.792	0.9255	0.4932		0.7845	0.7114
	0.04	11.949	39.352	17.188	40.477	1.0134	0.4426		0.8752	0.6586
	0.06	12.779	42.084	15.572	40.992	1.0838	0.4010		0.9497	0.6110
	0.08	13.458	44.320	14.226	41.394	1.1413	0.3664		1.0105	0.5679
	0.10	14.023	46.184	13.089	41.716	1.1893	0.3371		1.0598	0.5288
8	0.00	09.811	32.310	22.1601	39.001	0.8284	0.5682	37.031	0.6746	0.7698
	0.02	11.017	36.282	19.956	39.863	0.9303	0.5117		0.7717	0.7182
	0.04	11.984	39.469	18.121	40.500	1.0120	0.4646		0.8539	0.6712
	0.06	12.777	42.080	16.580	40.991	1.0789	0.4251		0.9232	0.6282
	0.08	13.438	44.256	15.271	41.383	1.1347	0.3916		0.9813	0.5888
	0.10	13.997	46.098	14.149	41.702	1.1819	0.3628		1.0299	0.5527
10	0.00	10.251	33.759	23.364	39.325	0.8585	0.5942	37.031	0.6746	0.7691
	0.02	11.279	37.145	21.467	40.040	0.9446	0.5459		0.7532	0.7277
	0.04	12.138	39.974	19.830	40.597	1.0165	0.5043		0.8222	0.6892
	0.06	12.865	42.370	18.412	41.045	1.0774	0.4682		0.8824	0.6533
	0.08	13.489	44.425	17.174	41.412	1.1297	0.4367		0.9349	0.6199
	0.10	14.030	46.205	16.087	41.720	1.1750	0.4091		0.9805	0.5887

TABLE No. A-4\*1.3

..... (continued)

The upper and the lower bound solutions for the drawing of square tube from round on a cylindrical plug.

Input tube size : 1.000 in o.d. x 0.2500 in gauge  
 Reduction of area : 48.45 %

Equivalent die semi-angle $\alpha_e^\circ$	Mean coeff. of friction $\mu$	UPPER BOUND						LOWER BOUND		
		Draw force P tonf	Mean draw stress $\sigma_{za}$ tonf in <sup>-2</sup>	Mean die pressure $P_m$ tonf in <sup>-2</sup>	Mean yield stress $\bar{Y}_m$ tonf in <sup>-2</sup>	Mean draw stress / yield stress	Mean die pressure / yield stress	Mean yield stress $Y_m$ tonf in <sup>-2</sup>	Mean draw stress / yield stress	Mean die pressure / yield stress
12	0.00	10.679	35.171	24.608	39.630	0.8875	0.6210	37.031	0.6746	0.7686
	0.02	11.583	38.147	22.917	40.241	0.9626	0.5783		0.7406	0.7340
	0.04	12.359	40.703	21.424	40.735	1.0271	0.5406		0.8000	0.7014
	0.06	13.032	42.919	20.101	41.144	1.0830	0.5072		0.8527	0.6706
	0.08	13.621	44.860	18.924	41.489	1.1320	0.4775		0.8999	0.6416
	0.10	14.141	46.572	17.872	41.782	1.1752	0.4510		0.9421	0.6143
14	0.00	11.101	36.561	25.908	39.920	0.9159	0.6490	37.031	0.6746	0.7679
	0.02	11.913	39.233	24.363	40.454	0.9828	0.6103		0.7313	0.7382
	0.04	12.624	41.574	22.975	40.898	1.0414	0.5755		0.7830	0.7100
	0.06	13.251	43.641	21.726	41.274	1.0932	0.5442		0.8300	0.6832
	0.08	13.809	45.479	20.598	41.596	1.1392	0.5160		0.8727	0.6577
	0.10	14.309	47.123	19.577	41.875	1.1804	0.4904		0.9115	0.6334
16	0.00	11.524	37.954	27.282	40.202	0.9441	0.6786	37.031	0.6746	0.7672
	0.02	12.265	40.392	25.844	40.677	1.0047	0.6428		0.7242	0.7412
	0.04	12.923	42.560	24.535	41.079	1.0587	0.6103		0.7700	0.7164
	0.06	13.513	44.502	23.342	41.426	1.1069	0.5806		0.8121	0.6926
	0.08	14.043	46.248	22.253	41.727	1.1504	0.5535		0.8509	0.6699
	0.10	14.523	47.828	21.256	41.992	1.1897	0.5287		0.8866	0.6481
18	0.00	11.894	39.172	28.605	40.442	0.9686	0.7073	37.031	0.6746	0.7664
	0.02	12.575	41.413	27.251	40.868	1.0240	0.6738		0.7186	0.7434
	0.04	13.188	43.431	26.007	41.236	1.0739	0.6431		0.7596	0.7212
	0.06	13.742	45.247	24.863	41.557	1.1190	0.6148		0.7977	0.6999
	0.08	14.246	46.916	23.809	41.840	1.1601	0.5887		0.8331	0.6794
	0.10	14.706	48.431	22.836	42.091	1.1975	0.5647		0.8660	0.6597
20	0.00	12.289	40.473	30.059	40.692	0.9946	0.7387	37.031	0.6746	0.7655
	0.02	12.922	42.557	28.768	41.079	1.0458	0.7070		0.7140	0.7448
	0.04	13.498	44.452	27.572	41.417	1.0924	0.6776		0.7510	0.7249
	0.06	14.023	46.182	26.463	41.716	1.1349	0.6503		0.7857	0.7056
	0.08	14.504	47.767	25.434	41.982	1.1739	0.6250		0.8182	0.6870
	0.10	14.947	49.224	24.478	42.221	1.2097	0.6015		0.8487	0.6690
22	0.00									
	0.02									
	0.04									
	0.06									
	0.08									
	0.10									

TABLE No. A-4.2.1

The upper and the lower bound solutions for the drawing of hexagonal tube from round on a cylindrical plug.

Input tube size : 1.0000 in o.d. x 0.3750 in gauge  
 Reduction of area : 18.45%

Equivalent die semi-angle $\alpha_d$	Mean coeff. of friction $\mu$	UPPER BOUND					LOWER BOUND			
		Draw force P tonf	Mean draw stress $\sigma_{za}$ tonf in <sup>-2</sup>	Mean die pressure $p_m$ tonf in <sup>-2</sup>	Mean yield stress $\bar{Y}_m$ tonf in <sup>-2</sup>	Mean draw stress/ yield stress	Mean die pressure/ yield stress	Mean yield stress $Y_m$ tonf in <sup>-2</sup>	Mean draw stress/ yield stress	Mean die pressure/ yield stress
2	0.00	09.530	15.872	47.068	34.114	0.4653	1.3797	28.172	0.2070	0.9221
	0.02	14.344	23.889	39.508	36.845	0.6484	1.0723		0.3331	0.8584
	0.04	17.579	29.277	33.571	38.284	0.7647	0.8769		0.4414	0.8005
	0.06	19.886	33.120	29.064	39.184	0.8452	0.7417		0.5344	0.7470
	0.08	21.610	35.990	25.580	39.802	0.9042	0.6427		0.6141	0.6994
	0.10	22.945	38.214	22.822	40.254	0.9493	0.5670		0.6823	0.6553
4	0.00	10.203	16.993	50.506	34.555	0.4918	1.4616	28.172	0.2070	0.9220
	0.02	13.051	21.787	46.270	36.195	0.6005	1.2783		0.2724	0.8895
	0.04	15.351	25.567	42.391	37.319	0.6851	1.3591		0.3329	0.8584
	0.06	17.238	28.710	38.983	38.143	0.7527	1.0220		0.3891	0.8288
	0.08	18.811	31.329	36.012	38.776	0.8080	0.9289		0.4411	0.8005
	0.10	20.140	33.543	33.488	39.278	0.8540	0.8513		0.4894	0.7735
6	0.00	10.826	18.031	53.798	34.943	0.5160	1.5396	28.172	0.2070	0.9219
	0.02	12.912	21.504	50.761	36.122	0.5953	1.4053		0.2510	0.9001
	0.04	14.713	24.504	47.850	37.022	0.6619	1.2925		0.2929	0.8789
	0.06	16.280	27.115	45.148	37.735	0.7186	1.1965		0.3327	0.8584
	0.08	17.654	29.403	42.672	38.315	0.7674	1.1137		0.3705	0.8385
	0.10	18.867	31.423	40.415	38.798	0.8099	1.0417		0.4065	0.8192
7	0.00	11.120	18.520	55.395	35.120	0.5273	1.5773	28.172	0.2070	0.9218
	0.02	12.973	21.607	52.707	36.154	0.5976	1.4578		0.2448	0.9031
	0.04	14.606	24.327	50.103	36.971	0.6580	1.3552		0.2811	0.8849
	0.06	16.053	26.737	47.648	37.635	0.7104	1.2660		0.3158	0.8671
	0.08	17.343	28.884	45.362	38.186	0.7564	1.1879		0.3490	0.8498
	0.10	18.497	30.807	43.247	38.653	0.7970	1.1189		0.3808	0.8330
8	0.00	11.402	18.991	56.962	35.286	0.5381	1.6143	28.172	0.2070	0.9218
	0.02	13.076	21.778	54.540	36.208	0.6014	1.5063		0.2402	0.9054
	0.04	14.574	24.273	52.175	36.956	0.6568	1.4118		0.2721	0.8894
	0.06	15.920	26.514	49.919	37.576	0.7056	1.3285		0.3028	0.8737
	0.08	17.134	28.536	47.794	38.099	0.7490	1.2545		0.3324	0.8584
	0.10	18.233	30.368	45.805	38.549	0.7878	1.1882		0.3609	0.8434
10	0.00	11.935	19.877	60.025	35.591	0.5585	1.6865	28.172	0.2070	0.9216
	0.02	13.348	22.231	57.977	36.349	0.6116	1.5950		0.2355	0.9085
	0.04	14.640	24.383	55.958	36.987	0.6592	1.5129		0.2593	0.8956
	0.06	15.824	26.355	54.005	37.533	0.7022	1.4388		0.2842	0.8830
	0.08	16.913	28.168	52.134	38.006	0.7414	1.3717		0.3084	0.8706
	0.10	17.916	29.839	50.421	38.421	0.7766	1.3105		0.3319	0.8584

TABLE No. A-4. 2.1

..... (continued)

The upper and the lower bound solutions for the drawing of hexagonal tube from round on a cylindrical plug.

Input tube size : 1.0000 in o.d. x 0.3750 in gauge  
 Reduction of area : 18.45%

Equivalent die semi-angle $\alpha_0$	Mean coeff. of friction $\mu$	UPPER BOUND						LOWER BOUND		
		Draw force	Mean draw stress	Mean die pressure	Mean yield stress	Mean draw stress	Mean die pressure	Mean yield stress	Mean draw stress	Mean die pressure
		P tonf	$\sigma_{za}$ tonf in <sup>-2</sup>	$P_m$ tonf in <sup>-2</sup>	$\bar{Y}_m$ tonf in <sup>-2</sup>	/yield stress	/yield stress	$Y_m$ tonf in <sup>-2</sup>	/yield stress	/yield stress
12	0.00	12.430	20.703	63.025	35.865	0.5772	1.7573	28.172	0.2070	0.9215
	0.02	13.662	22.753	61.228	36.508	0.6232	1.6771		0.2291	0.9105
	0.04	14.804	24.656	59.448	37.065	0.6652	1.6039		0.2506	0.8998
	0.06	15.866	26.424	57.709	37.552	0.7037	1.5368		0.2715	0.8892
	0.08	16.854	28.070	56.027	37.981	0.7390	1.4751		0.2920	0.8787
	0.10	17.776	29.605	54.407	38.364	0.7717	1.4182		0.3120	0.8685
14	0.00	12.892	21.471	65.979	36.112	0.5946	1.8271	28.172	0.2070	0.9212
	0.02	13.988	23.296	64.362	36.671	0.6353	1.7551		0.2259	0.9119
	0.04	15.015	25.008	62.756	37.164	0.6729	1.6886		0.2443	0.9027
	0.06	15.979	26.614	61.178	37.602	0.7078	1.6270		0.2623	0.8936
	0.08	16.886	28.123	59.639	37.995	0.7402	1.5697		0.2800	0.8846
	0.10	17.739	29.544	58.148	38.349	0.7704	1.5162		0.2973	0.8757
16	0.00	13.341	22.224	69.012	36.347	0.6114	1.8987	28.172	0.2070	0.9210
	0.02	14.336	23.876	67.528	36.841	0.6481	1.8329		0.2234	0.9128
	0.04	15.273	25.436	66.051	37.283	0.6822	1.7716		0.2395	0.9048
	0.06	16.149	26.912	64.594	37.681	0.7142	1.7142		0.2553	0.8968
	0.08	16.998	28.310	63.167	38.042	0.7442	1.6604		0.2708	0.8889
	0.10	17.793	29.634	61.775	38.371	0.7723	1.6099		0.2860	0.8811
18	0.00	13.458	22.414	70.402	36.405	0.6157	1.9338	28.172	0.2070	0.9207
	0.02	14.344	23.890	69.052	36.845	0.6484	1.8741		0.2215	0.9135
	0.04	15.187	25.294	67.707	37.244	0.6791	1.8179		0.2358	0.9064
	0.06	15.989	26.630	66.377	37.607	0.7081	1.7650		0.2498	0.8993
	0.08	16.753	27.902	65.069	37.939	0.7355	1.7151		0.2636	0.8923
	0.10	17.481	29.114	63.789	38.244	0.7613	1.6679		0.2771	0.8853
20	0.00	15.198	25.312	80.486	37.249	0.6794	2.1607	28.172	0.2070	0.9204
	0.02	16.096	26.807	79.703	37.653	0.7119	2.1005		0.2200	0.9140
	0.04	16.953	28.235	77.703	38.024	0.7426	2.0435		0.2327	0.9076
	0.06	17.773	29.601	76.327	38.363	0.7716	1.9896		0.2453	0.9012
	0.08	18.558	30.908	74.971	38.677	0.7991	1.9384		0.2577	0.8949
	0.10	19.309	32.158	73.639	38.967	0.8253	1.8898		0.2699	0.8897
22	0.00									
	0.02									
	0.04									
	0.06									
	0.08									
	0.10									

TABLE No. A-42.2

The upper and the lower bound solutions for the drawing of hexagonal tube from round on a cylindrical plug.

Input tube size : 1.0000 in o.d. x 0.1875 in gauge  
 Reduction of area : 28.39 %

Equivalent die semi-angle $\alpha_0$	Mean coeff. of friction $\mu$	UPPER BOUND					LOWER BOUND			
		Draw force	Mean draw stress	Mean die pressure	Mean yield stress	Mean draw stress/ yield stress	Mean die pressure/ yield stress	Mean yield stress	Mean draw stress/ yield stress	Mean die pressure/ yield stress
		P tonf	$\sigma_{za}$ tonf in <sup>-2</sup>	$p_m$ tonf in <sup>-2</sup>	$\bar{Y}_m$ tonf in <sup>-2</sup>			$Y_m$ tonf in <sup>-2</sup>		
2	0.00	06.376	18.605	31.001	35.150	0.5293	0.8820	31.586	0.3392	0.8756
	0.02	09.445	27.559	22.107	37.850	0.7281	0.5841		0.5694	0.7547
	0.04	11.042	32.218	17.018	38.981	0.8265	0.4366		0.7343	0.6551
	0.06	12.016	35.062	13.806	39.607	0.8852	0.3486		0.8514	0.5727
	0.08	12.672	36.976	11.605	40.005	0.9243	0.2901		0.9338	0.5041
	0.10	13.144	38.352	10.006	40.281	0.9521	0.2484		0.9911	0.4469
4	0.00	06.835	19.944	33.316	35.613	0.5600	0.9354	31.586	0.3392	0.8755
	0.02	08.784	25.630	27.826	37.336	0.6865	0.7453		0.4636	0.8122
	0.04	10.122	29.534	23.750	38.347	0.7702	0.6194		0.5691	0.7547
	0.06	11.094	32.371	20.672	39.015	0.8297	0.5294		0.6585	0.7025
	0.08	11.832	34.523	18.281	39.491	0.8742	0.4629		0.7339	0.6551
	0.10	12.410	36.210	16.378	39.848	0.9087	0.4110		0.7976	0.6120
6	0.00	07.259	21.180	35.523	36.019	0.5880	0.9862	31.586	0.3392	0.8754
	0.02	08.727	25.465	31.427	37.291	0.6829	0.8427		0.4242	0.8325
	0.04	09.854	28.753	28.070	38.154	0.7586	0.7357		0.5005	0.7923
	0.06	10.744	31.351	25.315	38.781	0.8084	0.6528		0.5688	0.7547
	0.08	11.464	33.452	23.031	39.257	0.8521	0.5867		0.6299	0.7194
	0.10	12.058	35.185	21.112	39.633	0.8878	0.5327		0.6845	0.6862
7	0.00	07.458	21.763	36.596	36.203	0.6011	1.0108	31.586	0.3392	0.8753
	0.02	08.775	25.605	32.926	37.329	0.6859	0.8820		0.4126	0.8384
	0.04	09.821	28.656	29.831	38.130	0.7515	0.7823		0.4794	0.8035
	0.06	10.670	31.133	27.223	38.730	0.8038	0.7029		0.5402	0.7705
	0.08	11.372	33.171	25.012	39.197	0.8465	0.6381		0.5955	0.7393
	0.10	11.961	34.902	23.120	39.572	0.8820	0.5842		0.6458	0.7097
8	0.00	07.550	22.323	37.653	36.377	0.6137	1.0351	31.586	0.3392	0.8752
	0.02	08.848	25.819	34.311	37.388	0.6906	0.9117		0.4037	0.8428
	0.04	09.825	28.668	31.431	38.133	0.7518	0.8243		0.4631	0.8120
	0.06	10.635	31.032	28.944	38.706	0.8017	0.7481		0.5178	0.7826
	0.08	11.317	33.022	26.718	39.161	0.8432	0.6848		0.5682	0.7546
	0.10	11.899	34.719	24.961	39.533	0.8782	0.6314		0.6146	0.7289
10	0.00	08.015	23.388	39.732	36.698	0.6373	1.0827	31.586	0.3392	0.8750
	0.02	09.038	26.37	36.864	37.538	0.7025	0.9821		0.3910	0.8490
	0.04	09.904	28.894	34.316	38.190	0.7567	0.8986		0.4395	0.8240
	0.06	10.645	31.061	32.060	38.713	0.8023	0.8281		0.4850	0.8000
	0.08	11.287	32.933	30.059	39.142	0.8414	0.7680		0.5276	0.7769
	0.10	11.847	34.568	28.280	39.501	0.8751	0.7159		0.5675	0.7546

TABLE No. A-4.2.2

..... (continued)

The upper and the lower bound solutions for the drawing of hexagonal tube from round on a cylindrical plug.

Input tube size : 1.0000 in o.d. x 0.1875 in gauge  
 Reduction of area : 28.39%

Equivalent die semi-angle $\alpha_e$	Mean coeff. of friction $\mu$	UPPER BOUND					LOWER BOUND			
		Draw force P tonf	Mean draw stress $\sigma_{za}$ tonf in <sup>-2</sup>	Mean die pressure $P_m$ tonf in <sup>-2</sup>	Mean yield stress $Y_m$ tonf in <sup>-2</sup>	Mean draw stress / yield stress	Mean die pressure / yield stress	Mean yield stress $Y_m$ tonf in <sup>-2</sup>	Mean draw stress / yield stress	Mean die pressure / yield stress
12	0.00	08.360	24.393	41.800	36.990	0.6594	1.1300	31.586	0.3392	0.8747
	0.02	09.259	27.016	39.254	37.709	0.7164	1.0410		0.3824	0.8530
	0.04	10.040	29.295	36.947	38.288	0.7651	0.9650		0.4233	0.8320
	0.06	10.724	31.291	34.862	38.767	0.8072	0.8993		0.4621	0.8117
	0.08	11.327	33.052	32.978	39.169	0.8438	0.8420		0.4989	0.7921
	0.10	11.864	34.617	31.274	39.512	0.8761	0.7915		0.5337	0.7730
14	0.00	08.691	25.359	43.893	37.262	0.6806	1.1780	31.586	0.3392	0.8743
	0.02	09.498	27.713	41.578	37.890	0.7314	1.0973		0.3762	0.8558
	0.04	10.212	29.796	39.450	38.411	0.7757	1.0270		0.4115	0.8377
	0.06	10.848	31.652	37.500	38.851	0.8147	0.9652		0.4452	0.8202
	0.08	11.417	33.314	35.713	39.227	0.8493	0.9104		0.4774	0.8031
	0.10	11.930	34.811	34.075	39.553	0.8801	0.8615		0.5082	0.7863
16	0.00	09.016	26.307	46.520	37.520	0.7011	1.2273	31.586	0.3392	0.8739
	0.02	09.751	28.452	43.905	38.078	0.7472	1.1530		0.3714	0.8577
	0.04	10.411	30.377	41.914	38.551	0.7880	1.0872		0.4024	0.8419
	0.06	11.006	32.115	40.069	38.957	0.8244	1.0285		0.4322	0.8265
	0.08	11.546	33.690	38.361	39.310	0.8570	0.9759		0.4608	0.8114
	0.10	12.037	35.123	36.779	39.620	0.8865	0.9283		0.4883	0.7967
18	0.00	09.341	27.258	48.307	37.772	0.7216	1.2789	31.586	0.3392	0.8735
	0.02	10.020	29.236	46.293	38.274	0.7639	1.2095		0.3677	0.8591
	0.04	10.635	31.033	44.406	38.706	0.8018	1.1473		0.3953	0.8451
	0.06	11.197	32.671	42.643	39.083	0.8350	1.0911		0.4218	0.8313
	0.08	11.710	34.169	40.998	39.419	0.8669	1.0402		0.4475	0.8179
	0.10	12.182	35.545	39.462	39.709	0.8951	0.9938		0.4723	0.8047
20	0.00	09.680	28.245	50.727	38.021	0.7428	1.3340	31.586	0.3392	0.8730
	0.02	10.312	30.090	48.809	38.482	0.7819	1.2684		0.3647	0.8601
	0.04	10.892	31.781	47.002	38.880	0.8147	1.2089		0.3894	0.8475
	0.06	11.424	33.335	45.303	39.231	0.8497	1.1547		0.4134	0.8351
	0.08	11.915	34.768	43.706	39.544	0.8792	1.1052		0.4366	0.8230
	0.10	12.369	36.092	42.205	39.823	0.9063	1.0598		0.4591	0.8111
22	0.00									
	0.02									
	0.04									
	0.06									
	0.08									
	0.10									

TABLE No. A-4. 2.3

The upper and the lower bound solutions for the drawing of hexagonal tube from round on a cylindrical plug.

Input tube size : 1.0625 in o.d. x 0.2500 in gauge  
 Reduction of area : 37.16%

Equivalent die semi-angle $\alpha_0$	Mean coeff. of friction $\mu$	UPPER BOUND					LOWER BOUND			
		Draw force	Mean draw stress	Mean die pressure	Mean yield stress	Mean draw stress/ yield stress	Mean die pressure/ yield stress	Mean yield stress	Mean draw stress/ yield stress	Mean die pressure/ yield stress
		P tonf	$\sigma_{za}$ tonf in <sup>-2</sup>	$p_m$ tonf in <sup>-2</sup>	$\bar{Y}_m$ tonf in <sup>-2</sup>	stress	stress	$Y_m$ tonf in <sup>-2</sup>	stress	stress
2	0.00	08.802	21.949	24.356	36.262	0.6053	0.6717	34.101	0.4697	0.8150
	0.02	12.607	31.438	17.331	38.801	0.8102	0.4780		0.7353	0.6704
	0.04	14.592	36.438	13.345	39.884	0.9123	0.3680		0.9020	0.5584
	0.06	15.804	39.414	10.830	40.489	0.9734	0.2987		1.0042	0.4711
	0.08	16.624	41.455	09.106	40.876	1.0141	0.2511		1.0648	0.4023
	0.10	17.212	42.922	07.854	41.145	1.0432	0.2166		1.0988	0.3476
4	0.00	09.327	23.259	25.853	36.660	0.6345	0.7052	34.101	0.4697	0.8149
	0.02	11.714	29.212	21.557	38.268	0.7633	0.5880		0.6170	0.7380
	0.04	13.355	33.305	18.395	39.225	0.8491	0.5018		0.7350	0.6704
	0.06	14.550	36.283	16.013	39.863	0.9102	0.4368		0.8282	0.6110
	0.08	15.457	38.544	14.164	40.319	0.9560	0.3864		0.9017	0.5585
	0.10	16.168	40.319	12.692	40.663	0.9915	0.3462		0.9592	0.5122
6	0.00	09.830	24.512	27.321	37.024	0.6621	0.7379	34.101	0.4697	0.8148
	0.02	11.613	28.961	24.140	38.206	0.7581	0.6520		0.5717	0.7625
	0.04	12.984	32.379	21.554	39.017	0.8299	0.6520		0.6593	0.7145
	0.06	14.068	35.082	19.438	39.611	0.8857	0.5822		0.7346	0.6705
	0.08	14.946	37.270	17.686	40.065	0.9302	0.4777		0.7991	0.6300
	0.10	15.670	39.078	16.216	40.424	0.9667	0.4380		0.8542	0.5929
7	0.00	10.072	25.118	28.046	37.195	0.6753	0.7540	34.101	0.4697	0.8147
	0.02	11.667	29.095	25.206	38.239	0.7609	0.6777		0.5579	0.7696
	0.04	12.935	32.257	22.828	38.989	0.8273	0.6138		0.6354	0.7278
	0.06	13.965	34.826	20.832	39.556	0.8804	0.5601		0.7035	0.6889
	0.08	14.818	36.952	19.142	40.008	0.9238	0.5146		0.7632	0.6528
	0.10	15.535	38.741	17.697	40.358	0.9599	0.4758		0.8154	0.6192
8	0.00	10.310	25.710	28.766	37.358	0.6882	0.7700	34.101	0.4697	0.8146
	0.02	11.757	29.319	26.189	38.294	0.7656	0.7010		0.5474	0.7750
	0.04	12.938	32.264	23.983	38.991	0.8275	0.6420		0.6168	0.7392
	0.06	13.919	34.709	22.093	39.531	0.8780	0.5914		0.6788	0.7031
	0.08	14.745	36.770	20.454	39.963	0.9201	0.5478		0.7340	0.6705
	0.10	15.45	38.530	19.050	40.317	0.9557	0.5099		0.7832	0.6399
10	0.00	10.768	26.854	30.193	37.666	0.7129	0.8016	34.101	0.4697	0.8143
	0.02	11.999	29.923	27.995	38.442	0.7784	0.7432		0.5323	0.7826
	0.04	13.042	32.524	26.054	39.050	0.8329	0.6917		0.5895	0.7524
	0.06	13.936	34.753	24.340	39.541	0.8789	0.6462		0.6419	0.7237
	0.08	14.711	36.684	22.824	39.946	0.9184	0.6060		0.6896	0.6965
	0.10	15.388	38.372	21.476	40.286	0.9525	0.5702		0.7322	0.6706

TABLE No. A-4.2.3

..... (continued)

The upper and the lower bound solutions for the drawing of Hexagonal tube from round on a cylindrical plug.

Input tube size : 1.0625 in o.d. x 0.2500 in gauge  
 Reduction of area : 37.16%

Equivalent die semi-angle $\alpha_0$	Mean coeff. of friction $\mu$	UPPER BOUND						LOWER BOUND		
		Draw force	Mean draw stress	Mean die pressure	Mean yield stress	Mean draw stress	Mean die pressure	Mean yield stress	Mean draw stress	Mean die pressure
		P tonf	$\sigma_{za2}$ tonf in <sup>-2</sup>	$P_m$ tonf in <sup>-2</sup>	$\bar{Y}_m$ tonf in <sup>-2</sup>	/yield stress	/yield stress	$Y_m$ tonf in <sup>-2</sup>	/yield stress	/yield stress
12	0.00	11.208	27.949	31.610	37.951	0.7365	0.8329	34.101	0.4697	0.8141
	0.02	12.286	30.638	29.672	38.613	0.7935	0.7819		0.5220	0.7875
	0.04	13.224	32.977	27.924	39.152	0.8423	0.7358		0.5706	0.7621
	0.06	14.047	35.028	26.350	39.599	0.8845	0.6943		0.6157	0.7378
	0.08	14.773	36.840	24.930	39.977	0.9215	0.6569		0.6575	0.7145
	0.10	15.420	38.452	23.646	40.301	0.9541	0.6231		0.6963	0.6921
14	0.00	11.629	29.001	33.025	38.216	0.7589	0.8642	34.101	0.4697	0.8137
	0.02	12.594	31.406	31.276	38.794	0.8096	0.8184		0.5145	0.7910
	0.04	13.449	33.538	29.674	39.277	0.8539	0.7765		0.5566	0.7691
	0.06	14.212	35.441	28.210	39.687	0.8930	0.7382		0.5962	0.7480
	0.08	14.895	37.145	26.872	40.040	0.9277	0.7032		0.6332	0.7277
	0.10	15.512	38.683	25.646	40.347	0.9587	0.6711		0.6680	0.7080
16	0.00	12.036	30.016	34.446	38.464	0.7803	0.8955	34.101	0.4697	0.8133
	0.02	12.912	32.200	32.840	38.976	0.8261	0.8538		0.5088	0.7935
	0.04	13.700	34.164	31.353	39.413	0.8668	0.8151		0.5459	0.7743
	0.06	14.411	35.938	29.979	39.391	0.9032	0.7794		0.5810	0.7557
	0.08	15.057	37.548	28.709	40.121	0.9359	0.7464		0.6142	0.7377
	0.10	15.646	39.016	27.533	40.412	0.9654	0.7158		0.6456	0.7202
18	0.00	12.431	31.001	35.883	38.699	0.8011	0.9272	34.101	0.4697	0.8129
	0.02	13.236	33.006	34.388	39.158	0.8429	0.8886		0.5044	0.7953
	0.04	13.967	34.830	32.993	39.557	0.8805	0.8526		0.5374	0.7783
	0.06	14.635	36.495	31.692	39.907	0.9145	0.8189		0.5689	0.7617
	0.08	15.247	38.021	30.479	40.216	0.9454	0.7876		0.5988	0.7455
	0.10	15.809	39.423	29.348	40.491	0.9736	0.7584		0.6274	0.7298
20	0.00	12.817	31.963	37.341	38.922	0.8212	0.9494	34.101	0.4697	0.8124
	0.02	13.562	33.820	35.936	39.339	0.8597	0.9233		0.5007	0.7967
	0.04	14.246	35.525	34.615	39.705	0.8947	0.8893		0.5304	0.7813
	0.06	14.875	37.095	33.375	40.029	0.9267	0.8575		0.5589	0.7664
	0.08	15.457	38.544	32.211	40.319	0.9560	0.8276		0.5861	0.7518
	0.10	15.995	39.887	31.118	40.580	0.9829	0.7995		0.6122	0.7376
22	0.00									
	0.02									
	0.04									
	0.06									
	0.08									
	0.10									

TABLE No. A-4. 2.4

The upper and the lower bound solutions for the drawing of hexagonal tube from round on a cylindrical plug.

Input tube size : 1.0625 in o.d. x 0.1875 in gauge  
 Reduction of area : 46.00%

Equivalent die semi-angle $\alpha_e$	Mean coeff. of friction $\mu$	UPPER BOUND						LOWER BOUND		
		Draw force	Mean draw stress	Mean die pressure	Mean yield stress	Mean draw stress/ yield stress	Mean die pressure/ yield stress	Mean yield stress	Mean draw stress/ yield stress	Mean die pressure/ yield stress
		P tonf	$\sigma_{za}$ tonf in <sup>-2</sup>	$p_m$ tonf in <sup>-2</sup>	$\bar{Y}_m$ tonf in <sup>-2</sup>			$Y_m$ tonf in <sup>-2</sup>		
2	0.00	07.386	26.542	20.355	37.583	0.7062	0.5416	36.413	0.6239	0.7615
	0.02	10.281	36.945	13.473	39.999	0.9236	0.3585		0.9358	0.5796
	0.04	11.643	41.839	10.008	40.947	1.0218	0.2663		1.0876	0.4524
	0.06	12.433	44.676	07.954	41.456	1.0776	0.2116		1.1543	0.3519
	0.08	12.948	46.526	06.593	41.775	1.1137	0.1754		1.1772	0.2963
	0.10	13.310	47.827	05.630	41.992	1.1389	0.1498		1.1786	0.2479
4	0.00	07.781	27.962	21.480	37.954	0.7367	0.5659	36.413	0.6239	0.7615
	0.02	09.638	34.632	17.150	39.515	0.8764	0.4519		0.8063	0.6623
	0.04	10.828	38.910	14.216	40.391	0.9633	0.3746		0.9355	0.5797
	0.06	11.655	41.880	12.123	40.955	1.0226	0.3194		1.0257	0.5105
	0.08	12.261	44.060	10.560	41.348	1.0656	0.2783		1.0873	0.4525
	0.10	12.726	45.728	09.351	41.639	1.0982	0.2464		1.1282	0.4035
6	0.00	08.157	29.312	22.579	38.292	0.7655	0.5897	36.413	0.6239	0.7614
	0.02	09.553	34.330	19.449	39.449	0.8702	0.5051		0.7520	0.6933
	0.04	10.571	37.988	16.871	40.209	0.9447	0.4406		0.8541	0.6331
	0.06	11.345	40.768	14.942	40.748	1.0005	0.3902		0.9351	0.5797
	0.08	11.953	42.951	13.400	41.150	1.0437	0.3499		0.9988	0.5323
	0.10	12.442	44.709	12.143	41.462	1.0783	0.3171		1.0485	0.4901
7	0.00	08.338	29.962	23.122	38.451	0.7792	0.6013	36.413	0.6239	0.7613
	0.02	09.588	34.453	20.224	39.476	0.8728	0.5260		0.7353	0.7025
	0.04	10.536	37.860	17.932	40.184	0.9422	0.4664		0.8271	0.6495
	0.06	11.279	40.530	16.089	40.703	0.9957	0.4184		0.9024	0.6018
	0.08	11.876	42.676	14.581	41.100	1.0383	0.3792		0.9640	0.5589
	0.10	12.367	44.438	13.327	41.415	1.0730	0.3466		1.0140	0.5198
8	0.00	08.514	30.595	23.660	38.603	0.7926	0.6129	36.413	0.6239	0.7611
	0.02	09.649	34.673	21.027	39.523	0.8773	0.5447		0.7224	0.7094
	0.04	10.537	37.863	18.886	40.184	0.9422	0.4892		0.8055	0.6622
	0.06	11.249	40.424	17.124	40.683	0.9936	0.4436		0.8756	0.6191
	0.08	11.834	42.523	15.653	41.073	1.0353	0.4055		0.9345	0.5797
	0.10	12.321	44.274	14.410	41.386	1.0698	0.3733		0.9837	0.5437
10	0.00	08.854	31.818	24.726	38.889	0.8182	0.6358	36.413	0.6239	0.7608
	0.02	09.819	35.284	22.478	39.654	0.8898	0.5780		0.7037	0.7192
	0.04	10.608	38.120	20.576	40.235	0.9474	0.5291		0.7735	0.6804
	0.06	11.265	40.481	18.956	40.693	0.9948	0.4874		0.8344	0.6445
	0.08	11.820	42.475	17.563	41.064	1.0344	0.4516		0.8875	0.6110
	0.10	12.295	44.182	16.335	41.370	1.0680	0.4206		0.9337	0.5798

TABLE No. A-4.2.4

..... (continued)

The upper and the lower bound solutions for the drawing of Hexagonal tube from round on a cylindrical plug.

Input tube size : 1.0625 in o.d. x 0.1875 in gauge  
 Reduction of area : 46.00 %

Equivalent die semi-angle $\alpha_0$	Mean coeff. of friction $\mu$	UPPER BOUND					LOWER BOUND			
		Draw force	Mean draw stress	Mean die pressure	Mean yield stress	Mean draw stress	Mean die pressure	Mean yield stress	Mean draw stress	Mean die pressure
		P tonf	$\sigma_{za_2}$ tonf in <sup>-2</sup>	$P_m$ tonf in <sup>-2</sup>	$\bar{Y}_m$ tonf in <sup>-2</sup>	/yield stress	/yield stress	$Y_m$ tonf in <sup>-2</sup>	/yield stress	/yield stress
12	0.00	09.179	32.986	25.787	39.154	0.8425	0.6586	36.413	0.6239	0.7604
	0.02	10.024	36.020	23.805	39.808	0.9048	0.6080		0.6908	0.7256
	0.04	10.736	38.579	22.082	40.326	0.9566	0.5640		0.7507	0.6929
	0.06	11.345	40.767	20.578	40.747	1.0005	0.5256		0.8043	0.6620
	0.08	11.871	42.656	19.257	41.097	1.0379	0.4918		0.8521	0.6330
	0.10	12.329	44.304	18.090	41.391	1.0704	0.4620		0.8947	0.6057
14	0.00	09.429	34.108	26.850	38.401	0.8657	0.6815	36.413	0.6239	0.7600
	0.02	10.246	36.818	25.061	39.973	0.9211	0.6361		0.6814	0.7301
	0.04	10.897	39.156	23.476	40.439	0.9683	0.5958		0.7338	0.7018
	0.06	11.464	41.194	22.068	40.828	1.0090	0.5601		0.7813	0.6749
	0.08	11.962	42.984	20.8112	41.159	1.0444	0.5282		0.8246	0.6493
	0.10	12.403	44.569	19.684	41.438	1.0756	0.4996		0.8638	0.6250
16	0.00	09.794	35.195	27.923	39.635	0.8880	0.7045	36.413	0.6239	0.7595
	0.02	10.478	37.651	26.282	40.142	0.9379	0.6631		0.6742	0.7334
	0.04	11.0781	39.808	24.808	40.565	0.9813	0.6259		0.7206	0.7085
	0.06	11.609	41.715	23.476	40.924	1.0193	0.5923		0.7632	0.6846
	0.08	12.082	43.415	22.274	41.233	1.0529	0.5620		0.8025	0.6618
	0.10	12.505	44.937	21.184	41.502	1.0828	0.5345		0.8386	0.6400
18	0.00	10.089	36.254	29.014	39.857	0.9096	0.7279	36.413	0.6239	0.7589
	0.02	10.715	38.505	27.487	40.312	0.9552	0.6897		0.6685	0.7358
	0.04	11.273	40.509	26.099	40.699	0.9953	0.6548		0.7100	0.7136
	0.06	11.773	42.304	24.835	41.033	1.0310	0.6231		0.7486	0.6922
	0.08	12.222	43.920	23.680	41.323	1.0628	0.5941		0.7845	0.6717
	0.10	12.629	45.382	22.623	41.579	1.0915	0.5676		0.8178	0.6520
20	0.00	10.379	37.297	30.131	40.070	0.9308	0.7520	36.413	0.6239	0.7583
	0.02	10.959	39.380	28.697	40.483	0.9727	0.7162		0.6639	0.7376
	0.04	11.480	41.254	27.380	40.839	1.0102	0.6833		0.7014	0.7176
	0.06	11.952	42.942	26.170	41.150	1.0437	0.6531		0.7365	0.6982
	0.08	12.381	44.489	25.057	41.424	1.0740	0.6253		0.7694	0.6796
	0.10	12.772	45.895	24.029	41.667	1.1014	0.5997		0.8002	0.6616
22	0.00									
	0.02									
	0.04									
	0.06									
	0.08									
	0.10									

TABLE No. A-4.3.1

The upper and the lower bound solutions for the drawing of octagonal tube from round on a cylindrical plug.

Input tube size : 1.000 in o.d. x 0.1875 in gauge  
 Reduction of area : 16.36%

Equivalent die semi-angle $\alpha_0$	Mean coeff. of friction $\mu$	UPPER BOUND						LOWER BOUND		
		Draw force	Mean draw stress	Mean die pressure	Mean yield stress	Mean draw stress/ yield stress	Mean die pressure/ yield stress	Mean yield stress	Mean draw stress/ yield stress	Mean die pressure/ yield stress
		P tonf	$\sigma_{za}$ tonf in <sup>-2</sup>	$p_m$ tonf in <sup>-2</sup>	$\bar{Y}_m$ tonf in <sup>-2</sup>			$Y_m$ tonf in <sup>-2</sup>		
2	0.00	05.234	13.076	44.845	32.891	0.3976	1.3634	27.317	0.1813	0.9313
	0.02	08.068	20.155	33.302	35.684	0.5648	0.9332		0.3237	0.8593
	0.04	09.626	24.047	26.170	36.891	0.6518	0.7094		0.4438	0.7944
	0.06	10.606	26.495	21.497	37.971	0.7052	0.5722		0.5499	0.7360
	0.08	11.278	28.174	18.222	38.008	0.7413	0.4794		0.6301	0.6832
	0.10	11.767	29.396	15.806	38.313	0.7673	0.4125		0.7016	0.6356
4	0.00	05.662	14.144	48.606	33.381	0.4237	1.4561	27.317	0.1813	0.9312
	0.02	07.450	18.612	41.596	35.153	0.5295	1.1833		0.2554	0.8943
	0.04	08.724	21.795	36.089	36.214	0.6018	0.9966		0.3235	0.8593
	0.06	09.674	24.167	31.783	36.925	0.6545	0.8607		0.3861	0.8260
	0.08	10.408	26.000	28.359	37.437	0.6945	0.7575		0.4435	0.7944
	0.10	10.992	27.458	25.583	37.824	0.7259	0.6764		0.4962	0.7645
6	0.00	06.030	21.065	51.947	33.780	0.4460	1.5378	27.317	0.1813	0.9312
	0.02	07.373	18.420	46.761	35.084	0.5250	1.3328		0.2313	0.9063
	0.04	08.433	21.067	42.318	35.983	0.5855	1.1761		0.2786	0.8824
	0.06	09.288	23.203	38.560	36.643	0.6332	1.0523		0.3232	0.8593
	0.08	09.991	24.959	35.371	37.150	0.6718	0.9521		0.3655	0.8369
	0.10	10.579	26.428	32.646	37.553	0.7038	0.8693		0.4053	0.8153
7	0.00	06.196	15.480	53.495	33.953	0.4559	1.5755	27.317	0.1813	0.9311
	0.02	07.398	18.482	48.867	35.106	0.5265	1.3920		0.2243	0.9098
	0.04	08.377	20.924	44.804	35.937	0.5823	1.2467		0.2652	0.8891
	0.06	09.186	22.940	41.282	36.567	0.6276	1.1289		0.3042	0.8691
	0.08	09.867	24.648	38.229	37.063	0.6650	1.0315		0.3414	0.8496
	0.10	10.446	26.095	35.571	37.463	0.6965	0.9495		0.3769	0.8307
8	0.00	06.353	15.870	54.982	34.113	0.4652	1.6118	27.317	0.1813	0.9310
	0.02	07.353	18.596	50.786	35.147	0.5291	1.4450		0.2189	0.9124
	0.04	09.121	20.868	47.034	35.918	0.5810	1.3095		0.2551	0.8942
	0.06	09.121	22.787	43.720	36.518	0.6240	1.1972		0.2897	0.8765
	0.08	09.778	24.426	40.798	37.000	0.6602	1.1026		0.3229	0.8593
	0.10	10.345	25.842	38.215	37.394	0.6911	1.0219		0.3547	0.8425
10	0.00	06.644	16.598	57.847	34.402	0.4825	1.6815	27.317	0.1819	0.9309
	0.02	07.572	18.915	53.273	35.260	0.5364	1.5392		0.2114	0.9160
	0.04	08.372	20.914	50.996	35.933	0.5820	1.4192		0.2406	0.9013
	0.06	09.068	22.652	48.022	35.478	0.6210	1.3165		0.2688	0.8870
	0.08	09.678	24.177	45.335	36.928	0.6547	1.2276		0.2960	0.8730
	0.10	10.217	25.524	42.905	37.307	0.6841	1.1500		0.3224	0.8593

TABLE No. A-4. 3.1

..... (continued)

The upper and the lower bound solutions for the drawing of octagonal tube from round on a cylindrical plug.

Input tube size : 1.000 in o.d. x 0.1875 in gauge  
 Reduction of area : 16.36%

Equivalent die semi-angle $\alpha_e^\circ$	Mean coeff. of friction $\mu$	UPPER BOUND					LOWER BOUND			
		Draw force	Mean draw stress	Mean die pressure	Mean yield stress	Mean draw stress	Mean die pressure	Mean yield stress	Mean draw stress	Mean die pressure
		P tonf	$\sigma_{za}^2$ tonf in <sup>-2</sup>	$P_m$ tonf in <sup>-2</sup>	$\bar{Y}_m$ tonf in <sup>-2</sup>	/yield stress	/yield stress	stress	$Y_m$ tonf in <sup>-2</sup>	/yield stress
12	0.00	06.920	17.287	60.682	34.667	0.4986	1.7504	27.317	0.1813	0.9307
	0.02	07.733	19.317	57.530	35.400	0.5457	1.6251		0.2064	0.9183
	0.04	08.450	21.110	54.592	35.996	0.5864	1.5166		0.2308	0.9061
	0.06	09.088	24.702	51.880	36.493	0.6221	1.4216		0.2545	0.8941
	0.08	09.657	24.124	49.385	36.913	0.6535	1.3379		0.2775	0.8823
	0.10	10.168	25.402	47.092	37.273	0.6815	1.2634		0.3000	0.8707
14	0.00	07.194	17.972	63.611	34.921	0.5145	1.8215	27.317	0.1813	0.9306
	0.02	07.922	19.791	60.759	35.562	0.5565	1.7085		0.2027	0.9199
	0.04	08.576	21.425	58.071	36.097	0.5935	1.6087		0.2236	0.9094
	0.06	09.166	22.899	55.558	36.552	0.6265	1.5199		0.2441	0.8991
	0.08	08.701	24.233	53.217	36.944	0.6559	1.4404		0.2640	0.8889
	0.10	10.187	25.447	51.039	37.286	0.6825	1.3688		0.2835	0.8789
16	0.00	07.478	18.681	66.740	35.177	0.5311	1.8972	27.317	0.1813	0.9303
	0.02	08.142	20.341	64.105	35.746	0.5690	1.7933		0.1999	0.9211
	0.04	08.747	21.851	61.602	36.231	0.6031	1.7008		0.2182	0.9119
	0.06	09.298	23.228	59.240	36.651	0.6338	1.6163		0.2361	0.9029
	0.08	09.803	24.490	57.020	37.018	0.6616	1.5403		0.2537	0.8939
	0.10	10.267	25.648	54.935	37.341	0.6869	1.4711		0.2708	0.8851
18	0.00	07.783	19.442	70.164	35.443	0.5485	1.9796	27.317	0.1813	0.9301
	0.02	08.398	20.978	67.689	35.954	0.5835	1.8826		0.1978	0.9219
	0.04	08.963	22.390	65.324	36.398	0.6151	1.7947		0.2140	0.9138
	0.06	09.483	23.690	63.075	36.787	0.6440	1.7146		0.2298	0.9057
	0.08	09.964	24.891	60.946	37.131	0.6704	1.6414		0.2455	0.8978
	0.10	10.409	26.004	58.932	37.438	0.6946	1.5741		0.2608	0.8899
20	0.00	08.114	20.269	73.945	35.722	0.5674	2.0700	27.317	0.1813	0.9298
	0.02	08.690	21.702	71.586	36.187	0.5999	1.9782		0.1960	0.9225
	0.04	09.224	23.043	69.321	36.595	0.6297	1.8942		0.2105	0.9152
	0.06	09.720	24.281	67.157	36.958	0.6570	1.8171		0.2248	0.9080
	0.08	10.181	25.433	65.095	37.282	0.6822	1.7460		0.2388	0.9008
	0.10	10.611	26.507	63.134	37.574	0.7055	1.6802		0.2526	0.8938
22	0.00									
	0.02									
	0.04									
	0.06									
	0.08									
	0.10									

TABLE No. A-4. 3.2

The upper and the lower bound solutions for the drawing of octagonal tube from round on a cylindrical plug.

Input tube size : 1.1250 in o.d. x 0.3125 in gauge  
 Reduction of area : 35.97%

Equivalent die semi-angle $\alpha_0$	Mean coeff. of friction $\mu$	UPPER BOUND						LOWER BOUND		
		Draw force	Mean draw stress	Mean die pressure	Mean yield stress	Mean draw stress/ yield stress	Mean die pressure/ yield stress	Mean yield stress	Mean draw stress/ yield stress	Mean die pressure/ yield stress
		P tonf	$\sigma_{za}$ tonf in <sup>-2</sup>	$P_m$ tonf in <sup>-2</sup>	$\bar{Y}_m$ tonf in <sup>-2</sup>			$Y_m$ tonf in <sup>-2</sup>		
2	0.00	10.657	20.965	24.577	35.657	0.5809	0.6843	33.777	0.4489	0.8096
	0.02	15.286	29.928	18.056	38.443	0.7785	0.5027		0.6948	0.6772
	0.04	17.821	34.892	14.148	39.570	0.8818	0.3939		0.8563	0.5726
	0.06	19.414	38.011	11.607	40.214	0.9452	0.3232		0.9605	0.6892
	0.08	20.507	40.150	09.833	40.631	0.9882	0.2738		1.0262	0.4224
	0.10	21.302	41.707	08.526	40.923	1.0192	0.2374		1.0663	0.3583
4	0.00	11.262	22.050	25.992	36.293	0.6075	0.7162	33.777	0.4489	0.8095
	0.02	14.120	27.645	22.082	37.873	0.7290	0.6084		0.5843	0.7395
	0.04	16.149	31.618	19.098	38.843	0.8140	0.5262		0.6945	0.6773
	0.06	17.659	34.575	16.790	39.502	0.8752	0.4626		0.7838	0.6620
	0.08	18.826	36.859	14.966	39.981	0.9219	0.4124		0.8559	0.5727
	0.10	19.753	38.675	13.492	40.345	0.9596	0.3718		0.9139	0.5287
6	0.00	11.846	23.194	27.376	36.640	0.6330	0.7472	33.777	0.4489	0.8095
	0.02	13.966	27.344	24.511	37.794	0.7235	0.6690		0.5420	0.7619
	0.04	15.634	30.609	22.118	38.606	0.7929	0.6036		0.6233	0.7180
	0.06	16.978	33.241	20.118	39.211	0.8477	0.5491		0.6941	0.6774
	0.08	18.083	35.404	18.434	39.679	0.8923	0.5031		0.7557	0.6399
	0.10	19.006	37.213	17.000	40.053	0.9291	0.4640		0.8091	0.6051
7	0.00	12.131	23.751	28.057	36.805	0.6453	0.7623	33.777	0.4489	0.8094
	0.02	14.021	27.452	25.510	37.822	0.7258	0.6931		0.5294	0.7685
	0.04	15.556	30.457	23.325	38.570	0.7896	0.6338		0.6011	0.7303
	0.06	16.825	32.941	21.455	39.144	0.8415	0.5830		0.6647	0.6945
	0.08	17.890	35.027	19.846	39.599	0.8845	0.5392		0.7213	0.6611
	0.10	18.797	36.803	18.452	39.970	0.9208	0.5013		0.7714	0.6298
8	0.00	12.410	24.298	28.731	36.963	0.6574	0.7773	33.777	0.4489	0.8094
	0.02	14.122	27.650	26.828	37.874	0.7300	0.7150		0.5197	0.7784
	0.04	15.546	30.650	24.414	38.565	0.7892	0.6605		0.5837	0.7396
	0.06	16.747	32.790	22.657	39.110	0.8384	0.6130		0.6415	0.7077
	0.08	17.773	34.799	21.120	39.550	0.8798	0.5714		0.6936	0.6776
	0.10	18.660	36.534	19.767	39.915	0.9153	0.5348		0.7405	0.6492
10	0.00	12.955	25.365	30.061	37.263	0.6807	0.8067	33.777	0.4489	0.8092
	0.02	14.407	28.207	28.110	38.016	0.7420	0.7544		0.5059	0.7804
	0.04	15.656	30.654	26.356	38.617	0.7938	0.7073		0.5585	0.7529
	0.06	16.743	32.781	24.784	39.108	0.8382	0.6651		0.6070	0.7267
	0.08	17.695	34.646	23.374	39.518	0.8767	0.6273		0.6517	0.7017
	0.10	18.537	36.293	22.105	39.865	0.9104	0.5932		0.6928	0.6779

TABLE No. A-4.3.2

..... (continued)

The upper and the lower bound solutions for the drawing of octagonal tube from round on a cylindrical plug.

Input tube size : 1.1250 in o.d. x 0.3125 in gauge  
 Reduction of area : 35.97%

Equivalent die semi-angle $\alpha_0^\circ$	Mean coeff. of friction $\mu$	UPPER BOUND					LOWER BOUND			
		Draw force	Mean draw stress	Mean die pressure	Mean yield stress	Mean draw stress	Mean die pressure	Mean yield stress	Mean draw stress	Mean die pressure
		P tonf	$\sigma_{za}$ tonf in <sup>-2</sup>	$P_m$ tonf in <sup>-2</sup>	$\bar{Y}_m$ tonf in <sup>-2</sup>	/yield stress	/yield stress	$Y_m$ tonf in <sup>-2</sup>	/yield stress	/yield stress
12	0.00	13.483	26.398	31.368	37.545	0.7031	0.8355	33.777	0.4489	0.8091
	0.02	14.752	28.883	29.661	38.186	0.7564	0.7900		0.4965	0.7851
	0.04	15.871	31.074	28.096	38.716	0.8026	0.7483		0.5411	0.7620
	0.06	16.865	33.020	26.668	39.161	0.8432	0.7103		0.5827	0.7398
	0.08	17.752	34.757	25.363	39.542	0.8790	0.6755		0.6217	0.7184
	0.10	18.550	36.318	24.170	39.871	0.9109	0.6438		0.6580	0.6979
14	0.00	13.995	27.400	32.661	37.809	0.7247	0.8638	33.777	0.4487	0.8089
	0.02	15.128	29.619	31.130	38.368	0.7719	0.8234		0.4897	0.7884
	0.04	16.145	31.610	29.710	38.841	0.8138	0.7858		0.5283	0.7649
	0.06	17.062	33.406	28.395	39.241	0.8512	0.7510		0.5647	0.7493
	0.08	17.893	35.034	27.178	39.601	0.8847	0.7188		0.5990	0.7307
	0.10	18.650	36.514	26.052	39.911	0.9149	0.6891		0.6314	0.7127
16	0.00	14.493	28.375	33.942	38.059	0.7456	0.8918	33.777	0.4489	0.8087
	0.02	15.520	30.387	32.547	38.553	0.7882	0.8552		0.4845	0.7908
	0.04	16.455	32.218	31.240	38.980	0.8264	0.8208		0.5184	0.7734
	0.06	17.308	33.888	30.017	39.353	0.8611	0.7887		0.5507	0.7565
	0.08	18.090	35.418	28.875	39.682	0.8925	0.7587		0.5813	0.7400
	0.10	18.808	36.825	27.808	39.974	0.9212	0.7307		0.6105	0.7241
18	0.00	14.980	29.329	35.220	38.297	0.7658	0.9196	33.777	0.4489	0.8085
	0.02	15.923	31.175	33.932	38.740	0.8047	0.8860		0.4804	0.7926
	0.04	16.789	32.871	32.716	39.128	0.8401	0.8543		0.5106	0.7771
	0.06	17.588	34.435	31.569	39.472	0.8724	0.8243		0.5395	0.7621
	0.08	18.326	35.880	30.490	39.779	0.9020	0.7962		0.5671	0.7474
	0.10	19.010	37.219	29.474	40.055	0.9292	0.7696		0.5936	0.7331
20	0.00	15.458	30.266	36.498	38.524	0.7856	0.9474	33.777	0.4489	0.8082
	0.02	16.331	31.975	35.298	38.925	0.8214	0.9162		0.4771	0.7940
	0.04	17.140	33.558	34.157	39.281	0.8543	0.8866		0.5042	0.7801
	0.06	17.891	35.029	33.075	39.600	0.8846	0.8585		0.5303	0.7666
	0.08	19.591	36.399	32.049	39.887	0.9125	0.8319		0.5554	0.7533
	0.10	19.243	37.677	31.078	40.147	0.9385	0.8067		0.5795	0.7404
22	0.00									
	0.02									
	0.04									
	0.06									
	0.08									
	0.10									

TABLE No. A-4.3.3

The upper and the lower bound solutions for the drawing of octagonal tube from round on a cylindrical plug.

Input tube size : 1.1250 in o.d. x 0.2500 in gauge  
 Reduction of area : 41.75%

Equivalent die semi-angle $\alpha_e$	Mean coeff. of friction $\mu$	UPPER BOUND						LOWER BOUND		
		Draw force	Mean draw stress	Mean die pressure	Mean yield stress	Mean draw stress/ yield stress	Mean die pressure/ yield stress	Mean yield stress	Mean draw stress/ yield stress	Mean die pressure/ yield stress
		P tonf	$\sigma_{za}$ tonf in <sup>-2</sup>	$p_m$ tonf in <sup>-2</sup>	$\bar{Y}_m$ tonf in <sup>-2</sup>			$Y_m$ tonf in <sup>-2</sup>		
2	0.00	09.430	23.557	21.653	36.748	0.6410	0.5892	35.320	0.5446	0.7731
	0.02	13.303	33.233	14.981	39.209	0.8476	0.4077		0.8287	0.6138
	0.04	15.245	38.083	11.372	40.228	0.9467	0.3095		0.9883	0.4962
	0.06	16.407	40.988	09.150	40.789	1.0049	0.2490		1.0739	0.4084
	0.08	17.181	42.919	07.651	41.144	1.0431	0.2082		1.1163	0.3419
	0.10	17.732	44.297	06.572	41.390	1.0702	0.1788		1.1340	0.2909
4	0.00	09.942	24.837	22.848	37.116	0.6692	0.6156	35.320	0.5546	0.7731
	0.02	12.386	30.941	18.737	38.685	0.7998	0.5048		0.7063	0.6873
	0.04	14.022	35.029	15.899	39.599	0.8846	0.4259		0.8284	0.6139
	0.06	15.191	37.949	13.651	40.201	0.9440	0.3678		0.9200	0.5507
	0.08	16.067	40.138	12.002	40.628	0.9879	0.3234		0.9880	0.4963
	0.10	16.748	41.839	10.704	40.947	1.0218	0.2884		1.0378	0.4493
6	0.00	10.437	26.074	24.018	37.457	0.6961	0.6412	35.320	0.5446	0.7730
	0.02	12.264	30.638	20.973	38.613	0.7934	0.5592		0.6571	0.7145
	0.04	13.641	34.076	18.560	39.394	0.8550	0.4955		0.7505	0.6617
	0.06	14.713	36.754	16.622	39.960	0.9198	0.4438		0.8280	0.6140
	0.08	15.571	38.897	15.039	40.389	0.9631	0.4015		0.8920	0.5709
	0.10	16.272	40.650	13.726	40.727	0.9981	0.3664		0.9445	0.5319
7	0.00	10.679	26.677	24.594	37.619	0.7091	0.6538	35.320	0.5446	0.7729
	0.02	12.311	30.755	21.879	38.641	0.7959	0.5816		0.6421	0.7225
	0.04	13.587	33.942	19.656	39.365	0.8622	0.5225		0.7254	0.6762
	0.06	14.609	36.495	17.822	39.907	0.9145	0.4738		0.7963	0.6339
	0.08	15.446	38.586	16.289	40.328	0.9568	0.4330		0.8566	0.5951
	0.10	16.144	40.329	14.993	40.665	0.9917	0.3986		0.9077	0.5595
8	0.00	10.916	27.269	25.165	37.775	0.7219	0.6662	35.320	0.5446	0.7729
	0.02	12.397	30.969	22.705	38.691	0.8004	0.6011		0.6306	0.7285
	0.04	13.587	33.941	20.642	39.365	0.8622	0.5464		0.7056	0.6875
	0.06	14.562	36.378	18.642	39.883	0.9121	0.5004		0.7708	0.6495
	0.08	15.376	38.411	17.421	40.293	0.9533	0.4612		0.8274	0.6142
	0.10	16.065	40.132	16.148	40.627	0.9878	0.4275		0.8765	0.5816
10	0.00	11.380	28.428	26.295	38.072	0.7469	0.6907	35.320	0.5446	0.7727
	0.02	12.638	31.570	24.205	38.832	0.8130	0.6358		0.6141	0.7371
	0.04	13.690	34.200	22.390	39.421	0.8675	0.5881		0.6764	0.7036
	0.06	14.583	36.430	20.810	39.421	0.9132	0.5466		0.7322	0.6720
	0.08	15.349	38.344	19.427	40.280	0.9519	0.5103		0.7821	0.6424
	0.10	16.014	40.005	18.209	40.603	0.9853	0.4783		0.8266	0.6145

TABLE No. A-4.3.3

..... (continued)

The upper and the lower bound solutions for the drawing of octagonal tube from round on a cylindrical plug.

Input tube size : 1.1250 in o.d. x 0.2500 in gauge  
 Reduction of area : 41.75%

Equivalent die semi-angle $\alpha_0^\circ$	Mean coeff. of friction $\mu$	UPPER BOUND					LOWER BOUND			
		Draw force P tonf	Mean draw stress $\sigma_{za}$ tonf in <sup>-2</sup>	Mean die pressure $P_m$ tonf in <sup>-2</sup>	Mean yield stress $\bar{Y}_m$ tonf in <sup>-2</sup>	Mean draw stress / yield stress	Mean die pressure / yield stress	Mean yield stress $Y_m$ tonf in <sup>-2</sup>	Mean draw stress / yield stress	Mean die pressure / yield stress
12	0.00	11.830	29.554	27.414	38.352	0.7706	0.7148	35.320	0.5446	0.7725
	0.02	12.932	32.305	25.580	39.000	0.8283	0.6670		0.6028	0.7428
	0.04	13.879	34.672	23.941	39.523	0.8773	0.6244		0.6559	0.7145
	0.06	14.703	36.730	22.497	39.955	0.9193	0.5866		0.7044	0.6877
	0.08	15.425	38.533	21.201	40.317	0.9557	0.5528		0.7487	0.6622
	0.10	16.062	40.125	20.039	40.626	0.9877	0.5225		0.7890	0.6379
14	0.00	12.271	30.654	28.528	38.617	0.7938	0.7387	35.320	0.5446	0.7723
	0.02	13.255	33.114	26.881	39.182	0.8451	0.6961		0.5945	0.7468
	0.04	14.120	35.274	25.391	39.652	0.8896	0.6575		0.6408	0.7225
	0.06	14.885	37.185	24.044	40.048	0.9285	0.6226		0.6835	0.6991
	0.08	15.567	38.887	22.822	40.387	0.9629	0.5910		0.7231	0.6768
	0.10	16.177	40.412	21.713	40.681	0.9934	0.5622		0.7596	0.6554
16	0.00	12.704	31.736	29.643	38.870	0.8164	0.7626	35.320	0.5446	0.7721
	0.02	13.597	33.968	28.139	39.371	0.8628	0.7239		0.5882	0.7498
	0.04	14.395	35.960	26.762	39.796	0.9036	0.6885		0.6290	0.7284
	0.06	15.110	37.743	25.500	40.161	0.9399	0.6560		0.6670	0.7078
	0.08	15.755	39.359	24.343	40.479	0.9723	0.6263		0.7028	0.6880
	0.10	16.340	40.819	23.281	40.757	1.0015	0.5989		0.7361	0.6689
18	0.00	13.132	32.805	30.767	39.113	0.8387	0.7866	35.320	0.5446	0.7718
	0.02	13.952	34.855	29.376	39.562	0.8810	0.7510		0.5833	0.7521
	0.04	14.694	36.706	28.089	39.950	0.9188	0.7182		0.6197	0.7331
	0.06	15.366	38.386	26.899	40.288	0.9528	0.6877		0.6540	0.7147
	0.08	15.979	39.917	25.798	40.586	0.9835	0.6596		0.6864	0.6969
	0.10	16.540	41.318	24.777	40.851	1.0114	0.6335		0.7168	0.6796
20	0.00	13.558	33.870	31.907	39.349	0.8607	0.8109	35.320	0.5446	0.7715
	0.02	14.318	35.769	30.607	39.756	0.8997	0.7778		0.5792	0.7539
	0.04	15.012	37.502	29.395	40.112	0.9349	0.7470		0.6121	0.7368
	0.06	15.647	39.089	28.215	40.426	0.9669	0.7183		0.6432	0.7202
	0.08	16.231	40.547	27.212	40.706	0.9961	0.6915		0.6727	0.7040
	0.10	16.770	41.892	26.229	40.957	1.0228	0.6666		0.7007	0.6884
22	0.00									
	0.02									
	0.04									
	0.06									
	0.08									
	0.10									

TABLE No. A-4.3.4

The upper and the lower bound solutions for the drawing of octagonal tube from round on a cylindrical plug.

Input tube size : 1.1250 in o.d. x 0.1875 in gauge  
 Reduction of area : 51.95 %

Equivalent die semi-angle $\alpha_c$	Mean coeff. of friction $\mu$	UPPER BOUND					LOWER BOUND			
		Draw force	Mean draw stress	Mean die pressure	Mean yield stress	Mean draw stress/ yield stress	Mean die pressure/ yield stress	Mean yield stress	Mean draw stress/ yield stress	Mean die pressure/ yield stress
		P tonf	$\sigma_{za}$ tonf in <sup>-2</sup>	$p_m$ tonf in <sup>-2</sup>	$\bar{Y}_m$ tonf in <sup>-2</sup>			$Y_m$ tonf in <sup>-2</sup>		
2	0.00	08.074	30.433	18.477	38.564	0.7891	0.4791	37.909	0.7402	0.7032
	0.02	10.992	41.432	11.834	40.872	1.0137	0.3069		1.0551	0.5064
	0.04	12.305	46.381	08.661	41.750	1.1109	0.2246		1.1753	0.3788
	0.06	13.050	49.188	06.823	42.215	1.1652	0.1769		1.2084	0.2938
	0.08	13.530	50.996	05.626	42.503	1.1998	0.1459		1.2053	0.2355
	0.10	13.864	52.257	04.786	42.699	1.2238	0.1241		1.1891	0.1943
4	0.00	08.445	31.830	19.341	38.892	0.8184	0.4973	37.909	0.7402	0.7031
	0.02	10.324	38.914	15.134	40.392	0.9634	0.3891		0.9321	0.5939
	0.04	11.493	43.319	12.388	41.216	1.0510	0.3185		1.0549	0.5065
	0.06	12.289	46.318	10.474	41.739	1.1097	0.2693		1.1308	0.4361
	0.08	12.865	48.490	09.067	42.101	1.1517	0.2331		1.1753	0.3798
	0.10	13.301	50.135	07.991	42.367	1.1833	0.2054		1.1986	0.3323
6	0.00	08.800	33.167	20.181	39.194	0.8462	0.5149	37.909	0.7402	0.7030
	0.02	10.212	38.490	17.040	40.309	0.9549	0.4347		0.8769	0.6276
	0.04	11.218	42.281	14.710	41.028	1.0305	0.3753		0.9790	0.5627
	0.06	11.970	45.115	12.928	41.533	1.0862	0.3299		1.0545	0.5066
	0.08	12.552	47.312	11.525	41.906	1.1290	0.2941		1.1093	0.4581
	0.10	13.017	49.064	10.394	42.195	1.1628	0.2652		1.1482	0.4159
7	0.00	08.972	33.816	20.594	39.337	0.8596	0.5235	37.909	0.7402	0.7029
	0.02	10.234	38.574	17.788	40.325	0.9566	0.4522		0.8595	0.6377
	0.04	11.172	42.110	15.625	40.997	1.0271	0.3972		0.9527	0.5803
	0.06	11.896	44.838	13.918	41.485	1.0808	0.3538		1.0248	0.5300
	0.08	12.471	47.005	12.541	41.855	1.1230	0.3188		1.0800	0.4851
	0.10	12.938	48.767	11.408	42.146	1.1571	0.2900		1.1216	0.4456
8	0.00	09.140	34.451	21.002	39.471	0.8727	0.5320	37.909	0.7402	0.7028
	0.02	10.285	38.765	18.458	40.363	0.9604	0.4676		0.8460	0.6454
	0.04	11.164	42.715	16.437	40.991	1.0265	0.4164		0.9313	0.5940
	0.06	11.860	44.700	14.803	41.461	1.0781	0.3750		0.9996	0.5481
	0.08	12.42	46.825	13.457	41.825	1.1195	0.3409		1.0539	0.5069
	0.10	12.889	48.581	12.332	42.116	1.1535	0.3124		1.0967	0.4698
10	0.00	09.468	35.687	21.809	39.739	0.8980	0.5488	37.909	0.7402	0.7026
	0.02	10.439	39.344	19.648	40.476	0.9720	0.4944		0.8263	0.6563
	0.04	11.220	42.291	17.351	41.030	1.0307	0.4493		0.8989	0.6139
	0.06	11.863	44.713	16.351	41.463	1.0784	0.4115		0.9600	0.5752
	0.08	12.401	46.739	15.074	41.811	1.1179	0.3793		1.0108	0.5397
	0.10	12.857	48.458	13.978	42.096	1.1511	0.3518		1.0523	0.5071

TABLE No. A-4. 3.4

..... (continued)

The upper and the lower bound solutions for the drawing of octagonal tube from round on a cylindrical plug.

Input tube size : 1.1250 in o.d. x 0.1875 in gauge  
 Reduction of area : 51.95 %

Equivalent die semi-angle $\alpha_0^\circ$	Mean coeff. of friction $\mu$	UPPER BOUND					LOWER BOUND			
		Draw force	Mean draw stress	Mean die pressure	Mean yield stress	Mean draw stress	Mean die pressure	Mean yield stress	Mean draw stress	Mean die pressure
		P tonf	$\sigma_{za}^2$ tonf in <sup>-2</sup>	$P_m$ tonf in <sup>-2</sup>	$\bar{Y}_m$ tonf in <sup>-2</sup>	/yield stress	/yield stress	$Y_m$ tonf in <sup>-2</sup>	/yield stress	/yield stress
12	0.00	09.786	36.886	22.607	39.987	0.9224	0.5654	37.909	0.7402	0.7024
	0.02	10.633	40.077	20.713	40.617	0.9867	0.5180		0.8127	0.6636
	0.04	11.338	42.736	19.095	41.111	1.0395	0.4775		0.8756	0.6277
	0.06	11.935	44.983	17.700	41.510	1.0837	0.4427		0.9300	0.5943
	0.08	12.445	46.906	16.490	41.839	1.1211	0.4124		0.9771	0.5632
	0.10	12.887	48.571	15.430	42.114	1.1533	0.3859		1.0176	0.5343
14	0.00	10.097	38.056	23.403	40.223	0.9461	0.5818	37.909	0.7402	0.7021
	0.02	10.851	40.899	21.706	40.772	1.0003	0.5396		0.8026	0.6688
	0.04	11.495	43.420	20.224	41.217	1.0511	0.5028		0.8579	0.6377
	0.06	12.051	45.420	18.922	41.586	1.0922	0.4704		0.9069	0.6084
	0.08	12.535	47.246	17.772	41.896	1.1277	0.4418		0.9502	0.5809
	0.10	12.961	48.851	16.949	42.160	1.1587	0.4164		0.9883	0.5550
16	0.00	10.402	39.208	24.204	40.449	0.9632	0.5984	37.909	0.7402	0.7017
	0.02	11.085	41.779	22.658	40.936	1.0206	0.5601		0.7949	0.6727
	0.04	11.678	44.015	21.285	41.340	1.0647	0.5262		0.8441	0.6452
	0.06	12.198	45.977	20.060	41.681	1.1031	0.4959		0.8885	0.6192
	0.08	12.659	47.712	18.964	41.973	1.1367	0.4688		0.9283	0.5946
	0.10	13.068	49.251	17.977	42.226	1.1665	0.4444		0.9640	0.5713
18	0.00	10.707	40.355	25.018	40.670	0.9922	0.6151	37.909	0.7402	0.7014
	0.02	11.331	42.706	23.590	41.106	1.0389	0.5800		0.7888	0.6756
	0.04	11.882	44.783	22.306	41.475	1.0797	0.5485		0.8330	0.6511
	0.06	12.371	46.629	21.148	41.792	1.1157	0.5200		0.8734	0.6278
	0.08	12.810	48.281	20.098	42.067	1.1477	0.4942		0.9101	0.6055
	0.10	13.204	49.767	19.144	42.308	1.1763	0.4707		0.9435	0.5843
20	0.00	11.012	41.505	25.849	40.885	1.0151	0.6322	37.909	0.7402	0.7001
	0.02	11.588	43.676	24.518	41.280	1.0580	0.5997		0.7834	0.6779
	0.04	12.103	45.617	23.308	41.620	1.0960	0.5701		0.8239	0.6558
	0.06	12.566	47.361	22.205	41.912	1.1299	0.5431		0.8608	0.6347
	0.08	12.984	48.937	21.197	42.174	1.1604	0.5185		0.8948	0.6144
	0.10	13.363	50.368	20.274	42.404	1.1878	0.4959		0.9260	0.5951
22	0.00									
	0.02									
	0.04									
	0.06									
	0.08									
	0.10									

TABLE No. A-4.4.1

The upper and the lower bound solutions for the drawing of decagonal tube from round on a cylindrical plug.

Input tube size : 1.0625 in o.d. x 0.3750 in gauge  
 Reduction of area : 18.75%

Equivalent die semi-angle $\alpha_p$	Mean coeff. of friction $\mu$	UPPER BOUND						LOWER BOUND		
		Draw force	Mean draw stress	Mean die pressure	Mean yield stress	Mean draw stress/ yield stress	Mean die pressure/ yield stress	Mean yield stress	Mean draw stress/ yield stress	Mean die pressure/ yield stress
		P tonf	$\sigma_{za}$ tonf in <sup>-2</sup>	$p_m$ tonf in <sup>-2</sup>	$\bar{Y}_m$ tonf in <sup>-2</sup>			$Y_m$ tonf in <sup>-2</sup>		
2	0.00	09.122	13.863	40.671	33.255	0.4169	1.2230	28.290	0.2089	0.9083
	0.02	13.757	20.906	33.506	35.931	0.5818	0.9326		0.3392	0.8425
	0.04	16.775	25.493	28.104	37.299	0.6835	0.7535		0.4503	0.7829
	0.06	18.883	28.696	24.110	38.140	0.7524	0.6321		0.5449	0.7288
	0.08	20.434	31.053	21.077	38.711	0.8022	0.5445		0.6252	0.6796
	0.10	21.622	32.859	18.708	39.125	0.8398	0.4781		0.6935	0.6349
4	0.00	09.769	14.845	43.576	33.687	0.4407	1.2936	28.290	0.2089	0.9083
	0.02	12.535	19.049	39.519	35.307	0.5395	1.1193		0.2766	0.8746
	0.04	14.726	22.049	35.901	36.395	0.6149	0.9864		0.3391	0.8425
	0.06	16.498	25.071	32.785	37.182	0.6743	0.8818		0.3968	0.8120
	0.08	17.956	27.287	30.117	37.780	0.7223	0.7972		0.4501	0.7829
	0.10	19.176	29.142	27.823	38.250	0.7619	0.7274		0.4992	0.7553
6	0.00	10.369	15.758	46.297	34.067	0.4626	1.3590	28.290	0.2089	0.9082
	0.02	12.401	18.545	43.386	35.235	0.5348	1.2313		0.2545	0.8856
	0.04	14.133	21.477	40.760	36.114	0.5947	1.1256		0.2978	0.8638
	0.06	15.623	23.742	38.149	36.802	0.6451	1.0366		0.3387	0.8426
	0.08	16.916	25.707	35.887	37.357	0.6881	0.9606		0.3778	0.8221
	0.10	18.048	27.427	33.847	37.816	0.7253	0.8950		0.4147	0.8023
7	0.00	10.653	16.190	47.591	34.241	0.4728	1.3899	28.290	0.2089	0.9082
	0.02	12.460	18.936	45.020	35.267	0.5369	1.2765		0.2481	0.8888
	0.04	14.034	21.329	42.569	36.066	0.5913	1.1803		0.2856	0.8700
	0.06	15.416	23.427	40.290	36.710	0.6382	1.0975		0.3214	0.8516
	0.08	16.635	25.281	38.194	37.240	0.6789	1.0256		0.3556	0.8338
	0.10	17.719	26.927	36.274	37.685	0.7145	0.9626		0.3883	0.8165
8	0.00	10.926	16.605	48.845	34.405	0.4826	1.4197	28.290	0.2089	0.9082
	0.02	12.560	19.087	46.532	35.320	0.5404	1.3174		0.2433	0.8912
	0.04	14.007	21.286	44.306	36.053	0.5904	1.2289		0.2763	0.8746
	0.06	15.295	23.244	42.210	36.655	0.6341	1.1515		0.3080	0.8585
	0.08	16.449	24.997	40.257	37.161	0.6727	1.0833		0.3385	0.8427
	0.10	17.486	26.573	38.447	37.591	0.7069	1.0227		0.3678	0.8273
10	0.00	11.443	17.391	51.235	34.706	0.5011	1.4763	28.290	0.2089	0.9081
	0.02	12.824	19.488	49.292	35.458	0.5496	1.3901		0.2364	0.8945
	0.04	14.076	21.391	47.399	36.086	0.5928	1.3135		0.2630	0.8812
	0.06	15.215	23.123	45.585	36.619	0.6314	1.2448		0.2888	0.8682
	0.08	16.256	24.704	43.865	37.078	0.6663	1.1830		0.3138	0.8554
	0.10	17.209	26.152	42.240	37.478	0.6978	1.1271		0.3381	0.8428

TABLE No. A-4. 4.1

..... (continued)

The upper and the lower bound solutions for the drawing of decagonal tube from round on a cylindrical plug.

Input tube size : 1.0625 in o.d. x 0.3750 in gauge  
 Reduction of area : 18.75%

Equivalent die semi-angle $\alpha_2^\circ$	Mean coeff. of friction $\mu$	UPPER BOUND						LOWER BOUND		
		Draw force	Mean draw stress	Mean die pressure	Mean yield stress	Mean draw stress	Mean die pressure	Mean yield stress	Mean draw stress	Mean die pressure
		P tonf	$\sigma_{za}$ tonf in <sup>-2</sup>	$P_m$ tonf in <sup>-2</sup>	$\bar{Y}_m$ tonf in <sup>-2</sup>	/yield stress	/yield stress	$Y_m$ tonf in <sup>-2</sup>	/yield stress	/yield stress
12	0.00	11.924	18.121	53.481	34.976	0.5181	1.5292	28.290	0.2089	0.9080
	0.02	13.137	19.950	51.796	35.615	0.5601	1.4543		0.2318	0.8967
	0.04	14.236	21.635	50.138	36.163	0.5983	1.3864		0.2541	0.8856
	0.06	15.261	23.192	48.532	36.646	0.6330	1.3246		0.2758	0.8747
	0.08	16.210	24.634	46.990	37.059	0.6547	1.2680		0.2969	0.8639
	0.10	17.090	25.971	45.517	37.429	0.6939	1.2161		0.3175	0.8534
14	0.00	12.376	18.808	55.630	35.222	0.5340	1.5794	28.290	0.2089	0.9079
	0.02	13.447	20.435	54.125	35.799	0.5712	1.5128		0.2285	0.8983
	0.04	14.446	21.953	42.641	36.264	0.6054	1.4516		0.2475	0.8885
	0.06	15.379	23.371	51.195	36.693	0.6369	1.3952		0.2662	0.8794
	0.08	16.251	24.697	49.794	37.076	0.6661	1.3430		0.2845	0.8701
	0.10	17.069	25.940	48.443	37.421	0.6932	1.2945		0.3023	0.8610
16	0.00	12.806	19.461	57.697	35.449	0.5490	1.6276	28.290	0.2089	0.9078
	0.02	13.774	20.932	56.334	35.939	0.5824	1.5675		0.2259	0.8994
	0.04	14.685	22.316	54.334	36.375	0.6135	1.5116		0.2426	0.8911
	0.06	15.543	23.620	53.554	36.766	0.6434	1.4596		0.2590	0.8829
	0.08	16.351	24.849	52.378	37.119	0.6694	1.4110		0.2750	0.8748
	0.10	17.115	26.010	51.129	37.440	0.6947	1.3656		0.2907	0.8668
18	0.00	13.236	20.106	59.761	35.668	0.5637	1.6755	28.290	0.2089	0.9077
	0.02	14.116	21.453	58.508	36.106	0.5941	1.6205		0.2239	0.9003
	0.04	14.956	22.728	57.267	36.501	0.6227	1.5689		0.2387	0.8929
	0.06	15.751	23.937	56.047	36.859	0.6494	1.5206		0.2532	0.8856
	0.08	16.506	25.085	54.853	37.185	0.6746	1.4751		0.2675	0.8784
	0.10	17.224	26.175	53.689	37.485	0.6983	1.4323		0.2815	0.8713
20	0.00	13.636	20.723	61.760	35.871	0.5777	1.7217	28.290	0.2089	0.9076
	0.02	14.454	21.150	60.598	36.267	0.6057	1.6709		0.2223	0.9009
	0.04	15.233	23.150	59.446	36.627	0.6320	1.6230		0.2356	0.8943
	0.06	15.976	24.278	58.309	36.957	0.6569	1.5777		0.2486	0.8878
	0.08	16.684	25.354	57.193	37.260	0.6805	1.5350		0.2614	0.8813
	0.10	17.360	26.382	56.102	37.540	0.7028	1.4944		0.2740	0.8749
22	0.00									
	0.02									
	0.04									
	0.06									
	0.08									
	0.10									

TABLE No. A-4.4.2

The upper and the lower bound solutions for the drawing of decagonal tube from round on a cylindrical plug.

Input tube size : 1.1250 in o.d. x 0.3125 in gauge.  
 Reduction of area : 32.50%

Equivalent die semi-angle $\alpha_e$	Mean coeff. of friction $\mu$	UPPER BOUND					LOWER BOUND			
		Draw force	Mean draw stress	Mean die pressure	Mean yield stress	Mean draw stress/ yield stress	Mean die pressure/ yield stress	Mean yield stress	Mean draw stress/ yield stress	Mean die pressure/ yield stress
		P tonf	$\sigma_{za}$ tonf in <sup>-2</sup>	$p_m$ tonf in <sup>-2</sup>	$\bar{Y}_m$ tonf in <sup>-2</sup>	yield stress	yield stress	$Y_m$ tonf in <sup>-2</sup>	yield stress	yield stress
2	0.00	10.653	19.788	27.377	35.561	0.5564	0.7699	32.805	0.3952	0.8274
	0.02	15.469	28.732	20.360	38.149	0.7532	0.5725		0.6234	0.7066
	0.04	18.150	33.713	16.056	39.315	0.8575	0.4515		0.7821	0.6085
	0.06	19.851	36.872	13.225	39.984	0.9222	0.3719		0.8914	0.5283
	0.08	21.025	39.052	11.233	40.419	0.9662	0.3159		0.9657	0.4624
	0.10	21.883	40.646	09.759	40.725	0.9981	0.2744		1.0152	0.4080
4	0.00	11.274	20.942	28.987	35.942	0.5826	0.8065	32.805	0.3952	0.8274
	0.02	14.238	26.446	24.805	37.558	0.7042	0.6901		0.5194	0.7639
	0.04	16.365	30.398	21.560	38.556	0.7884	0.5999		0.6231	0.7067
	0.06	17.961	33.362	19.025	39.238	0.8503	0.5293		0.7097	0.6551
	0.08	19.201	35.615	17.005	39.734	0.8976	0.4731		0.7818	0.6086
	0.10	20.192	37.504	15.364	40.112	0.9350	0.4275		0.8416	0.5665
6	0.00	11.871	22.050	30.544	36.293	0.6076	0.8416	32.805	0.3952	0.8273
	0.02	14.067	26.129	27.489	37.472	0.6973	0.7574		0.4803	0.7843
	0.04	15.809	29.365	24.905	38.306	0.7660	0.6862		0.5558	0.7442
	0.06	17.222	31.990	22.725	38.928	0.8217	0.6261		0.6228	0.7068
	0.08	18.390	34.158	20.875	39.412	0.8667	0.5752		0.6822	0.6719
	0.10	19.370	35.979	19.293	39.800	0.9040	0.5316		0.7348	0.6393
7	0.00	12.161	22.588	31.305	36.458	0.6196	0.8586	32.805	0.3952	0.8273
	0.02	14.118	26.224	28.592	37.265	0.6993	0.7842		0.4686	0.7903
	0.04	15.720	29.199	26.238	38.265	0.7631	0.7197		0.5349	0.7555
	0.06	17.052	31.672	24.206	38.844	0.8151	0.6639		0.5948	0.7226
	0.08	18.175	33.759	22.445	39.325	0.8585	0.6156		0.6488	0.6917
	0.10	19.135	35.543	20.911	39.708	0.8951	0.5736		0.6975	0.6625
8	0.00	12.445	23.116	32.053	36.617	0.6313	0.8754	32.805	0.3952	0.8273
	0.02	14.217	26.408	29.604	37.547	0.7033	0.8085		0.4598	0.7948
	0.04	15.701	29.165	27.439	38.256	0.7623	0.7493		0.5188	0.7640
	0.06	16.960	31.503	25.534	38.816	0.8116	0.6973		0.5728	0.7348
	0.08	18.041	33.510	23.856	39.270	0.8533	0.6515		0.6222	0.7071
	0.10	18.977	35.249	23.373	39.646	0.8891	0.6110		0.6674	0.6807
10	0.00	12.997	24.141	33.520	36.918	0.6539	0.9080	32.805	0.3952	0.8272
	0.02	14.499	26.931	31.450	37.686	0.7145	0.8519		0.4471	0.8012
	0.04	15.800	29.347	29.572	38.301	0.7662	0.8010		0.4955	0.7762
	0.06	16.936	31.458	27.875	38.806	0.8106	0.7551		0.5405	0.7523
	0.08	17.936	33.316	26.344	39.227	0.8493	0.7136		0.5825	0.7293
	0.10	18.823	34.963	24.960	39.585	0.8832	0.6761		0.6215	0.7073

TABLE No. A-4.4.2

..... (continued)

The upper and the lower bound solutions for the drawing of decagonal tube from round on a cylindrical plug.

Input tube size : 1.1250 in o.d. x 0.3125 in gauge  
 Reduction of area : 32.50 %

Equivalent die semi-angle $\alpha_0^\circ$	Mean coeff. of friction $\mu$	UPPER BOUND					LOWER BOUND			
		Draw force P tonf	Mean draw stress $\sigma_{za}$ tonf in <sup>-2</sup>	Mean die pressure $P_m$ tonf in <sup>-2</sup>	Mean yield stress $\bar{Y}_m$ tonf in <sup>-2</sup>	Mean draw stress /yield stress	Mean die pressure /yield stress	Mean yield stress $Y_m$ tonf in <sup>-2</sup>	Mean draw stress /yield stress	Mean die pressure /yield stress
12	0.00	13.530	25.132	34.951	37.199	0.6756	0.9363	32.804	0.3952	0.8271
	0.02	14.843	27.571	33.142	37.853	0.7284	0.8909		0.4385	0.8054
	0.04	16.007	29.732	31.937	38.395	0.7744	0.8461		0.4794	0.7845
	0.06	17.045	31.659	29.937	38.852	0.8149	0.8048		0.5179	0.7643
	0.08	17.975	33.387	28.527	39.243	0.8508	0.7668		0.5542	0.7447
	0.10	18.813	34.944	27.232	39.581	0.8828	0.7321		0.5884	0.7259
14	0.00	14.048	26.094	36.354	37.463	0.6965	0.9704	32.804	0.3952	0.8270
	0.02	15.226	28.271	34.737	38.033	0.7433	0.9272		0.4323	0.8084
	0.04	16.220	30.234	33.225	38.516	0.7849	0.8869		0.4676	0.7904
	0.06	17.234	32.010	31.81	39.933	0.8222	0.8493		0.5011	0.7730
	0.08	18.103	33.626	30.509	39.290	0.8557	0.8144		0.5330	0.7560
	0.10	18.897	35.100	29.292	39.615	0.8860	0.7819		0.5634	0.7396
16	0.00	14.553	27.032	37.738	37.713	0.7168	1.0007	32.805	0.3952	0.8268
	0.02	15.616	29.007	36.268	38.217	0.7590	0.9617		0.4276	0.8107
	0.04	16.587	30.809	34.881	38.654	0.7971	0.9249		0.4585	0.7949
	0.06	17.476	32.460	33.577	39.036	0.8316	0.8903		0.4882	0.7796
	0.08	18.293	33.978	32.353	39.373	0.8630	0.8579		0.5166	0.7646
	0.10	19.046	35.377	31.204	39.673	0.8917	0.8274		0.5437	0.7501
18	0.00	15.050	27.954	39.112	37.952	0.7366	1.0306	32.805	0.3952	0.8267
	0.02	16.025	29.765	37.758	38.403	0.7751	0.9949		0.4238	0.8124
	0.04	16.924	31.435	36.472	38.800	0.8102	0.9610		0.4514	0.7984
	0.06	17.756	32.980	35.254	39.152	0.8423	0.9289		0.4779	0.7848
	0.08	18.526	34.412	34.101	39.467	0.8719	0.8985		0.5034	0.7714
	0.10	19.243	35.743	33.013	39.750	0.8992	0.8699		0.5279	0.7584
20	0.00	15.541	28.866	40.485	38.182	0.7560	1.0603	32.805	0.3952	0.8265
	0.02	16.443	30.542	39.225	38.590	0.7914	1.0273		0.4208	0.8137
	0.04	17.282	32.101	38.022	38.954	0.8241	0.9958		0.4456	0.8012
	0.06	18.064	33.553	36.876	39.280	0.8542	0.9658		0.4695	0.7883
	0.08	18.795	34.910	35.786	39.574	0.8821	0.9372		0.4926	0.7769
	0.10	19.478	36.179	34.749	34.749	0.9081	0.9101		0.5149	0.7651
22	0.00									
	0.02									
	0.04									
	0.06									
	0.08									
	0.10									

TABLE No. A-4. 4.3

The upper and the lower bound solutions for the drawing of decagonal tube from round on a cylindrical plug.

Input tube size : 1.1250 in o.d. x 0.2500 in gauge  
 Reduction of area : 37.73 %

Equivalent die semi-angle $\alpha_d$	Mean coeff. of friction $\mu$	UPPER BOUND					LOWER BOUND			
		Draw force P tonf	Mean draw stress $\sigma_{za}$ tonf in <sup>-2</sup>	Mean die pressure $P_m$ tonf in <sup>-2</sup>	Mean yield stress $\bar{Y}_m$ tonf in <sup>-2</sup>	Mean draw stress/yield stress	Mean die pressure / yield stress	Mean yield stress $Y_m$ tonf in <sup>-2</sup>	Mean draw stress/yield stress	Mean die pressure / yield stress
2	0.00	09.3716	21.899	23.979	36.246	0.6042	0.6616	34.256	0.4766	0.7950
	0.02	13.4183	31.355	16.8381	38.782	0.8085	0.4645		0.7441	0.6488
	0.04	15.4873	36.190	12.874	39.844	0.9083	0.3552		0.9082	0.5368
	0.06	16.7390	39.115	10.403	40.431	0.9674	0.2870		1.0063	0.4505
	0.08	17.5770	41.073	08.722	40.805	1.0066	0.2406		1.0627	0.3830
	0.10	18.1770	42.476	07.507	40.064	1.0344	0.2071		1.0931	0.3300
4	0.00	09.8962	23.125	25.334	36.620	0.6315	0.6918	34.256	0.4766	0.7950
	0.02	12.4391	29.067	20.963	38.232	0.7603	0.5725		0.6261	0.7170
	0.04	14.1649	33.100	17.792	39.179	0.8448	0.4859		0.7439	0.6489
	0.06	15.4093	36.008	15.427	39.806	0.9046	0.4213		0.8361	0.5893
	0.08	16.3480	38.202	13.605	40.252	0.9491	0.3715		0.9079	0.5370
	0.10	17.0810	39.915	12.163	40.586	0.9835	0.3321		0.9635	0.4911
6	0.00	10.3999	24.302	26.645	36.964	0.6574	0.7208	34.256	0.4766	0.7949
	0.02	12.2985	28.739	23.419	38.150	0.7533	0.6336		0.5800	0.7418
	0.04	13.7435	32.115	20.824	38.957	0.8244	0.5634		0.6682	0.6933
	0.06	14.8778	34.766	18.718	39.543	0.8792	0.5064		0.7434	0.6490
	0.08	15.7910	36.900	16.986	39.990	0.9227	0.4595		0.8038	0.6085
	0.10	16.5416	38.654	15.539	40.341	0.9582	0.4204		0.8616	0.5713
7	0.00	10.6444	24.873	27.281	37.126	0.6700	0.7350	34.256	0.4766	0.7949
	0.02	12.3406	28.837	24.413	38.174	0.7554	0.6576		0.5661	0.7491
	0.04	13.6778	31.962	22.030	38.922	0.8212	0.5934		0.6443	0.7068
	0.06	14.7573	34.484	20.043	39.483	0.8734	0.5399		0.7124	0.6676
	0.08	15.6462	36.562	18.371	39.920	0.9159	0.4948		0.7718	0.6313
	0.10	16.3904	38.301	16.949	40.271	0.9511	0.4565		0.8235	0.5977
8	0.00	10.8844	25.434	27.918	37.282	0.6822	0.7488	34.256	0.4766	0.7948
	0.02	12.4224	29.028	25.318	38.222	0.7595	0.6791		0.5554	0.7547
	0.04	13.6684	31.940	23.111	38.917	0.8207	0.6199		0.6255	0.7171
	0.06	14.6968	34.343	21.231	39.452	0.8705	0.5695		0.6877	0.6821
	0.08	15.5593	36.358	19.621	39.878	0.9117	0.5263		0.7428	0.6493
	0.10	16.2926	38.072	18.229	40.226	0.9464	0.4889		0.7917	0.6186
10	0.00	11.3523	26.528	29.160	37.579	0.7059	0.7763	34.256	0.4766	0.7947
	0.02	12.6582	29.579	26.956	38.358	0.7711	0.7173		0.5402	0.7625
	0.04	13.7586	32.151	25.022	38.965	0.8251	0.6658		0.5981	0.7319
	0.06	14.6974	34.344	23.324	39.453	0.8705	0.6207		0.6507	0.7030
	0.08	15.5071	36.237	21.828	39.853	0.9092	0.5809		0.6986	0.6756
	0.10	16.2124	37.885	20.504	40.189	0.9427	0.5456		0.7421	0.6496

TABLE No. A-4.4.3

..... (continued)

The upper and the lower bound solutions for the drawing of Decagonal tube from round on a cylindrical plug.

Input tube size : 1.1250 in o.d. x 0.2500 in gauge  
 Reduction of area : 37.73%

Equivalent die semi-angle $\alpha_0$	Mean coeff. of friction $\mu$	UPPER BOUND					LOWER BOUND			
		Draw force	Mean draw stress	Mean die pressure	Mean yield stress	Mean draw stress	Mean die pressure / yield stress	Mean yield stress	Mean draw stress / yield stress	Mean die pressure / yield stress
		P tonf	$\sigma_{za}$ tonf in <sup>-2</sup>	$P_m$ tonf in <sup>-2</sup>	$\bar{Y}_m$ tonf in <sup>-2</sup>	/yield stress	stress	$Y_m$ tonf in <sup>-2</sup>	stress	stress
12	0.00	11.806	27.590	30.380	37.858	0.7288	0.8025	34.256	0.4766	0.7946
	0.02	12.949	30.260	28.450	38.523	0.7855	0.7515		0.5298	0.7677
	0.04	13.939	32.573	26.718	39.061	0.8339	0.7057		0.5789	0.7420
	0.06	14.803	34.592	25.165	39.506	0.8756	0.6647		0.6244	0.7175
	0.08	15.564	36.370	23.770	39.881	0.9120	0.6279		0.6664	0.6939
	0.10	16.239	37.947	22.513	40.201	0.9439	0.5947		0.7053	0.6715
14	0.00	12.251	28.629	31.588	38.123	0.7510	0.8286	34.256	0.4766	0.7945
	0.02	13.273	31.016	29.859	38.702	0.8014	0.7832		0.5222	0.7715
	0.04	14.175	33.124	28.282	39.185	0.8453	0.7419		0.5648	0.7493
	0.06	14.977	34.998	26.847	39.593	0.8839	0.7042		0.6047	0.7280
	0.08	15.694	36.674	25.538	39.943	0.9181	0.6699		0.6420	0.7075
	0.10	16.339	38.181	24.342	40.248	0.9486	0.6385		0.6769	0.6877
16	0.00	12.690	29.655	32.794	38.377	0.7727	0.8545	34.256	0.4766	0.7943
	0.02	13.618	31.822	31.218	38.890	0.8183	0.8135		0.5164	0.7742
	0.04	14.449	33.765	29.326	39.326	0.8586	0.7756		0.5540	0.7548
	0.06	15.198	35.515	28.426	39.703	0.8945	0.7407		0.5894	0.7361
	0.08	15.876	37.100	27.191	40.030	0.9268	0.7085		0.6229	0.7179
	0.10	16.493	38.542	26.051	40.319	0.9559	0.6788		0.6544	0.7003
18	0.00	13.128	30.678	34.008	38.623	0.7943	0.8805	34.256	0.4766	0.7941
	0.02	13.980	32.668	32.555	39.082	0.8359	0.8429		0.5119	0.7764
	0.04	14.752	34.474	31.201	39.481	0.8732	0.8078		0.5453	0.7591
	0.06	15.456	36.119	29.942	39.829	0.9068	0.7752		0.5772	0.7424
	0.08	15.100	37.623	28.770	40.136	0.9374	0.7449		0.6074	0.7261
	0.10	16.691	39.004	27.680	40.410	0.9652	0.7167		0.6361	0.7103
20	0.00	13.568	31.707	35.242	38.8636	0.8158	0.9068	34.256	0.4766	0.7939
	0.02	14.358	33.551	33.887	39.279	0.8542	0.8719		0.5082	0.7780
	0.04	15.081	35.241	32.615	39.645	0.8889	0.8392		0.5383	0.7626
	0.06	15.746	36.795	31.424	39.968	0.9206	0.8086		0.5671	0.7475
	0.08	16.359	38.228	30.307	40.257	0.9496	0.7798		0.5946	0.7328
	0.10	16.926	39.553	29.260	40.516	0.9762	0.7529		0.6209	0.7185
22	0.00									
	0.02									
	0.04									
	0.06									
	0.08									
	0.10									

TABLE No. A-4.4.4

The upper and the lower bound solutions for the drawing of decagonal tube from round on a cylindrical plug.

Input tube size : 1.1250 in o.d. x 0.1875 in gauge  
 Reduction of area : 46.95%

Equivalent die semi-angle $\alpha_0$	Mean coeff. of friction $\mu$	UPPER BOUND						LOWER BOUND		
		Draw force P tonf	Mean draw stress $\sigma_{za}$ tonf in <sup>-2</sup>	Mean die pressure $P_m$ tonf in <sup>-2</sup>	Mean yield stress $\bar{Y}_m$ tonf in <sup>-2</sup>	Mean draw stress/yield stress	Mean die pressure/yield stress	Mean yield stress $Y_m$ tonf in <sup>-2</sup>	Mean draw stress/yield stress	Mean die pressure/yield stress
2	0.00	07.884	26.912	20.104	37.681	0.7142	0.5335	36.653	0.6390	0.7335
	0.02	10.949	37.378	13.136	40.087	0.9324	0.3486		0.9484	0.5506
	0.04	12.365	42.210	09.678	41.015	1.0291	0.2574		1.0915	0.4253
	0.06	13.178	44.986	07.678	41.510	1.0837	0.2038		1.1500	0.3378
	0.08	13.705	46.786	06.351	41.818	1.1188	0.1686		1.1668	0.2753
	0.10	14.075	48.048	05.415	42.029	1.1432	0.1437		1.1634	0.2297
4	0.00	08.232	28.103	21.004	37.990	0.7397	0.5529	36.653	0.6390	0.7335
	0.02	10.190	34.786	16.642	39.548	0.8796	0.4381		0.8216	0.6333
	0.04	11.430	39.018	13.726	40.412	0.9655	0.3613		0.9481	0.5507
	0.06	12.284	41.933	11.664	40.965	1.0236	0.3070		1.0342	0.4823
	0.08	12.907	44.060	10.135	41.348	1.0656	0.2668		1.0913	0.4253
	0.10	13.382	45.681	08.958	41.631	1.0973	0.2358		1.1278	0.3779
6	0.00	08.561	29.226	21.863	38.271	0.7637	0.5713	36.653	0.6390	0.7334
	0.02	10.025	34.222	18.628	39.426	0.8680	0.4867		0.7676	0.6646
	0.04	11.082	37.831	16.185	40.178	0.9416	0.4229		0.8688	0.6041
	0.06	11.880	40.555	14.291	40.708	0.9962	0.3734		0.9477	0.5509
	0.08	12.504	42.683	12.787	41.102	1.0385	0.3341		1.0088	0.5040
	0.10	13.004	44.391	11.565	41.406	1.0721	0.3022		1.0556	0.4625
7	0.00	08.719	29.765	22.278	38.403	0.7751	0.5801	36.653	0.6390	0.7334
	0.02	10.025	34.222	19.398	39.426	0.8680	0.5051		0.7509	0.6739
	0.04	11.007	37.576	17.139	40.127	0.9364	0.4463		0.8421	0.6207
	0.06	11.772	40.188	15.336	40.638	0.9889	0.3993		0.9160	0.5730
	0.08	12.385	42.277	13.867	41.028	1.0304	0.3611		0.7656	0.5302
	0.10	12.885	43.986	12.651	41.335	1.0641	0.3294		1.0232	0.4918
8	0.00	08.873	30.289	22.686	38.530	0.7861	0.5888	36.653	0.6390	0.7333
	0.02	10.054	34.322	20.082	39.448	0.8701	0.5212		0.7380	0.6810
	0.04	10.972	37.455	17.981	40.102	0.9340	0.4667		0.8208	0.6335
	0.06	11.705	39.956	16.262	40.594	0.9843	0.4221		0.8898	0.5904
	0.08	12.303	41.998	14.835	40.976	1.0249	0.3850		0.9471	0.5512
	0.10	12.800	43.694	13.633	41.283	1.0584	0.3538		0.9948	0.5155
10	0.00	09.170	31.302	23.481	38.769	0.8074	0.6057	36.653	0.6390	0.7322
	0.02	10.167	34.709	21.281	39.531	0.8780	0.5489		0.7193	0.6911
	0.04	10.979	37.480	19.432	40.107	0.9345	0.5012		0.7890	0.6521
	0.06	11.652	39.777	17.864	40.559	0.9807	0.4608		0.8494	0.6160
	0.08	12.218	41.710	16.522	40.923	1.0192	0.4262		0.9015	0.5825
	0.10	12.701	43.359	15.363	41.223	1.0518	0.3963		0.9463	0.5515

TABLE No. A-4.4.4

..... (continued)

The upper and the lower bound solutions for the drawing of decagonal tube from round on a cylindrical plug.

Input tube size : 1.1250 in o.d. x 0.1875 in gauge  
 Reduction of area : 46.95%

Equivalent die semi-angle $\alpha_d$	Mean coeff. of friction $\mu$	UPPER BOUND						LOWER BOUND		
		Draw force	Mean draw stress	Mean die pressure	Mean yield stress	Mean draw stress	Mean die pressure	Mean yield stress	Mean draw stress	Mean die pressure
		P tonf	$\sigma_{za}$ tonf in <sup>-2</sup>	$P_m$ tonf in <sup>-2</sup>	$\bar{Y}_m$ tonf in <sup>-2</sup>	/yield stress	/yield stress	$Y_m$ tonf in <sup>-2</sup>	/yield stress	/yield stress
12	0.00	09.455	32.277	24.257	38.994	0.8277	0.6221	36.653	0.6390	0.7330
	0.02	10.323	35.241	22.340	39.645	0.8889	0.5729		0.7064	0.6978
	0.04	11.053	37.730	20.681	40.158	0.9394	0.5304		0.7664	0.6648
	0.06	11.673	39.849	19.239	40.573	0.9821	0.4934		0.8196	0.6339
	0.08	12.208	41.674	17.978	40.917	1.0185	0.4610		0.8668	0.6048
	0.10	12.673	43.262	16.866	41.206	1.0499	0.4325		0.9085	0.5776
14	0.00	09.734	33.227	25.021	39.208	0.8475	0.6383	36.653	0.6390	0.7327
	0.02	10.505	35.859	23.316	39.775	0.9016	0.5947		0.6970	0.7027
	0.04	11.168	38.123	21.806	40.230	0.9475	0.5562		0.7494	0.6741
	0.06	11.744	40.090	20.469	40.619	0.9870	0.5221		0.7968	0.6471
	0.08	12.249	41.814	19.280	40.943	1.0213	0.4917		0.8396	0.6215
	0.10	12.695	43.336	18.216	41.219	1.0513	0.4646		0.8782	0.5973
16	0.00	10.009	34.167	25.796	39.414	0.8669	0.6545	36.653	0.6390	0.7325
	0.02	10.704	36.541	24.246	39.916	0.9154	0.6151		0.6897	0.7063
	0.04	11.313	38.620	22.855	40.334	0.9575	0.5799		0.7362	0.6812
	0.06	11.851	40.455	21.606	40.689	0.9943	0.5482		0.7788	0.6572
	0.08	12.329	42.087	20.480	40.993	1.0266	0.5196		0.8179	0.6344
	0.10	12.756	43.546	19.461	41.257	1.0555	0.4937		0.8535	0.6126
18	0.00	10.285	35.109	26.579	39.617	0.8862	0.6709	36.653	0.6390	0.7324
	0.02	10.920	37.277	25.154	40.066	0.9304	0.6349		0.6840	0.7091
	0.04	11.484	39.202	23.862	40.448	0.9692	0.6023		0.7257	0.6867
	0.06	11.988	40.924	22.687	40.777	1.0036	0.5727		0.7643	0.6653
	0.08	12.442	42.472	21.616	41.063	1.0343	0.5456		0.8000	0.6447
	0.10	12.851	43.871	20.637	41.315	1.0619	0.5209		0.8330	0.6250
20	0.00	10.566	36.068	27.385	39.818	0.9058	0.6877	36.653	0.6390	0.7321
	0.02	11.151	38.067	26.062	40.225	0.9463	0.6545		0.6793	0.7112
	0.04	11.677	39.863	24.850	40.576	0.9824	0.6241		0.7170	0.6911
	0.06	12.153	41.485	23.737	40.882	1.0148	0.5961		0.7522	0.6718
	0.08	12.584	42.859	22.715	41.151	1.0439	0.5705		0.7850	0.6531
	0.10	12.977	44.301	21.772	41.391	1.0703	0.5468		0.8156	0.6351
22	0.00									
	0.02									
	0.04									
	0.06									
	0.08									
	0.10									

TABLE No. A-4.5.1

The upper and the lower bound solutions for the drawing of round tube from round on a cylindrical plug.

Input tube size : 1.0625 in o.d. x 0.3125 in gauge  
 Reduction of area : 13.75%

Equivalent die semi-angle $\alpha_0$	Mean coeff. of friction $\mu$	UPPER BOUND					LOWER BOUND			
		Draw force	Mean draw stress	Mean die pressure	Mean yield stress	Mean draw stress/ yield stress	Mean die pressure/ yield stress	Mean yield stress	Mean draw stress/ yield stress	Mean die pressure/ yield stress
		P tonf	$\sigma_{za}$ tonf in <sup>-2</sup>	$p_m$ tonf in <sup>-2</sup>	$\bar{Y}_m$ tonf in <sup>-2</sup>			$Y_m$ tonf in <sup>-2</sup>		
2	0.00	3.0611	4.8201	30.235	27.254	0.1768	1.1094	26.147	0.1054	0.8946
	0.02	5.0951	8.0229	27.716	29.999	0.2674	0.9239		0.2129	0.7871
	0.04	6.6523	10.474	24.970	31.545	0.3321	0.7916		0.3081	0.6919
	0.06	6.8673	12.388	22.542	32.557	0.3805	0.6924		0.3922	0.6078
	0.08	8.8371	13.915	20.476	33.278	0.4181	0.6153		0.4665	0.5335
	0.10	9.6274	15.159	18.724	33.800	0.4482	0.5536		0.5322	0.4678
4	0.00	3.5929	5.6575	35.487	28.089	0.2014	1.2634	26.147	0.1054	0.8946
	0.02	4.8702	7.6688	34.180	29.745	0.2578	1.1491		0.1607	0.8393
	0.04	5.9874	9.4279	32.588	30.925	0.3048	1.0538		0.2128	0.7872
	0.06	6.9655	10.968	30.962	31.819	0.3447	0.9730		0.2618	0.7382
	0.08	7.8257	12.322	29.397	32.525	0.3789	0.9038		0.3078	0.6922
	0.10	8.5865	13.520	27.928	33.098	0.4085	0.8438		0.3511	0.6489
6	0.00	4.1427	6.5232	40.918	28.852	0.2262	1.4182	26.147	0.1054	0.8946
	0.02	5.1494	8.1085	40.016	30.059	0.2697	1.3312		0.1426	0.8574
	0.04	6.0723	9.5616	38.895	31.007	0.3085	1.2544		0.1783	0.8217
	0.06	6.9175	10.892	37.685	31.778	0.3428	1.1859		0.2126	0.7874
	0.08	7.6921	12.112	36.456	32.520	0.3736	1.1245		0.2455	0.7545
	0.10	8.4034	13.232	35.244	32.964	0.4014	1.0691		0.2771	0.7229
7	0.00	4.4244	6.9668	43.700	29.212	0.2385	1.4960	26.147	0.1054	0.8946
	0.02	5.3535	8.4298	42.920	30.280	0.2784	1.4174		0.1373	0.8627
	0.04	6.2170	9.7896	41.945	31.145	0.3143	1.3467		0.1682	0.8318
	0.06	7.0186	11.051	40.876	31.865	0.3468	1.2828		0.1980	0.8020
	0.08	7.7629	12.223	39.770	32.576	0.3764	1.2246		0.2267	0.7733
	0.10	8.4546	13.312	38.661	33.002	0.4034	1.1715		0.2545	0.7455
8	0.00	4.7108	7.4177	46.529	29.559	0.2509	1.5741	26.147	0.1054	0.8946
	0.02	5.5823	8.7900	45.845	30.520	0.2880	1.5021		0.1333	0.8667
	0.04	6.4007	10.078	44.986	31.316	0.3218	1.4365		0.1605	0.8395
	0.06	7.1685	11.287	44.031	31.992	0.3528	1.3763		0.1868	0.8132
	0.08	7.8885	12.421	43.030	32.574	0.3813	1.3210		0.2123	0.7877
	0.10	8.5641	13.485	42.013	33.082	0.4076	1.2700		0.2371	0.7629
10	0.00	5.2979	8.3423	52.328	30.220	0.2760	1.7315	26.147	0.1054	0.8946
	0.02	6.0910	9.5911	51.794	31.025	0.3091	1.6694		0.1277	0.8723
	0.04	6.8471	10.781	51.115	31.717	0.3399	1.6116		0.1496	0.8504
	0.06	7.5672	11.915	50.344	32.320	0.3687	1.5577		0.1709	0.8291
	0.08	8.2525	12.994	49.515	32.852	0.3955	1.5072		0.1917	0.8083
	0.10	8.9047	14.021	48.654	33.326	0.4207	1.4599		0.2119	0.7880

TABLE No. A-4. 5.1

..... (continued)

The upper and the lower bound solutions for the drawing of round tube from round on a cylindrical plug.

Input tube size : 1.0625 in o.d. x 0.3125 in gauge  
 Reduction of area : 13.75 %

Equivalent die semi-angle $\alpha_0^\circ$	Mean coeff. of friction $\mu$	UPPER BOUND					LOWER BOUND			
		Draw force P tonf	Mean draw stress $\sigma_{za}$ tonf in <sup>-2</sup>	Mean die pressure $P_m$ tonf in <sup>-2</sup>	Mean yield stress $\bar{Y}_m$ tonf in <sup>-2</sup>	Mean draw stress /yield stress	Mean die pressure /yield stress	Mean yield stress $Y_m$ tonf in <sup>-2</sup>	Mean draw stress /yield stress	Mean die pressure /yield stress
12	0.00	5.9051	9.2983	58.325	30.845	0.3014	1.8909	26.147	0.1054	0.8946
	0.02	6.6492	10.470	57.914	31.542	0.3319	1.8361		0.1240	0.8760
	0.04	7.3662	11.599	57.378	32.156	0.3607	1.7843		0.1422	0.8578
	0.06	8.0562	12.685	56.755	32.703	0.3879	1.7354		0.1600	0.8400
	0.08	8.7198	13.730	56.071	33.195	0.4136	1.6891		0.1775	0.8225
	0.10	9.3578	14.735	55.345	33.639	0.4380	1.6452		0.1947	0.8053
14	0.00	6.5336	10.288	64.534	31.438	0.3272	2.0527	26.147	0.1054	0.8946
	0.02	7.2464	11.410	54.235	32.057	0.3559	2.0038		0.1212	0.8788
	0.04	7.9385	12.500	63.826	32.613	0.3833	1.9571		0.1368	0.8632
	0.06	8.6099	13.557	63.334	33.115	0.4094	1.9125		0.1522	0.8478
	0.08	9.2607	14.582	62.780	33.573	0.4343	1.8699		0.1673	0.8327
	0.10	9.8914	15.575	62.180	33.992	0.4582	1.8292		0.1821	0.8179
16	0.00	7.1851	11.313	70.969	32.006	0.3535	2.2173	26.147	0.1054	0.8946
	0.02	7.8780	12.404	70.781	32.566	0.3809	2.1735		0.1192	0.8808
	0.04	8.5549	13.470	70.493	33.075	0.4073	2.1312		0.1328	0.8672
	0.06	9.2158	14.511	70.127	33.542	0.4326	2.0907		0.1462	0.8538
	0.08	9.8605	15.526	69.699	33.972	0.4570	2.0516		0.1594	0.8406
	0.10	10.489	16.516	69.222	34.370	0.4805	2.0140		0.1724	0.8276
18	0.00	7.8615	12.378	77.649	32.553	0.3803	2.3853	26.147	0.1054	0.8946
	0.02	8.5425	13.451	77.576	33.066	0.4068	2.3460		0.1176	0.8824
	0.04	9.2115	14.504	77.411	33.539	0.4325	2.3080		0.1296	0.8704
	0.06	9.8679	15.538	77.171	33.977	0.4573	2.2712		0.1415	0.8585
	0.08	10.511	16.552	76.870	34.384	0.4814	2.2356		0.1532	0.8468
	0.10	11.142	17.545	76.519	34.764	0.5047	2.2011		0.1648	0.8352
20	0.00	8.5649	13.486	84.597	33.083	0.4076	2.5571	26.147	0.1054	0.8946
	0.02	9.2404	14.550	84.645	33.559	0.4336	2.5222		0.1163	0.8837
	0.04	9.9068	15.599	84.608	34.002	0.4586	2.4883		0.1270	0.8730
	0.06	10.563	16.634	84.501	34.416	0.4833	2.4552		0.1377	0.8623
	0.08	11.210	17.653	84.333	34.804	0.5072	2.4231		0.1482	0.8518
	0.10	11.848	18.656	84.113	35.168	0.5305	2.3918		0.1586	0.8414
22	0.00									
	0.02									
	0.04									
	0.06									
	0.08									
	0.10									

TABLE No. A-4.5.2

The upper and the lower bound solutions for the drawing of round tube from round on a cylindrical plug.

Input tube size : 1.0625 in o.d. x 0.1875 in gauge  
 Reduction of area : 19.64%

Equivalent die semi-angle $\alpha_d$	Mean coeff. of friction $\mu$	UPPER BOUND					LOWER BOUND			
		Draw force P tonf	Mean draw stress $\sigma_{za}$ tonf in <sup>-2</sup>	Mean die pressure $p_m$ tonf in <sup>-2</sup>	Mean yield stress $\bar{Y}_m$ tonf in <sup>-2</sup>	Mean draw stress/yield stress	Mean die pressure/yield stress	Mean yield stress $Y_m$ tonf in <sup>-2</sup>	Mean draw stress/yield stress	Mean die pressure/yield stress
2	0.00	3.1716	7.6575	31.326	29.737	0.2575	1.0534	28.630	0.1823	0.8177
	0.02	5.4442	13.144	27.512	32.923	0.3992	0.8356		0.3530	0.6470
	0.04	7.0498	17.021	23.936	34.566	0.4924	0.6925		0.4905	0.5095
	0.06	8.2300	19.870	21.039	35.588	0.5583	0.5912		0.6010	0.3990
	0.08	9.1306	22.045	18.717	36.291	0.6074	0.5157		0.6899	0.3101
	0.10	9.8391	23.755	16.834	36.806	0.6454	0.4576		0.7612	0.2388
4	0.00	3.5184	8.4950	31.326	30.324	0.2802	1.1460	28.630	0.1823	0.8177
	0.02	4.8957	11.820	27.512	32.271	0.3663	1.0147		0.2722	0.7278
	0.04	6.0461	14.597	23.936	33.580	0.4347	0.9104		0.3528	0.6472
	0.06	7.0139	16.934	21.039	34.532	0.4904	0.8255		0.4252	0.5478
	0.08	7.8365	18.920	18.717	35.261	0.5366	0.7552		0.4902	0.5098
	0.10	8.5427	20.625	16.834	35.839	0.5755	0.6958		0.5484	0.4516
6	0.00	3.8736	9.3626	38.260	30.878	0.3029	1.2391	28.630	0.1823	0.8177
	0.02	4.9175	11.873	36.876	32.298	0.3676	1.1417		0.2432	0.7568
	0.04	5.8443	14.110	35.321	33.366	0.4229	1.0586		0.2998	0.7002
	0.06	6.6684	16.100	33.752	34.205	0.4707	0.9867		0.3525	0.6475
	0.08	7.4039	17.876	32.236	34.886	0.5124	0.9240		0.4016	0.5984
	0.10	8.0631	19.467	30.800	35.451	0.5491	0.8688		0.4472	0.5528
7	0.00	4.0545	9.7894	40.473	31.145	0.3143	1.2858	28.630	0.1823	0.8177
	0.02	5.0005	12.073	38.845	32.400	0.3726	1.1989		0.2347	0.7653
	0.04	5.8555	13.127	37.484	33.378	0.4235	1.1230		0.2839	0.7161
	0.06	6.6290	16.005	36.086	34.167	0.4684	1.0561		0.3302	0.6700
	0.08	7.3301	17.698	34.709	34.820	0.5082	0.9968		0.3737	0.6262
	0.10	7.9675	19.237	33.383	35.372	0.5438	0.9438		0.4147	0.5853
8	0.00	4.2377	10.231	41.857	31.405	0.3258	1.3328	28.630	0.1823	0.8177
	0.02	5.1098	12.337	40.795	32.532	0.3792	1.2540		0.2282	0.7718
	0.04	5.9090	14.267	39.586	33.435	0.4267	1.1840		0.2718	0.7282
	0.06	6.6415	16.035	38.328	34.179	0.4691	1.1214		0.3130	0.6870
	0.08	7.3137	17.658	37.070	34.806	0.5073	1.0650		0.3521	0.6479
	0.10	7.9319	19.151	35.841	35.342	0.5419	1.0141		0.3891	0.6109
10	0.00	4.6115	11.134	45.549	31.910	0.3489	1.4274	28.630	0.1823	0.8177
	0.02	5.3804	12.990	44.694	32.850	0.3954	1.3605		0.2191	0.7809
	0.04	6.0991	14.726	43.714	33.635	0.4378	1.2996		0.2544	0.7456
	0.06	6.7706	16.347	42.673	34.304	0.4765	1.2440		0.2882	0.7118
	0.08	7.3981	17.862	41.609	34.881	0.5121	1.1929		0.3205	0.6795
	0.10	7.9852	19.279	40.546	35.387	0.5448	1.1458		0.3515	0.6485

TABLE No. A-4. 5.2 ..... (continued)

The upper and the lower bound solutions for the drawing of round tube from round on a cylindrical plug.

Input tube size : 1.0625 in o.d. x 0.1875 in gauge  
 Reduction of area : 19.64%

Equivalent die semi-angle $\sigma_a$	Mean coeff. of friction $\mu$	UPPER BOUND					LOWER BOUND			
		Draw force	Mean draw stress	Mean die pressure	Mean yield stress	Mean draw stress	Mean die pressure	Mean yield stress	Mean draw stress	Mean die pressure
		P tonf	$\sigma_{za}^2$ tonf in <sup>-2</sup>	$P_m$ tonf in <sup>-2</sup>	$\bar{Y}_m$ tonf in <sup>-2</sup>	/yield stress	/yield stress	$Y_m$ tonf in <sup>-2</sup>	/yield stress	/yield stress
12	0.00	4.9959	12.062	49.345	32.394	0.3723	1.5232	28.630	0.1823	0.8177
	0.02	5.6973	13.755	48.645	33.206	0.4142	1.4649		0.2130	0.7870
	0.04	6.3619	15.360	47.835	33.904	0.4530	1.4109		0.2425	0.7575
	0.06	6.9912	16.879	46.960	34.511	0.4891	1.3607		0.2711	0.7289
	0.08	7.5871	18.318	46.052	35.047	0.5227	1.3140		0.2986	0.7014
	0.10	8.1515	19.681	45.128	35.524	0.5540	1.2703		0.3252	0.6748
14	0.00	5.3917	13.018	53.255	32.863	0.3961	1.6205	28.630	0.1823	0.8177
	0.02	6.0467	14.599	52.682	33.581	0.4347	1.5688		0.2085	0.7915
	0.04	6.6737	16.113	52.011	34.211	0.4710	1.5203		0.2339	0.7661
	0.06	7.2734	17.561	51.275	34.770	0.5051	1.4747		0.2586	0.7414
	0.08	7.8468	18.945	50.499	35.270	0.5371	1.4318		0.2825	0.7175
	0.10	8.3952	20.269	49.699	35.722	0.5674	1.3913		0.3057	0.6943
16	0.00	5.8002	14.004	57.290	33.318	0.4203	1.7195	28.630	0.1823	0.8177
	0.02	6.4225	15.506	56.829	33.964	0.4565	1.6732		0.2051	0.7949
	0.04	7.0228	16.956	56.281	34.541	0.4909	1.6294		0.2274	0.7726
	0.06	7.6017	18.353	55.669	35.060	0.5235	1.5875		0.2490	0.7510
	0.08	8.1595	19.700	55.012	35.531	0.5544	1.5483		0.2701	0.7299
	0.10	8.6970	20.998	54.325	35.960	0.5839	1.5107		0.2906	0.7094
18	0.00	6.2227	15.024	61.463	33.763	0.4450	1.8204	28.630	0.1823	0.8177
	0.02	6.8216	16.470	61.109	34.352	0.4794	1.7789		0.2025	0.7975
	0.04	7.4032	17.874	60.674	34.886	0.5124	1.7392		0.2222	0.7778
	0.06	7.9677	19.237	60.177	35.372	0.5438	1.7013		0.2414	0.7585
	0.08	8.5151	20.559	59.634	35.817	0.5740	1.6649		0.2602	0.7398
	0.10	9.0461	21.841	59.057	36.228	0.6029	1.6301		0.2786	0.7214
20	0.00	6.6605	16.081	65.787	34.198	0.4702	1.9237	28.630	0.1823	0.8177
	0.02	7.2430	17.487	65.539	34.742	0.5033	1.8864		0.2003	0.8000
	0.04	7.8119	18.861	65.215	35.241	0.5352	1.8505		0.2180	0.7820
	0.06	8.3670	20.201	64.830	35.699	0.5659	1.8160		0.2353	0.7647
	0.08	8.9084	21.505	64.399	36.123	0.5954	1.7827		0.2522	0.7478
	0.10	9.4363	22.783	63.930	36.517	0.6239	1.7507		0.2688	0.7312
22	0.00									
	0.02									
	0.04									
	0.06									
	0.08									
	0.10									

TABLE No. A-4.5.3

The upper and the lower bound solutions for the drawing of round tube from round on a cylindrical plug.

Input tube size : 1.1250 in o.d. x 0.2500 in gauge  
 Reduction of area : 30.36 %

Equivalent die semi-angle $\alpha_d$	Mean coeff. of friction $\mu$	UPPER BOUND					LOWER BOUND			
		Draw force	Mean draw stress	Mean die pressure	Mean yield stress	Mean draw stress/yield stress	Mean die pressure/yield stress	Mean yield stress	Mean draw stress/yield stress	Mean die pressure/yield stress
		P tonf	$\sigma_{za}$ tonf in <sup>-2</sup>	$p_m$ tonf in <sup>-2</sup>	$\bar{Y}_m$ tonf in <sup>-2</sup>			$Y_m$ tonf in <sup>-2</sup>		
2	0.00	6.4225	13.419	30.784	33.052	0.4060	0.9314	32.179	0.2877	0.7123
	0.02	10.358	21.648	26.000	36.166	0.5984	0.7189		0.5258	0.4742
	0.04	12.995	27.152	22.094	37.744	0.7194	0.5854		0.5933	0.3067
	0.06	14.867	31.064	19.111	38.7139	0.8024	0.4937		0.8106	0.1894
	0.08	16.261	33.976	16.804	39.373	0.8629	0.4268		0.8922	0.1078
	0.10	17.338	36.227	14.979	39.851	0.9090	0.3759		0.9485	0.0515
4	0.00	6.8784	14.371	32.970	33.481	0.4292	0.9847	32.179	0.2877	0.7123
	0.02	9.2157	19.255	30.376	35.378	0.5442	0.8586		0.4170	0.5830
	0.04	11.104	23.201	27.889	36.643	0.6332	0.7611		0.4156	0.4744
	0.06	12.652	26.437	25.669	37.555	0.7039	0.6835		0.6167	0.3833
	0.08	13.942	29.131	23.723	38.248	0.7616	0.6202		0.6930	0.3070
	0.10	15.030	31.404	22.023	38.793	0.8095	0.5677		0.7659	0.2431
6	0.00	7.3422	15.341	35.194	33.985	0.4526	1.0383	32.179	0.2877	0.7123
	0.02	9.0702	18.951	33.386	35.272	0.5373	0.9465		0.3762	0.6238
	0.04	10.567	22.080	31.571	36.302	0.6082	0.8697		0.4550	0.5450
	0.06	11.872	24.806	29.847	37.107	0.6685	0.8043		0.5252	0.4748
	0.08	13.017	27.198	28.248	37.756	0.7204	0.7482		0.5876	0.4124
	0.10	14.028	29.311	26.778	38.292	0.7654	0.6993		0.6431	0.3569
7	0.00	7.5775	15.832	36.321	34.097	0.4643	1.0652	32.179	0.2877	0.7123
	0.02	9.1243	19.064	34.747	35.312	0.5399	0.9840		0.3641	0.6359
	0.04	10.493	21.924	33.146	36.254	0.6047	0.9143		0.4332	0.5667
	0.06	11.708	24.464	31.599	37.010	0.6610	0.8538		0.4959	0.5041
	0.08	12.793	26.730	30.137	37.633	0.7103	0.8008		0.5525	0.4475
	0.10	13.766	28.763	28.770	38.156	0.7538	0.7540		0.6038	0.3962
8	0.00	7.815	16.329	37.461	34.296	0.4761	1.0923	32.179	0.2877	0.7123
	0.02	9.224	19.273	36.064	35.384	0.5447	1.0192		0.3548	0.6452
	0.04	10.491	21.921	34.634	36.253	0.6047	0.9553		0.4164	0.5836
	0.06	11.633	24.307	33.231	36.965	0.6576	0.8990		0.4729	0.5271
	0.08	12.666	26.465	31.887	37.563	0.7046	0.8489		0.4246	0.4754
	0.10	13.604	28.425	30.613	38.071	0.7466	0.8041		0.5720	0.4280
10	0.00	8.2983	17.338	39.777	34.686	0.4999	1.1468	32.179	0.2877	0.7123
	0.02	9.5134	19.877	38.640	35.591	0.5585	1.0857		0.3417	0.6583
	0.04	10.631	22.213	37.462	36.343	0.6112	1.0308		0.3921	0.6079
	0.06	11.661	24.364	36.285	36.982	0.6588	0.9812		0.4391	0.5609
	0.08	12.611	26.350	35.134	37.532	0.7021	0.9361		0.4830	0.5170
	0.10	13.490	28.186	34.020	38.011	0.7415	0.8950		0.5239	0.4761

TABLE No. A-4.5.3

..... (continued)

The upper and the lower bound solutions for the drawing of round tube from round on a cylindrical plug.

Input tube size : 1.1250 in o.d. x 0.2500 in gauge  
 Reduction of area : 30.36 %

Equivalent die semi-angle $\alpha_0^\circ$	Mean coeff. of friction $\mu$	UPPER BOUND					LOWER BOUND			
		Draw force	Mean draw stress	Mean die pressure	Mean yield stress	Mean draw stress	Mean die pressure / yield stress	Mean yield stress	Mean draw stress / yield stress	Mean die pressure / yield stress
		P tonf	$\sigma_{za}$ tonf in <sup>-2</sup>	$P_m$ tonf in <sup>-2</sup>	$\bar{Y}_m$ tonf in <sup>-2</sup>	/yield stress	stress	$Y_m$ tonf in <sup>-2</sup>	/yield stress	stress
12	0.00	8.7929	18.372	42.147	35.067	0.5239	1.2019	32.179	0.2877	0.7123
	0.02	9.8789	20.641	41.196	35.844	0.5758	1.1493		0.3327	0.6678
	0.04	10.894	22.762	40.203	36.511	0.6234	1.1011		0.3753	0.6247
	0.06	11.843	24.746	39.197	37.090	0.6672	1.0568		0.4154	0.5845
	0.08	12.732	26.603	38.197	37.599	0.7075	1.0159		0.4534	0.5466
	0.10	13.565	28.344	37.216	38.051	0.7449	0.9781		0.4892	0.5108
14	0.00	9.3004	19.432	44.580	35.439	0.5483	1.2579	32.179	0.2877	0.7123
	0.02	10.295	21.511	43.774	36.124	0.5955	1.2117		0.3262	0.6737
	0.04	11.237	23.478	42.925	36.725	0.6394	1.1688		0.3630	0.6370
	0.06	12.127	25.339	42.057	37.256	0.6801	1.1289		0.3980	0.6020
	0.08	12.970	27.101	41.185	37.731	0.7183	1.0915		0.4313	0.5687
	0.10	13.769	28.769	40.318	38.158	0.7539	1.0566		0.4630	0.5370
16	0.00	9.8058	20.522	47.080	35.505	0.5732	1.3149	32.179	0.2877	0.7132
	0.02	10.751	22.464	46.396	36.420	0.6168	1.2739		0.3213	0.6787
	0.04	11.638	24.317	45.669	36.938	0.6578	1.2354		0.3536	0.6464
	0.06	12.485	26.087	44.919	37.461	0.6964	1.1991		0.3845	0.6155
	0.08	13.294	27.777	44.157	37.906	0.7328	1.1649		0.4141	0.5892
	0.10	14.066	29.391	43.392	38.312	0.7671	1.1326		0.4425	0.5575
18	0.00	10.359	21.646	49.658	36.167	0.5985	1.3730	32.179	0.2877	0.7123
	0.02	11.240	23.485	49.080	36.727	0.6394	1.3363		0.3174	0.6826
	0.04	12.087	25.255	48.452	37.233	0.6783	1.3016		0.3461	0.6539
	0.06	12.901	26.956	47.816	37.693	0.7151	1.2686		0.3737	0.6263
	0.08	13.684	28.593	47.155	38.114	0.7502	1.2372		0.4003	0.5997
	0.10	14.438	30.167	46.484	38.500	0.7835	1.2074		0.4259	0.5741
20	0.00	10.915	22.805	52.321	36.524	0.6244	1.4325	32.179	0.2877	0.7123
	0.02	11.759	24.570	51.842	37.040	0.6633	1.3996		0.3143	0.6857
	0.04	12.576	26.276	51.323	37.512	0.7005	1.3682		0.3400	0.6599
	0.06	13.366	27.928	50.776	37.945	0.7360	1.3381		0.3649	0.6350
	0.08	14.131	29.526	50.209	38.345	0.7700	1.3094		0.3890	0.6110
	0.10	14.871	31.072	49.628	38.716	0.8026	1.2819		0.4123	0.5877
22	0.00									
	0.02									
	0.04									
	0.06									
	0.08									
	0.10									

TABLE No. A-4.5.4

The upper and the lower bound solutions for the drawing of round tube from round on a cylindrical plug.

Input tube size : 1.1250 in o.d. x 0.1875 in gauge  
 Reduction of area : 37.78%

Equivalent die semi-angle $\alpha_0$	Mean coeff. of friction $\mu$	UPPER BOUND					LOWER BOUND			
		Draw force	Mean draw stress	Mean die pressure	Mean yield stress	Mean draw stress	Mean die pressure	Mean yield stress	Mean draw stress	Mean die pressure
		P tonf	$\sigma_{za_2}$ tonf in <sup>-2</sup>	$P_m$ tonf in <sup>-2</sup>	$\bar{Y}_m$ tonf in <sup>-2</sup>	/yield stress	/yield stress	$Y_m$ tonf in <sup>-2</sup>	/yield stress	/yield stress
2	0.00	6.5008	18.918	31.160	35.261	0.5365	0.8837	34.269	0.4055	0.5945
	0.02	10.347	30.114	25.088	38.488	0.7824	0.6518		0.6959	0.3041
	0.04	12.736	37.066	20.666	40.023	0.9261	0.5164		0.8691	0.1309
	0.06	14.351	41.766	17.499	40.934	1.0203	0.4275		0.9705	0.0295
	0.08	15.513	45.148	15.151	41.539	1.0869	0.3647		1.0282	-0.0282
	0.10	16.389	47.698	13.348	41.970	1.1364	0.3180		1.0594	-0.0591
4	0.00	6.8355	19.893	32.765	35.596	0.5588	0.9205	34.269	0.4055	0.5945
	0.02	9.1246	26.554	29.395	37.586	0.7065	0.7821		0.5689	0.4311
	0.04	10.889	31.692	26.418	38.860	0.8155	0.6798		0.6956	0.3044
	0.06	12.285	35.752	23.901	39.752	0.8994	0.6013		0.7935	0.2065
	0.08	13.413	39.035	21.782	40.416	0.9658	0.5389		0.8688	0.1312
	0.10	14.342	41.740	19.988	40.929	1.0198	0.4883		0.9264	0.0736
6	0.00	7.175	20.881	34.392	35.922	0.5813	0.9574	34.269	0.4055	0.5945
	0.02	8.852	25.761	32.033	37.372	0.6893	0.8571		0.5187	0.4813
	0.04	10.257	29.851	29.812	38.424	0.7769	0.7759		0.6144	0.3856
	0.06	11.447	33.314	27.799	39.227	0.8493	0.7087		0.6951	0.3049
	0.08	12.466	36.279	25.994	39.862	0.9101	0.6522		0.7631	0.2363
	0.10	13.347	38.843	24.390	40.378	0.9620	0.6040		0.8203	0.1797
7	0.00	7.346	21.381	35.216	36.083	0.5925	0.9760	34.269	0.4055	0.5945
	0.02	8.839	25.725	33.158	37.362	0.6885	0.8875		0.5036	0.4964
	0.04	10.121	29.457	31.186	38.328	0.7685	0.8137		0.5885	0.4115
	0.06	11.232	32.688	29.362	39.087	0.8363	0.7521		0.6619	0.3381
	0.08	12.200	35.507	27.697	39.706	0.8944	0.6796		0.7254	0.2746
	0.10	13.051	37.984	26.185	40.209	0.9447	0.6512		0.7801	0.2199
8	0.00	7.520	21.885	36.045	36.242	0.6039	0.9946	34.269	0.4055	0.5945
	0.02	8.872	25.820	34.220	37.388	0.6906	0.9152		0.4919	0.5081
	0.04	10.056	29.255	32.448	38.281	0.7656	0.8476		0.5682	0.4318
	0.06	11.098	32.300	30.782	38.999	0.8282	0.7893		0.6354	0.3646
	0.08	12.022	34.988	29.237	39.591	0.8837	0.7385		0.6945	0.3055
	0.10	12.845	37.384	27.813	40.088	0.9325	0.6938		0.7465	0.2535
10	0.00	7.871	22.908	37.732	36.555	0.6267	1.0322	34.269	0.4055	0.5945
	0.02	9.023	26.260	36.240	37.508	0.7001	0.9662		0.4753	0.5247
	0.04	10.060	29.277	34.767	38.284	0.7647	0.9081		0.5384	0.4616
	0.06	10.996	32.003	33.351	38.931	0.8220	0.8567		0.5955	0.4045
	0.08	11.845	34.474	32.007	39.481	0.8732	0.8107		0.6471	0.3529
	0.10	12.618	36.722	30.741	39.953	0.9191	0.7694		0.6937	0.3063

TABLE No. A-4.5.4

..... (continued)

The upper and the lower bound solutions for the drawing of round tube from round on a cylindrical plug.

Input tube size : 1.1250 in o.d. x 0.1875 in gauge  
 Reduction of area : 37.75%

Equivalent die semi-angle $\alpha_0$	Mean coeff. of friction $\mu$	UPPER BOUND					LOWER BOUND			
		Draw force P tonf	Mean draw stress $\sigma_{za}$ tonf in <sup>-2</sup>	Mean die pressure $P_m$ tonf in <sup>-2</sup>	Mean yield stress $\bar{Y}_m$ tonf in <sup>-2</sup>	Mean draw stress /yield stress	Mean die pressure /yield stress	Mean yield stress $Y_m$ tonf in <sup>-2</sup>	Mean draw stress /yield stress	Mean die pressure /yield stress
12	0.00	8.2307	23.953	39.452	36.863	0.6498	1.0702	34.269	0.4055	0.5945
	0.02	9.2476	26.913	38.196	37.196	0.7142	1.0136		0.4638	0.5361
	0.04	10.180	29.628	36.941	38.370	0.7722	0.9628		0.5176	0.4824
	0.06	11.039	32.126	35.715	38.959	0.8246	0.9167		0.5670	0.4330
	0.08	11.829	34.428	34.533	39.471	0.8722	0.8749		0.6125	0.3875
	0.10	12.560	36.554	33.401	39.919	0.9157	0.8367		0.6543	0.3457
14	0.00	8.598	25.022	41.213	37.168	0.6732	1.1088	34.269	0.4055	0.5945
	0.02	9.519	27.703	40.136	37.887	0.7312	1.0593		0.4555	0.5445
	0.04	10.376	30.198	39.050	38.508	0.7842	1.0141		0.5022	0.4978
	0.06	11.175	32.523	37.977	39.050	0.8329	0.9725		0.5456	0.4544
	0.08	11.921	34.693	36.929	39.528	0.8777	0.7342		0.5861	0.4139
	0.10	12.618	36.723	35.913	39.953	0.9191	0.8989		0.6238	0.3762
16	0.00	8.975	26.119	43.020	37.470	0.6971	1.1481	34.269	0.4005	0.5945
	0.02	9.825	28.593	42.087	38.114	0.7502	1.1042		0.4492	0.5508
	0.04	10.625	30.922	41.140	38.680	0.7994	1.0636		0.4903	0.5097
	0.06	11.379	33.115	40.195	39.183	0.8451	1.0258		0.5290	0.4710
	0.08	12.089	35.183	39.263	39.632	0.8877	0.9907		0.5653	0.4346
	0.10	12.766	37.135	38.349	40.038	0.9275	0.9578		0.5995	0.4005
18	0.00	9.362	27.247	44.878	37.769	0.7214	1.1882	34.269	0.4055	0.5945
	0.02	10.159	29.565	44.068	38.355	0.7708	1.1490		0.4442	0.5558
	0.04	10.915	31.766	43.240	38.877	0.8171	1.1122		0.4809	0.5191
	0.06	11.634	33.858	42.407	39.347	0.8605	1.0778		0.5156	0.4844
	0.08	12.317	35.846	41.577	39.772	0.9013	1.0454		0.5485	0.4515
	0.10	12.967	37.737	40.757	40.159	0.9397	1.0149		0.5797	0.4203
20	0.00	9.762	28.410	46.794	38.068	0.7453	1.2292	34.269	0.4055	0.5945
	0.02	10.517	30.608	46.093	38.606	0.7928	1.1939		0.4401	0.5598
	0.04	11.240	32.711	45.371	39.092	0.8368	1.1606		0.4732	0.5268
	0.06	11.931	34.723	44.639	39.534	0.8783	1.1291		0.5047	0.4953
	0.08	12.593	36.650	43.903	39.938	0.9177	1.0993		0.5346	0.4654
	0.10	13.227	38.495	43.171	40.310	0.8550	1.0710		0.5632	0.4368
22	0.00									
	0.02									
	0.04									
	0.06									
	0.08									
	0.10									

A-5 EXPERIMENTAL RESULTS

TABLE No. A-5.1.1 Experimental results of the drawing of square tube from round on a cylindrical plug  
 mean draw speed = 5 ft min<sup>-1</sup> lubricant : TD 50

Test No.	Tube reference No.	Die	Equiv. Die semi angle $\alpha_e$	Tube o d (in) x gauge (in)	Internal dia. (i.d. <sub>b</sub> in)	Actual plug dia. (d <sub>p</sub> in)	Reduction of area (%)	Plug force, F <sub>p</sub> (tonf)	Draw force, P (tonf)	Mean draw stress $\sigma_{za}$ (tonf/in <sup>2</sup> )	Remarks
007*	4/a25007/02-80	4JB	7	1 x 1/4	0.500	0.437	40.58	0.5092	10.5641	30.1821	
014	4/a2507*/08-80	4JB		1 x 1/4	0.500	0.470	44.57	0.8143	11.2634	34.4969	
033*	2/a18709/08-80	4JB		1 x 3/16	0.625	0.557	46.44	-	-	-	T. failure
034*	4/a25008/08-80	4JB		1 x 1/4	0.500	0.495	47.79	-	11.6129	37.7584	T. failure
035*	4/a25008/08-80	4JB		1 x 1/4	0.500	0.495	47.79	-	11.4561	37.2486	T. failure
038*	4/a25008/08-80	4JB		1 x 1/4	0.500	0.495	47.79	-	11.4516	37.2340	T. failure
036*	3/a21908/08-80	4JB		1 x 7/32	0.5625	0.495	42.71	0.9413	10.9140	35.9407	
102	15/a2197*/04-81	4GB	8	1 x 7/32	0.5625	0.470	39.19	0.9722	9.4355	28.8984	
138	15/a2197**/05-81	4GB		1 x 7/32	0.5625	0.485	41.28	1.3426	9.6775	30.6731	
096	15/a21908/04-81	4GB		1 x 7/32	0.5625	0.488	41.71	1.5741	9.9193	31.6950	T. failure
103	14/a18708*/04-81	4GB		1 x 3/16	0.625	0.488	34.61	1.5092	10.0968	32.2619	
137	16/a2507*/04-81	4GB		1 x 1/4 (.255)	0.490	0.470	45.29	1.8518	11.2903	34.5792	T. failure
101	16/a25008/04-81	4GB		1 x 1/4 (.255)	0.490	0.485	47.56	1.5741	11.8548	36.3082	T. failure
126	15/a2197*/05-81	4HA	8	1 x 7/32	0.5625	0.470	39.19	1.8055	10.4032	31.8623	T. failure
130	15/a2197**/05-81	4HA		1 x 7/32	0.5625	0.485	41.28	1.4815	11.2903	35.8133	
132	16/a2507*/05-81	4HA		1 x 1/4 (.255)	0.490	0.470	45.29	1.9599	12.2581	37.5432	
133	16/a2507**/05-81	4HA		1 x 1/4 (.255)	0.490	0.485	47.56	1.7940	12.1371	38.7813	
127	15/a2197*/05-81	4DA	7	1 x 7/32	0.5625	0.470	39.19	1.8518	10.6452	32.6033	T. failure
056*	15/a21908/01-81	4MC	7	1 x 7/32	0.5625	0.495	42.71	2.5926	12.0968	39.3318	T. failure
057*	16/a2507*/01-81	4MC		1 x 1/4	0.500	0.470	44.57	1.5741	11.9355	36.5552	T. failure
124	15/a2197*/05-81	4MC		1 x 7/32	0.5625	0.470	39.19	1.3796	8.7097	26.6754	
128	15/a2197**/05-81	4MC		1 x 7/32	0.5625	0.485	41.28	1.2685	9.2097	29.2134	
131	16/a2507*/05-81	4MC		1 x 1/4 (.255)	0.490	0.470	45.29	2.2222	11.7742	36.0612	T. failure
125	15/a2197*/05-81	4KD	7	1 x 7/32	0.5625	0.470	39.19	1.0833	8.5968	26.3296	
129	15/a2197**/05-81	4KD		1 x 7/32	0.5625	0.485	41.28	1.3889	9.4355	29.9297	T. failure

Test number with asterisk (\*) denotes the first stock of tubing, batch A

T. failure: Tensile failure

TABLE No. A-5.1.2.1 Experimental results of the drawing of hexagonal tube from round on a cylindrical plug  
 mean draw speed = 5 ft min<sup>-1</sup> lubricant : TD 50

Test No.	Tube reference No.	Die	Equiv. Die semi angle $\alpha_e$	Tube o d (in) x gauge (in)	Internal dia. (i.d. <sub>b</sub> in)	Actual plug dia. (d <sub>p</sub> in)	Reduction of area (%)	Plug force, F <sub>p</sub> (tonf)	Draw force, P (tonf)	Mean draw stress $\sigma_{za}$ (tonf/in <sup>2</sup> )	Remarks
009*	5/b12811/2-80	6NB	7	1 1/16 x 10g	0.806(5)	0.677	22.95	1.1574	7.2581	25.0686	
013	11/b17711/3-80	6NB		1 1/16 x 7g	0.708(5)	0.677	41.20	2.3148	8.7097	30.0823	
017*	7/b21910/8-80	6NB		1 1/16 x 7/32	0.624(5)	0.620	40.05	2.0648	13.6710	39.3305	
018	11/b17710/8-80	6NB		1 1/16 x 7g	0.708(5)	0.620	29.40	1.1481	7.1048	20.4401	
021*	2/a18710/8-80	6NB		1 x 3/16	0.625	0.620	27.37	2.0222	10.8742	31.2843	
037*	3/a21909/8-80	6NB		1 x 7/32	0.562(5)	0.557	24.41	1.5336	9.5363	23.4982	
047	11/b17711/01-81	6NB		1 1/16 x 7g	0.708(5)	0.682	42.28	2.2222	9.8387	32.9127	
039*	5/b12811/12-80	6WB	8	1 1/16 x 10g	0.806(5)	0.682	24.37	0.9954	7.0564	24.8295	
040	11/b17711/12-80	6WB		1 1/16 x 7g	0.708(5)	0.682	42.28	2.0833	9.5693	31.2476	
041*	8/c16011/12-80	6WB		1 1/8 x 8g	0.805	0.682	41.14	1.8518	11.1290	39.1600	
042*	6/b16011/12-80	6WB		1 1/16 x 8g	0.748	0.682	37.35	1.9444	11.7742	41.4304	
043*	2/a18710/12-80	6WB		1 x 3/16	0.625	0.620	27.37	1.6088	9.6774	27.8412	
044	11/b17710/12-80	6WB		1 1/16 x 7g	0.708(5)	0.620	29.40	0.8680	6.6734	19.1989	
045*	7/b21910/12-80	6WB		1 1/16 x 7/32	0.624(5)	0.620	40.05	1.6898	12.7419	36.6575	
046*	1/a17610/12-80	6WB		1 x 7g (.177)	0.648	0.620	23.70	1.2963	8.2258	23.6650	
083	16/a2507**/03-81	6NB	7	1 x 1/4 (.255)	0.490	0.485	22.13	1.0339	8.1720	17.5835	
084	15/a21909/03-81	6NB		1 x 7/32	0.562(5)	0.557	24.41	0.8218	7.3185	18.0335	
085	14/a18710/03-81	6NB		1 x 3/16	0.625	0.620	27.37	1.4043	8.5484	24.5931	
086	17/b16011/03-81	6NB		1 1/16 x 8g	0.748	0.682	37.35	1.9290	8.7634	30.8363	
088	16/a2507**/08-81	6WB	8	1 x 1/4 (.255)	0.490	0.485	22.13	1.0741	7.3064	15.7211	
089	15/a21909/03-81	6WB		1 x 7/32	0.562(5)	0.557	24.41	0.6481	6.3710	15.6986	
090	14/a18710/03-81	6WB		1 x 3/16	0.625	0.620	27.37	1.5586	8.0376	23.1237	
091	1/a17610/03-81	6WB		1 x 7g (.176)	0.648	0.620	23.70	1.2963	7.9032	22.7370	
092	17/b16011/03-81	6WB		1 1/16 x 8g	0.748	0.682	37.35	1.4815	8.0645	28.3769	
093	9/c18711/03-81	6WB		1 1/8 x 3/16	0.750	0.682	48.54	-	-	-	T. failure

Test number with asterisk (\*) denotes the first stock of tubing, batch A

T. failure: Tensile failure



TABLE No. A-5.1.3.1 Experimental results of the drawing of octagonal tube from round on a cylindrical plug  
 mean draw speed = 5 ft min<sup>-1</sup> lubricant : TD 50

Test No.	Tube reference No.	Die	Equiv. Die semi angle $\alpha_e$	Tube o d (in) x gauge (in)	Internal dia. (i.d. <sub>b</sub> in)	Actual plug dia. (d <sub>p</sub> in)	Reduction of area (%)	Plug force, F <sub>p</sub> (tonf)	Draw force, P (tonf)	Mean draw stress $\sigma_{za}$ (tonf/in <sup>2</sup> )	Remarks
004	11/b17711/1-80	8PB	7	1 1/16 x 7g	0.708(5)	0.677	29.50	0.7246	5.8871	16.9589	
008*	8/c16011/2-80	8PB		1 1/8 x 8g	0.805	0.677	28.43	1.2963	8.8710	25.5546	
010*	5/b12812/2-80	8PB		1 1/16 x 10g	0.806(5)	0.740	26.28	1.4815	6.5726	23.7256	
012*	10/c25010/2-80	8PB		1 1/8 x 1/4	0.625	0.615	40.33	2.1296	14.2742	34.8106	
020*	7/b21910/8-80	8PB		1 1/16 x 7/32	0.625	0.620	30.12	1.3229	10.8089	26.6753	
028*	8/c16012/8-80	8PB		1 1/8 x 8g	0.805	0.745	44.09	2.5463	11.2097	41.3345	
029*	6/b16011/8-80	8PB		1 1/16 x 8g	0.742	0.682	24.65	1.3194	8.8710	25.9536	
058	11/b17711/01-81	8PB		1 1/16 x 7g	0.708(5)	0.682	30.58	1.0818	6.0484	17.6956	
068	16/a2507**/03-81	8PB		1 x 1/4 (.255)	0.490	0.485	12.48	0.4333	4.2200	8.0786	
069	15/a21909/03-81	8PB		1 x 7/32	0.562(5)	0.557	13.68	0.4630	3.9314	8.4831	
070	14/a187 10/03081	8PB		1 x 3/16	0.625	0.620	15.34	0.7870	4.7581	11.7425	
071	19/c18711/03-81	8PB		1 1/8 x 3/16	0.750	0.682	38.10	2.5463	11.2500	32.9137	
072	19/c18712/03-81	8PB		1 1/8 x 3/16	0.750	0.745	50.89	1.3426	11 2500	41.4832	
079	17/b16012/03-81	8PB		1 1/16 x 8g	0.748	0.745	40.22	1.2500	7.7218	28.4733	
082	11/b17711/03081	8PB		1 1/16 x 7g	0.708(5)	0.682	30.58	1.0802	6.1021	17.8528	
073	16/a2507**/03-81	8WB	8	1 x 1/4 (.255)	0.490	0.485	12.48	0.5401	4.8387	9.2631	
073	15/a21909/03-81	8WB		1 x 7/32	0.562(5)	0.557	13.68	0.4961	4.2338	9.1356	
075	14/a18710/03-81	8WB		1 x 3/16	0.625	0.620	15.34	0.9259	5.1613	12.7376	
076	19/c18711/03-81	8WB		1 1/8 x 3/16	0.750	0.750	38.10	1.8518	9.8790	28.9026	
077	17/b16012/o3-81	8WB		1 1/16 x 8g	0.748	0.745	40.22	1.1111	7.1371	26.3173	
078	19/c18712/03-81	8WB		1 1/8 x 3/16	0.750	0.750	50.89	1.4444	10.4516	38.5319	
080	11/b17710/o3-81	8WB		1 1/16 x 7g	0.708(5)	0.620	17.71	0.0926	3.8710	9.5532	
081	11/b17711/03-81	8WB		1 1/16 x 7g	0.708(5)	0.682	30.58	1.2778	6.6935	19.5829	
113	20/b 23509/05-81	8WB		1.040 x .235	0.570	0.557	22.02	0.9259	6.9355	14.9652	
112	20/b 23509/05-81	8PB	7	1.040 x .235	0.570	0.557	22.02	0.9259	6.8952	14.8782	

Test number with asterisk (\*) denotes the first stock of tubing, batch A

T. failure: Tensile failure









TABLE No. A-5.2 .2.1 Tensile test results of the drawn hexagonal tube from round on a cylindrical plug

TEST No.	Tensile test No.	Tube ref. No.	Die	Equiv. die semi-angle $\alpha_0$	Tube o d (in) x gauge (in)	Tube inlet area ( $A_b$ in <sup>2</sup> )	Actual plug dia ( $d_p$ in)	Reduction of area (%)	Tensile force (tonf)	Mean flow stress $\sigma_f$ (tonf/in <sup>2</sup> )	Mean yield stress, $Y_m$ (ton/in <sup>2</sup> )
009*	17	5/b12811/	6NB	7	1 1/16 x 10g	0.3758	0.677	22.95	11.85	41.4851	30.9899
037*	18	3/a21909/	6NB		1 x 7/32	0.5369	0.557	24.41	17.50	43.5699	34.1615
021*	19	2/a18710/	6NB		1 x 3/16	0.4786	0.620	27.37	15.75	46.0094	35.2348
013	20	11/b17711/	6NB		1 1/16 x 7g	0.4924	0.677	41.20	12.5	43.3505	34.8225
018	21	11/b17710/	6NB		1 1/16 x 7g	0.4924	0.620	29.40	13.5	39.3240	31.3922
017*	22	7/b11910/	6NB		1 1/16 x 7/32	0.5798	0.620	40.05	17.9	51.7957	41.0992
085	49	14/a18710/	6NB		1 x 3/16	0.4786	0.620	27.37	14.60	42.2762	34.7238
083	50	16/a2507**/	6NB		1 x 1/4 (.25)	0.5968	0.485	22.13	16.5	36.0884	29.6414
086	51	17/b16011/	6NB		1 1/16 x 8g	0.4536	0.682	37.35	10.7	38.2723	31.4409
084	52	15/a21909/	6NB		1 x 7/32	0.5369	0.557	24.41	14.4	36.0647	29.6219
088	53	16/a2507**/	6WB	8	1 x 1/4	0.5968	0.485	22.13	16.5	36.0351	29.5976
087	54	16/a2507**/	6WB		1 x 1/4 (.25)	0.5968	0.485	22.13	16.5	36.1345	29.5976
091	55	1/a <sup>h</sup> 17610/	6WB		1 x 7g (.175)	0.4556	0.620	23.70	15.0	43.5121	35.7389
089	56	15/a21909/	6WB		1 x 7/32	0.5369	0.557	24.41	14.25	35.5661	29.2124
090	57	14/a18710/	6WB		1 x 3/16	0.4786	0.620	27.37	14.75	42.7360	35.1014
092	58	17/b16011/	6WB		1 1/16 x 8g	0.4536	0.682	37.54	11.00	39.1938	32.1920
094	66	2/a <sup>h</sup> 18710/	6WB		1 x 3/16	0.4786	0.620	27.37	18.75	54.6652	44.8995
114	67	20 <sup>-</sup> /b <sup>-</sup> 23509/	6WB		1.040 x .235	0.5943	0.557	31.71	17.3	43.1486	35.4403
105	68	9/e <sup>h</sup> 18710/	6WB		1 1/8 x 3/16	0.5522	0.620	37.06	15.5	44.9224	36.8972
106	69	8/e <sup>h</sup> 16011/	6WB		1 1/8 x 8g	0.4851	0.682	41.14	14.5	51.5932	42.3762
123	70	1/a <sup>h</sup> 17610/	6NB	7	1 x 7g (.175)	0.4556	0.620	23.70	18.25	53.1655	43.6678
115	71	20 <sup>-</sup> /b <sup>-</sup> 23509/	6NB		1.040 x .235	0.5943	0.557	31.71	17.25	43.0239	35.3379
136	72	16/a2507**/	6BA	7	1 x 1/4 (.25)	0.5968	0.485	22.13	16.35	35.7075	29.3285
122	73	1/a <sup>h</sup> 17610/	6BA		1 x 7g (.175)	0.4556	0.620	23.70	13.15	38.3537	31.5020
119	74	15/a21909/	6BA		1 x 7/32	0.5369	0.557	24.41	14.26	35.4783	29.1403

Test number with asterisk (\*) denotes the first stock of tubing, batch A



TABLE No. A-5.2.3.1 Tensile test results of the drawn octagonal tube from round on a cylindrical plug

TEST No.	Tensile test No.	Tube ref. No.	Die	Equiv. die semi-angle $\alpha_p^0$	Tube o d (in) x gauge (in)	Tube inlet area ( $A_b$ in <sup>2</sup> )	Actual plug dia ( $d_p$ in)	Reduction of area (%)	Tensile force (tonf)	Mean flow stress $\sigma_f$ (tonf/in <sup>2</sup> )	Mean yield stress, $Y_m$ (ton/in <sup>2</sup> )
004	10	11/b17711/	8PB	7	1 1/16 x 7g	0.4924	0.677	29.50	13.5	39.2237	31.4207
029*	11	6/b16011/	8PB		1 1/16 x 8g	0.4536	0.682	24.65	19.75	58.1170	47.1691
010*	12	5/b12812/	8PB		1 1/16 x 10g	0.3758	0.740	26.28	12.5	45.2936	36.7613
008*	13	8/c16011/	8PB		1 1/8 x 8g	0.4851	0.677	28.43	15.4	44.8151	34.6722
020*	14	7/b21910/	8PB		1 1/16 x 7/32	0.5798	0.620	30.12	21.0	52.3441	41.2915
012*	15	10/c25010/	8PB		1 1/8 x 1/4	0.6872	0.615	40.33	21.5	53.0667	42.2959
028*	16	8/c16012/	8PB		1 1/8 x 8g	0.4851	0.745	44.09	13.1	48.8241	39.1239
068	34	16/a2507**/	8PB		1 x 1/4 (.255)	0.5968	0.485	12.48	16.0	31.0710	25.5203
069	35	15/a21909/	8PB		1 x 7/32	0.5369	0.557	13.68	13.4	29.2900	24.0575
070	36	14/a18710/	8PB		1 x 3/13	0.4786	0.620	15.34	15.0	37.5441	30.8370
082	37	11/b17711/	8PB		1 1/16 x 7g	0.4924	0.682	30.58	13.5	40.0968	32.9337
071	38	19/c18711/	8PB		1 1/8 x 3/16	0.5522	0.682	38.10	16.65	49.5210	40.6743
079	39	17/b16012/	8PB		1 1/16 x 8g	0.4536	0.745	40.22	11.45	42.8370	35.1844
072	40	19/c18712/	8PB		1 1/8 x 3/16	0.5522	0.745	50.89	14.6	54.1159	44.4484
073	41	16/a2507**/	8WB	8	1 x 1/4 (.255)	0.5968	0.485	12.48	16.55	32.0947	26.3611
074	42	15/a21909/	8WB		1 x 7/32	0.5369	0.557	13.68	14.50	31.7288	26.0606
075	43	14/a18710/	8WB		1 x 3/16	0.4786	0.620	15.34	15.65	39.1479	32.1543
080	44	11/b17710/	8WB		1 1/16 x 7g	0.4924	0.620	17.71	13.20	33.0454	27.1420
081	45	11/b17711/	8WB		1 1/16 x 7g	0.4924	0.682	30.58	12.6	37.3537	30.6807
077	46	17/616012/	8WB		1 1/16 x 8g	0.4536	0.745	40.22	10.65	39.9697	32.8293
076	47	19/c18711/	8WB		1 1/4 x 3/16	0.5522	0.682	38.10	16.0	47.5456	39.0518
078	48	19/c18712/	8WB		1 1/8 x 3/16	0.5522	0.745	50.89	13.35	49.5220	40.6752
113	62	20/b-23509/	8WB		1.040 x .235	0.5943	0.557	22.02	18.5	40.5176	33.2793
112	63	20/b-23509/	8PB	7	1.040 x .235	0.5943	0.557	22.02	18.65	39.5476	32.4826
117	64	20/b-123509/	8SD	7	1.040 x .235	0.5943	0.557	22.02	18.75	41.0165	33.6891

Test number with asterisk (\*) denotes the first stock of tubing, batch A









TABLE No. A-5.4.1

The mean coefficient of friction from the experimental determination of redundant work and the apparent strain method

mean draw speed = 5 ft min<sup>-1</sup>

lubricant : TD 50

Test No.	Tube reference code	Die	Tube o d (in) x gauge (in)	Inlet area $A_b$ in <sup>2</sup>	Reduction of area 'r' (%)	Homogeneous strain $\epsilon_h$	Mean draw stress $\sigma_{za}$ tonf in <sup>-2</sup>	Mean flow stress $\sigma_f$ tonf in <sup>-2</sup>	Mean equivalent strain $\epsilon_m$	Mean yield stress $\gamma_m$ tonf in <sup>-2</sup>	Homogeneous yield stress $\gamma_h$ tonf in <sup>-2</sup>	Homogeneous work $W_h$ tonf in <sup>-2</sup>	Friction work $W_f$ tonf in <sup>-2</sup>	Mean pressure $P_m$ tonf in <sup>-2</sup>	Mean coeff. of friction $\mu$
103	14/a18708	4GB	1 x 3/16	0.8786	34.61	0.425	32.262	42.761	0.715	35.122	31.363	13.323	7.156	7.751	0.039
126	15/a2197**	4HA	1 x 7/32	0.5369	39.18	0.497	31.862	43.238	0.752	35.514	32.455	16.136	5.146	7.971	0.022
130	15/a2197**	4HA	1 x 7/32	0.5369	41.27	0.532	34.813	43.179	0.748	35.465	32.940	17.532	9.302	8.144	0.044
132	16/a2507*	4HA	1 x 1/4 (.255)	0.5962	45.29	0.603	37.543	43.554	0.778	35.774	33.848	20.416	9.715	8.595	0.040
124	15/a2197*	4MC	1 x 7/32	0.5369	39.18	0.497	26.675	38.560	0.444	31.671	26.675	16.136	12.603	5.915	0.118
128	15/a2197**	4MC	1 x 7/32	0.5369	41.27	0.532	29.213	38.430	0.437	31.565	32.940	17.532	15.404	5.667	0.172
088	16/a2507**	6WB	1 x 1/4 (.255)	0.5968	22.13	0.250	15.721	36.035	0.325	29.598	27.949	6.989	6.088	10.592	0.062
089	15/a11909/	6WB	1 x 7/32	0.5369	24.40	0.280	15.699	35.566	0.306	29.212	28.637	8.008	6.747	8.237	0.074
092	17/b16011/	6WB	1 1/16 x 8g	0.4536	37.35	0.468	28.377	39.194	0.479	32.192	32.025	14.975	12.959	5.512	0.092
083	16/a2507**	6NB	1 x 1/4 (.255)	0.5968	22.13	0.250	17.583	36.088	0.328	29.641	27.949	6.989	7.871	11.499	0.082
084	15/a21909/	6NB	1 x 7/32	0.5369	24.40	0.280	18.033	36.065	0.327	29.622	28.637	8.008	8.356	9.305	0.086
009*	5/b12811/	6NB	1 1/16 x 8g	0.3758	22.95	0.313	25.069	38.183	0.313	30.990	29.703	7.743	15.371	4.787	0.148
032*	3/a21909/	6NB	1 x 7/32	0.5369	24.40	0.476	23.498	42.090	0.476	34.161	30.191	8.443	7.231	11.617	0.042
021	2/a18710/	6NB	1 x 3/16	0.4786	27.37	0.544	31.284	43.413	0.544	35.235	31.146	9.960	12.114	11.893	0.061
118	15/a2507**	6AA	1 x 7/32	0.5369	24.40	0.280	19.309	36.086	0.328	29.640	28.637	8.008	9.599	9.772	0.101
120	11/b17710/	6AA	1 1/16 x 7g	0.4924	29.40	0.348	22.505	37.437	0.399	30.946	30.035	10.458	10.144	6.039	0.076
135	16/a2507**	6AA	1 x 1/4 (.255)	0.5968	22.13	0.250	20.692	36.545	0.347	30.016	27.949	6.989	10.271	13.134	0.102
119	15/a21909/	6BA	1 x 7/32	0.5369	24.40	0.280	19.077	35.478	0.303	29.140	28.649	8.008	10.248	9.394	0.122
121	11/b17710/	6BA	1 1/16 x 7g	0.4924	29.40	0.348	23.955	39.437	0.493	32.391	30.035	10.458	7.995	6.631	0.043
122	1/a <sup>h</sup> 17610/	6BA	1 x 7g	0.4556	23.70	0.271	23.433	38.354	0.434	31.502	28.431	7.692	9.776	10.301	0.063
136	16/a2507**	6BA	1 x 1/4 (.255)	0.5968	22.13	0.250	19.521	35.707	0.312	29.328	27.949	6.989	10.368	12.079	0.120
073	16/a2507**	8WB	1 x 1/4 (.255)	0.5968	12.48	0.133	9.263	32.095	0.191	26.361	24.373	3.248	4.255	12.181	0.086

TABLE No. A-5.4.2

The mean coefficient of friction from the experimental determination of redundant work and the apparent strain method

mean draw speed = 5 ft min<sup>-1</sup>

lubricant : TD 50

Test No.	Tube reference code	Die	Tube o d (in) x gauge (in)	Inlet area $A_b$ in <sup>2</sup>	Reduction of area 'r' (%)	Homogeneous strain $\epsilon_h$	Mean draw stress $\sigma_{za}$ tonf in <sup>-2</sup>	Mean flow stress $\sigma_f$ tonf in <sup>-2</sup>	Mean equivalent strain $\epsilon_m$	Mean yield stress $Y_m$ tonf in <sup>-2</sup>	Homogeneous yield stress $Y_h$ tonf in <sup>-2</sup>	Homogeneous work $W_h$ tonf in <sup>-2</sup>	Friction work $W_f$ tonf in <sup>-2</sup>	Mean pressure $P_m$ tonf in <sup>-2</sup>	Mean coeff. of friction $\mu$
074	15/a21909/	BWB	1 x 7/32	0.5369	13.67	0.147	9.136	31.148	0.181	26.061	24.897	3.659	4.411	9.620	0.092
080	11/b17710/	BWB	1 1/16 x 7g	0.4924	17.71	0.195	9.553	33.045	0.219	27.142	26.474	5.160	3.621	4.281	0.048
081	11/b17711/	BWB	1 1/16 x 7g	0.4924	30.58	0.365	9.583	37.354	0.384	30.681	30.346	11.078	3.804	6.117	0.072
077	17/b16012/	BWB	1 1/16 x 8g	0.4536	40.22	0.514	26.317	39.970	0.524	32.829	32.697	16.823	9.111	5.880	0.065
068	16/a2507**/	BPB	1 x 1/4 (.255)	0.5968	12.48	0.133	8.079	31.071	0.165	25.520	24.373	3.248	3.879	10.496	0.083
004	11/b17711/	BPB	1 1/16 x 7g	0.4924	29.50	0.350	16.959	38.888	0.416	31.421	25.321	10.573	3.899	5.075	0.026
008*	8/c16011/	BPB	1/8 x 8g	0.4851	28.43	0.335	25.555	42.720	0.508	34.672	31.474	10.530	7.954	5.212	0.034
116	15/a21909/	BSD	1 x 7/32	0.5369	13.67	0.147	8.445	32.012	0.189	26.293	24.897	3.659	13.480	15.477	0.272
117	20/b23509/	BSD	1.040 x .235	0.5943	22.02	0.249	24.101	41.016	0.590	24.101	27.916	6.944	4.216	15.551	0.019
067	16/a2507**/	LOQB	1 x 1/4 (.255)	0.5968	7.85	0.082	6.452	30.346	0.148	24.925	21.914	1.791	2.770	14.261	0.064
065	17/b16012/	LOQB	1 1/16 x 8g	0.4536	34.13	0.417	23.750	39.286	0.484	32.267	21.267	13.044	8.128	7.005	0.052
061	17/b16012/	ccRA	1 1/16 x 8g	0.4536	22.96	0.261	14.307	35.023	0.286	28.767	28.207	7.358	6.094	7.341	0.067
108	20/b23509/	ccRA	1.040 x .235	0.5943	8.85	0.093	5.955	31.377	0.172	25.772	22.520	2.086	1.516	10.307	0.027

- A68 -

A-6 SPECIFICATIONS FOR THE EQUIPMENT AND INSTRUMENTATION

A-6.1 'Brookes' hydraulic drawbench

Manufacturer: Brookes Ltd.

Primary drive: 3-phase induction motor;  
40 hp, 50 Hz and  $1440 \text{ rev min}^{-1}$

Hydraulic delivery:  $25.2 \text{ g min}^{-1}$  at  $1440 \text{ rev min}^{-1}$  and  
a pressure of  $100 \text{ lbf in}^{-2}$ ;  
maximum working pressure of  
 $2000 \text{ lbf in}^{-2}$  at 30 tonf

Nominal speed range: 0 to  $15 \text{ ft min}^{-1}$

Stroke: 54 in

A-6.1.1 Rotary drive

Primary drive: 3-phase induction motor; 7.5 hp and  
 $1435 \text{ rev min}^{-1}$

Variable speed unit: 'Crofts' belt drive with speed ratio  
of 4:1

Reduction gear unit: 'Crofts' gear unit with reduction  
ratio 16.61:1

'Reynolds' chain: Duplex chain  $5/8$  in pitch;  
Serial No.

A-6.2 'Sheffield' hydraulic drawbench

Manufacturer: Department of Mechanical Engineering,  
Sheffield University

Primary drive: 'Crompton Parkinson' 50 hp motor;  
3-phase, 50 c/s, M.C. rating,  
 $1440 \text{ rev min}^{-1}$ ; 415 V Ellison starter:  
50 c/s, and 76 Amp

Hydraulic delivery: DS 240 pump ('Langdale Engineering Co.');

29.5 g min<sup>-1</sup> at 1250 rev min<sup>-1</sup> for a pressure of 4400 lbf in<sup>-2</sup> on continuous duty; working intermittently at 1500 rev min<sup>-1</sup> pressures of 5500 lbf in<sup>-2</sup> are developed; at a maximum speed of 1650 rev min<sup>-1</sup> the oil pressure is 6500 lbf in<sup>-2</sup>

Nominal speed range: 0 to 100 ft min<sup>-1</sup>

Stroke: 120 in

Capacity: Capable of 30 tonf at 100 ft min<sup>-1</sup>

'Reynolds' chain: Duplex chain 1 in pitch; No. 114 088

### A-6.3 Equipment for the measurement of drawing parameters

#### A-6.3.1 Load transducers

A summary of the load transducers on the 'Brookes' bench is given on Table A-6.1.

#### A-6.3.2 Speed measurements

- (i) Rotational speed: 'Smith' type tachogenerator; 25 volts d.c./1000 rev min<sup>-1</sup>; output maximum current 100 mA; armature resistance 39 ohm
- (ii) Draw speed: 'LAS - 15' photo-cell; supply voltage 11-20 kHz; light source: 2.5 volts

#### A-6.3.3 Other data recording accessories

Voltage supply: 'Farnell L30 BT' stabilised power source; 0 to 30 volts d.c. and 1 Amp maximum

Bridge amplifier: 'SGA 300 KAP'; provides supply voltage

virtually independent of the source  
voltage; potentiometers for zero, span  
and bridge supply adjustments

Ultra-violet recorder: 'S.E. Oscillograph 3006'; 12 channels

Calibrating meter: Type 'TCAA' advance electronics

#### A-6.4 Testing machines

##### Load cells calibration

'Denison' universal hydraulic testing machine

Model 7104 DCJ

Machine No. E62404

##### Tensile testing machine

'Denison' universal testing machine

Model T42B4

Serial No. 28176

##### Metrology equipment (for the verification of die angles)

'Nikon', Nippon Kogaku (Japan)

Model Shadowgraph 5A

Serial No. 2368

TABLE No. A-6.1

## Load transducers

'BROOKES' DRAWBENCH					
Reference name of the transducer	Measured parameter	Strain gauge resistance	Manufacturer of the gauges	Galvanometer code	U-V recorder channel No.
TAG LOAD	Draw force	75 ohm	Saunders - Roe	M100 9043	4
	Torque	29 ohm	"	M40 9435	5
PLUG LOAD	Plug force	120 ohm	Tinsley Tylcon	B450 2-165	8
RING LOAD (split-die)	Axial force	100 ohm	"	A1000 2-298	9
CUP LOAD (split-die)	Drag force	120 ohm	"	M20 9037	1
	Torque	50 ohm	"		

A-7 CALIBRATION CURVES

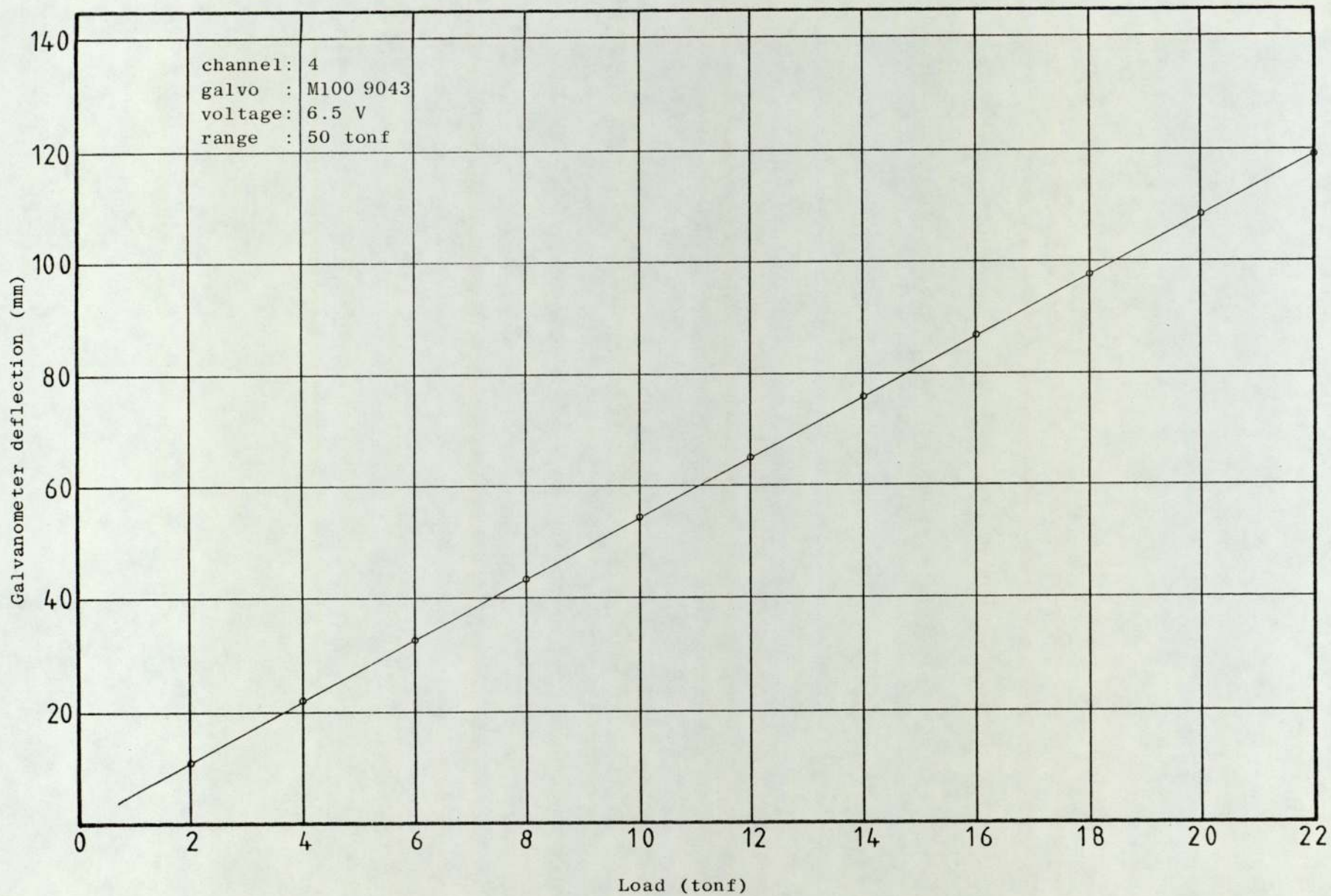
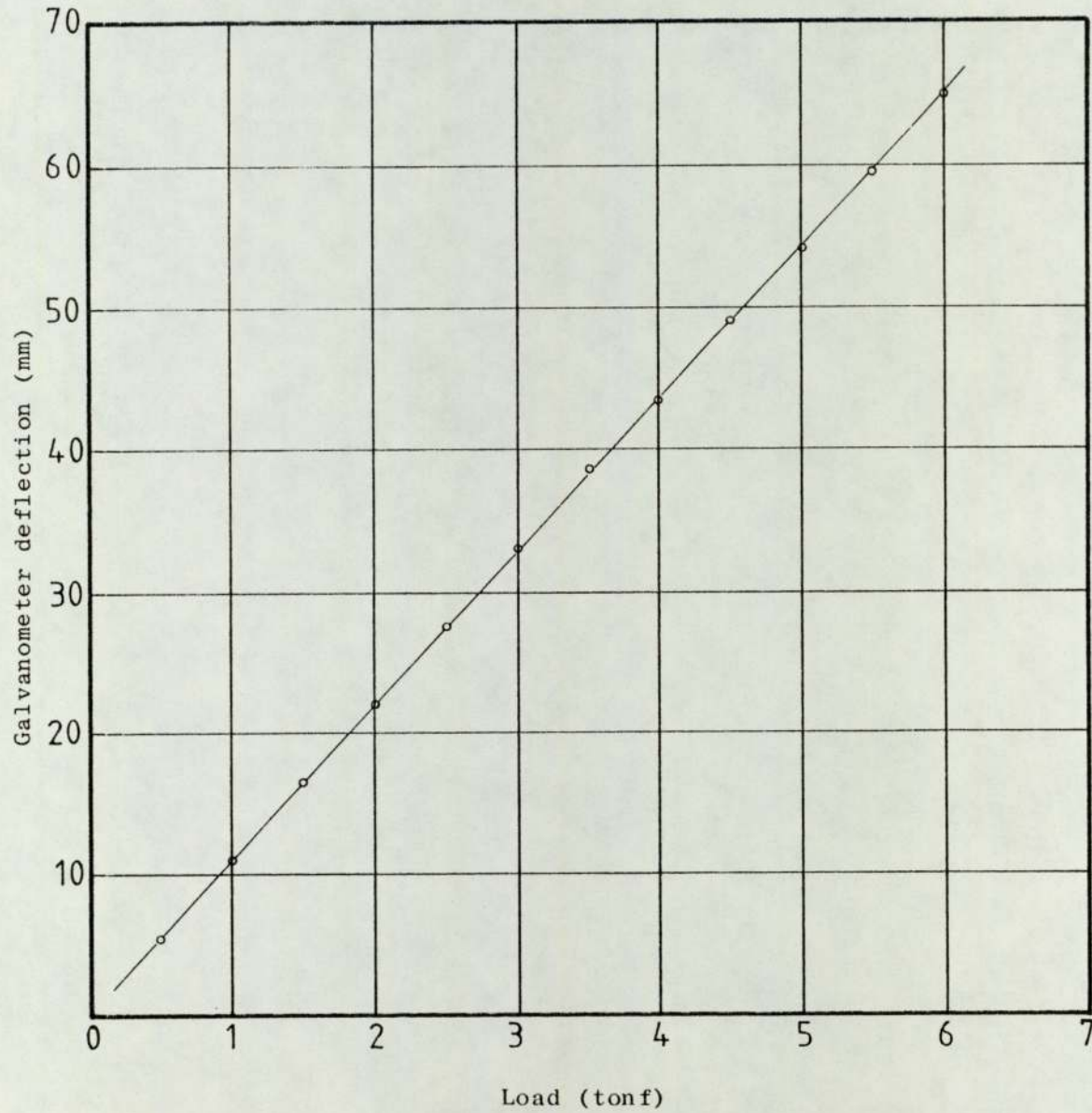


Fig. A-7.1 Calibration curve of the load transducer at the tag holder.



channel : 8  
galvo : B-450 2-165  
voltage : 6.5 V  
range : 10 tonf

Fig. A-7.2 Calibration curve of the plug load cell

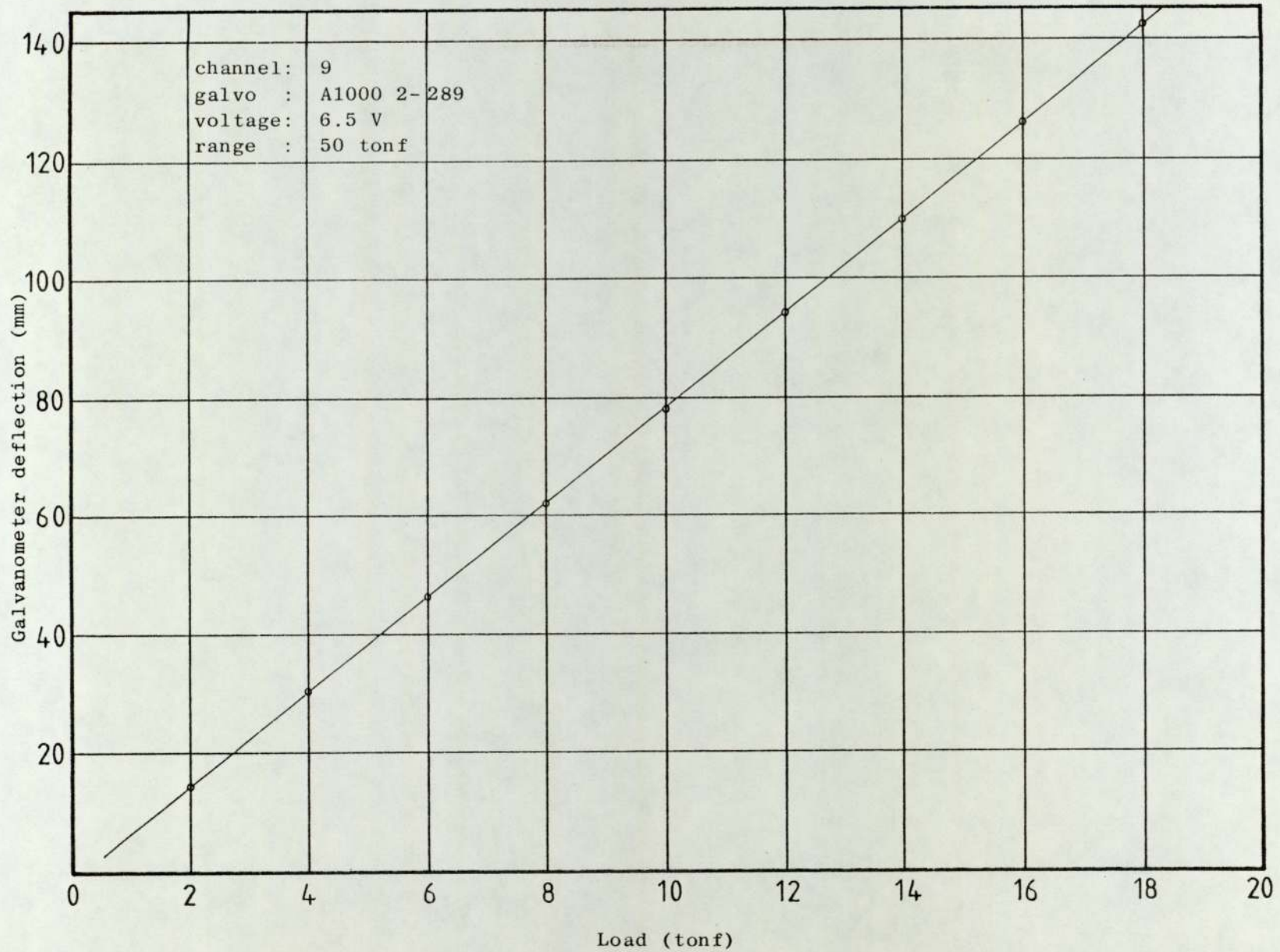


Fig. A-7.3 Calibration curve of the ring load cell of the split rotating die.

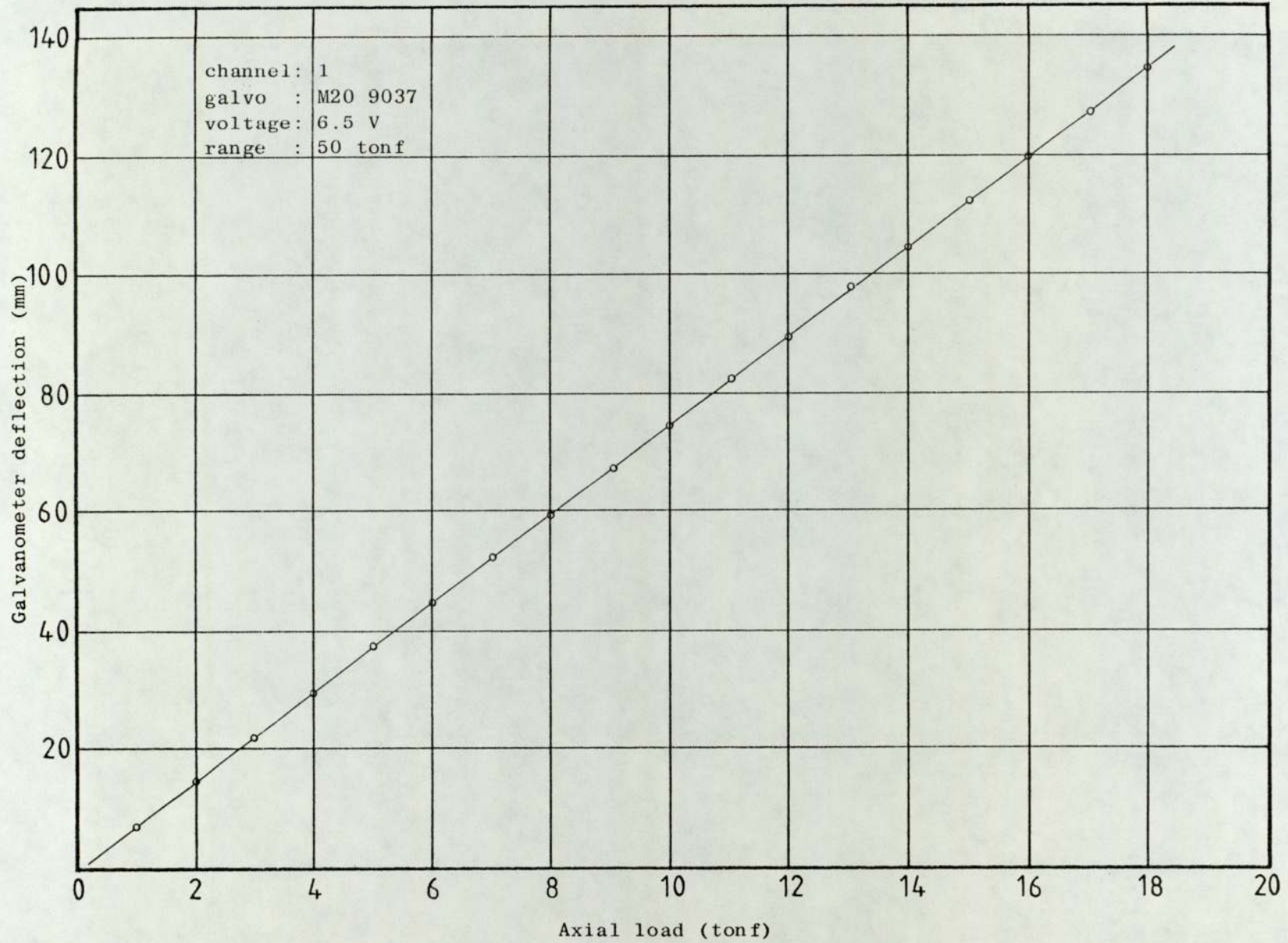


Fig. A-7.4 Calibration curve of the cup-load cell of the split rotating die.

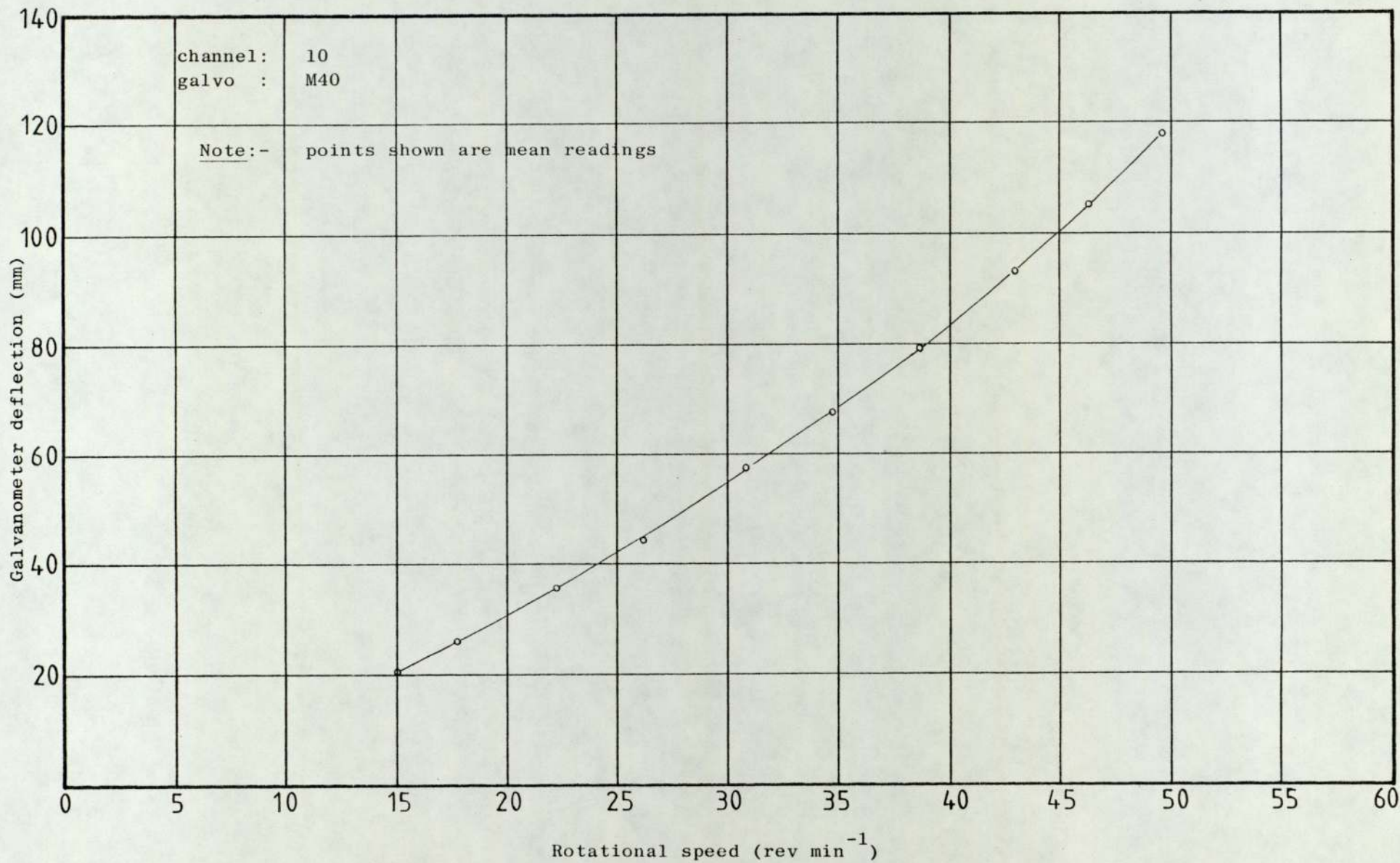


Fig. A-7.5 Calibration curve of the rotational speed transducer of the split die rig.

A-8 Deformation pattern for the upper bound solution of the drawing of polygonal tubes from round stock on a cylindrical plug.

A-8.1 Banding the exit plane with N-2 hyperbolic curves.

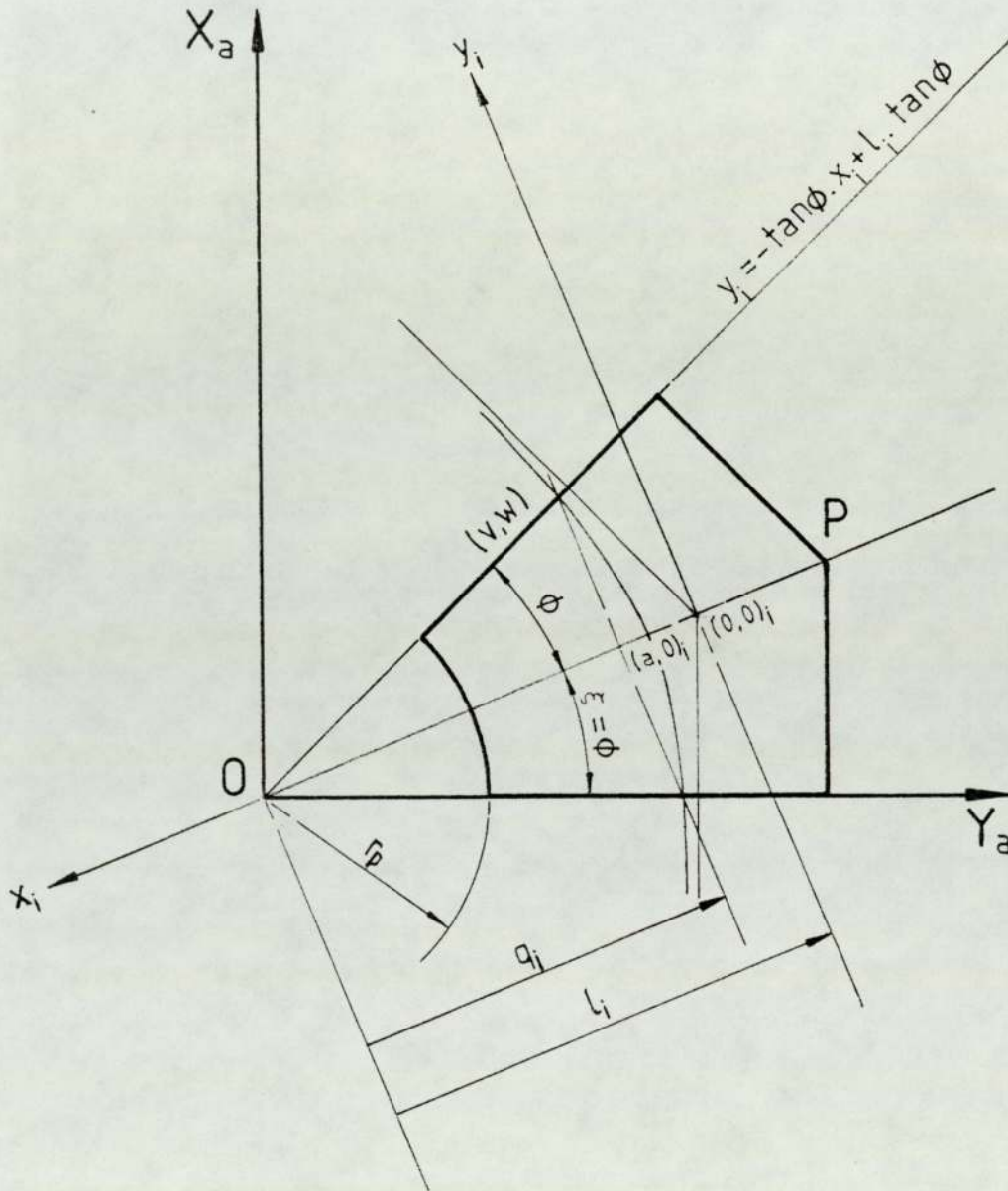


Fig. A-8.1 Double symmetric section at the exit plane.

$OP$  is a line of symmetry and the included angle  $\phi = \beta = \frac{\pi}{N_s}$ .

The section is banded by N-2 hyperbolic curves and the inner limiting curve corresponds to the plug surface.

The equation of the hyperbola is given by:-

$$\frac{x_i^2}{a_i^2} - \frac{y_i^2}{b_i^2} = 1 \quad (\text{A-8.1})$$

with respect to  $x_i, y_i$  axes, or

$$\frac{(X_a \sin \xi + Y_a \cos \xi - l_i)^2}{a_i^2} - \frac{(X_a \cos \xi - Y_a \sin \xi)^2}{b_i^2} = 1 \quad (\text{A-8.2})$$

where 
$$\begin{pmatrix} x_i \\ y_i \end{pmatrix} = \begin{pmatrix} -\sin \xi - \cos \xi \\ \cos \xi - \sin \xi \end{pmatrix} \begin{Bmatrix} X_a - l_i \sin \xi \\ Y_a - l_i \cos \xi \end{Bmatrix} \quad (\text{A-8.3})$$

and  $\xi = \phi$

The intersection of the hyperbola  $i$  and the straight line

$y_i = -\tan \phi \cdot x_i + l_i \tan \phi$  is denoted by  $(v, w) \equiv (x_i, y_i)$ , where

$$v = x_i = \frac{-l_i \tan^4 \phi + \sqrt{l_i^2 \tan^8 \phi + (1 - \tan^4 \phi)(a_i^2 + l_i^2 \tan^4 \phi)}}{(1 - \tan^4 \phi)}$$

for  $\phi = \beta < \pi/4$  (A-8.4)

or 
$$v = x_i = \frac{a_i^2 + l_i^2}{2l_i} \quad \text{for } \phi = \beta = \pi/4$$

and  $w = y_i = \tan \phi (-v + l_i)$  (A-8.5)

The cross-sectional area enclosed by the hyperbola  $i$ , the straight line  $y_i = -\tan \phi x_i + l_i \tan \phi$ , the plug surface and the  $Y_a$  axis is found

to be

$$A_T(i) = \cot\phi \left[ v \sqrt{v^2 - a_i^2} - a_i^2 \ln \left\{ \frac{v + \sqrt{v^2 - a_i^2}}{a_i} \right\} \right] + q_i^2 \cdot \tan\phi - \phi \cdot r_p^2 \quad (\text{A-8.6})$$

$$q_i = l_i - v \quad (\text{A-8.7})$$

$a_i$ , the distance from the origin  $(0,0)_i$  to the vertex of the hyperbola  $i$  is adjusted as the  $(x_i, y_i)$  axes translate along the straight line  $X_a = \tan\xi \cdot Y_a$  or the line of symmetry. The value of  $a_i$  is selected to suit the corners of the asymptotes drawn for every  $l_i$ . In particular,  $a_i = N^{-1} < 0.1$ , so that the hyperbola corresponding to the outer surface of the polygon is almost coincident with the asymptote.

e.g.  $a_i = 1 - \frac{(i-1)}{N}$ , where  $i = 2, \dots, = N$

The diagonal wall thickness,  $t_a = \kappa H_a$  is divided into  $N - 2$  elemental lengths. Let the elemental lengths be  $\Delta t_2, \Delta t_3, \dots, \Delta t_{N-1}$  such that  $\sum_{i=2} \Delta t_i = t_a$ . Then,

$$l_i = l_2 + \sum_{n=2}^i \Delta t_{n-1}, \quad 3 \leq i \leq N$$

If  $\Delta t_2 = \Delta t_3 \dots = \Delta t_{N-1} = \Delta t$ , then

$$\Delta t = \frac{\kappa H_a}{(N-1)} \quad \text{and}$$

$$l_i = l_2 + (i-2)\Delta t = r_p + (i-2) \cdot \Delta t \quad 3 \leq i \leq N \quad (\text{A-8.8})$$

A-8.2 Dividing the entry plane into  $(N-2) \times (M-1)$  sectors.  
 Each sector is further sub-divided into a small and a large triangle.

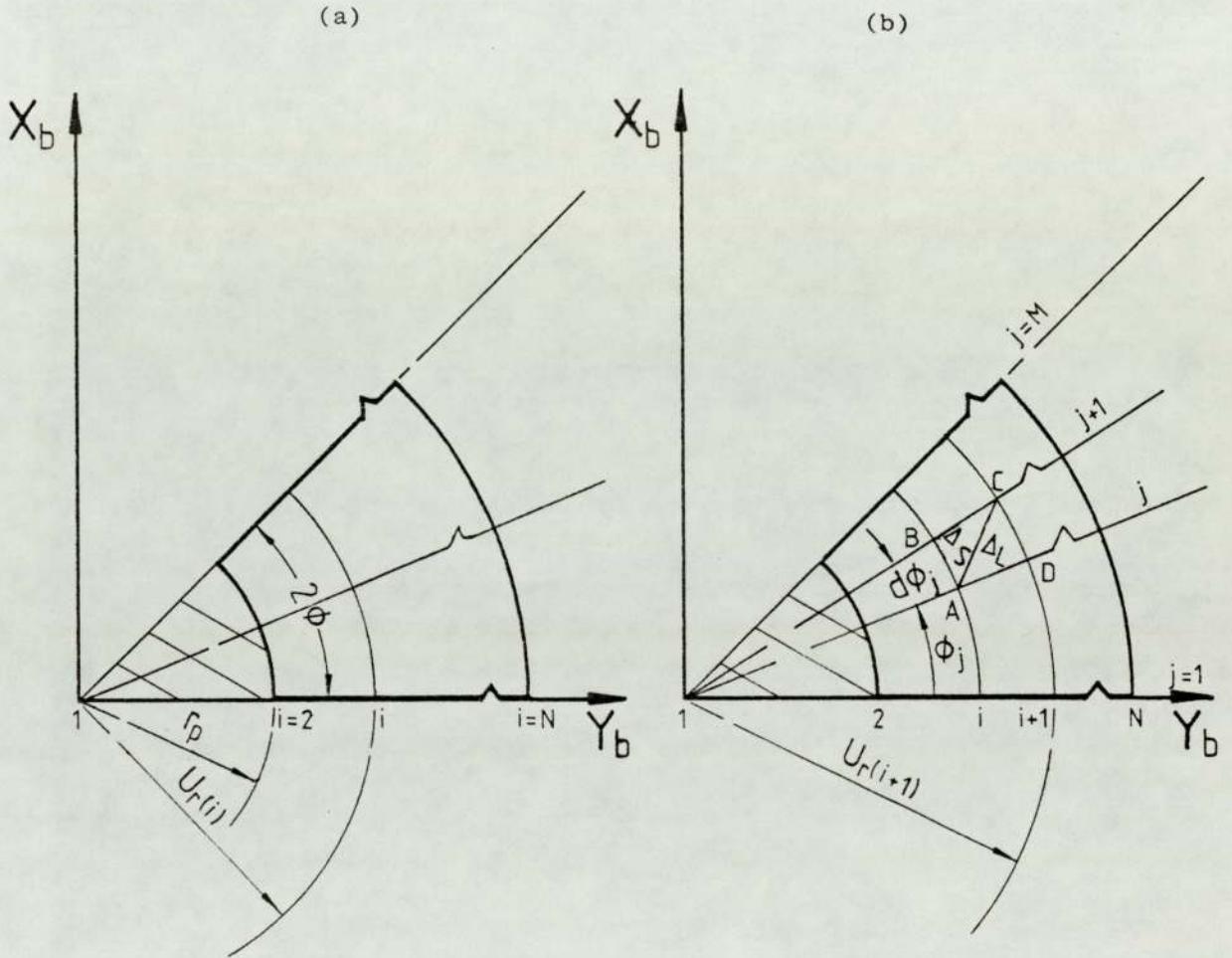


Fig. A-8.2 Section at the entry plane.

Assuming a constant reduction of area, the outer radius  $U_r(i)$  of the cross-sectional area at the entry plane corresponding to the material enclosed by the hyperbola  $i$  and the plug at the exit, can be determined.

$$\text{If } A_r = \frac{\text{Area at entry}}{\text{Area at exit}} = \frac{A_b}{A_a},$$

$$\text{then } \left( \frac{2\phi}{2\pi} \right) \cdot \pi U_r^2(i) = A_T(i) \cdot A_r + \frac{2\phi}{2\pi} \cdot \pi r_p^2$$

$$\text{i.e. } \phi \cdot U_r^2(i) = A_T(i) \cdot A_r + \phi \cdot r_p^2$$

By substituting for  $A_T(i)$  and simplifying,

$$U_r(i) = \text{SQRT} \left\{ \frac{1}{\phi} \left\{ \cot\phi \cdot \left[ v \sqrt{v^2 - a_i^2} - a_i^2 \right. \right. \right. \right. \quad (\text{A-8.9})$$

$$\left. \left. \left. \ln \left\{ \frac{v + \sqrt{v^2 - a_i^2}}{a_i} \right\} \right] + q_i^2 \cdot \tan\phi \right\} A_r + r_p^2 (1 - A_r) \right\}$$

The area banded by the radii  $U_r(i+1)$  and  $U_r(i)$  is divided into  $M-1$  sectors each subtending an angle  $d\phi_j$ , where  $j$  refers to the element between the radial lines  $j$  and  $j+1$ . If the inclination of the radial line  $j$  to the  $Y_b$  axis is  $\phi_j$ , then  $d\phi_j = \phi_{j+1} - \phi_j$ .

$$\text{Also note (i) } \sum d\phi_j = d\phi_1 + d\phi_2 + \dots +$$

$$d\phi_{M-1} = 2\phi, \text{ and}$$

if  $d\phi_1 = d\phi_2, \dots = d\phi_{m-1} = d\phi$ , then

$$d\phi = \frac{2\phi}{M-1} \quad (\text{A-8.10})$$

$$\text{(ii) } \phi_j = \phi_{j-1} + d\phi_{j-1}$$

$$\begin{aligned}
&= d\phi_1 + d\phi_2 + \dots + d\phi_{j-1} \\
&= (j-1) d\phi \\
&= (j-1) \cdot \frac{2\phi}{M-1} \tag{A-8.11}
\end{aligned}$$

The elemental area of each sector, say ABCD in fig. A-8.2(b) is divided into a large triangle ADC and a small triangle ABC. If the angle subtended at the centre is  $d\phi_j = d\alpha$  and the radial increment  $AD = \delta R$ , where  $U_r(i) = R$ , then the area of the large triangle ADC,

$$\begin{aligned}
\Delta_L &= \frac{1}{2} \delta R (R + \delta R) \delta \alpha \\
&= \frac{1}{2} R \cdot \delta R \cdot \delta \alpha + \frac{1}{2} \delta R^2 \cdot \delta \alpha \tag{A-8.12}
\end{aligned}$$

and the small triangle ABC,

$$\Delta_S = \frac{1}{2} R \cdot \delta R \cdot \delta \alpha \tag{A-8.13}$$

From equations (A-8.12) and (A-8.13),

$$\Delta_d = \Delta_L - \Delta_S = \frac{1}{2} \delta R^2 \cdot \delta \alpha \tag{A-8.14}$$

$$\text{and } \Delta_L + \Delta_S = \text{ABCD} \tag{A-8.15}$$

From equations (A-8.14) and (A-8.15),

$$\Delta_L = \frac{1}{2} (\text{ABCD} + \Delta_d) \tag{A-8.16a}$$

$$\Delta_S = \frac{1}{2} (\text{ABCD} - \Delta_d) \tag{A-8.17a}$$

Substituting for area ABCD and  $\Delta_d$ , the general expressions for the areas of the large and small triangles are:

$$\Delta_L = \frac{1}{2} \cdot \frac{\phi}{M-1} \left\{ \left( U_r^2(i+1) - U_r^2(i) \right) + \left( U_r(i+1) - U_r(i) \right)^2 \right\} \tag{A-8.16b}$$

$$\Delta_S = \frac{1}{2} \cdot \frac{\phi}{M-1} \left\{ \left( U_r^2(i+1) - U_r^2(i) \right) - \left( U_r(i+1) - U_r(i) \right)^2 \right\} \tag{A-8.17b}$$

The co-ordinates of A, B, C, D, are readily determined. e.g. at B,

$$X_b(i, j + 1) = U_r(i) \sin \phi_{j + 1} \quad (A-8.18)$$

$$Y_b(i, j + 1) = U_r(i) \cos \phi_{j + 1}$$

With known co-ordinates of A, B, C, D the centroids of the large and the small triangles are calculated. The centroid of the large triangle ACD,

$$X_b CL(i, j) = \left\{ X_b(i, j) + X_b(i + 1, j + 1) + X_b(i + 1, j) \right\} / 3$$

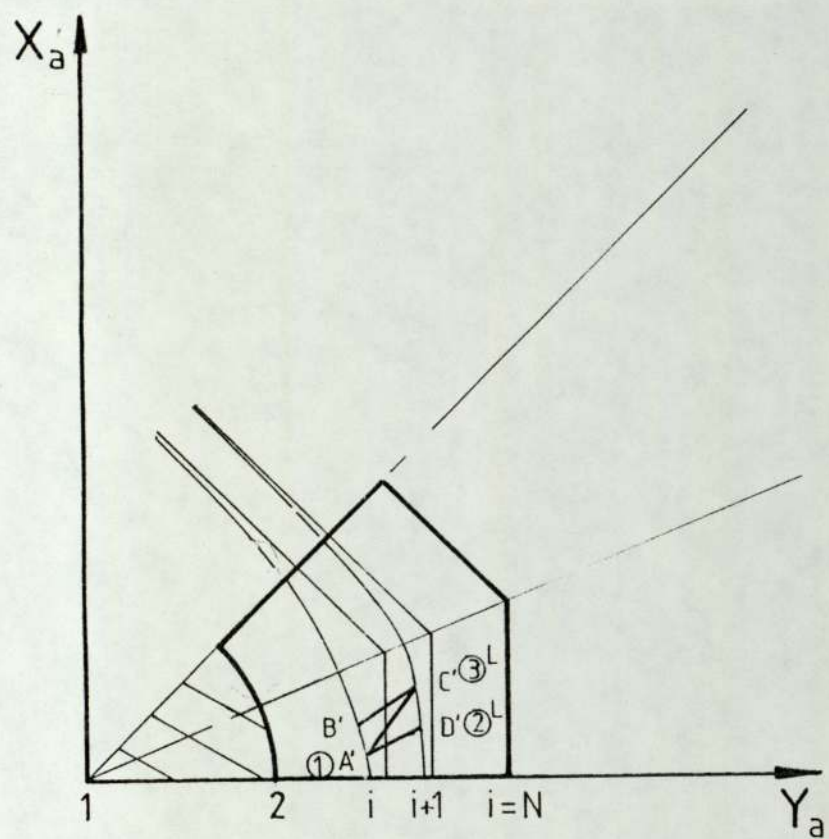
$$Y_b CL(i, j) = \left\{ Y_b(i, j) + Y_b(i + 1, j + 1) + Y_b(i + 1, j) \right\} / 3 \quad (A-8.19)$$

and the centroid of the small triangle ACB,

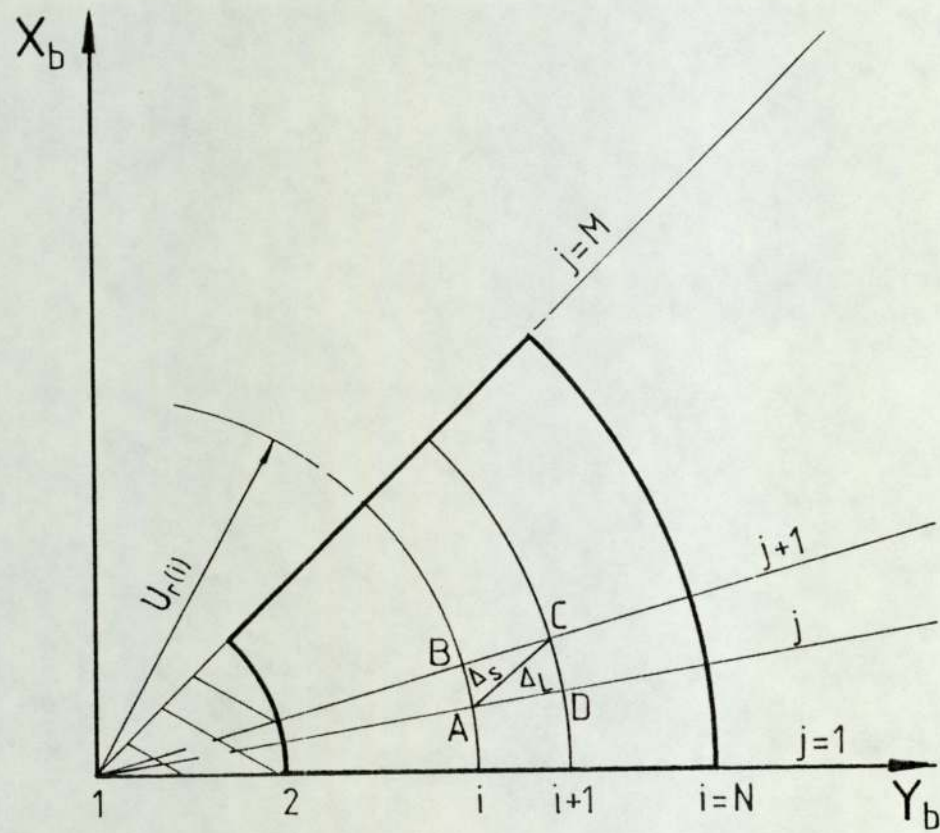
$$X_b CS(i, j) = \left\{ X_b(i, j) + X_b(i + 1, j + 1) + X_b(i, j + 1) \right\} / 3$$

$$Y_b CS(i, j) = \left\{ Y_b(i, j) + Y_b(i + 1, j + 1) + Y_b(i, j + 1) \right\} / 3 \quad (A-8.20)$$

A-8.3 Mapping the exit plane with triangles corresponding to those at entry plane (Fig. A-8.3).



(a) Exit plane



(b) Entry plane

Fig. A-8.3 Conformal mapping of triangular elements on the inlet and exit plane surfaces.

Each triangle at the entry plane is transformed into a corresponding triangle at the exit section, with the constant reduction of area  $A_r$ ,

$$\Delta_L' = \Delta_L / A_r \quad (A-8.21)$$

$$\Delta_S' = \Delta_S / A_r$$

Starting from the  $Y_a$  axis, and with the intersection of  $Y_a$  axis and the hyperbolae  $i$  and  $i + 1$ , the vertices ① and ② (or  $(X_a, Y_a)_{i,j}$  and  $(X_a, Y_a)_{i+1,j}$ , where  $j = 1$ ) of the large triangle are known. The problem now remains to find the third point of the triangle. Since area ( $\Delta_L'$ ) is known and the third point is known to lie on the hyperbola  $i + 1$ , the co-ordinates of the vertex ③ (or  $(X_a, Y_a)_{i+1,j+1}$ ) can be determined. The vertex ③ of the large triangle now becomes the vertex ② of the smaller triangle ( $\Delta_S'$ ) and in a similar manner the third vertex known to lie on the hyperbola  $i$ , can be determined.

The same procedure is repeated until the whole band area ( $i$ ), between hyperbolae  $i + 1$  and  $i$  is mapped with large and small triangles. The next band is similarly mapped to complete the whole exit plane.

Finally the centroids of the mapped triangles are located as in the entry plane.

#### Location of the third vertex of the triangle

Area of the triangle,

$$\Delta' = \frac{1}{2} \left\{ (Y_2 X_1 - Y_1 X_2) + Y_3 (X_2 - X_1) + X_3 (Y_1 - Y_2) \right\} \quad (A-8.22)$$

Two vertices are known and the third lies on the hyperbola, i.e.

$$\frac{(X_3 \sin \xi + Y_3 \cos \xi - 1)^2}{a^2} - \frac{(X_3 \cos \xi - Y_3 \sin \xi)^2}{b^2} = 1 \quad (A-8.23)$$

Equations (A-8.22) and (A-8.23) are solved simultaneously to yield,

$$X_3 = \frac{-(c_2 - d_2) \pm \sqrt{(c_2 - d_2)^2 - 4(c_3 - d_3)(c_1 - d_1 - a^2)}}{2(c_3 - d_3)} \quad (\text{A-8.24})$$

The computer selects the appropriate value and calculates,

$$Y_3 = m_1 - k_1 X_3 \quad (\text{A-8.25})$$

where,

$$m_1 = \frac{2\Delta' - (Y_2 X_1 - Y_1 X_2)}{(X_2 - X_1)}$$

$$k_1 = \frac{Y_1 - Y_2}{X_2 - X_1}$$

$$c_3 = \sin^2 \xi - k_1 \sin 2\xi + k_1^2 \cos^2 \xi$$

$$c_2 = m_1 \sin 2\xi - 2l \sin \xi - 2k_1 m_1 \cos^2 \xi + 2k_1 l \cos \xi$$

$$c_1 = m_1^2 \cos^2 \xi - 2m_1 l \cos \xi + l^2$$

$$d_3 = \tan^2 \phi \left\{ \cos^2 \xi + k_1 \sin 2\xi + k_1^2 \sin^2 \xi \right\}$$

$$d_2 = \tan^2 \phi \left\{ -m_1 \sin 2\xi - 2k_1 m_1 \sin^2 \xi \right\}$$

$$d_1 = \tan^2 \phi \cdot m_1^2 \cdot \sin 2\xi$$

The inner curve is a circle and the third point of the triangle will therefore be calculated from the simultaneous solution of the equations of the circle and the area of a triangle

$$\text{i.e. } (X_3, Y_3) \text{ satisfies } X^2 + Y^2 = r_p^2 \quad (\text{A-8.26})$$

$$X_3 = \frac{m_1 k_1 + \sqrt{(m_1 k_1)^2 - (1 + k_1^2)(m_1^2 - r_p^2)}}{(1 + k_1^2)} \quad (\text{A-8.27})$$

The computer selects the larger positive value and determines

$$Y_3 = m_1 - k_1 X_3 \quad (\text{A-8.28})$$

The centroids of triangles at the exit plane

For the large triangle:

$$\begin{aligned} X_{a\text{CL}}(i, j) &= \left\{ X_a(i, j) + X_a(i + 1, j + 1) + X_a(i + 1, j) \right\} / 3 \\ Y_{a\text{CL}}(i, j) &= \left\{ Y_a(i, j) + Y_a(i + 1, j + 1) + Y_a(i + 1, j) \right\} / 3 \end{aligned} \quad (\text{A-8.29})$$

For the small triangle:

$$\begin{aligned} X_{a\text{CS}}(i, j) &= \left\{ X_a(i, j) + X_a(i + 1, j + 1) + X_a(i, j + 1) \right\} / 3 \\ Y_{a\text{CS}}(i, j) &= \left\{ Y_a(i, j) + Y_a(i + 1, j + 1) + Y_a(i, j + 1) \right\} / 3 \end{aligned} \quad (\text{A-8.30})$$

A-8.4 Shear surfaces defining the plastic deforming zone at the die,  
Fig. A-8.4 and A-8.5

A triangular element at the die entry is assumed to shear at an elemental surface inclined at an angle  $t\theta$  to the die axis. The position of the element is defined on a general spherical surface  $(\rho_b, \theta, \phi)$  with the centre at the virtual apex of the equivalent die cone. The parameter  $t$  is used to optimize the shear surface by minimising the total shear work.

Similarly a general pyramidal shear surface is defined at the exit of the deforming zone and the parameter  $t$  optimizes the geometry of the surface.

Defining the 'entry' plane  $(X_b, Y_b)$  as the plane perpendicular to the die axis through the point where the outermost tube elements (i.e. at  $r = R_b$ ) come into contact with the die, and forming starts; similarly the 'exit' plane is defined as the plane perpendicular to the die axis which passes through the point where the outermost material elements start to flow parallel to the die axis, thus:-

- (i)  $\delta_b(i, j)$  is the horizontal distance an element with its centroid denoted by  $(i, j)$ , travels after shearing at the assumed discontinuity boundary, measured to the 'entry' plane.
- (ii)  $\delta_a(i, j)$  is the horizontal distance the particle travels after shear at the assumed pyramidal discontinuity boundary, measured to the 'exit' plane.

Therefore, the total horizontal distance covered by the particle in the deforming zone becomes:-

$$Z_s(i, j) = DIEH + \delta_b(i, j) - \delta_a(i, j) \quad (A-8.31)$$

A-8.5 Derivation of  $Z_t$ ,  $\eta$  and  $\psi$

If the centroid of a triangular element at entry is  $(X_b, Y_b)'$  (i,j) and the centroid of its corresponding transformed triangular element at the exit is  $(X_a, Y_a)'$  (i,j), then the vector joining the two centroids defines the flow.  $(X_b, Y_b)'$  denotes a plane through the centroid of the triangular element on the assumed shear surface and parallel to the 'entry' plane  $(X_b, Y_b)$ . Plane  $(X_a, Y_a)'$  is similarly defined on the exit shear boundary.

The length of the flow path  $Z_t$  for each element, and the relative angular deflexions  $\eta$  and  $\psi$  as the element flows through the deforming zone are determined from the geometry (see fig. A-8.6). The results are summarised below.

$$\delta_b(i,j) = \rho_b (\cos \theta(i,j) - \cos \alpha_e) \quad (\text{A-8.32})$$

$$\text{where } \theta(i,j) = \sin^{-1} \left\{ \frac{R_b(i,j)}{\rho_b} \right\} \quad (\text{A-8.33})$$

$$\text{and } R_b(i,j) = \sqrt{X_b^2(i,j) + Y_b^2(i,j)}$$

$$\phi_A(i,j) = \tan^{-1} \left\{ \frac{X_a(i,j)}{Y_a(i,j)} \right\} \quad (\text{A-8.34})$$

$$\phi_B(i,j) = \tan^{-1} \left\{ \frac{X_b(i,j)}{Y_b(i,j)} \right\}$$

$$\delta_a(i,j) = \delta_a \left\{ \frac{H_a}{2R_a(i,j) \cos \phi_A(i,j)} - 1 \right\} \quad (\text{A-8.35})$$

$$\text{where } \phi_A(i,j) = \begin{cases} \tan^{-1} \left\{ \frac{X_a(i,j)}{Y_a(i,j)} \right\}, & \text{for } \phi_A \leq \beta \\ 2\beta - \tan^{-1} \left\{ \frac{X_a(i,j)}{Y_a(i,j)} \right\}, & \text{for } \phi_A > \beta \end{cases} \quad (\text{A-8.36})$$

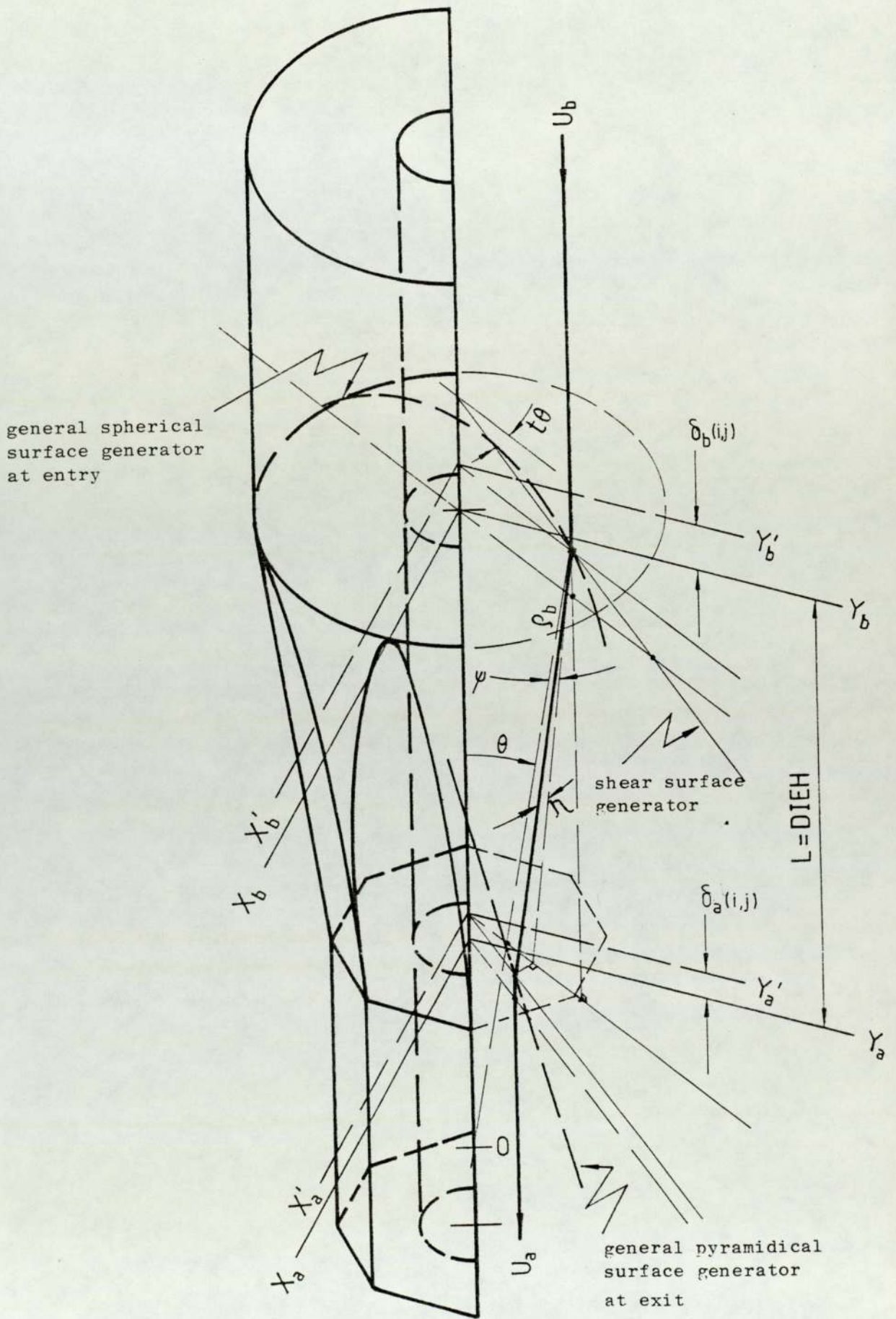


Fig. A-8.4 Plastic deformation zone in the drawing of polygonal tube from round stock on a cylindrical plug.

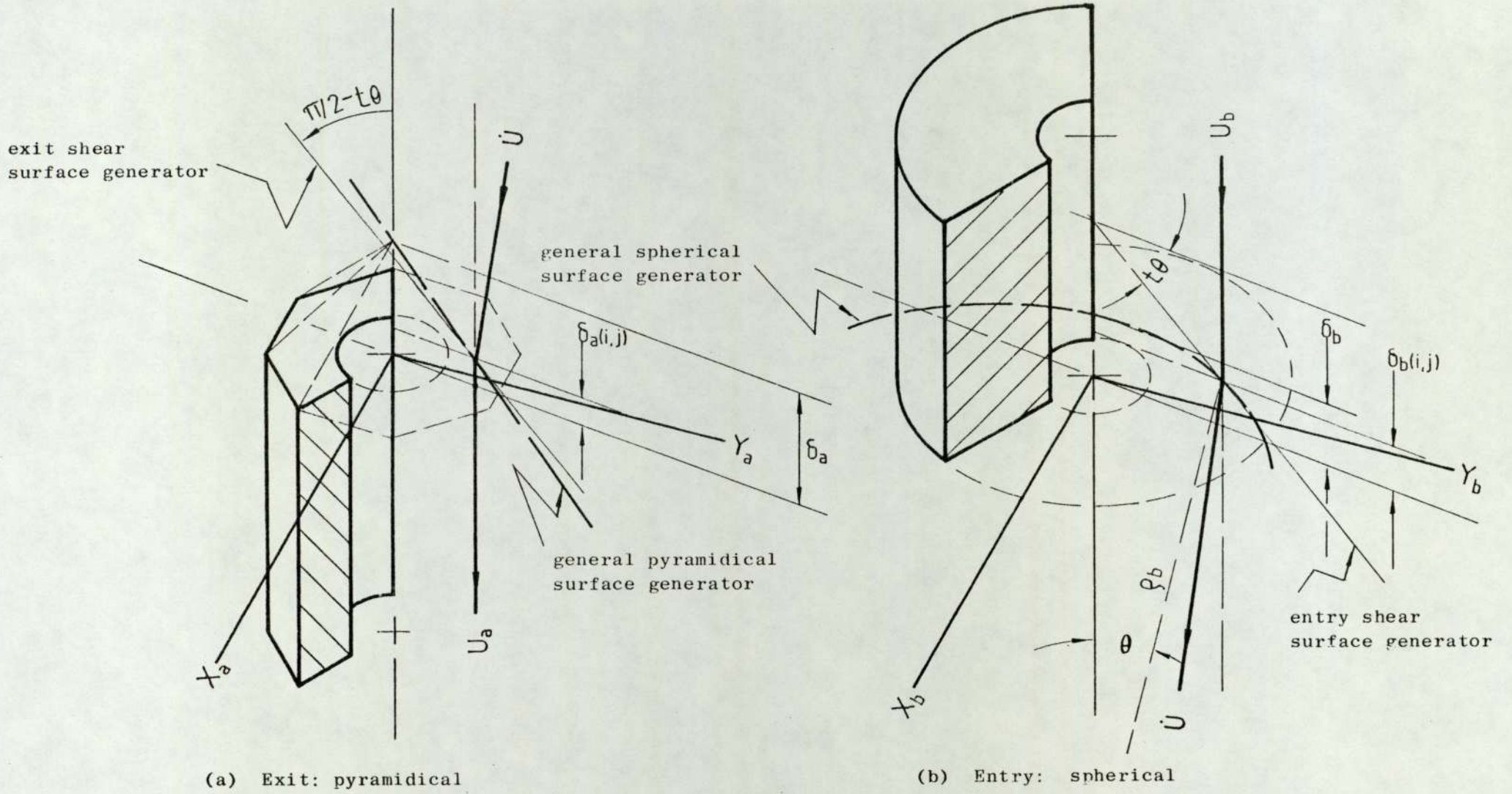


Fig. A-8.5 General position of shear surfaces at the exit and entry to the deformation zone.

- A92 -



$$\text{and } R_a(i, j) = \sqrt{X_a^2(i, j) + Y_a^2(i, j)} \quad (\text{A-8.37})$$

$$Z_t(i, j) = \left[ \left\{ X_b(i, j) - X_a(i, j) \right\}^2 + \left\{ Y_b(i, j) - Y_a(i, j) \right\}^2 + Z_s^2(i, j) \right]^{\frac{1}{2}} \quad (\text{A-8.38})$$

$$\eta(i, j) = \tan^{-1} \left\{ \frac{R_a(i, j) \sin \phi_{B/A}(i, j)}{Z_p(i, j)} \right\} \quad (\text{A-8.39})$$

$$\text{where } \phi_{B/A}(i, j) = \tan^{-1} \left\{ \frac{X_b(i, j)}{Y_b(i, j)} \right\} - \tan^{-1} \left\{ \frac{X_a(i, j)}{Y_a(i, j)} \right\} \quad (\text{A-8.40})$$

$$\text{and } Z_p(i, j) = \left[ \left\{ R_b(i, j) - R_a(i, j) \cos \phi_{B/A}(i, j) \right\}^2 + Z_s^2(i, j) \right]^{\frac{1}{2}} \quad (\text{A-8.41})$$

$$\psi(i, j) = \left| \theta_{(i, j)} - \theta_{(i, j)} \right| \quad (\text{A-8.42})$$

$$\text{where } \theta_{(i, j)} = \tan^{-1} \left\{ \frac{R_b(i, j) - R_a(i, j) \cos \phi_{B/A}(i, j)}{Z_s(i, j)} \right\} \quad (\text{A-8.43})$$

#### A-8.6 Velocity discontinuities, $\dot{U}_{ra}$ and $\dot{U}_{rb}$

The resultant velocity of the tangential components on both sides of shear surface gives the velocity discontinuity.

From Fig. A-8.7 and A-8.8, the entry shear surface yields,

$$\dot{U}_{rb} = \left[ \dot{U}_\phi^2 + \left\{ -U_b \sin t\theta + \dot{U}_\theta \cos(1-t)\theta + \dot{U}_\rho \sin(1-t)\theta \right\}^2 \right]^{\frac{1}{2}} \quad (\text{A-8.44})$$

Substituting for the values of velocity components derived in equations (3.6), the above equation reduces to,

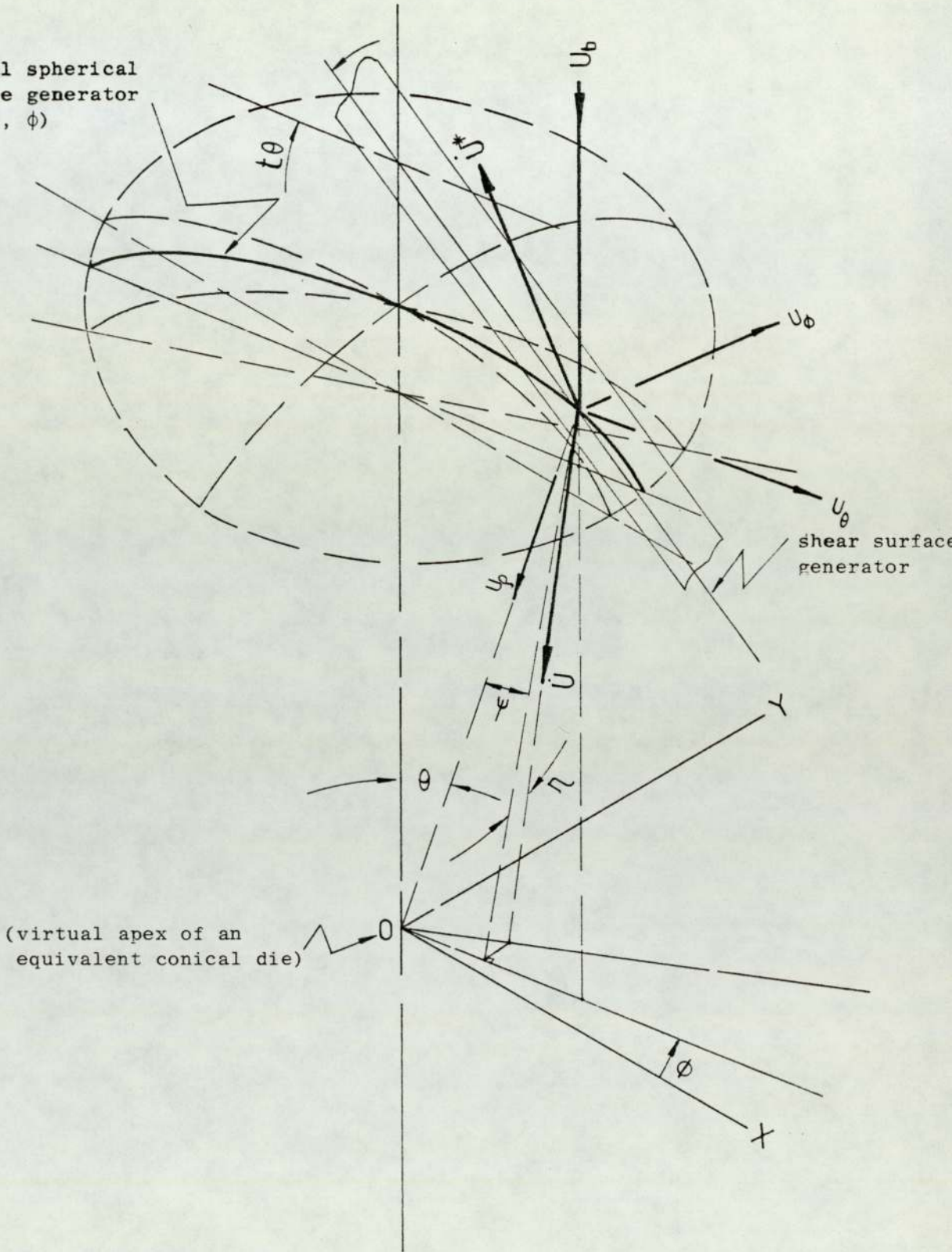
$$\dot{U}_{rb} = U_b \left[ \left\{ \frac{\cos t\theta}{\cos(1-t)\theta} \cdot \frac{\tan \eta}{\cos \psi} \right\}^2 + \left\{ -\sin t\theta + \cos t\theta \tan \psi + \cos t\theta \tan(1-t)\theta \right\}^2 \right]^{\frac{1}{2}} \quad (\text{A-8.45})$$

A similar situation occurs at the exit shear surface boundary when the velocity of the particle just before shear is  $(\dot{U}_\rho, \dot{U}_\theta, \dot{U}_\phi)$ , but after shear the particle travels parallel to the tube axis with a velocity  $U_a$ . From the assumption of an equivalent divergent deformation passage,

$$\dot{U}_{ra} = \dot{U}_{rb} \cdot \left( \frac{\rho_b'}{\rho_a'} \right)^2 \quad (\text{A-8.46})$$

where  $\rho_b'^2$  and  $\rho_a'^2$  are given by equations (3.5).

general spherical  
surface generator  
( $\rho_b, \theta, \phi$ )

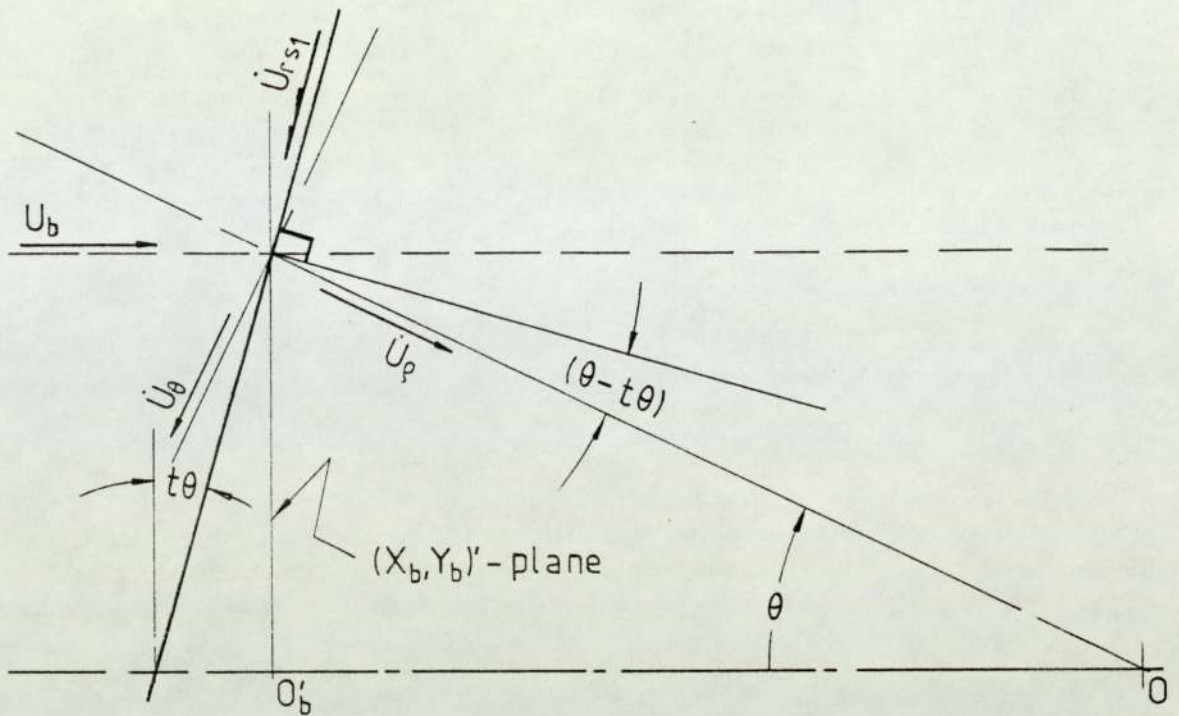


(virtual apex of an  
equivalent conical die)

$$(\dot{U}_\rho = U_\rho, \dot{U}_\theta = U_\theta, \dot{U}_\phi = U_\phi ;$$

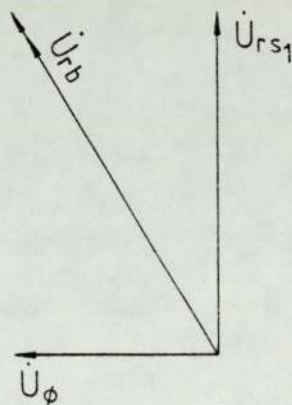
$$\dot{U}^2 = \dot{U}_\rho^2 + \dot{U}_\theta^2 + \dot{U}_\phi^2)$$

Fig. A-8.7 Velocity discontinuity  $\dot{U}^*$  at the entry shear surface in the drawing of polygonal tube from round stock on a cylindrical plug.



$$\dot{U}_{rs1} = -U_b \sin t\theta + \dot{U}_\theta \cos(\theta - t\theta) + \dot{U}_\rho \sin(\theta - t\theta)$$

- (a) Resultant velocity component ( $\dot{U}_{rs1}$ ) tangential to the shear surface and the  $\rho - \theta$  plane



( $\dot{U}_\phi$  = component of velocity normal to  $\rho - \theta$  plane)

- (b) The resultant velocity tangential to the shear surface (or the velocity discontinuity suffered by an element entering the deformation zone)

$$\begin{aligned} \dot{U}_{rb} &= \left\{ \dot{U}_\phi^2 + U_{rs1}^2 \right\}^{\frac{1}{2}} \\ &= \left\{ \dot{U}_\phi^2 + \left[ -U_b \sin t\theta + \dot{U}_\theta \cos(\theta - t\theta) + \dot{U}_\rho \sin(\theta - t\theta) \right]^2 \right\}^{\frac{1}{2}} \end{aligned}$$

Fig. A-8.8 The derivation of the velocity discontinuity of an element at the entry shear surface.

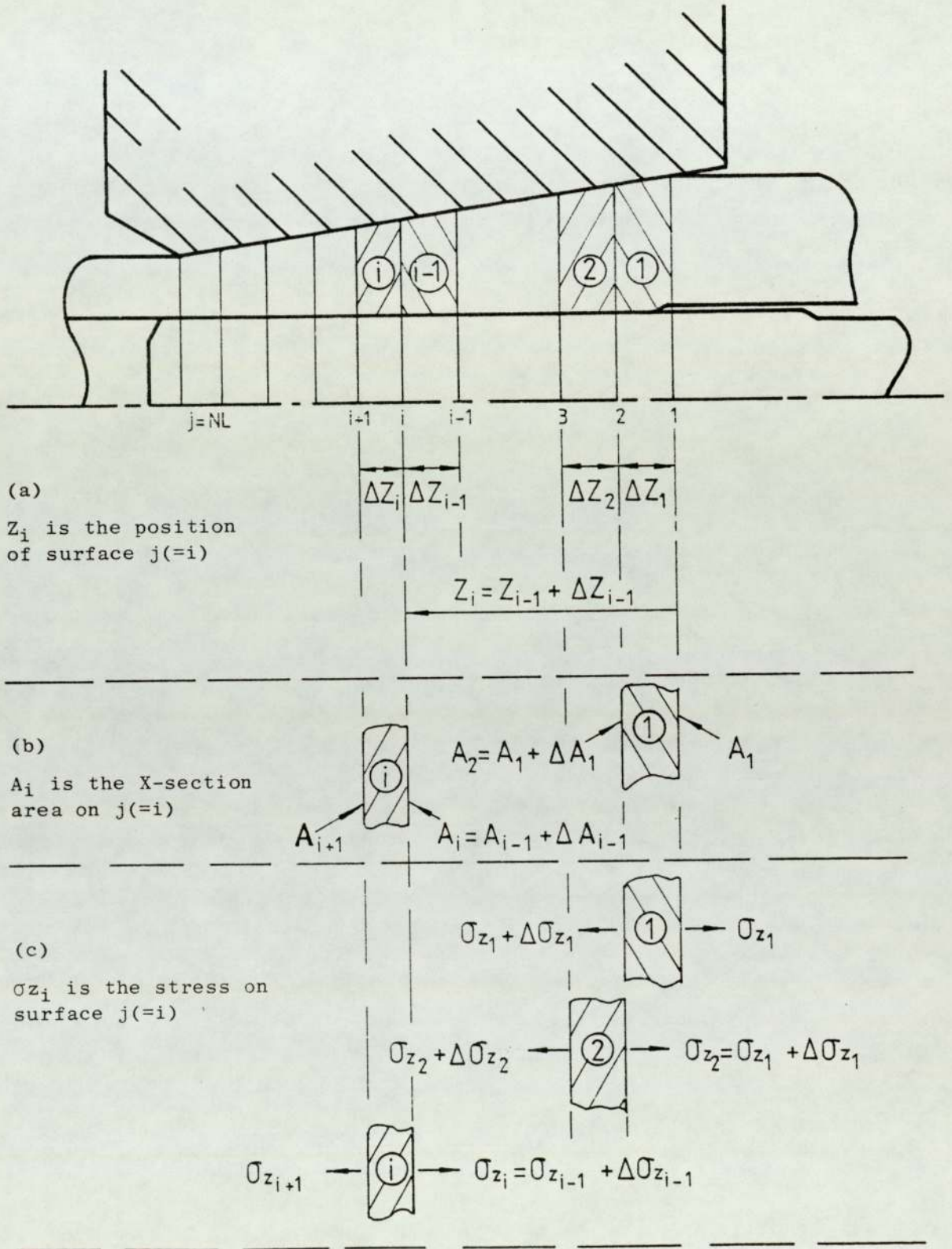


Fig. A-9.1 Round tube drawn through an elliptical polygonal die on a cylindrical plug divided into elements for the lower bound solution.

### A-9.1 Geometrical derivations

The die length (L) is divided into (NL-1) elemental lengths such that,

$$\sum_{i=1}^{NL-1} \Delta Z_i = L \quad (A-9.1)$$

Using the geometrical relationship shown in Chapter 3.3.2 and Fig. 3.6, and starting from the inlet plane, where  $Z_{i=1} = 0$ , the following calculations are performed:-

- (a) At any section  $Z_i$ , calculate  $R(i)$ ,  $\lambda_s(i)$ ,  $\lambda_c(i)$ ,  $A(i)$ . The following relationship is developed in Fig. A-9.1:-

$$A_i = A_1 + \sum_{j=2}^i \Delta A_{j-1} \quad (A-9.2)$$

$$Z_i = Z_1 + \sum_{j=2}^i \Delta Z_{j-1} \quad (A-9.3)$$

- (b) For the tube element  $i$ , between the surfaces  $i$  and  $i + 1$ , the die/tube surface areas  $\Delta A_{s1}$  and  $\Delta A_{c1}$ , and the plug/tube surface area  $\Delta A_{s2}$  are calculated. The change of the cross-sectional area of the tube over the element  $i$ ,  $\Delta A(i)$  is determined.

A-9.2 Development of recursive equations to calculate the draw stress and the mean pressure.

Starting from the inlet plane, surface  $i = 1$ , since there is no backpull  $\sigma_{Z_1} = 0$ , the stress on the surface  $i = 2$  can be determined from the equilibrium equation (3.82). The calculated value of  $\sigma_{Z_2}$  is used to obtain  $\sigma_{Z_3}$ , etc. The general equation to determine the

stress on surface i is given by,

$$\sigma_{z_i} = \sigma_{z_1} + \sum_{j=2}^i \Delta\sigma_{z_{j-1}} \quad (\text{A-9.4})$$

The stress equation (3.82) established from the equilibrium of the element i in the horizontal direction and the use of Tresca's yield criterion, can be conveniently re-written as,

$$\Delta \left( \frac{\sigma_{z_i}}{Y} \right) = \frac{1}{(A_i + \Delta A_i)} \left\{ - \left( \frac{\sigma_{z_i}}{Y} \right) \cdot \Delta A_i + \left[ 1 - \left( \frac{\sigma_{z_i}}{Y} \right) \right] \left[ K_{s_1} \cdot \Delta A_{s_1}(i) + K_{c_1} \cdot \Delta A_{c_1}(i) + K_{s_2} \cdot \Delta A_{s_2}(i) \right] \right\} \quad (\text{A-9.5})$$

where,

$$K_{s_1} = (\sin\alpha_s + \mu\cos\alpha_s) = \text{constant 1}$$

$$K_{c_1} = (\sin\alpha_c + \mu\cos\alpha_c) = \text{constant 2} \quad (\text{A-9.6})$$

$$K_{s_2} = \mu = \text{constant 3}$$

Example:

Starting from  $Z_{i=1} = 0$  and the known conditions of stress the change of stress over element  $i = 1$ , can be determined. Say  $\left( \frac{\sigma_{z_1}}{Y} \right) = 0$ , for element  $i = 1$ ,

$$\Delta \left( \frac{\sigma_{z_1}}{Y} \right) = \frac{1}{(A_1 + \Delta A_1)} \left\{ - (0) \cdot \Delta A_1 + \left[ 1 - (0) \right] \left[ K_{s_1} \cdot \Delta A_{s_1}(1) + K_{c_1} \cdot \Delta A_{c_1}(1) + K_{s_2} \cdot \Delta A_{s_2}(1) \right] \right\}$$

for element  $i = 2$ ,

$$\left( \frac{\sigma_{z_2}}{Y} \right) = \left( \frac{\sigma_{z_1}}{Y} \right) + \Delta \left( \frac{\sigma_{z_1}}{Y} \right) = \Delta \left( \frac{\sigma_{z_1}}{Y} \right)$$

$$\therefore \Delta \left( \frac{\sigma_{z_2}}{Y} \right) = \frac{1}{(A_2 + \Delta A_2)} \left\{ - \left( \frac{\sigma_{z_2}}{Y} \right) \cdot \Delta A_2 + \left[ 1 - \left( \frac{\sigma_{z_2}}{Y} \right) \right] \right.$$

$$\left. \left[ K_{s_1} \cdot \Delta A_{s_1}(2) + K_{c_1} \cdot \Delta A_{c_1}(2) + K_{s_2} \cdot \Delta A_{s_2}(2) \right] \right\}$$

..... etc.

The mean pressure at the die/tube interface can be calculated from the total normal force for elements  $i = 1, 2, \dots, NL$  divided by the total die/tube surface area.

The normal force at the die/tube interface of the element  $i$ ,

$$\begin{aligned} NF_1(i) &= p_i \cdot \left( \Delta A_{s_1}(i) + \Delta A_{c_1}(i) \right) \\ &= p_i \cdot \Delta A_{sT}(i) \end{aligned}$$

$$\text{or } \frac{NF_1(i)}{Y} = \left\{ 1 - \left( \frac{\sigma_{z_i}}{Y} \right) \right\} \cdot \Delta A_{sT}(i) \quad (\text{A-9.7})$$

\(\therefore\) the total normal force for elements  $i = 1, \dots, NL$ ,

$$\begin{aligned} \frac{NF_1}{Y} &= \sum_{i=1}^{NL-1} \frac{NF_1(i)}{Y} \\ &= \sum_{i=1}^{NL-1} \left\{ 1 - \left( \frac{\sigma_{z_i}}{Y} \right) \right\} \cdot \Delta A_{sT}(i) \end{aligned} \quad (\text{A-9.8})$$

The dimensionless mean pressure becomes,

$$\left( \frac{p_m}{Y} \right) = \frac{(NF_1/Y)}{\sum \Delta A_{sT}(i)}$$

$$\begin{aligned}
&= \frac{\sum \left\{ 1 - \left( \frac{\sigma_{z_i}}{Y} \right) \right\} \cdot \Delta A_{sT}(i)}{\sum \Delta A_{sT}(i)} \\
&= 1 - \frac{\sum \left( \frac{\sigma_{z_i}}{Y} \right) \cdot \Delta A_{sT}(i)}{\sum \Delta A_{sT}(i)} \qquad (A-9.9)
\end{aligned}$$

A-10 PARAMETERS FOR THE DESIGN OF DIES FOR THE DRAWING OF  
POLYGONAL TUBE FROM ROUND ON A CYLINDRICAL PLUG

A-10.1 Equivalent die semi-angle

In the drawing of polygonal tube from round stock on a cylindrical plug, a circular section on entry transforms to a polygonal section at the exit in a single pass; the die passage comprises the conical and the plane surfaces of different inclinations to the tube axis to allow for gradual transformation. The conventional term of the die semi-angle is therefore, inapplicable; the die angle changes from a minimum at the diagonals to a maximum at the mid section of the die. An equivalent die semi-angle ' $\alpha_e$ ' is, therefore, defined to facilitate the comparison between the dies drawing tubes with the same number of sides and with different numbers of sides.

The equivalent die semi-angle ' $\alpha_e$ ' is the semi-cone angle of the axisymmetric tube drawing die which produces the same reduction of area as the polygonal tube drawing die, for the same die length. See Fig. A-10.1.

From the equivalent axisymmetric drawing, Fig. A-10.1 (b), the die length is given by,

$$L = \frac{D_b - D_e}{\tan \alpha_e} \quad (\text{A-10.1})$$

Therefore, the inclinations of the conical and plane surfaces of the polygonal tube drawing die become:-

$$\alpha_c = \tan^{-1} \left\{ \frac{D_b - H_a}{2L} \right\} \quad (\text{A-10.2})$$

$$\alpha_s = \tan^{-1} \left\{ \frac{D_b - H_a \cos \beta}{2L} \right\} \quad (\text{A-10.3})$$

(a) Square tube drawing die

(b) axisymmetric tube drawing die

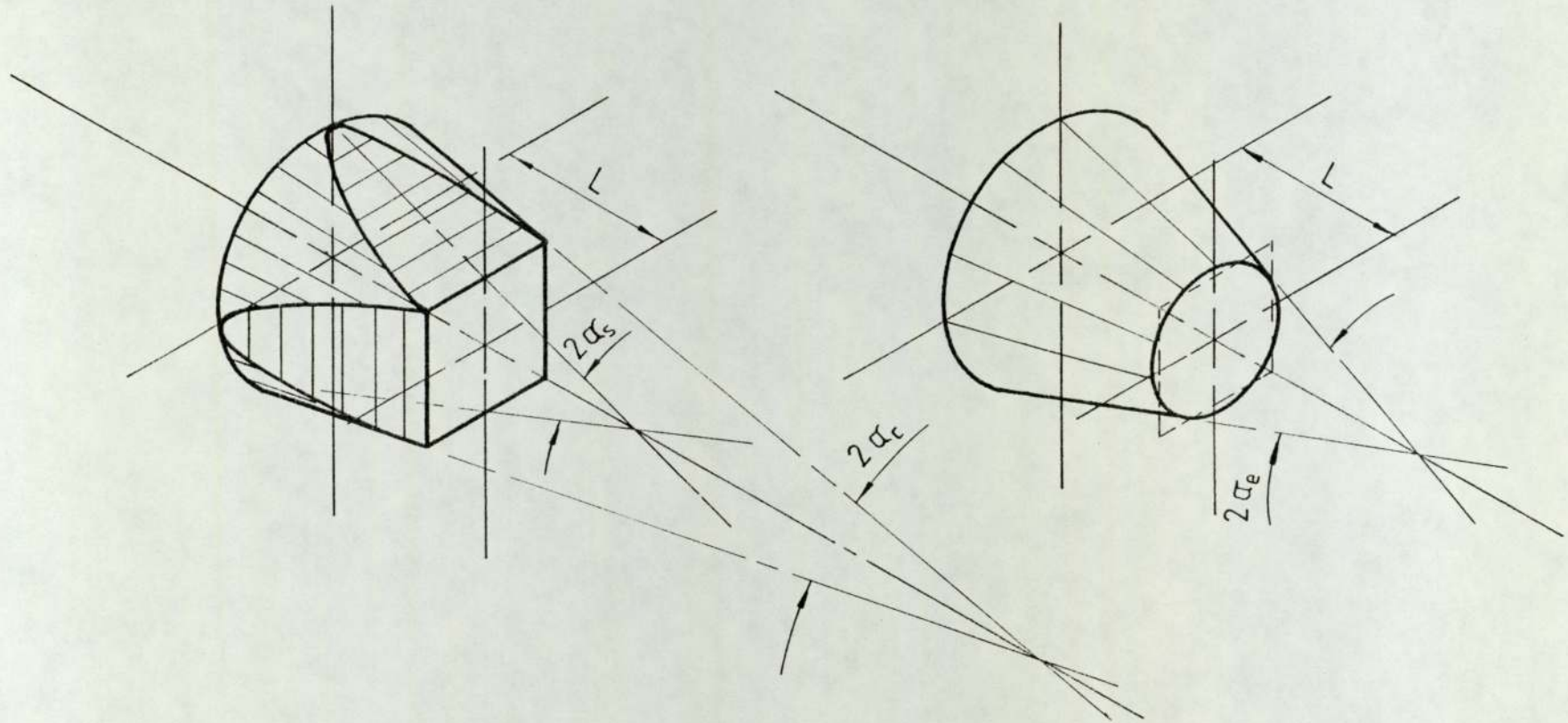


Fig. A-10.1 Isometric drawing of the square and the corresponding axisymmetric tube drawing dies.

For the pyramidal and triangular plane surface die shapes, if the diameter of the input stock is different from that used in the design, the deformation pattern does not change; however, the equivalent die semi-angle changes. If the outside diameter of the new stock is  $D_b'$ , then the effective length,

$$L_e = \frac{D_b' - H_a \cos\beta}{2 \tan\alpha_s} \quad (\text{A-10.4})$$

and the equivalent die semi-angle becomes:-

$$\alpha_e' = \tan^{-1} \left\{ \frac{D_b' - D_e}{2L_e} \right\} \quad (\text{A-10.5})$$

#### A-10.2 Design data

Tables A-10.1 and A-10.2 show die design parameters for the input stock of outside diameter of 1 in and 1 1/16 in and 1 1/8 in and 1 3/16 in respectively, for different die semi-angles. The optimum equivalent die semi-angle of  $8^\circ$  was used in the design of dies for drawing of polygonal tube from round on a cylindrical plug.

A-10.2.1 Details of dies manufactured for the drawing of polygonal tube from round (mechanical drawings are given on pages A109, A110 and A111)

##### (1) Square die

Reference: 4WB

Exit section diagonal length  $H_a = 1.000$  in

Inlet stock o.d.  $D_b = 1$  in

Die length  $L = 0.7191$  in

Conical angle  $\alpha_c = 0^\circ$

Angle of inclination of the plane surface to the die axis

$$\alpha_s = 11^\circ 31'$$

Equivalent die semi-angle  $\alpha_e = 8^\circ$

However, this die was manufactured with the exit diagonal length  $H_a = 1$  in, but a conical angle  $\alpha_c = 1^\circ 54'$  in order to draw tubes with o.d. of  $1 \frac{1}{16}$  in and an equivalent angle of  $7^\circ 54'$ .

(2) Hexagonal die

Reference: 6WB

Exit diagonal length  $H_a = 1.000$  in

Inlet stock o.d.  $D_b = 1 \frac{1}{8}$  in

Die length  $L = 0.767$  in

Conical angle  $\alpha_c = 4^\circ 40'$

Angle of inclination of the plane surface to the die axis

$$\alpha_s = 9^\circ 36'$$

Equivalent die semi-angle

$$\alpha_e = 8^\circ$$

(3) Octagonal die

Reference: 8WB

Exit diagonal length  $H_a = 1.000$  in

Inlet stock o.d.  $D_b = 1 \frac{1}{8}$  in

Die length  $L = 0.627$  in

Conical angle  $\alpha_c = 5^\circ 42'$

Angle of inclination of the plane surface to the die axis

$$\alpha_s = 9^\circ 07'$$

Equivalent die semi angle

$$\alpha_e = 8^\circ$$

TABLE No. A-10.1

Parameters for the design of dies for drawing polygonal tube from round

		Nominal tube o.d. = 1.0000 in EQUIVALENT DIE SEMI-ANGLE $\alpha_e$ (degrees)							Nominal tube o.d. = 1.0625 in EQUIVALENT DIE SEMI-ANGLE $\alpha_e$ (degrees)						
		4	5	6	7*	8	9	10	4	5	6	7*	8	9	10
SQUARE TUBE	$L$	1.445	1.155	0.961	0.823	0.719	0.638	0.573	1.892	1.512	1.259	1.077	0.941	0.835	0.750
	$\alpha_c$	0.00	0.00	0.00	0.00	0.00	0.00	0.00	0.946	1.184	1.422	1.661	1.901	2.142	2.385
	$\alpha_B$	5.786	7.225	8.660	10.089	11.511	12.927	14.334	5.365	6.702	8.035	9.364	10.689	12.003	13.323
	$L_e$				0.823	0.719						0.999	0.872		
	$\alpha_{e'}$				7.000	8.000						7.550	8.623		
HEXAGONAL TUBE	$L$	0.648	0.518	0.431	0.369	0.322	0.286	0.256	1.095	0.875	0.728	0.623	0.545	0.483	0.434
	$\alpha_c$	0.00	0.00	0.00	0.00	0.00	0.00	0.00	1.635	2.045	2.457	2.869	3.283	3.699	4.117
	$\alpha_B$	5.903	7.371	8.833	10.290	11.739	13.180	14.613	5.127	6.406	7.681	8.954	10.223	11.489	12.750
	$L_e$				0.454	0.397						0.666	0.582		
	$\alpha_{e'}$				5.700	6.514						6.560	7.495		
OCTAGONAL TUBE	$L$	0.366	0.292	0.243	0.208	0.182	0.161	0.145	0.813	0.649	0.540	0.463	0.404	0.359	0.322
	$\alpha_c$	0.00	0.00	0.00	0.00	0.00	0.00	0.00	2.202	2.754	3.308	3.863	4.419	4.978	5.538
	$\alpha_B$	5.941	7.418	8.890	10.355	11.813	13.263	14.703	4.875	6.091	7.305	8.517	9.727	10.934	12.138
	$L_e$				0.281	0.237						0.511	0.432		
	$\alpha_{e'}$				5.210	6.154						6.350	7.494		
DECAGONAL TUBE	$L$	0.234	0.187	0.156	0.133	0.117	0.103	0.093	0.681	0.545	0.453	0.388	0.339	0.301	0.270
	$\alpha_c$	0.00	0.00	0.00	0.00	0.00	0.00	0.00	2.626	3.284	3.943	4.604	5.266	5.931	6.597
	$\alpha_B$	5.958	7.439	8.915	10.384	11.846	13.300	14.744	4.675	5.42	7.007	8.171	9.334	10.494	11.652
	$L_e$				0.186	0.158						0.423	0.360		
	$\alpha_{e'}$				5.050	5.926						6.430	7.546		
CIRCULAR TUBE	$L$	-	-	-	-	-	-	-		0.357	0.297	0.254	0.222	0.197	0.177
	$\alpha_c$	-	-	-	-	-	-	-	4	5	6	7	8	9	10

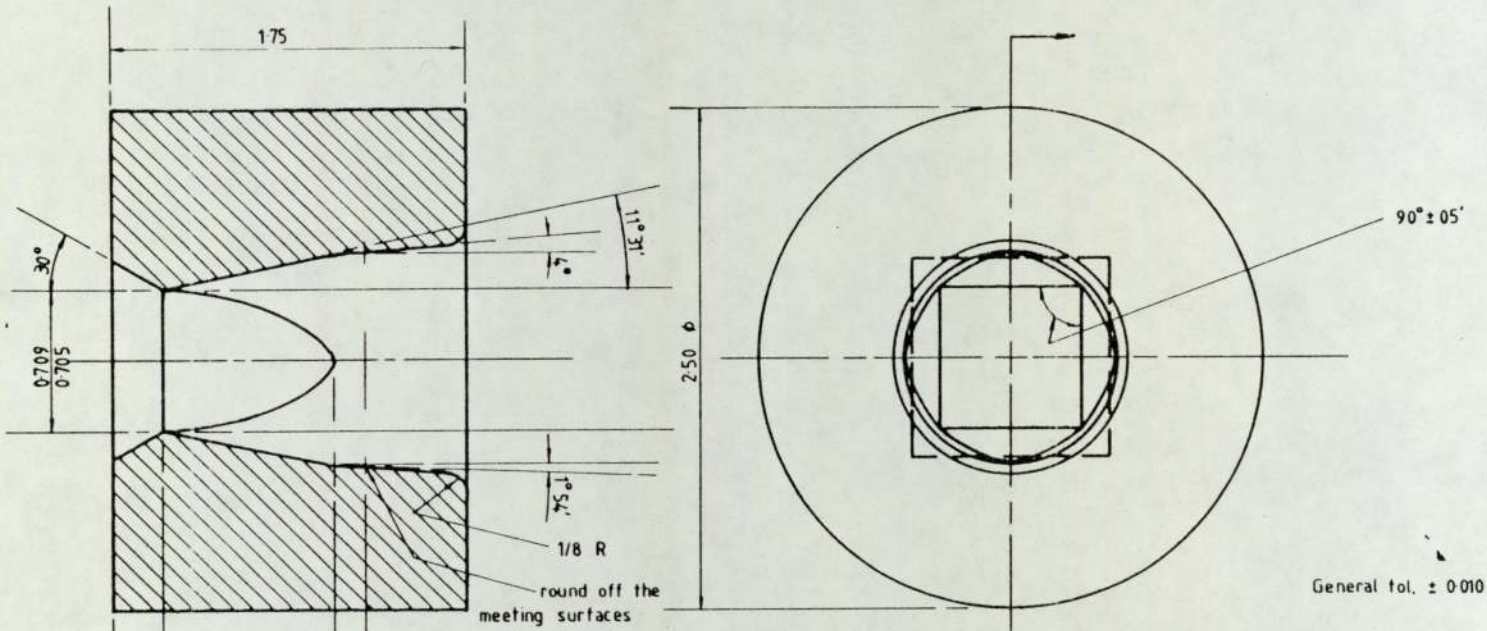
\* optimal equivalent die semi-angle for the section bar drawing dies

TABLE No. A-10.2

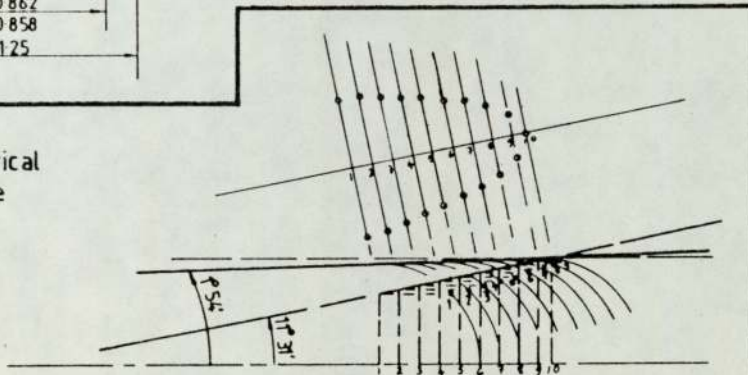
Parameters for the design of dies for drawing polygonal tube from round

		Nominal tube o.d. = 1.125 in							Nominal tube o.d. = 1.1875 in						
		EQUIVALENT DIE SEMI-ANGLE $\alpha_e$ (degrees)							EQUIVALENT DIE SEMI-ANGLE $\alpha_e$ (degrees)						
		4	5	6	7*	8	9	10	4	5	6	7*	8	9	10
SQUARE TUBE	L	2.339	1.869	1.556	1.332	1.164	1.033	0.927	2.786	2.227	1.853	1.586	1.386	1.230	1.105
	$\alpha_c$	1.543	1.915	2.300	2.686	3.074	3.463	3.855	1.927	2.411	2.896	3.382	3.869	4.358	4.850
	$\alpha_s$	5.105	6.377	7.647	8.915	10.178	11.437	12.694	4.928	6.157	7.384	8.609	9.831	11.050	12.266
	$L_e$				1.174	1.026									
	$\alpha_{e'}$				7.930	9.058									
HEXAGONAL TUBE	L	1.542	1.232	1.026	0.878	0.767	0.680	0.611	1.989	1.589	1.323	1.132	0.989	0.878	0.789
	$\alpha_c$	2.321	2.904	3.487	4.071	4.658	5.246	5.837	2.699	3.375	4.053	4.737	5.412	6.095	6.772
	$\alpha_s$	4.801	5.999	7.195	8.389	9.582	10.771	11.958	4.621	5.774	6.927	8.078	9.227	10.374	11.520
	$L_e$				0.878	0.767									
	$\alpha_{e'}$				7.000	8.000									
OCTAGONAL TUBE	L	1.259	1.007	0.838	0.717	0.627	0.556	0.499	1.706	1.364	1.135	0.972	0.849	0.753	0.677
	$\alpha_c$	2.841	3.552	4.265	4.980	5.695	6.413	7.132	3.145	3.932	4.721	5.510	6.301	7.093	7.887
	$\alpha_s$	4.565	5.704	6.843	7.980	9.116	10.250	11.383	4.417	5.520	6.622	7.724	8.824	9.924	11.022
	$L_e$				0.741	0.627						0.972			
	$\alpha_{e'}$				6.770	8.000						7.000			
DECAGONAL TUBE	L	1.128	0.902	0.751	0.642	0.561	0.498	0.447	1.575	1.259	1.048	0.897	0.784	0.695	0.625
	$\alpha_c$	3.171	3.964	4.759	5.555	6.353	7.151	7.952	3.407	4.259	5.112	5.966	6.821	7.678	8.535
	$\alpha_s$	4.408	5.509	6.609	7.708	8.806	9.904	11.000	4.292	5.364	6.436	7.507	8.578	9.648	10.717
	$L_e$				0.659	0.562						0.897			
	$\alpha_{e'}$				6.820	8.000						7.00			
CIRCULAR TUBE	L	0.894	0.714	0.595	0.509	0.445	0.395	0.354	1.341	1.071	0.892	0.763	0.667	0.592	0.532
	$\alpha_c$	4	5	6	7	8	9	10	4	5	6	7.000	8	9	10

\* optimal equivalent die semi-angle for the section bar drawing dies



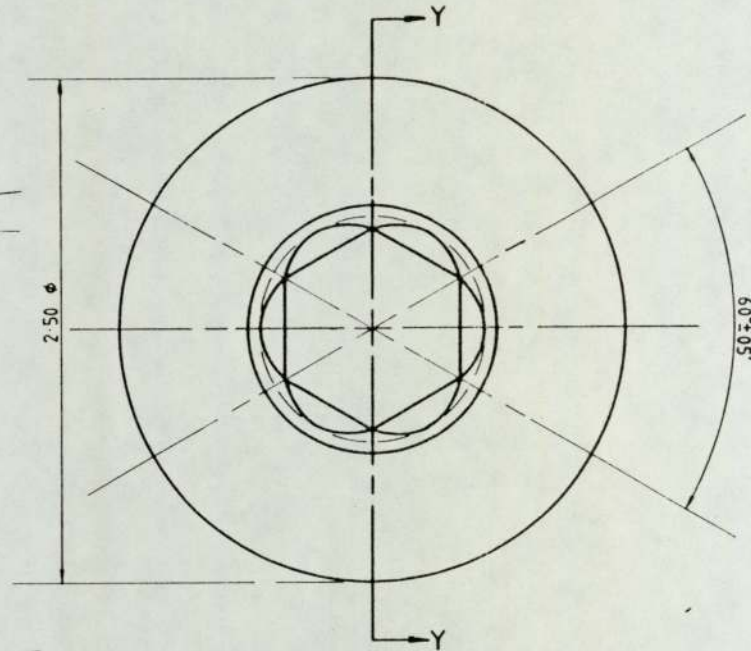
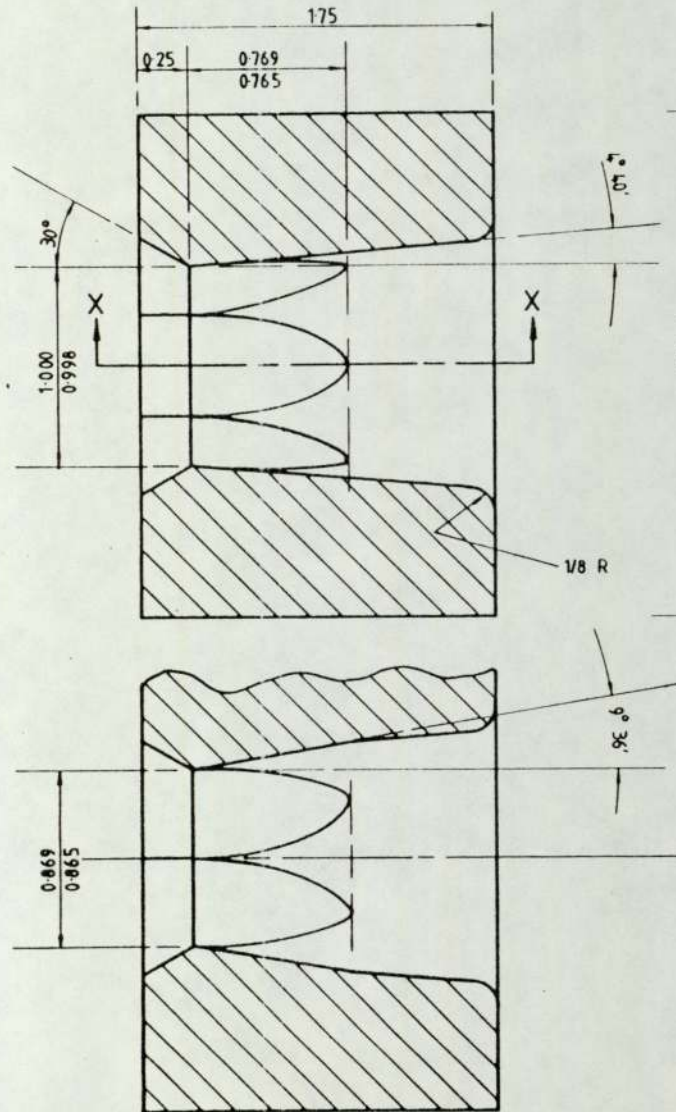
Developing an elliptical surface from a cone



NOTES

- [1] Elliptical surface is obtained when a cone of semi-angle  $1^{\circ} 54'$  is cut by a plane inclined at  $11^{\circ} 31'$  to the cone axis.
- [2] Die surface heat treated to 64 RC, ground and lapped.

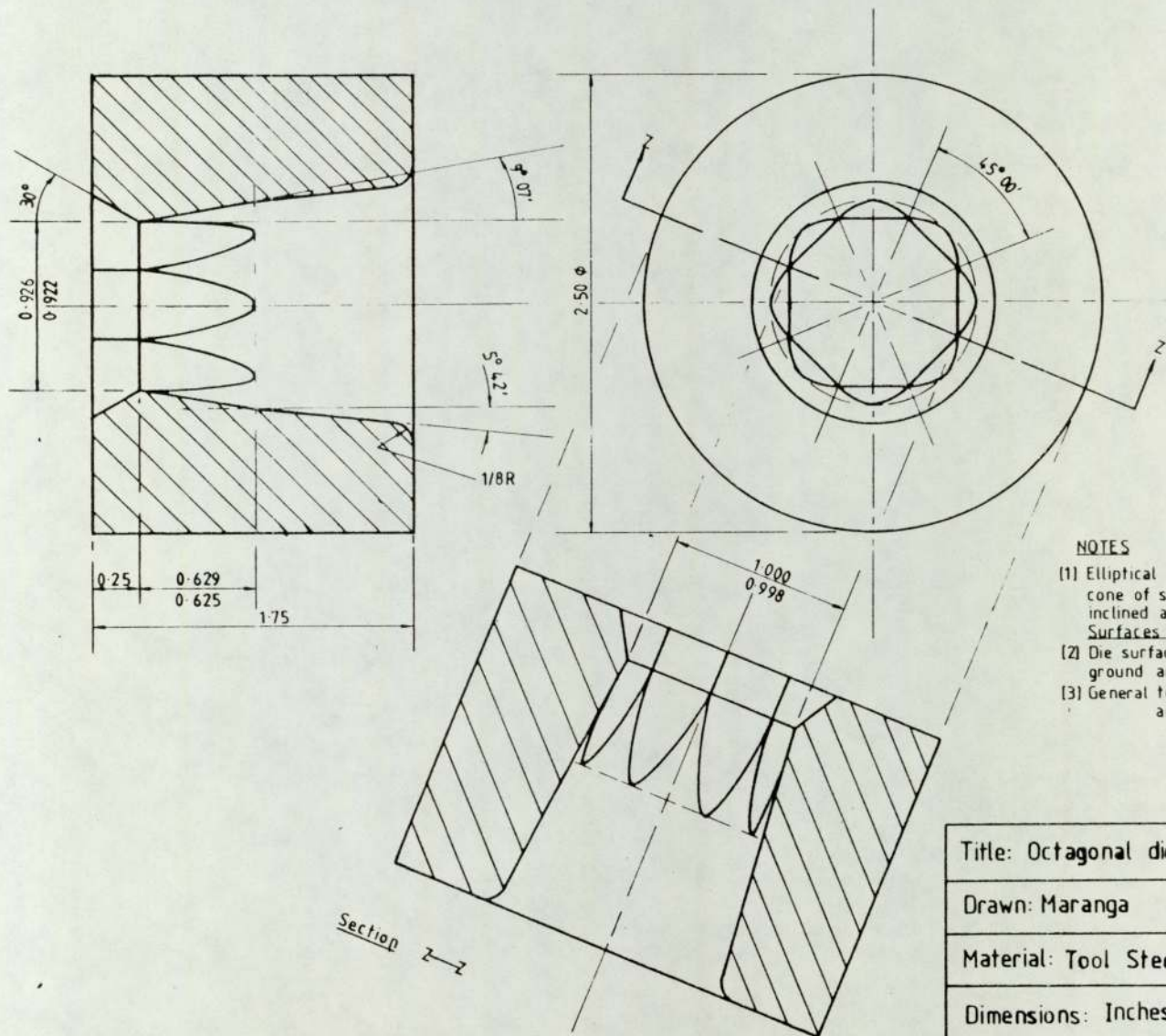
Title: Square die insert		
Drawn: Maranga	26/1/80	Draw 41/80
Material: Tool Steel	No. of parts 1	
Dimensions: Inches	Scale: 2:1	



**NOTES**

- [1] Elliptical surfaces generated from a cone of semi-angle  $4^{\circ} 40'$  cut by six planes inclined at  $9^{\circ} 36'$  to the cone axis. SURFACES NOT DRAWN TO SCALE.
- [2] Die surface heat treated to 64 RC, ground and lapped to mirror finish.
- [3] General tol.  $\pm 0.010$ ; angular tol.  $\pm 05'$

Title: Hexagonal die insert		
Drawn: Maranga	19/1/80	Draw 41/80
Material: Tool Steel	No. of parts 1	
Dimensions: Inches	Scale: 2:1	



NOTES

- (1) Elliptical plane surfaces generated from a cone of semi-angle  $5^{\circ} 42'$  cut by 8 planes inclined at  $9^{\circ} 7'$  to the cone axis  
Surfaces are not drawn to scale
- (2) Die surface heat treated to 64 RC, ground and lapped to mirror finish
- (3) General tolerance  $\pm 0.010$   
angular tolerance  $\pm 5'$

Title: Octagonal die insert		
Drawn: Maranga	23/8/80	Draw 43/80
Material: Tool Steel	No. of parts 1	
Dimensions: Inches	Scale: 2:1	

Section Z-Z

A-11 DIES USED IN THE DRAWING EXPERIMENTS

Table A-11.1 shows the set of dies used in the investigations on the drawing of polygonal tube from round on a cylindrical plug.

To facilitate cross-referencing the dies were given 3-part identification numbers. The first digit refers to the number of sides of the polygon required, followed by a letter designating the die and ends with one of the four letters A, B, C and D indicating the shape of the deforming zone.

TABLE No. A-11.1 Dies used in the drawing of polygonal tube from round stock on a cylindrical plug

	Die Ref. Number	Deforming shape	Radius / straight	Material of the die	$\alpha_e$ (degrees)	Remarks
SQUARE SECTION	4DA	pyramidical	straight	special alloy steel		
	4HA	"	radius (1.50 in)	tungsten carbide		
	4JB	elliptical	straight	"	7	
	4MC	triangular	"	tool steel (ARNE)	7	
	4GD	inverted parabolic	"	special alloy steel	7	
	4KD	"	"	tool steel (ARNE)	7	
	4WB	elliptical	"	"	8	Design for tube drawing
	4GB	elliptical	"	"	8	Design for tube drawing
HEXAGONAL	6BA	pyramidical	"	tungsten carbide		Industrial die
	6AA	pyramidical	radius (1.375 in)	"		"
	6NB	elliptical	straight	tool steel (ARNE)	7	
	6WB	"	"	"	8	Design for tube drawing
OCTAGONAL	8PB	"	"	"	7	
	8SD	inverted parabolic	"	"	7	
	8WB	elliptical	"	"	8	Design for tube drawing
DECAGONAL	10QB	elliptical	straight	tool steel (ARNE)	7	
CIRCULAR	ORA	conical	straight	tool steel	7	

The rotating die arrangement consisted mainly of the die shaft (4), the conical die (27) and the driving chain wheel (25). The die shaft had a cup form of 6 in bore which enclosed the conical die, and rotated about its axis in the die casing (2) by means of the chain wheel (25) fixed on its external surface. The die shaft was supported by the three anti-friction bearings (23, 24 and 26), arranged to carry the reaction of the chain and transmit the thrust from the conical die to the die casing through a compact axial thrust load cell (15).

The die inserts (10) consisted of  $N_s$  number of blades, equal to the number of sides of the polygonal section being drawn. They enclosed a converging pyramidal die forming orifice, while their exterior formed a surface around which a conical die rotated. The holder (5) of the die inserts functioned as a load cell and measured the drag force 'Q' (see Fig. 4.2). The special die tip seat (7) (and a mechanical drawing on page A118) enabled the die inserts to be changed without removing the die insert holder. The same feature transmitted the drag force 'Q' to the cup load cell (5) through a thrust roller bearing (22). This arrangement also made it possible to restrict or permit twisting by engaging or releasing the dog clutch (6, 11).

The axial thrust 'R' (see Fig. 4.2) exerted on the conical die resulted from the bursting force on the die inserts, as the metal deformed. The axial thrust was transmitted from the die to the die shaft and through the ring load cell to the die casing fixed to the bed of the drawbench.

A holder (5) was used as a load cell to measure the reaction 'Q'

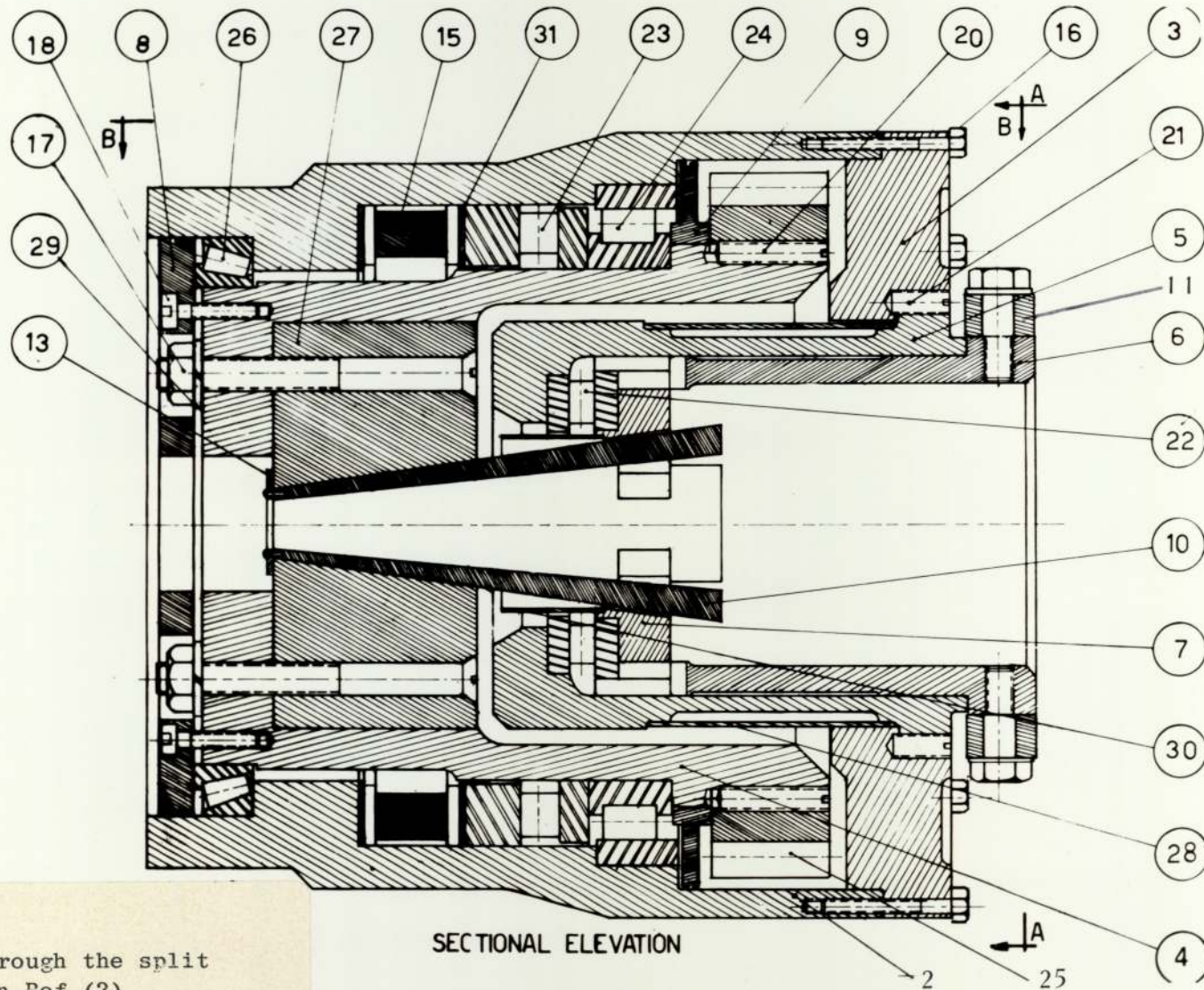


PLATE A-12.1

A cross-section through the split rotating die rig in Ref (2)

SECTIONAL ELEVATION

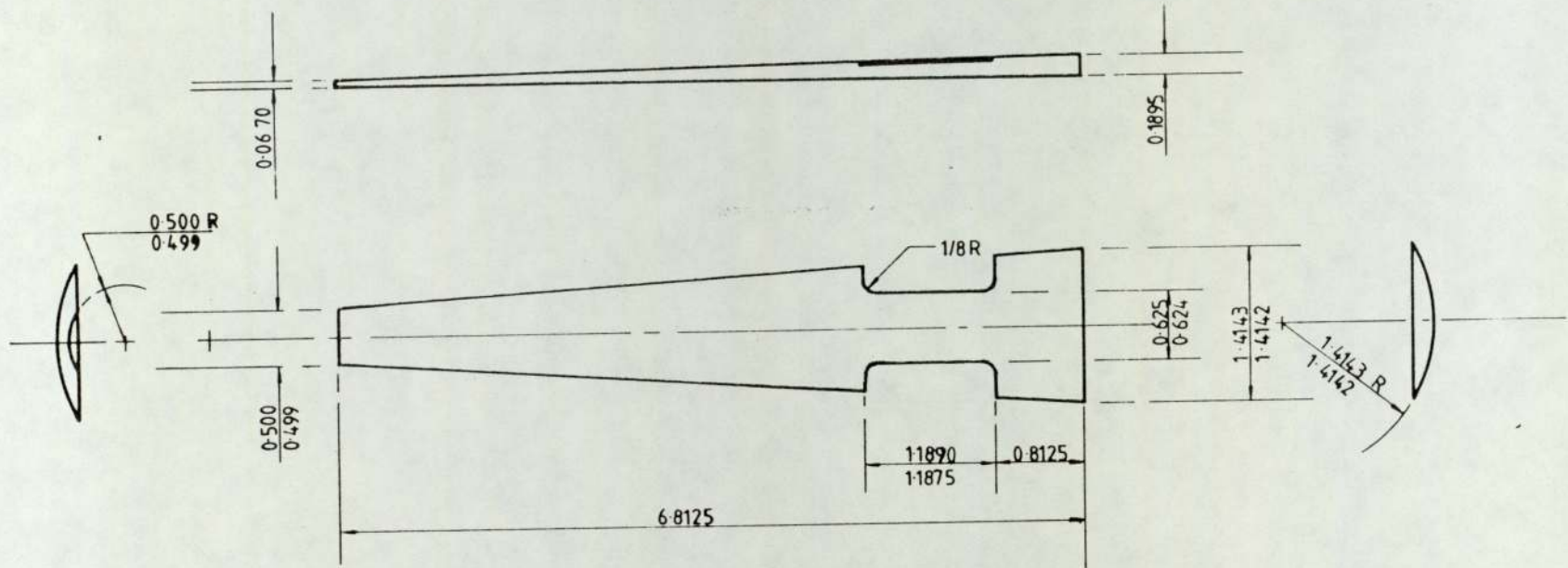
2 25

TABLE No. A-12.1 Components of the split rotating die rig shown in Table A-12.1

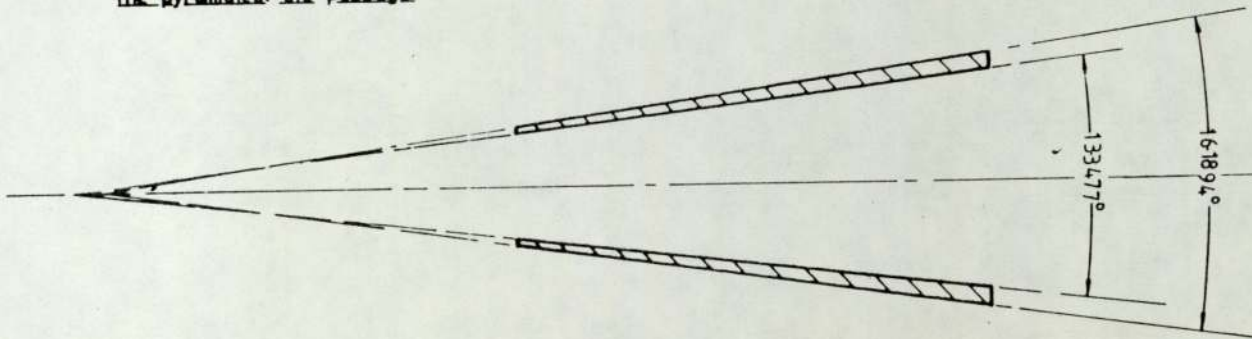
Part No.	No. of parts	Part Name/Description	Material	Part No.	No. of parts	Part Name/Description	Material
1	2	Rivet bolt	Mild steel	19	1	Set screw 1/2 x 7.75 x 1	—
2	1	Thrust block casing	Mild steel	20	6	Grubb socket screw 3/8 x 1.75	—
3	1	Thrust block cover	Mild steel	21	4	Grubb socket screw 3/8 x 1	—
4	1	Thrust block shaft	High S.steel	22	1	Thrust roller bearing Nth-4472 Torrington	
5	1	Thrust block die housing	Vibrac 30	23	1	Thrust roller bearing K81138/GS89328/WS81138INA	
6	1	Sliding key bush	Mild steel	24	1	Cylindrical roller bearing xLRJ 7 1/2 R & E	
7	1	Die tip seat	Vibrac 30	25	1	Duplex chain wheel 213634 Reynold	
8	1	Back bearing seal	Brass	26	1	Taper roller bearing LL735449/LL735410 TIMKEN	
9	1	Front bearing seal	Brass	27	1	Conical die	
10	Ns	Die tip	High S.steel	28	2	Gauge cover	Mild steel
11	1	Die clutch lever	EN 11	29	2	Spring washer	—
12	1	Hinge seal	Mild steel	30	1	Sealing sleeve	Brass
13	1	Die tip spacer	Silver steel	31	2	Copper ring	Copper
14	2	Sliding pin	EN 11				
15	1	Back load cell	Vibrac 30				
16	12	Set screw 1/2 x 2 x 1.5	—				
17	4	Set screw 1/2 x 4.5 x 2	—				
18	4	Set screw 5/16 x 1.5 x 1	—				

on the die inserts. The central part of the cupwall was reduced in thickness and two sets of strain gauges bonded on the outer surface of this thin walled portion. One set measured the traction 'Q' exerted on the die inserts, and the other set measured the torque exerted and transmitted to the die insert holder when the dog clutch was engaged. The dog clutch was used to prevent the drawn tube from twisting due to the torque transmitted by friction from the rotating conical die.

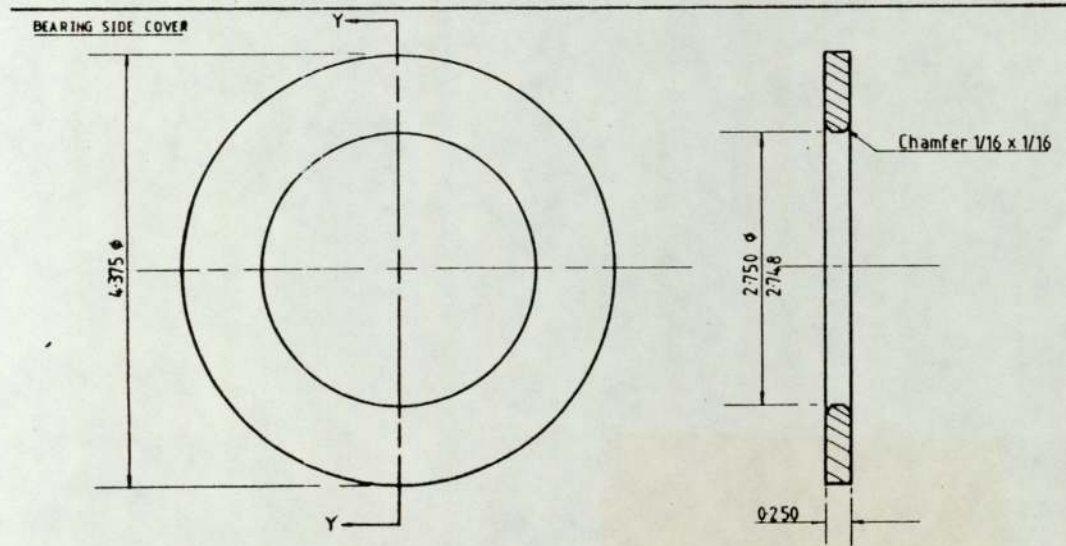
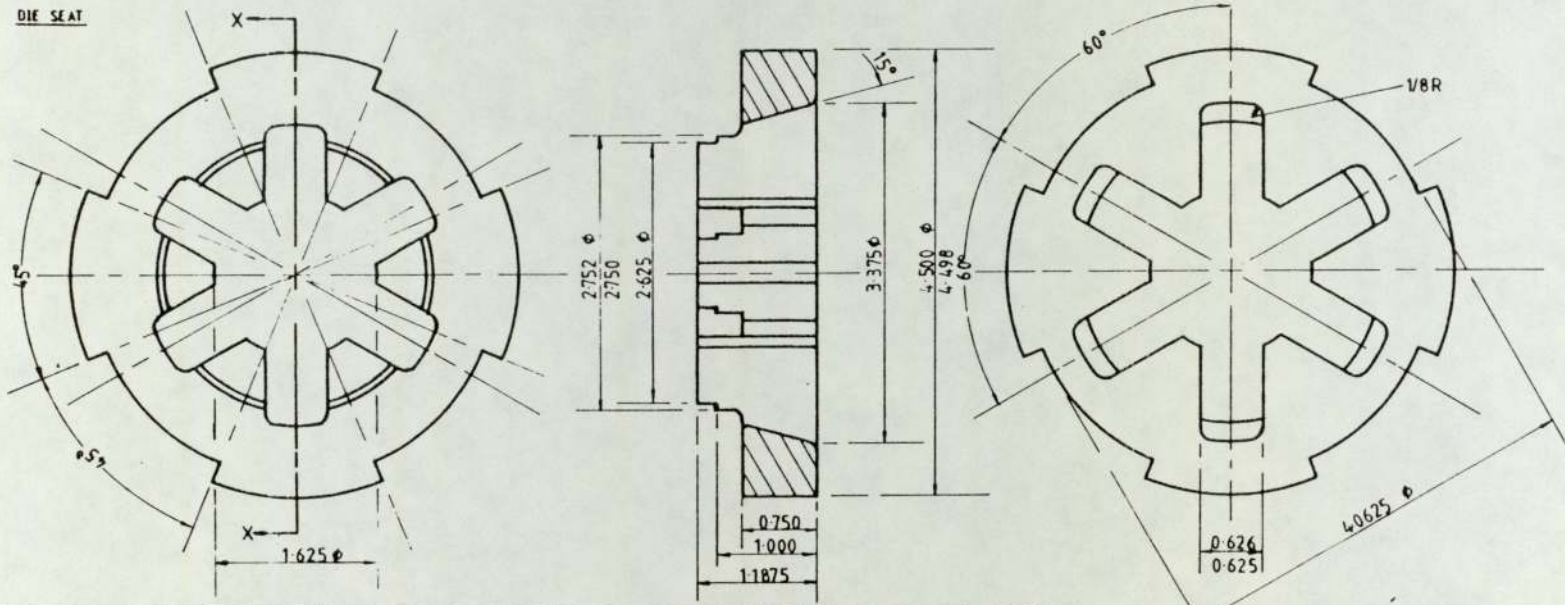
The drive (see Plate A-12.2) consisted of a 7.5 h.p., 3-phase motor coupled to a Crofts variable speed belt-cone unit with a speed ratio of 4:1. The output shaft of the combined motor-speed unit was coupled to a 16.61:1 reduction gear unit to provide a rotational speed range of 30 to 120 rev min<sup>-1</sup>. A duplex chain transmitted the power to the shaft of the rotating die and drove it with infinitesimally variable speed range from a minimum of 15 rev min<sup>-1</sup> to a maximum of 60 rev min<sup>-1</sup>. A marine tachogenerator measured the speed of the rotating die. The output shaft of the variable speed unit drove the tachogenerator through a chain and sprocket with a speed ratio of 1:2.



The pyramidal die passage.

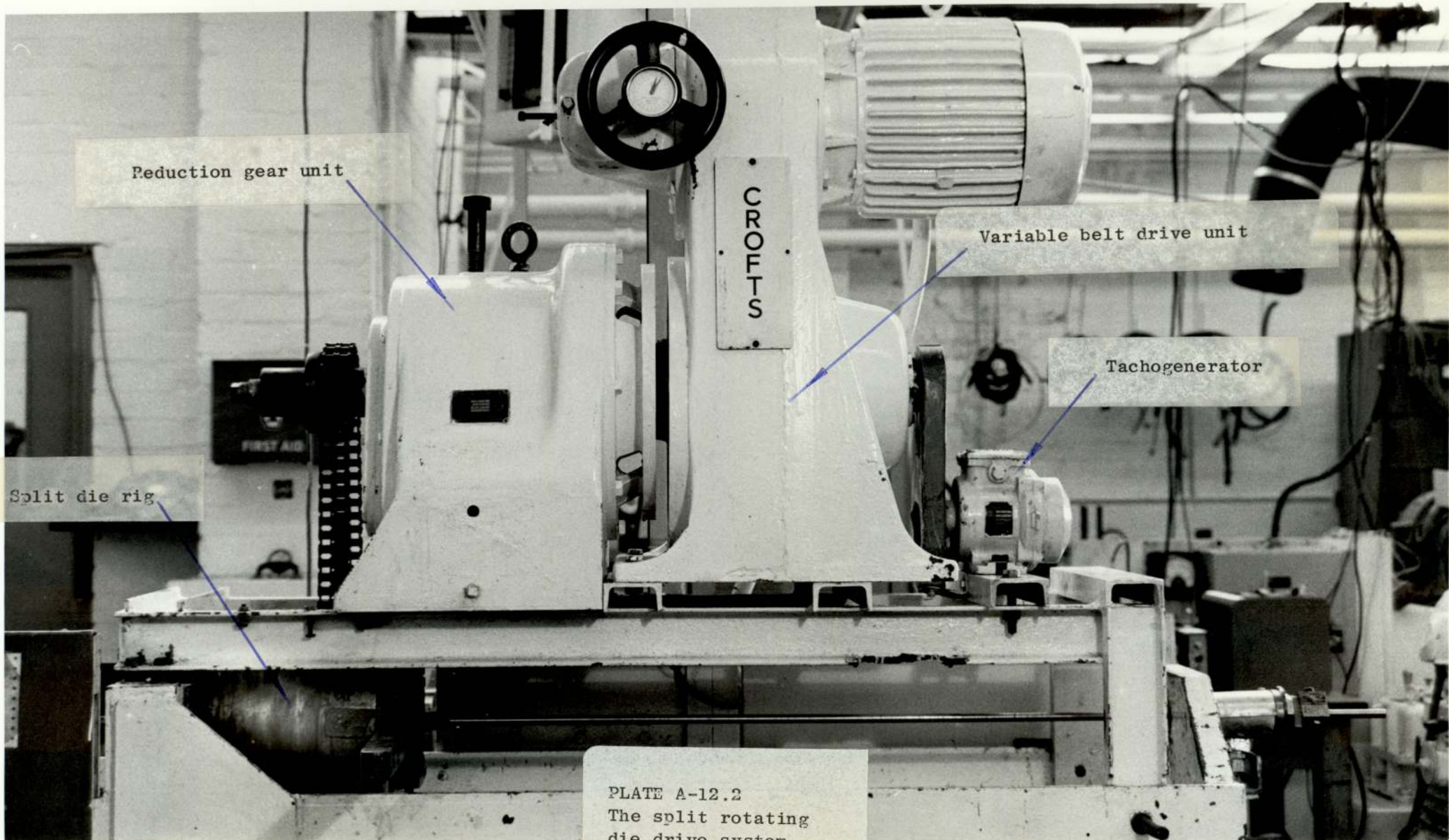


Title: Hexagonal split die tips		
Drawn: S.M. Maranga	4/10/80	Draw 44/80
Material: High speed steel	No. of parts 6	
Dimensions: Inches	Scale: 1:1	



**NOTE**  
 General tol.  $\pm 0.005$   
 angular tol.  $\pm 5'$

Title: Tip-die seat		
Drawn: S. M. Maranga	5/10/80	Draw 44b/80
Material: Vibrac 30	No. of parts: 1 of each	
Dimensions: Inches	Scale: 1:1	



Reduction gear unit

Variable belt drive unit

Tachogenerator

Split die rig

PLATE A-12.2  
The split rotating  
die drive system

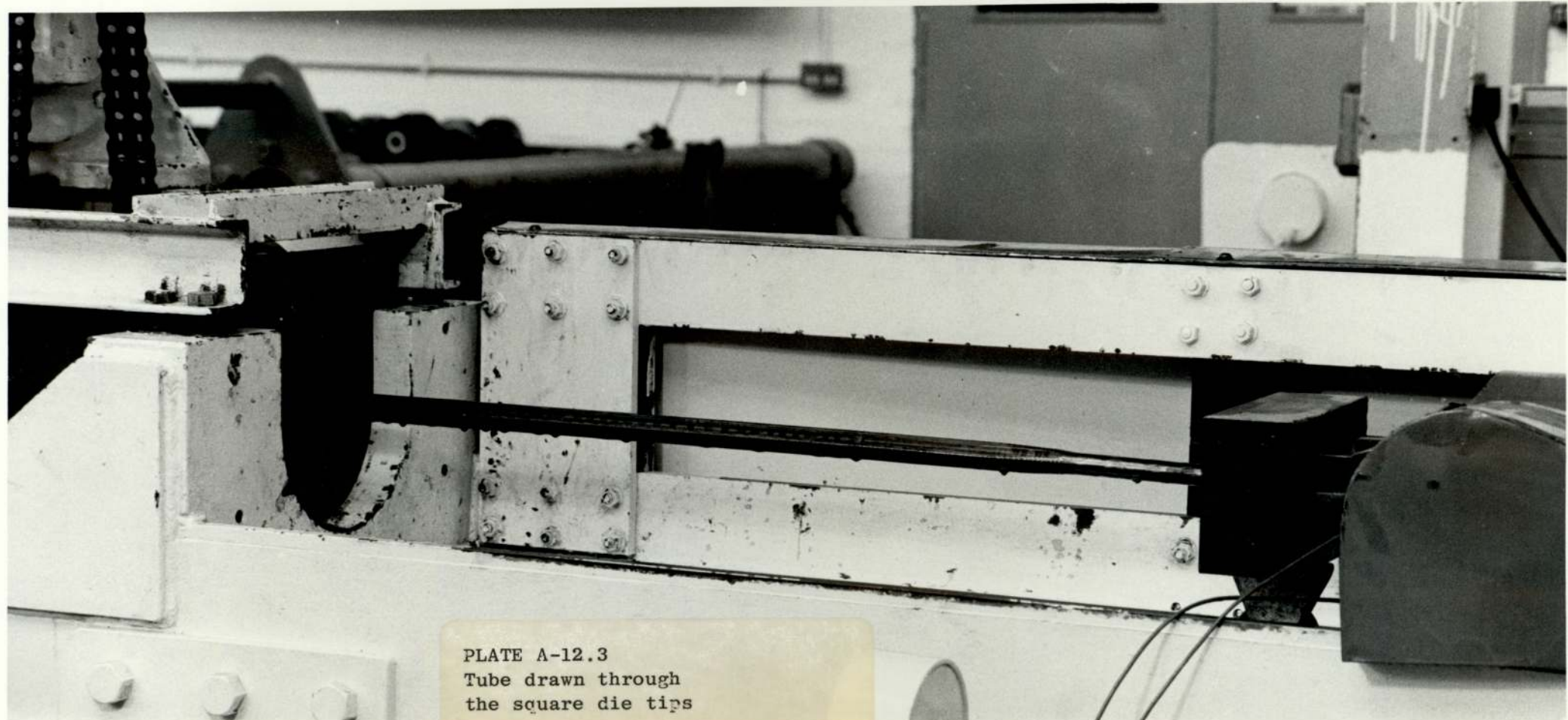


PLATE A-12.3  
Tube drawn through  
the square die tips

TUBE DIRECTLY FROM ROUND STOCK ON A CYLINDRICAL PLUG†

```

2      MASTER MAINPROG
3      DIMENSION XA(11,11),YA(11,11),XB(11,11),YB(11,11),XACS(11,11),
4      1YACS(11,11),XBCS(11,11),YBCS(11,11),XACL(11,11),YACL(11,11),
5      2XBCL(11,11),YBCL(11,11),A(10),PL(10),ER(10),ARLTA(10),ARLTB(10),
6      3ARSTA(10),ARSTB(10),RAS(11,11),RAL(11,11),RBS(11,11),RBL(11,11),
7      4THETA(11,11),THETAS(11,11),DBL(11,11),DBS(11,11),DAL(11,11),
8      5DAS(11,11),PHILBA(11,11),PHISBA(11,11),CKIL(11,11),CKIS(11,11),
9      6BETAS(11,11),BETAL(11,11),EITAL(11,11),EITAS(11,11),ZS(11,11),
10     7ZL(11,11),ZTS(11,11),ZTL(11,11),URBL(11,11),URBS(11,11),X(10),
11     1Y(10),AT(10),XXH(11),YYN(11),XXM(11),YYM(11),XXM1(8),YYM1(8)
12 C
13 C DIMENSION FOR THE INCOMING STOCK (TUBES) AND THE PROCESSED PRODUCT (SECTION)
14 C GAUGE (T1), TUBING O.D (DO1) AND THE DIAGONAL
15 C LENGTH OF THE POLYGONAL STOCK (DHE)-----
16 C
17     READ(1,200) T1,DO1,DHE
18     200 FORMAT(3F0.0)
19 C
20     WRITE(2,2200) DO1,T1,DHE
21     2200 FORMAT(//15X,'STOCK DIMENSIONS:',/20X,'TUBE DIAMETER      = ',F6.4,
22     1' INCHES',/20X,'TUBE THICKNESS   = ',F6.4,' INCHES',/20X,'SECTI
23     2ON DIAGONAL = ',F6.4,' INCHES')
24 C
25 C
26 C
27 C
28 C SPECIFY DRAWING VELOCITY (INCHES/SECOND)
29 C SPECIFY STRESS-STRAIN CURVE FOR THE DRAWING STOCK
30 C SIGMA=K*EPSILON**N WHERE K IS IN TON-FORCE/SQ.IN.
31 C
32 C     DATA VLA,YK,YN/3.0,50.20,0.2321/
33     READ(1,200) VLA,YK,YN
34     PI=3.1415927
35 C
36 C DEFINE LINEAR AND AREA SCALE (LISC :20 UNITS/IN, LASC :400 UNITS/SQ.IN)
37 C
38     LISC=20
39     LASC=LISC**2
40 C DIMENSIONS OF THE DRAWING AND THE UNDRAWN STOCK TO THE ABOVE SCALE
41     T1=T1*LISC
42     DO1=DO1*LISC
43     DHE=DHE*LISC
44 C
45 C TO GENERATE THE NUMBER OF SIDES OF THE SECTION REQUIRED
46     DO DO NOSIDE=2,6
47 C     READ(1,205) NOSIDE
48 C     205 FORMAT(I3)
49 C
50 C WHEN NOSIDE IS 6,THE DRAWN SECTION IS ROUND
51 C

```

† The flow chart is given in Figure 3.7

```

52     IF (NOSIDE.EQ.6) GO TO 2561
53     NS=NOSIDE*2
54     WRITE(2,2000) NS
55 2000 FORMAT(1H1,5X,'NUMBER OF SIDES OF DRAWN SECTION = ',I2,/)
56     GO TO 2562
57 2561 WRITE(2,2500)
58 2500 FORMAT(1H1,5X,'NUMBER OF SIDES OF DRAWN SECTION = INFINITY',/)
59 C
60 C CALCULATE SECTION PARAMETERS, INCLUDED ANGLE(BETA), PLUG RADIUS(RP)
61 C INLET AREA(AB), OUTLET AREA(AA), AREA RATIO(AR), PLUG AREA(AP) AND
62 C REDUCTION(RED); REMEMBER THE SCALE TO OBTAIN ABSOLUTE VALUES WHERE APPROP.
63 C
64 2562 BETA=PI/NS
65 C WHAT IF NS=INFINITY
66 C ----- EASIER OF COURSE BUT -----
67     IF (NOSIDE.EQ.6) GO TO 2510
68     SPARAM=NS*COS(BETA)*SIN(BETA)/4.0
69     GO TO 2511
70 2510 SPARAM=PI/4.0
71 2511 RP=0.5*T1*(D01/T1-2.0)
72     CK=0.5*(1.0-2.0*RP/DHE)
73     AB=PI*T1**2*(D01/T1-1.0)
74     AA=DHE**2*(SPARAM-PI*0.25*(1.0-2.0*CK)**2)
75     AR=AB/AA
76     AP=PI*RP**2
77     RED=1.0-1.0/AR
78     RED100=RED*100.0
79     AAA=AA/LASC
80     ABB=AB/LASC
81     DD01=D01/LISC
82     RPP=RP/LISC
83     WRITE(2,2152) ABB,AAA,RED100
84 2152 FORMAT(/20X,'AREA AT INLET = ',F8.4,' SQ INCHES',/20X,'AREA A
85 1T OUTLET = ',F8.4,' SQ INCHES',/20X,'REDUCTION OF AREA = ',F8.
86 24,' PER CENT')
87 C RADIUS OF CIRCUMSCRIBING CIRCLE AT INLET(RB) AND AT OUTLET(RA)
88     RB=D01/2.0
89     RA=DHE/2.0
90 C IN CASE OF AXISYMMETRIC DRAWING MAPPING IS GENERALLY
91 C OVERLOOKED, SO A BIG JUMP -----
92     IF (NOSIDE.EQ.6) GO TO 2570
93 C RADIUS OF INSCRIBED CIRCLE AT THE EXIT(RAI)
94     RAI=DHE*COS(BETA)/2.0
95 C
96 C ...<<< NOTE THAT TO SAVE COMPUTER TIME INSTEAD OF WORKING WITH
97 C DOUBLE SYMMETRIC SECTION A SINGLE SYMMETRIC SECTION IS
98 C USED; DENOTED HEREAFTER BY (DOUBLE) SYMMETRIC >>>>-----
99 C
100 C BANDING INLET (DOUBLE) SYMMETRIC SECTION INTO M-1 EQUAL SECTORS AND
101 C MAP OUTLET WITH N-2 HYPERBOLIC CURVES; (I,J) DEFINES GENERAL

```

```

102 C INTERSECTION AND (1,1) DENOTES THE ORIGIN
103 C
104     N=10
105     M=10
106 C THE FIRST CURVE OF OUTLET SECTION CORRESPONDS TO THE CIRCULAR PLUG
107 C PL(I) REFERS TO THE POSITION OF THE HYPERBOLA VIRTUAL ORIGIN ALONG
108 C THE LINE OF SYMMETRY AND A(I) IS THE FOCAL LENGTH
109     T2=DHE/2.0-RP
110     PL(2)=RP
111     PL(1)=0.0
112 C
113 C T2 IS THE THICKNESS OF THE SECTION TUBE ALONG THE DIAGONAL AND IS
114 C DIVIDED INTO N-2 EQUAL LENGTHS
115     DT=(T2-RP*(1.0/COS(BETA)-1.0))/(N-2)
116 C INCLUDED AREA OF THE PLUG AT(2) ;AT(1) CORRESPONDS TO THE ORIGIN
117     AT(2)=AP/(NS*2.0)
118     AT(1)=0.0
119     ER(2)=RP
120     ER(1)=0.0
121 C DIFFERENT FUNCTIONS OF THE SYMMETRIC ANGLE (BETA)
122 C
123     TABETA=TAN(BETA)
124     COBETA=1.0/TABETA
125     TB2=TABETA**2
126     TB4=TB2**2
127     TB8=TB4**2
128     T2B=TAN(BETA*2.0)
129     T2B2=T2B**2
130 C
131 C ??? REAL JOB OF MAPPING STARTS HERE iiiiiiii
132 C
133     DO 65 I=3,N
134     PL(I)=RP/COS(BETA)+(I-2)*DT
135     A(I)=1.0-(I-1)*1.0/N
136 C TO CALCULATE CO-ORDINATES AT INTERSECTION OF THE HYPERBOLA AND THE
137 C LINE INCLINED TO (DOUBLE)BETA BY THE YA-AXIS
138     IF (NS.EQ.4) GO TO 66
139     X(I)=(-PL(I)*TB4+SQRT(PL(I)**2*TB8+(1.0-TB4)*(A(I)**2+
140     1PL(I)**2*TB4)))/(1.0-TB4)
141     GO TO 67
142 66 X(I)=(PL(I)**2+A(I)**2)/(2.0*PL(I))
143 67 Y(I)=TABETA*(-X(I)+PL(I))
144 C
145 C CO-ORDINATES OF INTERSECTION TO GLOBAL XA-YA AXES
146     V=X(I)
147     W=Y(I)
148     XA(I,M)=W
149     YA(I,M)=-V+PL(I)
150 C AREA ENCLOSED BY THE HYPERBOLA I AND THE PLUG I=2 DENOTED BY AT(I)
151     PIL=PL(I)-V

```

```

152      AT(I)=CBETA*(V*SQRT(V**2-A(I)**2)-A(I)**2*ALOG((V+SQRT(V**2-A(I)*
153      1+2))/A(I)))/2.0+PIL**2*TABETA/2.0-AT(2)
154 C
155 C AREA ENCLOSED BY THE CURVE AND THE PLUG REFERRED TO THE OUTLET
156      ABT=AT(I)*AR
157 C EQUIVALENT RADIUS AT INLET ER(I)
158      ER(I)=SQRT((ABT+AP/(NS*2))/BETA*2.0)
159 C
160 C AREA OF BAND AT THE INLET ENCLOSED BY THE CIRCULAR ARC I AND I-1
161      ABAND=BETA*(ER(I)**2-ER(I-1)**2)/2.0
162 C DIVIDE AREA OF THE BAND INTO M-1 EQUAL SECTORS AND ALSO CALCULATE
163 C THE RADIAL WIDTH OF THE BAND
164      ABCD=ABAND/(M-1)
165      DR=ER(I)-ER(I-1)
166      DOA=BETA/(M-1)
167 C
168 C CALCULATE AREAS OF LARGE AND SMALL TRIANGLES AT INLET PLANE
169      DD=0.5*DR**2*DOA
170      ARLTB(I)=0.5*(ABCD+DD)
171      ARSTB(I)=0.5*(ABCD-DD)
172 C EQUIVALENT TRIANGULAR AREAS AT THE EXIT PLANE
173      ARLTA(I)=ARLTB(I)/AR
174      ARSTA(I)=ARSTB(I)/AR
175 C
176 C INTERSECTION OF HYPERBOLA I AND YA-AXIS
177      XA(I,1)=0.0
178      YA(I,1)=PL(I)-A(I)
179      65 CONTINUE
180 C CURVE I=2 IS A CIRCLE AND THE CO-ORDINATES FOR INTERSECTION WITH
181 C LINE INCLINED AT BETA TO YA-AXIS CAN BE FOUND
182      YA(2,M)=RP*SQRT(1.0/(1.0+TB2))
183      XA(2,M)=YA(2,M)*TABETA
184      GO TO 69
185      69 YA(2,1)=RP
186      XA(2,1)=0.0
187 C DEFINE ORIGIN AT EXIT
188      XA(1,1)=0.0
189      YA(1,1)=0.0
190      WRITE(2,2992)
191      2998 FORMAT(5X,'THE LIMITING CO-ORDINATES OF CURVES AT EXIT XA/YA ',/)
192      WRITE(2,2999) (XA(I,M),I=1,N)
193      WRITE(2,2999) (YA(I,M),I=1,N)
194      2999 FORMAT(7X,10(2X,F8.6),/)
195 C
196 C CO-ORDINATES OF TRIANGLES AT INLET
197      DO 70 I=2,N
198      DO 71 J=1,M
199      OJ=(J-1)*BETA/(M-1)
200      XB(I,J)=ER(I)*SIN(OJ)
201      YB(I,J)=ER(I)*COS(OJ)

```

```

202 71 CONTINUE
203 70 CONTINUE
204 C
205 C LOCATE CENTROIDS OF LARGE AND SMALL TRIANGLES AT INLET
206 DO 75 I=2,N-1
207 DO 76 J=1,M-1
208 X3CL(I+1,J+1)=(XB(I,J)+XB(I+1,J)+XB(I+1,J+1))/3.0
209 Y3CL(I+1,J+1)=(YB(I,J)+YB(I+1,J)+YB(I+1,J+1))/3.0
210 X3CS(I+1,J+1)=(XB(I,J)+XB(I+1,J+1)+XB(I,J+1))/3.0
211 Y3CS(I+1,J+1)=(YB(I,J)+YB(I+1,J+1)+YB(I,J+1))/3.0
212 76 CONTINUE
213 75 CONTINUE
214 C
215 C MAPPING CORRESPONDING TRIANGLES AT OUTLET PLANE
216 C DIFFERENT FUNCTIONS OF BETA
217 CBETA=COS(BETA)
218 CBETA2=CBETA**2
219 SBETA=SIN(BETA)
220 SBETA2=SBETA**2
221 AZERO=0.0
222 DO 80 I=2,N-1
223 DO 81 J=1,M-1
224 C MAPPING LARGE TRIANGLES
225 AREA=ARLTA(I+1)
226 X1=XA(I,J)
227 Y1=YA(I,J)
228 X2=XA(I+1,J)
229 Y2=YA(I+1,J)
230 IF (J.EQ.1) GO TO 82
231 C
232 C SUBSTITUTE FOR Y3 AND SOLVE FOR X3 USING THE EQUATIONS OF THE CURVE
233 C AND THE AREA OF THE TRIANGLE
234 DM1=(2.0*AREA-(X2*Y1-X1*Y2))/(X1-X2)
235 DK1=(Y2-Y1)/(X1-X2)
236 C3=DK1**2-TB2
237 C2=-2.0*DM1*DK1+2.0*DK1*PL(I+1)
238 C1=DM1**2+PL(I+1)**2-2.0*PL(I+1)*DM1
239 SQT=SQRT(C2**2-4.0*C3*(C1-A(I+1)**2))
240 X3R1=(-C2+SQT)/(2.0*C3)
241 X3R2=(-C2-SQT)/(2.0*C3)
242 Y3R1=DM1-DK1*X3R1
243 Y3R2=DM1-DK1*X3R2
244 C
245 C SELECT THE CO-ORDINATE OF THE THIRD VERTEX
246 IF (Y3R1.LT.Y3R2) GO TO 83
247 YA(I+1,J+1)=Y3R2
248 XA(I+1,J+1)=X3R2
249 GO TO 84
250 83 YA(I+1,J+1)=Y3R1
251 XA(I+1,J+1)=X3R1

```

```

252 84 GO TO 85
253 C
254 C MAPPING THE INITIAL LARGE TRIANGLES BY SUBSTITUTING X AND SOLVE FOR Y
255 82 DM1=(2.0*AREA-(X2*Y1-X1*Y2))/(Y2-Y1)
256 DK1=(X1-X2)/(Y2-Y1)
257 C1=PL(I+1)**2-TB2*DM1**2
258 C2=-2.0*PL(I+1)+2.0*DK1*DM1*TB2
259 C3=1.0-DK1**2*TB2
260 C
261 SQT=SQRT(C2**2-4.0*C3*(C1-A(I+1)**2))
262 Y3R1=(-C2+SQT)/(2.0*C3)
263 Y3R2=(-C2-SQT)/(2.0*C3)
264 X3R1=DM1-DK1*Y3R1
265 X3R2=DM1-DK1*Y3R2
266 C
267 C THE THIRD VERTEX OF THE TRIANGLE
268 IF (X3R1.GT.X3R2) GO TO 86
269 XA(I+1,J+1)=X3R2
270 YA(I+1,J+1)=Y3R2
271 GO TO 85
272 86 XA(I+1,J+1)=X3R1
273 YA(I+1,J+1)=Y3R1
274 C
275 85 IF (I.GT.2) GO TO 89
276 C TO MAP SMALL TRIANGLES AT INLET WHERE ONE OF THE CURVES IS CIRCULAR
277 X2=XA(I+1,J+1)
278 Y2=YA(I+1,J+1)
279 AREA=ARSTA(I+1)
280 FM1=(2.0*AREA-(X2*Y1-X1*Y2))/(X1-X2)
281 FK1=(Y2-Y1)/(X1-X2)
282 SQT=SQRT((FM1*FK1)**2-(1.0+FK1**2)*(FM1**2-PP**2))
283 X3S1=((FM1*FK1)+SQT)/(1.0+FK1**2)
284 X3S2=((FM1*FK1)-SQT)/(1.0+FK1**2)
285 C
286 C THE THIRD VERTEX OF THE TRIANGLE
287 IF (X3S1.GT.X3S2) GO TO 87
288 XA(I,J+1)=X3S2
289 GO TO 88
290 87 XA(I,J+1)=X3S1
291 88 YA(I,J+1)=FM1-FK1*XA(I,J+1)
292 C
293 GO TO 81
294 C
295 C
296 C MAPPING SMALL TRIANGULAR ELEMENTS BANDED BY HYPERBOLAE I & I+1
297 89 X2=XA(I+1,J+1)
298 Y2=YA(I+1,J+1)
299 AREA=ARSTA(I+1)
300 DM1=(2.0*AREA-(X2*Y1-X1*Y2))/(X1-X2)
301 DK1=(Y2-Y1)/(X1-X2)

```

```

302 C
303     C3=DK1**2-TB2
304     C2=-2.0*DM1*DK1+2.0*DK1*PL(I)
305     C1=DM1**2+PL(I)**2-2.0*PL(I)*DM1
306     SQT=SQRT(C2**2-4.0*C3*(C1-A(I)**2))
307     X3R1=(-C2+SQT)/(2.0*C3)
308     X3R2=(-C2-SQT)/(2.0*C3)
309     Y3R1=DM1-DK1*X3R1
310     Y3R2=DM1-DK1*X3R2
311 C
312 C SELECT THE CO-ORDINATE OF THE THIRD VERTEX
313     IF (Y3R1.LT.Y3R2.AND.X3R1.GT._AZERO) GO TO 870
314     XA(I,J+1)=X3R2
315     YA(I,J+1)=Y3R2
316     GO TO 81
317 870 XA(I,J+1)=X3R1
318     YA(I,J+1)=Y3R1
319 81 CONTINUE
320 80 CONTINUE
321 C
322 C LOCATING THE CENTROIDS OF MAPPED TRIANGLES AT THE EXIT PLANE
323     DO 90 I=2,N-1
324     DO 91 J=1,M-1
325     XACL(I+1,J+1)=(XA(I,J)+XA(I+1,J)+XA(I+1,J+1))/3.0
326     YACL(I+1,J+1)=(YA(I,J)+YA(I+1,J)+YA(I+1,J+1))/3.0
327     XACS(I+1,J+1)=(XA(I,J)+XA(I,J+1)+XA(I+1,J+1))/3.0
328     YACS(I+1,J+1)=(YA(I,J)+YA(I,J+1)+YA(I+1,J+1))/3.0
329 91 CONTINUE
330 90 CONTINUE
331 C
332 C DEFINE X-Y AT THE ORIGIN
333     DO 95 J=1,M
334     XA(1,J)=0.0
335     YA(1,J)=0.0
336     XB(1,J)=0.0
337     YB(1,J)=0.0
338 95 CONTINUE
339 C THE CARD BELOW IS USED TO CALL FOR A FRESH PAGE
340 C WRITE(2,2001)
341 C2001 FORMAT(1H1)
342 C
343 C PRINT CO-ORDINATE OF INLET TRIANGLES AND THE EQUIVALENT RADIUS
344     WRITE(2,2002)
345 2002 FORMAT(5X,'VALUES OF XB,YB AT INLET PLANE AND EQUIV RADIUS ER',/)
346     WRITE(2,2003)
347 2003 FORMAT(5X,'I=',5X,'J=1',8X,'J=2',8X,'J=3',8X,'J=4',8X,'J=5',8X,'J=
348 16',8X,'J=7',8X,'J=9',8X,'J=10',2X,'AS SHOWN',/)
349     DO 100 I=1,N
350     WRITE(2,2005) ((I,(XB(I,J),J=1,M),ER(I)))
351     WRITE(2,2006) (YB(I,J),J=1,M)

```

```

352 2005 FORMAT(5X,I2,10(2X,F8.6),2X,F8.4)
353 2006 FORMAT(7X,10(2X,F8.6))
354 100 CONTINUE
355 C
356 C CENTROIDS OF THE TRIANGLES AT INLET PLANE AND THE RESPECTIVE AREAS
357 WRITE(2,2009)
358 2009 FORMAT(/5X,'VALUES OF XBCS,YBCS,XBCL,YBCL AND AREAS OF TRIANGLES'
359 1,/)
360 DO 105 I=3,N
361 WRITE(2,2010) ((I,(XBCS(I,J),J=2,M),ARSTB(I)))
362 WRITE(2,2011) (YBCS(I,J),J=2,M)
363 WRITE(2,2010) ((I,(XBCL(I,J),J=2,M),ARLTB(I)))
364 WRITE(2,2011) (YBCL(I,J),J=2,M)
365 2010 FORMAT(5X,I2,8X,9(2X,F8.6),2X,F8.4)
366 2011 FORMAT(15X,9(2X,F8.6))
367 105 CONTINUE
368 C OUTLET PLANE .....
369 WRITE(2,2015)
370 2015 FORMAT(/5X,'VERTICES OF TRIANGLES XA,YA AND FOCAL LENGTH A(I) OF
371 HYPERBOLA I',/)
372 WRITE(2,2003)
373 A(2)=RP*(1.0/COS(BETA)-1.0)
374 A(1)=0.0
375 DO 110 I=1,N
376 WRITE(2,2005) ((I,(XA(I,J),J=1,M),A(I)))
377 WRITE(2,2006) (YA(I,J),J=1,M)
378 110 CONTINUE
379 C
380 WRITE(2,2020)
381 2020 FORMAT(/5X,'CENTROIDS OF TRIANGLES XACS,YACS,XACL AND YACL AND
382 AREAS OF TRIANGLES',/)
383 DO 115 I=3,N
384 WRITE(2,2010) ((I,(XACS(I,J),J=2,M),ARSTA(I)))
385 WRITE(2,2011) (YACS(I,J),J=2,M)
386 WRITE(2,2010) ((I,(XACL(I,J),J=2,M),ARLTA(I)))
387 WRITE(2,2011) (YACL(I,J),J=2,M)
388 115 CONTINUE
389 C
390 C MAPPING PER CENTAGE ERROR IN AREA AT OUTLET OBTAINED FROM MAPPING
391 C AND GEOMETRICAL VALUE (AA)
392 AST=AA/(NS*2)
393 DE=((AST-AT(N))/AST)*100.0
394 WRITE(2,2021) DE
395 2021 FORMAT(/5X,'PER CENTAGE DIFFERENCE OF TOTAL X-SECTION AREA = ',
396 1F8.4,/)
397 C
398 C
399 C
400 C ***** PLOTTING ON THE RESULTING ENTRY AND EXIT PLANES *****
401 C

```

```

472 C CALL GINO THE PLOTTER AND OBSERVE THE -----
473     CALL OPENINGP
474 C SHIFT THE ORIGIN BY 50 MM IN THE X- DIRECTION AND
475 C BY 30 MM IN THE Y-DIRECTION FOR THE EXIT PLANE MAPPING....
476     CALL SHIFT2(50.0,30.0)
477 C DEFINE NATURAL ORIGIN TO BE AT (0,0); EACH AXIS OF LENGTH 100 MM
478     CALL AXIPOS(0.0,0.0,0.0,100.0,1)
479     CALL AXIPOS(0.0,0.0,0.0,100.0,2)
480 C DEFINE SCALING EQUAL AND LINEAR IN BOTH AXES;10 INTERVALS RANGE 0 TO 10
481     CALL AXISCA(3,10,0.0,10.0,1)
482     CALL AXISCA(3,10,0.0,10.0,2)
483 C DRAW X-AXIS WITH TICK MARKS AT INTERVALS AND SCALING ON
484 C CLOCKWISE SIDE OF AXIS -----
485     CALL AXIDRA(1,1,1)
486 C THE SAME TREATMENT FOR Y AXIS BUT SCALING ON ANTI-CLOCKWISE SIDE OF AXIS
487     CALL AXIDRA(-1,-1,2)
488 C LABEL X-AXIS BUT FIRST MOVE PEN TO START POSITION
489     CALL MOVT02(40.0,-15.0)
490 C DEFINE CHARACTER SIZE: 2.5 MM WIDE BY 3.0 MM HIGH
491     CALL CHASIZ(2.5,3.0)
492 C LABEL X-AXIS
493     CALL CHAHOL(10HX-A*LXIS*.)
494     CALL CHAHOL(10HIN X 0.1*.)
495 C MOVE PEN FOR LABELLING Y-AXIS
496     CALL MOVT02(-15.0,40.0)
497 C DEFINE ROTATION OF 90 DEGREES FOR ALL FOLLOWING CHARACTER OUTPUT
498     CALL CHAANG(90.0)
499 C LABEL Y-AXIS
500     CALL CHAHOL(10HY-A*LXIS*.)
501     CALL CHAHOL(10HIN X 0.1*.)
502 C RETURN CHARACTER ORIENTATION TO HORIZONTAL
503     CALL CHAANG(0.0)
504 C START DRAWING HYPERBOLIC CURVES AT THE EXIT PLANE NOW >>> -----
505     DO 2450 I=2,N
506     DO 2451 J=1,M
507     XXN(J)=YA(I,J)
508     YYN(J)=XA(I,J)
509 2451 CONTINUE
510     CALL GRACUR(XXN,YYN,M)
511 2450 CONTINUE
512 C
513 C DRAW LINE OF SYMMETRY AT THE EXIT SECTION
514     CALL MOVT02(0.0,0.0)
515     XXNN=XXN(M)*10.0
516     YYNN=YYN(M)*10.0
517     CALL LINBY2(XXNN,YYNN)
518 C
519     NL2=N-2
520 C JOIN CENTRES OF LARGE TRIANGLES -----
521     DO 2440 J=2,M

```

```

452      DO 2441 I=3,N
453      XXM(I)=YA CL(I,J)
454      YYM(I)=XA CL(I,J)
455 2441 CONTINUE
456      K=3
457      DO 2442 IK=1,NL2
458      XXM1(IK)=XXM(K)
459      YYM1(IK)=YYM(K)
460      K=K+1
461 2442 CONTINUE
462      CALL GRAPOL(XXM1,YYM1,NL2)
463 2440 CONTINUE
464 C
465 C SHIFT THE ORIGIN FOR THE MAPPING OF THE ENTRY PLANE ----
466      CALL SHIFT2(0.0,130.0)
467 C CHANGE LENGTH OF AXES AT ENTRY TO ACCOMMODATE DIFFERENT O.D.'S
468      CALL AXIPOS(0,0.0,0.0,140.0,1)
469      CALL AXIPOS(0,0.0,0.0,140.0,2)
470      CALL AXISCA(3,14,0.0,14.0,1)
471      CALL AXISCA(3,14,0.0,14.0,2)
472 C
473 C DRAW AXES FOR THE ENTRY PLANE
474      CALL AXIDRA(1,1,1)
475      CALL AXIDRA(-1,-1,2)
476 C LABEL AXES; FIRST MOVE PEN TO START POSITION RELATIVE TO NEW ORIGIN
477      CALL MOVTO2(50.0,-15.0)
478 C CALL CHAHOL(11HXB-A*LXIS*.)
479      CALL CHAHOL(10HIN X 0.1*.)
480 C MOVE PEN TO LABEL Y-AXIS
481      CALL MOVTO2(-15.0,50.0)
482 C ROTATE CHARACTER BY 90 DEGREES FOR Y-LABELLING
483      CALL CHAANG(90.0)
484 C LABEL Y-AXIS
485 C CALL CHAHOL(11HYB-A*LXIS*.)
486      CALL CHAHOL(10HIN X 0.1*.)
487 C RETURN CHARACTER ORIENTATION TO THE HORIZONTAL
488      CALL CHAANG(0.0)
489 C START DRAWING CIRCULAR CURVES AT THE ENTRY SECTION
490      DO 2460 I=2,N
491      DO 2461 J=1,M
492      XXN(J)=YB(I,J)
493      YYN(J)=XB(I,J)
494 2461 CONTINUE
495      CALL GRACUR(XXN,YYN,M)
496 2460 CONTINUE
497 C JOIN THE CENTROIDS OF THE LARGE TRIANGLES BY STRAIGHT LINES
498      DO 2470 J=2,M
499      DO 2471 I=3,N
500      XXM(I)=YBCL(I,J)
501      YYM(I)=XBCL(I,J)

```

```

502 2471 CONTINUE
503     K=3
504     DO 2472 IK=1,NL2
505     XXM1(IK)=XXM(K)
506     YYM1(IK)=YYM(K)
507     K=K+1
508 2472 CONTINUE
509     CALL GRAPOL(XXM1,YYM1,NL2)
510 2470 CONTINUE
511 C     DRAW LINE OF SYMMETRY BUT MOVE PEN FIRST TO THE ORIGIN
512     CALL MOVTO2(0.0,0.0)
513     XXNN=XXN(M)*10.0
514     YYNN=YYN(M)*10.0
515     CALL LINBY2(XXNN,YYNN)
516 C
517 C     CLOSE PLOT -----
518     CALL DEVEND
519 C
520 2570 WRITE(2,2022)
521 2022 FORMAT(10X,'PART TWO BEGINS HERE')
522 C
523 C TO CALCULATE THE EQUIVALENT RADIUS (RE) AT THE OUTLET
524     RE=SQRT((AA+AP)/PI)
525 C     DEFINE THE HOMOGENEOUS STRAIN--EPSILON-H..
526     EPSILOH=ALOG(AR)
527     EQSTH=EPSILOH
528 C     CALCULATIONS FOR THE AXISYMMETRIC TUBE DRAWING; NON-FUNCTIONS
529 C     OF THE EQUIVALENT DIE SEMI-CONE ANGLE (ALFAE).....
530     RE2=RE**2
531     RB2=RB**2
532     RP2=RP**2
533     BHA=RE-RP
534     BHB=RB-RP
535     VM=SQRT(3.0)
536     BFACTO=1.0/(1.0+YN)
537 C     A MEAN YIELD STRESS OVER THE STRAIN RANGE 0 TO EPSILON-H
538 C     IS DEFINED AND THE UNITS ARE IN TONF/SQ IN.....
539     YM=YK*EPSILOH**YN/(1.0+YN)
540     YMEST=YM
541     BFACT=BFACTO
542 C     TERMS APPEARING IN THE MEAN EQUIVALENT STRAIN EXPRESSION FOR THE
543 C     AXISYMMETRIC CASE.....
544     AJP=ALOG((RB2-RP2)/(RE2-RP2))
545     BJP=ALOG(RE2*(RE2-RP2)/(RB2*(RE2-RP2)))/6.0
546     CJP=RE/(RB2-RP2)**2*(RB**3-3.0*RB*RP2+2.0*RP**3)
547     DJP=RE/(RE2-RP2)**2*(RE**3-3.0*RE*RP2+2.0*RP**3)
548 C     TERMS FOR FACTORS I2 IN THE EXPRESSION FOR APPARENT STRAIN CALCULATIONS
549     FACTOZ1=ALOG((RB-RP)/(RB+RP)*(RE+RP)/(RE-RP))
550     FACTOZ2=ALOG((RB2-RP2)/(RE2-RP2))
551 C

```

```

552 C      TO GENERATE THE EQUIVALENT DIE SEMI-CONE ANGLES (2,4,6,7,8,.....
553 C      20 DEGREES)
554
555      DO 120 KONE=1,11
556 C      TO PERFORM CALCULATIONS FOR AN ANGLE OF 7 DEGREES.....
557      IF (KONE.EQ.11) GO TO 1111
558      LONE=KONE*2
559      GO TO 1117
560 1111 LONE=KONE*4
561 1117 ALFAE=LONE*PI/180.0
562 C ANGLES EXPRESSED IN RADIANS
563      SALFAE=SIN(ALFAE)
564      CALFAE=COS(ALFAE)
565      TALFAE=TAN(ALFAE)
566      COTFAE=1.0/TALFAE
567 C LENGTH OF THE DIE ALONG THE DRAW AXIS
568      DIEH=(RB-RE)/TALFAE
569 C RADIUS OF THE SHEAR SURFACE AT THE INLET (ROOB)
570      ROOB=DIEH*RB/(CALFAE*(RB-RE))
571      RC=ROOB
572 C
573      DIEHH=DIEH/LISC
574      WRITE(2,2025) LONE,DIEHH
575 2025 FORMAT(/5X,'SEMI-DIE ANGLE = ',I3,' DEGREES',/5X,'DIE HEIGHT
576      1 = ',F8.4,' INCHES',/)
577 C      BRANCH OFF IF NS=INFINITY, I.E. ROUND TO ROUND
578      IF (NSIDE.EQ.6) GO TO 2571
579 C
580 C      ***** UPPER BOUND PROBLEM FOR POLYGONAL DRAWING *****
581      WRITE(2,2300)
582 2300 FORMAT(/15X,'***** UPPER BOUND SOLUTION FOR POLYGONAL DRAWIN
583      1G *****',/)
584 C
585 C CALCULATION OF RADIAL DISTANCE OF THE PARTICLE(R) FROM THE AXIS
586 C PHI,NU, ...ETC, AND THE LENGTH OF THE FLOW PATH
587 C
588 C CALCULATIONS FOR THE SMALL TRIANGLES AT EXIT(A) AND ENTRY(B)
589      DO 125 I=3,N
590      DO 126 J=2,M
591      RAS(I,J)=SQRT(XACS(I,J)**2+YACS(I,J)**2)
592      RBS(I,J)=SQRT(XBCS(I,J)**2+YBCS(I,J)**2)
593      RRBS=RBS(I,J)/RC
594      THETAS(I,J)=ASIN(RRBS)
595      DB=RC*(1.0-CALFAE)
596      DA=DB
597      DBS(I,J)=RC*(COS(THETAS(I,J))-CALFAE)
598      PHIA=ATAN(XACS(I,J)/YACS(I,J))
599      BET2=2.0*BETA
600      IF (PHIA.GT.BETA) GO TO 127
601      DAS(I,J)=DA*(DHE/(2.0*COS(PHIA))-RAS(I,J))/RAS(I,J)

```

```

602      GO TO 128
603      127 DAS(I,J)=DA*(DHE/(2.0*COS(BET2-PHIA))-RAS(I,J))/RAS(I,J)
604      128 PHIB=ATAN(XBCS(I,J)/YBCS(I,J))
605      PHISBA(I,J)=PHIB-PHIA
606      ZS(I,J)=DIEH+DBS(I,J)-DAS(I,J)
607 C THE LENGTH OF THE PATH OF FLOW IN THE DIE ZONE
608 C
609      ZTS(I,J)=SQRT((XBCS(I,J)-XACS(I,J))**2+(YBCS(I,J)-YACS(I,J))**2+
610      1ZS(I,J)**2)
611 C
612      ZPS=SQRT((RBS(I,J)-RAS(I,J)*COS(PHISBA(I,J)))**2+ZS(I,J)**2)
613      EITAS(I,J)=ATAN(RAS(I,J)*SIN(PHISBA(I,J))/ZPS)
614      BETAS(I,J)=ATAN((RBS(I,J)-RAS(I,J)*COS(PHISBA(I,J)))/ZS(I,J))
615      CKIS(I,J)=ABS(BETAS(I,J)-THETAS(I,J))
616      126 CONTINUE
617      125 CONTINUE
618 C
619 C CALCULATIONS FOR THE LARGE TRIANGLES AT EXIT(A) AND INLET(B)
620      DO 130 I=3,N
621      DO 131 J=2,M
622      RAL(I,J)=SQRT(XACL(I,J)**2+YACL(I,J)**2)
623      RBL(I,J)=SQRT(XBCL(I,J)**2+YBCL(I,J)**2)
624      RRBL=RBL(I,J)/RC
625      THETAL(I,J)=ASIN(RRBL)
626      DBL(I,J)=RC*(COS(THETAL(I,J))-CALFAE)
627      PHIA=ATAN(XACL(I,J)/YACL(I,J))
628      IF (PHIA.GT.BETA) GO TO 132
629      DAL(I,J)=DA*(DHE/(2.0*COS(PHIA))-RAL(I,J))/RAL(I,J)
630      GO TO 133
631      132 DAL(I,J)=DA*(DHE/(2.0*COS(BET2-PHIA))-RAL(I,J))/RAL(I,J)
632      133 PHIB=ATAN(XBCL(I,J)/YBCL(I,J))
633      PHILBA(I,J)=PHIB-PHIA
634      ZL(I,J)=DIEH+DBL(I,J)-DAL(I,J)
635 C THE LENGTH OF THE PATH OF FLOW IN THE DEFORMATION ZONE
636 C
637      ZTL(I,J)=SQRT((XBCL(I,J)-XACL(I,J))**2+(YBCL(I,J)-YACL(I,J))**2+
638      1ZL(I,J)**2)
639 C
640      ZPL=SQRT((RBL(I,J)-RAL(I,J)*COS(PHILBA(I,J)))**2+ZL(I,J)**2)
641      EITAL(I,J)=ATAN(RAL(I,J)*SIN(PHILBA(I,J))/ZPL)
642      BETAL(I,J)=ATAN((RBL(I,J)-RAL(I,J)*COS(PHILBA(I,J)))/ZL(I,J))
643      CKIL(I,J)=ABS(BETAL(I,J)-THETAL(I,J))
644      131 CONTINUE
645      130 CONTINUE
646 C
647      GO TO 2700
648      WRITE(2,2040)
649      2040 FORMAT(5X,'LENGTH OF PATH OF FLOW IN THE DIE ZONE ZTS/ZTL',/)
650      WRITE(2,2003)
651      DO 134 I=3,N

```

```

652      WRITE(2,2041) (I,(ZTS(I,J),J=2,M))
653      WRITE(2,2042) (ZTL(I,J),J=2,M)
654 2042 FORMAT(15X,9(3X,F8.5))
655 2041 FORMAT(5X,12,3X,9(3X,F8.5))
656 134 CONTINUE
657 C
658 C OPTIMIZATION OF THE SHEAR WORK ; FIND THE VALUE OF T THAT
659 C MINIMIZES THE SHEAR WORK FACTOR R(S)
660 C
661 2700 UA=VLA
662      UB=UA/AR
663      WRITE(2,2045)
664 2045 FORMAT(5X, 'PARAMETER T   SHEAR FACTOR R(S)',/)
665 C
666 C GENERATE VALUES OF T BETWEEN 0 AND 1 (.....LATER TRY 0.....,-1)
667 C
668      DO 135 ITGEN=1,10
669      T=ITGEN*0.1
670      TP=1.0-T
671      RS=0.0
672      DO 136 I=3,N
673      DO 137 J=2,M
674 C VALUE OF R(S) FOR THE SMALL TRIANGULAR ELEMENTS
675      AREA=ARSTB(I)
676      THETA=THETAS(I,J)
677      EITA=KITAS(I,J)
678      CKI=CKIS(I,J)
679 C RESULTANT TANGENTIAL VELOCITY
680      URBS(I,J)=UB*SQRT((COS(T*THETA)*TAN(EITA)/(COS(TP*THETA)*COS(CKI))
681      1)**2+(-SIN(T*THETA)+COS(T*THETA)*TAN(CKI)+COS(T*THETA)*TAN(TP*THET
682      2A))**2)
683      RSS=URBS(I,J)*AREA/(UB*COS(T*THETA))
684 C VALUE OF R(S) FOR THE LARGE TRIANGULAR ELEMENTS
685      AREA=ARLTB(I)
686      THETA=THETAL(I,J)
687      EITA=EITAL(I,J)
688      CKI=CKIL(I,J)
689 C THE RESULTANT TANGENTIAL VELOCITY
690      URBL(I,J)=UB*SQRT((COS(T*THETA)*TAN(EITA)/(COS(TP*THETA)*COS(CKI))
691      1)**2+(-SIN(T*THETA)+COS(T*THETA)*TAN(CKI)+COS(T*THETA)*TAN(TP*THET
692      2A))**2)
693      RSL=URBL(I,J)*AREA/(UB*COS(T*THETA))
694 C
695      RS=RS+RSS+RSL
696 137 CONTINUE
697 136 CONTINUE
698      WRITE(2,2046) T,RS
699 2046 FORMAT(9X,F5.3,3X,F10.6)
700      RSV=RS
701      IF (ITGEN.EQ.1) GO TO 138

```

```

702 C SELECT THE MINIMUM SHEAR FACTOR AS THE COMPUTER PLOUGHS.....
703     IF (RSV.LT.RSM) GO TO 138
704     GO TO 135
705     138 RSM=RSV
706     TM=T
707     135 CONTINUE
708 C
709     WRITE(2,2047) TM,RSM
710     2047 FORMAT(//5X,'OPTIMAL T = ',F5.3,5X,'AND MINIMUM R(S) = '
711     1,F10.6,/)
712 C
713     T=TM
714     RS=RSM
715     TP=1.0-T
716 C CALCULATE SHAPE FACTOR F(S) USING THE OPTIMAL T FOR THE INTERNAL POWER
717 C
718     GVALUE=AP/(PI*SALFAE**2)
719     ROOBD=ROOB**2-GVALUE
720     ROOA=ROOB-DIEH/CALFAE
721     ROOAD=ROOA**2-GVALUE
722 C
723     FS=0.0
724     DO 140 I=3,N
725     DO 141 J=2,M
726 C THE VALUE OF F(S) FOR THE SMALL TRIANGULAR ELEMENTS
727     AREA=ARSTB(I)
728     THETA=THETAS(I,J)
729     EITA=EITAS(I,J)
730     CKI=CKIS(I,J)
731     RAD=RAS(I,J)
732     ROE=(RC-ZS(I,J))*COS(THETA)
733     PHI=PHISBA(I,J)
734     BETTY=BETAS(I,J)
735     ZDIEH=ZS(I,J)
736 C
737     SKA=4.0*(ROOA**4/ROOAD**2)
738     SKB=4.0*(ROOB**4/ROOBD**2)
739     TK=(1.0+TAN(CKI)*(-T*TAN(T*THETA)+1.0/COS(CKI)+TP*TAN(TP*THETA)))
740     T**2
741     UK=(1.0+RAD*COS(PHI)/((RC-ROE)*COS(THETA)*SIN(THETA)*COS(CKI))+
742     T*TAN(CKI)/TAN(THETA))**2
743     VKA=(-TAN(CKI)*(2.0*(ROOA**2/ROOAD)+1.0)-T*TAN(T*THETA)+TP*TAN(
744     T*THETA))**2
745     VKB=(-TAN(CKI)*(2.0*(ROOB**2/ROOBD)+1.0)-T*TAN(T*THETA)+TP*TAN(
746     T*THETA))**2
747     WK=((TAN(EITA)/COS(CKI))*(-T*TAN(TP*THETA)+TAN(CKI)+TAN(THETA)+
748     T*TP*TAN(TP*THETA)-1.0/TAN(THETA)))**2
749     XKA=((TAN(EITA)/COS(CKI))*(2.0*(ROOA**2/ROOAD)+1.0))**2
750     XKB=((TAN(EITA)/COS(CKI))*(2.0*(ROOB**2/ROOBD)+1.0))**2
751 C CALCULATE ROOT (K) FOR SMALL TRIANGLES AND HENCE F(S)

```

```

752      ROOTKA=SQRT(2.0*(SKA+TK+UK)+(VKA+WK+XKA))
753      ROOTKB=SQRT(2.0*(SKB+TK+UK)+(VKB+WK+XKB))
754 C
755      ROOTK=0.5*(ROOTKA*ROOA/ROOAD+ROOTKB*ROOB/ROOBD)*ZDIEH/COS(BETTY)
756      FSS=ROOTK*COS(T*THETA)*AREA/COS(TP*THETA)
757 C
758 C THE VALUE OF F(S) FOR THE LARGE TRIANGULAR ELEMENTS
759      AREA=ARLTB(I)
760      THETA=THETAL(I,J)
761      EITA=ETAL(I,J)
762      CKI=CKIL(I,J)
763      RAD=RAL(I,J)
764      ROE=(RC-ZL(I,J))*COS(THETA)
765      PHI=PHILBA(I,J)
766      BETTY=BETAL(I,J)
767      ZDIEH=ZL(I,J)
768 C
769      SKA=4.0*(ROOA**4/ROOAD**2)
770      SKB=4.0*(ROOB**4/ROOBD**2)
771      TK=(1.0+TAN(CKI))*(-T*TAN(T*THETA)+1.0/COS(CKI)+TP*TAN(TP*THETA))
772      **2
773      UK=(1.0+RAD*COS(PHI))/((RC-ROE)*COS(THETA)*SIN(THETA)*COS(CKI))+
774      1TAN(CKI)/TAN(THETA))**2
775      VKA=(-TAN(CKI))*(2.0*(ROOA**2/ROOAD)+1.0)-T*TAN(T*THETA)+TP*TAN(
776      1TP*THETA))**2
777      VKB=(-TAN(CKI))*(2.0*(ROOB**2/ROOBD)+1.0)-T*TAN(T*THETA)+TP*TAN(
778      1TP*THETA))**2
779      WK=((TAN(EITA)/COS(CKI))*(-T*TAN(TP*THETA)+TAN(CKI)+TAN(THETA)+
780      1TP*TAN(TP*THETA)-1.0/TAN(THETA))**2
781      XKA=((TAN(EITA)/COS(CKI))*(2.0*(ROOA**2/ROOAD)+1.0))**2
782      XKB=((TAN(EITA)/COS(CKI))*(2.0*(ROOB**2/ROOBD)+1.0))**2
783 C CALCULATE ROOT (K) FOR LARGE TRIANGLES AND HENCE F(S)
784      ROOTKA=SQRT(2.0*(SKA+TK+UK)+(VKA+WK+XKA))
785      ROOTKB=SQRT(2.0*(SKB+TK+UK)+(VKB+WK+XKB))
786 C
787      ROOTK=0.5*(ROOTKA*ROOA/ROOAD+ROOTKB*ROOB/ROOBD)*ZDIEH/COS(BETTY)
788      FSL=ROOTK*COS(T*THETA)*AREA/COS(TP*THETA)
789 C
790      FS=FS+FSS+FSL
791      141 CONTINUE
792      140 CONTINUE
793 C
794      WRITE(2,2050) FS
795      2050 FORMAT(5X,'THE VALUE OF F(S) = ',F10.6,/)
796 C
797      FS=FS*1.0/(2.0*PI*SQRT(3.0)*RB**2)
798 C
799 C CALCULATE THE MEAN EQUIVALENT STRAIN (EPSILON(M))--EQSTM AND THE
800 C HOMOGENEOUS EQUIV STRAIN (EQSTH)
801 C

```

```

802      RS=RS*1
803 C
804 C
805      VOL=UB*AB
806      EQSTM=(UB*AB*FS+(2.0/SQRT(3.0))*UB*RS)*2.0*NS/VOL+
807      1ALFAE/SALFAE**2-COTFAE
808 C TRAPPING VALUES TO SEE WHAT'S UP !!!!!!!!!!!!!!!....
809 C
810      EQSTR=2.0*UB*RS*2.0*NS/(VOL*SQRT(3.0))+ALFAE/SALFAE**2-COTFAE
811      EQSTIN=FS*2.0*NS
812      WRITE(2,2090) EQSTR,EQSTIN
813 2090 FORMAT(5X,'REDUNDANT STRAIN = ',F10.6/5X,'INTERNAL WORK STRAIN = '
814      1,F10.6,/)
815      WRITE(2,2051) EQSTM,EQSTH
816 2051 FORMAT(5X,'THE MEAN EQUIVALENT STRAIN = ',F10.6,/,5X,'THE HOMOG.
817      1 EQUIVALENT STRAIN = ',F10.6,/)
818 C
819      WRITE(2,2240)
820 2240 FORMAT(2X,'COEFFICIENT APPARENT YIELD STRESS DRAW FORCE DRAW S
821      1TRESS MEAN DIE-PRESS DRAW POWER DRAW/YIELD MEAN-PRESS/YIELD')
822      WRITE(2,2241)
823 2241 FORMAT(2X,'OF FRICTION STRAIN (TONF/SQ IN) (TONF) (TONF/S
824      1Q IN) (TONF/SQ IN) (H-POWER) STRESS STRESS RATIO',/)
825 C
826 C TO FIND FRICTION FACTORS I1* AND I2*
827 C
828 C
829 C
830      FAI21=2.0/SIN(ALFAE*2.0)*ALOG(AR)
831      FAI22=COTFAE*ALOG((RB-RP)/(RB+RP)*(RE+RP)/(RE-RP))
832      FAI2=FAI21+FAI22
833      ABAR=2.0*BETA*RB/(M-1)
834 C GENERATE COEFFICIENT OF FRICTION (0,0.02,0.04,.....,0.1)
835      DO 145 ICOEF=1,6
836      CMU=(ICOEF-1)*0.02
837 C
838      GO TO 5001
839 C
840      FI1=0.0
841      FI2=0.0
842 C INTEGRATE THE RESPECTIVE TERMS OVER THE DIE/TUBE INTERFACE
843      DO 146 J=1,M-1
844      THETA=THETAL(N,J+1)
845      BETA=BETAL(N,J+1)
846      CKI=CKIL(N,J+1)
847 C
848      ADBD=SQRT((XA(N,J+1)-XA(N,J))**2+(YA(N,J+1)-YA(N,J))**2)
849 C MEAN SLIDING ELEMENTAL SURFACE AREA
850      SLAREA=0.5*(ADBD+ABAR)*ZTL(N,J+1)
851      FI1=FI1+SLAREA*(SIN(THETA)+CMU*COS(THETA))

```

```

852      FI2=FI2+SLAREA
853      146 CONTINUE
854 C
855      FACT1D=(FI1+CMU*DIEH*2.0*BETA*RP)/AA
856 C
857      FACT2D=(FI2*ALOG(AR)/RED*CALFAE*UB+PLUGTOT/(2.0*NS))*CMU/VOL
858 C FACTORS THUS FOUND FOR COMPLETE SECTION
859      FACT1=FACT1D*2.0*NS
860      FACT2=FACT2D*2.0*NS
861 C
862 C
863      5001 FACT1=((AB-AA)*(1.0+CMU*COTFAE)+CMU*2.0*PI*RP*DIEH)/AA
864      FACT2=FAI2*CMU
865 C
866      FACT2=((AB-AA)*ALOG(AR)/SALFAE+PI*RP*DIEH*(1+AE))*UB*CMU/VOL
867 C
868 C MATERIAL HARDENING FACTOR ( YM/YMF) ....BFACTOR...
869 C ALSO AT THIS STAGE CALCULATE THE FRICTION WORK RATIO
870      BFACT=1.0/(1.0+YN)
871      PFACTO=BFACT*FACT2/FACT1
872 C HENCE THE CALCULATION OF THE OBJECT OF ALL THIS          ...APPARENT STRAIN
873      EQSTA=EQSTM/(1.0-PFACTO)
874 C
875 C DEFINE THE MEAN YIELD STRESS          ..... YIELDM UP TO MEAN EQUIVALENT
876 C STRAIN AND YMBAR OVER THE WHOLE STRAIN RANGE (EPSILON-A)
877      YMBAR=YK*EQSTA**YN/(1.0+YN)
878      YIELDM=YK*EQSTM**YN/(1.0+YN)
879 C
880 C CALCULATE THE DRAW STRESS, FORCE, AND THE CORRESPONDING POWER OF THE
881 C MACHINE ... ALSO THE RATIO OF THE STRESS TO THE MEAN YIELD STRESS
882 C
883      SIGMAZ=YMBAR*EQSTA
884      DRAWF=SIGMAZ*AA/LASC
885      RSIGYM=SIGMAZ/YMBAR
886 C
887      DIEPM=EQSTA*YMBAR/FACT1
888      RDI=YM DIEPM/YIELDM
889      DRAWP=DRAWF*VLA*2240.0/(550.0*12.0)
890 C
891      WRITE(2,2055) CMU,EQSTA,YMBAR,DRAWF,SIGMAZ,DIEPM,DRAWP,RSIGYM,
892      1RDI,YM
893      2055 FORMAT(4X,F5.3,6X,F8.6,4X,F8.4,5X,F8.4,4X,F8.4,7X,F8.4,6X,F7.3,5X,
894      1F8.5,6X,F8.5)
895      145 CONTINUE
896 C
897 C ***** LOWER BOUND SOLUTION FOR POLYGONAL DRAWING *****
898 C THE SUB-PROGRAM CALCULATES THE LOWER BOUND BY NUMERICAL INTEGRATION
899      WRITE(2,2640)
900      2640 FORMAT(///,15X,'***** THE LOWER BOUND SOLUTION OF SECTION DRAWING *
901      1*****')

```

```

902 C      PRINT THE HEADING FOR THE FINAL TABLE OF RESULTS
903      WRITE(2,2655)
904 2655  FORMAT(/,2X,'COEFFICIENT YIELD STRESS DRAW LOAD DRAW STRESS DI
905      1E PRESSURE PLUG PRESSURE DRAW/YIELD DIE P/YIELD PLUG P/YIELD'
906      2)
907      WRITE(2,2656)
908 2656  FORMAT(2X,'OF FRICTION (TONF/SQ IN) (TONF) (TONF/SQ IN) (TON
909      1F/SQ IN) (TONF/SQ IN) STRESS RATIO STRESS STRESS*')
910 C
911 C      CALCULATE CONICAL AND FLAT SURFACE ANGLES -----
912      ALFAC=ATAN((DD1-DHE)/(2.0*DIEH))
913      ALFAS=ATAN((DD1-DHE*COS(BETA))/(2.0*DIEH))
914      SALFAC=SIN(ALFAC)
915      CALFAC=COS(ALFAC)
916      SALFAS=SIN(ALFAS)
917      CALFAS=COS(ALFAS)
918 C      CONSTANTS FOR THE ELLIPSE -----
919      ASE=DD01*CALFAC/(2.0*SIN(ALFAC+ALFAS))
920      BSE=DD01*SQRT(CALFAC**2-CALFAS**2)/(2.0*SIN(ALFAC+ALFAS))
921 C
922 C      TO GENERATE THE MEAN COEFFICIENT OF FRICTION (0.0,0.02,-----,0.1)
923      DO 2645 ICoeff=1,6
924      CMU=(ICoeff-1)*0.02
925 C      NUMERICAL INTEGRATION OF THE DRAW STRESS -----
926 C      ACCUMULATIVE SURFACE AT DIE(TSURF1) AND PLUG(TSURF2) AND,
927 C      NORMAL FORCE ACCUMULATIVE (SUMF1 AND SUMF2)
928      TSURF1=0.0
929      TSURF2=0.0
930      SUMF1=0.0
931      SUMF2=0.0
932 C
933 C      FOR NO BACK-PULL, THE NORMAL STRESS AT THE INLET PLANE IS ZERO...
934      SIGMAZ=0.0
935 C      CONSTANTS -----
936      CKS1=SALFAS+CMU*CALFAS
937      CKC1=SALFAC+CMU*CALFAC
938      CKS2=CMU
939 C      DIE LENGTH (DIEHH) IS DIVIDED INTO 50 EQUAL ELEMENTS.....
940      NH=51
941      DZI=DIEHH/(NH-1)
942 C
943      AI1=A&B/(2.0*NS)
944 C      I REFERS TO THE SECOND FACE OF THE ELEMENT DENOTED BY I-1
945      DO 2647 I=2,NH
946      ZI=(I-1)*DZI
947      RI=DD01/2.0-ZI*TAN(ALFAC)
948 C      Y-VALUE OF THE ELLIPSE
949      YI=BSE*SQRT(2.0*ASE*ZI*CALFAS-ZI**2)/(ASE*CALFAS)
950      SYRI=YI/RI
951 C      CONICAL AND FLAT SURFACE INCLUDED ANGLES ALONG Z-XIS

```

```

952      CAMDAS=ASIN(SYRI)
953      CAMDAC=BETA-CAMDAS
954 C     AREA AT SECTION ZI .....
955      AI=0.5*RI**2*(COS(CAMDAS)*SIN(CAMDAS)+CAMDAC)-0.5*BETA*RPP**2
956      GO TO 2646
957 C     CHANGE OF X-SECTIONAL AREA OVER THE ELEMENT I .....
958      DAI=-RI*DZI*((COS(CAMDAS)*SIN(CAMDAS)+CAMDAC)*TAN(ALFAC)+((BSE*
959      1SIN(CAMDAS)**2/(ASE+CALFAS**2*RI))*(RI*(ASE+CALFAS-ZI)/SQRT(2.0*
960      1ASE*ZI+CALFAS-ZI**2)+TAN(ALFAC)*SQRT(2.0*ASE*ZI+CALFAS-ZI**2))))
961 C
962 C     CALCULATE SURFACE AREA OF ELEMENTS .....
963 C
964      2646 DAI=AI-AI1
965      DAS1=BSE*SQRT(2.0*ASE*ZI+CALFAS-ZI**2)*DZI/(ASE+CALFAS**2)
966      DACI=RI*CAMDAC*DZI/CALFAC
967      DASTI=DASI+DACI
968      DAS2I=BETA*RPP*DZI
969 C     ACCUMULATIVE SIGMAZ/Y(DASTI) AND SIGMAZ/(DAS2I)
970      SUMF1=SUMF1+SIGMAZ*DASTI
971      SUMF2=SUMF2+SIGMAZ*DAS2I
972 C     ACCUMULATIVE SURFACE AREAS .....
973      TSURF1=TSURF1+DASTI
974      TSURF2=TSURF2+DAS2I
975 C
976 C     DIMENSIONLESS STRESS .....
977      DSIGMAZ=(1.0/AI)*(-SIGMAZ*DAI+(1.0-SIGMAZ)*(CKS1*DASI+
978      1CKC1*DACI+CKS2*DAS2I))
979 C     STRESS ON SECOND FACE BECOMES STRESS FOR FACE I OF ELEMENT
980 C     I+1 .....
981      SIGMAZ=SIGMAZ+DSIGMAZ
982      GO TO 2648
983      WRITE(2,2626) YI,SYRI,CAMDAC,AI,DAI,SIGMAZ,TSURF1,TSURF2,SUMF1,
984      1SUMF2
985      2625 FORMAT(5X,5(3X,F13.4),/5X,5(3X,F13.4),/)
986      2648 AI1=AI
987      2647 CONTINUE
988 C
989      ANA=AI
990      AAS=AAA/(2.0*NS)
991      ANS=(AAS-ANA)/AAS
992 C     MEAN DRAW STRESS AND FORCE FOR THE LOWER BOUND .....
993 C     THE MEAN YIELD STRESS, YMEST, EXPRESSED IN TONF/SQ IN
994      SIGMAD=SIGMAZ*YMEST
995      RSIGYM=SIGMAZ
996      DRAWF=SIGMAD*ANA*2.0*NS
997 C     DIE/WORKPIECE MEAN PRESSURE
998      PM1=(1.0-SUMF1/TSURF1)*YMEST
999      RPM1YM=PM1/YMEST
1000 C     PLUG/WORKPIECE MEAN PRESSURE
1001      PM2=(1.0-SUMF2/TSURF2)*YMEST

```

```

1002      RPM2YM=PM2/YMEST
1003 C      PRINT COEFFICIENT OF FRICTION
1004 C      PRINT DRAW LOADS,STRESSES,DIE AND PLUG PRESSURE....
1005 C
1006      WRITE(2,2665) CMU,YMEST,DRAWF,SIGMAD,PM1,PM2,RSIGYM,RPM1YM,
1007      1RPM2YM
1008 2665  FORMAT(4X,F8.3,8X,F8.4,2(4X,F8.4),2(6X,F8.4),6X,F8.5,2(5X,F8.5))
1009 2645  CONTINUE
1010 C
1011 C      ***** THIS ENDS THE LOWER BOUND FOR POLYGONAL DRAW *****
1012 C
1013 C      ***** AXISYMMETRIC PROBLEM *****
1014 C
1015      WRITE(2,2580)
1016 2580  FORMAT(///,8X,'LOWER AND UPPER BOUND SOLUTIONS FOR AXISYMMETRIC DR
1017      1AWING',/)
1018 C      CALCULATE THE MEAN EQUIVALENT STRAIN(EPSILON-M) & THE REDUNDANT
1019 C      STRAIN (EPSILON-R) -----
1020 2571  EPSILOM=AJP+BJP+2.0/(3.0+VM)*ALFAE+(CJP+DJP)
1021      EPSILOR=EPSILOM-EPSILOH
1022      WRITE(2,2590) EPSILOH,EPSILOR,EPSILOM
1023 2590  FORMAT(5X,'THE HOMOG. EQUIVALENT STRAIN = ',F8.6,/5X,'THE REDUNDA
1024      INT EQUIVALENT STRAIN = ',F8.6,/5X,'THE MEAN EQUIVALENT STRAIN
1025      2 = ',F8.6,/)
1026 C      THE HEADING FOR THE FINAL TABLE OF RESULTS -----
1027      WRITE(2,2592)
1028 2592  FORMAT(11X,'I',27X,'UPPER BOUND SOLUTION',28X,'I',6X,'LOWER BOUND
1029      1SOLUTION',6X,'I')
1030      WRITE(2,2540)
1031 2540  FORMAT(2X,'COEFF OF YIELD STRESS DRAW FORCE DRAW STRESS MEAN D
1032      1IE-PRESS APPARENT PRESS/YIELD YIELD STRESS DRAW/YIELD PRESS/YI',/
1033      22X,'FRICTION (TONF/SQ IN) (TONF) (TONF/QS IN) (TONF/SQ IN)
1034      3 STRAIN STRESS RATIO (TONF/SQ IN) STRESS -STRESS',/)
1035 C
1036 C      TO GENERATE THE MEAN COEFFICIENT OF FRICTION MU=0.00,0.02,.....,0.10
1037      DO 2545 ICOEFF=1,6
1038      CMU=(ICOEFF-1)*0.02
1039 C      EVALUATE THE FACTORS I1 AND I2 -----
1040      FACTOI1=1.0/AA*((AB-AA)*(1.0+CMU*COTFAE)+CMU*2.0*PI*RP*DIEH)
1041      FACTOI2=CMU*COTFAE*FACTO21+2.0+CMU/SIN(ALFAE*2.0)*FACTO22
1042 C      USING THE MATERIAL WORK HARDENING FACTOR (B-FACTOR), EVALUATE
1043 C      THE PHI-FACTOR, THE APPARENT STRAIN(EPSILON-A),HENCE THE APPARENT
1044 C      FRICTIONAL STRAIN(EPSILON-F) AND THE MEAN STRESS(YM-BAR) OVER THE
1045 C      STRAIN RANGE 0 TO EPSILON-A -----
1046      PHIFACT=BFACTO*FACTOI2/FACTOI1
1047      EPSILOA=EPSILOM/(1.0-PHIFACT)
1048      EPSILOR=EPSILOA-EPSILOM
1049      YMBAR=YK*EPSILOA**YN/(1.0+YN)
1050 C      HENCE THE MEAN DRAW STRESS(SIGMAD OR THE DIMENSIONLESS DSIGMAD) &
1051 C      THE MEAN TOOL/TUBE PRESSURE(P-MEAN OR D-MEAN) FOR U-BOUND SOLUTION

```



A-14 THE AXISYMMETRIC TUBE DRAWING SOLUTIONS CORRESPONDING TO  
THE POLYGONAL TUBE DRAWING ON A CYLINDRICAL PLUG

In tube drawing the depth of metal shearing at the entry and exit to the deformation zone is small. Hence, the redundant work calculated at both the exit and the entry shear surfaces will not differ appreciably whether the velocity discontinuity assumed is tangential to a spherical, a conical or a plane surface. Furthermore, the range of the die semi-angles is restricted to  $20^\circ$  (78). A plane surface of velocity discontinuity and the convenient cylindrical co-ordinate system  $(r, \theta, z)$  were, therefore, selected for the theoretical analysis of the axisymmetric tube drawing.

A-14.1 Upper bound

For the axisymmetric case equation (3.69) gives the mean equivalent strain,

$$\begin{aligned} \bar{\epsilon}_m = & \ln \left\{ \frac{R_b^2 - R_p^2}{R_e^2 - R_p^2} \right\} + \frac{1}{6} \ln \left\{ \frac{R_e^2}{R_b^2} \cdot \frac{R_b^2 - R_p^2}{R_e^2 - R_p^2} \right\} \\ & + \frac{2}{3\sqrt{3}} \tan \alpha_e \left\{ \frac{R_b}{(R_b^2 - R_p^2)^2} \left[ R_b^3 - 3R_b R_p^2 + 2R_p^3 \right] \right. \\ & \left. + \frac{R_e}{(R_e^2 - R_p^2)^2} \left[ R_e^3 - 3R_e R_p^2 + 2R_p^3 \right] \right\} \end{aligned} \quad (A-14.1)$$

The factors  $I_1$  and  $I_2$  in equations (3.52) and (3.56) reduce to

$$I_1 = \frac{1}{A_a} \left\{ (A_b - A_a)(1 + \mu_m \cot \alpha_e) + \mu_m \cdot 2\pi R_p L \right\} \quad (A-14.2)$$

$$\begin{aligned} I_2 = & \mu_m \cot \alpha_e \ln \left\{ \frac{R_b - R_p}{R_b + R_p} \cdot \frac{R_e + R_p}{R_e - R_p} \right\} + \\ & 2\mu_m \operatorname{cosec} 2\alpha_e \ln \left\{ \frac{R_b^2 - R_p^2}{R_e^2 - R_p^2} \right\} \end{aligned} \quad (A-14.3)$$

∴ the draw stress is evaluated from equation (3.62), i.e.

$$\sigma_{za} = \bar{Y}_m \cdot \frac{\bar{\epsilon}_m}{(1 - \psi)}$$

where  $\psi = B \frac{I_2}{I_1}$  as given by equation (3.59) and equation (3.57)

gives the value of  $B = \frac{1}{1 + n}$

The mean pressure  $p_m$  is obtained from equation (3.61),

$$\text{i.e. } p_m = \frac{\bar{Y}_m}{I_1} \cdot \left( \frac{\bar{\epsilon}_m}{1 - \psi} \right)$$

#### A- 14.2 The lower bound solution

The integration of equation (3.82) for the axisymmetric tube drawing reduces to

$$\sigma_{za} = Y_m \frac{1 + \beta^*}{\beta^*} \left[ 1 - \left( \frac{h_a}{h_b} \right)^{\beta^*} \right] \quad (\text{A-14.4})$$

Where,  $\beta^* = 2\mu_m \cot \alpha_e$

$h_a$ ,  $h_b$  are the wall thicknesses of the exit equivalent circular tube and the inlet tubular stock respectively.

A-15 COMPUTER SUB-PROGRAMS TO CALCULATE THE  
MEAN COEFFICIENT OF FRICTION IN POLYGONAL  
TUBE DRAWING USING EQUATIONS (4.10) AND (4.19)

A-15.1 Evaluation of mean coefficient of friction by the  
 semi-analytical method (equation 4.10)

```

1     MASTER SEMIMETHOD
2 C   A COMPUTER PROGRAM TO EVALUATE THE EXPRESSION TO DETERMINE THE
3 C   MEAN COEFFICIENT OF FRICTION AND THE MEAN PRESSURE IN THE
4 C   SEMI-ANALYTICAL METHOD BASED ON AN EQUIVALENT CONICAL DIE
5 C   SPECIFY THE DIAGONAL LENGTH OF THE OUTPUT STOCK HA=HE=1.000 INCH
6 C   THE EQUIVALENT DIE SEMI-ANGLE (ALFAE IN DEGREES)
7     READ(1,299) DHE,IKONE
8     299 FORMAT(F5.3,2X,I2)
9 C   SPECIFY THE DRAWING VELOCITY (INCHES/SECOND) AND THE STRESS-STRAIN
10 C  CHARACTERISTIC OF THE UNDRAWN METAL, SIGMA=K*EPSILON**N, WHERE K
11 C  IS IN TONS/SQ_IN
12     READ(1,200) VLA,YK,YN
13     200 FORMAT(3F0.0)
14     PI=3.1415927
15 C  NUMBER OF TESTS SO FAR .....IDATE
16     READ(1,202) IDATE
17     202 FORMAT(I3)
18 C
19 C  THESE SET OF CARDS WRITE THE HEADINGS FOR THE OUTPUT.....IGNORE
20 C  WRITE(2,2000)
21 C2000 FORMAT(2X,'DRAW DATE      SIDES OF INPUT TUBE      SIZE OF EQUIVA
22 C  1LENT REDUCTION FLOW STRESS DRAW STRESS MEAN PRESS MEAN',/2X,
23 C  2'TEST OF          POLYGONAL O.D.(IN) X          PLUG      DIAM SINK  OF A
24 C  3REA      (SIGMA-F)      (SIGMAD)      (P-MEAN)      COEFF OF',/2X,'NO.
25 C  4DRAW TUBE (NS) GAUGE (IN)      (IN)      (/1000 IN) (PER CENT)
26 C  5TONF/SQ IN  TONF/SQ IN  TONF/SQ IN  FRICTION',/)
27 C
28 C  WRITE(2,2002)
29 C2002' FORMAT(2X,'DRAW DATE      SIDES OF INPUT TUBE      SIZE OF EQUIVA
30 C  1LENT REDUCTION FLOW STRESS DRAW STRESS YIELD STRESS MEAN',/2X,
31 C  2'TEST OF          POLYGONAL O.D.(IN) X          PLUG      DIAM SINK  OF A
32 C  3REA      (SIGMA-F)      (SIGMAD)      (Y-MEAN)      COEFF OF',/2X,'NO.
33 C  4DRAW TUBE (NS) GAUGE (IN)      (IN)      (/1000 IN) (PER CENT)
34 C  5TONF/SQ IN  TONF/SQ IN  TONF/SQ IN  FRICTION',/)
35 C
36     WRITE(2,2001)
37     2001 FORMAT(1X,'DRAW          EQUIVALENT REDUCTION  FLOW STRESS DRAW STRESS
38     1 MEAN PRESS HOMOGEN REDUNDAN HOMOG REDUND FRICTI MEAN EQ APPARE',/
39     21X,'TEST      DIAM SINK  OF AREA      (SIGMA-F)  (SIGMA-D)  (P-MEAN
40     3)  WORK      WORK      STRN STRAIN STRAIN STRAIN STRAIN',/1X,'NO.
41     4 (NS) (/1000 IN) (PER CENT) TONF/SQ IN TONF/SQ IN TONF/SQ IN (
42     SWH)  (WR)      (EH)  (ER)  (EF)  (EM)  (EA)',/)
43 C  READ THE DATA FOR INDIVIDUAL POLYGONAL TUBE DRAWING FROM ROUND
44 C  THE INPUT DATA INCLUDE THE TEST NUMBER, DATE OF THE DRAW, POLYGONAL
45 C  TUBE, TUBE O.D. X GAUGE, PLUG SIZE, DRAW STRESS, AND THE FLOW
46 C  STRESS OF THE DRAWN MATERIAL .....
47     DO 60 ITEST=1, IDATE
48     READ(1,205) NOTEST, IDAY, IMON, IYEAR, NOSIDE, TUBEOD, TGAUGE, PSIZE,
49     1SIGMAD, SIGMAF
50     205 FORMAT(I3,4(2X,I2),2(2X,F6.4),2X,F5.3,2(2X,F7.4))

```

```

51 C   CALCULATIONS FOR SECTION PARAMETERS, INCLUDING ANGLE(BETA), PLUG
52 C   RADIUS(RP), INLET AREA(AB), OUTLET AREA(AA), AREA RATIO(AR), PLUG
53 C   AREA(AP), REDUCTION OF AREA(RED), EQUIVALENT RADIUS AT EXIT(RE)
54     NS=NOSIDE
55     BETA=PI/NS
56     DO1=TUBEOD
57     T1=TGAUGE
58     RP=PSIZE/2.0
59 C   OTHERWISE FOR CLOSE PASS DRAW IN GENERAL RP=0.5*T1*(DO1/T1-2.0)
60     IF (NS.EQ.99) GO TO 101
61     SPARAM=NS*COS(BETA)*SIN(BETA)/4.0
62     GO TO 102
63 101 SPARAM=PI/4.0
64 102 CK=0.5*(1.0-2.0*RP/DHE)
65     AB=PI*T1**2*(DO1/T1-1.0)
66     AA=DHE**2*(SPARAM-PI*0.25*(1.0-2.0*CK)**2)
67     AR=AB/AA
68     AP=PI*RP**2
69     RED=1.0-1.0/AR
70     RED100=RED*100.0
71 C   CALCULATE THE EQUIVALENT RADIUS AT THE EXIT SECTION
72     RE=SQRT((AA+AP)/PI)
73     RB=DO1/2.0
74     RA=DHE/2.0
75 C   NOMINAL DIAMETRAL SINK -----EQSINK
76     RPCLOSE=0.5*T1*(DO1/T1-2.0)
77     EQSINK=(RPCLOSE-RP)*1000.0
78     LONE=IKONE
79     ALFAE=LONE*PI/180.0
80 C   THEREFORE -----
81     TALFAE=TAN(ALFAE)
82     COTFAE=1.0/TALFAE
83 C
84 C   CALCULATION FOR THE MEAN COEFFICIENT OF FRICTION AND THE MEAN
85 C   PRESSURE STARTS FROM HERE -----DIE LENGTH=DIEH-----
86     DIEH=(RB-RE)/TALFAE
87     WT=SIGMAD
88 C   CALCULATE THE MEAN EQUIVALENT STRAIN (EPSILON-*) CORRESPONDING TO
89 C   THE FLOW STRESS, AND THE MEAN APPARENT STRAIN (EPSILON-2) AND
90 C   HENCE THE FRICTIONAL WORK (WF)-----
91     EPSILOM=EXP(1.0/YN*ALOG(SIGMAF/YK))
92     EPSILOA=EXP(1.0/(1.0+YN)*ALOG(WT*(1.0+YN)/YK))
93     WF=WT-YK/(1.0+YN)*EPSILOM**(1.0+YN)
94     EPSILOH=ALOG(AR)
95     EPSILOR=EPSILOM-EPSILOH
96     EPSILOF=EPSILOA-EPSILOM
97     WH=YK/(1.0+YN)*EPSILOH**(1+YN)
98     WR=WT-WF-WH
99 C   WHERE WF AND WR ARE THE HOMOGENEOUS AND REDUNDANT WORK RESPECTIVELY....
100 C

```

```

101 C      DETERMINE THE MEAN COEFFICIENT OF FRICTION (CMU)
102 C      THE DENOMINATOR (CMUDE) AND THE NUMERATOR (CMUNU)
103      CMUNU=WF*RED/(1.0-RED)
104 C
105      CMUDE1=WT*(2.0/SIN(ALFAE*2.0)*ALOG(AR)+COTFAE*ALOG((RB-RP)/(RB+RP)
106      1*(RE+RP)/(RE-RP)))
107      CMUDE2=WF/AA*((AS-AA)*COTFAE+2.0*PI*RP*DIEH)
108      CMUDE=CMUDE1-CMUDE2
109      CMU=CMUNU/CMUDE
110 C      TO CALCULATE THE MEAN PRESSURE(P-MEAN) EVALUATE THE FACTOR I1....
111      FACTI1=RED/(1.0-RED)*(1.0+CMU*COTFAE)+2.0*PI*RP*DIEH/AA
112      PMEAN=SIGMAD/FACTI1
113 C      DEFINE THE RESULTING MEAN YIELD STRESS OVER THE STRAIN
114 C      RANGE 0 TO EPSILON-M -----
115      YMEAN=YK/(1.0+YN)*EPSILOA**YN
116      YMBAR=YMEAN
117      YSIGMA=SIGMAD/YMEAN
118      YPM=AN=PMEAN/YMEAN
119 C
120 C      TABULATE THE RESULTS -----
121 C      WRITE(2,2005) NOTEST, IDAY, IMON, IYEAR, NOSIDE, TUBEOD, TGAUGE, PSIZE,
122 C      1EQSINK, RED100, SIGMAF, SIGMAD, PMEAN, CMU, YPMEAN
123 C      1EQSINK, RED100, SIGMAF, SIGMAD, YMEAN, CMU, YSIGMA
124 C2005 FORMAT(2X, I3, 2X, 2(I2, '/ '), I2, 4X, I2, 4X, F6.4, 1X, 'X', 1X, F6.4, 3X, F5.3,
125 C      16X, F4.1, 7X, F5.2, 3(6X, F7.4), 4X, F6.4, 2X, F6.4
126 C A NEW SET OF WRITING
127      WRITE(2,2006) NOTEST, NOSIDE, EQSINK, RED100, SIGMAF, SIGMAD, PMEAN,
128      1WH, WR, EPSILOH, EPSILOR, EPSILOF, EPSILOM, EPSILOA, WF
129      2006 FORMAT(1X, I3, 3X, I2, 5X, F4.1, 6X, F5.2, 6X, F7.4, 2(5X, F7.4), 2(2X, F7.4),
130      14(2X, F5.3), 3X, F5.3, 1X, F7.4)
131 C
132      60 CONTINUE
133      STOP
134      END

```

A-15.2 Evaluation of mean coefficient of friction by the  
split rotating die method (equation 4.19)

```

1 MASTER SPLITDIE
2 C COMPUTER PROGRAM TO EVALUATE THE MEAN COEFFICIENT OF FRICTION FROM
3 C THE SPLIT ROTATING DIE EXPERIMENTS
4 C THESE SET OF CARDS PRINT THE HEADINGS FOR THE INPUT AND OUTPUT VALUES
5 WRITE(2,2000)
6 2000 FORMAT(2X,'DRAW DATE SIDES OF INPUT TUBE SIZE OF EQUIVA
7 1LENT REDUCTION DRAW AXIAL MEAN APPLIED CHECKING'
8 2,/2X,'TEST OF POLYGONAL O.D.(IN) X PLUG DIAM SINK'
9 3 OF AREA FORCE THRUST COEFF OF TORQUE TA QUADRATIC EQUA'
10 4,/2X,'NO. TEST TUBE (NS) GAUGE (IN) (IN) (/1000 IN)
11 5 (PER CENT) P(TONF) Q(TONF) FRICTION (TONF-IN) CMU1 CMU2',/
12 6)
13 C
14 C READ THE INPUT DATA..... AXIAL DRAG AT THE DIE (Q) AND THE DRAW
15 C FORCE (P). ALSO THE TEST NUMBER,DATE,TEST TUBE SPECIFICATIONS
16 C AND THE PLUG SIZE
17 PI=3.1415927
18 C USING DEGREES,DEFINE THE SEMI-ANGLE OF THE CONICAL DIE (ALFA-D)
19 C AND THE SEMI-ANGLE OF THE PLANE SURFACES OF THE SPLIT DIE (ALFA-S)
20 C FOR THE PARTICULAR DESIGN
21 C THE MEAN RADIUS OF THE SPLIT DIE R-MEAN (INCHES); DIAGONAL LENGTH
22 C DHE (=HA)
23 READ(1,299) ALFAD,ALFAS,RMEAN,DHE
24 299 FORMAT(4F0.0)
25 READ(1,200) ITDATE
26 DO 60 ITEST=1,ITDATE
27 READ(1,205) NOTEST,IDAY,IMON,IYEAR,NOSIDE,TUBEOD,TGAUGE,PSIZE,
28 1PDRAW,QAXIAL,PLUGFO,AFORCE
29 205 FORMAT(I3,4(2X,I2),2(2X,F6.4),2X,F5.3,4(2X,F7.4))
30 200 FORMAT(I3)
31 C CALCULATION OF SECTION PARAMETERS, INCLUDED ANGLE(BETA)
32 C PLUG RADIUS(RP),INLET AREA(AS),OUTLET AREA(AA),AREA RATIO(AR),
33 C PLUG AREA(AP),AND THE REDUCTION OF AREA(RED) .....
34 C
35 NS=NOSIDE
36 DO1=TUBEOD
37 T1=TGAUGE
38 BETA=PI/NS
39 RP=PSIZE/2.0
40 SPARAM=NS*COS(BETA)*SIN(BETA)/4.0
41 CK=0.5*(1.0-2.0*RP/DHE)
42 AB=PI*T1**2*(DO1/T1-1.0)
43 AA=DHE**2*(SPARAM-PI*0.25*(1.0-2.0*CK)**2)
44 AR=AB/AA
45 AP=PI*RP**2
46 RED=1.0-1.0/AR
47 RED100=RED*100.0
48 RPCLOSE=0.5*T1*(DO1/T1-2.0)
49 C NOMINAL DIAMETRAL SINK EXPRESSED IN 1/000 OF AN INCH.....
50 E2SINK=(RPCLOSE-RP)*1000.0

```

```

51     ALFAE=DALFAE*PI/180.0
52     ALFAD=DALFAD*PI/180.0
53 C   CALCULATE THE MEAN COEFFICIENT OF FRICTION(CMU) AND THE
54 C   CORRESPONDING APPLIED TORQUE TA (TONF-IN)
55     P=PDRAW
56     Q=P-PLUGFO-AFORCE
57     TALFAE=TAN(ALFAE)
58     TALFAD=TAN(ALFAD)
59     A=1.0
60     B=(P/Q)*(1.0/TALFAE+TALFAD)
61     C=(P/Q)*(1.0-TALFAD/TALFAE)
62     T2QUAD=SQRT(B**2-4.0*A*C)
63     CMU1=(-B-T2QUAD)/(2.0*A)
64     CMU2=(-B+T2QUAD)/(2.0*A)
65 C   TO CALCULATE THE APPROPRIATE VALUE -----
66     IF (CMU1.GT.CMU2) GO TO 101
67     CMU=CMU2
68     GO TO 102
69 101  CMU=CMU1
70 C   WITH CORRECT VALUE OF CMU, EVALUATE THE APPLIED TORQUE
71 102  TNUM=1.0-(CMU+TALFAE)/(1.0-CMU*TALFAE)
72     TA=RMEAN*CMU*P/COS(ALFAD)*1.0/TNUM
73 C   CALCULATE THE MEAN PRESSURE
74 C   DEFINE THE DIE LENGTH L (=DIEH)
75     DIEH=0.5*(D01-DHE*COS(BETA))/TALFAE
76     RB=D01/2.0
77     SINHET=1.0-DIEH/RB*TALFAE
78     THETA1=ASIN(SINHET)
79     AS=NS*RB**2/(4.0*SIN(ALFAE))*(-SIN(2.0*THETA1)+2.0*(PI/2.0-THETA1)
80     1)
81     PMEAN=P/(A3*(1.0-CMU**2)*SIN(ALFAE))
82 C   TABULATE THE RESULTS -----
83 C
84     WRITE(2,2005) NOTEST, IDAY, IMON, IYEAR, NOSIDE, TUBEOD, TGAUGE, PSIZE,
85     1EQSINK, RED100, PDRAW, QAXIAL, CMU, TA, CMU1, CMU2, PMEAN
86 2005 FORMAT(2X, I3, 2X, 2(I2, '/ '), I2, 4X, I2, 4X, F6.4, 1X, 'X', 1X, F6.4, 3X, F5.3,
87     16X, F4.1, 7X, F5.2, 4X, F7.4, 2(2X, F7.4), 4X, F8.4, 3(1X, F7.4))
88     60 CONTINUE
89     STOP
90     END

```

A-16 Hydraulic drawbench: Assembly and design of equipment<sup>†</sup>

<sup>†</sup> Footnote

The work set out in detail in this section took a substantial fraction of the research time. Initially, the object of the research incorporated the installation of the tube drawing rig, design and manufacture of the equipment to measure the required draw parameters. However, the persistent shortage of the technical assistance forced the work on this bench to be abandoned eventually and the entire experimental work, therefore, was carried out on the operating 'Brookes' bench. At the time of typing the thesis, all the parts had been manufactured and it remained only for the calibration of the load and speed measuring transducers and the final inspection of the hydraulic system.

## A-16.1 INTRODUCTION

The experimental investigations of the drawing of polygonal tube from round stock was initially to be carried out on two separate benches. An assembled "Brookes" drawbench with instrumentation (see Frontispiece) and a newly installed bench acquired from the Department of Mechanical Engineering, Sheffield University (see Plate A-16.1). The design capacity for the two benches is 30 tonf, but there are differences in the operating performances and the length of their strokes.

### A-16.1.1 "Brookes" hydraulic bench

The drawbench has a stroke of 54 in and a speed of 0 to 15 ft min<sup>-1</sup>. The bench previously used to draw polygonal bars from round stock and polygonal tubes from round on the corresponding polygonal plugs (2, 1), was complete with instrumentation. In addition, the drawbench was fitted with a split rotating die rig for the direct determination of the mean coefficient of friction and the mean pressure.

The technical specifications of this bench are reproduced in Appendix A-6.1.

The bench in operation is not as stiff as the "Sheffield" bench. When drawing, the dog was observed to lift off the bench, thus imparting a bending moment to the drawn tube. The dog assembly connected to the load cell through a trunion pin; the load cell was in turn, bolted to a cross-beam that pivoted freely between the tie-bars. The tie-bars were fixed to the head of the ram of the hydraulic cylinder and ran freely on the flanged wheels. The wheels tended to lift off the track especially when the rotating die was used.

#### A-16.1.2. "Sheffield" hydraulic drawbench

This drawbench designed for drawing tubes of  $2\frac{1}{8}$  in diameter and to withstand a load of 30 tonf at  $100 \text{ ft min}^{-1}$ , has a stroke of 120 in.

The technical details of this bench are given in Appendix A-6.2.

The carriage runs along the centre line between the beams fixed to the side frame of the drawbench. The sliding brass collars have just the minimum clearance needed to allow free relative motion. Therefore, during drawing, the carriage was restrained from lifting off the centre line of the bench.

To restore the drawbench to its operational condition, the main motor, the oil reservoir and some of the low pressure piping were required. The rest of the 'chapter' describes briefly the work done on the bench and the design of the essential equipment. The mechanical drawings of these components are given in Appendix A-17.

#### A-16.2 ASSEMBLY

The bench as received was disconnected and, therefore, the task undertaken included the installation, modification and the manufacture of equipment to measure the various parameters to verify the theory for the drawing of polygonal tubes from round stock. The drive motor and respective starter, the oil reservoir, and the low pressure pipework to the pump and the exhaust line, were acquired separately.

A platform of steel U-channels was constructed to mount the motor and the oil reservoir. Gravity flow to the pump was found adequate; the infeed pipe from the reservoir passed through a square manifold, fabricated in the Departmental workshop, before branching

off into the four pump inlets.

The condition of the seals and the valves was examined visually and the piping generally cleaned. To economise in space, the pipe layout was placed under the bench; this necessitated some bending and cutting of the pipes. These pipes were bent cold to avoid formation of scale and consequential weakening if heat had been used. General precautionary measures were observed also when cutting the pipes to ascertain that no abrasive particle or dirt was trapped in the pipe.

The temperature rise of the chain drive was not of great concern; periodical greasing of the chain replaced the initial cost of continuous lubrication. The power available to the drive, 50 hp, was less than a half of the design value. Furthermore, the work in the laboratory was intermittent.

#### A-16.3. MODIFICATION OF THE DRAWBENCH AND THE DESIGN OF EQUIPMENT

In the drawing tests, the following parameters were measured:

- (i) the draw load
- (ii) the torque at the tag end
- (iii) the draw speed
- (iv) the plug load
- (v) the load at the die and
- (vi) the mean coefficient of friction.

In order to fit the equipment for the measurement of the above quantities, some modifications of the drawbench were necessary.

These included:

- (1) the thrust block assembly to hold the die, the die load cell and the split rotating die rig (see mechanical drawings on pages A155, A156 and A157).
- (2) the dog assembly to transmit the draw load and the torque

reaction to the tag load cell (see mechanical drawings on page A158) and

- (3) the thrust blocks at the tail end of the bench to hold the plug load cell (see mechanical drawings on pages A159 and A165).

One major consideration put into the design of the thrust block assembly at the die was to keep the tag length of the tube as short as possible, to avoid wasting stock and to reduce the cost of tagging.

One plug thrust block consisted of a single plate fixed to the rear of the bench. The other block fabricated by welding four parts together, could be bolted anywhere on the U-channel between the rear of the bench and the die thrust block, depending on the length of the plug bar.

#### A-16.3.1. The dog assembly

The dog assembly consisted of a trunion pin, two jaw side holders, the block housing and the jaws. The conventional wedge-type jaws were used to grip the tagged tubes.

The jaw side holders fitted the ends of the trunion pin where it protruded from the cross-holes of the load cell at the tag, and carried the drawing force and the torque reaction, and formed the wedge angle for the jaws. These side jaw holders fitted inside the rectangular housing which resisted the splitting force in the jaws and held them in alignment against the torque reaction, but they did not carry any direct drawing force.

The dog pivoted freely on the trunion pin and a wheel was attached therefore to support it when not drawing. The height of the wheel was

such that it lifted clear off the track during the working stroke and did not interfere with the self-alignment of the load cell. To a lesser extent this arrangement reduced unnecessary pre-loading.

#### A-16.3.2. The measurement of the drawing parameters

The draw force and the torque were measured by a load cell at the tag holder of the drawbench, the plug force was measured by a load cell fixed at the rear of the bench and a ring load cell at the die thrust block measured the die load. The draw speed was obtained by a direct method, based on the measurement of finite distances and the time to cover them. The determination of the mean coefficient of friction by the split rotating die rig was carried out on the "Brookes" bench, but the rig could be transferred readily to this drawbench with a modified driving system.

##### A-16.3.2.1. The load cells

The load cells were designed for a nominal maximum of 0.1% strain in the active direction of the gauges, under the maximum expected loading conditions. They were heat treated and lapped before bonding the gauges. The three load cells are:

- (1) the load cell at the tag (see mechanical drawing on page A160).
- (2) the load cell at the plug end (see mechanical drawing on page A164) and
- (3) the ring load cell at the die (see mechanical drawing on page A166).

##### A-16.3.2.1.1. The tag load cell

This load cell, in addition to measuring the draw force, was designed also to measure the rotational torque. At a combined maximum draw load of 30 tonf and a torque of 500 lbf-in, the principal strains in the respective directions of the gauges were slightly less than 0.1%.

One end of the load cell was connected to the dog through a trunnion pin, while the other flanged end was bolted to the cross-plate of the sliding carriage. This load cell was fixed to the plate by passing it through from the rear. The clearance between the brass collars of the carriage and the two parallel beams along which the carriage slides is just the minimum distance required. Therefore, the movement is only very slight and is a characteristic of a stiff bench. The cross-plates on the carriage were modified to withstand the torque reaction in addition to the direct load (see mechanical drawings on page A159).

#### A-16.3.2.1.2 The plug load cell

The load cell was machined from a cylindrical block with a 2 in bore and designed for a maximum strain of 0.1% for a load of 10 tonf. One end of the flanged cell bolted to the rear plate of the drawbench with the axis aligned with that of the die.

#### A-16.3.2.1.3 The die load cell

The load cell designed for a maximum axial load of 30 tonf, consisted of a continuous ring of a square cross-section. On one side were eight integral supports equally spaced and on the other side were an equivalent number of the equispaced supports in positions equal to half the pitch. The ring was thus formed from a continuous series of circumferentially shaped beams which strained in terms of bending and torsion when subjected to an axial thrust. The stress and strain distribution, and the stiffness of this type of load cell is discussed elsewhere in detail by Basily (2).

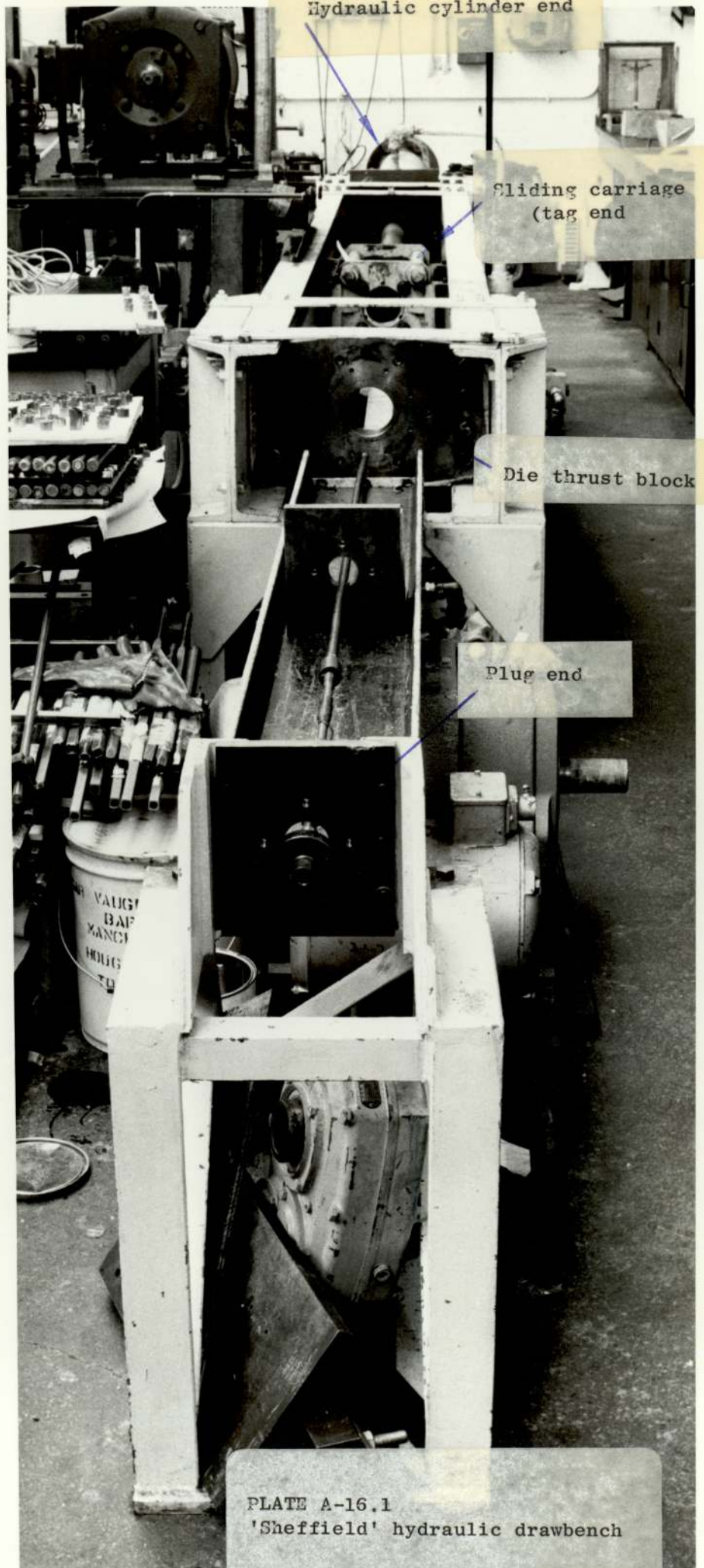
One set of the sectoral supports was bolted to the thrust block and the other set to the die holder plate. Care was taken to ensure that the presence of threads did not affect the stress

distribution at the points at which the strain gauges were bonded.

#### A-16.3.2.2. The draw speed measuring device

An aluminium angle of  $\frac{3}{4}$  in x  $\frac{3}{4}$  in x  $\frac{1}{8}$  in with a row of 2 mm diameter holes spaced at  $\frac{1}{4}$  in intervals, was fixed to the side frame of the drawbench. The photo-cell and the light source were mounted on a bracket on the carriage which was fixed to the ram of the hydraulic cylinder. Thus the light activated switch receives intermittently the illumination, for every  $\frac{1}{4}$  in movement of the ram.

The pulses from the photo-cell are recorded on the u-v chart against the time signals of the quartz timer installed in the recorder. The time lapse between the signals is, therefore, measured accurately and the mean draw speed derived. During the experiments, the time is set to give a pulse every 0.1 s depending on the drawing speed.



Hydraulic cylinder end

Sliding carriage  
(tag end)

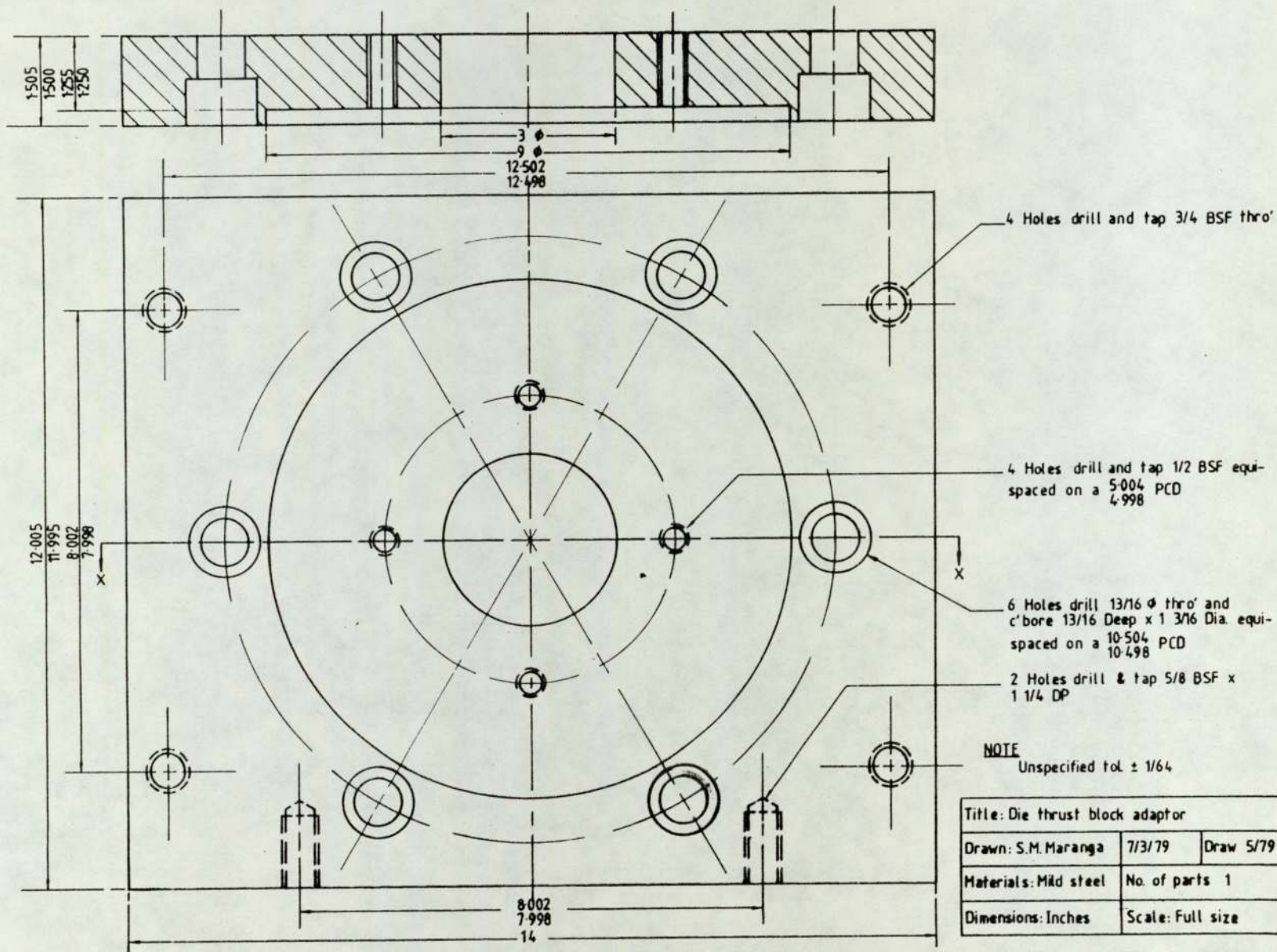
Die thrust block

Plug end

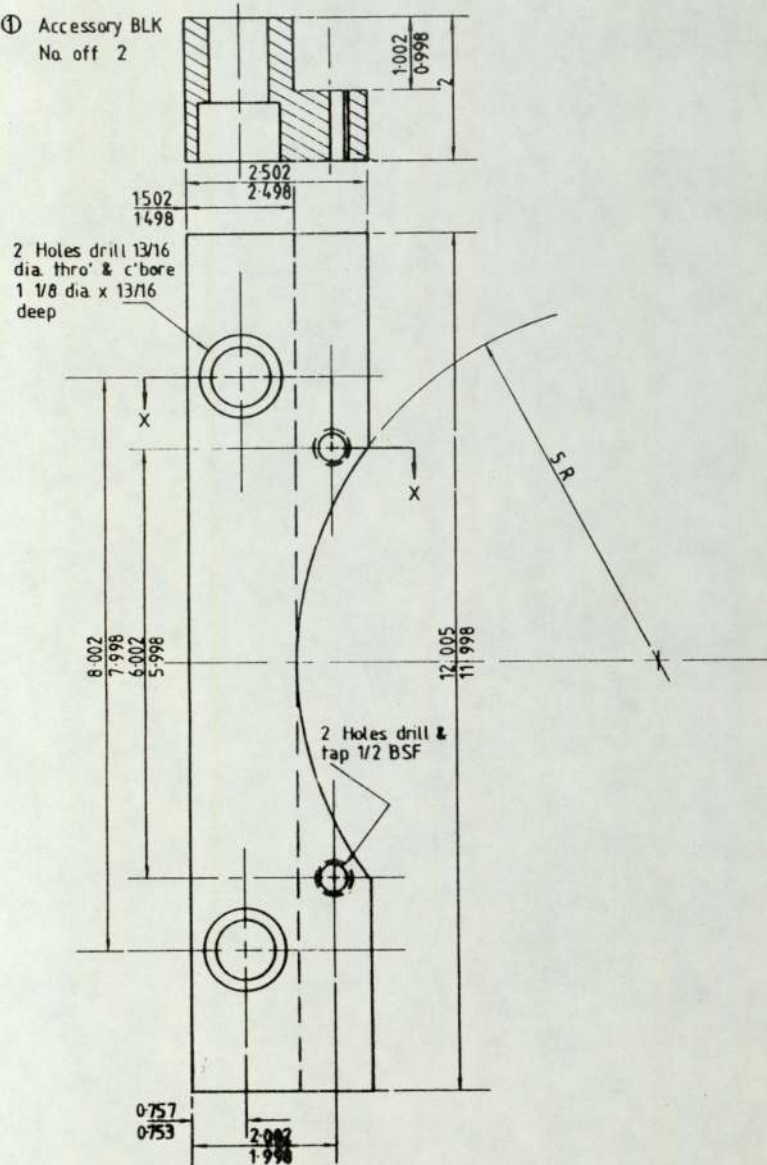
PLATE A-16.1  
'Sheffield' hydraulic drawbench

A-17 MECHANICAL DRAWINGS OF PARTS  
FOR THE 'SHEFFIELD' DRAWBENCH  
ASSEMBLY AND OTHER TUBE DRAWING  
ACCESSORIES

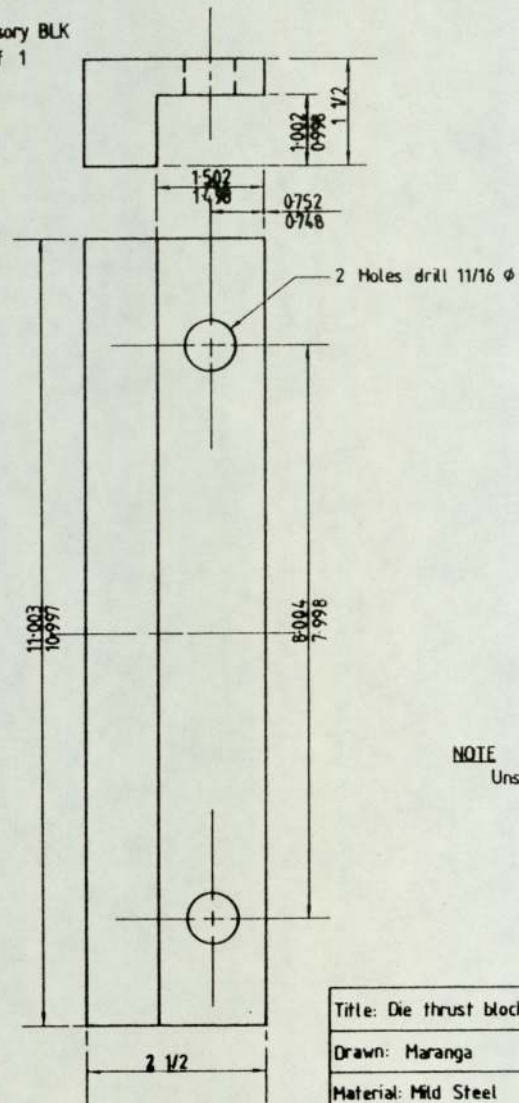
- A155 -



① Accessory BLK  
No off 2



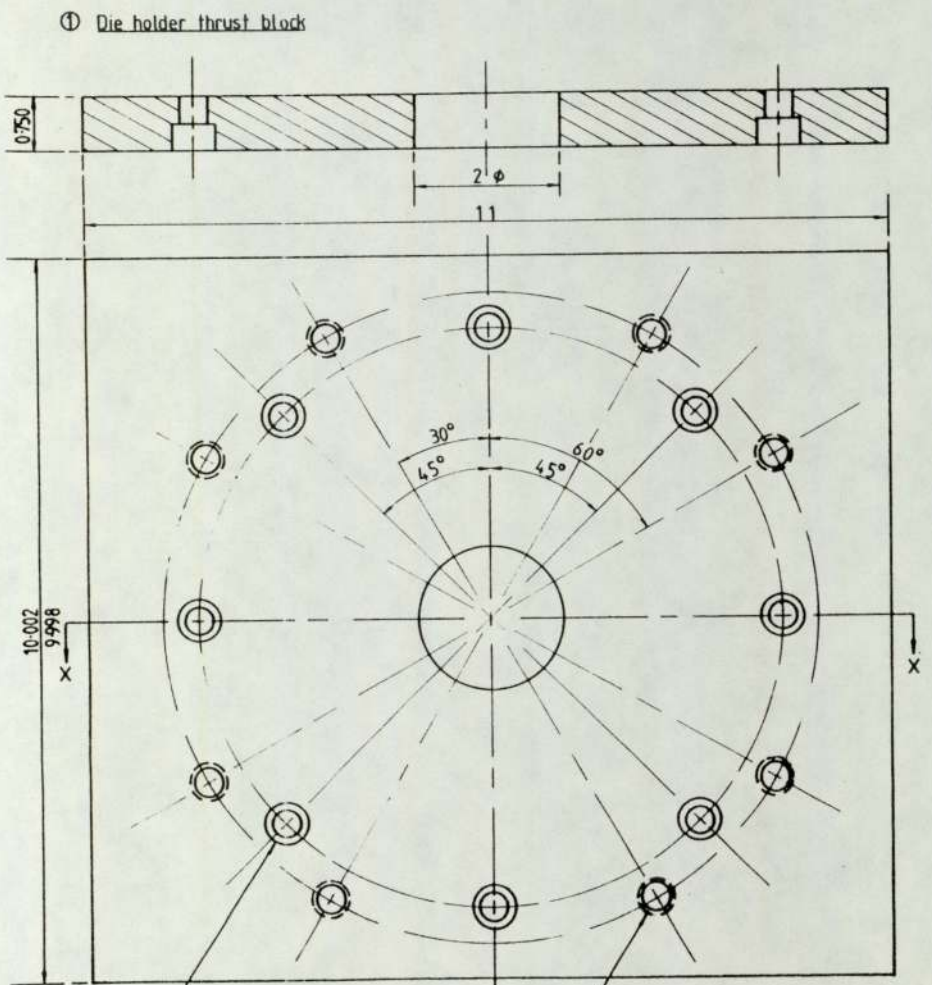
② Accessory BLK  
No off 1



NOTE  
Unspecified tol. ±1/64

Title: Die thrust block accessory		
Drawn: Maranga	7/3/79	Draw 5b/79
Material: Mild Steel	No. of parts specified	
Dimensions: Inches	Scale: 1:1	

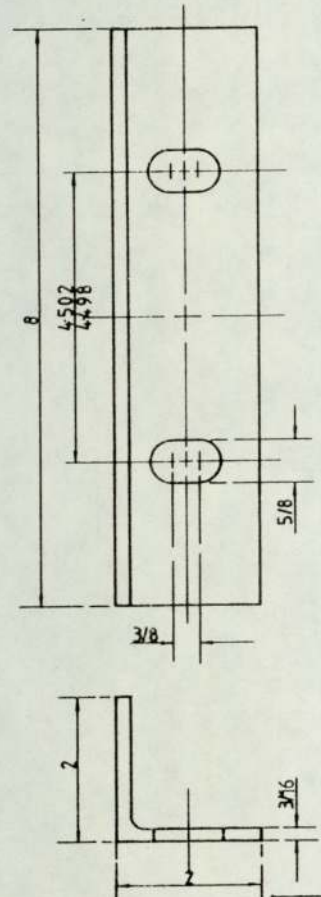
- A157 -



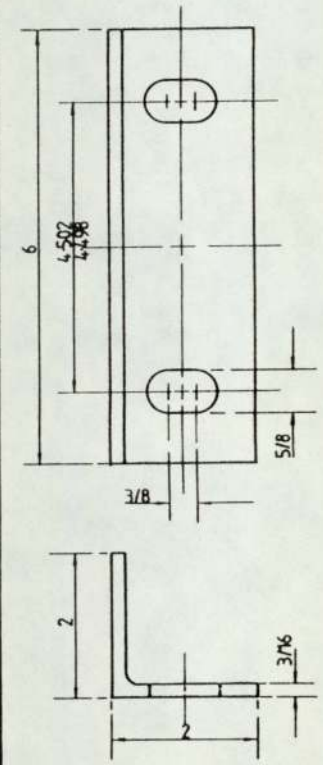
8 Holes drill  $7/16 \phi$  thro' and c'bore  
 $11/16 \phi \times 3/8$  DP equ-spaced on  
 8-102 PCD  
 8-098

8 Holes drill and tap  $1/2$  BSF  
 on 9-002 PCD  $5/8$  DP  
 8-998

② Holder block accessory 1  
 No. off 2

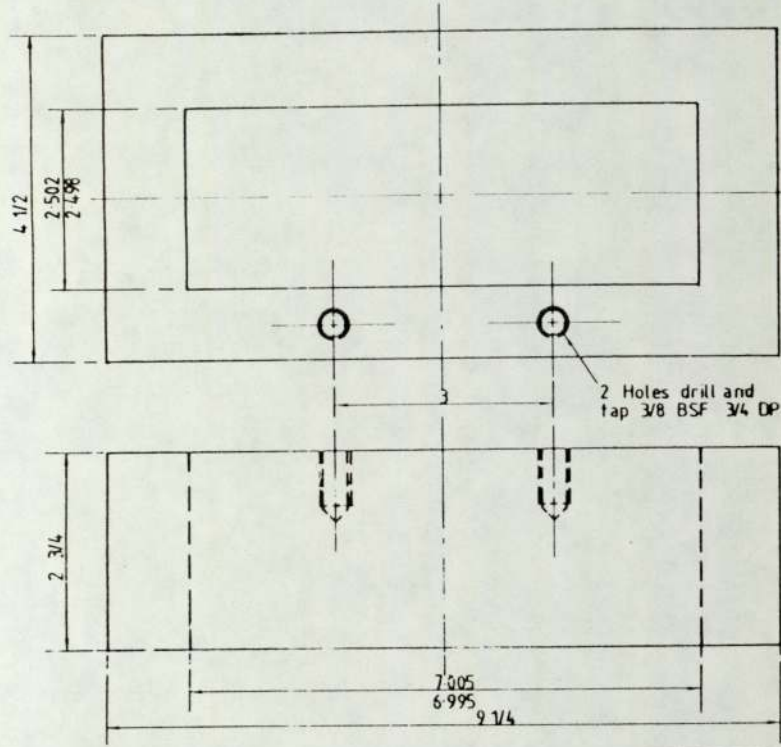


③ Holder block accessory 2  
 No. off 2

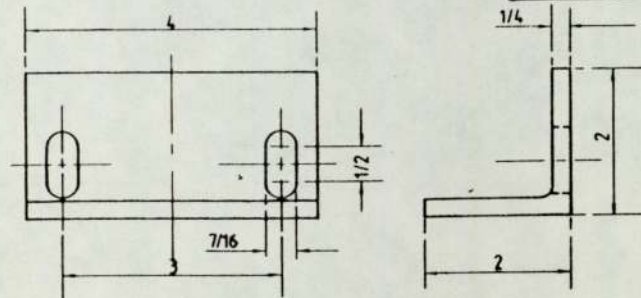


Title: Die holder block-assembly		
Drawn: S.M. Maranga	23/3/79	Draw 6/79
Material: Mild Steel	No. of parts stated for each	
Dimensions: Inches	Scale: 1:1	

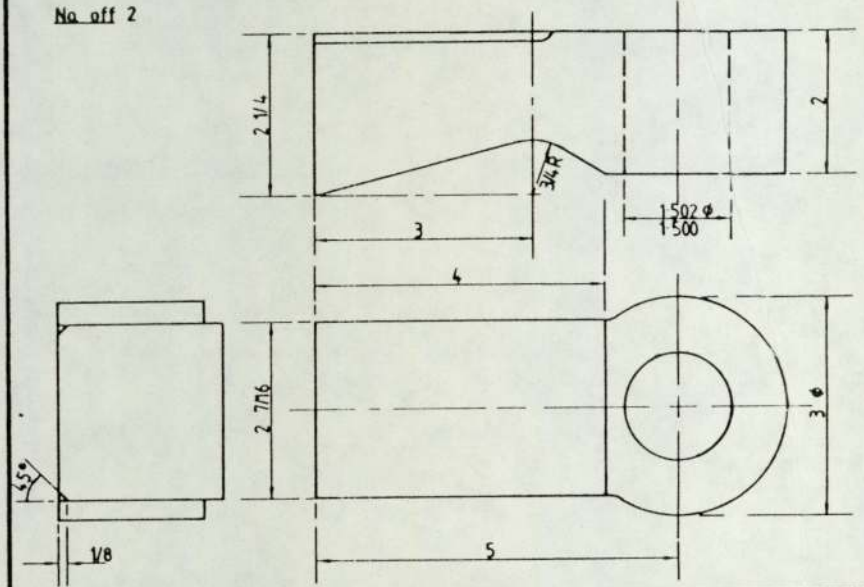
① Jaw block housing



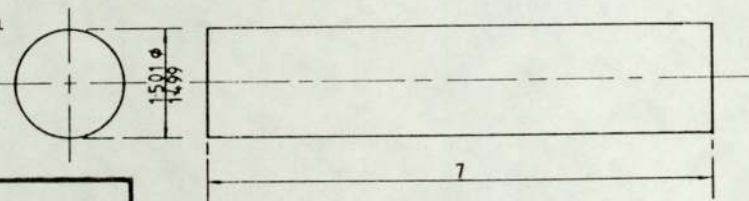
② Heel plate  
Material: Mild steel



③ Jaw side holders  
No. off 2

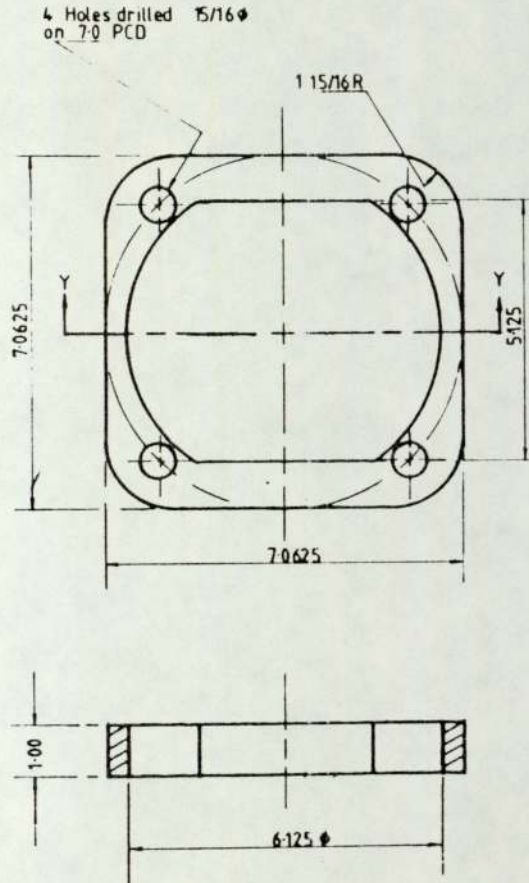


④ Trunion pin

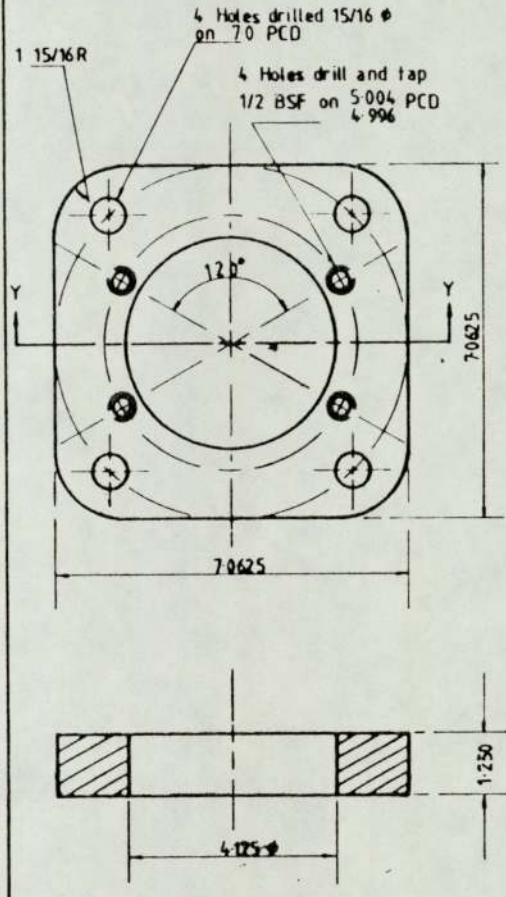


Title: Dog assembly-components		
Drawn: S. M. Maranga	2/4/80	Draw 2/79
Material: EN 24 unless stated	No. of parts 1 of each unless stated	
Dimensions: Inches	Scale: 1:1	

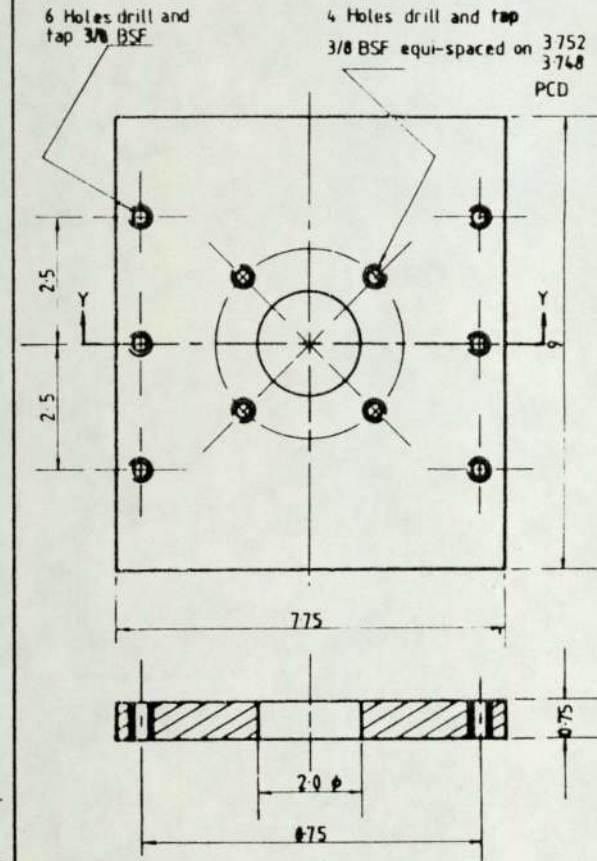
TAG LOAD CELL PLATE A



TAG LOAD CELL PLATE B



PLUG THRUST BLOCK



NOTE:  
General tol.  $\pm 0.013$

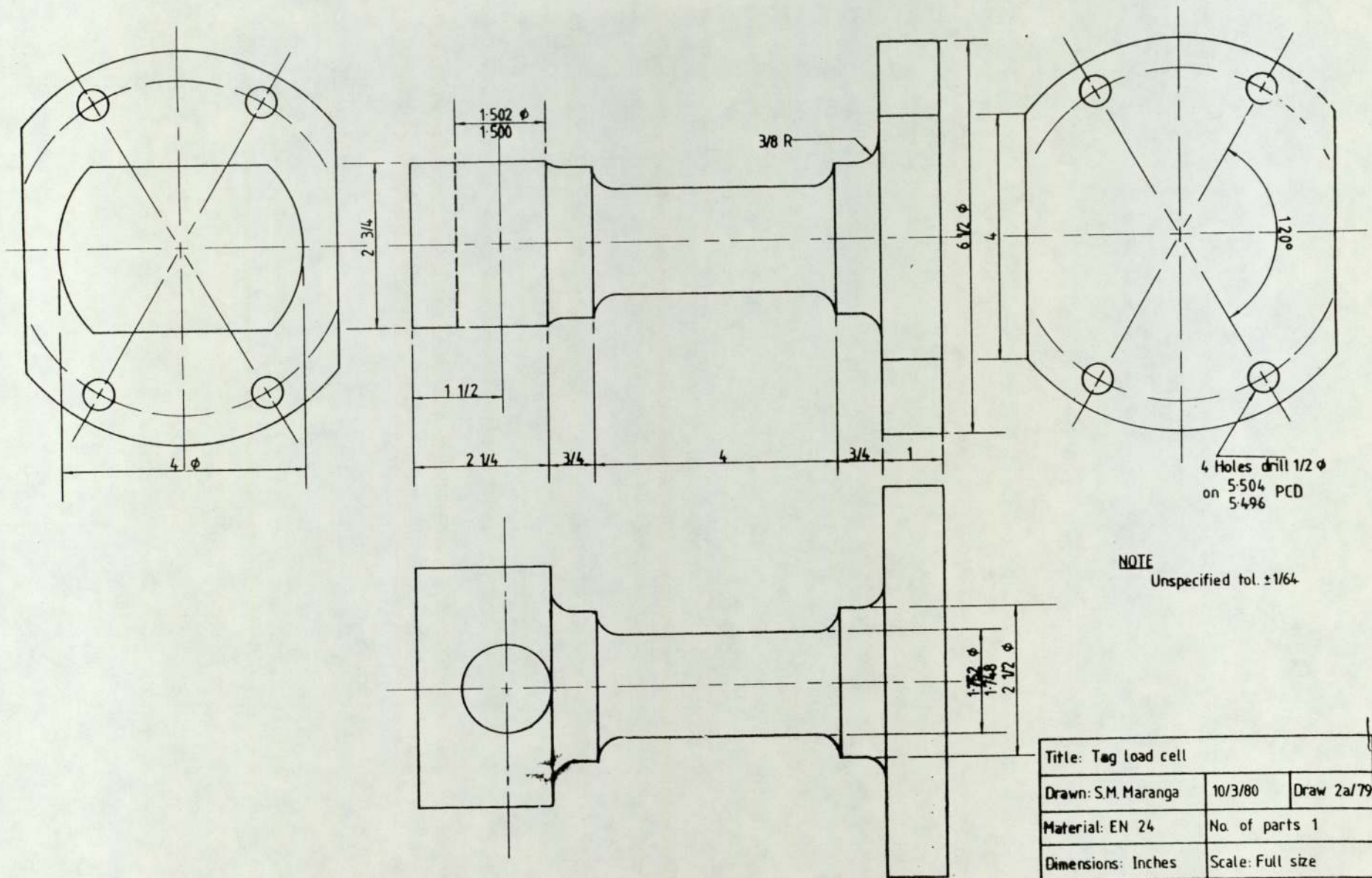
Title: Hydraulic bench accessory components

Drawn: Maranga 19/3/80 Draw 47/80

Material: Mild Steel No. of parts 3

Dimension: Inches Scale: 1:2

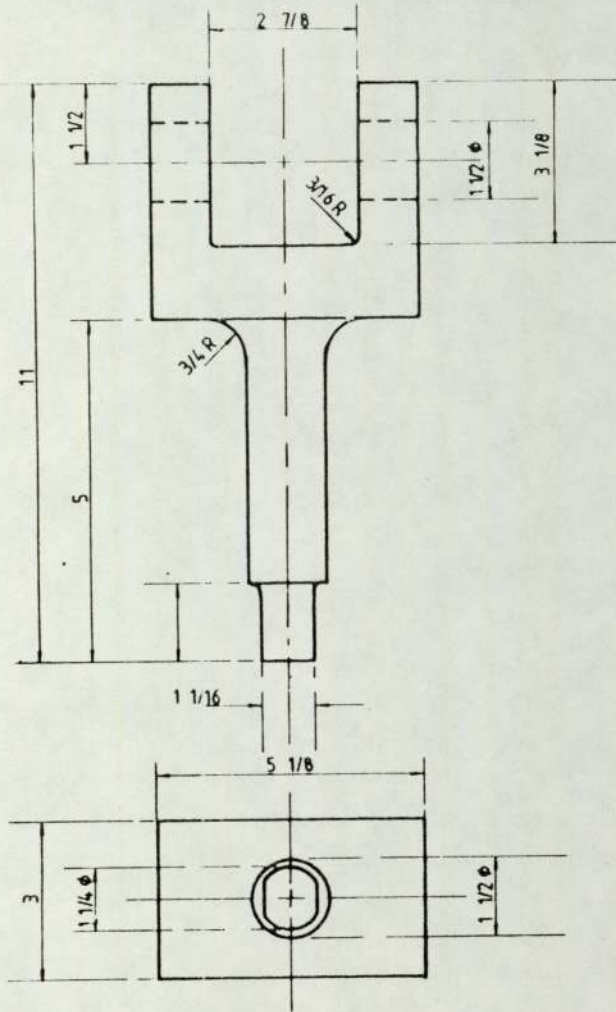
- A160 -



NOTE  
Unspecified tol.  $\pm 1/64$

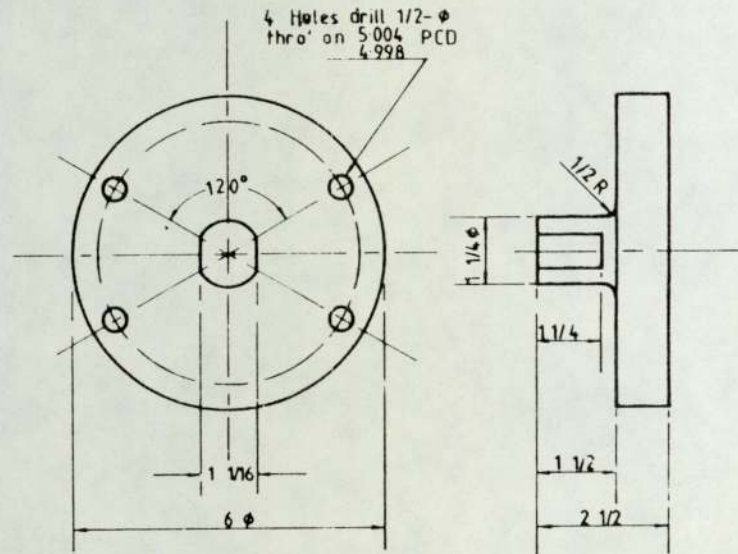
Title: Tag load cell		
Drawn: S.M. Maranga	10/3/80	Draw 2a/79
Material: EN 24	No. of parts 1	
Dimensions: Inches	Scale: Full size	

Force/torque calibrating adaptor



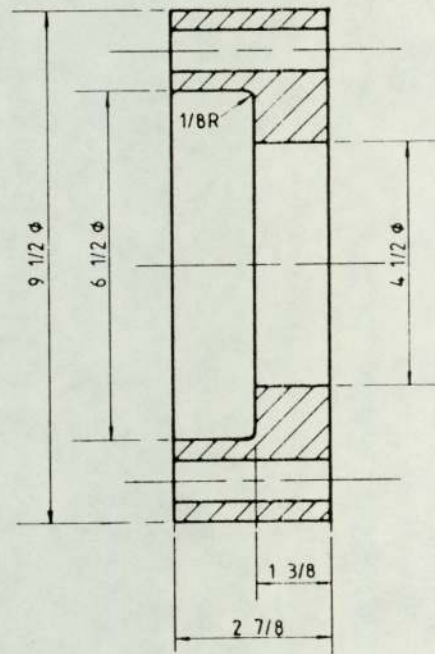
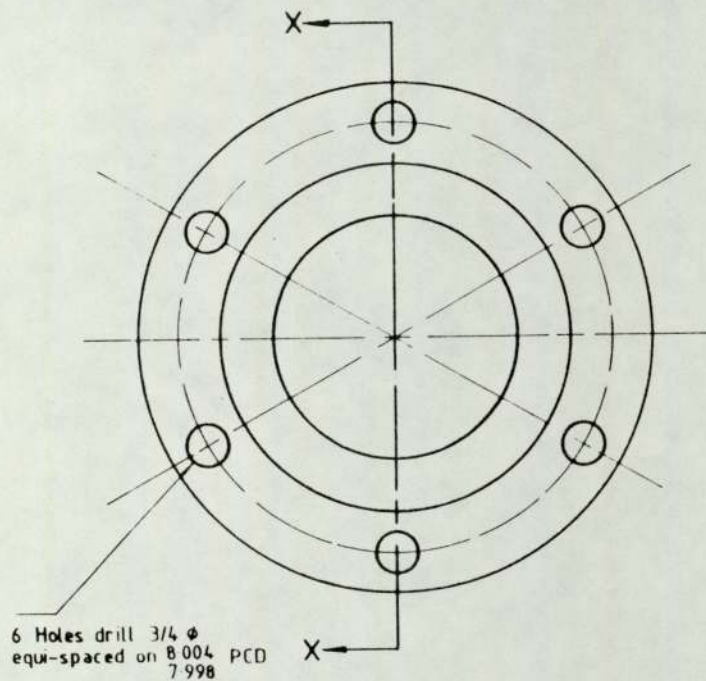
- A161 -

Torque calibrating adaptor



NOTE:  
General tol.  $\pm 1/64$

Title: Tag load cell calibrating adaptors		
Drawn: Maranga	19/3/80	Draw 52/80
Material: Mild Steel	No. of parts 2	
Dimensions: inches	Scale: 1:2	

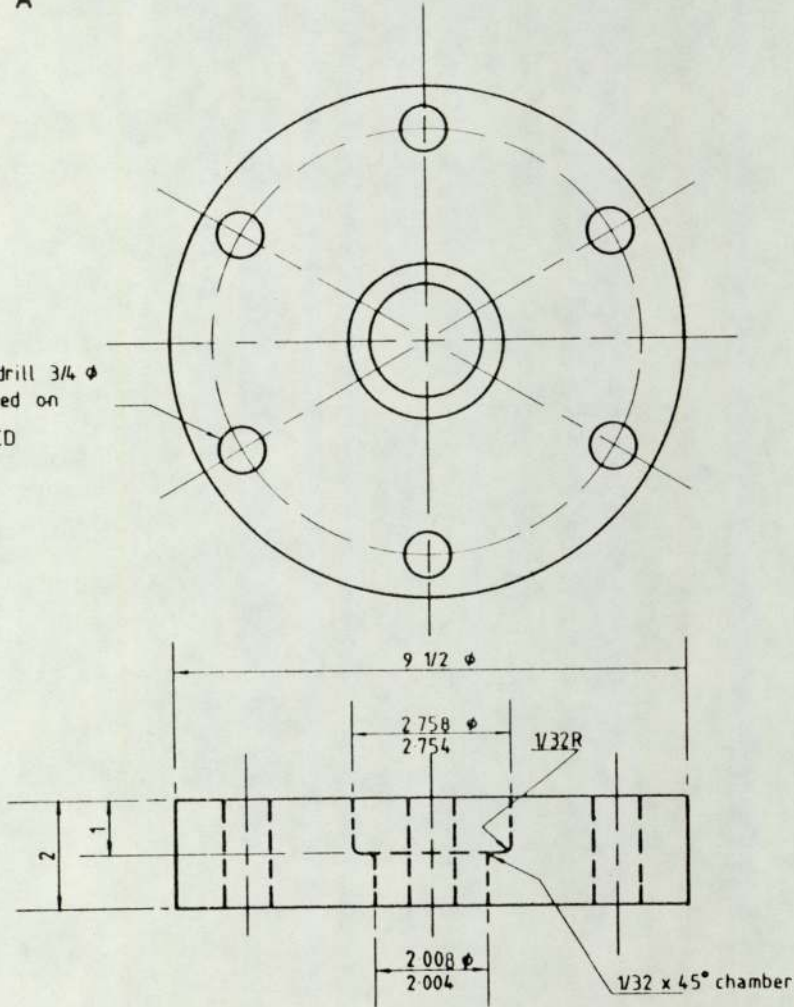


NOTE  
General tol.  $\pm 1/64$

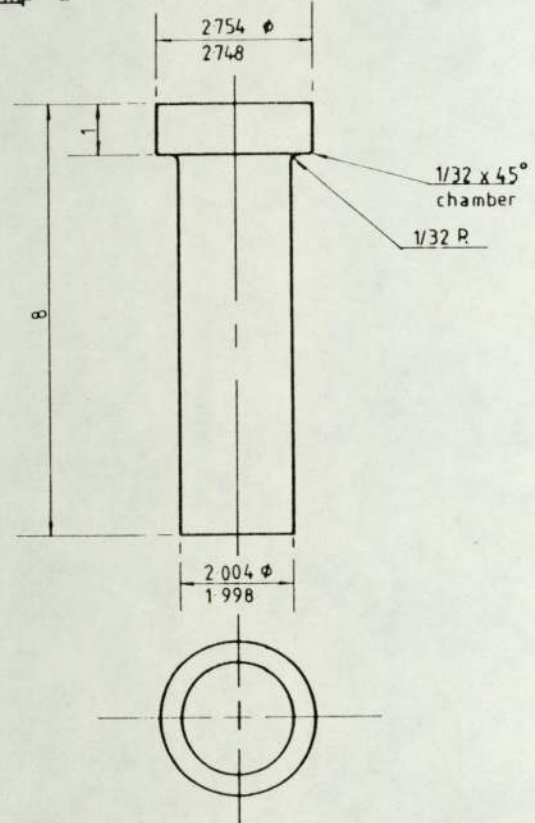
Title: Tag cell-Denxon adaptor		
Drawn: Maranga	19/3/80	Draw 45/80
Material: Mild Steel	No. of parts 1	
Dimensions: Inches	Scale: 1:2	

Comp. A

6 Holes drill  $3/4 \phi$   
equi-spaced on  
8.004 PCD  
7.998 PCD



Comp. B



Title: Tag cell-Denison adaptors

Drawn: Maranga

19/3/80

Draw 46/80

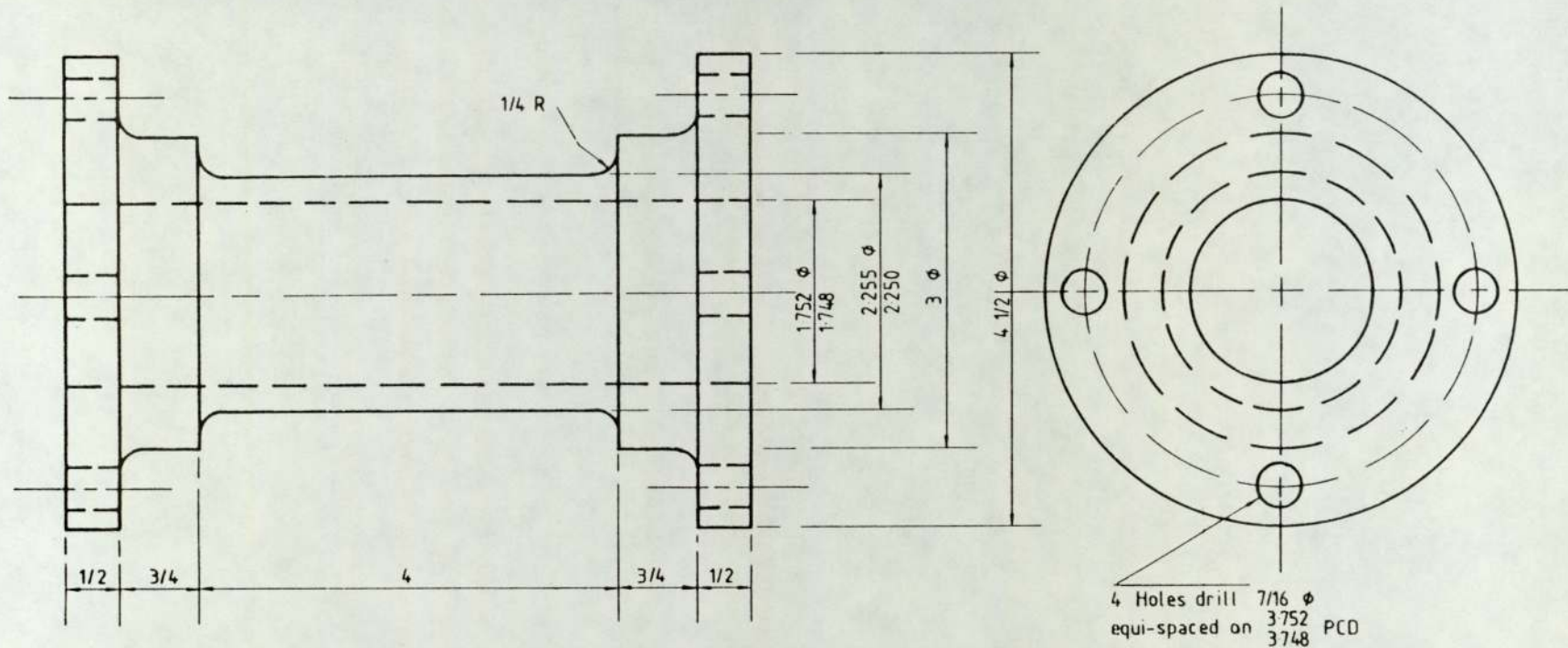
Material: Mild Steel

No of parts 1 of each

Dimensions: Inches

Scale: 1:2

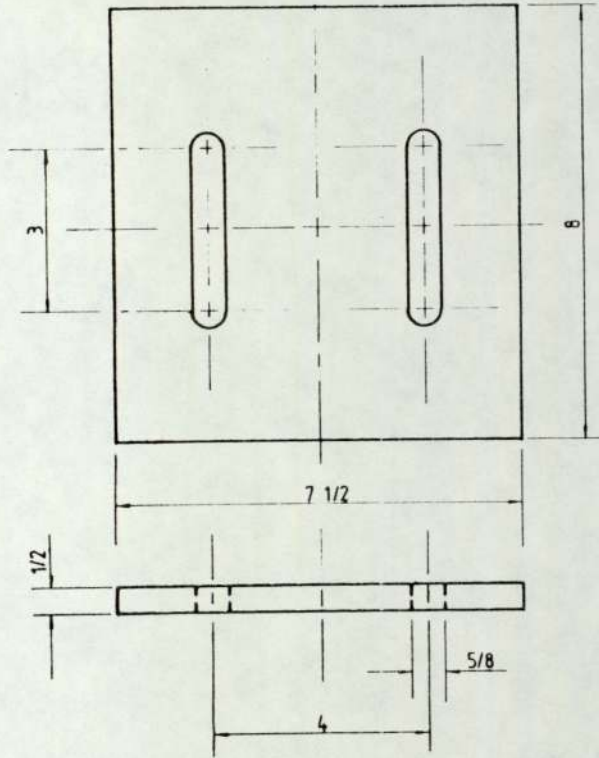
- A164 -



**NOTE**  
Unspecified tol.  $\pm 1/64$

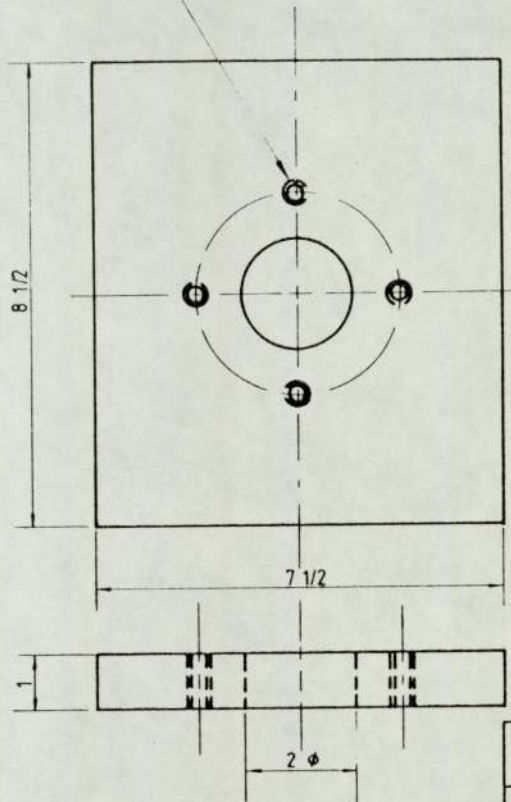
Title: Plug load cell		
Drawn: S.M. Maranga	6/3/79	Draw 1/79
Material: EN 24	No. of parts 1	
Dimensions: Inches	Scale: Full size	

Component A



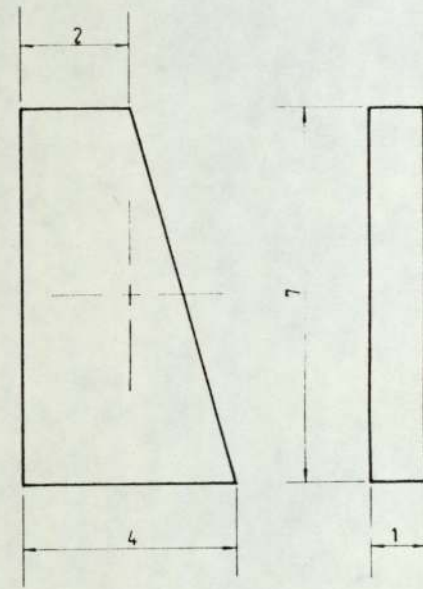
Component B

4 Holes drill and tap  $3/8 \phi$  BSF  
 equi-spaced on  $\frac{3.752}{3.748}$  PCD



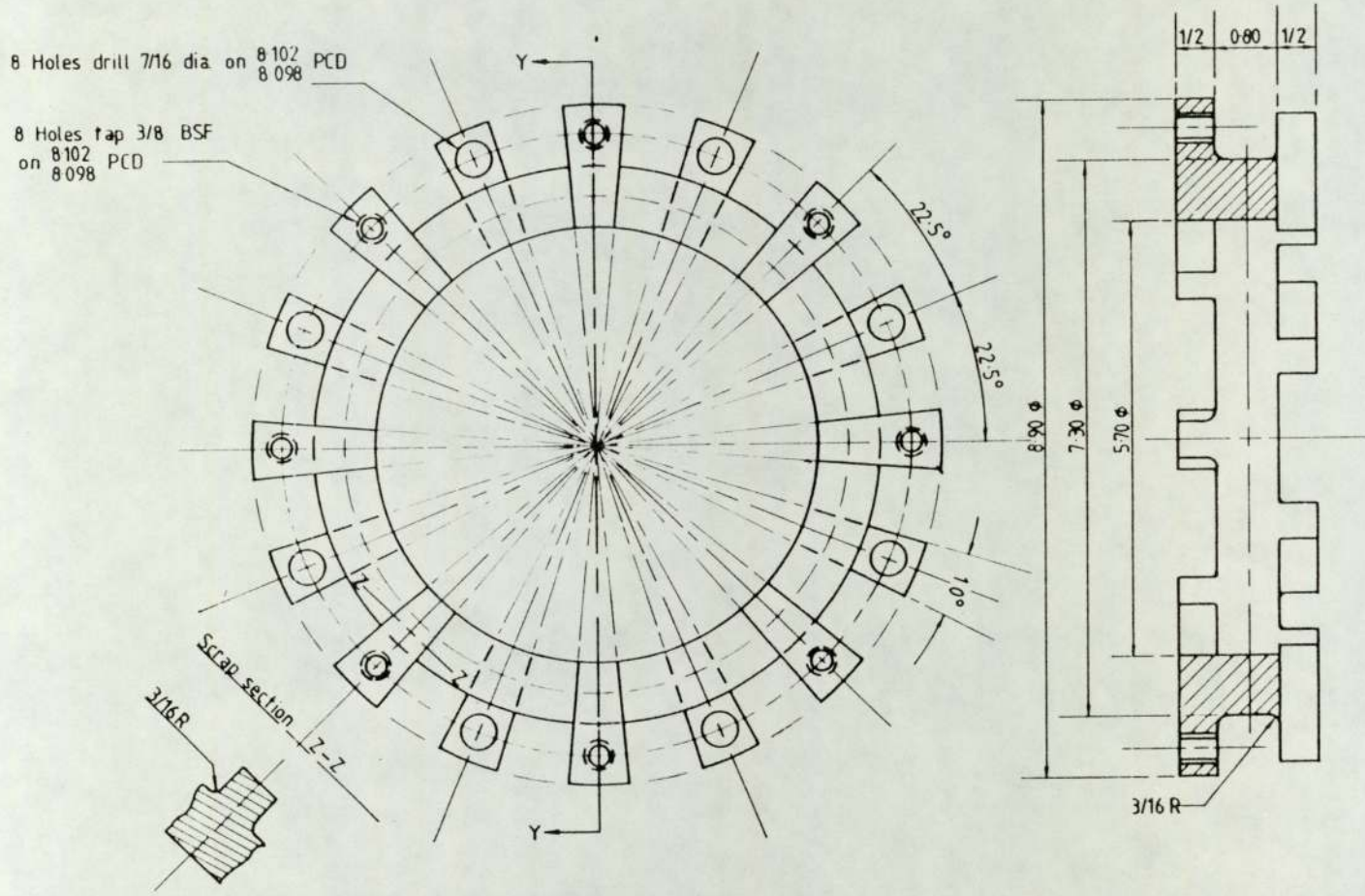
Component C

No. off 2



NOTE:  
 General tol.  $\pm 1/64$

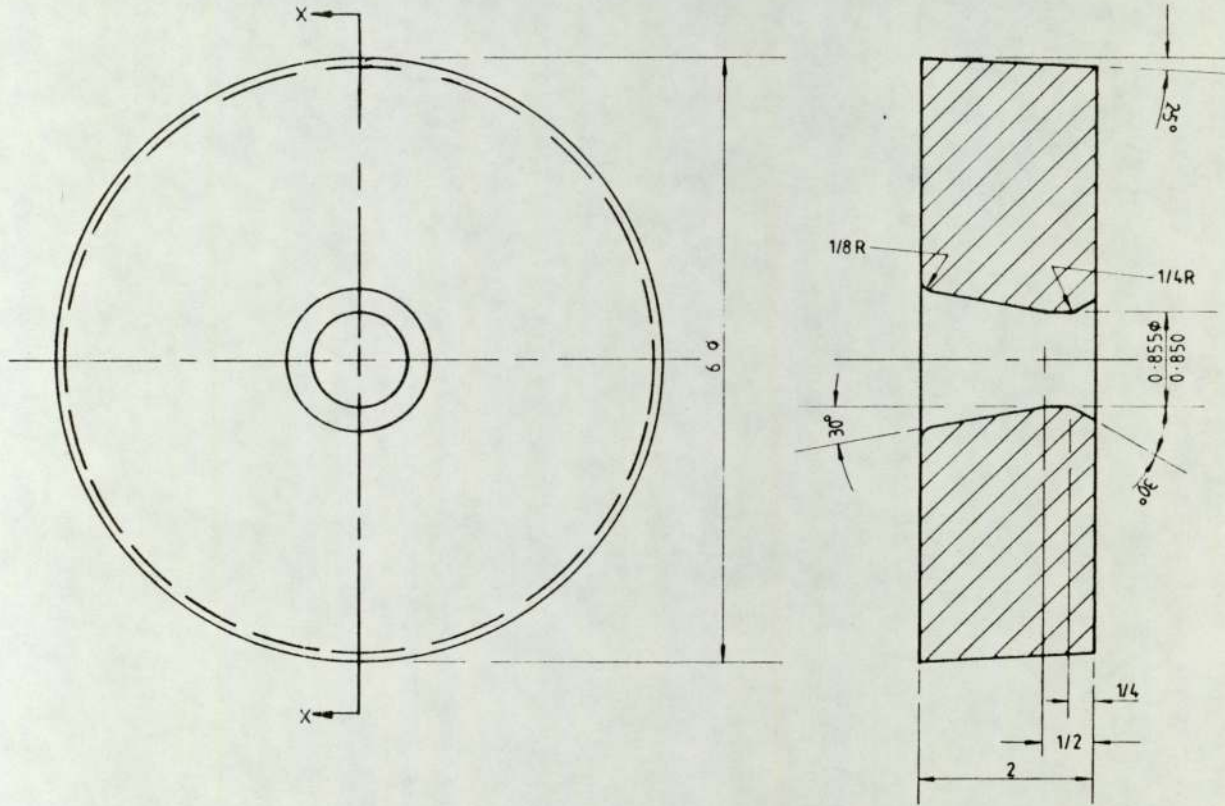
Title: Plug thrust block-adjustable		
Drawn: Maranga	20/3/80	Draw 51/80
Material: Mild Steel	No. of parts 1 of each unless stated	
Dimensions: all inches	Scale: 1:2	



**NOTE**

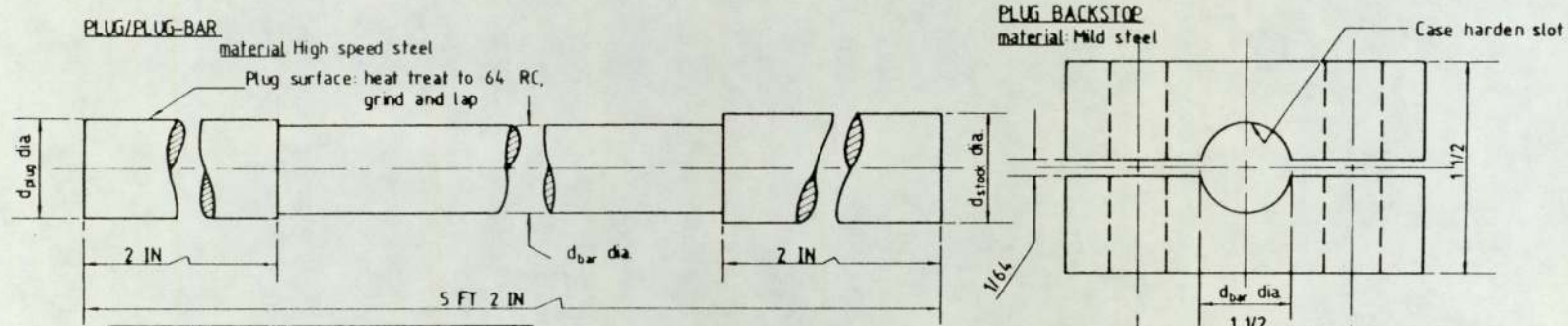
- [1] Unspecified Tol.  $\pm 0.005$
- [2] Angular Tol.  $\pm 01^\circ$

Title: Die load cell		
Drawn: Maranga	23/3/80	Draw 3/79
Material: EN 32	No. of parts 1	
Dimensions: Inches	Scale: 1:1	

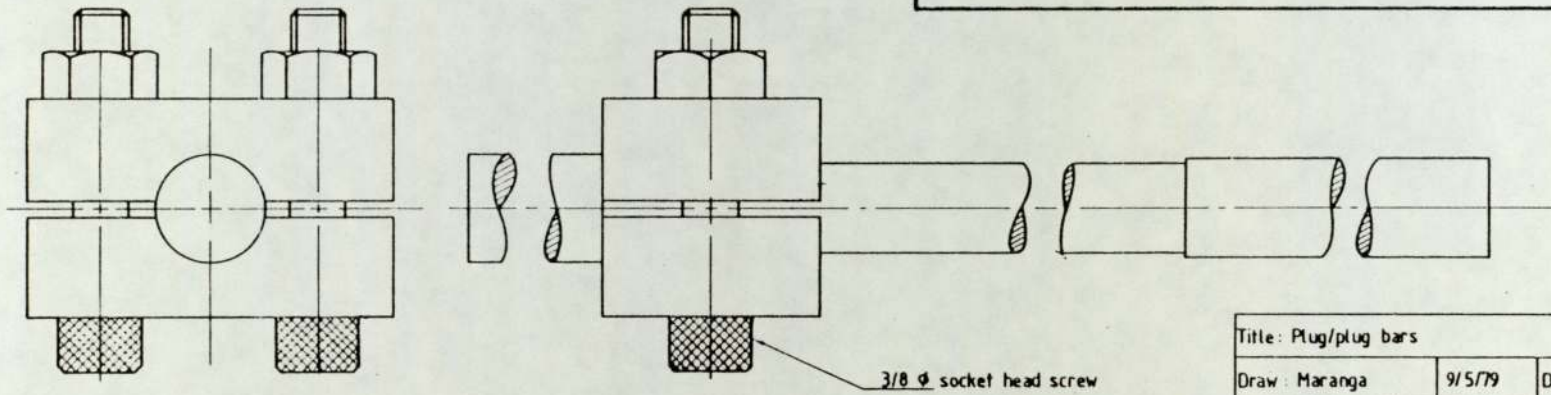


Title: Tagging die		
Drawn: S.M. Maranga	17/12/80	Draw 29/79
Material: Tool Steel	No. of parts 1	
Dimensions: Inches	Scale: 1:1	





Nominal plug size	Stock size $d_{stock}$	Plug size $d_{plug}$		$d_{bar}$
		Upper limit	Lower limit	
P- 7/16	7/16	0.433	0.431	0.423
15/32	31/64	0.471	0.469	0.454
31/64	1/2	0.486	0.484	0.480
1/2	1/2	0.496	0.494	0.486
9/16	9/16	0.558	0.556	0.548
5/8	5/8	0.621	0.619	0.611
11/16	11/16	0.683	0.681	0.673
3/4	3/4	0.746	0.744	0.736



PLUG BACKSTOP ASSEMBLY

Title: Plug/plug bars		
Draw: Maranga	9/5/79	Draw 23/79
Material: Stated for each	No. of parts 8 sets	
Dimensions: Inches unless stated otherwise	Scale: 2:1	

A-18 REDUCTION OF DRAW FORCE WITH DIE ROTATION

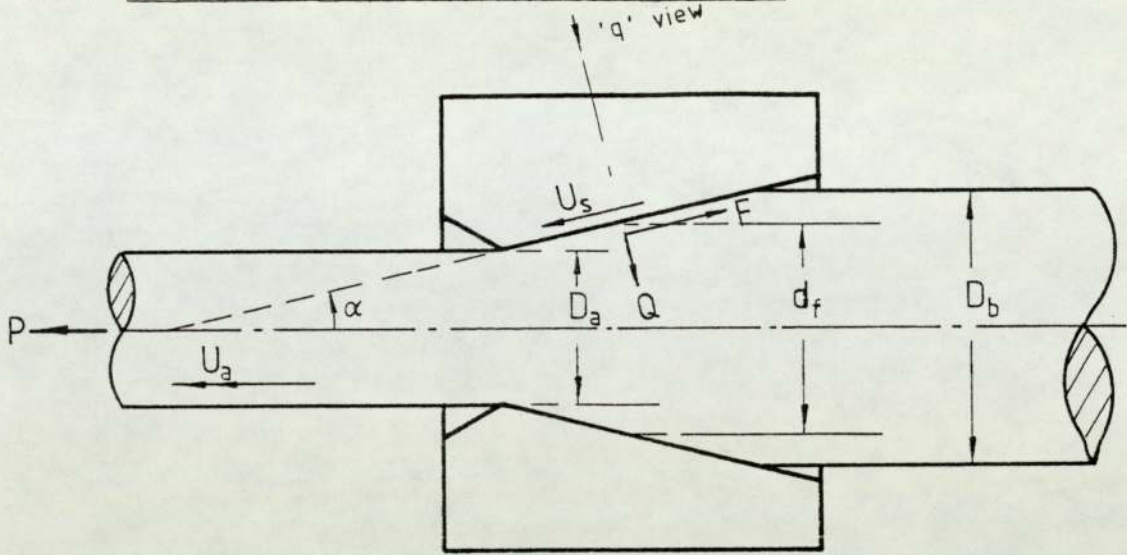


Figure A-18.1 Forces and velocities in axisymmetric drawing

From equilibrium of forces in the horizontal direction,

$$P = Q \sin\alpha + F \cos\alpha \quad (\text{A-18.1})$$

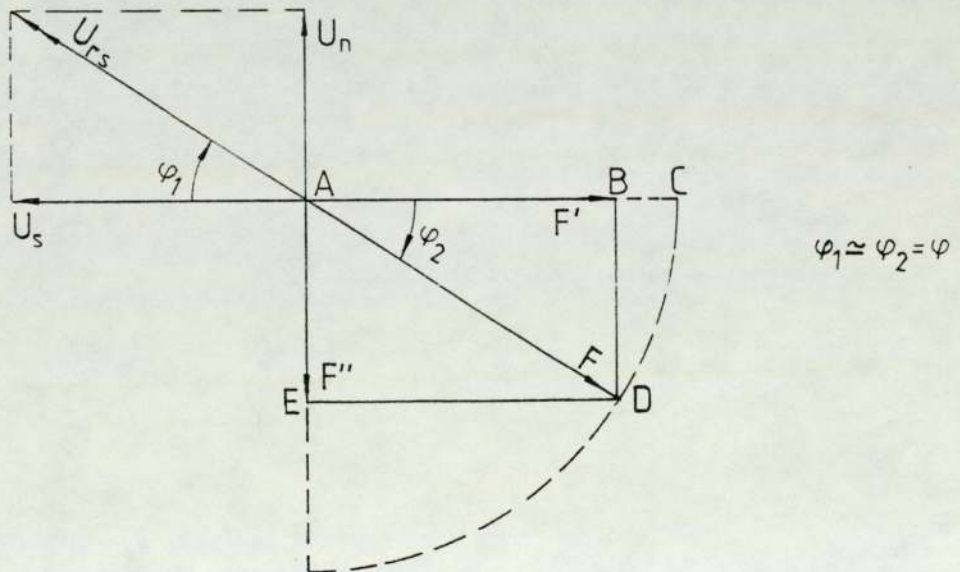


Figure A-18.2 Velocity and friction vector with die rotation at position f in Fig. A-18.1 (View normal to the die surface, 'q' direction)

$U_s$  : velocity of a point f moving along the die surface without rotation  
 $U_n$  : circumferential velocity of point f relative to the die during rotation

AC = F: friction force vector without die rotation

When the die rotates, AC swings round a position AD. Since the friction force acts in opposite direction to the relative motion between the two surfaces, and if  $\varphi_1 = \varphi_2 = \varphi$  and the magnitude of the force F is unchanged by the motion,

$$AD = AC = F \quad (A-18.2)$$

There will therefore be a reduction in draw force corresponding to  $BC \cos\alpha$ . By equilibrium of forces the draw force  $P_r$  with die rotation will be given by:

$$\begin{aligned} P_r &= Q \sin\alpha + F' \cos\alpha \\ &= Q \sin\alpha + F \cos\varphi \cos\alpha \end{aligned} \quad (A-18.3)$$

Combining equations (A-18.3) and (A-18.1) gives:

$$\frac{F}{Q} = \frac{(P - P_r) \tan\alpha}{(P_r - P \cos\varphi)} = \mu_P \quad (A-18.4)$$

Rotational torque is given by:

$$\begin{aligned} T &= F'' \frac{d_f}{2} \\ &= \frac{F}{2} \sin\varphi d_f \end{aligned} \quad (A-18.5)$$

Equations (A-18.1) and (A-18.5) can be combined to give:

$$\frac{F}{Q} = \frac{2T \sin\alpha}{(P d_f \sin\varphi - 2T \cos\alpha)} = \mu_T \quad (A-18.6)$$

## ITANYA RIA IBUKU RIRI

Matukũ-inĩ maya tũrĩ ũnyinyi wa mĩtukanio ĩrĩa iganda ihũthagĩra harĩ gũthondeka mĩthemba ya indo iria andũ mabataraga, wendi wa kũnyihia wĩra, o hamwe na ũnyinyi wa ihumo cia hinya ũria ũhũthĩkaga harĩ gũtwarithia macini na iganda nĩiratũma athondeki a mĩberethi-ya-cuuma ya mĩena mĩingĩ maambĩrĩrie gwĩcirĩria njĩra ingĩ cia kũmĩthondeka. Harĩ gĩcunji kĩmwe kĩa ũbundi ũcio wa mĩberethi kĩrĩ bata mũno iganda-inĩ na kĩagĩrĩire kwerekerio mecirĩa. Gĩcunji kũ nĩ kĩrĩa kĩĩgĩ ũthondeki wa mĩberethi ya mĩena mĩingĩ kuuma harĩ mĩberethi ya gĩthiũrũrĩ na njĩra ya kwamba kũingĩria mũberethi wa gĩthiũrũrĩ gĩkama-inĩ gĩa gĩthiũrũrĩ na kũũhĩtũkĩria gĩkama-inĩ kũ thabari ĩmwe nĩgetha uumĩre mwena ũũria ũngĩ ũrĩkĩtie gũcongwo ũgatuĩka wa mĩena mĩingĩ. Ta ũthondeki-inĩ wa nati iria ihũthĩkaga mwako-inĩ na harĩ kwoha cuuma ũbundi ũyũ no ũnyihie wĩra mũno o hamwe na mahũthĩro ma hinya wa gũtwarithia macini. O hamwe na ũguo ũbundi wa mĩthemba ũyũ no ũhote gũtũma cuuma ĩrĩa ĩthondekete nati ĩgĩe na hinya na yagĩrĩre makĩria mahũthĩro-ini mayo.

O na gũtuika wĩra mũingĩ wa iganda-inĩ wa kũgeria mawoni ma mĩthemba mĩingĩ na wa gwĩcirĩa nĩũrĩkĩtie kũrutwo ũkonĩ mũguĩrie wa mũberethi wa gĩthiũrũrĩ ũtonyetio mĩcuuma mĩraihi wa gĩthiũrũrĩ irima-inĩ rĩagwo kana na njĩra ya kũũguca ũhĩtũkĩrio gĩkama-inĩ gĩa gĩthiũrũrĩ, gũtiri wĩra mwandĩki wa ibuku rĩrĩ ooi kana aigũite ũrĩkĩtie kũrutwo wĩgĩ ũthondeki wa mĩberethi wa mĩena mĩingĩ kuuma harĩ mũberethi wa gĩthiũrũrĩ na njĩra ya kũhĩtũkĩria ũcio wa gĩthiũrũrĩ gĩkama-inĩ gĩa gĩthiũrũrĩ nĩgetha uumĩre mwene ũria ũngĩ ũrĩkĩtie gũcongwo ũgatuĩka wa mĩena mĩingĩ. Uhoro ũria wĩ thĩinĩ wa ibuku rĩrĩ ũkonĩ wĩra ũria mwandĩki warĩo arĩkĩtie kũruta wa gwĩcirĩa ũria ũbundi wa mĩthemba ta ũcio ũngĩhoteka o hamwe na wa kũgeria na ciiko ũria mecirĩa na mawoni maake mangĩhũthĩka ũbundi-inĩ thĩinĩ wa iganda.

Gũkĩrĩ ũguo-rĩ, itanya rĩa ibuku rĩrĩ nĩ gũkinyĩria athomi arĩo mecirĩa na mawoni ma mwandĩki o hamwe na cionererie cia ũria mecirĩa na mawoni maake mangĩhũthĩka iganda-inĩ harĩ gũthondeka mũberethi wa mĩena mĩingĩ kuuma harĩ wa gĩthiũrũrĩ na njĩra ya kũũguca thabari ĩmwe ũhĩtũkĩrio gĩkama-inĩ gĩa gĩthiũrũrĩ.

Mwandiki niagandũire wĩra-inĩ wake ati mwakĩre wa gĩkama kana mũhaanĩre wa gĩcunji kĩrĩa mũberethi wa gĩthiũrũrĩ ũkũingĩrĩra nĩgetha ũcoke uume ũrĩkĩtie gũcongwo ũgatuĩka wa mĩena mĩingĩ na irima riaguo rĩa gatagati rĩrĩ o ũrĩa riuma kiambĩrĩria-inĩ, nĩguo ũrĩ bata mũno makĩria. Mwakĩre kana mũhaanĩre wa gĩkama ũrĩa wagĩrĩire makĩria nĩ ũrĩa ũkũnyihia wĩra wa gũthondeka mũberethi na njĩra ĩrĩa ĩrendekana na ningĩ ũtũme ũitangi wa hinya wa macini ũkorwo ũrĩ mũnyinyi mũno makĩria o ũrĩa kũngĩhoteka.

Mwandiki wa ibuku nĩecirĩirie njĩra igĩrĩ cia kuonania muĩgana wa hinya ũrĩa mĩingĩ na ũrĩa mũnyinyi makĩria ũrĩa ĩngĩhũthĩka hari kũguucia mũberethi na wa gĩkama o hamwe na ũhĩhinyi ũrĩa ĩngĩendekana thĩinĩ wa gĩkama. Mũtaratara wa komubiuta (macini ya mathabu na ũhoru) nĩwathondekirwo wa gũkobia mathabu kuuma mageria-inĩ maingĩ na njĩra nyingĩ ndiganu cia kũguucia mũberethi. Maũndũ mamwe maria mangĩcenjia matũme hinya wa kũguucia mũberethi o hamwe na ũhĩhinyanu ũrĩa wĩ thĩinĩ wa gĩkama o nacio icenje nĩta muĩgana wa ũkumuthanu ũrĩa ũrĩ kũrĩa cuuma inyitanĩire o hamwe na mũhaanĩre wa gĩcunji kĩrĩa gĩcongaga mũberethi nĩgetha uume ũrĩ wa mĩena mĩingĩ. Mathabu maria maarutirwo nĩ komubiuta na maria mwandiki wa ibuku aambĩte gũthugunda meciria-inĩ maake moothe nĩ maiguanire na njĩra njega.

Njĩra igĩrĩ cia gũthima muĩgana wa ũkumuthanu gatagati-inĩ ga cuuma ya mũberethi na ya gĩkama nĩ ciecirĩirio na ikĩhũthĩrwo na ithimi iria cionekire kũhũthĩrĩtwo njĩra icio cieri ikĩiguana o wega.

Maranga wa Mũriũki